



Universidade Estadual Paulista

Faculdade de Engenharia de Ilha Solteira

Departamento de Física e Química

**Majorana bound states in hybrid quantum dot-topological
superconducting nanowires: detection and applications**

Luciano Henrique Siliano Ricco

Materials Science Graduate Program

PhD degree

March 19, 2020

Ilha Solteira, São Paulo, Brazil

UNIVERSIDADE ESTADUAL PAULISTA

Faculdade de Engenharia de Ilha Solteira

Departamento de Física e Química

Pós-Graduação em Ciência dos Materiais

**ESTADOS LIGADOS DE MAJORANA EM SISTEMAS HÍBRIDOS
COMPOSTOS POR PONTOS QUÂNTICOS E NANOFIOS
SUPERCONDUTORES TOPOLOGÍCOS: DETECÇÃO E
APLICAÇÕES**

LUCIANO HENRIQUE SILIANO RICCO

Orientador: Prof. Dr. Antonio Carlos Ferreira Seridonio

Tese apresentada à Faculdade de Engenharia
- UNESP - Campus de Ilha Solteira, para
obtenção do título de Doutor em Ciência dos
Materiais.

Área de concentração: Física da Matéria Con-
densada.

Ilha Solteira - SP

Março, 2020

FICHA CATALOGRÁFICA

Desenvolvido pelo Serviço Técnico de Biblioteca e Documentação

Ricco, Luciano Henrique Siliano.

R359m Majorana bound states in hybrid quantum dot-topological superconducting nanowires: detection and applications / Luciano Henrique Siliano Ricco. -- Ilha Solteira: [s.n.], 19/03/2020
202 f. : il.

Tese (doutorado) - Universidade Estadual Paulista. Faculdade de Engenharia de Ilha Solteira. Área de conhecimento: Física da Matéria Condensada, 2020

Orientador: Antonio Carlos Ferreira Seridonio
Inclui bibliografia

1. Majorana bound states. 2. Topological superconducting nanowires. 3. Quantum dot. 4. Hybrid systems. 5. Majorana nonlocality. 6. Zero-bias Conductance peak.


Raiane da Silva Santos

CERTIFICADO DE APROVAÇÃO

TÍTULO DA TESE: Estados Ligados de Majorana em Sistemas Híbridos Compostos por Pontos Quânticos e Nanofios Supercondutores Topológicos: Detecção e Aplicações

AUTOR: LUCIANO HENRIQUE SILIANO RICCO

ORIENTADOR: ANTONIO CARLOS FERREIRA SERIDONIO

Aprovado como parte das exigências para obtenção do Título de Doutor em CIÊNCIA DOS MATERIAIS, área: Física da Matéria Condensada pela Comissão Examinadora:

AC Seridonio

Prof. Dr. ANTONIO CARLOS FERREIRA SERIDONIO
Departamento de Física e Química / Faculdade de Engenharia de Ilha Solteira - UNESP

Prof. Dr. CLAUDIO LUIZ CARVALHO *CLC Carvalho*
Departamento de Física e Química / Faculdade de Engenharia de Ilha Solteira - UNESP

Prof. Dr. ELWIS CARLOS SARTORELLI DUARTE *ELC Duarte*
Departamento de Física e Química / Faculdade de Engenharia de Ilha Solteira - UNESP

LNO Oliveira
Prof. Dr. LUIZ NUNES DE OLIVEIRA
Instituto de Física de São Carlos / Universidade de São Paulo - USP

LK Castelano
Prof. Dr. LEONARDO KLEBER CASTELANO
Departamento de Física / Universidade Federal de São Carlos - UFSCAR

Ilha Solteira, 09 de março de 2020

© 2020 Luciano Henrique Siliano Ricco

All rights reserved

This study was supported by grant no. 2015/23539-8, São Paulo Research Foundation (FAPESP),

DEDICATÓRIA

*Dedico esse trabalho à meus pais, **Ricco e Janete**, por todo amor demonstrado à mim, por sempre estarem ao meu lado apoiando minhas decisões e escolhas sem questionamentos, por toda ajuda e por me mostrarem a necessidade de resiliência e perseverança nos momentos em que a vida, inevitavelmente, apresenta seu amargor.*

*Dedico também à minha esposa **Karen**, por seu companherismo e carinho ao longo desses anos, por estar ao meu lado nos momentos de maior dificuldade e por todo o seu altruísmo ao longo de nossa caminhada.*

AGRADECIMENTOS

Muitas pessoas, de forma direta ou indireta, contribuíram em minha jornada até aqui. Sem elas, com toda certeza a presente tese não passaria de duas meras páginas: capa e contra-capas. Expresso aqui, de forma igualitária, minha mais profunda e sincera gratidão a elas:

Ao meu orientador, Prof. Antonio Carlos F. Seridonio, por todo suporte, dedicação, sabedoria compartilhada e paciência em me orientar ao longo de todos esses anos frutíferos de boa física e amizade.

Aos meus companheiros de trabalho e amigos para a vida Yuri Marques, Willian Mizobata, José Eduardo e Mataus, por todo apoio profissional e pessoal e é claro, por muita conversa boa ao longo da boemia.

Aos colaboradores de longa data, Prof. Marcos Sérgio Figueira da Silva, Prof. Mariano de Souza e ao Prof. Ivan Shelykh, pela parceria e apoio ao longo desses bons anos.

Aos meus pais, Ricco e Janete, por todo amor, carinho, dedicação compreensão e paciência que sempre demonstraram de forma incondicional. Ao meu irmão Lucas, por toda a zoeira, alegria e risadas compartilhadas.

À minha esposa Karen, por todo amor, força, muita paciência e companherismo. Por sempre estar ao meu lado perante as dificuldades e desafios da vida.

Ao meu sogro e sogra, Marcos e Cristina, por me receberem como um filho em seu lar quando precisei.

Aos meus avós, Lourdes e Arlindo e aos meus padrinhos/tios, Paulo e Jane, por todo amor, preocupação, suporte e torcida.

Por fim, agradeço à Fundação de Amparo à Pesquisa do Estado de São Paulo (FAPESP), processo nº 2015/23539-8, pelo suporte financeiro, sem o qual o desenvolvimento do presente trabalho não seria possível. Também agradeço à Coordenação de Aperfeiçoamento de Pessoal de Nível Superior - Brasil (CAPES).



In our lives, change is unavoidable, loss is unavoidable. In the adaptability and ease with which we experience change lies our happiness and freedom. [Buddha]

The greatest enemy of knowledge is not ignorance, it is the illusion of knowledge. [Stephen Hawking]

Abstract

In the last years, the seeking for Majorana quasiparticles has been one of the hottest topics in condensed matter physics, owing to its potential application for achieving fault-tolerant quantum computing processes. Such exotic quasiparticles emerge as bound states at the ends of one-dimensional (1D) spinless p -wave superconductors within topologically protected phases. An indicative of this so-called Majorana bound states (MBSs) in these 1D systems is given by the emergence of a robust zero-bias conductance peak (ZBCP) in tunneling spectroscopy measurements. However, other physical phenomena can give rise to such a peak, as Kondo effect, disorder and Andreev bound states (ABSs), for instance. Concerning this later, such states can stick at zero energy even when parameters as magnetic field or chemical potential are changed, thus perfectly mimicking the MBSs hallmark. Hence, distinguishing between trivial ABSs and topologically protected MBSs is one of the current key issues in the field of Majorana detection. Aiming to enlarge the discussion concerning the MBS-ABS distinction, in this thesis we study the electronic transport features of a hybrid device composed by a quantum dot coupled to a topological superconducting nanowire hosting MBSs at the ends, wherein the so-called degree of Majorana nonlocality is taken into account. In this scenario [*Phys. Rev. B* 98, 075142 (2018)], we analyze the role of the Fano interference phenomenon in the well-known Majorana oscillations, showing that both shape and amplitude of such oscillatory patterns depend on the bias voltage, degree of MBSs nonlocality, and Fano parameter of the system. We also demonstrate that the spin-resolved density of states of the dot responsible for the zero-bias conductance peak strongly depends on the separation between the MBSs and their relative couplings with the dot [*Phys. Rev. B* 99, 155159 (2019)], suggesting that spin-resolved spectroscopy can be used as a tool for discriminating between ABSs and MBSs. It is worth noticing that in both works we recover experimental profiles, at least qualitatively. Moreover, along the current thesis we propose a quantum bit storing/reading mechanism [*Phys. Rev. B* 93, 165116 (2016)] and a thermoelectrical hybrid device [*Sci. Reports*, 8, 2790 (2018)], both based on MBSs properties.

Keywords: Majorana bound states, topological superconducting nanowires, quantum dot, hybrid systems, Majorana nonlocality, zero-bias conductance peak.

Resumo

Nos últimos anos, a busca pelas denominadas quasipartículas de Majorana tem sido um dos tópicos que mais tem atraído atenção na área de Física da Matéria Condensada. Esse fato deve-se à sua potencial aplicação em processos de computação quântica imunes a fenômenos de decoerência e portanto, tolerante à falhas. Tais quasipartículas emergem como estados ligados, localizados nas bordas de supercondutores *spinless* unidimensionais do tipo *p-wave*, quando esses encontram-se em uma fase topologicamente protegida. Nesses tipos de sistemas, em aparatos experimentais que envolvem espectroscopia de tunelamento eletrônico, o surgimento de um pico na condutância, localizado na voltagem zero e robusto perante variação de parâmetros do sistema, é um indicativo da presença dos chamados estados ligados de Majorana. No entanto, outros fenômenos físicos, tais como efeito Kondo, desordem e estados ligados de Andreev, por exemplo, podem dar origem a tal pico. No que diz respeito aos estados ligados de Andreev, os mesmos podem permanecer na voltagem zero com certa robustez à variação de campo magnético e potencial químico, emulando perfeitamente a assinatura dos estados de Majorana. Sendo assim, distinguir experimentalmente os estados de Andreev triviais dos estados de Majorana topologicamente protegidos é uma das questões fundamentais relacionadas a detecção de quasipartículas de Majorana a serem sanadas. Levando em conta tal cenário, na presente tese analisaram-se teoricamente as características de transporte eletrônico de um sistema híbrido, composto por um ponto quântico acoplado a um nanofio supercondutor topológico com estados ligados de Majorana localizados em suas bordas, em que o denominado grau de não-localidade de Majorana foi levado em consideração. Em uma primeira abordagem [*Phys. Rev. B* 98, 075142 (2018)], estudou-se qual o papel da interferência Fano nas chamadas oscilações de Majorana, onde pode-se constatar que a forma e a amplitude de tais oscilações são moduladas por alguns fatores, tais como a voltagem aplicada no ponto quântico, o grau de não-localidade de Majorana e o parâmetro de Fano em questão. No mesmo tipo de sistema [*Phys. Rev. B* 99, 155159 (2019)], demonstrou-se também que o tipo de spin da densidade de estados no ponto quântico responsável pelo pico em voltagem zero (assinatura Majorana) depende fortemente da separação entre os dois estados de Majorana nas bordas do fio, bem como dos acoplamentos entre o nanofio e o ponto quântico. Essa dependência sugere que medidas de transporte eletrônico com resolução de spin podem ser utilizadas para identificar qual o mecanismo responsável pelo surgimento do pico em voltagem zero. Vale a pena ressaltar que, em ambos os trabalhos, perfis experimentais conhecidos foram qualitativamente obtidos em nossas simulações. Ademais, ao longo da presente tese foi proposto um mecanismo de armazenamento e leitura de bit quântico [*Phys. Rev. B* 93, 165116 (2016)], além de um dispositivo termoelétrico híbrido [*Sci. Reports*, 8, 2790 (2018)], ambos baseados nas propriedades exóticas dos estados ligados de Majorana.

Palavras-chave: estados ligados de Majorana, nanofios supercondutores topológicos, ponto quântico, sistemas híbridos, não-localidade de Majorana, pico de condutância em voltagem zero.

List of Figures

1.1	Portrait of the Italian Physicist Ettore Majorana, who mysteriously disappeared on 25 March 1938 while travelling by ship from Palermo to Naples. His body was never found and his fate is inconclusive. The last investigations concerning the case pointed out that Majorana lived in Venezuela between 1955-1959. (Adapted from: Wikipedia and Ref. [1])	1
2.1	Sketch of the Kitaev chain in both (a) trivial and (b) topological phases. (a) In the trivial phase [Eq. (2.7)] Majorana operators of the same site are coupled to form a regular fermion. (b) In the topological regime [Eq. (2.8)], only Majoranas of adjacent sites are coupled, leading to unpaired Majoranas at the end of the chain, which are completely absent of the Hamiltonian. Adapted from [1]	7
2.2	Bulk energy dispersion $E(k)$ of the BdG Hamiltonian [Eq. (2.27)] for several values of chemical potential μ . In panel (a), the green dashed curve depicts the case of $\Delta = 0$, while the opposite situation is described by the orange curve, wherein a gap opens at $k = \pm \frac{\pi}{2}$ (orange curves). Panels (b) and (c) correspond to the trivial regime of gapped energy spectrum. The phase boundaries at $\mu = \pm t$ are shown in panels (d) and (e), in which the gap closes at $k = 0$ and $\pm\pi$, respectively.	11
2.3	Energy spectrum of the quasi-1D Rashba nanowire in absence of superconducting proximity effect, given by Eq. (A.42). (a): two spin-degenerated parabolas describing the free electron case with finite chemical potential μ . (b): the Rashba SOI breaks the spin-degeneracy along the k -axis. Each parabola carries one spin projection (red arrows). (c): The Zeeman splitting due to a magnetic field applied perpendicularly to the Rashba field removes the spin degeneracy at $k = 0$ and opens a gap of size $2E_Z$. The spin projection is locked to k for μ within the energy gap, defining a helical state.	14
2.4	Basic scheme to induce p -wave superconductivity in the 1D semiconducting nanowire, described by the Hamiltonian of Eq. (A.51). Adapted from [1].	14
2.5	Energy spectrum of proximitized Rashba nanowire for distinct cases. (a): free electron case, wherein the normal and inverted parabolas represent the kinetic energy of an electron and a hole, respectively. (b): The SOI shifts the parabolas along k -axis and cross with each other at $k = 0$. (c): The magnetic field opens a gap of $2E_Z$ at $k = 0$. (d): A gap of 2Δ is opened at the Fermi points (red circles) due to the induced pairing by proximity effect.	16
2.6	Energy spectrum of the proximitized Rashba nanowire for increasing values of Zeeman energy splitting. The critical value $E_{Zc} = \sqrt{\mu^2 + \Delta^2}$ points out the topological transition.	17

- 2.7 Left panel: Scanning electron microscope of the hybrid device from Delft experiment [20]. A semiconducting InSb nanowire is placed between S (niobium titanium nitride-NbTiN) and N (gold) reservoirs and is depleted by the gates numbered 1 to 4. The green line indicates the tunnel barrier between the contacts. Right panel: Differential conductance measurements at distinct magnetic fields B . A subgap ZBA emerges for B between 100 and 400mT, indicating the presence of MBSs at the opposite ends of the nanowire. Typical estimated parameters are the induced superconducting gap $\Delta = 250\mu eV$, the Rashba coupling $\alpha = 0.2eV \cdot \text{\AA}$ and the Zeeman energy splitting $E_Z/B \approx 1.5meV/T$ (g -factor $g \approx 50$). The measurements were performed at $T = 50mK$. Source: Ref. [3]. 20
- 2.8 (a) Scanning electron micrograph of the hybrid device from the Copenhagen experiment [68]. The blue part indicates the epitaxial growth of Al directly performed in two or three facets of the hexagonal semiconducting Indium arsenide (InAs) nanowire. The Ti/Au and Ti/Au/V are the metal and superconducting leads, respectively. The white brace indicates the quantum dot region, which spontaneously emerges due to disorder or band-bending. A magnetic field is applied parallel to the nanowire axis. (b) Differential conductance as a function of both source-drain voltage V_{SD} and magnetic field, wherein the two initial ABSs merges at $B = 0.75T$ into a stable zero-bias peak, which remains robust up to $B = 2T$. (c) Line cut plots from panel (b), showing the differential conductance for distinct values of B . The measurements were performed at $T = 20mK$. Adapted from Ref. [68] 21
- 2.9 (a) Scheme of a native quantum dot coupled to γ_L and γ_R MBSs, with finite hybridization δ between them. The dot couples with both Majoranas end modes due to finite size effects and displacement of the Majorana wave functions by tuning external magnetic field or chemical potential of the nanowire. Panels (b) and (c) show the expected low-energy spectrum of the nanowire as a function of the quantum dot gate voltage V_{dot} for overlapped and well separated MBSs, respectively. For the hybridized Majoranas (b), the zero-energy state is perturbed by the quantum dot states (anticrossing points). The energies $\epsilon_{\pm}^{M(D)}$ provide the information related to the degree of nonlocality $\Omega^2 = \frac{\epsilon_{\pm}^M}{\epsilon_{\pm}^D} \left| \frac{\sin \frac{1}{2} \theta_L}{\sin \frac{1}{2} \theta_R} \right| \approx \frac{t_R}{t_L}$, with the canting angles θ_L and θ_R related the spin-texture of left and right MBSs [69, 70], respectively. (d) False color micrograph of the hybrid device, wherein part the InAs nanowire (green) is partially covered by epitaxial Al (blue). The quantum dot region is indicated by the dashed circle. (e) Differential conductance at $B = 1T$, in agreement with the prediction of panel (b). Adapted from Ref. [69] 21
- 3.1 Sketch of the model described by Anderson: an atom with localized magnetic moment is adsorbed in a non-magnetic metallic host. V stands for the hybridization strength between the former and the later. 29
- 3.2 (a) Schematic DOS of an impurity (dot) adsorbed in a non-magnetic metallic host [Eq. (3.39)] described by the Anderson Hamiltonian [Eq. (3.18)] for the particle-hole symmetric regime $2\varepsilon_{d\sigma} + U = 0$. Both the peaks describe the Coulomb blockade physics acting within the impurity. The broadening of such peaks are given by the self-energy Γ owing to the coupling between the discrete state of the impurity and the continuum which describes the non-magnetic host. (b) if an electron with a spin up (\uparrow) for instance, is added at the level $\varepsilon_{d\sigma}$, another electron with opposite spin down (\downarrow) cannot be placed at the same energy level due to the Coulomb repulsion, thus opening a second electronic channel at $\varepsilon_{d\sigma} + U$ 33
- 7.1 Green's functions Tree showing a bird's eye view of evolution of each Green's function under application of EOM technique. The functions with a red X were thrown away due to Hubbard-I truncation scheme. 72

7.2	(a) Color scale plot of density of states for a QD under external magnetic field coupled to a normal lead as a function of QD energy level ε_d and spectral frequency ω . (b) Line cut in the above panel at $\omega = 0$ (dashed line in (a)). The arrows indicate the spin of each possible QD state. (c) Total occupation number of the QD state obtained by self-consistent numerical calculation [Eq. (14) of draft], showing a singlet-doublet-singlet transition.	83
7.3	Density of states as a function of ω with $\varepsilon_d = -2.5E_0$ in the Anderson symmetric regime ($U = 5E_0$), for distinct physical situations. The curves were shifted for better visualization.	84

Contents

1	Introduction	1
2	Majorana Fermions in Condensed Matter Physics	5
2.1	Overview	5
2.2	The Kitaev Model	6
2.3	MZMs in quasi-one dimensional Rashba nanowires	11
2.4	Experimental detection of Majorana bound states in semiconducting proximitized nanowires	18
2.4.1	First generation	19
2.4.2	Second generation	20
2.4.3	Outlook	22
3	Mathematical formalism	26
3.1	Green's function formalism and the equation of motion technique	26
3.2	The Single Impurity Anderson Model (SIAM)	28
4	Decay of bound states in the continuum of Majorana fermions induced by vacuum fluctuations: Proposal of qubit technology	36
4.1	Overview and Remarks	36
4.1.1	Methodology	36
4.2	Published Article	39
5	Tuning of heat and charge transport by Majorana fermions	46
5.1	Overview and remarks	46
5.2	Methodology	47
5.3	Published Paper	48
6	Majorana oscillations modulated by Fano interference and degree of nonlocality in a topological superconducting nanowire-quantum dot system	58
6.1	Overview and remarks	58
6.2	Methodology	59
6.3	Published paper	61

7	Spin-dependent zero-bias peak in a hybrid nanowire-quantum dot system: Distinguishing isolated Majorana fermions from Andreev bound states	70
7.1	Overview and Remarks	70
7.2	Theoretical Model and density of states calculations	70
7.3	Published Paper	73
7.4	Supplementary Results	83
8	Conclusions	85
A	Obtaining the DOS of Majorana quasiparticles	86
A.1	Finding the Green's Function for the Majorana Quasiparticle η_1	87
A.1.1	Summary of mean relations	108
A.1.2	Grouping terms	109
A.1.3	Summary of Results for $\tilde{G}_{\eta_1\eta_1}$	112
A.2	Finding the Green's Function for the Majorana Quasiparticle η_2	113
B	DOS of the Quantum Dot for the Interacting Spinfull Model within Hubbard-I Approximation	117
B.1	Single particle Green's functions (two operators)	117
B.2	Hubbard-I approximation (1 st order)	136
B.2.1	EOM and decoupling scheme in $G_{d_\sigma n_{d\bar{\sigma}}, d_\sigma}^r(\omega)$	137
B.2.2	EOM and decoupling scheme in $G_{d_\sigma^\dagger n_{d\bar{\sigma}}, d_\sigma}^r(\omega)$	165
B.2.3	Resulting system of Green's functions	183
B.2.4	Results for Hubbard-I approximation	184
C	Curriculum Vitae and List of Publications	186

Chapter 1

Introduction

There is no doubt at all that the first half of the twentieth century was pivotal for the understanding of the quantum nature of matter. In this period, despite substantial contributions of many genius of Physics, as the Bohr atomic model in 1911, the Werner Heisenberg and his matrix formulation in 1925 and the non-relativistic wave equation developed by Erwin Schrödinger half a year later, there are two theoretical breakthroughs proposed by the british physicist Paul Dirac which deserves special attention [1]. The first one is related to the development of operators acting on the Hilbert space and can be considered the genesis of quantum field theory. The second [2] concerns to the proposal of an equation which bears his name: the relativistic version of Schrödinger's equation. Besides the conciliation between quantum mechanics and special relativity, the Dirac equation allowed the prediction the antimatter, which was confirmed four years later with the discovery of the positron by Carl Anderson in 1932 [3].



Figure 1.1: Portrait of the italian Physicist Ettore Majorana, who mysteriously disappeared on 25 March 1938 while was travelling by ship from Palermo to Naples. His body was never found and his fate is inconclusive. The last investigations concerning the case pointed out that Majorana lived in Venezuela between 1955-1959. (Adapted from: [Wikipedia](#) and Ref. [1])

Almost ten years after the Dirac's prediction of antimatter, the young italian physicist Ettore Majorana¹ (Fig. 1.1) solved the Dirac equation in terms of real solutions, allowing the description of particles that are their own antiparticles [4], unlike electrons and positrons. According to Majorana's idea, these exotic particles could be neutrinos [2]. Interestingly enough, recent experimental advances in particle physics [6, 7] can reveal that neutrinos indeed are their own antiparticles by measuring a process called neutrinoless double-beta decay, which would lead to violation of the conservation of lepton number, a fundamental law in nature within the standard model.

For many years, the impact of Majorana's solution for Dirac equation remained obviously restricted to areas belonging to high energy physics [1, 2]. No one could imagine that such a proposal would have a huge impact in a completely unexpected field: the condensed matter physics [8]. Nowadays, the searching for Majoranas in condensed matter systems has caused a true healthy competition between researchers of such a field and undoubtedly has become one of "trend top-

¹Quoting his advisor, Enrico Fermi : "There are several categories of scientists in the world; those of second or third rank do their best but never get very far. Then there is the first rank, those who make important discoveries, fundamental to scientific progress. But then there are the geniuses, like Galilei and Newton. Majorana was one of these". (Source: [Wikipedia](#))

ics” in physics. The reason behind that comes from the possibility of applications of such Majorana excitations as building blocks for fault-tolerant quantum computation owing to their exotic non-Abelian exchange statistics [9] and even giant technology companies as [Microsoft](#), for instance, have been investing a lot of money and efforts in this seek for Majorana fermions.

Motivated by such a flurry around the searching for Majoranas in condensed matter physics, as well as by the intrinsic beauty of the theoretical physics in such a field, in this thesis we present our tiny contribution to better understand the electronic transport mechanisms of Majorana fermions in condensed matter, focusing on hybrid systems constituted by one dimensional p -wave superconducting nanowires coupled to quantum dots. This understanding allowed us to provide new insights about Majorana detection protocols and propose new applications for such devices.

Basically, this thesis is a compendium of the main papers published along the PhD period and is organized as follows:

- **Chapter 2:** we start with a brief introduction concerning the theoretical framework supporting the emergence of the so-called Majorana bound states in 1D superconducting nanowires. In this sense, we review the Kitaev toy model, which is considered the simplest Hamiltonian wherein isolated Majorana zero-modes appears at the nanowire ends when the system enters into the topological phase. Next, we explore the well-established features of quasi-1D Rashba nanowires in presence of magnetic field and proximity effect, which have been considered the most promising platforms to perform Majorana excitations. Lastly, we discuss the main tunneling spectroscopy conductance experiments for Majorana detection in these quasi-1D hybrid devices.
- **Chapter 3:** we present the theoretical tool used in all our papers: the equation of motion (EOM) technique applied to Anderson-type Hamiltonians. We start with a brief explanation concerning Green’s functions followed by the EOM method. We also discuss the single impurity Anderson Model by calculating the corresponding density of states via EOM within the Hubbard-I approximation. The full version of the calculations related to our works can be seen in Appendices [A](#) and [B](#).
- **Chapter 4:** we show the published article *Decay of bound states in the continuum of Majorana fermions induced by vacuum fluctuations: Proposal of qubit technology* [[Phys. Rev. B 93, 165116 \(2016\)](#)], wherein we have proposed a new way to read/storage the qubit information in a setup composed by two semi-infinite Kitaev nanowires within the topological phase coupled to a quantum dot between metallic reservoirs. It was found that such an exotic read/storage mechanism is based on the interplay between vacuum fluctuations, Majorana quasiparticle excitations and formation of bound states in the continuum.
- **Chapter 5:** we present the paper *Tuning of heat and charge transport by Majorana fermions*, [[Sci. Reports, 8 2790 \(2018\)](#)]. In such a work, we have theoretically explored both electric and heat transport features in a topological U-shaped Kitaev chain coupled to a quantum dot. We have shown that the topological thermoelectric device works as a tuner electricity and heat owing to the presence of Majorana bound states in the system. We emphasize that such work was subject of an article at “[Agência Fapesp](#)” website and chosen as “*Destaque em Física*” by *Sociedade Brasileira de Física (SBF)*.

- **Chapter 6:** another article entitled *Majorana oscillations modulated by Fano interference and degree of nonlocality in a topological superconducting nanowire-quantum dot system* [*Phys. Rev. B* 98, 075142 (2018)] is shown, wherein we have explored a T-shaped hybrid setup, allowing us to determine the role of Fano interference processes in the so-called Majorana oscillations, discussed previously in Sec. 2.3.
- **Chapter 7:** we present our most recent paper *Spin-dependent zero-bias peak in a hybrid nanowire-quantum dot system: Distinguishing isolated Majorana fermions from Andreev bound states* [*Phys. Rev. B* 99, 155159 (2019)]. In such a work, we have analysed a hybrid system composed by a semiconducting nanowire with proximity-induced superconductivity coupled to a quantum dot. We have shown that spin-resolved measurements performed at the dot are able to solve one of the key issues concerning the Majorana detection: distinguish between truly topological Majorana bound states and the so-called trivial Andreev bound states.

It is worth mentioning that some results of the papers corresponding to chapters 5, 6 and 7 qualitatively resembles recent experimental data, once we have taken into account the so-called degree of Majorana nonlocality. Such a concept is introduced in Sec. 2.4.2 (Fig. 2.9) and also discussed along the aforementioned papers.

Bibliography

- [1] R. Aguado, Riv. Nuovo Cimento **40**, 523 (2017).
- [2] Dirac P. A. M., Proc. R. Soc. A, **117** (1928) 610.
- [3] Carl D. Anderson, Phys. Rev. **43**, 491 (1933).
- [4] Majorana E., Il Nuovo Cimento, **14** 171 (1937).
- [5] S. R. Elliott and M. Franz, Rev. Mod. Phys. **87**, 137 (2015).
- [6] C. E. Aalseth *et al.* (Majorana Collaboration), Phys. Rev. Lett. **120**, 132502 (2018).
- [7] M. Agostini *et al.* (GERDA Collaboration), Phys. Rev. Lett. **120**, 132503 (2018).
- [8] J. Alicea, Reports on Progress in Physics **75**, 076501 (2012).
- [9] C. Nayak, S. H. Simon, A. Stern, M. Freedman, and S. Das Sarma, Rev. Mod. Phys. **80**, 1083 (2008).

Chapter 2

Majorana Fermions in Condensed Matter Physics

2.1 Overview

Distinct from high energy physics, Majorana fermions are not elementary particles in condensed matter physics, but rather quasiparticle excitations [1–3]. Such Majorana quasiparticles must fulfill the condition of a particle being equal to its own antiparticle, *i.e.*, an electron equal to its correspondent hole, which is expressed in the operator language as:

$$\gamma^\dagger = \gamma. \quad (2.1)$$

By following this criteria, superconductors seems to provide a natural environment for the emergence of such exotic excitations, since quasiparticles in a superconductor involve superpositions of electrons and holes. It is worth mentioning that the Bogoliubov-de Gennes (BdG) and the Majorana equation share the same structure [3–6]. However, the usual *s*-wave superconductivity is not sufficient for the appearance of Majorana quasiparticles, once it arises due to paired electrons with opposite spins, breaking the condition of Eq. (2.1). Such a trouble is overcome by considering “spinless” quasiparticles excitations to describe superconductivity (time reversal symmetry is broken) [1].

The aforementioned spinless feature results in a *p*-wave superconductivity in one dimension or in a $p_x + ip_y$ superconductivity in two dimensional systems, where Majoranas emerge as edge states in exotic topological superconducting phases. However, this does not seem to be useful, since *p*-wave superconductors are very rare in nature: only the Sr_2RuO_4 [7, 8], $\nu = 5/2$ fractional quantum Hall state [9] and superfluid ^3He [10–12] are known to allow such a exotic kind of pairing. The tables turned in 2008, when Fu and Kane [13] demonstrated in a seminal paper that *p*-wave pairing can be induced by an usual *s*-wave superconductor by the so-called proximity effect in the surface of a three dimensional topological insulator. Following such a idea, just two years later Lutchyn *et al* [14] and Oreg *et al* [15] independently showed that is possible to engineer a *p*-wave superconductor in a hybrid one dimensional system composed by a semiconducting nanowire with strong Rashba spin-orbit interaction (SOI) close to a *s*-wave superconductor and under external magnetic field. As will be seen later, such a 1D setup exhibits a topological phase as the magnetic field exceeds a critical value, wherein Majorana zero-modes (MZMs) emerge as bound states at the opposite ends of the superconducting nanowire.

In what follows, we present some theoretical aspects concerning the emergence of MZMs in these 1D topological superconducting nanowires (TSNWs). After, we will discuss some experimental realizations of such a device, which have been evolving since the first claim for Majorana observation in 2012.

2.2 The Kitaev Model

We start by reviewing the toy model proposed by Kitaev in 2001 [16], which is the simplest description of topological superconductivity in 1D spinless systems. Despite its simplicity, the Kitaev model has profound implications, since MZMs emerge in an extremely intuitive fashion. Basically, Kitaev wrote a Hamiltonian of a chain with N spinless fermions with a long-range-ordered p -wave pairing, which reads [1]

$$H = -\mu \sum_{j=1}^N c_j^\dagger c_j - \frac{1}{2} \sum_{j=1}^{N-1} \left(t c_j^\dagger c_{j+1} + \Delta c_j c_{j+1} + \text{h.c.} \right), \quad (2.2)$$

wherein μ is the onsite chemical potential, t is the nearest-neighbor hopping strength and Δ is the p -wave pairing amplitude (assumed as real here). The operator $c_j^\dagger(c_j)$ creates (annihilates) an electron in the site j and obey the standard anticommutation relations for fermions [17]

$$\left[c_i, c_j^\dagger \right]_+ = \delta_{ij} \quad \text{and} \quad \left[c_i, c_j \right]_+ = \left[c_i^\dagger, c_j^\dagger \right]_+ = 0, \quad (2.3)$$

where δ_{ij} is the Kronecker delta.

To understand how the non-trivial properties emerge in such a model, its instructive to rewrite the fermionic operators of the Kitaev Hamiltonian [Eq. (2.2)] in terms of two Majorana operators γ_{A_j} and γ_{B_j} as follows:

$$c_j = \frac{1}{2}(\gamma_{B_j} + \nu\gamma_{A_j}) \quad \text{and} \quad c_j^\dagger = \frac{1}{2}(\gamma_{B_j} - \nu\gamma_{A_j}). \quad (2.4)$$

This means that an usual fermionic operator can be decomposed into real and imaginary parts, corresponding to Majorana fermions. In this sense, the Majorana can be interpreted as a ‘‘half-regular fermion’’. By using the standard anticommutators of Eq. (2.3), it is easy to verify that the Majorana operators obey the following algebra [1]

$$\left[\gamma_{\alpha i}, \gamma_{\beta j} \right]_+ = 2\delta_{\alpha\beta}\delta_{ij}, \quad \gamma_{\alpha j}^2 = (\gamma_{\alpha j}^\dagger)^2 = 1 \quad \text{and} \quad \gamma_{\alpha j} = \gamma_{\alpha j}^\dagger. \quad (2.5)$$

The last relation above ensures the Majorana condition of particle being equal to its own antiparticle [Eq. (2.1)]. Using Eq. (2.4), the Hamiltonian [Eq. (2.2)] reads

$$H = -\frac{\mu}{2} \sum_{j=1}^N (1 + \nu\gamma_{B_j}\gamma_{A_j}) - \frac{i}{4} \sum_{j=1}^{N-1} [(\Delta + t)\gamma_{B_j}\gamma_{A_{j+1}} + (\Delta - t)\gamma_{A_j}\gamma_{B_{j+1}}]. \quad (2.6)$$

Let us now analyze two limiting cases of the Kitaev proposal [16]. The first one corresponds to $t = \Delta = 0$, wherein the second term of Eq. (2.6) vanishes, *i.e.*,

$$H = -\frac{\mu}{2} \sum_{j=1}^N (1 + \nu\gamma_{B_j}\gamma_{A_j}), \quad (2.7)$$

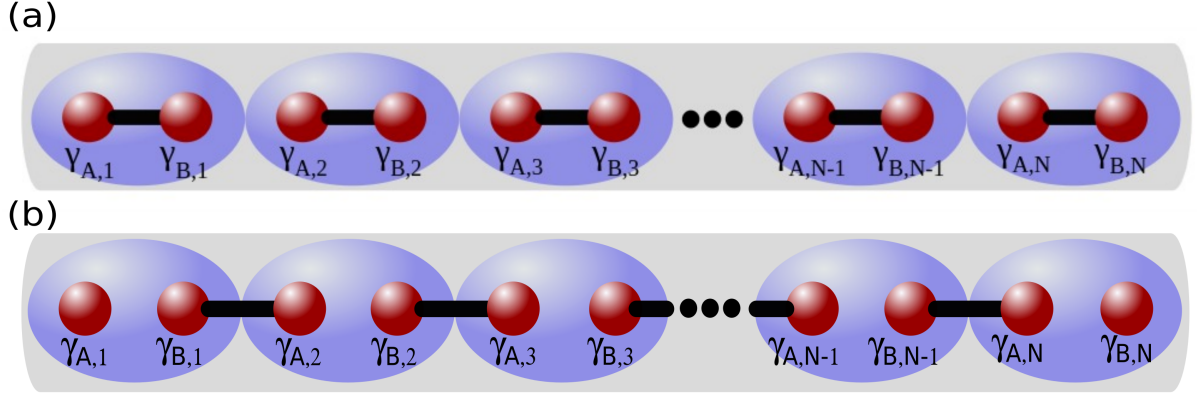


Figure 2.1: Sketch of the Kitaev chain in both (a) trivial and (b) topological phases. (a) In the trivial phase [Eq. (2.7)] Majorana operators of the same site are coupled to form a regular fermion. (b) In the topological regime [Eq. (2.8)], only Majoranas of adjacent sites are coupled, leading to unpaired Majoranas at the end of the chain, which are completely absent of the Hamiltonian. Adapted from [1]

which describes the trivial case, wherein two Majorana operators from same lattice site are coupled to form a regular fermion [Fig. 2.1(a)]. Moreover, there is an energy cost of μ to introduce a spinless fermion in the lattice. The second limiting situation arises when $\mu = 0$ and $\Delta = t \neq 0$, described by the following Hamiltonian:

$$H = -i\frac{t}{2} \sum_{j=1}^{N-1} \gamma_{Bj}\gamma_{Aj+1} = -i\frac{t}{2} (\gamma_{B1}\gamma_{A2} + \gamma_{B2}\gamma_{A3} + \gamma_{B3}\gamma_{A4} + \dots + \gamma_{B,N-1}\gamma_{AN}), \quad (2.8)$$

which represents the so-called topological phase, wherein only the Majorana fermions of adjacent lattice sites are coupled [Fig. 2.1(b)]. The most important feature concerning this phase comes from the fact that the Majorana operators γ_{A1} and γ_{BN} at the end of the lattice are explicitly absent of the Hamiltonian [Eq. (2.8)] and consequently, $[H, \gamma_{A1}] = [H, \gamma_{BN}] = 0$ [3]. To enlighten the significance of such a nontrivial property, let us rewrite Eq. (2.8) by introducing the following new fermionic operator [1, 3]:

$$d_j = \frac{1}{2}(\gamma_{Aj+1} + i\gamma_{Bj}) \quad \text{and} \quad d_j^\dagger = \frac{1}{2}(\gamma_{Aj+1} - i\gamma_{Bj}). \quad (2.9)$$

In this new basis, the Hamiltonian within the topological phase becomes

$$H = t \sum_{j=1}^{N-1} \left(d_j^\dagger d_j - \frac{1}{2} \right). \quad (2.10)$$

This form seems to be very usual, since it diagonalizes the superconducting Hamiltonian, wherein an energy $t = \Delta$ must be paid to add a d_j fermion at the lattice site. However, distinct from its original proposal [Eq. (2.2)], such a diagonal form contains only $N - 1$ new operators, which means that a fermionic degree of freedom is out of the Hamiltonian [Eq. (2.10)]. Remarkably, this missing operator is formed by the unpaired Majorana bound states (MBSs) situated at opposite ends of the Kitaev chain [Fig. 2.1(b)], *i.e.*,

$$f = \frac{1}{2}(\gamma_{A1} + i\gamma_{BN}). \quad (2.11)$$

Although it seems just another ordinary Dirac operator, $f(f^\dagger)$ shares some nontrivial features. First, it has a highly non-local nature, since the MBSs are located far apart from each other. Second, such fermionic operator is not in the Hamiltonian of Eq. (2.10) and therefore costs zero energy to be added or removed in the topological chain. In other words, a pair of delocalized Majoranas can be created without changing the energy of the ground state of the Eq. (2.8).

Bulk properties

In order to investigate the bulk properties of the Kitaev model and establish a relation with the BdG Hamiltonian for superconductors, let us analyze the system in the k -momentum space within periodic boundary conditions [1–3]. We start by rewriting the site space operators from original Hamiltonian [Eq. (2.2)] in the momentum space considering a Fourier series as follows [17, 18]:

$$c_j = \frac{1}{\sqrt{N}} \sum_k e^{-ikx_j} c_k \quad \text{and} \quad c_j^\dagger = \frac{1}{\sqrt{N}} \sum_k e^{ikx_j} c_k^\dagger, \quad (2.12)$$

wherein $x_j = ja$, with the lattice parameter a . According to such a definition,

$$\begin{aligned} \sum_{j=1}^N c_j^\dagger c_j &= \sum_{j=1}^N \frac{1}{\sqrt{N}} \sum_k e^{ikx_j} c_k^\dagger \frac{1}{\sqrt{N}} \sum_q e^{-iqx_j} c_q = \sum_{j=1}^N \frac{1}{N} \sum_{kq} e^{i(k-q)x_j} c_k^\dagger c_q, \\ &= \sum_{kq} c_k^\dagger c_q \sum_{j=1}^N \frac{1}{N} e^{i(k-q)x_j} = \sum_{kq} c_k^\dagger c_q \delta_{kq} = \sum_k c_k^\dagger c_k, \end{aligned} \quad (2.13)$$

where we recognize the discrete Kronecker delta definition

$$\delta_{kq} = \sum_{j=1}^N \frac{1}{N} e^{i(k-q)x_j} = \begin{cases} 0, & \text{if } k \neq q \\ 1, & \text{if } k = q \end{cases}. \quad (2.14)$$

In the same way,

$$\begin{aligned} \sum_{j=1}^{N-1} c_j^\dagger c_{j+1} &= \sum_{j=1}^{N-1} \frac{1}{\sqrt{N}} \sum_k e^{ikx_j} c_k^\dagger \frac{1}{\sqrt{N}} \sum_q e^{-iqx_{j+1}} c_q = \sum_{j=1}^{N-1} \frac{1}{N} \sum_k e^{ikx_j} \sum_q e^{-iq(x_j+a)} c_k^\dagger c_q \\ &= \sum_{kq} e^{-iqa} c_k^\dagger c_q \sum_{j=1}^{N-1} \frac{1}{N} e^{i(k-q)x_j} = \sum_{kq} e^{-iqa} c_k^\dagger c_q \delta_{kq} \\ &= \sum_k e^{-ika} c_k^\dagger c_k \end{aligned} \quad (2.15)$$

and

$$c_{j+1}^\dagger c_j = \sum_k e^{ika} c_k^\dagger c_k, \quad (2.16)$$

with $x_{j+1} = (j+1)a = x_j + a$. Moreover,

$$\begin{aligned}
 \sum_{j=1}^{N-1} c_j c_{j+1} &= \sum_{j=1}^{N-1} \frac{1}{\sqrt{N}} \sum_k e^{-ikx_j} c_k \frac{1}{\sqrt{N}} \sum_k e^{-iqx_{j+1}} c_q = \sum_{j=1}^{N-1} \frac{1}{N} \sum_{kq} e^{-i(k+q)x_j} \sum_k e^{-iqa} c_k c_q \\
 &= \sum_{kq} \sum_k e^{-iqa} c_k c_q \sum_{j=1}^{N-1} \frac{1}{N} e^{-i(k+q)x_j} = \sum_{kq} e^{-iqa} c_k c_q \delta_{k,-q} \\
 &= \sum_k e^{ika} c_k c_{-k} = \sum_k e^{-ika} c_{-k} c_k
 \end{aligned} \tag{2.17}$$

and

$$\sum_{j=1}^{N-1} c_{j+1}^\dagger c_j^\dagger = \sum_k e^{ika} c_k^\dagger c_{-k}^\dagger. \tag{2.18}$$

Thus, the Hamiltonian in the momentum space reads

$$H = \sum_k \epsilon_k c_k^\dagger c_k - \frac{\Delta}{2} \sum_k \left(e^{-ika} c_{-k} c_k + e^{ika} c_k^\dagger c_{-k}^\dagger \right), \tag{2.19}$$

with the kinetic energy $\epsilon_k = -\mu - t \cos(ka)$. Since our goal is to write such a Hamiltonian in a BdG fashion [1, 5, 6], we make use of the following tricks:

$$\begin{aligned}
 \sum_k \epsilon_k c_k^\dagger c_k &= \frac{1}{2} \sum_k (\epsilon_k c_k^\dagger c_k + \epsilon_k c_k^\dagger c_k) \\
 &= \frac{1}{2} \sum_k \left[\epsilon_k c_k^\dagger c_k + \epsilon_k (1 - c_k c_k^\dagger) \right] \\
 &= \frac{1}{2} \sum_k (\epsilon_k c_k^\dagger c_k - \epsilon_{-k} c_{-k} c_{-k}^\dagger) + \frac{1}{2} \sum_k \epsilon_k,
 \end{aligned} \tag{2.20}$$

$$\begin{aligned}
 \sum_k e^{-ika} c_{-k} c_k &= \frac{1}{2} \sum_k (e^{-ika} c_{-k} c_k + e^{-ika} c_{-k} c_k) \\
 &= \frac{1}{2} \sum_k (e^{-ika} c_{-k} c_k - e^{-ika} c_k c_{-k}) \\
 &= \frac{1}{2} \sum_k (e^{-ika} c_{-k} c_k - e^{ika} c_{-k} c_k) \\
 &= \frac{1}{2} \sum_k (e^{-ika} - e^{ika}) c_{-k} c_k \\
 &= - \sum_k i \sin(ka) c_{-k} c_k
 \end{aligned} \tag{2.21}$$

and

$$e^{ika} c_k^\dagger c_{-k}^\dagger = \sum_k i \sin(ka) c_k^\dagger c_{-k}^\dagger. \tag{2.22}$$

Now, the Hamiltonian is written as

$$H = \frac{1}{2} \sum_k \left[\epsilon_k c_k^\dagger c_k - \epsilon_{-k} c_{-k} c_{-k}^\dagger + \Delta_k^* c_k^\dagger c_{-k}^\dagger + \Delta_k c_{-k} c_k \right] + \frac{1}{2} \sum_k \epsilon_k. \quad (2.23)$$

wherein $\Delta_k = -t\Delta \sin(ka)$ is the Fourier-transformed superconducting pairing energy [1]. In an equivalent matrix representation (omitting the constant),

$$H = \frac{1}{2} \sum_k \begin{pmatrix} c_k^\dagger & c_{-k} \end{pmatrix} \begin{pmatrix} \epsilon_k & \Delta_k^* \\ \Delta_k & -\epsilon_{-k} \end{pmatrix} \begin{pmatrix} c_k \\ c_{-k}^\dagger \end{pmatrix}. \quad (2.24)$$

In superconducting systems, it is natural to define the Nambu spinors [17]

$$\psi_k^\dagger = \begin{pmatrix} c_k^\dagger & c_{-k} \end{pmatrix} \quad (2.25)$$

and finally

$$H = \frac{1}{2} \sum_k \psi_k^\dagger H_{BdG} \psi_k, \quad (2.26)$$

with

$$H_{BdG} = \begin{pmatrix} \epsilon_k & \Delta_k^* \\ \Delta_k & -\epsilon_{-k} \end{pmatrix} \quad (2.27)$$

as being the BdG Hamiltonian, with the pairing energy Δ_k odd in k , indicating the p -wave superconducting nature.

Aiming to analyze the bulk properties, we calculate the energy spectrum of H_{BdG} as follows:

$$|H_{BdG} - E(k)I| = 0, \quad (2.28)$$

wherein I is a 2x2 identity matrix and $E(k)$ are the eigenstates associated to the corresponding BdG Hamiltonian. Thus [1],

$$E(k)_\pm = \pm \sqrt{\epsilon_k^2 + |\Delta_k|^2} = \pm \sqrt{(\mu + t \cos(ka))^2 + \Delta^2 \sin^2(ka)}. \quad (2.29)$$

Figure 2.2 shows the bulk energy dispersion $E(k)$ [Eq. (2.29)] of the Kitaev model for distinct physical situations, with the lattice parameter $a = 1$. Panel (a) reveals that a finite p -wave pairing opens a gap of 2Δ at $k = \pm \frac{\pi}{2}$ (orange curves) for $|\mu| < t$ ($\mu = 0$). Moreover, $E(k)$ is gapped (independent of Δ_k), when $|\mu| > t$, as can be seen in panels (b) and (c) of the same figure. The former case describes the weak pairing situation, while the latter is called strong pairing regime. Also according to Eq. (2.29), the system will be gapless as the both elements of the square root vanishes simultaneously [3]. In this sense, $|\Delta_k| \equiv \Delta \sin(ka) = 0$ for $k = 0, \pm\pi$ and the kinetic energy normal dispersion $\epsilon_k = -\mu - t \cos(ka)$ is zero when k coincides with the Fermi momentum k_F [$\epsilon_k(k_F) = 0$], which is fulfilled for $-\mu - t \cos(ka) = 0$. Thus, the gap closes for $k_F = 0, \pm\pi$, which happens for $\mu = -t$ [Fig. 2.2(d)] and $\mu = t$ [Fig. 2.2(e)], respectively.

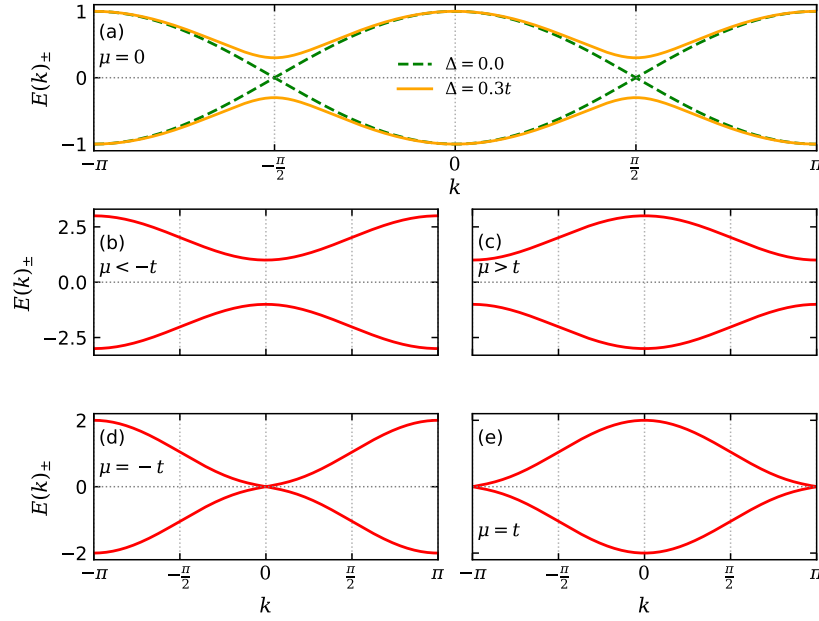


Figure 2.2: Bulk energy dispersion $E(k)$ of the BdG Hamiltonian [Eq. (2.27)] for several values of chemical potential μ . In panel (a), the green dashed curve depicts the case of $\Delta = 0$, while the opposite situation is described by the orange curve, wherein a gap opens at $k = \pm \frac{\pi}{2}$ (orange curves). Panels (b) and (c) corresponds to the trivial regime of gapped energy spectrum. The phase boundaries at $\mu = \pm t$ are shown in panels (d) e (e), in which the gap closes at $k = 0$ and $\pm\pi$, respectively.

It should be emphasized that the transition between weak [$|\mu| < t$, Fig. 2.2(a)] and strong [$|\mu| > t$, Fig. 2.2(b)-(c)] pairing regimes necessarily involves the closing of the bulk gap at $\mu = \pm t$. It is precisely such a phase transition in which the gap closes that gives to the system its topological feature, wherein unpaired MBSs emerge as zero modes in the weak regime [1, 3]. As will be seen in next section, such a bulk gap closure behavior can be indeed verified in quasi-1D semiconducting nanowires with strong Rashba SOI, close to a s -wave superconductor and under external magnetic field.

2.3 MZMs in quasi-one dimensional Rashba nanowires

As aforementioned in the beginning of the current chapter, in 2010 Lutchyn *et al* [14] and Oreg *et al* [15] demonstrated the possibility of engineering exotic p -wave pairing through proximity effect in quasi-1D semiconductors with strong SOI, as InAs and InSb, for instance. Such a theoretical prediction paved the way for experimental achievements of topological superconductivity with MZMs features.

In order to understand better the manifestation of p -wave superconductivity in these devices, let us start by considering a quasi-1D nanowire with SOI and Zeeman splitting in absence of the proximitized s -wave superconductor, which is described by the following Hamiltonian [1, 3]

$$H = \int dx \Psi^\dagger(x) H_0 \Psi(x), \quad (2.30)$$

with

$$\Psi(x) = \begin{pmatrix} \psi_\uparrow \\ \psi_\downarrow \end{pmatrix}, \quad (2.31)$$

and

$$H_0 = H_{kin} + H_{Rashba} + H_{Zeeman}, \quad (2.32)$$

wherein

$$H_{kin} = \frac{p_x^2}{2m} - \mu \quad (2.33)$$

describes the kinetic energy of an electron of effective mass m , with $p_x \equiv -i\hbar\partial_x$ as being the momentum operator and μ the chemical potential,

$$H_{Rashba} = -\frac{\alpha}{\hbar}\sigma_y p_x \quad (2.34)$$

and

$$H_{Zeeman} = E_Z\sigma_x \quad (2.35)$$

stands for Rashba SOI interaction of strength α along the y -axis and Zeeman energy splitting $E_Z = g\mu_B B/2$, respectively, wherein g is the nanowire's g -factor, μ_B is the Bohr magneton and B is the applied magnetic field along the x -axis¹. Moreover, σ_x and σ_y are the Pauli matrices along x and y directions, respectively². Later on, we will see the importance of the perpendicularity between Rashba and Zeeman fields.

According to the Schrödinger equation, $H_0\Psi = E\Psi$ and thus one can find the eigenvalues E of H_0 with the correspondent eigenvectors Ψ . In order to solving such a equation, let us suppose that the eigenvectors in k -space are two dimensional spinors given in terms of plane waves, *i.e.*, $\Psi_k(r) = \phi e^{ikr} = (c_1, c_2)^T e^{ikr}$, wherein r is the radius of the quasi-1D nanowire [18]. First, let us find the eigenvalues:

$$|H_0 - EI| = \mathbf{0} \Rightarrow \begin{vmatrix} \varepsilon_k - E & i\alpha k + E_Z \\ -i\alpha k + E_Z & \varepsilon_k - E \end{vmatrix} = \begin{pmatrix} 0 \\ 0 \end{pmatrix}, \quad (2.36)$$

resulting in

$$E_{\pm}(k) = \varepsilon_k \pm \sqrt{(\alpha k)^2 + E_Z^2}, \quad (2.37)$$

with $\varepsilon_k = \frac{\hbar^2 k^2}{2m} - \mu$. By using such eigenvalues, we can now find the eigenvectors according to the eigenvalue equation, which reads

$$[H_0 - E_{\pm}(k)I]\Psi_k(r) = \mathbf{0} \Rightarrow \begin{pmatrix} \varepsilon_k - E_{\pm}(k) & i\alpha k + E_Z \\ -i\alpha k + E_Z & \varepsilon_k - E_{\pm}(k) \end{pmatrix} \begin{pmatrix} c_1 \\ c_2 \end{pmatrix} = 0, \quad (2.38)$$

giving rise to the following coupled equations:

$$\begin{cases} (\varepsilon_k - E_{\pm}(k)) c_1 + (i\alpha k + E_Z) c_2 = 0, \\ (-i\alpha k + E_Z) c_1 + (\varepsilon_k - E_{\pm}(k)) c_2 = 0. \end{cases} \quad (2.39)$$

¹For InSb, the typical values are $m = 0.015m_e$ and $\alpha = 20meV \cdot nm$ [20].

² $\sigma_x = \begin{pmatrix} 0 & 1 \\ 1 & 0 \end{pmatrix}$, $\sigma_y = \begin{pmatrix} 0 & -i \\ i & 0 \end{pmatrix}$, $\sigma_z = \begin{pmatrix} 1 & 0 \\ 0 & -1 \end{pmatrix}$.

Now, let us write c_1 in terms of c_2 ³:

$$c_1 = -\frac{(i\alpha k + E_Z)}{(\varepsilon_k - E_{\pm}(k))} c_2 \quad (2.40)$$

and consequently

$$\Psi_k(r) = \begin{pmatrix} c_1 \\ c_2 \end{pmatrix} e^{ikr} \Rightarrow \Psi_{k,\pm}(r) = c_2 \begin{pmatrix} -\frac{(i\alpha k + E_Z)}{(\varepsilon_k - E_{\pm}(k))} \\ 1 \end{pmatrix} e^{ikr}. \quad (2.41)$$

Moreover, $\varepsilon_k - E_{\pm}(k) = \mp \sqrt{(\alpha k)^2 + E_Z^2}$. Thus,

$$\Psi_{k,\pm}(r) = c_2 \begin{pmatrix} \pm \frac{(i\alpha k + E_Z)}{\sqrt{(\alpha k)^2 + E_Z^2}} \\ 1 \end{pmatrix} e^{ikr}. \quad (2.42)$$

According to the normalization condition $|\Psi_{k,\pm}(r)|^2 = 1$ one can find c_2 as follows:

$$|\Psi_{k,\pm}(r)|^2 = \Psi_{k,\pm}^*(r) \Psi_{k,\pm}(r) = c_2^* \begin{pmatrix} \pm \frac{(-i\alpha k + E_Z)}{\sqrt{(\alpha k)^2 + E_Z^2}}, & 1 \end{pmatrix} e^{-ikr} c_2 \begin{pmatrix} \pm \frac{(i\alpha k + E_Z)}{\sqrt{(\alpha k)^2 + E_Z^2}} \\ 1 \end{pmatrix} e^{ikr} = 1 \Rightarrow$$

$$|c_2| = \frac{1}{\sqrt{2}}. \quad (2.43)$$

Finally, the eigenvectors normalized by the finite length of the nanowire L , are given by

$$\Psi_{k,\pm}(r) = \frac{1}{\sqrt{L}} \phi_{k,\pm} e^{ikr}, \quad \phi_{k,\pm} = \frac{1}{\sqrt{2}} \begin{pmatrix} \pm \nu_k \\ 1 \end{pmatrix}, \quad (2.44)$$

with $\nu_k = \frac{(i\alpha k + E_Z)}{\sqrt{(\alpha k)^2 + E_Z^2}}$.

Figure 2.3 illustrates the energy dispersion $E_{\pm}(k)$ [Eq. (2.38)] of the Rashba nanowire with Zeeman splitting for distinct situations. Panel (a) shows the simplest free electron case ($\alpha = E_Z = 0$) described by two spin-degenerated parabolas shifted down by finite μ . The Rashba SOI breaks such a spin-degeneracy along the k -axis by shifting the spin up and down parabolas by an amount of $k_{SOI} = m\alpha/\hbar^2$ and $E_{SOI} = m\alpha^2/2\hbar^2$ in the energy axis, as shown in Fig. 2.3(b). Each spin species is aligned along the y -axis, following the quantization direction defined the the Rashba coupling, *i.e.*, σ_y . Hence, for $E_Z = 0$, the energy dispersion exhibits opposite spin directions associated to opposite momenta for a given value of chemical potential and thus, only singlet states are allowed to form when a s -wave superconductor is taken into account. An external magnetic field applied perpendicularly to Rashba intrinsic field fix this issue [Fig. 2.3(c)]: for $E_Z \neq 0$ there is an opening gap of $2E_Z$, which removes the spin-degeneracy at $k = 0$. Moreover, when μ is within such a gap, the spin projection is now a mix of both spin up and down directions due to the competition of Rashba (σ_y) and Zeeman fields (σ_x), yielding a canting angle dependent of k and thus characterizing a helical spin state. It is precisely this behaviour that allows p -wave pairing in the nanowire when placed next to s -wave superconductor, since the induced triplet states are favoured due to the Zeeman energy splitting along σ_x .

³if we had considered the inverse, the result wouldn't change.

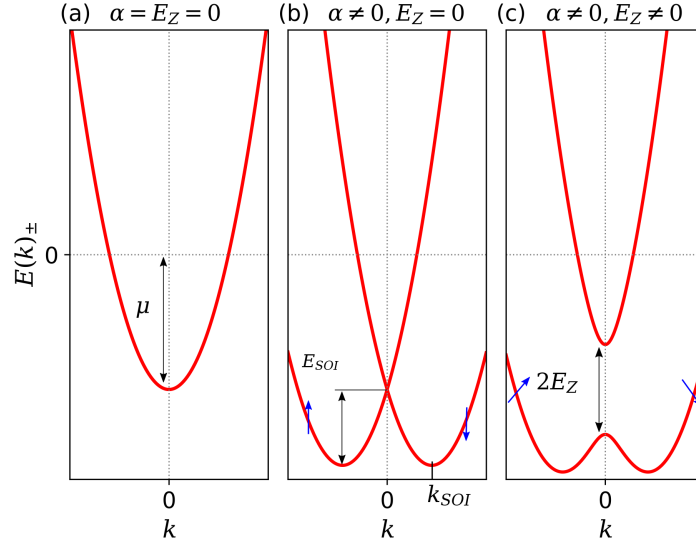


Figure 2.3: Energy spectrum of the quasi-1D Rashba nanowire in absence of superconducting proximity effect, given by Eq. (A.42). (a): two spin-degenerated parabolas describing the free electron case with finite chemical potential μ . (b): the Rashba SOI breaks the spin-degeneracy along the k -axis. Each parabola carries one spin projection (red arrows). (c): The Zeeman splitting due to a magnetic field applied perpendicularly to the Rashba field removes the spin degeneracy at $k = 0$ and opens a gap of size $2E_Z$. The spin projection is locked to k for μ within the energy gap, defining a helical state.

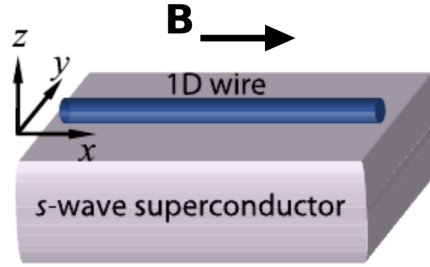


Figure 2.4: Basic scheme to induce p -wave superconductivity in the 1D semiconducting nanowire, described by the Hamiltonian of Eq. (A.51). Adapted from [1].

Aiming to analyze the energy spectrum of the nanowire when the proximity effect is taken into account, let us consider the following Hamiltonian [1, 18]

$$H_{sc} = \int dx \left(\Delta \psi_{\uparrow, k}^\dagger \psi_{\downarrow, -k}^\dagger + \Delta^* \psi_{\downarrow, -k} \psi_{\uparrow, k} \right), \quad (2.45)$$

describing the standard s -wave pairing of electrons with opposite spin and momenta within the Bardeen-Cooper-Schrieffer (BCS) theory, with pairing potential Δ . The Hamiltonian representing the full system (see Figure 2.4) now reads

$$H = H_0 + H_{sc}, \quad (2.46)$$

with H_0 given by Eq. (2.32). Since the Hamiltonian describes a superconducting system, is convenient to write it in a BdG form using the Nambu representation as follows [see Eqs. (2.24)-(2.27)]:

$$H = \frac{1}{2} \int dx \Psi(k) H_{BdG} \Psi(k), \quad (2.47)$$

with

$$\Psi(k) = \begin{pmatrix} \psi_{\uparrow,k} \\ \psi_{\downarrow,k} \\ \psi_{\uparrow,-k}^\dagger \\ \psi_{\downarrow,-k}^\dagger \end{pmatrix} \quad (2.48)$$

and

$$H_{BdG} = \left(\frac{p_x^2}{2m} - \mu \right) \tau_z \otimes \sigma_0 - \frac{\alpha}{\hbar} (\tau_z \otimes \sigma_y) p_x + E_Z (\tau_z \otimes \sigma_x) + \Delta (\tau_y \otimes \sigma_y), \quad (2.49)$$

wherein the τ_i and σ_i are the Pauli matrices acting on the electron-hole and spin subspaces, respectively. In the equivalent matrix form,

$$H_{BdG} = \begin{bmatrix} \varepsilon_k & (i\alpha k + E_Z) & 0 & -\Delta \\ (-i\alpha k + E_Z) & \varepsilon_k & \Delta & 0 \\ 0 & \Delta & -\varepsilon_k & (-i\alpha k + E_Z) \\ -\Delta & 0 & (i\alpha k + E_Z) & -\varepsilon_k \end{bmatrix}. \quad (2.50)$$

Again, by solving the Schrödinger equation $H_{BdG}\Psi = E\Psi$ and its corresponding eigenvalue equation, one can find the following energy dispersion relation [3]:

$$E_{\pm}^2(k) = \varepsilon_k^2 + (\alpha k)^2 + E_Z^2 + \Delta^2 \pm 2\sqrt{(E_Z\Delta)^2 + \varepsilon_k^2(E_Z^2 + \alpha^2 k^2)}. \quad (2.51)$$

In Figure 2.5 we explore the role of the proximity effect in the energy spectrum of the Rashba nanowire, given by Eq. (2.51). The free electron case is depicted in panel (a), wherein the inverted parabola describes the kinetic energy of a hole which emerges in the spectrum owing to the Nambu description [Eq. (2.48)]. As we have seen in previous situation [Fig. 2.3(b)], the finite Rashba SOI split such parabolas along the k -axis, with a crossing point only at $k = 0$ [panel (b)]. Such a feature is removed by the finite Zeeman splitting, since it opens a gap of $2E_Z$ at $k = 0$ [panel (c)]. As can be noticed in panel (d), the role of the induced superconducting pairing is to open a gap at the Fermi points, indicated by red circles in panel (c).

In what follows, we investigate the competition between the Zeeman splitting E_Z and the superconducting pairing potential Δ , both the mechanisms responsible for the gap opening process in the Rashba proximitized nanowire. For this propose, it is appropriate to rewrite the Hamiltonian which describes the superconducting pairing [Eq. (2.45)] in terms of

$$\psi(k) = \phi_-(k)\psi_-(k) + \phi_+(k)\psi_+(k), \quad (2.52)$$

wherein the operators $\psi_{\pm}(k)$ annihilates states with momentum k in the upper/lower bands and $\phi_{\pm}(k)$ are the renormalized wavefunctions given by Eq. (2.44). Such upper/lower functions, in turn, can be decomposed into two spinor components, *i.e.*,

$$\phi_-(k) = \begin{pmatrix} \phi_{\uparrow-}(k) \\ \phi_{\downarrow-}(k) \end{pmatrix} = \frac{1}{\sqrt{2}} \begin{pmatrix} -\nu_k \\ 1 \end{pmatrix} \quad \text{and} \quad \phi_+(k) = \begin{pmatrix} \phi_{\uparrow+}(k) \\ \phi_{\downarrow+}(k) \end{pmatrix} = \frac{1}{\sqrt{2}} \begin{pmatrix} +\nu_k \\ 1 \end{pmatrix}, \quad (2.53)$$

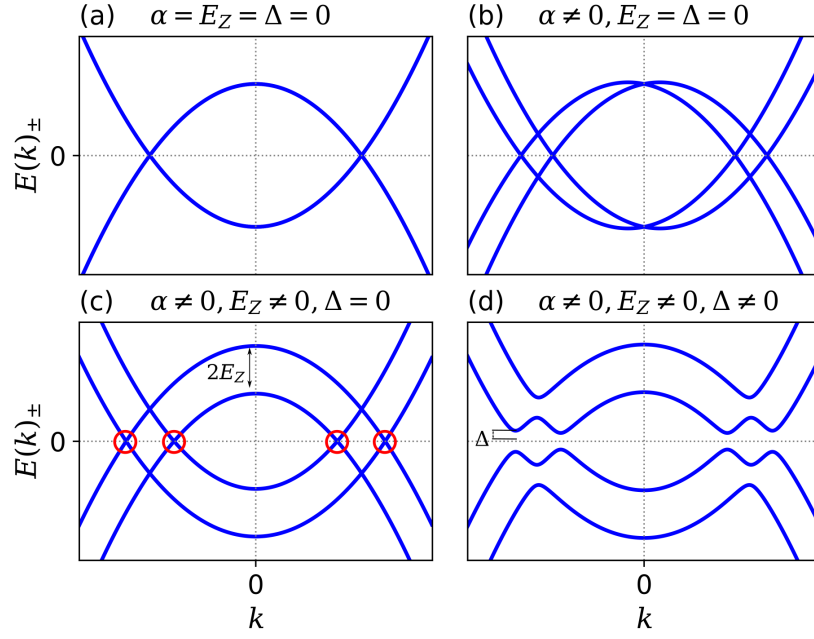


Figure 2.5: Energy spectrum of proximitized Rashba nanowire for distinct cases. (a): free electron case, wherein the normal and inverted parabolas represent the kinetic energy of an electron and a hole, respectively. (b): The SOI shifts the parabolas along k -axis and cross with each other at $k = 0$. (c): The magnetic field opens a gap of $2E_Z$ at $k = 0$. (d): A gap of 2Δ is opened at the Fermi points (red circles) due to the induced pairing by proximity effect.

with $\nu_k = \frac{i\alpha k + E_Z}{\sqrt{(\alpha k)^2 + E_Z^2}}$. Now, we can consider this spinorial representation in Eq. (2.52):

$$\begin{aligned}\psi_\uparrow(k) &= \phi_{\uparrow-}(k)\psi_-(k) + \phi_{\uparrow+}(k)\psi_+(k) = \frac{1}{\sqrt{2}}\nu_k [-\psi_-(k) + \psi_+(k)] \\ \psi_\downarrow(k) &= \phi_{\downarrow-}(k)\psi_-(k) + \phi_{\downarrow+}(k)\psi_+(k) = \frac{1}{\sqrt{2}}[\psi_-(k) + \psi_+(k)].\end{aligned}\quad (2.54)$$

In this helical basis, Eq. (2.45) reads [3]

$$H_{sc} = \int \frac{dk}{2\pi} \left[\frac{\Delta_\mp^p(k)}{2} \psi_\mp^\dagger(k) \psi_\mp^\dagger(-k) + \frac{\Delta_\mp^p(k)}{2} \psi_\mp^\dagger(k) \psi_\mp^\dagger(-k) + \frac{\Delta^s(k)}{2} \psi_\mp^\dagger(k) \psi_\mp^\dagger(-k) + \text{h.c.} \right], \quad (2.55)$$

wherein one can see the emergence of

$$\Delta_\mp^p(k) = \frac{\pm i\alpha k \Delta}{\sqrt{(\alpha k)^2 + E_Z^2}} \quad \text{and} \quad \Delta^s(k) = \frac{E_Z \Delta}{\sqrt{(\alpha k)^2 + E_Z^2}}, \quad (2.56)$$

which explicitly describe distinct pairing processes at the nanowire owing to interplay between the Zeeman splitting (E_Z), Rashba SOI (α) and proximity effect Δ . The first one accounts for the pairing between states of the same lower/upper (\mp) band, while the second mix states of distinct bands. Furthermore, $\Delta_\mp^p(k)$ is odd function of k , thus describing a p -wave paring, while $\Delta^s(k)$ is even, which corresponds to a s -wave superconductivity process.

Moreover, one can verify how the topological superconductivity emerges in the proximitized Rashba nanowire by analyzing the gap opening process in the energy spectrum given by Eq. (2.51), which comes from distinct superconducting pairings [Eq. (2.56)] for finite Δ . In this sense, it can be shown that a

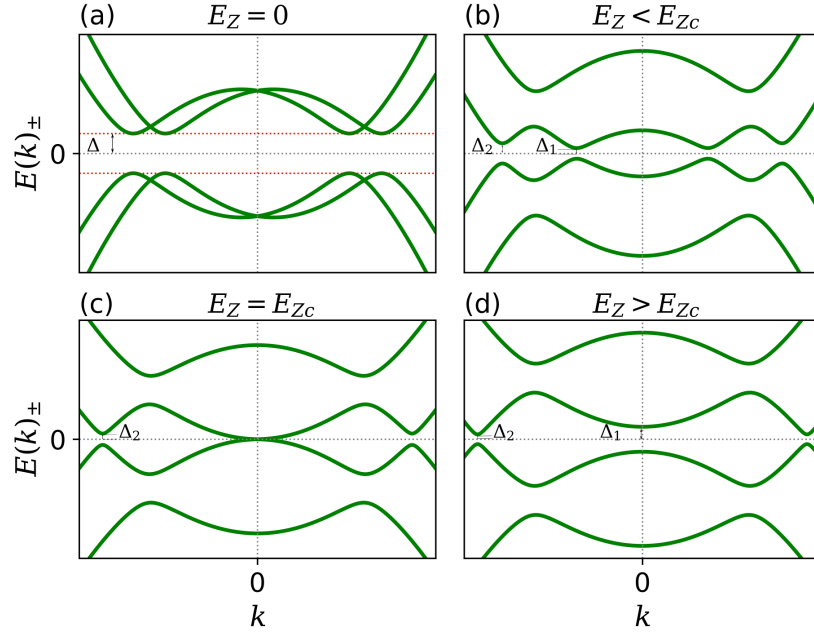


Figure 2.6: Energy spectrum of the proximitized Rashba nanowire for increasing values of Zeeman energy splitting. The critical value $E_{Zc} = \sqrt{\mu^2 + \Delta^2}$ points out the topological transition.

topological phase transition occurs for a critical Zeeman energy splitting [1]

$$E_{Zc} = \sqrt{\mu^2 + \Delta^2} \quad (\text{topological criterion}). \quad (2.57)$$

Let us label the inner and outer gaps in such spectrum as Δ_1 (lower momentum gap) and Δ_2 (higher momentum gap), respectively. Panel (a) of Figure 2.6 shows that $\Delta_1 = \Delta_2 = \Delta$ for $E_Z = 0$. However, as E_Z approaches the critical value [panel (b)], the lower momentum gap Δ_1 starts to close, followed by a complete closing at $E_Z = E_{Zc}$ [panel (c)] and reopening for $E_Z > E_{Zc}$ [panel (d)], while Δ_2 keeps finite and approximately constant for all Zeeman energy values. Such a closing and reopening of Δ_1 , also known as gap inversion, is the fingerprint of the topological transition, wherein the nontrivial superconducting phase ($E_Z > E_{Zc}$) hosts MZMs at the nanowire ends, protected by an effective gap $\Delta_{eff} = \text{Min}(\Delta_1, \Delta_2)$ [3].

One can make a clear connection between the Rashba nanowire within the topological phase and the Kitaev p -wave superconducting chain with periodic boundary conditions by considering the regime of stronger magnetic fields ($E_Z \gg m\alpha^2, \Delta$) [3], wherein the upper band of the energy spectrum is projected out of the problem. In this situation, the full Hamiltonian in the helical basis reads

$$H = \int \frac{dk}{2\pi} \left\{ \xi_{k-} \psi_-^\dagger(k) \psi_-(k) + \left[\frac{\Delta_-^p(k)}{2} \psi_-^\dagger(k) \psi_-^\dagger(-k) + \text{h.c.} \right] \right\}, \quad (2.58)$$

with $\xi_{k-} = \varepsilon_k - \sqrt{(\alpha k)^2 + E_Z^2}$ and $\Delta_-^p(k) = \frac{i\alpha k \Delta}{\sqrt{(\alpha k)^2 + E_Z^2}}$ is the pairing potential with p -wave symmetry (odd function in k). In this scenario, one can rewrite the Hamiltonian in a BdG form as

$$H_{BdG} = \begin{bmatrix} \xi_{k-} & \Delta_-^p(k) \\ \Delta_-^{p*}(k) & \xi_{-k-} \end{bmatrix}, \quad (2.59)$$

with the following energy spectrum

$$E(k) = \pm \sqrt{\xi_{k-}^2 + |\Delta_-^p(k)|^2}. \quad (2.60)$$

Thus,

$$H = \frac{1}{2} \int \frac{dk}{2\pi} \Psi(k) H_{BdG} \Psi(k), \quad \text{with } \Psi(k) = \begin{pmatrix} \psi_-(k) \\ \psi_-^\dagger(-k) \end{pmatrix}. \quad (2.61)$$

Formidably, the energy dispersion given by Eq. (2.60) has the same p -wave superconducting nature of the Kitaev toy model [Eq. (2.29)], ensuring that the Rashba proximitized nanowire in the topological phase ($E_Z \gg E_{Zc}$) indeed hosts p -wave superconductivity with protected MBSs.

It should be mentioned that the MBSs are not strictly zero-modes in realistic nanowires with finite length L , once the Majorana wave function [21]

$$\psi(x) \sim e^{-\frac{x}{\xi_M}} e^{\pm i k_F x} \quad (2.62)$$

exponentially decays into the nanowire, wherein k_F and ξ_M are the Fermi wave vector and is the superconducting coherence length associated to the MBSs, respectively. Thus, the MBSs residing at opposite ends of the nanowire can hybridize with each other, yielding a fermionic quasiparticle excitation with energy [22–26]

$$\delta E \sim \frac{\hbar^2 k_F e^{-\frac{2L}{\xi_M}}}{m \xi_M} \cos(k_F L), \quad (2.63)$$

wherein m is the effective electron's mass in the nanowire. Such a finite overlap leads to an energy splitting of the associated zero modes and its magnitude depends on the ratio L/ξ_M , whose the Majorana coherence length $\xi_M \sim 2 \left(\frac{E_Z}{\Delta} \right) l_{SOI}$ [21, 27], with the spin-orbit length $l_{SOI} = \frac{\hbar^2}{m\alpha}$. Therefore, for finite-length nanowires within the topological phase, the energy spectrum can exhibit an oscillatory pattern around the zero energy as a function of the magnetic field. This phenomenon is known as Majorana oscillations and we have investigated it in one of our papers, as we shall see in chapter 6.

2.4 Experimental detection of Majorana bound states in semiconducting proximitized nanowires

Based on the theoretical background of previous sections, we have realized the possibility of achieving p -wave superconductivity in a quasi-1D semiconducting nanowire by considering the following key ingredients: strong Rashba SOI coupling, induced superconducting pairing and external magnetic field perpendicular to the Rashba field. When such components are put together in the right way, a topological superconducting phase of p -wave nature emerges with MBSs as zero-energy modes at the opposite ends of the proximitized nanowire.

In present section, we shall see that the “ p -wave Majorana recipe” indeed works in the laboratory. Although other setups have been proposed to accomplish MBSs, such as superconductor-normal-superconductor (Josephson) junctions [28, 29], Coulomb blockade effect in the so-called Majorana islands [30, 31], proximitized edges of 2D topological insulators [32] and atomic magnetic chains [33–37], we will focus just on quasi-1D semiconducting nanowires of previous section (Sec. 2.3). In these kind of

systems, the so-called zero-bias anomaly (ZBA) in tunneling spectroscopy measurements is considered the hallmark which testifies the presence of the MBSs [1–3]. We shall realize, however, that nowadays the key issue concerning these experiments is to make sure that the Majorana excitations were indeed accomplished at the nanowire and besides that, how to distinguish them from other subgap excitations, as trivial Andreev levels [38–44], Kondo effect [45, 46] and disorder [47], for instance.

2.4.1 First generation

The first claim of Majorana observation in semiconducting nanowires with strong Rashba SOI, Zeeman splitting and induced superconductivity by proximity effect was done by Prof. Kouwenhoven’s group in 2012 [20]. A scanning electron microscope image of the so-called Delft experiment is shown in left panel of Figure 2.7: an Indium antimonide (InSb) semiconducting nanowire with strong Rashba SOI is placed between normal-metallic (N) and superconducting (S) electrodes. While distinct tunnel barriers (1 to 4 in the figure) vary the nanowire electron density between the N and S leads, an external magnetic field B is applied parallel to such a wire. As we discussed in previous section, when this a field exceeds the critical value $E_{Zc} = \sqrt{\mu^2 + \Delta^2}$, the system experiences a topological phase transition with emergence of MBSs at the ends of the nanowire. Right panel shows differential conductance curves for increasing magnetic fields in $10mT$ steps. For $B = 0$ there are two peaks at $V = \pm 250\mu eV$ (green arrows), indicating the formation of a gap due to induced superconductivity in the InSb nanowire owing to proximity effect to S electrode. For a range of magnetic fields between 100 and $400mT$, a subgap ZBA emerges in such conductance profiles, thus suggesting that the MBSs were created in the nanowire. Other experiments verified similar behaviour [48–51].

Although the promising results of Delft experiment have generated an initial excitement in the scientific community, it was not long before the first objections came to light, since the following relevant features of the experiment disagreed with theory [14, 15]: (i) the amplitude of the zero-bias peak was of $\approx 0.05G_0$, which is much smaller than the theoretical prediction $G = G_0 = 2e^2/h$; (ii) there was no data showing the gap inversion which characterizes the topological phase transition (see Fig. 2.6 of previous section); (iii) the spin-orbit length $l_{SOI} \approx 200nm$ ($\alpha = 0.2eV \cdot \text{\AA}$) generated a relevant Majorana coherence length ξ_M when compared to the length of the nanowire section close to the superconductor, leading to overlapped MBSs [see Eq. (2.63)] and hence, an oscillatory pattern around zero energy should be verified. However, the Majorana oscillations were absent in the experimental data. Both (i) and (ii) issues can be explained by considering the formation of multiple subbands in the nanowire [23], while the absence of Majorana oscillations can be understood by taken into account strong Coulomb repulsion in the system [24].

Another relevant issue in the results of Delft experiment comes from the fact that another physical phenomena can give rise to the ZBA. Disorder, for instance, can create subgap states around the zero-energy, mimicking the signature of the MBSs [52–54]. However, these disorder effects are fragile against the change of parameters, as the magnetic field, which discards such a possibility in the experimental data [Fig. 2.7(right panel)]. Other mechanism that can generate ZBAs is the Kondo effect [45, 46]. Such a phenomenon becomes more relevant for situations wherein a quantum dot is formed in the nanowire by depleting gates. In this situation, there is a competition between the superconducting proximity effect (singlet ground state) and the Coulomb repulsion (doublet ground state) in the quantum dot, which is controlled by the ratio Δ/T_K , with T_k is the Kondo temperature [55]. Thus, for $\Delta \ll T_K$ a Kondo peak

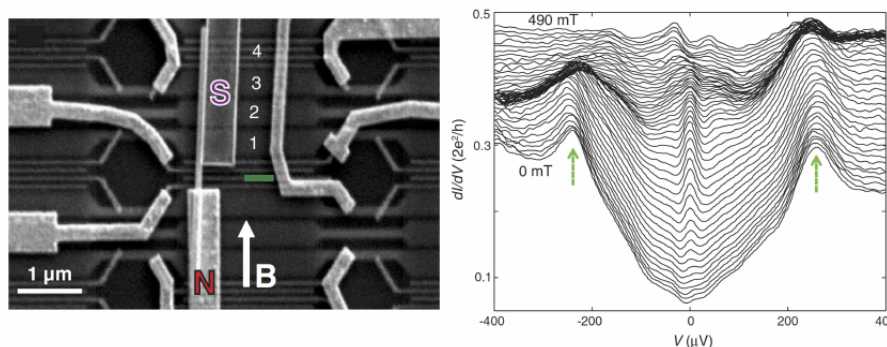


Figure 2.7: Left panel: Scanning electron microscope of the hybrid device from Delft experiment [20]. A semiconducting InSb nanowire is placed between S (niobium titanium nitride-NbTiN) and N (gold) reservoirs and is depleted by the gates numbered 1 to 4. The green line indicates the tunnel barrier between the contacts. Right panel: Differential conductance measurements at distinct magnetic fields B . A subgap ZBA emerges for B between 100 and 400 mT, indicating the presence of MBSs at the opposite ends of the nanowire. Typical estimated parameters are the induced superconducting gap $\Delta = 250 \mu\text{eV}$, the Rashba coupling $\alpha = 0.2 \text{eV} \cdot \text{\AA}$ and the Zeeman energy splitting $E_Z/B \approx 1.5 \text{meV}/T$ (g -factor $g \approx 50$). The measurements were performed at $T = 50 \text{mK}$. Source: Ref. [3].

emerges at zero energy. Nevertheless [56], one can distinguish the ZBAs coming from Kondo and MBSs by analyzing the splitting of the Kondo peak under increasing magnetic field.

Moreover, in hybrid devices of Fig. 2.7 (left), the transport between normal and superconducting segments is given by Andreev reflection processes [57], which can yield either the so-called Andreev bound states (ABSs) or Yu-Shiba-Rusinov (YSR) states [58–60]. These states can stick at zero energy for a wide range of magnetic fields⁴, thus mimicking exactly the ZBA signature of the MBSs [61]. Distinguish Andreev from Majorana bound states is nowadays one of the greatest challenges in Majorana hybrid devices, since they are indistinguishable for local conductance measurements [62].

2.4.2 Second generation

The criticism to the results from Delft boosted relevant improvements in the fabrication of hybrid setups, such as the epitaxial growth of superconducting cells on the surface of the nanowire [63] or high-quality semiconductor-superconductor interfaces [64, 65], for instance. These advances have allowed to obtain cleaner hybrid devices, with very good induced hard gaps and almost perfect Andreev reflection processes.

The aforementioned experimental progress could be verified in 2016 at Prof. Charles Marcus lab (Copenhagen) [68], wherein a native quantum dot at the end of the nanowire [66, 67] allowed to obtain detailed transport features of the Majorana hybrid device [Fig. 2.8(a)]. It was shown, for instance, that the MBSs can emerge from coalescing ABSs when either a gate voltage (chemical potential) or a Zeeman field is applied to the nanowire [Fig. 2.8(b)-(c)]. However, such a finding was promptly challenged by Das Sarma *et al* [62], who theoretically proved that trivial ABSs can indeed mimic the Majorana signature, as we have discussed in the section above.

Also at Charles Marcus lab [69], such a native quantum dot structure was recently used as a spectroscopy tool to experimentally investigate the so-called degree of Majorana non-locality [70, 71] (Figure 2.9). According to such a proposal, it is possible to quantify “how non-local” are the MBSs at the

⁴The range of magnetic fields is of order of the broadening of the ABSs resonances, *i.e.*, $\delta B \sim \Gamma_A$.

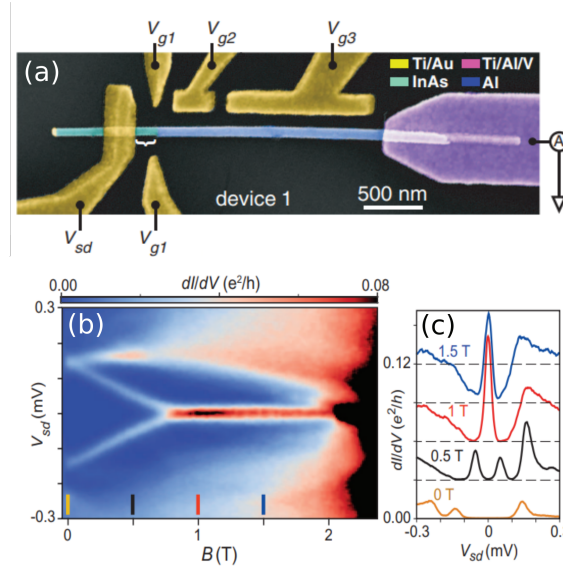


Figure 2.8: (a) Scanning electron micrograph of the hybrid device from the Copenhagen experiment [68]. The blue part indicates the epitaxial growth of Al directly performed in two or three facets of the hexagonal semiconducting Indium arsenide (InAs) nanowire. The Ti/Au and Ti/Au/V are the metal and superconducting leads, respectively. The white brace indicates the quantum dot region, which spontaneously emerges due to disorder or band-bending. A magnetic field is applied parallel to the nanowire axis. (b) Differential conductance as a function of both source-drain voltage V_{SD} and magnetic field, wherein the two initial ABSs merge at $B = 0.75T$ into a stable zero-bias peak, which remains robust up to $B = 2T$. (c) Line cut plots from panel (b), showing the differential conductance for distinct values of B . The measurements were performed at $T = 20mK$.

Adapted from Ref. [68]

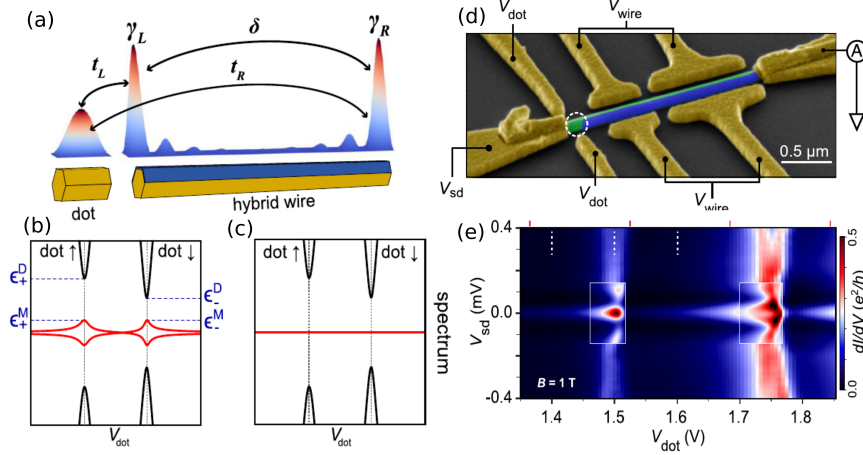


Figure 2.9: (a) Scheme of a native quantum dot coupled to γ_L and γ_R MBSs, with finite hybridization δ between them. The dot couples with both Majoranas end modes due to finite size effects and displacement of the Majorana wave functions by tuning external magnetic field or chemical potential of the nanowire. Panels (b) and (c) show the expected low-energy spectrum of the nanowire as a function of the quantum dot gate voltage V_{dot} for overlapped and well separated MBSs, respectively. For the hybridized Majoranas (b), the zero-energy state is perturbed by the quantum dot states (anticrossing points). The energies $\epsilon_{\pm}^{M(D)}$ provide the information related to the degree of nonlocality $\Omega^2 = \frac{\epsilon_{\pm}^M}{\epsilon_{\pm}^D} \left| \frac{\sin \frac{1}{2} \theta_L}{\sin \frac{1}{2} \theta_R} \right| \approx \frac{t_R}{t_L}$, with the canting angles θ_L and θ_R related to the spin-texture of left and right MBSs [69, 70], respectively. (d) False color micrograph of the hybrid device, wherein part of the InAs nanowire (green) is partially covered by epitaxial Al (blue). The quantum dot region is indicated by the dashed circle. (e) Differential conductance at $B = 1T$, in agreement with the prediction of panel (b). Adapted from Ref. [69]

opposite ends of the superconducting section of the nanowire by analyzing the typical differential conductance profiles showing anticrossings between the quantum dot and MBSs. The information coming from such a degree of nonlocality can settle the intriguing issue concerning the distinction between trivial zero-energy Andreev levels and highly nonlocal MBSs. Furthermore, the spin structure of the Majorana wave functions also can be experimentally accessed.

2.4.3 Outlook

There is no doubt that there was a remarkable progress concerning the Majorana detection since the original Fu and Kane proposal [13]. The second generation of proximitized Rashba nanowires, for instance, have shown better signatures of MBSs, as well as how to differentiate between the zero-bias peak emerging from Majorana excitations and those from other sub-gap mechanisms. Moreover, further advance was performed in other experimental platforms, as high energy frequency measurements in Josephson junctions based on quantum spin Hall insulators [72, 73], ferromagnetic atomic chains on top of superconductors [33–37], STM measurements of vortices in superconductor-topological insulator heterostructures [74] and graphene-based hybrid systems [75, 76].

All this outstanding progress points out that the recipe works, *i.e.*, the p -wave superconductivity can be achieved through proximity effect and time reversal symmetry break, allowing to create and measure Majorana excitations in a variety of platforms. However, there is a long way to achieve the holy grail of exponentially protected topological qubits based on Majorana physics. The next and more tangible challenge to be overcome is demonstrating the spacial nonlocality of MBSs and finding better ways to differentiate the Majorana signatures from other many-body phenomena, as we have discussed along sec. 2.4. The second and hardest challenge to be shot down is demonstrating the exotic non-Abelian braiding statistics in Majorana-based devices and how to control such a process for performing quantum computing operations, which will raise the bar of the research area. As we shall see along the following chapters, part of our work is basically focused in helping to beat the first challenge.

Bibliography

- [1] J. Alicea, Reports on Progress in Physics **75**, 076501 (2012).
- [2] S. R. Elliott and M. Franz, Rev. Mod. Phys. **87**, 137 (2015).
- [3] R. Aguado, Riv. Nuovo Cimento **40**, 523 (2017).
- [4] Chamon C., Jackiw R., Nishida Y., Pi S.-Y. and Santos L., Phys. Rev. B, **81** 224515 (2000).
- [5] Bogoliubov, N. N., Sov. Phys. JETP, **7** 41 (1958).
- [6] de Gennes, P.-G., Superconductivity of Metals and Alloys, (Benjamin, New York) 1966.
- [7] A. P. Mackenzie and Y. Maeno, Rev. Mod. Phys. **75**, 657 (2003).
- [8] Das Sarma S., Nayak C., and Tewari S., Phys. Rev. B, **73** 220502(R) (2006).
- [9] Moore G. and Read N., Nucl. Phys. B, **360** 362 (1991).
- [10] Kopnin N. B., Salomaa M. M., Phys. Rev. B, **44** 9667 (1991).
- [11] Volovik G., JETP Lett., **70** 609 (1999).
- [12] Kitaev A. Yu., Ann. Phys., **303** 2 (2003).
- [13] L. Fu and C. L. Kane, Phys. Rev. Lett. **100**, 096407 (2008).
- [14] R. M. Lutchyn, J. D. Sau, and S. Das Sarma, Phys. Rev. Lett. **105**, 077001 (2010).
- [15] Y. Oreg, G. Refael, and F. von Oppen, Phys. Rev. Lett. **105**, 177002 (2010).
- [16] A. Y. Kitaev, Physics-Uspekhi **44**, 131 (2001).
- [17] H. Bruus and K. Flensberg, Many-Body Quantum Theory in Condensed Matter Physics: An Introduction, Oxford Graduate Texts (Oxford University Press, 2004).
- [18] Jorge Cayao, arXiv PhD Thesis, arXiv:1703.07630v1 [cond-mat.mes-hall] (2017).
- [19] C. Nayak, S. H. Simon, A. Stern, M. Freedman, and S. Das Sarma, Rev. Mod. Phys. **80**, 1083 (2008).
- [20] V. Mourik, K. Zuo, S. M. Frolov, S. R. Plissard, E. P. A. M. Bakkers, and L. P. Kouwenhoven, Science **336**, 1003 (2012).
- [21] J. Klinovaja and D. Loss, Phys. Rev. B, **86** 085408 (2012).
- [22] Lim J. S., Serra L., Lopez R., Aguado R., Phys. Rev. B, **86** 121103 (2012).
- [23] Prada E., San-Jose P., and Aguado R., Phys. Rev. B, **86** 180503(R) (2012).
- [24] Das Sarma S., Sau J. D. , and Stanescu T. D, Phys. Rev. B, **86** 220506 (2012).
- [25] Rainis D., Trifunovic L., Klinovaja J., and Loss D., Phys. Rev. B, **87** 024515 (2013).

-
- [26] J. Danon, E. B. Hansen, and K. Flensberg, *Phys. Rev. B* **96**, 125420 (2017).
- [27] Mishmash R. V., Aasen D., Higginbotham A. P. , and Alicea J., *Phys. Rev. B*, **93** 245404 (2016).
- [28] Fu L. and Kane, C. L., *Phys. Rev. B*, **79** 161408 (2009).
- [29] Kwon H., Sengupta K., and Yakovenko V., *Eur. Phys. J. B*, **37** 349 (2003).
- [30] Fu L., *Phys. Rev. Lett.*, **104** 056402 (2010).
- [31] R., Zazunov A., Braunecker B., Levy Yeyati A. and Egger R., *Phys. Rev. Lett.*, **109** 166403 (2012).
- [32] Oostinga J. B., Maier L., Schüffelgen P., Knott D., Ames C., Brüne C.,Tkachov G., Buhmann H., and Molenkamp L. W., *Phys. Rev. X*, **3** 021007 (2013).
- [33] Nadj-Perge S., Drozdov I. K., Li J., Chen H., Jeon S., Seo J., MacDonald A. H., Bernevig B. A., and Yazdani A., *Science*, **346** 602 (2014).
- [34] Pawlak R., Kisiel M., Klinovaja J., Meier T., Kawai S., Glatzel T., Loss D.,and Meyer E., *npj Quantum Information*, **2** 16035 (2016).
- [35] Ruby M., Pientka F., Peng Y., von Oppen F., Heinrich B. W. , and Franke K. J. , *Phys. Rev. Lett.*, **115** 197204 (2015).
- [36] Feldman B. E., Randeria M. T., Li J., Jeon S., Xie Y., Wang Z., Drozdov I. K., A. H., Bernevig B. A., and Yazdani A., *Nature Physics*, **13** 286 (2017).
- [37] Jeon S., Xie Y., Li J., Wang Z., Bernevig B. A., and Yazdani A., *Science*, **358** 772 (2017).
- [38] G. Kells, D. Meidan, and P. W. Brouwer, *Phys. Rev. B* **86**, 100503 (2012).
- [39] C.-X. Liu, J. D. Sau, T. D. Stanescu, and S. Das Sarma, *Phys. Rev. B* **96**, 075161 (2017).
- [40] C.-X. Liu, J. D. Sau, and S. Das Sarma, *Phys. Rev. B* **97**, 214502 (2018).
- [41] M. Hell, K. Flensberg, and M. Leijnse, *Phys. Rev. B* **97**, 161401 (2018).
- [42] P. Marra and M. Nitta, arXiv e-prints , **arXiv:1907.05416** (2019), arXiv:1907.05416 [cond-mat.supr-con].
- [43] Y.-H. Lai, J. D. Sau, and S. Das Sarma, *Phys. Rev. B* **100**, 045302 (2019).
- [44] J. Chen, B. D. Woods, P. Yu, M. Hocevar, D. Car, S. R. Plissard, E. P. A. M. Bakkers, T. D. Stanescu, and S. M. Frolov, *Phys. Rev. Lett.* **123**, 107703 (2019).
- [45] S. M. Cronenwett, T. H. Oosterkamp, and L. P. Kouwenhoven, *Science* **281**, 540 (1998).
- [46] D. Goldhaber-Gordon, H. Shtrikman, D. Mahalu, D. Abusch-Magder, U. Meirav, and M. A. Kastner, *Nature (London)* **391**, 156 (1998).
- [47] D. Bagrets and A. Altland, *Phys. Rev. Lett.* **109**, 227005 (2012).
- [48] Deng M. T., Yu C. L., Huang G. Y., Larsson M., Caroff P., and Xu H. Q., *Nanoletters*, **12** 6414 (2012).
- [49] Das A., Ronen Y., Most Y., Oreg Y., Heiblum M., and Shtrikman H., *Nature Phys.*, **8** 887 (2012).
- [50] Finck A. D. K., Van Harlingen D. J., Mohseni P. K., Jung K., and Li X., *Phys. Rev. Lett.*, **110** 126406 (2013).
- [51] H. O. H. Churchill, V. Fatemi, K. Grove-Rasmussen, M. T. Deng, P. Caroff, H. Q. Xu, C. M. Marcus, *Phys. Rev. B*, **87** 241401(R) (2013).
- [52] Liu, J., Potter, A. C., Law K. and Lee P. A., *Phys. Rev. Lett.*, **109** 267002 (2012).
- [53] Pikulin D. I., Dahlhaus J., Wimmer M., Schomerus H. and Beenakker C. W. J., *New Journal of Physics*, **14** 125011 (2012).

-
- [54] Bagrets D. and Altland A., Phys. Rev. Lett., **109** 227005 (2012).
- [55] Lee E. J. H., Jiang X., Zitko R., Aguado R., Lieber C. M., De Franceschi S., Phys. Rev. B, **95** 180502(R) (2017).
- [56] Zitko R., Lim J. S., Lopez R., Aguado R., Phys. Rev. B, **91** 045441 (2015).
- [57] A. F. Andreev, J. Exp. Teor. Phys **19**, 1228 (1964).
- [58] Yu, L. Bound state in superconductors with paramagnetic impurities. Acta Phys. Sin. **21**, 75?91 (1965).
- [59] Shiba, H. Classical spins in superconductors. Prog. Theor. Phys. **40**, 435?451 (1968).
- [60] Rusinov, A. I. Superconductivity near a paramagnetic impurity. JETP Lett. **9**, 85?87 (1969). [Zh. Eksp. Teor. Fiz. **9**, 146 (1968)].
- [61] Lee E. J. H., Jiang X., Houzet M., Aguado R., Lieber C. M., De Franceschi S., Nature Nanotechnology, **9** 79 (2014).
- [62] Liu C. X., Sau J. D., Stanescu T. D., Das Sarma S., Phys. Rev. B, **96** 075161 (2017).
- [63] Krogstrup P., Ziino N. L. B., Chang W., Albrecht S. M., Madsen M. H., Johnson E., Nygard J., Marcus C. M., and Jespersen T. S., Nature Materials, **14** 400 (2015).
- [64] Zhang H., Gul O., Conesa-Boj S., Zuo K., Mourik V., de Vries F. K., van Veen J., van Woerkom D. J., Nowak M. P., Wimmer M, Car D., Plissard S. R.,Bakkers E. P.A.M., Goswami S., Watanabe K., Taniguchi T., and Kouwenhoven L. P., Nature Communications, **8** 16025 (2017).
- [65] Gul O., Zhang H., de Vries F. K., van Veen J., Zuo K., Mourik V., Conesa-Boj S., Nowak M. P., van Woerkom D. J., Quintero-Perez M., Cassidy M. C., Geresdi A., Kollig S., Car D., Plissard S. R., Bakkers E. P.A.M., and Kouwenhoven L.P., Nanoletters, **17** 2690 (2017).
- [66] Liu D. E., and Baranger H. U., Phys. Rev. B, **84** 201308 (2011).
- [67] Vernek E., Penteado P. H.,Seridonio A. C., and Egues J. C., Phys. Rev. B, **89** 165314 (2014).
- [68] Deng M. T., Vaitiekėnas S., Hansen E. B., Danon J., Leijnse M., Flensberg K., Nygard J., Krogstrup P., and Marcus C. M., Science, **354** 1557 (2016).
- [69] M-T. Deng, S. Vaitiekėnas, E. Prada, P. San-Jose, J. Nygard, P. Krogstrup, R. Aguado, and C. M. Marcus, Phys. Rev. B **98**, 085125 (2018).
- [70] Prada E., Aguado R., and San-Jose P., Phys. Rev. B, **96** 085418(2017) .
- [71] Clark D. J., Phys. Rev. B, **96** 201109(R) (2017).
- [72] Bocquillon E., Deacon R. S., Wiedenmann J., Leubner P., Klapwijk T. M., Bru?ne C., Ishibashi K., Buhmann H., and Molenkamp L. W., Nature Nanotechnology, **12** 137 (2017).
- [73] Deacon R. S., Wiedenmann J., Bocquillon E., Dominguez F., Klapwijk T. M., Leubner P., Bru?ne C., Hankiewicz E. M., Tarucha S., Ishibashi K., Buhmann H., and Molenkamp L. W., Phys. Rev. X, **7** 021011 (2017).
- [74] Sun H. H., Zhang K. W., Hu L. H., Li C., Wang G. Y., Ma H. Y., Xu Z. A., Gao C. L., Guan D. D., Li Y. Y., Liu C., Qian D., Zhou Y., Fu L., Li S. C., Zhang F. C., and Jia J. F., Phys. Rev. Lett., **116** 257003 (2016).
- [75] Amet F., Ke C. T., Borzenets I. V., Wang J., Watanabe K., Taniguchi T., Deacon R. S., Yamamoto M., Bomze Y., Tarucha S., Finkelstein G., Science, **352** 966 (2016).
- [76] Bretheau L., Wang J. I., Pisoni R., Watanabe K., Taniguchi T., and Jarillo-Herrero P., Nature Physics, **13** 756 (2017).

Chapter 3

Mathematical formalism

In what follows, we will present the theoretical tools employed in all our works: the equation of motion (EOM) technique using the Green's functions formalism at equilibrium [1–3] applied to Anderson-type Hamiltonians [4]. Such a framework allows us to compute, for instance, the density of electronic states (DOS) of an impurity adsorbed in a metallic host or, equivalently, the DOS of a quantum dot between metallic reservoirs. This quantity provides important information concerning the electronic transport, once the differential conductance through a given impurity/dot within the Landauer-Büttiker formalism reads [1]

$$\mathcal{G} = \frac{2e^2}{h} \int d\omega \left(-\frac{\partial f_F}{\partial \omega} \right) \pi \Gamma \rho_d(\omega), \quad (3.1)$$

wherein $2e^2/h$ is the quantum of conductance, f_F is the Fermi-Dirac distribution, Γ is known as Anderson parameter [4] and

$$\rho(\omega) = -\left(\frac{1}{\pi} \right) \text{Im} [G_{dd}^r(\omega)] \quad (3.2)$$

is the related DOS, with $G_{dd}^R(\omega)$ as being the retarded Green's function of a quantum dot/impurity in the spectral (energy) domain ω . As we shall see later on, such a quantity describes the electron propagation behaviour through the system in question.

3.1 Green's function formalism and the equation of motion technique

The Green's functions formalism are widely employed to solve linear differential equations in many branches of Physics and Mathematics [5]. In the context of classical physics, for instance, one can use the Green's functions as a solution of linear differential equations with Dirac delta inhomogeneous source and homogeneous boundary conditions. A practical example is the Poisson's equation $\nabla^2 \varphi = -\rho/\epsilon_0$ [1], connecting a given charge density distribution ρ with its electric potential φ . In quantum mechanics, the Green's functions formalism allows to obtain the eigenvalues of a given Hamiltonian with external potential associated to the Schrödinger equation [1]. In this picture, the Green's functions are also known as a propagators, since they describe the time evolution of the related wave function from a given time and position to another time and space points [3].

Despite extensive discussion concerning distinct uses of Green's functions in many-particle physics, here we focus on the definition of retarded Green's functions, which are specifically used for obtaining

the DOS [Eq. (3.2)] via EOM technique. Such a kind of function is defined for fermions as¹ [1]:

$$G^R(\mathbf{r}\sigma t, \mathbf{r}'\sigma't') = -i\theta(t-t')\langle[\psi_\sigma(\mathbf{r}t), \psi_\sigma^\dagger(\mathbf{r}'t')]_+\rangle, \quad (3.3)$$

wherein $\theta(t-t')$ is the Heaviside function, being non-zero only for $t > t'$, which means that such a Green's function provide the information of the system after it has been perturbed. Moreover, $[\dots, \dots]_+$ holds the anticommutation relation for fermions belonging to a given Hamiltonian and

$$\langle[\psi_\sigma(\mathbf{r}t), \psi_\sigma^\dagger(\mathbf{r}'t')]_+\rangle = \mathcal{Z}^{-1}\text{Tr}\{e^{-\beta H}[\psi_\sigma(\mathbf{r}t), \psi_\sigma^\dagger(\mathbf{r}'t')]_+\}, \quad (3.4)$$

i.e., it represents the thermal average between the annihilation and creation operators $\psi_\sigma(\dots, \dots)$ and $\psi_\sigma^\dagger(\dots, \dots)$ respectively, with $\mathcal{Z} = \text{Tr}\{e^{-\beta H}\}$ as being the partition function, wherein $\beta = \frac{1}{k_B T}$. By defining $|n\rangle$ as an eigenstate of the Hamiltonian H with associated energy E_n , one can write Eq. (3.3) as

$$G^R(\mathbf{r}\sigma t, \mathbf{r}'\sigma't') = -i\theta(t-t') \sum_n \mathcal{Z}^{-1} e^{-\beta E_n} \langle n | [\psi_\sigma(\mathbf{r}t), \psi_\sigma^\dagger(\mathbf{r}'t')]_+ | n \rangle. \quad (3.5)$$

Here one can explicitly notice the propagating character of such Green's functions: they compute the amplitude of a particle at initial point (\mathbf{r}', t') evolving to the position \mathbf{r} and time t .

In order to calculate the corresponding DOS associated to a given Hamiltonian H , one should get the retarded Green's function in the spectral domain ω . One way of achieving this is to employ the EOM technique, which consists of determining the time evolution of a given Green's function, followed by a Fourier transform. As an example, we consider a retarded Green's function which relates two fermionic operators c_i and c_j belonging to H [1], *i.e.*,

$$G^R(it, jt') \equiv G_{c_i; c_j}^R(t, t') = -i\theta(t-t')\langle[c_i(t), c_j^\dagger(t')]_+\rangle, \quad (3.6)$$

wherein the position dependency was omitted for sake of simplicity. Let us derive such a Green's function with respect to time t :

$$\begin{aligned} \partial_t G_{c_i; c_j}^R(t, t') &= -i\partial_t \theta(t-t')\langle[c_i(t), c_j^\dagger(t')]_+\rangle \\ &+ (-i)\theta(t-t')\langle[\partial_t c_i(t), c_j^\dagger(t')]_+\rangle \\ &= -i\delta(t-t')\langle[c_i(t), c_j^\dagger(t')]_+\rangle \\ &+ (-i)\theta(t-t')\langle[-i[c_i(t), H], c_j^\dagger(t')]_+\rangle, \end{aligned} \quad (3.7)$$

wherein we employed the Heisenberg picture $\partial_t c_i(t) = -i[c_i(t), H]$ to evolve the operator in the time domain. In the last line of Eq. (3.7), one can see that the Hamiltonian will determine the new set of Green's functions, once it depends on the commutator of the operator c_i with H . Furthermore, Eq. (3.7) can be written as

$$\partial_t G_{c_i; c_j}^R(t, t') = -i\delta(t-t')\langle[c_i(t), c_j^\dagger(t')]_+\rangle + (-i)G_{[c_i, H]; c_j}^R(t, t'). \quad (3.8)$$

In order to apply the Fourier transform, let us now multiply the both sides of Eq. (3.8) by $e^{i(\omega+i0^+)t}$ and

¹We assume $\hbar = 1$.

integrate over all the temporal domain t :

$$\begin{aligned} \int dt \partial_t G_{c_i; c_j}^R(t, t') e^{i(\omega + i0^+)t} &= -i \int dt \delta(t - t') \langle [c_i(t), c_j(t')]_+ \rangle e^{i(\omega + i0^+)t} \\ &+ (-i) \int dt G_{[c_i H]; c_j}^R(t, t') e^{i(\omega + i0^+)t}. \end{aligned} \quad (3.9)$$

The left-hand-side of the equation above can be solved by using partial integration

$$\int u dv = uv - \int v du, \quad (3.10)$$

with $u = e^{i\omega t}$ and $dv = \partial_t G_{c_i; c_j}^R(t, t') dt$, yielding

$$\begin{aligned} \int dt \partial_t G_{c_i; c_j}^R(t, t') e^{i\omega t} &= G_{c_i; c_j}^R(t, t') e^{i\omega t} - i\omega \int G_{c_i; c_j}^R(t, t') e^{i\omega t} dt \\ &= -i\omega \int G_{c_i; c_j}^R(t, t') e^{i\omega t} dt, \end{aligned} \quad (3.11)$$

with $\omega \equiv \omega + i0^+$. Thus, Eq. (3.9) is reduced to

$$\begin{aligned} -i\omega \int G_{c_i; c_j}^R(t, t') e^{i\omega t} dt &= -i \int dt \delta(t - t') \langle [c_i(t), c_j(t')]_+ \rangle e^{i(\omega + i0^+)t} \\ &+ (-i) \int dt G_{[c_i H]; c_j}^R(t, t') e^{i(\omega + i0^+)t}. \end{aligned} \quad (3.12)$$

By using the definition of Fourier transform $G^R(\omega) = \int dt G_{c_i; c_j}^R(t, t') e^{i\omega t} dt$ and the Dirac-delta property, the expression above reads

$$\omega G_{c_i; c_j}^R(\omega) = \delta_{ij} + G_{[c_i H]; c_j}^R(\omega), \quad (3.13)$$

or in the Zubarev notation [3]

$$\omega \langle \langle c_i; c_j^\dagger \rangle \rangle = \delta_{ij} + \langle \langle [c_i, H]; c_j^\dagger \rangle \rangle. \quad (3.14)$$

The Eqs. (3.13) and (3.14) ensure that the calculation of $G_{c_i; c_j}^R(\omega)$ gives rise to a new Green's function $G_{[c_i H]; c_j}^R(\omega)$, whose the dynamics is determined by the Hamiltonian of the system.

3.2 The Single Impurity Anderson Model (SIAM)

By a way of example, we will apply the EOM technique in the celebrated model proposed by P. W. Anderson² in 1961 [4], which describes the formation of a local magnetic moment of a magnetic ion embedded in a non-magnetic metallic host (Fig. 3.1). According to the Anderson proposal, only the external shell of the magnetic ion contributes for the charge transport process, which is typically the d -shell. Thus, the magnetic impurity is described by the Hamiltonian

$$H_{imp} = \varepsilon_{d\sigma} n_{d\sigma} + U n_{d\uparrow} n_{d\downarrow}, \quad (3.15)$$

²Was awarded the Nobel Prize in Physics in 1977, "for their fundamental theoretical investigations of the electronic structure of magnetic and disordered systems." Source: [Nobel Prize website](#)

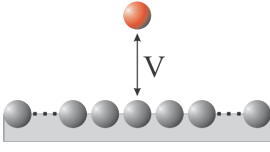


Figure 3.1: Sketch of the model described by Anderson: an atom with localized magnetic moment is adsorbed in a non-magnetic metallic host. V stands for the hybridization strength between the former and the later.

Coulomb interaction can be neglected in the host Hamiltonian, once the states which form the conduction band are s -states and therefore, more extended in space [1].

The electrons of the metallic host overlap with those ones occupying the d -state of magnetic impurity, giving rise to the Hamiltonian

$$H_{hyb} = \sum_{\mathbf{k}\sigma} V(d_{\sigma}^{\dagger}c_{\mathbf{k}\sigma} + \text{h.c.}), \quad (3.17)$$

with hybridization amplitude V . Thus, the SIAM is fully modelled as

$$H = H_{host} + H_{imp} + H_{hyb}. \quad (3.18)$$

Besides its simplicity, the SIAM has a very complicated full solution due to the interacting term [Eq. (3.15)], as we shall see. However, it has been employed to describe a variety of strong correlated systems in condensed matter.

Now, let us making use of the EOM technique³ to obtain the DOS of the ion impurity [Eq. (3.2)]. According to Eq. (3.14):

$$\omega \langle\langle d_{\sigma}; d_{\sigma}^{\dagger} \rangle\rangle = 1 + \langle\langle [d_{\sigma}, H]; d_{\sigma}^{\dagger} \rangle\rangle \quad (3.19)$$

with

$$[d_{\sigma}, H] = [d_{\sigma}, H_{host}] + [d_{\sigma}, H_{imp}] + [d_{\sigma}, H_{hyb}]. \quad (3.20)$$

Let us calculate each of these commutators separately, using the following anticommutation relations for fermions

$$[d_{\sigma}, d_{\bar{\sigma}}^{\dagger}]_{+} = \delta_{\sigma\bar{\sigma}}, \quad [c_{\mathbf{k}\sigma}, c_{\mathbf{q}\bar{\sigma}}^{\dagger}]_{+} = \delta_{\mathbf{k}\mathbf{q}}\delta_{\sigma\bar{\sigma}}, \quad (3.21)$$

$$[d_{\sigma}, d_{\bar{\sigma}}]_{+} = [d_{\sigma}^{\dagger}, d_{\bar{\sigma}}^{\dagger}]_{+} = 0 \quad \text{and} \quad (3.22)$$

$$[c_{\mathbf{k}\sigma}, c_{\mathbf{q}\bar{\sigma}}]_{+} = [c_{\mathbf{k}\sigma}^{\dagger}, c_{\mathbf{q}\bar{\sigma}}^{\dagger}]_{+} = 0. \quad (3.23)$$

Starting with

$$[d_{\sigma}, H_{host}] = [d_{\sigma}, \sum_{\mathbf{k}} \varepsilon_{\mathbf{k}} c_{\mathbf{k}\sigma}^{\dagger} c_{\mathbf{k}\sigma}] = 0, \quad (3.24)$$

once the operators of the ion impurity and host belong to distinct subspaces. We also must compute

$$[d_{\sigma}, H_{imp}] = [d_{\sigma}, \sum_{\bar{\sigma}} \varepsilon_{d\bar{\sigma}} d_{\bar{\sigma}}^{\dagger} d_{\bar{\sigma}} + U n_{d\uparrow} n_{d\downarrow}], \quad (3.25)$$

³The full calculations related to our works are shown in Appendices A and B.

$$\begin{aligned}
 [d_\sigma, \sum_{\bar{\sigma}} \varepsilon_{d\bar{\sigma}} d_{\bar{\sigma}}^\dagger d_{\bar{\sigma}}] &= \sum_{\bar{\sigma}} \varepsilon_{d\bar{\sigma}} (d_\sigma d_{\bar{\sigma}}^\dagger d_{\bar{\sigma}} - d_{\bar{\sigma}}^\dagger d_{\bar{\sigma}} d_\sigma) \\
 &= \sum_{\bar{\sigma}} \varepsilon_{d\bar{\sigma}} (d_\sigma d_{\bar{\sigma}}^\dagger d_{\bar{\sigma}} + d_{\bar{\sigma}}^\dagger d_\sigma d_{\bar{\sigma}}) \\
 &= \sum_{\bar{\sigma}} \varepsilon_{d\bar{\sigma}} (d_\sigma d_{\bar{\sigma}}^\dagger d_{\bar{\sigma}} + \delta_{\sigma\bar{\sigma}} d_{\bar{\sigma}} - d_\sigma d_{\bar{\sigma}}^\dagger d_{\bar{\sigma}}) \\
 &= \varepsilon_{d\sigma} d_\sigma,
 \end{aligned} \tag{3.26}$$

$$\begin{aligned}
 [d_\sigma, U n_{d\uparrow} n_{d\downarrow}] &= U (d_\sigma d_{\uparrow}^\dagger d_{\uparrow} d_{\downarrow}^\dagger d_{\downarrow} - d_{\uparrow}^\dagger d_{\uparrow} d_{\downarrow}^\dagger d_{\downarrow} d_\sigma) \\
 &= U (d_\sigma d_{\uparrow}^\dagger d_{\uparrow} d_{\downarrow}^\dagger d_{\downarrow} + d_{\uparrow}^\dagger d_{\uparrow} d_{\downarrow}^\dagger d_\sigma d_{\downarrow}) \\
 &= U (d_\sigma d_{\uparrow}^\dagger d_{\uparrow} d_{\downarrow}^\dagger d_{\downarrow} + \delta_{\downarrow\sigma} d_{\uparrow}^\dagger d_{\uparrow} d_{\downarrow} - d_{\uparrow}^\dagger d_{\uparrow} d_\sigma d_{\downarrow}^\dagger d_{\downarrow}) \\
 &= U (d_\sigma d_{\uparrow}^\dagger d_{\uparrow} d_{\downarrow}^\dagger d_{\downarrow} + \delta_{\downarrow\sigma} d_{\uparrow}^\dagger d_{\uparrow} d_{\downarrow} + d_{\uparrow}^\dagger d_\sigma d_{\uparrow} d_{\downarrow}^\dagger d_{\downarrow}) \\
 &= U (d_\sigma d_{\uparrow}^\dagger d_{\uparrow} d_{\downarrow}^\dagger d_{\downarrow} + \delta_{\downarrow\sigma} d_{\downarrow} d_{\uparrow}^\dagger d_{\uparrow} + \delta_{\uparrow\sigma} d_{\uparrow} d_{\downarrow}^\dagger d_{\downarrow} - d_\sigma d_{\uparrow}^\dagger d_{\uparrow} d_{\downarrow}^\dagger d_{\downarrow}) \\
 &= U d_\sigma n_{d\bar{\sigma}},
 \end{aligned} \tag{3.27}$$

with $\bar{\sigma}$ as being the opposite of σ . Lastly,

$$\begin{aligned}
 [d_\sigma, H_{hyb}] &= [d_\sigma, \sum_{\mathbf{q}, \bar{\sigma}} V (d_{\bar{\sigma}}^\dagger c_{\mathbf{q}\bar{\sigma}} + c_{\mathbf{q}\bar{\sigma}}^\dagger d_{\bar{\sigma}})] \\
 &= \sum_{\mathbf{q}, \bar{\sigma}} V (d_\sigma d_{\bar{\sigma}}^\dagger c_{\mathbf{q}\bar{\sigma}} - d_{\bar{\sigma}}^\dagger c_{\mathbf{q}\bar{\sigma}} d_\sigma) \\
 &+ \sum_{\mathbf{q}, \bar{\sigma}} V (d_\sigma c_{\mathbf{q}\bar{\sigma}}^\dagger d_{\bar{\sigma}} - c_{\mathbf{q}\bar{\sigma}}^\dagger d_{\bar{\sigma}} d_\sigma) \\
 &= \sum_{\mathbf{q}, \bar{\sigma}} V (d_\sigma d_{\bar{\sigma}}^\dagger + d_{\bar{\sigma}}^\dagger d_\sigma) c_{\mathbf{q}\bar{\sigma}} \\
 &+ \sum_{\mathbf{q}, \bar{\sigma}} V (-d_\sigma d_{\bar{\sigma}} c_{\mathbf{q}\bar{\sigma}}^\dagger - d_{\bar{\sigma}} d_\sigma c_{\mathbf{q}\bar{\sigma}}^\dagger) \\
 &= \sum_{\mathbf{q}, \bar{\sigma}} V [d_\sigma, d_{\bar{\sigma}}^\dagger]_{+} c_{\mathbf{q}\bar{\sigma}} - \sum_{\mathbf{q}, \bar{\sigma}} V [d_\sigma, d_{\bar{\sigma}}]_{+} c_{\mathbf{q}\bar{\sigma}}^\dagger \\
 &= V \sum_{\mathbf{q}} c_{\mathbf{q}\sigma}.
 \end{aligned} \tag{3.28}$$

Thus,

$$[d_\sigma, H] = \varepsilon_{d\sigma} d_\sigma + V \sum_{\mathbf{q}} c_{\mathbf{q}\sigma} + U d_\sigma n_{d\bar{\sigma}} \tag{3.29}$$

and consequently,

$$(\omega - \varepsilon_{d\sigma}) \langle\langle d_\sigma; d_\sigma^\dagger \rangle\rangle = 1 + V \sum_{\mathbf{k}} \langle\langle c_{\mathbf{k}\sigma}; d_\sigma^\dagger \rangle\rangle + U \langle\langle d_\sigma n_{d\bar{\sigma}}; d_\sigma^\dagger \rangle\rangle. \tag{3.30}$$

As can be noticed, the running of EOM has generated new Green's functions, which in principle can be

found by applying again the same technique. Thus, let us compute $\langle\langle c_{\mathbf{k}\sigma}; d_{\sigma}^{\dagger} \rangle\rangle$:

$$\omega \langle\langle c_{\mathbf{k}\sigma}; d_{\sigma}^{\dagger} \rangle\rangle = \langle\langle [c_{\mathbf{k}\sigma}, H]; d_{\sigma}^{\dagger} \rangle\rangle, \quad (3.31)$$

with

$$[c_{\mathbf{k}\sigma}, H] = \varepsilon_{\mathbf{k}} c_{\mathbf{k}\sigma} + V d_{\sigma}, \quad (3.32)$$

yielding

$$(\omega - \varepsilon_{\mathbf{k}}) \langle\langle c_{\mathbf{k}\sigma}; d_{\sigma}^{\dagger} \rangle\rangle = V \langle\langle d_{\sigma}; d_{\sigma}^{\dagger} \rangle\rangle. \quad (3.33)$$

Now, let us substitute Eq. (3.33) into Eq. (3.30):

$$(\omega - \varepsilon_{d\sigma}) \langle\langle d_{\sigma}; d_{\sigma}^{\dagger} \rangle\rangle = 1 + V^2 \sum_{\mathbf{k}} \frac{\langle\langle d_{\sigma}; d_{\sigma}^{\dagger} \rangle\rangle}{(\omega - \varepsilon_{\mathbf{k}})} + U \langle\langle d_{\sigma} n_{d\bar{\sigma}}; d_{\sigma}^{\dagger} \rangle\rangle. \quad (3.34)$$

Since $\omega \equiv \omega + i0^+$, the sum over \mathbf{k} can be separated into correspondent real and imaginary parts (See Appendix A), which leads to

$$(\omega - \varepsilon_{d\sigma} + i\Gamma) \langle\langle d_{\sigma}; d_{\sigma}^{\dagger} \rangle\rangle = 1 + U \langle\langle d_{\sigma} n_{d\bar{\sigma}}; d_{\sigma}^{\dagger} \rangle\rangle, \quad (3.35)$$

wherein $\Gamma = \pi V^2 \sum_{\mathbf{k}} \rho_0$ is the self-energy contribution from the metallic host and $\rho_0 = 1/2D$, with D as being the characteristic band half-width of the metal. This self-energy term represents the way in which the impurity ‘‘feels’’ the presence of the host, leading to a renormalization of its energy levels. The quantity Γ also is known as Anderson parameter [4] and are related to the electron exchange rate between the impurity and the host via Fermi’s golden rule as follows [6]:

$$\tau = \frac{\hbar}{2\Gamma}, \quad (3.36)$$

with τ as being the electron lifetime in a given state of the impurity. As we will see later, Γ provides the half width at half maximum (HWHM) of the peaks in the DOS related to possible states at the impurity [6]. Therefore, broader peaks describes states in which the electron lifetime is shorter.

Let us continue to apply the EOM for obtaining $\langle\langle d_{\sigma}; d_{\sigma}^{\dagger} \rangle\rangle$. According to Eq. (3.35), the four-operator Green’s function $\langle\langle d_{\sigma} n_{d\bar{\sigma}}; d_{\sigma}^{\dagger} \rangle\rangle$ should be computed. Such kind of Green’s function describes a many-particle interaction owing to the presence of the correlation ($U \neq 0$). Using the definition of Eq. (3.14) again,

$$\omega \langle\langle d_{\sigma} n_{d\bar{\sigma}}; d_{\sigma}^{\dagger} \rangle\rangle = \langle\langle [d_{\sigma} n_{d\bar{\sigma}}, d_{\sigma}^{\dagger}]_+ \rangle\rangle + \langle\langle [d_{\sigma} n_{d\bar{\sigma}}, H]; d_{\sigma}^{\dagger} \rangle\rangle, \quad (3.37)$$

which leads to (see Appendix B)

$$\begin{aligned} (\omega - \varepsilon_{d\sigma} - U) \langle\langle d_{\sigma} n_{d\bar{\sigma}}; d_{\sigma}^{\dagger} \rangle\rangle &= \langle n_{d\bar{\sigma}} \rangle + V \sum_{\mathbf{k}} \langle\langle c_{\mathbf{k}\sigma} n_{d\bar{\sigma}}; d_{\sigma}^{\dagger} \rangle\rangle + V \sum_{\mathbf{k}} \langle\langle d_{\sigma}^{\dagger} c_{\mathbf{k}\bar{\sigma}} d_{\sigma}; d_{\sigma}^{\dagger} \rangle\rangle \\ &- V \sum_{\mathbf{k}} \langle\langle c_{\mathbf{k}\bar{\sigma}}^{\dagger} d_{\bar{\sigma}} d_{\sigma}; d_{\sigma}^{\dagger} \rangle\rangle, \end{aligned} \quad (3.38)$$

with the occupation average

$$\langle n_{d\bar{\sigma}} \rangle = - \left(\frac{1}{\pi} \right) \int d\omega f_F(\omega) \text{Im}[\langle\langle d_{\bar{\sigma}}; d_{\bar{\sigma}}^{\dagger} \rangle\rangle]. \quad (3.39)$$

As can be seen in Eq. (3.38), the running of the EOM procedure in the four-operator Green's function has generated new many-particle Green's functions. If we apply the EOM in each of them, we will get new Green's functions of same type and by running EOM in such functions, we will obtain again new Green's functions. In other words, the successive application of the EOM technique in many-particle Green's functions leads to an infinite growth of the system of coupled functions and thus, some approximation method becomes necessary to close the calculations. In this sense, we employ the well-established Hubbard-I truncation scheme [7], which allows to catch the Coulomb blockade peaks [1], also known as Hubbard peaks. Like every approximation in Physics, the Hubbard-I also has a disadvantage: it is unable to pick up the features of Kondo effect [8], once it throws away the Green's functions containing spin-flip processes between the host and the magnetic impurity. Hence, the Hubbard-I is valid only for $T \gg T_K$, wherein T_K is the characteristic Kondo temperature. It should be emphasized that a full description of the Kondo scattering process only can be obtained by the Numerical Renormalization Group (NRG) method [9, 10], developed by Kenneth G. Wilson⁴ in the 1970s.

Now, let us effectively apply the Hubbard-I approximation. The first step consists of transforming the many-particle Green's functions $\langle\langle d_{\sigma}^{\dagger} c_{\mathbf{k}\bar{\sigma}} d_{\sigma}; d_{\sigma}^{\dagger} \rangle\rangle$ and $\langle\langle c_{\mathbf{k}\bar{\sigma}}^{\dagger} d_{\bar{\sigma}} d_{\sigma}; d_{\sigma}^{\dagger} \rangle\rangle$ in an average of two operators multiplied by a single particle Green's functions and evaluate $\langle\langle c_{\mathbf{k}\sigma} n_{d\bar{\sigma}}; d_{\sigma}^{\dagger} \rangle\rangle$ with the EOM technique. From Eq. (3.38),

$$\begin{aligned} (\omega - \varepsilon_{d\sigma} - U) \langle\langle d_{\sigma} n_{d\bar{\sigma}}; d_{\sigma}^{\dagger} \rangle\rangle &= \langle n_{d\bar{\sigma}} \rangle + V \sum_{\mathbf{k}} \langle\langle c_{\mathbf{k}\sigma} n_{d\bar{\sigma}}; d_{\sigma}^{\dagger} \rangle\rangle + V \sum_{\mathbf{k}} d_{\bar{\sigma}}^{\dagger} c_{\mathbf{k}\bar{\sigma}} \langle\langle d_{\sigma}; d_{\sigma}^{\dagger} \rangle\rangle \\ &- V \sum_{\mathbf{k}} c_{\mathbf{k}\bar{\sigma}}^{\dagger} d_{\bar{\sigma}} \langle\langle d_{\sigma}; d_{\sigma}^{\dagger} \rangle\rangle. \end{aligned} \quad (3.40)$$

Since $d_{\bar{\sigma}}^{\dagger} c_{\mathbf{k}\bar{\sigma}} = c_{\mathbf{k}\bar{\sigma}}^{\dagger} d_{\bar{\sigma}}$, the equation above reads

$$(\omega - \varepsilon_{d\sigma} - U) \langle\langle d_{\sigma} n_{d\bar{\sigma}}; d_{\sigma}^{\dagger} \rangle\rangle = \langle n_{d\bar{\sigma}} \rangle + V \sum_{\mathbf{k}} \langle\langle c_{\mathbf{k}\sigma} n_{d\bar{\sigma}}; d_{\sigma}^{\dagger} \rangle\rangle. \quad (3.41)$$

Also according to EOM (see Appendix B),

$$\begin{aligned} (\omega - \varepsilon_{\mathbf{k}}) \langle\langle c_{\mathbf{k}\sigma} n_{d\bar{\sigma}}; d_{\sigma}^{\dagger} \rangle\rangle &= V \langle\langle d_{\sigma} n_{d\bar{\sigma}}; d_{\sigma}^{\dagger} \rangle\rangle + V \langle\langle d_{\bar{\sigma}}^{\dagger} c_{\mathbf{k}\bar{\sigma}} c_{\mathbf{k}\sigma}; d_{\sigma} \rangle\rangle \\ &- V \langle\langle c_{\mathbf{k}\bar{\sigma}}^{\dagger} d_{\bar{\sigma}} c_{\mathbf{k}\sigma}; d_{\sigma} \rangle\rangle. \end{aligned} \quad (3.42)$$

At this point of the process, we apply the second step of the Hubbard-I truncation scheme, by considering that

$$\begin{aligned} \langle\langle d_{\bar{\sigma}}^{\dagger} c_{\mathbf{k}\bar{\sigma}} c_{\mathbf{k}\sigma}; d_{\sigma} \rangle\rangle &= \langle d_{\bar{\sigma}}^{\dagger} c_{\mathbf{k}\bar{\sigma}} \rangle \langle\langle c_{\mathbf{k}\sigma}; d_{\sigma} \rangle\rangle, \\ \langle\langle c_{\mathbf{k}\bar{\sigma}}^{\dagger} d_{\bar{\sigma}} c_{\mathbf{k}\sigma}; d_{\sigma} \rangle\rangle &= \langle c_{\mathbf{k}\bar{\sigma}}^{\dagger} d_{\bar{\sigma}} \rangle \langle\langle c_{\mathbf{k}\sigma}; d_{\sigma} \rangle\rangle \end{aligned} \quad (3.43)$$

and consequently,

$$(\omega - \varepsilon_{\mathbf{k}}) \langle\langle c_{\mathbf{k}\sigma} n_{d\bar{\sigma}}; d_{\sigma}^{\dagger} \rangle\rangle = V \langle\langle d_{\sigma} n_{d\bar{\sigma}}; d_{\sigma}^{\dagger} \rangle\rangle. \quad (3.44)$$

⁴The Nobel Prize in Physics 1982 was awarded to Wilson "for his theory for critical phenomena in connection with phase transitions", related to the NRG technique.

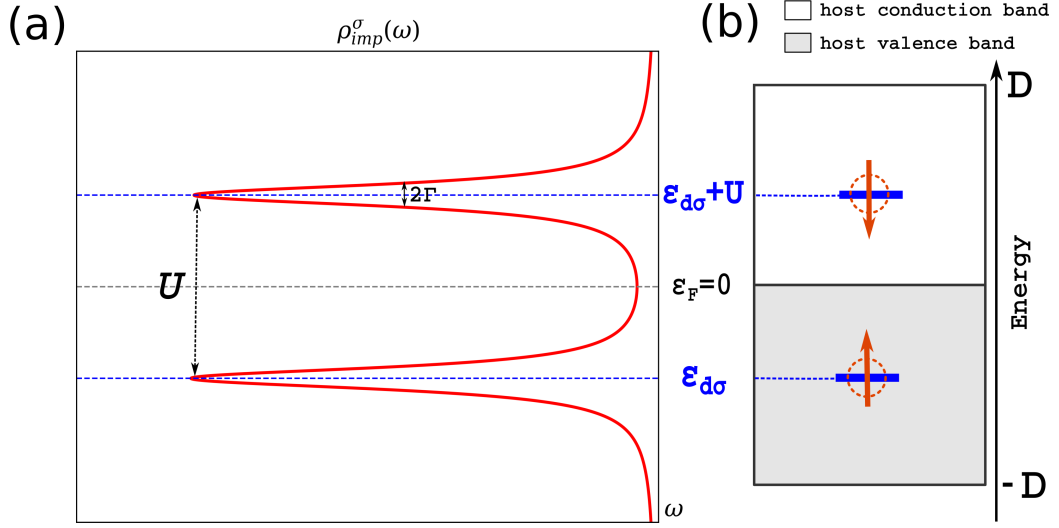


Figure 3.2: (a) Schematic DOS of an impurity (dot) adsorbed in a non-magnetic metallic host [Eq. (3.39)] described by the Anderson Hamiltonian [Eq. (3.18)] for the particle-hole symmetric regime $2\varepsilon_{d\sigma} + U = 0$. Both the peaks describe the Coulomb blockade physics acting within the impurity. The broadening of such peaks are given by the self-energy Γ owing to the coupling between the discrete state of the impurity and the continuum which describes the non-magnetic host. (b) if an electron with a spin up (\uparrow) for instance, is added at the level $\varepsilon_{d\sigma}$, another electron with opposite spin down (\downarrow) cannot be placed at the same energy level due to the Coulomb repulsion, thus opening a second electronic channel at $\varepsilon_{d\sigma} + U$.

By substituting Eq. (3.44) into Eq. (3.41), we obtain

$$(\omega - \varepsilon_{d\sigma} - U + i\Gamma)\langle\langle d_{\sigma}n_{d\bar{\sigma}}; d_{\sigma}^{\dagger} \rangle\rangle = \langle n_{d\bar{\sigma}} \rangle \quad (3.45)$$

wherein we recognize the definition of Anderson parameter [Eq. (3.34)]. Finally, by substituting Eq. (3.45) into Eq. (3.35) and performing some algebra, we get the following well-known expression for the Green's function describing an impurity embedded in a non-magnetic metallic host within the Hubbard-I approximation [1]:

$$G_{d\sigma;d\sigma}^R(\omega) = \frac{1 - \langle n_{d\bar{\sigma}} \rangle}{\omega - \varepsilon_{d\sigma} + i\Gamma} + \frac{\langle n_{d\bar{\sigma}} \rangle}{\omega - \varepsilon_{d\sigma} - U + i\Gamma}, \quad (3.46)$$

with the corresponding DOS $\rho_{imp}^{\sigma}(\omega) = -(\frac{1}{\pi})\text{Im}[G_{d\sigma;d\sigma}^R(\omega)]$, *i.e.*,

$$\rho_{imp}^{\sigma}(\omega) = \left(\frac{1}{\pi}\right) \frac{(1 - \langle n_{d\bar{\sigma}} \rangle)\Gamma}{(\omega - \varepsilon_{d\sigma})^2 + \Gamma^2} + \left(\frac{1}{\pi}\right) \frac{\langle n_{d\bar{\sigma}} \rangle\Gamma}{(\omega - \varepsilon_{d\sigma} - U)^2 + \Gamma^2}. \quad (3.47)$$

As can be seen in Figure 3.2(a), the first term of Eq. (3.47) gives rise to a Lorentzian peak centered at $\varepsilon_{d\sigma}$, with its height and width modulated by $(1 - \langle n_{d\bar{\sigma}} \rangle)$ ⁵ and Γ , respectively. Such a peak represents the DOS related for adding an electron with a given spin σ when the impurity (quantum dot) level is empty [Fig. 3.2(b)]. The second term of Eq. (3.47) describes another Lorentzian structure with same width $\propto \Gamma$, but with its amplitude modulated by $\langle n_{d\bar{\sigma}} \rangle$. This second peak, centered at $\varepsilon_{d\sigma} + U$, represents the DOS for adding an electron with opposite spin $\bar{\sigma}$ when the impurity (dot) is already occupied [Fig. 3.2(b)]. These two structures in Fig. 3.2(a) are known as Hubbard peaks and describe the physics of Coulomb

⁵The self-consistent integrals of the occupation averages [Eq. (3.39)] were numerically computed via *Python 3.6.9*, using *scipy.quad* package.

blockade regime.

The application of the Hubbard-I truncation scheme showed above corresponds to a simplest and well-known situation related to the original Anderson Hamiltonian. As we shall see in chapter 7, the presence of other terms in the system Hamiltonian, as those ones which describe electron hopping processes or superconducting pairing, leads to a more intricate calculations, once more many-particle Green's functions arise from these new physical mechanisms.

Bibliography

- [1] H. Bruus and K. Flensberg, *Many-Body Quantum Theory in Condensed Matter Physics: An Introduction*, Oxford Graduate Texts (Oxford University Press, 2004).
- [2] H. Haug and A. Jauho, *Quantum Kinetics in Transport and Optics of Semiconductors*, Springer Series in Solid-State Sciences (Springer Berlin Heidelberg, 2008).
- [3] M. M. Odashima, B. G. Prado and E. Vernek. *Revista Brasileira de Ensino de Física*, **39**, 1, e1303 (2017).
- [4] P. W. Anderson, *Phys. Rev.* **124**, 41 (1961).
- [5] D. G. Duffy, *Green's Functions with Applications*, 2nd edition. *Advances in Applied Mathematics* (Chapman and Hall/CRC, 2015).
- [6] P. Phillips. *Advanced Solid State Physics*. 2nd edition, Cambridge University Press, 2012.
- [7] J. Hubbard, *Proc. R. Soc. London, Ser. A* **276**, 238 (1963).
- [8] Hewson, A. *The Kondo Problem to Heavy Fermions* (Cambridge Studies in Magnetism). Cambridge: Cambridge University Press, 1993.
- [9] K. G. Wilson, *Rev. Mod. Phys.* **47**, 4 (1975).
- [10] R. Bulla, T.A. Costi, T. Pruschke, *Rev. Mod. Phys.* **80**, 2 (2008).

Chapter 4

Decay of bound states in the continuum of Majorana fermions induced by vacuum fluctuations: Proposal of qubit technology

L. S. Ricco, Y. Marques, F. A. Dessotti, R. S. Machado, M. de Souza, and A. C. Seridonio, Phys. Rev. B 93, 165116. Published April 14, 2016.

4.1 Overview and Remarks

As we have discussed in sec. 1, in recent years, the seeking for Majorana quasiparticles in condensed matter systems has attracted a huge attention of both theoretical and experimental physicists [2, 13], owing to its exotic non-Abelian exchange statistics [3], which opens the possibility of building Majorana-based qubits to realize fault-tolerant topological quantum computing [4–7] operations. In this sense, quantum apparatus which betake of Majorana quasiparticles(MQPs) properties have been acquired the status of the next generation of nanodevices and are expected to be responsible for the next technological breakthrough within the field of quantum information.

By considering this fruitful background, we have proposed theoretically a nanodevice [please, see Fig.1 of the corresponding paper (sec. 4.2)] constituted by two semi-infinite topological Kitaev wires [4] coupled to a quantum dot (QD), which is hybridized with metallic leads. Such a setup have allowed us to reveal an innovative method for reading the information trapped in the Majorana-based qubit. This new mechanism make use of the so-called bound states in the continuum (BICs) [8–10] to manipulate the information through the device. Basically, when the Kitaev wire-dot couplings are asymmetric, the BICs decay into the energy continuum and thus, the information can be read at the QD-leads part of the system. Our findings also revealed that such a decay process occurs when the vacuum of the qubit state fluctuates [11], instead of the usual unbalance mechanism of decaying owing to Fano interference phenomena [9, 10].

4.1.1 Methodology

In order to obtain the density of states(DOS) of the non-local fermions f composed by MQPs η_1 and η_2 , localized at the edges of the semi-infinite Kitaev wires, as well as the transmittance through the

QD, we have employed the equation-of-motion (EOM) approach (See Chapter 3.1), aiming to find the suitable retarded Green's functions in the energy domain ω , since

$$\text{DOS}_{ab} = -\frac{1}{\pi} \text{Im}(G_{a,b}^r(\omega)), \quad (4.1)$$

where $G_{a,b}^r(\omega)$ represents the retarded Green's function in the energy domain (spectral Green's function) for the fermionic operators a and b of the Hamiltonian (Eq.(2) of the published article). We also introduced $\mathcal{T} = -\Gamma \text{Im}(G_{d\dagger d}^r)$ as the transmittance through the QD, with Γ as being the Anderson broadening[13]. It's interesting to note that the poles of spectral Green's function allow to obtain the information about the system electronic excitations[14]. The calculations concerning the EOM applied to the present system Hamiltonian can be found in Appendix A.

Experimentally, the DOS can be accessed by zero-bias conductance measurements, as the Landauer-Büttiker formula states. More details can be found in the published article below.

Bibliography

- [1] J. Alicea, Rep. Prog. Phys. **75**, 076501 (2012).
- [2] S. R. Elliott and M. Franz, Rev. Mod. Phys. **87**, 137 (2015).
- [3] C. Nayak, S. H. Simon, A. Stern, M. Freedman, and S. Das Sarma Rev. Mod. Phys. **80**, 1083 (2008).
- [4] A.Y. Kitaev, Phys. Usp. **44**, 131 (2001).
- [5] K. Flensberg, Phys. Rev. Lett. **106**, 090503 (2012).
- [6] M. Leijnse and K. Flensberg, Phys. Rev. Lett. **107**, 210502 (2012).
- [7] M. Leijnse and K. Flensberg, Phys. Rev. B **86**, 134528 (2012).
- [8] J. von Neumann and E. Wigner, Phys. Z. **30**, 465 (1929).
- [9] L.H. Guessi, R.S. Machado, Y. Marques, L.S. Ricco, K. Kristinsson, M. Yoshida, I.A. Shelykh, M. de Souza, and A.C. Seridonio, Phys. Rev. B **92**, 045409 (2015).
- [10] L. H. Guessi, Y. Marques, R. S. Machado, K. Kristinsson, L. S. Ricco, I. A. Shelykh, M. S. Figueira, M. de Souza, and A. C. Seridonio, Phys. Rev. B **92**, 245107 (2015).
- [11] H. B. G. Casimir, Proc. K. Ned. Akad. Wet. **51**, 793 (1948).
- [12] H. Haug and A. P. Jauho, Quantum Kinetics in Transport and Optics of Semiconductors, Springer Series in Solid-State Sciences Vol. 123 (Springer, New York, 1996).
- [13] P.W. Anderson, Phys. Rev. **124**, 41 (1961).
- [14] H. Bruus, K. Flensberg, Many-Body Quantum Theory in Condensed Matter Physics, An Introduction (Oxford University Press, New York, 2004).
- [15] R. Bulla, T.A. Costi, T. Pruschke, Rev. Mod. Phys. **80**, 2 (2008).
- [16] A.C. Seridonio, M. Yoshida, and L.N. Oliveira, Europhys. Lett. **86**, 67006 (2009).
- [17] A.C. Seridonio, M. Yoshida, and L.N. Oliveira, Phys. Rev. B **80**, 235318, (2009).
- [18] M. Yoshida, A.C. Seridonio, and L.N. Oliveira, Phys. Rev. B **80**, 235317, (2009).
- [19] J. Hubbard, Proc. R. Soc. Lond. A 276 (1963) 238.
- [20] L.S. Ricco, Y. Marques, F.A. Dessotti, M. de Souza and A.C. Seridonio, Phys. E **78**, 25 (2015).

- [21] C. J.Lacroix, Phys. F. **11**, 2389(1981).
- [22] A. C. Seridonio, E. C. Siqueira, F. A. Dessotti, R. S. Machado, and M. Yoshida, J. Appl. Phys. **115**, 063706 (2014).
- [23] D.A. Ruiz-Tijerina, E. Vernek, L.G.G.V. Dias da Silva, J.C. Egues, Phys. Rev. B **91** 115435 (2015).
- [24] E. Prada, R. Aguado, and P. San-Jose, Phys. Rev. B, **96** 085418 (2017).

4.2 Published Article

Decay of bound states in the continuum of Majorana fermions induced by vacuum fluctuations: Proposal of qubit technology

L. S. Ricco¹, Y. Marques¹, F. A. Dessotti¹, R. S. Machado¹, M. de Souza^{2,*} and A. C. Seridonio^{1,2}

¹*Departamento de Física e Química, Unesp - Univ Estadual Paulista, 15385-000, Ilha Solteira, SP, Brazil*

²*IGCE, Unesp - Univ Estadual Paulista, Departamento de Física, 13506-900, Rio Claro, SP, Brazil*

We report on a theoretical investigation of the interplay between vacuum fluctuations, Majorana quasiparticles (MQPs) and bound states in the continuum (BICs) by proposing a new venue for qubit storage. BICs emerge due to quantum interference processes as the Fano effect and, since such a mechanism is unbalanced, these states decay as regular into the continuum. Such fingerprints identify BICs in graphene as we have discussed in detail in Phys. Rev. B **92**, 245107 and 045409 (2015). Here by considering two semi-infinite Kitaev chains within the topological phase, coupled to a quantum dot (QD) hybridized with leads, we show the emergence of a novel type of BICs, in which MQPs are trapped. As the MQPs of these chains far apart build a delocalized fermion and qubit, we identify that the decay of these BICs is not connected to Fano and it occurs when finite fluctuations are observed in the vacuum composed by electron pairs for this qubit. From the experimental point of view, we also show that vacuum fluctuations can be induced just by changing the chain-dot couplings from symmetric to asymmetric. Hence, we show how to perform the qubit storage within two delocalized BICs of MQPs and to access it when the vacuum fluctuates by means of a complete controllable way in quantum transport experiments.

PACS numbers: 72.10.Fk 73.63.Kv 74.20.Mn

I. INTRODUCTION

An astonishing aftermath in the underlying framework of quantum theory is the possibility of fluctuations within the corresponding quantum field describing the vacuum, in which pairs of virtual particles pop up leading to counterintuitive phenomena. In this regard, the Casimir effect¹ is the most known picture in Physics arising from the straight outcome of vacuum fluctuations. In particular, the Casimir effect manifests itself as an attractive force between two reflecting, plane and parallel plates, even when external fields are entirely absent.

On the ground of condensed matter Physics, we make explicit that the interplay between vacuum fluctuations and Majorana quasiparticles (MQPs)² is accomplishable by the setup proposed in Fig. 1, where we find peculiar bound states in the continuum (BICs)³ for a pair of semi-infinite Kitaev chains^{2,4-8} in the topological phase and coupled to a quantum dot (QD) connected to leads. Concerning on BICs, they were pioneering predicted by von Neumann and Wigner in 1929³ as quantum states for electrons described by localized square-integrable wave functions appearing in the continuum of those delocalized and exhibiting infinite lifetimes for such electrons. Hence, electrons within BICs do not decay into the continuum acting as fully invisible states from the perspective of conductance measurements. The issue on BICs had a revival after the works of Stillinger and Herrick in 1975⁹, followed by the experimental realization made by Capasso and co-workers in 1992, concerning semiconductor heterostructures¹⁰. Noteworthy, BICs are expected to emerge in several systems as in graphene¹¹⁻¹³, optics and photonics¹⁴⁻¹⁷, setups characterized by singular chirality¹⁸, Floquet-Hubbard states due to strong oscillating electric field¹⁹ and driven by A.C. fields²⁰.

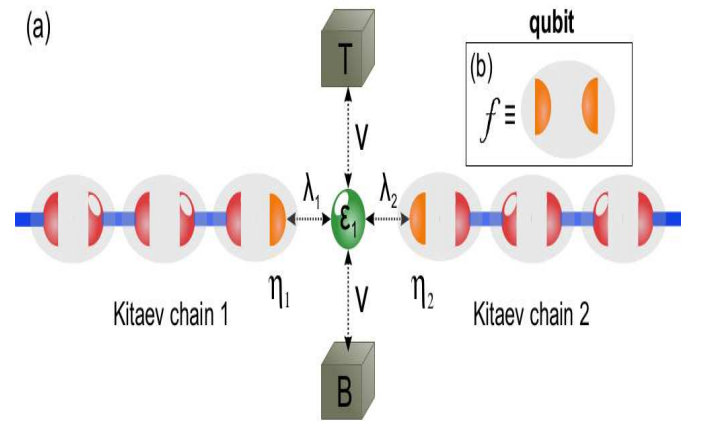


Figure 1. (Color online) For a off-resonance QD with the Fermi level of the top (T) and bottom (B) leads, together with couplings $\lambda_1 = \lambda_2$, BICs of the MQPs η_1 and η_2 emerge. V is the hybridization of the QD with the leads. The vacuum of electron pairs for the qubit f fluctuates when $\lambda_1 \equiv (t+\Delta) \neq \lambda_2 \equiv (t-\Delta)$, thus inducing the decay of the BICs into the system continuum of energies.

In this paper, we show that the setup proposed in Fig. 1 enables the observation of an unprecedented phenomenon: vacuum fluctuations yielding the decay of BICs into the continuum, in which the building blocks of the former are MQPs for qubit storage. We highlight two setups considered proper platforms for MQPs in Kitaev chains as well as for the experimental achievement of our proposal: i) an *s*-wave superconductor nearby a semiconducting nanowire where two magnetic fields exist perpendicular to each other, wherein one of them arises from the spin-orbit coupling of the semiconductor, while the second is applied externally to freeze the spin de-

gree of freedom of the system and to ensure topological superconductivity²¹, and ii) magnetic chains on top of superconductors characterized by a strong spin-orbit parameter^{22,23}. Moreover, MQPs are expected to rise among several setups as the fractional quantum Hall state with filling factor $\nu = 5/2$ ²⁴, in three-dimensional topological insulators²⁵ and at the center of superconducting vortices as well²⁶⁻²⁸.

To the best of our knowledge, the works up to date published in the literature have focused mainly on BICs assisted by Fano interference^{11,12,14,15}. The so-called Fano effect is a quantum interference phenomenon, wherein transport channels compete for the electron tunneling, mainly via a continuum of energies hybridized with discrete levels of nanoscale structures^{29,30}. Here, as an alternative we propose that quantum fluctuations in the vacuum of electron pairs arising from the regular fermion and qubit f composed by the MQPs $\eta_1 = \eta_1^\dagger$ and $\eta_2 = \eta_2^\dagger$, cf. shown in Fig.1, give rise to the decay of these peculiar BICs, the so-called quasi BICs. Otherwise, the BICs of MQPs remain intact.

In order to present our proposal in a comprehensive way, we begin by defining the qubit f as follows: $f = \frac{1}{\sqrt{2}}(\eta_1 + i\eta_2)$ and $f^\dagger = \frac{1}{\sqrt{2}}(\eta_1 - i\eta_2)$, in which the occupations

$$\langle f^\dagger f^\dagger \rangle = \int_{-\infty}^{+\infty} d\varepsilon \text{DOS}_{f^\dagger f^\dagger} = \langle ff \rangle = \int_{-\infty}^{+\infty} d\varepsilon \text{DOS}_{ff} = 0 \quad (1)$$

can be found³¹, here expressed in terms of the densities $\text{DOS}_{f^\dagger f^\dagger}$ and DOS_{ff} , since the pairings $f^\dagger f^\dagger$ and ff are not allowed in the system when both the Kitaev chains considered are equally coupled to the QD. Later on, such densities will be deduced from our model Hamiltonian. Furthermore, we will clarify that vacuum fluctuations can be tunable experimentally. To that end, we should take into account asymmetric Kitaev chain-dot couplings and a off-resonance QD with the Fermi level of the leads, since the symmetric case prevents vacuum fluctuations thus ensuring the qubit storage as MQPs delocalized at the edges of the Kitaev chains as sketched in Fig. 1. Hence, by means of BICs of MQPs, we propose a novel manner of qubit storage when a single QD and controllable vacuum fluctuations are accounted.

II. THE MODEL

To give a theoretical description of the setup depicted in Fig. 1 describing two semi-infinite Kitaev chains within the topological phase and connected to a QD coupled to leads, we employ an extension of the Hamiltonian inspired on the original proposal from Liu and Baranger, which is a spinless model to ensure topological superconductivity Ref. [32]:

$$\mathcal{H} = \sum_{\alpha k} \tilde{\varepsilon}_{\alpha k} c_{\alpha k}^\dagger c_{\alpha k} + \varepsilon_1 d_1^\dagger d_1 + V \sum_{\alpha k} (c_{\alpha k}^\dagger d_1 + \text{H.c.}) + \frac{(t + \Delta)}{\sqrt{2}} (d_1 - d_1^\dagger) \eta_1 + i \frac{(\Delta - t)}{\sqrt{2}} (d_1 + d_1^\dagger) \eta_2, \quad (2)$$

where the electrons in the lead $\alpha = T, B$ are described by the operator $c_{\alpha k}^\dagger$ ($c_{\alpha k}$) for the creation (annihilation) of an electron in a quantum state labeled by the wave number k and energy $\tilde{\varepsilon}_{\alpha k} = \varepsilon_k - \mu_\alpha$, with μ_α as the chemical potential. For the QD coupled to leads, d_1^\dagger (d_1) creates (annihilates) an electron in the state ε_1 . V stands for the hybridizations between the QD and the leads. The QD couples asymmetrically to the Kitaev chains with tunneling amplitudes proportional to $(t + \Delta) \equiv \lambda_1$ and $(t - \Delta) \equiv \lambda_2$, respectively for the left and right MQPs η_1 and η_2 . We stress that the prefactors $1/\sqrt{2}$ and $i/\sqrt{2}$, respectively for λ_1 and λ_2 constitute a convenient gauge that changes the last two terms of Eq. (2) into $td_1 f^\dagger - td_1^\dagger f + \Delta f^\dagger d_1^\dagger - \Delta f d_1 = td_1 f^\dagger + \Delta f^\dagger d_1^\dagger + \text{H.c.}$, when the representation f is adopted. As a result, we can notice that the electrons within f and d_1 beyond the normal tunneling t between them, become bounded as a Cooper pair with binding energy Δ . Particularly, with $\Delta \neq 0$ we will verify that the BICs here proposed decay into the continuum due to the emergence of these pairing terms.

In what follows, we use the Landauer-Büttiker formula for the zero-bias conductance G ³². Such a quantity is given by:

$$G = \frac{e^2}{h} \Gamma \int d\varepsilon \left(\frac{\partial f_F}{\partial \varepsilon} \right) \text{Im}(\tilde{\mathcal{G}}_{d_1^\dagger d_1}), \quad (3)$$

where $\Gamma = 2\pi V^2 \sum_k \delta(\varepsilon - \varepsilon_k)$ is the Anderson broadening³³, f_F stands for the Fermi-Dirac distribution, $\tilde{\mathcal{G}}_{d_1^\dagger d_1}$ is the retarded Green's function for the QD in energy domain ε , obtained from the time Fourier transform of $\tilde{\mathcal{G}}_{\mathcal{B}^\dagger \mathcal{A}} = \int d\tau \mathcal{G}_{\mathcal{B}^\dagger \mathcal{A}} e^{\frac{i}{h}(\varepsilon + i0^+)\tau}$. Furthermore, we introduced $\mathcal{T} = -\Gamma \text{Im}(\tilde{\mathcal{G}}_{d_1^\dagger d_1})$ as the transmittance through the QD. $\mathcal{G}_{\mathcal{B}^\dagger \mathcal{A}} = -\frac{i}{h} \theta(\tau) \text{Tr}\{\varrho[\mathcal{A}(\tau), \mathcal{B}^\dagger(0)]_+\}$ corresponds to the Green's function in time domain τ , here expressed in terms of the density matrix ϱ for Eq. (2) and the Heaviside function $\theta(\tau)$. From $\mathcal{G}_{\mathcal{B}^\dagger \mathcal{A}}$, it is possible to find the expectation value $\langle \mathcal{B}^\dagger \mathcal{A} \rangle = \int d\varepsilon \text{DOS}_{\mathcal{B}^\dagger \mathcal{A}}$ by using $\text{DOS}_{\mathcal{B}^\dagger \mathcal{A}} = -\frac{1}{\pi} \text{Im}(\mathcal{G}_{\mathcal{B}^\dagger \mathcal{A}})$ as the corresponding density of states, similarly to Eq.(1) for the vacuum. Particularly for Eq. (3), we used $\mathcal{A} = \mathcal{B} = d_1$ and to calculate $\tilde{\mathcal{G}}_{d_1^\dagger d_1}$ together with other Green's functions, we should employ the equation-of-motion (EOM) method³¹ summarized as follows: $\omega \tilde{\mathcal{G}}_{\mathcal{B}^\dagger \mathcal{A}} = (\varepsilon + i0^+) \tilde{\mathcal{G}}_{\mathcal{B}^\dagger \mathcal{A}} = [\mathcal{A}, \mathcal{B}^\dagger]_+ + \tilde{\mathcal{G}}_{\mathcal{B}^\dagger [\mathcal{A}, \mathcal{H}]}$. As a result, we find

$$(\varepsilon - \varepsilon_1 + i\Gamma) \tilde{\mathcal{G}}_{d_1^\dagger d_1} = 1 - t \tilde{\mathcal{G}}_{d_1^\dagger, f} - \Delta \tilde{\mathcal{G}}_{d_1^\dagger, f^\dagger}, \quad (4)$$

in addition to the Green's functions $\tilde{\mathcal{G}}_{d_1^\dagger, f}$ and $\tilde{\mathcal{G}}_{d_1^\dagger, f^\dagger}$. According to the EOM approach, we also have $\omega \tilde{\mathcal{G}}_{d_1^\dagger, f} =$

$(\Delta\tilde{\mathcal{G}}_{d_1^\dagger, d_1^\dagger} - t\tilde{\mathcal{G}}_{d_1^\dagger, d_1^\dagger})$, $\omega\tilde{\mathcal{G}}_{d_1^\dagger, f^\dagger} = (t\tilde{\mathcal{G}}_{d_1^\dagger, d_1^\dagger} - \Delta\tilde{\mathcal{G}}_{d_1^\dagger, d_1^\dagger})$ and $\tilde{\mathcal{G}}_{d_1^\dagger, d_1^\dagger} = -2t\Delta\tilde{K}\tilde{\mathcal{G}}_{d_1^\dagger, d_1^\dagger}$, in which $\tilde{K} = [\varepsilon + \varepsilon_1 - K(t, \Delta) + i\Gamma]^{-1}K$, $K(t, \Delta) = [\varepsilon^2 + 2i\varepsilon 0^+ - (0^+)^2]^{-1}\omega(t^2 + \Delta^2)$ and $K = [\varepsilon^2 + 2i\varepsilon 0^+ - (0^+)^2]^{-1}\omega$. Consequently, the Green's function of the QD reads

$$\tilde{\mathcal{G}}_{d_1^\dagger d_1} = \frac{1}{\varepsilon - \varepsilon_1 + i\Gamma - \Sigma_{\text{MQPs}}}, \quad (5)$$

where $\Sigma_{\text{MQPs}} = K(t, \Delta) + (2t\Delta)^2 K\tilde{K}$ accounts for the self-energy due to the MQPs connected to the QD and $\text{DOS}_{11} = -\frac{1}{\pi}\text{Im}(\tilde{\mathcal{G}}_{d_1^\dagger d_1})$ is the density of states for the QD. Particularly for $t = \Delta = \frac{\lambda}{\sqrt{2}}$, the expressions for \tilde{K} and Σ_{MQPs} found in Ref. [32] are recovered.

To perceive the emergence of BICs in the Kitaev chains and vacuum fluctuations, we need to find the densities for the MQPs η_1 and η_2 , namely $\text{DOS}_{\eta_1} = -\frac{1}{\pi}\text{Im}(\tilde{\mathcal{G}}_{\eta_1 \eta_1})$ and $\text{DOS}_{\eta_2} = -\frac{1}{\pi}\text{Im}(\tilde{\mathcal{G}}_{\eta_2 \eta_2})$, together with $\text{DOS}_{ff} = -\frac{1}{\pi}\text{Im}(\tilde{\mathcal{G}}_{ff})$ and $\text{DOS}_{f^\dagger f^\dagger} = -\frac{1}{\pi}\text{Im}(\tilde{\mathcal{G}}_{f^\dagger f^\dagger})$, in which the latter allows to determine the occupations $\langle f^\dagger f^\dagger \rangle$ and $\langle ff \rangle$ as Eq. (1) ensures for the vacuum of electron pairs. Thus the EOM gives rise to

$$\tilde{\mathcal{G}}_{\eta_1 \eta_1} = \frac{1}{2}(\tilde{\mathcal{G}}_{f^\dagger f^\dagger} + \tilde{\mathcal{G}}_{ff^\dagger} + \tilde{\mathcal{G}}_{f^\dagger f} + \tilde{\mathcal{G}}_{ff}) \quad (6)$$

and

$$\tilde{\mathcal{G}}_{\eta_2 \eta_2} = \frac{1}{2}(-\tilde{\mathcal{G}}_{f^\dagger f^\dagger} + \tilde{\mathcal{G}}_{ff^\dagger} + \tilde{\mathcal{G}}_{f^\dagger f} - \tilde{\mathcal{G}}_{ff}) \quad (7)$$

for the Green's functions of the MQPs, with

$$\omega\tilde{\mathcal{G}}_{f^\dagger f^\dagger} = (t\tilde{\mathcal{G}}_{f^\dagger d_1^\dagger} - \Delta\tilde{\mathcal{G}}_{f^\dagger d_1^\dagger}) \quad (8)$$

and

$$\omega\tilde{\mathcal{G}}_{ff} = (-t\tilde{\mathcal{G}}_{fd_1} + \Delta\tilde{\mathcal{G}}_{fd_1^\dagger}) \quad (9)$$

for those describing the aforementioned vacuum. To close the system of Green's functions above-described, we calculate via EOM the following $\omega\tilde{\mathcal{G}}_{ff^\dagger} = (1 + t\tilde{\mathcal{G}}_{fd_1^\dagger} - \Delta\tilde{\mathcal{G}}_{fd_1})$, $\omega\tilde{\mathcal{G}}_{f^\dagger f} = (1 - t\tilde{\mathcal{G}}_{f^\dagger d_1} + \Delta\tilde{\mathcal{G}}_{f^\dagger d_1^\dagger})$, $\omega\tilde{\mathcal{G}}_{f^\dagger d_1} = -t(1+2\Delta^2\tilde{K})\tilde{\mathcal{G}}_{d_1^\dagger d_1}$, $\omega\tilde{\mathcal{G}}_{fd_1} = -\Delta(1+2t^2\tilde{K})\tilde{\mathcal{G}}_{d_1^\dagger d_1}$, $\tilde{\mathcal{G}}_{f^\dagger d_1^\dagger} = \Delta\tilde{K}K^{-1}\omega^{-1} - 2t\Delta\tilde{K}\tilde{\mathcal{G}}_{f^\dagger d_1}$ and $\tilde{\mathcal{G}}_{fd_1^\dagger} = t\tilde{K}K^{-1}\omega^{-1} - 2t\Delta\tilde{K}\tilde{\mathcal{G}}_{fd_1}$.

Thus based on the theoretical framework developed up to here, shortly thereafter we will discuss the role of Eqs.(5), (6) and (7) in the connection with the novel qubit technology proposed in this paper.

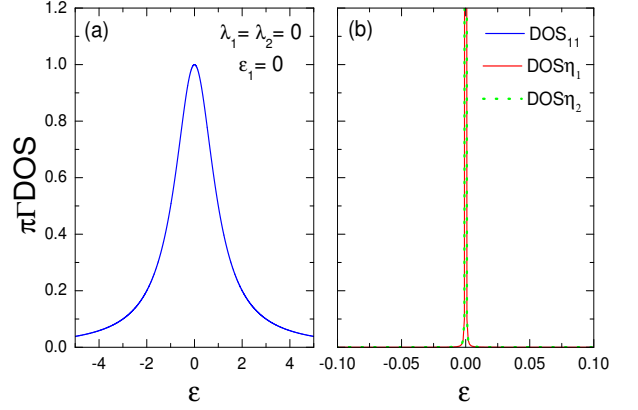


Figure 2. (Color online) (a) DOS of the QD in resonance with the Fermi level of the leads ($\varepsilon_F \equiv 0$) when the Kitaev chains are absent: a Lorentzian shape is observed. (b) DOSs of the MQPs by neglecting the couplings to the leads: a Delta function profile appears instead. Details in the main text.

III. RESULTS AND DISCUSSION

In the simulations discussed here we adopt $T = 0$ and the Anderson broadening $\Gamma = 2\pi V^2 \sum_k \delta(\varepsilon - \varepsilon_k)$ as the energy scale for the parameters from the system Hamiltonian of Eq. (2). In order to make explicit the phenomenon of qubit storage ruled by vacuum fluctuations, due to the Kitaev chains connected to the QD, we should begin by analyzing the cases in which both are decoupled from each other ($\lambda_1 = \lambda_2 = 0$). Within this situation, but for the QD in resonance with the Fermi level of the metallic leads ($\varepsilon_1 = \varepsilon_F \equiv 0$), the standard Lorentzian shape depicted in Fig. 2(a) for the DOS encoded by $\text{DOS}_{11} = -\frac{1}{\pi}\text{Im}(\tilde{\mathcal{G}}_{d_1^\dagger d_1})$ as a function of energy ε is verified. In the panel (b) of the same figure, we find coincident profiles for $\text{DOS}_{\eta_1} = -\frac{1}{\pi}\text{Im}(\tilde{\mathcal{G}}_{\eta_1 \eta_1})$ and $\text{DOS}_{\eta_2} = -\frac{1}{\pi}\text{Im}(\tilde{\mathcal{G}}_{\eta_2 \eta_2})$ describing the DOSs of the MQPs, respectively found at the edges of the Kitaev chains 1 and 2 nearby the QD. Once the MQPs are zero-energy modes for discrete states, the curves of DOS_{η_1} and DOS_{η_2} are indeed Dirac delta functions as expected, due to the absence of leads connected to the Kitaev chains. These Delta functions represent the complete storage of the qubit f composed by the MQPs η_1 and η_2 , since the zero broadening of such DOSs point out that the electron within f has an infinite lifetime and does not decay into the QD. Below, we will see that such a scenario is modified when the Kitaev chain-QD couplings are turned-on, i.e., $\lambda_1 = \lambda_2 \neq 0$.

Fig. 3(a) treats the symmetric regime $\lambda_1 = \lambda_2 = 10\Gamma$, in which the QD is still in resonance with the leads Fermi level. As both the QD and MQPs are zero-energy modes and share the same DOS profile ($\text{DOS}_{\eta_1} = \text{DOS}_{\eta_2} = \text{DOS}_{11}$), the outcome of this set is to exhibit the same splitting of the zero-peak, which was originally centered at the Fermi energy as showed in Figs. 2(a) and (b). Once the zero-peak is splitted, one can propose a manner of

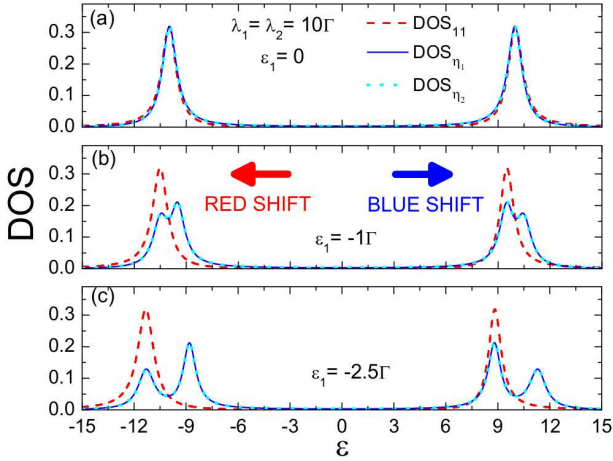


Figure 3. (Color online) (a) Scenario of Figs.2(a) and (b) modified when the Kitaev chain-QD symmetric couplings are turned-on: as the QD and the MQPs are in resonance, their DOSs split equally. (b) For the QD off-resonance, a new structure composed by four peaks emerges only in the DOSs for the MQPs. (c) Visualization of the red and blue shifts of the peaks found in (b) by placing the QD very far from the resonance.

controlling this splitting within the DOS_{11} . The way we have found is by placing the QD off-resonance in respect with the leads Fermi level. This picture can be visualized in Fig. 3(b) for the dashed-red curve with $\varepsilon_1 = -\Gamma$, where we can perceive the red and blue shifts of the peaks. On the other hand, the response of the MQPs due to the tuning of ε_1 is fully different compared to the QD: the original pattern given by a pair of peaks for the MQPs appearing in Fig. 3(a) evolves towards a novel structure, where four peaks emerge as depicted by the dotted and solid blue curves of Fig. 3(b). Note that this novel pattern is not well resolved for $\varepsilon_1 = -\Gamma$ yet, since the peaks within each pair of peaks are found partially merged. However, if we consider $\varepsilon_1 = -2.5\Gamma$ as in Fig. 3(c), the visibility of the four peaks becomes more pronounced and they appear completely resolved. We should draw attention in the manner that the pairs of peaks in the DOSs for the MQPs evolve from the pattern observed in Fig. 3(b) to that in panel (c). To reveal the underlying mechanism of such an electron-hole asymmetry, we should focus on panels (a)-(c) of Fig. 4 and, in particular, Eqs.(6) and (7) for $\text{DOS}_{\eta_1} = -\frac{1}{\pi}\text{Im}(\tilde{\mathcal{G}}_{\eta_1\eta_1})$ and $\text{DOS}_{\eta_2} = -\frac{1}{\pi}\text{Im}(\tilde{\mathcal{G}}_{\eta_2\eta_2})$, respectively.

Still in the symmetric regime $\lambda_1 = \lambda_2 = 10\Gamma$, we see that only $\tilde{\mathcal{G}}_{f\uparrow f}$ and $\tilde{\mathcal{G}}_{f\uparrow f}$ rise in Fig.4(a) respectively via the $\text{DOS}_{ff\uparrow} = -\frac{1}{\pi}\text{Im}(\tilde{\mathcal{G}}_{ff\uparrow})$ and $\text{DOS}_{f\uparrow f} = -\frac{1}{\pi}\text{Im}(\tilde{\mathcal{G}}_{f\uparrow f})$, while $\tilde{\mathcal{G}}_{f\uparrow f\uparrow}$ and $\tilde{\mathcal{G}}_{ff}$ contributes with $\text{DOS}_{f\uparrow f\uparrow} = \text{DOS}_{ff} = 0$ as aftermath of the vacuum $\langle f^\dagger f^\dagger \rangle = \langle ff \rangle = 0$ for the electron pairs. Besides, the structure of four peaks firstly displayed in Fig.3(c) and together with Fig.4(b) for the MQPs η_1 and η_2 considering $\varepsilon_1 = -3.5\Gamma$, then make explicit that the un-

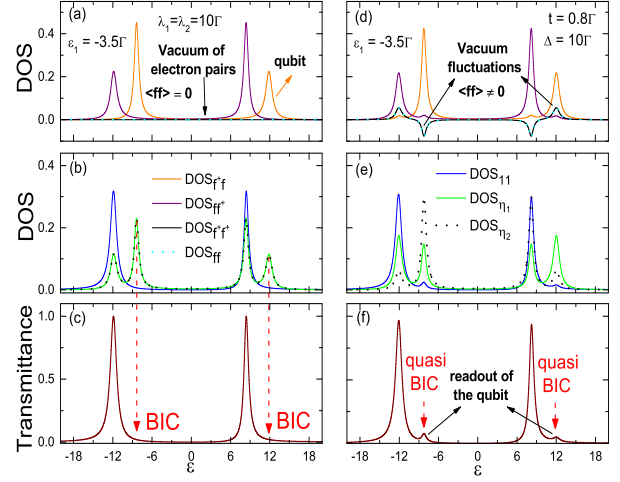


Figure 4. (Color online) Symmetric regime of Kitaev chain-QD couplings: (a) DOSs for electrons within the qubit f and absence of vacuum fluctuations outlined by the vertical arrow; (b) DOSs for the QD and MQPs in absence of vacuum fluctuations; (c) transmittance profile with BICs appearing denoted by dashed-vertical arrows, i.e., the lacking of the corresponding peaks found at the same positions within panel (b) for the DOSs of the MQPs is a BIC fingerprint, since these states do not contribute to the quantum transport. Only the peaks of the DOS for the QD remain in the transmittance. Asymmetric regime of Kitaev chain-QD couplings: (d) the vacuum fluctuates around the BICs verified in (c) and the DOSs for f also change; (e) DOSs for the QD and MQPs in presence of vacuum fluctuations; (f) As aftermath of the fluctuations observed in (d) which are denoted by arrows, the BICs of MQPs found in panel (c) decay as quasi BICs. They are found outlined by dashed-vertical arrows as we can visualize in the transmittance profile.

matched profiles of the $\text{DOS}_{ff\uparrow}$ and $\text{DOS}_{f\uparrow f}$ play the role of two spectral functions analogous to the possibilities DOS_\uparrow and DOS_\downarrow , due to spin-imbalance in ferromagnetic systems. Based on this, we can realize the features within Fig. 4(c), where the peaks appearing in the transmittance $\mathcal{T} = -\Gamma\text{Im}(\tilde{\mathcal{G}}_{d_1^\dagger d_1})$ determined by Eq.(3) do not correspond to those found in panel (a) for the $\text{DOS}_{f\uparrow f}$, but just to those from $\text{DOS}_{ff\uparrow}$. Equivalently, from those four peaks observed in Fig. 4(b) for the MQPs, solely two of them decay into the QD, thus contributing to the conductance. As a result, the peaks within $\text{DOS}_{\eta_1} = \text{DOS}_{\eta_2}$ that do not appear in \mathcal{T} correspond to BICs of MQPs, which constitute the building blocks of the delocalized qubit f characterized by the two peaks found in Fig. 4(a) for the $\text{DOS}_{f\uparrow f}$. These invisible peaks arising from the $\text{DOS}_{f\uparrow f}$ in \mathcal{T} , then provide a novel manner of qubit storage, wherein despite the coupling $\lambda_1 = \lambda_2 = 10\Gamma$ of the Kitaev chains with the QD, the decay of the state f is completely prevented. Such a forbiddance, we should highlight, occurs when the vacuum $\langle f^\dagger f^\dagger \rangle = \langle ff \rangle = 0$ does not fluctuate [Fig.4(a)]. In what follows, we will show that when $\langle f^\dagger f^\dagger \rangle = \langle ff \rangle \neq 0$, just in the vicinity of BICs, the suppression of the qubit storage occurs

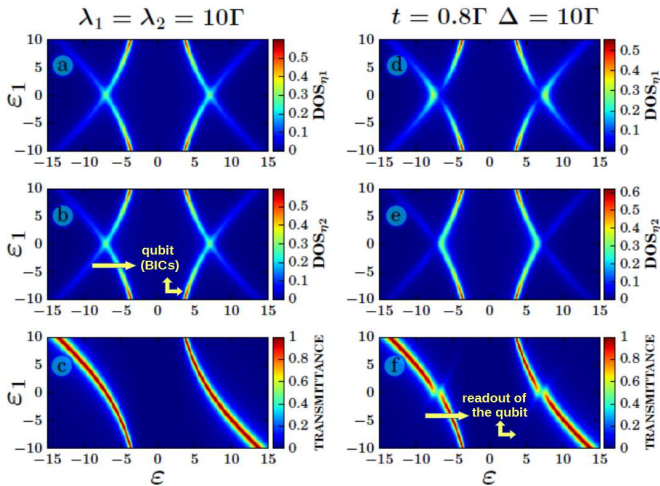


Figure 5. (Color online) Symmetric regime of Kitaev chain-QD couplings: in panels (a), (b) and (c) we see the density plots of the DOSs for the MQPs and transmittance spanned by the axis ε_1 and ε . Panel (c) for the transmittance shows only two bows from the set of four bows found in (a) and (b) describing the DOSs of the MQPs. The lack of such bows in the transmittance then denotes BICs of MQPs. Asymmetric regime of Kitaev chain-QD couplings: panels (d) and (e) are similar to (a) and (b), but in panel (f) quasi BICs appear as light bows in the transmittance in respect with those verified in panels (d) and (e).

and hence, the decay of the BICs as quasi BICs is allowed appearing thought out the transmittance.

To fluctuate the vacuum considered, it is demanded asymmetric couplings $\lambda_1 \neq \lambda_2$ by means of $\Delta = 10\Gamma$ and $t = 0.8\Gamma$, for instance. As a net effect we have $\text{DOS}_{f^\dagger f^\dagger} = \text{DOS}_{ff} \neq 0$ corresponding to fluctuations in the vacuum $\langle f^\dagger f^\dagger \rangle = \langle ff \rangle \neq 0$ around the BICs, which appear pointed out by black arrows in Fig. 4(d). In such a situation, pairing terms $d_1 f + f^\dagger d_1^\dagger$ appear, which allow the correlations above to become finite. Consequently, the profiles for DOS_{η_1} and DOS_{η_2} become distinct as showed in Fig. 4(e), resulting in the detection of the BICs by means of the quasi BICs, which appear as unpronounced states indicated by dashed-red arrows in Fig. 4(f). Noteworthy, the quasi BICs are placed exactly at the positions of the BICs found in Fig. 4(c). Moreover, it is worth noticing in opposite to the unbalance of Fano interference as the underlying mechanism for the rising of quasi BICs reported in graphene systems^{11,12}, here we

identify that vacuum fluctuations of the electron pairs described by the expectation value $\langle f^\dagger f^\dagger \rangle = \langle ff \rangle \neq 0$ as the trigger for the decay of these peculiar BICs of MQPs. When it occurs, the information within the qubit is read via transmittance.

To summarize the results presented up to here, we wrap up them in the density plots of \mathcal{T} spanned by the axis ε_1 and ε appearing in Fig. 5, where panels (a)-(c) and (d)-(e) designate respectively, the symmetric and asymmetric regimes of couplings between the QD and the Kitaev chains. Panels (a), (b), (d) and (e) of the same figure, in particular, share a main characteristic: all of them exhibit the structure of four peaks previously reported, which appear as four bows in the density plot format. As just two bows from the set of four found in Figs. 5(a) and (b) are displayed in (c), those absent are then BICs of MQPs, while the light pair of bows in (f) represent quasi BICs.

IV. CONCLUSIONS

In summary, we have proposed a setup based on two semi-infinite Kitaev chains presenting MQPs at their edges both coupled to a single QD crossed by a current due to source and drain reservoirs of electrons, in which BICs of MQPs are revealed as building blocks for the storage of a delocalized qubit. For absence of fluctuation in the vacuum of electron pairs as aftermath of the delocalized fermion and qubit built by these MQPs, the BICs do not decay into the system continuum and are still unperceived by conductance measurements, which then ensure the storage. Fluctuations of the aforementioned vacuum then trigger the decay of such states as quasi BICs. Distinct from the standard BICs formed by Fano effect^{11,12,14,15}, the corresponding for MQPs are ruled by vacuum fluctuations, thus constituting a novel phenomenon. Experimentally speaking, it can be feasible just by tuning the Kitaev chain-dot couplings from symmetric (intact BICs where the qubit is found) to asymmetric (vacuum fluctuations induced), when the QD is off-resonance with the Fermi energy of the metallic leads.

V. ACKNOWLEDGMENTS

This work was supported by CNPq, CAPES, 2014/14143-0 and 2015/23539-8 São Paulo Research Foundation (FAPESP).

* Current address: Institute of Semiconductor and Solid State Physics, Johannes Kepler University Linz, Austria.

¹ H.B.G. Casimir, Proc. K. Ned. Akad. Wet. **51**, 793 (1948).

² S.R. Elliott and M. Franz, Rev. Mod. Phys. **87**, 137 (2015).

³ J. von Neumann and E. Wigner, Phys. Z. **30**, 465 (1929).

⁴ F. Iemini, L. Mazza, D. Rossini, R. Fazio, and S. Diehl, Phys. Rev. Lett. **115**, 156402 (2015).

⁵ D. Roy, C. J. Bolech, and N. Shah, Phys. Rev. B **86**, 094503 (2012).

⁶ A.A. Zyuzin, D. Rainis, J. Klinovaja, and D. Loss, Phys. Rev. Lett. **111**, 056802 (2013).

- ⁷ E. Vernek, P.H. Penteado, A.C. Seridonio, and J.C. Egues, *Phys. Rev. B* **89**, 165314 (2014).
- ⁸ D.A.R.-Tijerina, E. Vernek, L.G.G.V. Dias da Silva, and J. C. Egues, *Phys. Rev. B* **91**, 115435 (2015).
- ⁹ F.H. Stillinger and D.R. Herrick, *Phys. Rev. A* **11**, 446 (1975).
- ¹⁰ F. Capasso, C. Sirtori, J. Faist, D.L. Sivco, S.-N.G. Chu, and A.Y. Cho, *Nature* **358**, 565 (1992).
- ¹¹ L.H. Guessi, Y. Marques, R.S. Machado, L.S. Ricco, K. Kristinsson, M.S. Figueira, I.A. Shelykh, M. de Souza, and A.C. Seridonio, *Phys. Rev. B* **92**, 245107 (2015).
- ¹² L.H. Guessi, R.S. Machado, Y. Marques, L.S. Ricco, K. Kristinsson, M. Yoshida, I.A. Shelykh, M. de Souza, and A.C. Seridonio, *Phys. Rev. B* **92**, 045409 (2015).
- ¹³ W.-J. Gong, X.-Y. Sui, Y. Wang, G.-D. Yu, and X.-H. Chen, *Nanoscale Research Letters* **8**, 330 (2013).
- ¹⁴ Y. Boretz, G. Ordonez, S. Tanaka, and T. Petrosky, *Phys. Rev. A* **90**, 023853 (2014).
- ¹⁵ A. Crespi, L. Sansoni, G.D. Valle, A. Ciamei, R. Ramponi, F. Sciarrino, P. Mataloni, S. Longhi, and R. Oselame, *Phys. Rev. Lett.* **114**, 090201 (2015).
- ¹⁶ C.W. Hsu, B. Zhen, J. Lee, S.-L. Chua, S.G. Johnson, J.D. Joannopoulos, and M. Soljačić, *Nature* **499**, 188 (2013).
- ¹⁷ Y. Plotnik, O. Peleg, F. Dreisow, M. Heinrich, S. Nolte, A. Szameit, and M. Segev, *Phys. Rev. Lett.* **107**, 183901 (2011).
- ¹⁸ J.M.-Petit and R.A. Molina, *Phys. Rev. B* **90**, 035434 (2014).
- ¹⁹ G.D. Valle and S. Longhi, *Phys. Rev. B* **89**, 115118 (2014).
- ²⁰ C. González-Santander, P.A. Orellana, and F. Domínguez-Adame, *Europhys. Lett.* **102**, 17012 (2013).
- ²¹ V. Mourik, K. Zuo, S.M. Frolov, S.R. Plissard, E.P.A.M. Bakkers, and L.P. Kouwenhoven, *Science* **336**, 1003 (2012).
- ²² S.N.-Perge, I.K. Drozdov, J. Li, H. Chen, S. Jeon, J. Seo, A.H. MacDonald, B.A. Bernevig, and A. Yazdani, *Science* **346**, 602 (2014).
- ²³ R. Pawlak, M. Kisiel, J. Klinovaja, T. Meier, S. Kawai, T. Glatzel, D. Loss, and E. Meyer, *arXiv:1505.06078v2* (2015).
- ²⁴ G. Moore, and N. Read, *Nucl. Phys.* **B360**, 362 (1991).
- ²⁵ L. Fu, C.L. Kane, and E.J. Mele, *Phys. Rev. Lett.* **98**, 106803 (2007).
- ²⁶ L. Fu and C.L. Kane, *Phys. Rev. Lett.* **100**, 096407 (2008).
- ²⁷ J.D. Sau, R.M. Lutchyn, S. Tewari, and S. Das Sarma, *Phys. Rev. Lett.* **104**, 040502 (2010).
- ²⁸ T.Kawakami and X. Hu, *Phys. Rev. Lett.* **115**, 177001 (2015).
- ²⁹ U. Fano, *Phys. Rev.* **124**, 1866 (1961).
- ³⁰ A.E. Miroshnichenko, S. Flach, and Y.S. Kivshar, *Rev. Mod. Phys.* **82**, 2257 (2010).
- ³¹ H. Haug and A.P. Jauho, *Quantum Kinetics in Transport and Optics of Semiconductors*, Springer Series in Solid-State Sciences 123 (Springer, New York, 1996).
- ³² D.E. Liu and H.U. Baranger, *Phys. Rev. B* **84**, 201308(R) (2011).
- ³³ P.W. Anderson, *Phys. Rev.* **124**, 41 (1961).

Chapter 5

Tuning of heat and charge transport by Majorana fermions

L. S. Ricco, F. A. Dessotti, I. A. Shelykh, M. S. Figueira and A. C. Seridonio, [Sci. Reports, 8, 2790](#). Published February 12, 2018.

5.1 Overview and remarks

As already discussed in previous chapters, setups based on the Majorana exotic physics have been keeping the status of next generation of technological nanodevices within electronic transport and quantum computing fields.

By considering this prolific scenario, we have proposed a device composed by a topological U-shaped Kitaev wire, hosting Majorana fermions (MFs) at their edges, which are coupled to a quantum dot via $(\Delta - t)$ and $(\Delta + t)$ strengths. The main idea was to analyse theoretically how the electronic and heat transport are affected by the presence of the Majoranas [1–4]. In this sense, we have found that, for MFs wave functions weakly overlapped (finite U-shaped wire), slight deviations from the superconducting-metallic boundary phase ($t = \Delta$) lead to the displacement of resonance positions in the electrical and thermal conductances simulations. Such a distinct behavior characterizes the capacity of tuning heat and electricity across the quantum dot. This feature is also revealed in the relevant thermoelectric quantities [5], as the thermopower (Seebeck coefficient) and figure of merit, as well as the periodic violation of the Wiedemann-Franz law. The intriguing heat/charge tunability observed in the device comes from the exotic Majorana ability of building a non-local fermion state. Such a delocalized quasiparticle is responsible for the transport in the system when the asymmetric coupling regime ($t \neq \Delta$) is taken into account. More details can be found in the paper at sec. 5.3.

It is worth mentioning that such a work was highlighted by the Fapesp Agency website ([Nanodispositivo termoelétrico é baseado em férmions de Majorana](#)) and by the Brazilian Physical Society ([Sintonizador termoelétrico assistido por férmions de Majorana](#)). Moreover, the paper was ranked in the list of the Top 100 most highly accessed physics articles in 2018, according to [nature.com web analytics](#).

5.2 Methodology

At first, we have employed the same approach used in the previous chapters, *i.e.*, the EOM technique to find the spectral Green's functions of the system, in order to obtain the transmittance through the quantum dot. Particularly, the Green's function of the dot can be obtained by following the steps of Appendix B, by considering the spinless case within the non-interacting picture ($U = 0$).

The procedure described above enabled us to calculate the thermoelectric coefficients \mathcal{L}_n [1, 2], which depends upon the transmittance according to the Eq.(2) of the paper. The electrical and thermal conductances, as well as the thermopower, Wiedemann-Franz law and figure of merit were obtained from relations with \mathcal{L}_n .

Bibliography

- [1] J. P. R. -Andrade, O. Á.- Ovando, P. A. Orellana, S. E. Ulloa, Phys. Rev. B **94**, 155436 (2016).
- [2] R. López, M. Lee, L. Serra, and J. S. Lim, Phys. Rev. B **89**, 205418 (2014).
- [3] M. Leijnse, New J. Phys. **16**, 015029 (2014).
- [4] S. Valentini, R. Fazio, V. Giovannetti, and F. Taddei, Phys. Rev. B **91**, 045430 (2015).
- [5] Y. Dubi and M. Di Ventra, Rev. Mod. Phys. **83**, 131 (2011).

5.3 Published Paper

Tuning of heat and charge transport by Majorana fermions

L. S. Ricco¹, F. A. Dessotti¹, I. A. Shelykh^{2,3}, M. S. Figueira⁴, and A. C. Seridonio^{1,5*}

¹*Departamento de Física e Química, Unesp - Univ Estadual Paulista, 15385-000, Ilha Solteira, SP, Brazil*

²*Science Institute, University of Iceland, Dunhagi-3, IS-107, Reykjavik, Iceland*

³*ITMO University, St. Petersburg 197101, Russia*

⁴*Instituto de Física, Universidade Federal Fluminense, 24210-340, Niterói, RJ, Brazil*

⁵*IGCE, Unesp - Univ Estadual Paulista, Departamento de Física, 13506-900, Rio Claro, SP, Brazil*

We investigate theoretically thermal and electrical conductances for the system consisting of a quantum dot (QD) connected both to a pair of Majorana fermions residing the edges of a Kitaev wire and two metallic leads. We demonstrate that both quantities reveal pronounced resonances, whose positions can be controlled by tuning of an asymmetry of the couplings of the QD and a pair of MFs. Similar behavior is revealed for the thermopower, Wiedemann-Franz law and dimensionless thermoelectric figure of merit. The considered geometry can thus be used as a tuner of heat and charge transport assisted by MFs.

* correspondent author: seridonio@dfq.feis.unesp.br

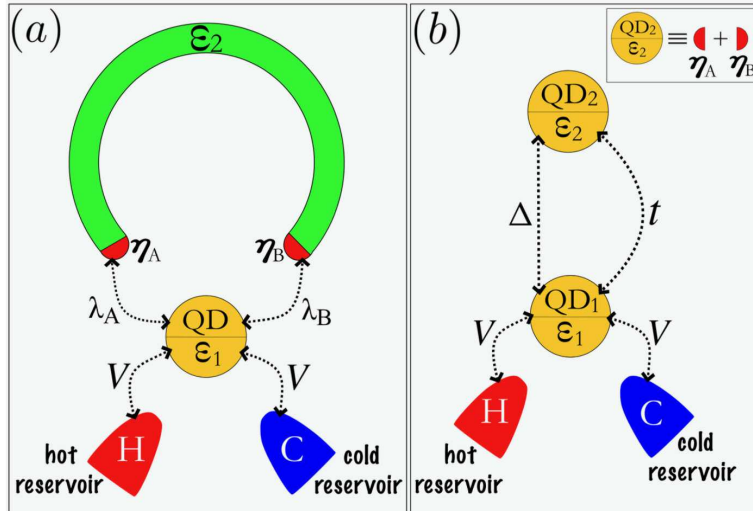


Figure 1. (a) The sketch of the geometry we consider. Topological U-shaped Kitaev wire with a pair of MFs η_A and η_B is placed in contact with a QD, which is connected as well to two metallic reservoirs. The coupling of the QD to the MFs is asymmetric and is characterized by tunneling matrix elements λ_A and λ_B , while coupling to the metallic leads is symmetric and is characterized by the tunneling matrix element V . ε_2 denotes the coupling between two MF states. (b) Equivalent auxiliary setup (Kitaev dimer) resulting from the mapping of the original system onto the system with nonlocal fermion residing in QD₂. t is tunneling matrix element between the QDs 1 and 2, Δ is the binding energy of the Cooper pair delocalized between them.

INTRODUCTION

Majorana fermions (MFs) are particles that are equivalent to their antiparticles. The corresponding concept was first proposed in the domain of high-energy physics, but later on existence of the elementary excitations of this type was predicted for certain condensed matter systems. Particularly, MFs emerge as quasiparticle excitations characterized by zero-energy modes[1, 2] appearing at the edges of the 1D Kitaev wire[3–7]. Kitaev model is used to describe the emerging phenomena of p -wave and spinless topological superconductivity.

Kitaev topological phase can be experimentally achieved in the geometry consisting of a semiconducting nanowire with spin-orbit interaction put in contact with s -wave superconducting material and placed in external magnetic field[8, 9]. Other condensed matter systems were also proposed as candidates for the observation of MFs. They include ferromagnetic chains placed on top of superconductors with spin-orbit interaction[10, 11], fractional quantum Hall state with filling factor $\nu = 5/2$ [12], three-dimensional topological insulators[13] and superconducting vortices[14–16].

MFs residing at the opposite edges of a Kitaev wire are elements of a robust nonlocal *qubit* which appears to be immune to the environment decoherence. This attracted the interest of the researchers working in the domain of quantum information and transport, as systems with MFs [17–19] can be in principle used as building blocks for the next generation of nanodevices, [20, 21] including current switches [20] and quantum memory elements[21]. At the same time, similar systems were proposed as thermoelectric nanodevices [22–25].

In this work, following the proposals of thermoelectric detection of MF states [22–25], we explore theoretically zero-bias thermal and electrical transport through one particular geometry consisting of an individual QD coupled both to a pair of MFs and metallic leads as shown in the Fig.1(a). The MFs reside at the edges of a topological U-shaped Kitaev wire, similar to the case of Ref.[19]. The QD coupling to the MFs is considered to be asymmetric, while coupling to the metallic leads is symmetric, and MFs are supposed to overlap with each other. The results of our calculations clearly show that thermoelectric conductance, thermopower, Wiedemann-Franz law[26] and dimensionless thermoelectric figure of merit (ZT) as function of the QD electron energy demonstrate resonant behavior. Moreover, the position of the resonance can be tuned by changing the coupling amplitudes between the QD and the MFs, which allows the system to operate as a tuner of heat and charge assisted by MFs.

MODEL

For theoretical treatment of the setup depicted in the Fig. 1(a), we use the Hamiltonian proposed by Liu and Baranger[27]:

$$\mathcal{H} = \sum_{\alpha k} \varepsilon_k c_{\alpha k}^\dagger c_{\alpha k} + \varepsilon_1 d_1^\dagger d_1 + V \sum_{\alpha k} (c_{\alpha k}^\dagger d_1 + \text{H.c.}) + \lambda_A (d_1 - d_1^\dagger) \eta_A + \lambda_B (d_1 + d_1^\dagger) \eta_B + i\varepsilon_2 \eta_A \eta_B, \quad (1)$$

where the electrons in the leads $\alpha = H, C$ (for hot and cold reservoirs, respectively) are described by the operators $c_{\alpha k}^\dagger$ ($c_{\alpha k}$) for the creation (annihilation) of an electron in a quantum state labeled by the wave number k and energy ε_k . For the QD d_1^\dagger (d_1) creates (annihilates) an electron in the state with the energy ε_1 . The energies of both electrons in the leads and QD are counted from the chemical potential μ (we consider only the limit of small source-drain bias, thus assuming that chemical potential is the same everywhere). V stands for the hybridization between the QD and the leads. The asymmetric coupling between the QD and MFs at the edges of the topological U-shaped Kitaev wire is described by the complex tunneling amplitudes λ_A and λ_B . Introduction of an asymmetry in the couplings can account for the presence of the magnetic flux which can be introduced via Peierls phase shift [27]. ε_2 stands for the overlap between the MFs.

Without the loss of generality, we can put: $\lambda_A = \frac{(t+\Delta)}{\sqrt{2}}$ and $\lambda_B = i\frac{(\Delta-t)}{\sqrt{2}}$, respectively for the left ($\eta_A = \eta_A^\dagger$) and right ($\eta_B = \eta_B^\dagger$) MFs, and introduce an auxiliary nonlocal fermion $d_2 = \frac{1}{\sqrt{2}}(\eta_A + i\eta_B)$ [20, 21]. The expressions for $\lambda_A = |\lambda_A|e^{i\phi_A}$ and $\lambda_B = |\lambda_B|e^{i\phi_B}$ constitute a convenient gauge for our problem. We put $\phi_A = 0$ and $\phi_B = (n + \frac{1}{2})\pi$ with integer $n = 0, 1, 2, \dots$ corresponding to the total flux through the ring of Fig. 1. This parameter is experimentally tunable by changing the external magnetic field. This fact gives certain advantages to our proposal with respect to the previous works with asymmetric couplings between a single QD and a pair of MFs at the ends of a topological Kitaev wire[28–31]. According to Ref.[32] the parameter ε_2 describing the overlap between the MFs depends on magnetic field in an oscillatory manner, the amplitudes $|\lambda_A| = \frac{t+\Delta}{\sqrt{2}}$ and $|\lambda_B| = \frac{|\Delta-t|}{\sqrt{2}}$ demonstrate the same behavior (see Sec.III-A of Ref.[30]) and thus external magnetic field affects not only the relative phase between λ_A and λ_B but their absolute values as well. To fulfill the condition $|\lambda_B| < |\lambda_A|$ one should place the QD closer the MF η_A than to the MF η_B .

We map the original Hamiltonian into one where the electronic states d_1 and d_2 are connected via normal tunneling t and bounded as delocalized Cooper pair, with binding energy Δ :

$$\mathcal{H} = \sum_{\alpha k} \varepsilon_k c_{\alpha k}^\dagger c_{\alpha k} + V \sum_{\alpha k} (c_{\alpha k}^\dagger d_1 + \text{H.c.}) + \varepsilon_1 d_1^\dagger d_1 + \varepsilon_2 d_2^\dagger d_2 + (td_1 d_2^\dagger + \Delta d_2^\dagger d_1^\dagger + \text{H.c.}) - \frac{\varepsilon_2}{2}. \quad (2)$$

This expression represents a shortened version of the microscopic model for the Kitaev wire corresponding to the Kitaev dimer (see Fig.1(b)). As it was shown in the Refs.[33] and [34] this model allows clear distinguishing between topologically trivial and Majorana-induced zero-bias peak in the conductance.

In what follows, we use the Landauer-Büttiker formula for the zero-bias thermoelectric quantities \mathcal{L}_n [22, 23]:

$$\mathcal{L}_n = \frac{1}{h} \int d\varepsilon \left(-\frac{\partial f_F}{\partial \varepsilon} \right) \varepsilon^n \mathcal{T}, \quad (3)$$

where h is Planck's constant, $\Gamma = 2\pi V^2 \sum_k \delta(\varepsilon - \varepsilon_k)$ is Anderson broadening[35] and f_F stands for Fermi-Dirac distribution. The quantity

$$\mathcal{T} = -\Gamma \text{Im}(\tilde{\mathcal{G}}_{d_1 d_1}) \quad (4)$$

is electronic transmittance through the QD, with $\tilde{\mathcal{G}}_{d_1 d_1}$ being retarded Green's function for the QD in the energy domain ε , obtained from the Fourier transform $\tilde{\mathcal{G}}_{AB} = \int d\tau \mathcal{G}_{AB} e^{\frac{i}{\hbar}(\varepsilon + i0^+)\tau}$, where

$$\mathcal{G}_{AB} = -\frac{i}{\hbar} \theta(\tau) \text{Tr}\{\varrho[\mathcal{A}(\tau), \mathcal{B}^\dagger(0)]_+\} \quad (5)$$

corresponds to the Green's function in time domain τ , expressed in terms of the Heaviside function $\theta(\tau)$ and thermal density matrix ϱ for Eq. (1).

Experimentally measurable thermoelectric coefficients can be expressed via $\mathcal{L}_0, \mathcal{L}_1$ and \mathcal{L}_2 as:

$$G = e^2 \mathcal{L}_0, \quad (6)$$

$$K = \frac{1}{T}(\mathcal{L}_2 - \frac{\mathcal{L}_1^2}{\mathcal{L}_0}) \quad (7)$$

and

$$S = -(\frac{1}{eT})\frac{\mathcal{L}_1}{\mathcal{L}_0} \quad (8)$$

for the electrical and thermal conductances and thermopower, respectively (T denotes a temperature of the system). We also investigate the violation of Wiedemann-Franz law, given by

$$WF = \frac{1}{T}(\frac{K}{G}), \quad (9)$$

in units of Lorenz number $L_0 = (\pi^2/3)(k_B/e)^2$ and corresponding behavior of the dimensionless figure of merit [22, 23]

$$ZT = \frac{S^2 GT}{K}. \quad (10)$$

For Eq. (4), we use equation-of-motion (EOM) method[36] summarized as follows:

$$(\varepsilon + i0^+)\tilde{\mathcal{G}}_{\mathcal{A}\mathcal{B}} = [\mathcal{A}, \mathcal{B}^\dagger]_+ + \tilde{\mathcal{G}}_{[\mathcal{A}, \mathcal{H}]\mathcal{B}}, \quad (11)$$

with $\mathcal{A} = \mathcal{B} = d_1$.

As our Hamiltonian given by Eqs. (1) and (2) is quadratic, the set of the EOM for the single particle Green's functions can be closed without any truncation procedure [37]. We find the following four coupled linear algebraic equations:

$$(\varepsilon - \varepsilon_1 - \Sigma)\tilde{\mathcal{G}}_{d_1 d_1} = 1 - t\tilde{\mathcal{G}}_{d_2 d_1} - \Delta\tilde{\mathcal{G}}_{d_1^\dagger d_1}, \quad (12)$$

where $\Sigma = -i\Gamma$ is the self-energy of the coupling with the metallic leads

$$\tilde{\mathcal{G}}_{d_2 d_1} = +\frac{\Delta\tilde{\mathcal{G}}_{d_1^\dagger d_1}}{(\varepsilon - \varepsilon_2 + i0^+)} - \frac{t\tilde{\mathcal{G}}_{d_1 d_1}}{(\varepsilon - \varepsilon_2 + i0^+)}, \quad (13)$$

$$\tilde{\mathcal{G}}_{d_1^\dagger d_1} = -\frac{\Delta\tilde{\mathcal{G}}_{d_1 d_1}}{(\varepsilon + \varepsilon_2 + i0^+)} + \frac{t\tilde{\mathcal{G}}_{d_1^\dagger d_1}}{(\varepsilon + \varepsilon_2 + i0^+)} \quad (14)$$

and

$$\tilde{\mathcal{G}}_{d_1^\dagger d_1} = -2t\Delta\tilde{K}\tilde{\mathcal{G}}_{d_1 d_1}, \quad (15)$$

with

$$\tilde{K} = \frac{K_{\text{MFS}}}{\varepsilon + \varepsilon_1 - \Sigma - K_-}, \quad (16)$$

$$K_{\text{MFS}} = \frac{(\varepsilon + i0^+)}{[\varepsilon^2 - \varepsilon_2^2 + 2i\varepsilon 0^+ - (0^+)^2]} \quad (17)$$

and

$$K_{\pm} = \frac{(\varepsilon + i0^+)(t^2 + \Delta^2) \pm \varepsilon_2(t^2 - \Delta^2)}{[\varepsilon^2 - \varepsilon_2^2 + 2i\varepsilon 0^+ - (0^+)^2]}. \quad (18)$$

This gives the Green's function of the QD:

$$\tilde{\mathcal{G}}_{d_1 d_1} = \frac{1}{\varepsilon - \varepsilon_1 - \Sigma - \Sigma_{\text{MFS}}}, \quad (19)$$

where the part of self-energy

$$\Sigma_{\text{MFS}} = K_+ + (2t\Delta)^2\tilde{K}K_{\text{MFS}} \quad (20)$$

describes the hybridization between MFs and QD.

Importantly, for the low temperatures regime, the substitution of Eq. (19) into Eq. (3) and its decomposition into Sommerfeld series [23, 26] allows to get analytical expressions for thermoelectric coefficients:

$$\frac{G}{G_0} = \frac{K}{G_0 L_0 T} \approx \mathcal{T}|_{\varepsilon=0}, \quad (21)$$

$$S \approx e L_0 T \left. \frac{1}{\mathcal{T}} \frac{d\mathcal{T}}{d\varepsilon} \right|_{\varepsilon=0}, \quad (22)$$

where

$$\mathcal{T} = \frac{\tilde{\Gamma}^2}{[\varepsilon - \varepsilon_1 - K_+ - \frac{(2t\Delta K_{\text{MFs}})^2(\varepsilon + \varepsilon_1 - K_-)}{(\varepsilon + \varepsilon_1 - K_-)^2 + \Gamma^2}]^2 + \tilde{\Gamma}^2}, \quad (23)$$

with

$$\tilde{\Gamma} = [1 + \frac{(2t\Delta K_{\text{MFs}})^2}{(\varepsilon + \varepsilon_1 - K_-)^2 + \Gamma^2}] \Gamma. \quad (24)$$

Comparison of the Eqs. (21) and (22) allows us to conclude that the peak values of the electric conductance are reached when $S = 0$ for which $d\mathcal{T}/d\varepsilon = 0$ which happens when

$$\varepsilon_1 = \frac{(t^2 - \Delta^2)}{\varepsilon_2}. \quad (25)$$

As we will see below, fulfillment of this condition corresponds to the presence of an electron-hole symmetry in the system. Note that as ε_2 enters in the denominator of the Eq. (25), even slight differences between t and Δ will be enough to change drastically the position of the resonance if hybridization between the MFs is small.

RESULTS AND DISCUSSION

In our further calculations, we scale the energy in units of the Anderson broadening $\Gamma = 2\pi V^2 \sum_k \delta(\varepsilon - \varepsilon_k)$ [35] and take the temperature of the system $k_B T = 10^{-4} \Gamma$. The Anderson broadening Γ defines the coupling between the QD and the metallic leads, which is assumed to be symmetrical for a sake of simplicity.

We start our analysis from the case when only a single MF (η_A) is coupled to the QD. In terms of the amplitudes t, Δ this corresponds to $t = \Delta$. To be specific, we fix $t = \Delta = 4\Gamma$. Looking at Eq. (2), we see that the terms $d_1 d_2^\dagger + \text{H.c.}$ and $d_2^\dagger d_1 + \text{H.c.}$ enter into Hamiltonian with equal weights, and thus we are in the superconducting (SC)-metallic boundary phase.

Fig. 2(a) shows the electrical conductance $G = e^2 \mathcal{L}_0$ scaled in units of the conductance quantum $G_0 = e^2/h$ as a function of the QD energy level ε_1 , for several coupling amplitudes ε_2 between the MFs. Note that, if MFs are completely isolated from each other ($\varepsilon_2 = 0$), the conductance reveals a plateau with $G = G_0/2$ whatever the value of ε_1 (black line), and similar trend is observed in the thermal conductance shown in the Fig. 2(b). The effect is due to the leaking of the Majorana fermion state into the QD [38]. The MF zero-mode becomes pinned at the Fermi level of the metallic leads, but within the QD electronic-structure. With increase of the coupling between the wire and the QD, the MF state of the Kitaev wire leaks into the QD. As a result, a peak at the Fermi energy emerges in the QD density of states (DOS), while in the DOS corresponding to the edge of the wire the corresponding peak becomes gradually suppressed. Consequently, the QD effectively becomes the new edge of the Kitaev wire. This scenario was reported experimentally in the Ref. [9].

To get resonant response of the thermoelectric conductances one should consider the case $\varepsilon_2 \neq 0$, corresponding to the splitting of the MF zero-bias peak. The resonant behavior of G and K can be understood as arising from the presence of an auxiliary fermion d_2 , in the Hamiltonian [Eq. (2)], whose energy ε_2 is now detuned from the Fermi level (see inset of Fig. 2(b)). In this case, the regular fermion state instead of the corresponding half-fermion provided by MF η_A gives the main contribution to the charge and heat current. In this scenario, filtering of the electricity and heat emerges: the maximal transmission occurs at $\varepsilon_1 = 0$. Our Figs. 2(a) and (b) recover the findings of Fig. 5(a) in Ref. [23]. Our work, however, have an important novel dimension: we demonstrate that even small deviations of the system from the SC-metallic boundary phase which can be achieved by the control of the asymmetry of the couplings

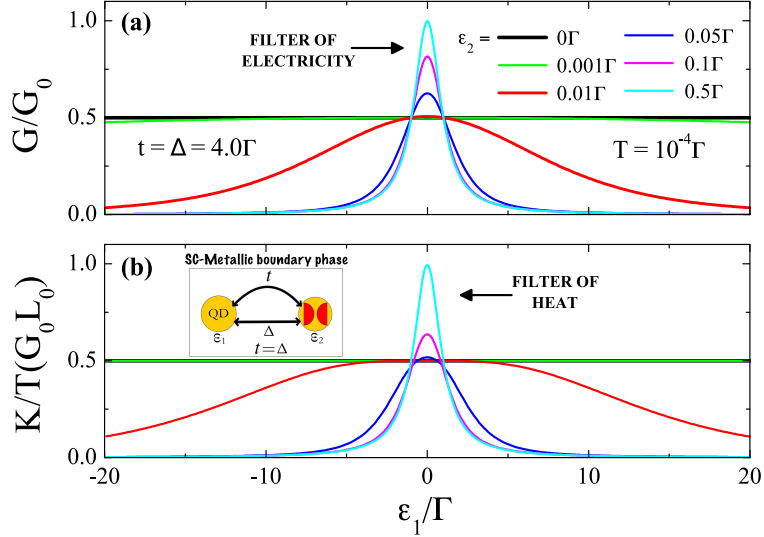


Figure 2. Electrical and thermal conductances of the system corresponding to SC-metallic boundary phase, $t = \Delta = 4\Gamma$: (a) Electrical conductance as function of the QD energy level ε_1 for several ε_2 values of the couplings between MFs. (b) Corresponding thermal conductance. For both cases the resonance at the Fermi energy $\varepsilon_1 = 0$ occurs if $\varepsilon_2 \neq 0$. For $\varepsilon_2 = 0$ the conductance plateau is observed (see main text for the corresponding discussion). The inset shows the equivalent circuit with an auxiliary fermion d_2 constructed from MFs η_A and η_B (red half-circles).

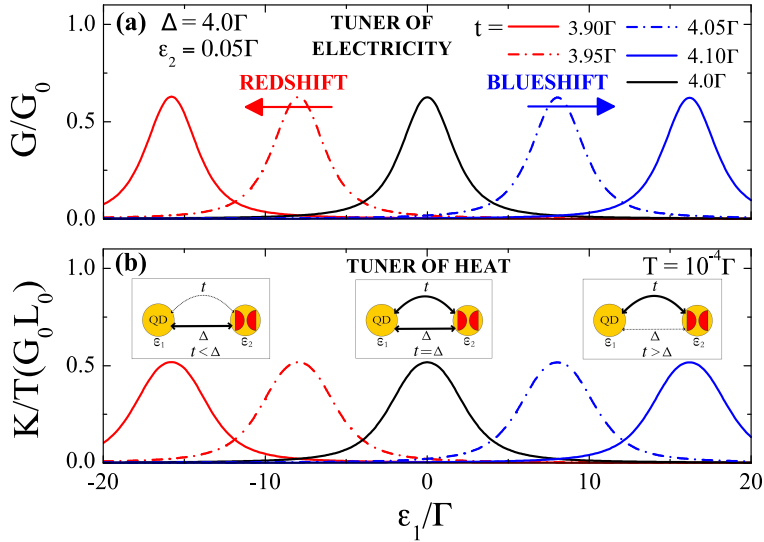


Figure 3. Electrical and thermal conductances as functions of the QD energy level outside SC-metallic boundary phase. Slight deviations from the condition $t = \Delta$, result in the shift of the resonance peak for the electrical (panel (a)) and thermal (panel (b)) conductances. The corresponding resonances are blueshifted for $t > \Delta$ and redshifted for $t < \Delta$ as compared to the case of the SC-metallic boundary phase. Insets show the equivalent circuit with auxiliary fermion d_2 constructed from MFs η_A and η_B (red half-circles).

allows realization of the efficient tuners of electricity and heat. This effect is shown in the Figs. 3(a) and (b). As one can see, even small detuning of the coefficient t from the value $t = \Delta$ leads to substantial blueshift (for the case $t > \Delta$) or redshift (for the case $t < \Delta$) of the conductance resonances. Such sensitivity is a direct consequence of the Eq. (25) defining the position of the resonances.

To shed more light on the effect of the tuning of charge and heat transport in the system, we make a plot of the quantity $\mathcal{T} = -\Gamma \text{Im}(\hat{G}_{d_1 d_1})$ appearing in the Eq. (3) and Eq. (4), as function of ε_1 and ε , see Figs. 4(a)-(d). Fig. 4(a) corresponds to the case $t = \Delta$, $\varepsilon_2 = 0$. One can recognize a ‘‘cat eye’’-shaped central structure, corresponding to the

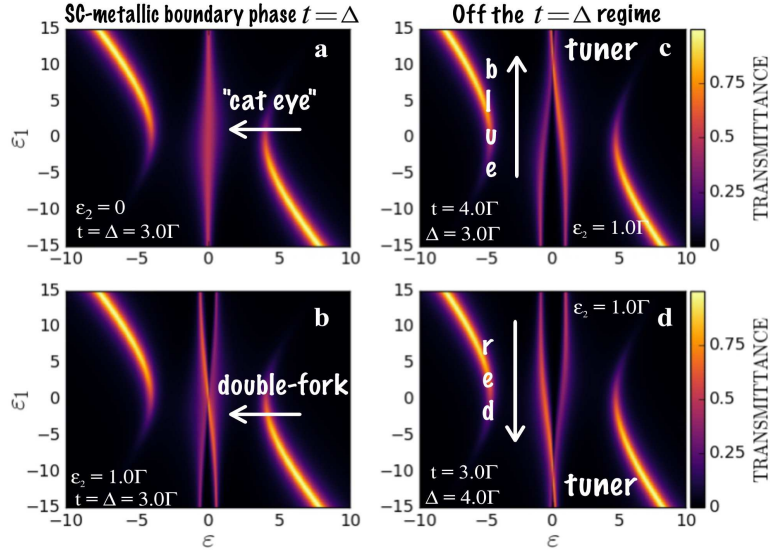


Figure 4. Transmittance \mathcal{T} spanned by the axes of ε_1 and ε . Panels (a) and (b) show the regime corresponding to SC-metallic boundary phase with $t = \Delta$, for $\varepsilon_2 = 0$ and finite ε_2 , respectively. Panel (a) reveals characteristic “cat eye”-shaped central structure at the Fermi level responsible for the onset of the conductance plateau. Panel (b) exhibits a double-fork structure responsible for the resonant character of the conductance for $\varepsilon_2 \neq 0$. Introduction of the asymmetry of the QD to MFs coupling leads to the vertical shift of the double-fork feature resulting in the blueshift (panel (c)) or redshift (panel (d)) of the resonant conductance curve. The bright arcs visualized in all panels represent poles of the Green’s function of the QD.

vertical line at $\varepsilon = 0$. Everywhere along this line $\mathcal{T} = \text{constant}$, which according to the Eq. (21) means that changes in ε_1 do not affect the conductance. This corresponds well to the conductance plateau in the Fig. 2. If ε_2 is finite, the “cat eye” structure transforms into a double-fork profile as it is shown in the Fig.4(b). Note that in this case, movement along the vertical line corresponding to $\varepsilon = 0$ lead to the change of the function \mathcal{T} , which according to the Eq. (21) leads to the modulation of the conductance. The maximal value is achieved at the point $\varepsilon_1 = 0$, which corresponds well to the resonant character of the curves shown in the Fig.2. The introduction of the finite value of ε_2 and the asymmetry of the coupling between the QD and MFs ($t \neq \Delta$) leads to the shifts of the double-fork structure either upwards by ε_1 scale for $t > \Delta$ (panel (c), blueshift of the resonant curves in the Fig.3) or downwards by ε_1 scale for $t < \Delta$ (panel (d), redshift of the resonant curves in the Fig.3). It should be noted that similar results to the transmittance were reported both theoretically (Ref.[30]) and experimentally (Ref.[31]) for the geometry of a linear Kitaev wire with a QD attached to one of its ends placed between source and drain metallic leads. Differently from the case considered in our work, the authors account for the spin degree of freedom and particularly for Ref.[31], they evaluate the dependence of the conductance on the energy level of the QD and magnetic field, while we further analyze ε and asymmetry of couplings dependencies relevant for the understanding of the tuner regime. Despite the distinct geometry and spinless regime, our results and those reported in Refs.[30,31] are in good correspondence with each other, thus validating the mechanism pointed out in Refs.[30,32] of field-assisted overlapping between MFs and tunnel-couplings with the QD.

The possibility to tune electric and thermal conductances opens a way for tuning the thermopower (S), Wiedemann-Franz law (WF) and dimensionless figure of merit (ZT) as it is shown in the Figs.5(a)-(c). In the Fig.5(a) the dependence of the thermopower on ε_1 is demonstrated. If $t > \Delta$, at $\varepsilon_1 = 0$, $S > 0$ and the setup behaves as a tuner of holes. On the contrary, for $t < \Delta$, at $\varepsilon_1 = 0$, $S < 0$ and the setup behaves as a tuner of electrons. Figs.5(b) and (c) illustrate the violation of WF law and the behavior of the dimensionless thermoelectric ZT , respectively. Note that ZT does not reach pronounced amplitudes, i.e. $ZT < 1$ [26], even for finite values of G and K as dependence on S^2 prevails if we take into account Eq. (21) into Eq. (10).

CONCLUSIONS

In summary, we considered theoretically thermoelectric conductances for the device consisting of an individual QD coupled to both pair of MFs and metallic leads. The charge and heat conductances of this system as functions of an electron energy in the QD reveal resonant character. The position of the resonance can be tuned by changing the

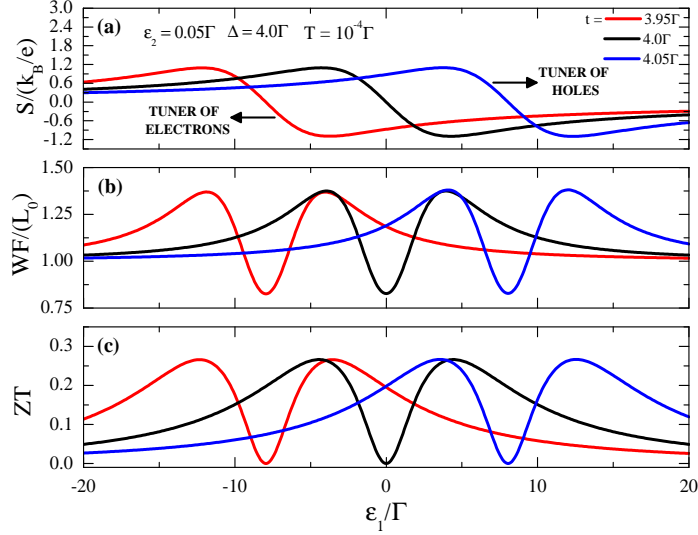


Figure 5. (a) Thermopower (S), (b) Wiedemann-Franz law (WF) and (c) the figure of merit (ZT) as function of the QD energy level ε_1 for several ε_2 values of the couplings between MFs. Deviation from the condition $t = \Delta$ leads to the shift of the curves.

degree of asymmetry between the QD and the MFs, which allows us to propose the scheme of the tuner of heat and charge. Thermopower, Wiedemann-Franz law and the figure of merit are found to be sensitive to the asymmetry of the coupling as well. Our findings will pave way for the development of thermoelectric nanodevices based on MFs.

ACKNOWLEDGEMENTS

This work was supported by the Brazilian funding agencies CNPq Grant No. 307573/2015-0, CAPES and São Paulo Research Foundation (FAPESP) Grant No. 2015/23539-8. I.A.S. acknowledges support from Horizon2020 RISE project CoExAN and the project No. 3.8884.2017/8.9 of the Ministry of Education and Science of the Russian Federation.

AUTHOR CONTRIBUTIONS

A.C.S., M.S.F. and I.A.S formulated the problem and wrote the manuscript. L.S.R and A.C.S. derived the expressions and M.S.F. performed their numerical computing. F.A.D. and L.S.R. plotted the figures. All co-authors taken part in the discussions and reviewed the manuscript as well.

Competing financial interests: The authors declare no competing financial interests.

-
- [1] J. Alicea, Rep. Prog. Phys. **75**, 076501 (2012).
 - [2] S. R. Elliott and M. Franz, Rev. Mod. Phys. **87**, 137 (2015).
 - [3] A. Y. Kitaev, Phys. Usp. **44**, 131 (2001).
 - [4] A. A. Zyuzin, D. Rainis, J. Klinovaja, and D. Loss, Phys. Rev. Lett. **111**, 056802 (2013).
 - [5] D. Rainis, J. Klinovaja, L. Trifunovic, and D. Loss, Phys. Rev. B **87**, 024515 (2013).
 - [6] A. Zazunov, P. Sodano, and R. Egger, New J. Phys **15**, 035033 (2013).
 - [7] D. Roy, C. J. Bolech, and N. Shah, Phys. Rev. B **86**, 094503 (2012).
 - [8] V. Mourik, K. Zuo, S. M. Frolov, S. R. Plissard, E. P. A. M. Bakkers, and L. P. Kouwenhoven, Science **336**, 1003 (2012).
 - [9] M. T. Deng, S. Vaitiekenas, E. B. Hansen, J. Danon, M. Leijnse, K. Flensberg, J. Nygard, P. Krogstrup, and C. M. Marcus, Science **354**, 6319 (2016).
 - [10] S. N.- Perge, I. K. Drozdov, J. Li, H. Chen, S. Jeon, J. Seo, A. H. MacDonald, B. A. Bernevig, and A. Yazdani, Science **346**, 602 (2014).

- [11] R. Pawlak, M. Kisiel, J. Klinovaja, T. Meier, S. Kawai, T. Glatzel, D. Loss, and E. Meyer, *Nature Partner Journals Quantum Information* **2**, 16035 (2016).
- [12] G. Moore and N. Read, *Nucl. Phys. B* **360**, 362 (1991).
- [13] L. Fu, C. L. Kane, and E. J. Mele, *Phys. Rev. Lett.* **98**, 106803 (2007).
- [14] L. Fu and C.L. Kane, *Phys. Rev. Lett.* **100**, 096407 (2008).
- [15] J. D. Sau, R. M. Lutchyn, S. Tewari, and S. Das Sarma, *Phys. Rev. Lett.* **104**, 040502 (2010).
- [16] T. Kawakami and X. Hu, *Phys. Rev. Lett.* **115**, 177001 (2015).
- [17] K. Flensberg, *Phys. Rev. Lett.* **106**, 090503 (2011).
- [18] M. Leijnse and K. Flensberg, *Phys. Rev. Lett.* **107**, 210502 (2011).
- [19] C.-K. Chiu, J. D. Sau, and S. Das Sarma, [arXiv:1709.04475](https://arxiv.org/abs/1709.04475) (2017).
- [20] F. A. Dessotti, L. S. Ricco, Y. Marques, L. H. Guessi, M. Yoshida, M. S. Figueira, M. de Souza, Pasquale Sodano, and A. C. Seridonio, *Phys. Rev. B* **94**, 125426 (2016).
- [21] L. S. Ricco, Y. Marques, F. A. Dessotti, R. S. Machado, M. de Souza, and A. C. Seridonio, *Phys. Rev. B* **93**, 165116 (2016).
- [22] J. P. R. -Andrade, O. A. -Ovando, P. A. Orellana, S. E. Ulloa, *Phys. Rev. B* **94**, 155436 (2016).
- [23] R. Lopez, M. Lee, L. Serra, and J. S. Lim, *Phys. Rev. B* **89**, 205418 (2014).
- [24] M. Leijnse, *New J. Phys.* **16**, 015029 (2014).
- [25] S. Valentini, R. Fazio, V. Giovannetti, and F. Taddei, *Phys. Rev. B* **91**, 045430 (2015).
- [26] Y. Dubi and M. Di Ventra, *Rev. Mod. Phys.* **83**, 131 (2011).
- [27] D. E. Liu and H. U. Baranger, *Phys. Rev. B* **84**, 201308(R) (2011).
- [28] D. J. Clarke, *Phys. Rev. B* **96**, 201109(R) (2017).
- [29] A. Schuray, L. Weithofer, and P. Recher, *Phys. Rev. B* **96**, 085417 (2017).
- [30] E. Prada, R. Aguado, and P. S.-Jose, *Phys. Rev. B* **96**, 085418 (2017).
- [31] M. T. Deng, S. Vaitiekenas, E. Prada, P. S.-Jose, J. Nygard, P. Krogstrup, R. Aguado, C. M. Marcus, [arXiv:1712.03536v1](https://arxiv.org/abs/1712.03536v1).
- [32] J. Danon, E. B. Hansen, and K. Flensberg, *Phys. Rev. B* **96**, 125420 (2017).
- [33] T. D. Stanescu and S. Tewari, *Phys. Rev. B* **89**, 220507(R) (2014).
- [34] D. Roy, N. Bondyopadhyaya, and S. Tewari, *Phys. Rev. B* **88**, 020502(R) (2013).
- [35] P. W. Anderson, *Phys. Rev.* **124**, 41 (1961).
- [36] H. Haug and A. P. Jauho, *Quantum Kinetics in Transport and Optics of Semiconductors*, Springer Series in Solid-State Sciences 123 (Springer, New York, 1996).
- [37] L. S. Ricco, Y. Marques, F. A. Dessotti, M. de Souza, and A. C. Seridonio, *Phys. E* **78**, 25 (2016).
- [38] E. Vernek, P. H. Penteado, A. C. Seridonio, and J.C. Egues, *Phys. Rev. B* **89**, 165314 (2014).

Chapter 6

Majorana oscillations modulated by Fano interference and degree of nonlocality in a topological superconducting nanowire-quantum dot system

L. S. Ricco, V. L. Campo Jr., I. A. Shelykh and A. C. Seridonio, Phys. Rev. B 98, 075142. Published August 28, 2018.

6.1 Overview and remarks

As already discussed in previous chapters, setups based on Majorana exotic physics have been keeping the status of next generation of quantum bits. As also briefly mentioned in Sec. 2, hybrid systems, composed by a quasi-one-dimensional nanowire with strong spin-orbit coupling, placed nearby s -wave superconductors, have been considered the most suitable platform to explore Majorana quasiparticles properties [1–4]. Under an applied magnetic field parallel to the intrinsic spin-orbit field, such a system enters into a p -wave superconducting topological phase, wherein a pair of zero-energy MBS emerges at the nanowire ends [4].

According to Liu and Baranger proposal [5], for a QD side-coupled to a Kitaev nanowire, the experimental signature of an isolated MBS is the emergence of a zero-bias peak (ZBP) with $e^2/2h$ amplitude in conductance profiles through the QD. Although the ZBP prediction already has been observed in a series of experiments [6–10], questionings whether such a peak emerges inside a truly topological phase still remains [11–14]. In this context, the ZBP splitting in conductance measurements, followed by an oscillatory pattern as a function of applied magnetic field, which are known as Majorana oscillations, have been looked upon as a smoking gun to claim the presence of MBSs and the transition to the topological phase [11, 15, 16].

Taking such a prolific scenario into account, we have investigated the influence of Fano interference process in the so-called Majorana oscillations in a hybrid T-shaped device, consisting of a quantum dot between metallic leads and side-coupled to a topological superconducting nanowire (TSNW) hosting Majorana bound states (MBSs) at opposite ends. As expected, we have observed a oscillatory pattern of

differential conductance as a function of external magnetic field, applied parallel to nanowire. However, both the amplitude and shape of such oscillations depend on the bias-voltage, Fano parameter of system and the so-called degree of Majorana nonlocality, which was previously discussed in sec. 2.4. We also have found the experimentally reported “bowtie” and “diamond” line shapes in differential conductance as a function of both bias-voltage and dot energy level [Ref.16 of published paper]. We believe that our findings can improve the comprehension of Majorana oscillations in hybrid nanowires and also can be used to estimate the degree of Majorana nonlocality and its topological properties. For more details, please see the paper below (sec. 6.3).

6.2 Methodology

We have employed the same approach used in previous chapters, i.e, the EOM technique (see Sec. 3.1), which allowed us to find the spectral Green’s function for the QD $G_{dd}^r(\omega)$ (see Appendix B, for spinless configuration, $U = 0$ and $\delta_M \equiv \varepsilon_M(l, B)$), in order to obtain the transmittance $\mathcal{T}(\omega)$. In linear response regime, the zero-bias conductance depends on transmittance as follows [18]:

$$\mathcal{G}(eV) = \frac{e^2}{h} \int \left(-\frac{\partial f_F(\omega, eV)}{\partial \omega} \right) \mathcal{T}(\omega) d\omega, \quad (6.1)$$

where e^2/h is the quantum of conductance and f_F is the Fermi-Dirac distribution function. For low temperature regime ($T \rightarrow 0$) [18],

$$\mathcal{G}(eV) \approx \frac{e^2}{h} \mathcal{T}(eV). \quad (6.2)$$

The pivotal difference between this work and those found in previous chapters is the overlap function between MBSs, given by [16]:

$$\varepsilon_M(l, B) = \frac{E_0}{\sqrt{b}} e^{-l/2b} \cos(l\sqrt{b}) \quad (6.3)$$

where, $b = B/E_0$, $l = \sqrt{2mE_0}L/\hbar$, with B being the Zeeman field applied longitudinally to the nanowire, L the wire length, $E_0 = (2m\alpha^2\Delta^2/\hbar^2)^{1/3}$, α the spin-orbit constant and Δ the superconducting gap induced in the wire [16]. We have adopt $E_0 \approx 0.23$ meV, the wire length $L = 1$ μm , and Anderson broadening $\Gamma \approx 0.17E_0$, which are in agreement with both experimental [6–8] and theoretical estimations [15, 17].

Bibliography

- [1] R. M. Lutchyn, J. D. Sau, and S. Das Sarma, Phys. Rev. Lett. **105**, 077001 (2010).
- [2] Y. Oreg, G. Refael, and F. von Oppen, Phys. Rev. Lett. **105**, 177002 (2010).
- [3] A. A. Zyuzin, D. Rainis, J. Klinovaja, and D. Loss, Phys. Rev. Lett. **111**, 056802 (2013).
- [4] A. Y. Kitaev, Physics-Uspekhi **44**, 131 (2001).
- [5] D. E. Liu and H. U. Baranger, Physical Review B **84**, 201308 (2011).
- [6] V. Mourik, K. Zuo, S. M. Frolov, S. Plissard, E. Bakkers, and L. Kouwenhoven, Science **336**, 1003 (2012).
- [7] S. M. Albrecht, A. Higginbotham, M. Madsen, F. Kuemmeth, T. S. Jespersen, J. Nygård, P. Krogstrup, and C. Marcus, Nature **531**, 206 (2016).
- [8] M. T. Deng, S. Vaitiekenas, E. B. Hansen, J. Danon, M. Leijnse, K. Flensberg, J. Nygård, P. Krogstrup, and C. M. Marcus, Science **354**, 1557 (2016).
- [9] H. Zhang, Ö. Gül, S. Conesa-Boj, K. Zuo, V. Mourik, F. K. de Vries, J. van Veen, D. J. van Woerkom, M. P. Nowak, M. Wimmer, D. Car, S. Plissard, E. P. A. M. Bakkers, M. Quintero-Pérez, S. Goswami, K. Watanabe, T. Taniguchi, and L. P. Kouwenhoven, ArXiv e-prints (2016), **arXiv:1603.04069** [cond-mat.mes-hall].
- [10] P. Krogstrup, N. L. B. Ziino, W. Chang, S. M. Albrecht, M. H. Madsen, E. Johnson, J. Nygård, C. M. Marcus, and T. S. Jespersen, Nat.Mater. **14**, 1476 (2015).
- [11] D. Rainis, L. Trifunovic, J. Klinovaja, and D. Loss, Phys. Rev. B **87**, 024515 (2013).
- [12] J. Liu, A. C. Potter, K. T. Law, and P. A. Lee, Phys. Rev. Lett. **109**, 267002 (2012).
- [13] R. V. Mishmash, D. Aasen, A. P. Higginbotham, and J. Alicea, Phys. Rev. B **93**, 245404 (2016).
- [14] C.-X. Liu, J. D. Sau, T. D. Stanescu, and S. Das Sarma, Phys. Rev. B **96**, 075161 (2017)
- [15] S. Das Sarma, J. D. Sau, and T. D. Stanescu, Phys. Rev. B **86**, 220506 (2012).
- [16] J. Danon, E. B. Hansen, and K. Flensberg, Phys. Rev. B **96**, 125420 (2017).
- [17] E. Vernek, P. H. Penteado, A. C. Seridonio, and J. C. Egues, Phys. Rev. B **89**, 165314 (2014).
- [18] J. A.-P. Hartmut Haug, *Quantum Kinetics in Transport and Optics of Semiconductors*, Vol. 123 (Springer-Verlag Berlin Heidelberg, 2008).

6.3 Published paper

Majorana oscillations modulated by Fano interference and degree of non-locality in a topological superconducting nanowire-quantum dot system

L. S. Ricco,¹ V. L. Campo Jr.,² I. A. Shelykh,^{3,4} and A. C. Seridonio^{1,5,*}

¹*Departamento de Física e Química, Unesp - Univ Estadual Paulista, 15385-000, Ilha Solteira, São Paulo, Brazil*

²*Departamento de Física, Universidade Federal de São Carlos, Rodovia Washington Luiz, km 235, Caixa Postal 676, 13565-905, São Carlos, São Paulo, Brazil*

³*Science Institute, University of Iceland, Dunhagi-3, IS-107, Reykjavik, Iceland*

⁴*ITMO University, St. Petersburg 197101, Russia*

⁵*Instituto de Geociências e Ciências Exatas - IGCE, Universidade Estadual Paulista, Departamento de Física, 13506-970, Rio Claro, São Paulo, Brazil*

(Dated: October 2, 2018)

We explore theoretically the influence of Fano interference in the so-called Majorana oscillations in a T-shaped hybrid setup formed by a quantum dot (QD) placed between conducting leads and side-coupled to a topological superconducting nanowire (TSNW) hosting zero-energy Majorana bound states (MBSs) at the ends. Differential conductance as a function of the external magnetic field reveals oscillatory behavior. Both the shape and amplitude of the oscillations depend on the bias-voltage, degree of MBSs non-locality and Fano parameter of the system determining the regime of interference. When the latter is such that direct lead-lead path dominates over lead-QD-lead path and the bias is tuned in resonance with QD zero-energy, pronounced fractional Fano-like resonances are observed around zero-bias for highly non-local geometries. Further, the conductance profiles as a function of both bias-voltage and QD energy level display “bowtie” and “diamond” shapes, in qualitative agreement with both previous theoretical and experimental works. These findings ensure that our proposal can be used to estimate the degree of MBS non-locality, thus allowing to investigate their topological properties.

I. INTRODUCTION

Ideas borrowed from high energy physics became ubiquitous in the domain of condensed matter. The concepts of quasi-relativistic particles in graphene and other Dirac materials, acoustic analogs of black holes in Bose-Einstein condensates, AdS-CFT duality in the theory of the quantum phase transitions are now among standard tools used by condensed matter specialists. Some of these concepts still remain playground for theoreticians; the others on the contrary appeared to be of high experimental relevance and even paved way to novel applications in the domains of nanoelectronics and quantum computing. Among these latter are Majorana quasiparticles^{1,2} which are currently considered as highly perspective candidates for practical realization of fault-tolerant quantum computation process³.

In the domain of condensed matter, Majorana quasiparticles appear in hybrid systems composed by a quasi-one-dimensional semiconducting nanowire with strong spin-orbit coupling placed nearby *s*-wave superconductors⁴⁻⁷. In this configuration, when magnetic (Zeeman) field is applied parallel to the wire, the latter enters into *p*-wave topological superconducting (SC) phase and a pair of gapless (zero-energy) Majorana bound states (MBSs) is formed at the nanowire edges⁷. To analyze the MBSs transport properties in hybrid systems with topological superconducting nanowire (TSNW), in several theoretical works was proposed the use of quantum dots (QDs) as tunneling spectrometers to reveal MBSs signatures and topological transitions⁸⁻¹³. Experiments on hybrid TSNW with a QD also were performed^{14,15}.

According to Liu and Baranger prediction⁸, the experimental signature of the onset of an isolated MBS is zero-bias peak (ZBP) with $e^2/2h$ amplitude in the conductance profile of a system consisting of an individual QD side-coupled to a TSNW.

Despite experimental observations of the quantized ZBP in sophisticated devices with hybrid TSNWs¹⁴⁻²⁰, questions regarding its amplitude and emergence inside a truly topological phase still remain^{11,12,21-24}. Indeed, only the observation of ZBP itself is not sufficiently for asserting that the system is into the topological regime, hosting robust MBSs. In this context, non-local Majorana features^{11,12}, as well as ZBP splitting, followed by the appearance of an oscillatory pattern in the differential conductance as function of an applied magnetic field^{21,25,26} have been viewed as smoking guns of the MBSs manifestation in the topologically non-trivial regime.

In the current work, we investigate the role of Fano interference processes in the so-called Majorana oscillations in a T-shaped nanodevice, consisting of a single-level QD placed between the conducting leads and side-coupled to a TSNW hosting MBSs at the ends (Fig. 1). We also explore features of the system when the Majorana non-locality is taken into account, by considering the coupling λ_2 between the QD and lower MBS (see Fig. 1). The degree of Majorana non-locality η was previously defined by Prada *et al.*¹² as the ratio between the lower and upper QD-MBSs coupling strengths, *i.e.*, $\eta^2 = |\lambda_2|/|\lambda_1|$. When $\eta \rightarrow 0$ ($|\lambda_2| \ll |\lambda_1|$), the MBSs are highly non-local, thus presenting the holy grail for the quantum computation: the topological protection feature. Ref. [12] also

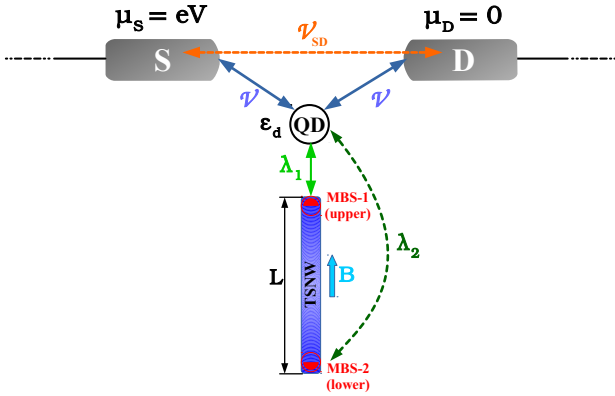


Figure 1. Sketch of the T-shaped geometry considered in the present paper: a single-level QD with energy ε_d is hybridized symmetrically (\mathcal{V}) with source-drain (S/D) conducting leads and side-coupled (λ_1) to a TSNW of length L , hosting zero-energy MBSs at the edges (half-filled red circles). The coupling λ_2 between the QD and MBS-2 is also taken into account due to the finite length of topological nanowire. Leads are also coupled with each other directly (\mathcal{V}_{SD}). External magnetic field B (light blue arrow) is applied parallel to the direction of the wire. The value of Zeeman splitting induced by magnetic field is considered to be large enough to achieve the full spin polarized regime in the setup. The QD-leads system operates as a tunneling spectrometer, allowing to investigate the properties of the MBSs by differential conductance measurements as a function of the external magnetic field and bias-voltage between leads. The presence of lead-lead tunneling path allows to explore how Fano interference process affects the MBSs signatures.

proposed a protocol to estimate experimentally such a degree of non-locality, which was recently performed by Deng *et al.*¹⁵ in a TSNW, with a QD working as spectrometer. The ratio between QD-MBSs couplings also can define the “*topological quality factor*”, being stated by Clarke¹¹ as $\mathcal{Q} = 1 - \eta^2$. In this context, the higher topological quality occurs when $\mathcal{Q} \approx 1$.

It is worth mentioning that T-shaped setups with QDs are suitable geometries to investigate the well-known Fano effect^{27–30}, once they have the key ingredients for its emergence: a localized state coupled to the continuum and distinct tunneling channels. Fano interference phenomenon can be used to explore Majorana properties, as theoretically proposed in earlier works^{9,13,31,32}.

In the current proposal, the quantities which define the tunneling conductance spectroscopy are Zeeman field, bias-voltage between the leads, energy level of QD, couplings between the MBSs and QD and Fano parameter, describing the relative importance of the direct lead-lead and lead-QD-lead tunneling paths. The conductance as a function of the magnetic field reveals pronounced oscillatory pattern, which are both dependent on Fano regime of interference and MBSs non-local features. In a nutshell, when the direct lead-lead tunneling prevails, the Majorana oscillations are suppressed at zero-bias and re-

veal unexpected fractional Fano-like resonances as a function of bias-voltage between the leads. The degree of MBSs non-locality also influences the behavior of such oscillations, which are attenuated as the local feature is increased (lower topological quality factor). We also report the ability to identify experimentally such a degree of non-locality in conductance measurements by changing the energy level of QD. Our results are in agreement with Ref. [12], despite differences between their system and ours, which will be discussed in due course.

This work is organized as follows: in Sec. II we present the theoretical model describing the system of Fig. 1. We also show the expression for zero-bias conductance and corresponding transmittance through the QD, which was obtained via equation of motion (EOM) technique. In Sec. III we show and discuss our findings, which are summarized in Sec. IV.

II. THE MODEL

The setup we consider is depicted in Fig. 1 and can be described by the following spinless model Hamiltonian⁸:

$$\mathcal{H} = \sum_{\alpha,k} \xi_{\alpha,k} c_{\alpha,k}^\dagger c_{\alpha,k} + \varepsilon_d d^\dagger d + \mathcal{V} \sum_{\alpha,k} (c_{\alpha,k}^\dagger d + \text{H.c.}) + \mathcal{V}_{SD} \sum_{k,l} (c_{S,k}^\dagger c_{D,l} + \text{H.c.}) + \mathcal{H}_M, \quad (1)$$

where the operator $c_{\alpha,k}^\dagger$ ($c_{\alpha,k}$) creates an electron (hole) in the metallic lead $\alpha = S/D$ (Source/Drain) with wave-number k and energy $\xi_{\alpha,k} = \varepsilon_k - \mu_\alpha$, where μ_α is chemical potential and $\mu_S - \mu_D = eV$ is the bias-voltage between the leads. The operator d^\dagger (d) creates an electron (hole) in the energy level ε_d of the QD, which is symmetrically coupled to the leads with coupling constant \mathcal{V} . The lead-lead coupling constant is \mathcal{V}_{SD} . No charging effect was taken into account in the QD energy level, since the MBS signatures remain in presence of Coulomb repulsion and possible Kondo physics, as Ruiz-Tijerina *et al.*³³ have shown.

Considering the even and odd conduction operators $c_{e,k} = c_{S,k} \cos \theta + c_{D,k} \sin \theta$ and $c_{o,k} = c_{S,k} \sin \theta - c_{D,k} \cos \theta$, with $\tan \theta = 1$, Eq. (1) can be rewritten as

$$\mathcal{H} = \sum_k \varepsilon_k c_{e,k}^\dagger c_{e,k} + \varepsilon_d d^\dagger d + \sqrt{2}\mathcal{V} \sum_k (c_{e,k}^\dagger d + \text{H.c.}) + \mathcal{V}_{SD} \sum_{k,q} c_{e,k}^\dagger c_{e,q} + \mathcal{H}_M + \mathcal{H}_o, \quad (2)$$

wherein $\mathcal{H}_o = \sum_k \varepsilon_k c_{o,k}^\dagger c_{o,k} - \mathcal{V}_{SD} \sum_{k,q} c_{o,k}^\dagger c_{o,q}$ describes the odd conduction states, which are decoupled from the QD⁹.

The term³⁴

$$\mathcal{H}_M = i\varepsilon_M \gamma_1 \gamma_2 + \lambda_1 (d - d^\dagger) \gamma_1 + \lambda_2 (d + d^\dagger) \gamma_2 \quad (3)$$

is the effective model Hamiltonian for a TSNW hosting zero-energy MBSs γ_i at the ends⁷. The Majorana operators have following algebra¹: $[\gamma_i, \gamma_j]_+ = \delta_{ij}$, $\gamma_{i(j)}^\dagger = \gamma_{i(j)}$. The parameter $\varepsilon_M \equiv \varepsilon_M(l, B) = \frac{E_0}{\sqrt{b}} e^{-l/2b} \cos(l\sqrt{b})$ describes the overlapping of unpaired gapless MBSs at the opposite sides of the wire²⁶, where $b = B/E_0$, $l = L\sqrt{2mE_0}/\hbar$ with B being longitudinal Zeeman field (light-blue arrow in the Fig. 1), L the length of the wire, $E_0 = (2m\alpha^2\Delta_{SC}^2/\hbar^2)^{1/3}$ ²⁶, α is spin-orbit constant and Δ_{SC} is the induced SC gap in the wire. The presence of the term $\cos(l\sqrt{b})$ in ε_M is responsible for the oscillatory pattern in conductance as function of the magnetic field. The couplings between the upper/lower MBSs and the QD are given by λ_1 and λ_2 , respectively³⁴. As known, the Hamiltonian of Eq. (3) can be rewritten with usual fermion operators¹ f , since $\gamma_1 = \frac{1}{\sqrt{2}}(f + f^\dagger)$ and $\gamma_2 = \frac{i}{\sqrt{2}}(f^\dagger - f)$. To see how \mathcal{H}_M stays in the fermionic basis, please see Ref. [34].

The differential conductance of the system is given by the following expression³⁵:

$$\mathcal{G}(eV) = \frac{e^2}{h} \int \left(-\frac{\partial f_F(\omega, eV)}{\partial \omega} \right) \mathcal{T}(\omega) d\omega = \frac{e^2}{h} \mathcal{T}(eV), \quad (4)$$

where e^2/h is quantum of conductance and f_F is Fermi-Dirac distribution function. The last equality holds for $T = 0$. $\mathcal{T}(\omega)$ is the transmittance across the system which can be obtained using equation of motion (EOM) method^{35,36}, yielding:

$$\mathcal{T}(\omega) = \mathcal{T}_b + \sqrt{\mathcal{T}_b \mathcal{R}_b} \tilde{\Gamma} \text{Re}[G_{dd}^r(\omega)] - (1 - 2\mathcal{T}_b) \frac{\tilde{\Gamma}}{2} \text{Im}[G_{dd}^r(\omega)], \quad (5)$$

where $\tilde{\Gamma} = \Gamma/(1+x)$ is dot-lead effective coupling, $\Gamma = 2\pi\mathcal{V}^2 \sum_k \rho_0$ is Anderson broadening³⁷, $x = (\pi\mathcal{V}_{SD}\rho_0)^2$, $\rho_0 = \sum_k \delta(\omega - \varepsilon_k)$ is the density of states (DoS) of the leads, $\mathcal{T}_b = 4x/(x+1)^2$ and $\mathcal{R}_b = 1 - \mathcal{T}_b$ are the background transmittance and reflectance, respectively^{9,38}.

We also define the Fano parameter³⁰ $q_b = \sqrt{\frac{\mathcal{R}_b}{\mathcal{T}_b}} = \frac{(1-x)}{2\sqrt{x}}$. For asymmetric couplings between the QD and leads³⁹, \mathcal{H}_o of Eq. (2) remains decoupled from the QD, with $\tan \theta = \mathcal{V}_S/\mathcal{V}_D$. The only differences are an effective Anderson broadening $\Gamma' = 2\Gamma_S\Gamma_D/(\Gamma_S + \Gamma_D)$ and an effective QD-even conduction band coupling $\mathcal{V}' = \sqrt{\mathcal{V}_S^2 + \mathcal{V}_D^2}$ instead of $\sqrt{2}\mathcal{V}$.

To calculate the spectral retarded Green's function of the QD $G_{dd}^r(\omega)$ in the Eq. (5), we use again EOM technique, which allows us to get the following expression:

$$G_{dd}^r(\omega) = \frac{1}{\omega^+ - \varepsilon_d - \Sigma - \Sigma_{\text{MBSs}}(\omega)}, \quad (6)$$

where $\Sigma = -(\sqrt{x} + i)\Gamma/(1+x)$, $\Sigma_{\text{MBSs}}(\omega) = K_+(\omega) + (|\lambda_1|^2 - |\lambda_2|^2)\tilde{K}(\omega)K(\omega)$ is the part of self-energy provided by the presence of MBSs^{8,9}, $\tilde{K}(\omega) = K(\omega)/(\omega^+ + \varepsilon_d + \Sigma^* - K_-(\omega))$, $K(\omega) = \omega^+ / [(\omega^+)^2 - \varepsilon_M^2]$ and

$$K_{\pm}(\omega) = \frac{\omega^+ (|\lambda_1|^2 + |\lambda_2|^2) \mp 2\varepsilon_M |\lambda_1| |\lambda_2|}{[(\omega^+)^2 - \varepsilon_M^2]}, \quad (7)$$

with $\omega^+ = \omega + i0^+$. Imaginary part of the Green's function given by Eq. (6) defines the DoS of the QD,

$$\rho_{\text{dot}}(\omega) = -\frac{1}{\pi} \text{Im}[G_{dd}^r(\omega)]. \quad (8)$$

III. RESULTS AND DISCUSSION

We investigate the effects of applied longitudinal Zeeman field on differential conductance of the system restricting ourselves to the temperature $T = 0$. Our goal is to analyze the changes in the conductance oscillation patterns introduced by the bias-voltage between leads for distinct Fano regimes of interference and couplings between the QD and MBSs. The tuning of QD-lower MBS coupling strength $|\lambda_2|$ allows to study the degree of MBS non-locality η , as discussed in Sec. I. Concerning the Fano interference process, one should discriminate between the cases when tunneling between the leads goes preferably via QD as intermediate ($x = 0$, $q_b \rightarrow \infty$, $\mathcal{T}_b = 0$) and the opposite case when direct lead-lead tunneling prevails ($x = 1$, $q_b = 0$, $\mathcal{T}_b = 1$). Intermediary situations are also considered ($0 < x < 1$). The parameters of the system are taken as: $E_0 \approx 0.23$ meV the wire length $L = 1 \mu\text{m}$, and Anderson broadening $\Gamma \approx 0.17E_0$. This is in agreement with both experiment^{14,16,17} and existing theoretical estimations^{10,25}.

Before discussing in detail our findings, we define the Zeeman critical value B_c , corresponding to $b = (\pi/2l)^2$, as the value in which MBSs begin to overlap with each other. It is important to mention that the Hamiltonian which describes the system [Eq. (1)] is an effective model that previously takes into account a Zeeman field to break the spin degeneracy, thus ensuring the spinless feature considered here and appearance of MBSs. Besides this field, intrinsic to the model, there is an applied longitudinal Zeeman field B in the TSNW, which overlaps the MBSs for $B > B_c$ and is responsible for oscillatory pattern in the conductance, as we shall see.

A. Majorana Oscillations and Fano interference

In this section, we study the role of Fano interference effect in the Majorana oscillations emerging in differential conductance, for $\varepsilon_d = 0$. Fig. 2 shows the differential conductance as a function of both eV and Zeeman field, considering different TSNW-QD couplings ($|\lambda_1|$) for the case when lead-QD-lead tunneling path is dominant

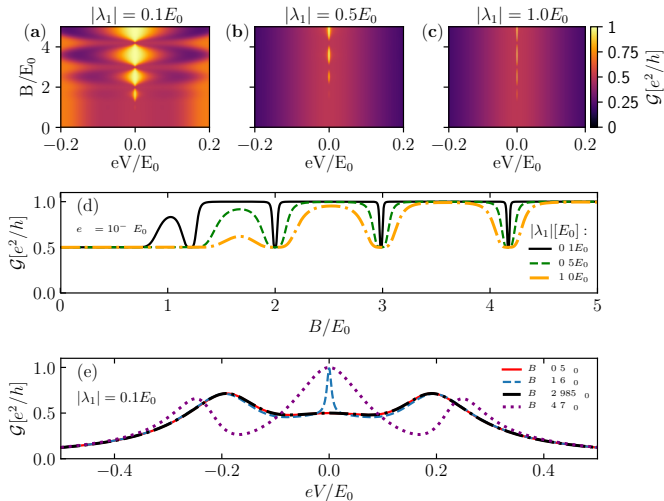


Figure 2. (a)-(c): Plots of differential conductance [Eq. (4)] as a function of the Zeeman field B and bias-voltage eV for the case when lead-QD-lead tunneling path is dominant ($x = 0, q_b \rightarrow \infty$) and $|\lambda_2| = 0$. The QD energy level $\varepsilon_d = 0$, the values of TSNW-QD coupling are $|\lambda_1| = 0.1E_0, 0.5E_0$ and $E_0 = 1.0E_0$. (d) Differential conductance at $eV = 10^{-6}E_0$ as function of the Zeeman field, for distinct values of TSNW-QD coupling $|\lambda_1|$. (e) Differential conductance as a function of eV for several values of the Zeeman field.

($x = 0, q_b \rightarrow \infty$) and $|\lambda_2| = 0$. In such a case the MBSs can overlap via ε_M , but the wire is long enough to ensure that there is no connection between the MBS-2 and QD (See Fig. 1). If the value of magnetic field is below critical, $B < B_c$, we observe typical plateau in differential conductance with $\mathcal{G} = e^2/2h$, which indicates that MBSs remain isolated from each other. When magnetic field exceeds the critical value, $B > B_c$, an oscillatory pattern in differential conductance as function of the magnetic field arises. The value of the conductance oscillates between the minimal value of $e^2/2h$ and maximal value which in certain cases can reach e^2/h . This latter points to a regular fermion signature arising due to the finite overlap between the MBSs⁸.

These effects become visible at the panel (d), where the differential conductance is plotted as function of the magnetic field for $eV = 10^{-6}E_0$: the oscillations between isolated MBSs ($\varepsilon_M \rightarrow 0, \mathcal{G} \rightarrow e^2/2h$) and nonlocal fermion state formed by overlapping MBSs ($\mathcal{G} \rightarrow e^2/h$) are clearly visible. The increase of TSNW-QD coupling λ_1 broadens the dips in the conductance and decreases the amplitudes of the oscillations. Note however, that for big values of magnetic field the maxima of the conductance still reach the values of the conductance quantum. Effects of the overlap between MBSs assisted by Zeeman field are clearly seen at panel (e), where differential conductance is plotted versus eV . Indeed, for certain values of B (corresponding e.g. to dashed-blue and dotted purple lines), conductance reaches maximum value at $eV = 0$, which is a signature of a regular fermion state, whereas for other values of Zeeman field (corresponding e.g. to red filled

and dash-dotted black lines), \mathcal{G} has minima at $eV = 0$, which corresponds to the case of isolated MBSs.

The change of the Fano interference regime to the case where $q_b = 0$, corresponding to the dominance of the direct lead-lead tunneling, brings dramatic changes in the differential conductance pattern, as can be seen at Fig. 3. Two qualitatively new phenomena are observed here as compare to the case $q_b \rightarrow \infty$. First, at $eV = 0$, $\mathcal{G} = e^2/2h$ and is independent on the values of $|\lambda_1|$ and applied field B . Moreover, differential conductance as function of bias-voltage reveals fractional Fano-like resonances around $eV = 0$ with intriguing minimal and maximal values equal to $e^2/4h$ and $3e^2/4h$ ^{31,38}. Similar fractional Fano interference process was already reported by Barański *et al.*³² in a T-shaped geometry with a QD between metallic and superconducting leads, side-coupled to a MBS. In such a system, the fractional interferometric behavior is related to the presence of MBS in the system, which scatters the electron waves, changing their phase³². We highlight that the fractional oscillatory pattern reported here only can be verified for low temperatures ($T \leq mK$). Otherwise, the thermal effects can smear out such Fano-like resonances, making the effect unobservable.

We also examine the corresponding dimensionless QD DoS for the case $q_b = 0$. The results are shown in the Fig. 4 for $|\lambda_1| = 1.0E_0$. As it can be clearly seen, DoS reveal the resonant asymmetric pattern, which is inverted with respect to the pattern observed in the differential conductance: the dips in the DoS correspond to the peaks in \mathcal{G} and vice versa. This inversion is a straight aftermath of the system electrical charge conservation: in the lead-lead Fano regime the better is localization of the electron on the dot the poorer is the conductance. In order to catch both charge conservation and fractional Fano-like lineshapes, we present horizontal line cuts of the color plot of the Fig. 4(a) along red, blue and black horizontal bars, as shown in the Fig. 4(b). As can be seen, for both values of $B > B_c$ considered (dashed blue and dash-dotted black lines), the amplitudes of the fractional profile remain the same.

To understand better the fractional Fano interference process, we analyze differential conductance as a function of eV for several values of coupling between the QD and lower MBS ($|\lambda_2|$), which allows to verify how the fractional feature is modified by decreasing the degree of MBS non-locality¹². Fig. 5 shows that, for smaller values of $|\lambda_2|$, the fractional lineshape persists with slight changes in amplitude. However, for $|\lambda_2| = 10^{-2}E_0$ (purple dashed-line) the fractional resonances invert and, for bigger values, vanish. This behavior suggests that the fractional Fano effect appears just for high degrees of MBS non-locality, i.e. $|\lambda_2| \leq 10^{-2}E_0 \ll |\lambda_1|$, yielding $\eta = 0.1$.

Fig. 6 shows the differential conductance as a function of eV for distinct Fano interference processes ($0 < x < 1$). When the lead-QD-lead path is dominant ($x = 0$), the conductance reaches maximum e^2/h , indicating that the

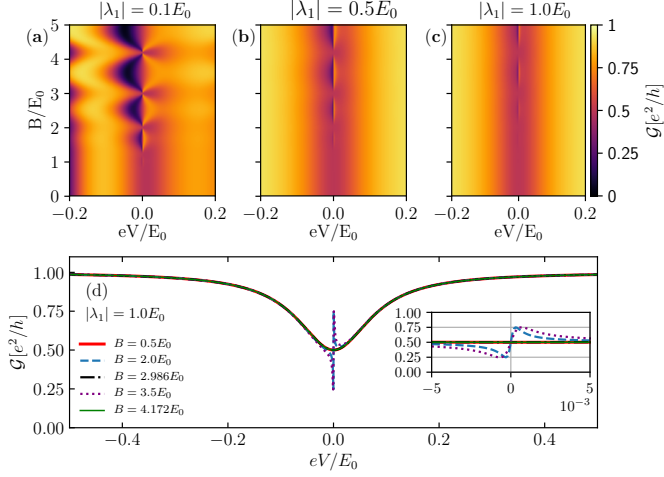


Figure 3. (a)-(b): Plots of differential conductance [Eq. (4)] as function of the Zeeman field B and eV , for the case when direct lead-lead tunneling path is dominant ($x = 1, q_b = 0$) and $|\lambda_2| = 0$. The QD energy level $\varepsilon_d = 0$, the values of TSNW-QD coupling are $|\lambda_1| = 0.1E_0, 0.5E_0$, and $E_0 = 1.0E_0$. (d) Differential conductance as function of eV for several values of Zeeman field. Conductance reveals sharp resonant asymmetric profile.

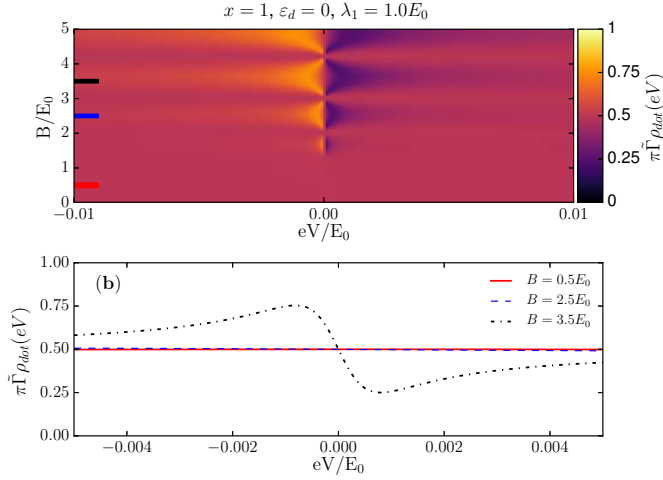


Figure 4. (a) Dimensionless DoS of the QD for the case of the dominant direct lead-lead tunneling ($x = 1, q_b = 0$) as a function of the Zeeman field and eV , with $|\lambda_1| = 1.0E_0$ and $|\lambda_2| = 0$. (b) Dimensionless DoS of the QD as function of eV for three different values of the magnetic field, corresponding to the colored horizontal bars at the panel (a).

MBSs are overlapped via Zeeman field ($\varepsilon_M(B) \neq 0$). As we enhance the direct lead-lead transport, the Fano-like fractional resonance begins to take shape. Such a behavior can be verified for $x \geq 0.15 (q_b \leq 1.10)$. For higher values of x , which describes the predominance of direct lead-lead tunneling ($x \geq 0.75 (q_b \leq 0.14)$), the fractional resonances becomes more evident, showing the same line-

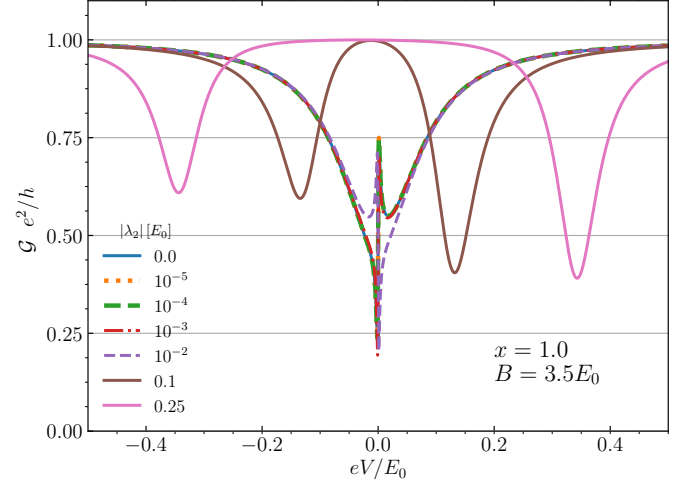


Figure 5. Differential conductance [Eq. (4)] as function of eV for the situation which the fractional Fano-like resonances are present ($x = 1, q_b = 0$). Several values of the coupling between the QD and the lower MBS are considered ($|\lambda_2|$).

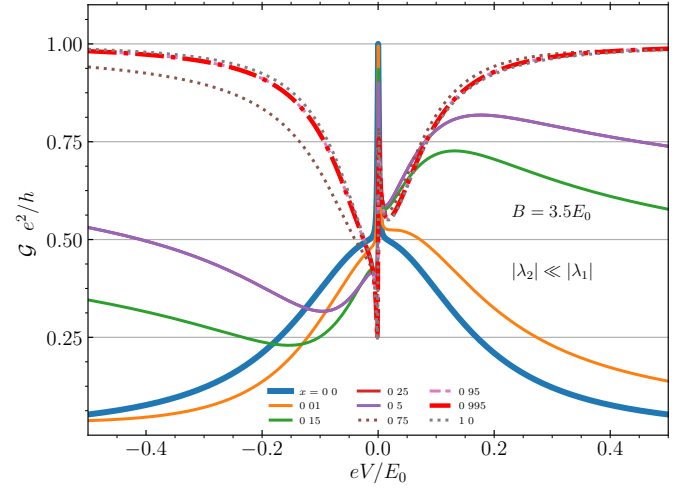


Figure 6. Differential conductance [Eq. (4)] as function of eV for the several Fano regimes of interference ($0 \leq x \leq 1$) and highly non-local situation ($|\lambda_2| \ll |\lambda_1|$).

shape, with small deviations in amplitude. These features state that the fractional Fano interference effect takes place when direct lead-lead tunneling process is dominant over those lead-QD-lead, thus indicating that the measurement system (metallic leads and QD) can distort the MBSs local/non-local signatures due to interference phenomena.

In order to have an overview about the influence of Fano interference in the Majorana oscillations, in Fig. 7 we analyze the differential conductance for $eV = 0$ as a function of Zeeman field, considering several values of $x(q_b)$. For the highly non-local situation ($|\lambda_2| = 0, \eta = 0$) [Fig. 7(a)], we verify that as x increases, the am-

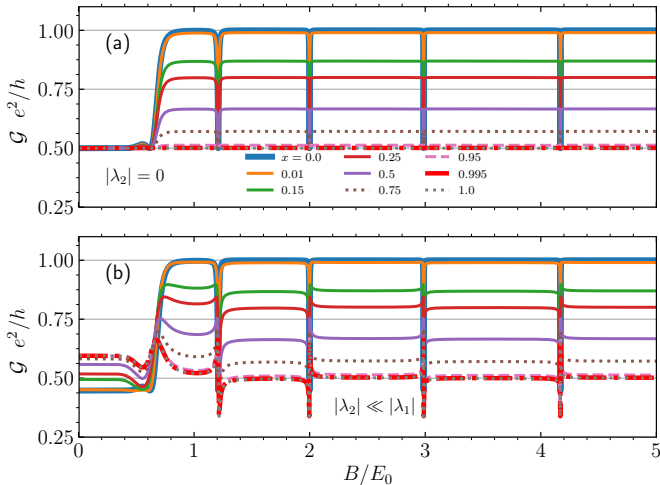


Figure 7. Differential conductance [Eq. (4)] as function of Zeeman field, for $eV = 0$ and several Fano regimes of interference ($0 \leq x \leq 1$). In panel (a) the coupling between the QD and the lower MBS is neglected $|\lambda_2| = 0$, while in (b) is considered.

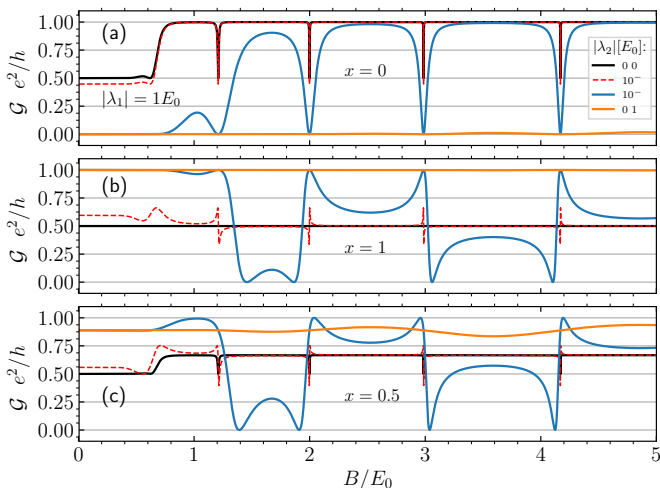


Figure 8. Differential conductance [Eq. (4)] as function of Zeeman field, for $eV = 0$ and several values of $|\lambda_2|$. Panel (a) exhibits the Fano regime $x = 0$, while (b) and (c) show the situation for $x = 1$ and $x = 0.5$, respectively.

plitude of oscillations are suppressed until total quench for $x = 1$ ($q_b = 0$). Thereby, the enhancement of direct lead-lead tunneling process ($x \geq 0.95$) can destroy the oscillatory behavior at zero-bias voltage ($eV = 0$), hiding the information about the overlap between MBSs via Zeeman field. The suppression of oscillations amplitude is also verified for $|\lambda_2| \neq 0$, even for a high degree of MBSs non-locality ($\eta \sim 10^{-3}$), as depicted in Fig. 7(b). The main difference is that for the finite $|\lambda_2|$ situation, the oscillatory pattern is not completely quenched for $x = 1$.

Fig. 8 exhibits how the degree of MBSs non-locality af-

fects the Majorana oscillations at zero-bias voltage. The oscillatory behavior is well defined just for higher non-local situations in all the three interference processes considered here [(a) $x = 0$, (b) $x = 1.0$ and (c) $x = 0.5$]. As we decrease the Majorana non-local property (enhancing $|\lambda_2|$), the oscillation pattern is totally suppressed due to the MBSs peak splitting, which points out that the MBSs can experience each other. The data indicates that for $|\lambda_2| = 0.1E_0$ (orange solid line), yielding $\eta = 0.32$, the oscillatory pattern is completely absent, which shows that the presence of well-defined oscillations at $eV = 0$ in the differential conductance as a function of Zeeman field is a feature of highly non-local MBSs ($\eta \rightarrow 0$). These findings suggest that our device can work as a fine tunneling spectrometer to investigate the non-local MBSs features, once it catches changes in oscillations amplitude appearing in differential conductance at zero-bias, even for small values of η .

B. Degree of MBS non-locality and experimental protocol

In Sec. I, we recall the concept of degree of MBSs non-locality η proposed by Prada *et al.*¹², who also indicated a protocol to measure it in a QD-TSNW hybrid system. Such a theoretical proposal was followed by its experimental achievement by Deng *et al.*¹⁵. We also introduced that η is related to a topological quality factor, as stated in Ref. [11]. In this subsection, we present that our simplest effective Hamiltonian (spinless carriers, absence of charging effect and additional ABSs) is also able to catch the information of the degree of MBSs non-locality using the same protocol previously proposed^{12,15}. Before presenting our findings, it is worth mentioning that the QD setup in our device is distinct from the original proposal¹². Here, the transport is through the QD, placed between metallic leads and side-coupled to the TSNW, while in previous works^{11,12,14,15,26}, the transport is through the QD-TSNW system, placed between metallic and superconducting leads. Furthermore, in such works the QD belongs to the nanowire structure and, therefore is not a separated entity as in our device.

Fig. 9 shows contour plots of differential conductance as a function of bias-voltage eV and QD energy level ε_d , for several values of $\varepsilon_M(B)$ and $|\lambda_2|$. The QD energy level can be experimentally accessed by a gate potential V_d , which can be tuned separately from the gate voltage eV between metallic leads by changing both in a compensatory way¹⁵. Panel (a) describes the higher non-local situation, *i.e.*, there is no overlap between the MBSs ($\varepsilon_M(B) = |\lambda_2| = 0$). This highly non-local property is characterized by a plateau at $\mathcal{G}(eV = 0) = e^2/h$, independent from the value of ε_d . It is known from previous works^{14,24} that Andreev bound states (ABSs) can transmute in a topological MBS as they become merged at zero-energy. However, the ABSs also can coalesce forming near-zero energy mid-gap states in a nontopological

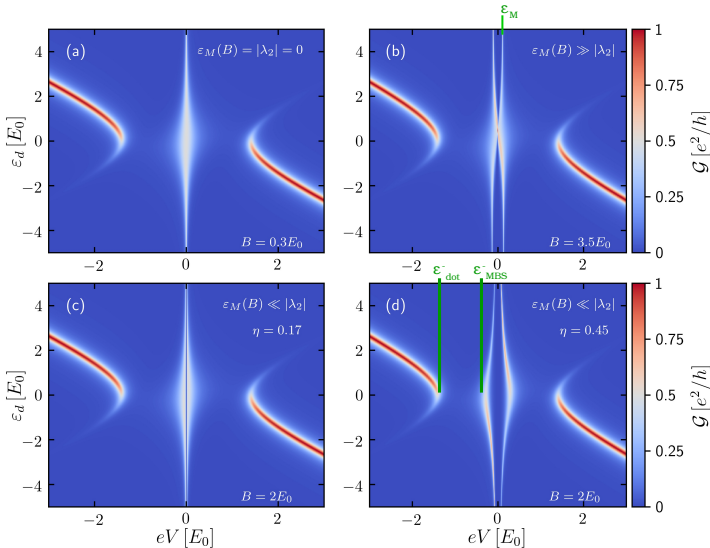


Figure 9. Differential conductance [Eq. (4)] as function of both QD energy level ε_d and bias voltage eV . Panel (a) shows the highly non-local situation of isolated MBSs ($\varepsilon_M(B) = |\lambda_2| = 0$). (b) exhibits a non-local situation, wherein the $\varepsilon_M(B)$ is dominant (“bowtie” overlapping MBSs in Ref. [12]), while (c) and (d) show the case correspondent to “diamond” of same reference, described by the dominance of $|\lambda_2|$ over $\varepsilon_M(B)$. The difference between (c) and (d) is the degree of MBSs non-locality $\eta = \sqrt{|\lambda_2|/|\lambda_1|}$, with $|\lambda_1| = 1.0E_0$ for all the situations considered. The values $\varepsilon_{\text{dot}}^-$ and $\varepsilon_{\text{MBS}}^-$ allows to obtain experimentally $\eta \approx \Omega$.

regime, mimicking MBS signatures. Such ABSs analysis does not belong to scope of this work, since no additional ABSs were included.

Now, let us consider the situation in which MBSs overlap with each other via $\varepsilon_M(B) \gg |\lambda_2|$. We verify in panel (b) the “bowtie” pattern, in qualitative agreement with the same situation reported in Fig. 4(b) of Ref. [12] and 3(b) of Ref. [15]. As indicated in Fig. 9(b), such a measurement is able to provide the value of $\varepsilon_M(B)$, which is $\approx 0.12E_0$ for $B = 3.5E_0$. Figs. 9(c)-(d) depict the situation wherein $\varepsilon_M(B) \ll |\lambda_2|$, which reveal information about the degree of MBSs non-locality using the same protocol previously stated¹²: $\Omega \approx \eta$ can be obtained experimentally by the ratio $\varepsilon_{\text{MBS}}^\pm/\varepsilon_{\text{dot}}^\pm$. Let us pick out the values indicated in Fig. 9(d): $\varepsilon_{\text{MBS}}^- \approx -0.30E_0$ and $\varepsilon_{\text{dot}}^- \approx -1.5E_0$. Since $\Omega^2 = \varepsilon_{\text{MBS}}^-/\varepsilon_{\text{dot}}^-$ ^{12,15}, we find $\Omega \approx 0.45$, in agreement with the theoretical parameters adopted ($|\lambda_2| = 0.2E_0$, $|\lambda_1| = 1.0E_0$ and

$\eta = \sqrt{|\lambda_2|/|\lambda_1|} = 0.45$). In such panels, we also confirm the “diamond” shape, which was previously verified in Figs. 4(d) and 3(c) of Refs. [12] and [15], respectively. By comparing panels (c) and (d), it can be noticed that the enhancement of Ω , *i.e.*, the reduction of MBSs non-local properties, is characterized by the opening of the “diamond” shape. Qualitative agreement between our results of Fig. 9 and those found in Ref. [12], which were experimentally verified in Ref. [15], evidence that our device can be used to explore the MBSs non-local properties.

IV. CONCLUSIONS

To summarize, we studied Majorana oscillations in a T-shaped hybrid device composed by a QD embedded between a pair of conducting leads and side-coupled to a TSNW hosting zero-energy MBSs at its ends. Analyzing the differential conductance profiles of the system as a function of the applied Zeeman field and bias-voltage eV between the leads, we found that Majorana oscillations are very sensitive to the changes of the regime of Fano interference and degree of Majorana non-locality η . This latter can be tuned by changing the coupling between the QD and lower MBS. Unexpected fractional Fano-like resonances were unveiled for high non-local situations ($\eta \rightarrow 0$), in the regime where direct lead-lead tunneling prevails. Moreover, differential conductance as a function of both bias-voltage and energy level of QD revealed “bowtie” and “diamond” shapes, in qualitative agreement with the original theoretical proposal¹², despite differences between the models. Such correspondences indicate that our device also can be used as a tunneling spectrometer to obtain experimentally the degree of Majorana non-locality and investigate its topological properties following the same protocol proposed by Prada *et al.*¹² and experimentally performed by Deng *et al.*¹⁵.

ACKNOWLEDGMENTS

We thank the funding Brazilian agencies CNPq (Grant No. 307573/2015-0), CAPES, and São Paulo Research Foundation (FAPESP) Grant No. 2015/23539-8. I.A.S. acknowledge support from Russian Science Foundation Project 17-12-01359 and Horizon2020 project CoExAN.

* correspondent author: acfseridonio@gmail.com

¹ J. Alicea, Reports on Progress in Physics **75**, 076501 (2012).

² S. R. Elliott and M. Franz, Rev. Mod. Phys. **87**, 137 (2015).

³ C. Nayak, S. H. Simon, A. Stern, M. Freedman, and S. Das Sarma, Rev. Mod. Phys. **80**, 1083 (2008).

⁴ R. M. Lutchyn, J. D. Sau, and S. Das Sarma, Phys. Rev. Lett. **105**, 077001 (2010).

- ⁵ Y. Oreg, G. Refael, and F. von Oppen, *Phys. Rev. Lett.* **105**, 177002 (2010).
- ⁶ A. A. Zyuzin, D. Rainis, J. Klinovaja, and D. Loss, *Phys. Rev. Lett.* **111**, 056802 (2013).
- ⁷ A. Y. Kitaev, *Physics-Uspekhi* **44**, 131 (2001).
- ⁸ D. E. Liu and H. U. Baranger, *Physical Review B* **84**, 201308 (2011).
- ⁹ F. A. Dessotti, L. S. Ricco, M. de Souza, F. M. Souza, and A. C. Seridonio, *J. of Appl. Phys.* **116**, 173701 (2014).
- ¹⁰ E. Vernek, P. H. Penteado, A. C. Seridonio, and J. C. Egues, *Phys. Rev. B* **89**, 165314 (2014).
- ¹¹ Clarke, David J., *Phys. Rev. B* **96**, 201109 (2017).
- ¹² Prada, Elsa and Aguado, Ramón and San-Jose, Pablo, *Phys. Rev. B* **96**, 085418 (2017).
- ¹³ Schuray, Alexander and Weithofer, Luzie and Recher, Patrik, *Phys. Rev. B* **96**, 085417 (2017).
- ¹⁴ M. T. Deng, S. Vaitiekėnas, E. B. Hansen, J. Danon, M. Leijnse, K. Flensberg, J. Nygård, P. Krogstrup, and C. M. Marcus, *Science* **354**, 1557 (2016).
- ¹⁵ Deng, M. T. and Vaitiekėnas, S. and Prada, E. and San-Jose, P. and Nygård, J. and Krogstrup, P. and Aguado, R. and Marcus, C. M., *ArXiv e-prints* (2017), [arXiv:1712.03536 \[cond-mat.mes-hall\]](https://arxiv.org/abs/1712.03536).
- ¹⁶ V. Mourik, K. Zuo, S. M. Frolov, S. Plissard, E. Bakkers, and L. Kouwenhoven, *Science* **336**, 1003 (2012).
- ¹⁷ S. M. Albrecht, A. Higginbotham, M. Madsen, F. Kuemmeth, T. S. Jespersen, J. Nygård, P. Krogstrup, and C. Marcus, *Nature* **531**, 206 (2016).
- ¹⁸ P. Krogstrup, N. L. B. Ziino, W. Chang, S. M. Albrecht, M. H. Madsen, E. Johnson, J. Nygård, C. M. Marcus, and T. S. Jespersen, *Nat.Mater.* **14**, 1476 (2015).
- ¹⁹ H. Zhang, Ö. Gül, S. Conesa-Boj, K. Zuo, V. Mourik, F. K. de Vries, J. van Veen, D. J. van Woerkom, M. P. Nowak, M. Wimmer, D. Car, S. Plissard, E. P. A. M. Bakkers, M. Quintero-Pérez, S. Goswami, K. Watanabe, T. Taniguchi, and L. P. Kouwenhoven, *Nature Nanotechnology* **13**, 1748 (2018).
- ²⁰ H. Zhang, C.-X. Liu, S. Gazibegovic, D. Xu, J. A. Logan, G. Wang, N. van Loo, J. D. S. Bommer, M. W. A. de Moor, D. Car, R. L. M. Op het Veld, P. J. van Veldhoven, S. Koelling, M. A. Verheijen, M. Pendharkar, D. J. Pennachio, B. Shojaei, J. S. Lee, C. J. Palmstrm, E. P. A. M. Bakkers, S. D. Sarma, and L. P. Kouwenhoven, *Nature* **556**, 74 (2018).
- ²¹ D. Rainis, L. Trifunovic, J. Klinovaja, and D. Loss, *Phys. Rev. B* **87**, 024515 (2013).
- ²² J. Liu, A. C. Potter, K. T. Law, and P. A. Lee, *Phys. Rev. Lett.* **109**, 267002 (2012).
- ²³ R. V. Mishmash, D. Aasen, A. P. Higginbotham, and J. Alicea, *Phys. Rev. B* **93**, 245404 (2016).
- ²⁴ C.-X. Liu, J. D. Sau, T. D. Stanescu, and S. Das Sarma, *Phys. Rev. B* **96**, 075161 (2017).
- ²⁵ S. Das Sarma, J. D. Sau, and T. D. Stanescu, *Phys. Rev. B* **86**, 220506 (2012).
- ²⁶ J. Danon, E. B. Hansen, and K. Flensberg, *Phys. Rev. B* **96**, 125420 (2017).
- ²⁷ U. Fano, *Phys. Rev.* **124**, 1866 (1961).
- ²⁸ A. E. Miroshnichenko, S. Flach, and Y. S. Kivshar, *Rev. Mod. Phys.* **82**, 2257 (2010).
- ²⁹ Kobayashi, Kensuke and Aikawa, Hisashi and Sano, Akira and Katsumoto, Shingo and Iye, Yasuhiro, *Phys. Rev. B* **70**, 035319 (2004).
- ³⁰ W. Hofstetter, J. König, and H. Schoeller, *Phys. Rev. Lett.* **87**, 156803 (2001).
- ³¹ A. C. Seridonio, E. C. Siqueira, F. A. Dessotti, R. S. Machado, and M. Yoshida, *J. of Appl. Phys.* **115**, 063706 (2014).
- ³² J Baranski and A Kobianka and T Domanski, *Journal of Physics: Condensed Matter* **29**, 075603 (2017).
- ³³ Ruiz-Tijerina, David A. and Vernek, E. and Dias da Silva, Luis G. G. V. and Egues, J. C., *Phys. Rev. B* **91**, 115435 (2015).
- ³⁴ Ricco, L. S. and Dessotti, F. A. and Shelykh, I. A. and Figueira, M. S. and Seridonio, A. C., *Sci. Reports* **8**, 2790 (2018).
- ³⁵ J. A.-P. Hartmut Haug, *Quantum Kinetics in Transport and Optics of Semiconductors*, Vol. 123 (Springer-Verlag Berlin Heidelberg, 2008).
- ³⁶ F. Dessotti, L. Ricco, Y. Marques, R. Machado, L. Guessi, M. Figueira, M. de Souza, and A. Seridonio, *Phys. E* **83**, 297 (2016).
- ³⁷ P. W. Anderson, *Phys. Rev.* **124**, 41 (1961).
- ³⁸ F. A. Dessotti, L. S. Ricco, Y. Marques, L. H. Guessi, M. Yoshida, M. S. Figueira, M. de Souza, P. Sodano, and A. C. Seridonio, *Phys. Rev. B* **94**, 125426 (2016).
- ³⁹ Campo, V. L. and Ricco, L. S. and Seridonio, A. C., *Phys. Rev. B* **96**, 045135 (2017).

Chapter 7

Spin-dependent zero-bias peak in a hybrid nanowire-quantum dot system: Distinguishing isolated Majorana fermions from Andreev bound states

*L. S. Ricco, M. de Souza, M. S. Figueira, I. A. Shelykh and A. C. Seridonio, [Phys. Rev. B 98, 075142](#).
Published August 24, 2018*

7.1 Overview and Remarks

The current work concerns the detection of Majorana bound states (MBSs) in hybrid nanowire-quantum dot devices. The pivotal difference between such a work and those found in previous sections is the full spin description in our system Hamiltonian, instead of a spinless model adopted in our earlier papers. Parallel to this, we also have considered the Coulomb repulsion between the charge carriers at dot energy level (intradot correlation). As we already have done in sec. 6, the coupling of dot with both MBSs was kept, as well as the direct overlap between them. The consideration of all these ingredients allowed us to theoretically analyze a physical system more faithful to recent experimental devices and also propose a way to solve a key issue in the area of Majorana detection: Differentiate the truly topological MBSs from the so-called Andreev bound states (ABSs). For further information, please see the paper at the end of this chapter. We also present some supplementary results.

7.2 Theoretical Model and density of states calculations

In this section we will provide some details concerning the theoretical calculations of the Green's function of quantum dot, which are in a summarized way in the paper. The full procedure can be found in Appendix B, at the end of current thesis.

Let us start by writing the Hamiltonian which describes the hybrid system that is being considered

[please, see Fig. 1 of draft]:

$$\begin{aligned}
 H &= \sum_{\mathbf{k}\sigma} \varepsilon_{\mathbf{k}\sigma} e_{\mathbf{k}\sigma}^\dagger e_{\mathbf{k}\sigma} + \sum_{\sigma} \varepsilon_{d\sigma} n_{d\sigma} + U n_{d\uparrow} n_{d\downarrow} \\
 &+ \sqrt{2}V \sum_{\mathbf{k}\sigma} (e_{\mathbf{k}\sigma}^\dagger d_{\sigma} + d_{\sigma}^\dagger e_{\mathbf{k}\sigma}) + H_{Nw},
 \end{aligned} \tag{7.1}$$

where $n_{d\sigma} = d_{\sigma}^\dagger d_{\sigma}$ is the number operator for electrons in the QD single-level and $e_{\mathbf{k}\sigma}^\dagger (e_{\mathbf{k}\sigma})$ depicts electrons (holes) in the normal (N) lead with wave number \mathbf{k} , spin $\sigma = \uparrow, \downarrow$ and energy $\varepsilon_{\mathbf{k}\sigma}$. The energy level of QD is $\varepsilon_{d\sigma} = \varepsilon_d - \sigma V_Z$, wherein V_Z is the Zeeman energy splitting induced by external magnetic field and U accounts for the charging energy. The dot is coupled to N-lead with strength $\sqrt{2}V$. H_{Nw} represents the effective model Hamiltonian for a SC nanowire hosting MBSs γ_i at opposite ends and coupled to the QD and is given by:

$$H_{Nw} = i\delta_M \gamma_L \gamma_R + (\lambda_L d_{\sigma} - \lambda_L^* d_{\sigma}^\dagger) \gamma_L + (\lambda_R d_{\sigma} + \lambda_R^* d_{\sigma}^\dagger) \gamma_R, \tag{7.2}$$

wherein the Majorana operators γ_i are self-conjugated ($\gamma_i = \gamma_i^\dagger$) and obey the algebraic relation $\{\gamma_i, \gamma_j\} = \delta_{ij}$. The dot is coupled to left and right MBSs, with hoppings λ_L and λ_R , respectively. The direct hybridization δ_M between MBSs is the same which we have adopt in Sec. 6.3, *i.e.*,

$$\delta_M = \frac{e^{-l/2b}}{\sqrt{b}} \cos(l\sqrt{b}) E_0, \tag{7.3}$$

which is function of both Zeeman energy splitting $b = V_Z/E_0$ and SC nanowire length l . This theoretical prediction can be related to experiments by choosing the energy scale $E_0 = (2m^* \alpha^2 \Delta_{SC}^2 / \hbar^2)^{1/3}$ and $l = L\sqrt{2m^* E_0} / \hbar$, where L is the actual SC nanowire length, m^* is the electron effective mass, α is spin-orbit constant and Δ_{SC} is the induced SC gap.

As already have established in previous sections, H_{Nw} [Eq. (7.2)] can be rewritten in a regular fermionic basis, since a Majorana excitation can be decomposed into a pair of fermionic operators, *i.e.*, $\gamma_L = (f_{\uparrow} + f_{\uparrow}^\dagger) / \sqrt{2}$ and $\gamma_R = i(f_{\uparrow}^\dagger - f_{\uparrow}) / \sqrt{2}$. In such a basis, H_{Nw} becomes into

$$\mathcal{H}_{Nw} = \delta_M \left(f_{\uparrow}^\dagger f_{\uparrow} - \frac{1}{2} \right) + t_{hp} \sum_{\sigma} (d_{\sigma} f_{\uparrow}^\dagger + f_{\uparrow} d_{\sigma}^\dagger) + \Delta \sum_{\sigma} (d_{\sigma} f_{\uparrow} + f_{\uparrow}^\dagger d_{\sigma}^\dagger) \tag{7.4}$$

wherein the hopping term t_{hp} and the binding energy between the delocalized Cooper pair Δ are given by $t_{hp} = (|\lambda_L| - |\lambda_R|) / \sqrt{2}$ and $\Delta = (|\lambda_L| + |\lambda_R|) / \sqrt{2}$, respectively.

Our goal is to obtain the total density of states (DOS) in the QD, which reads:

$$\text{DOS}(\omega) = \pi \Gamma \sum_{\sigma} \rho_{\sigma}(\omega), \tag{7.5}$$

where the constant $\Gamma = 2\pi V^2 \rho_0$ is the QD-N lead effective coupling, with ρ_0 being the DOS of lead. The quantity $\rho_{\sigma}(\omega) = -\frac{1}{\pi} \text{Im}[G_{d,d}^{r,\sigma}(\omega)]$ accounts for DOS per spin orientation, which depends on the retarded Green's function of the QD $G_{d,d}^{r,\sigma}(\omega)$ in spectral domain ω . To obtain such a function, we apply the EOM procedure as described in Sec. 3.1. We remember the reader that this technique can be summarized as

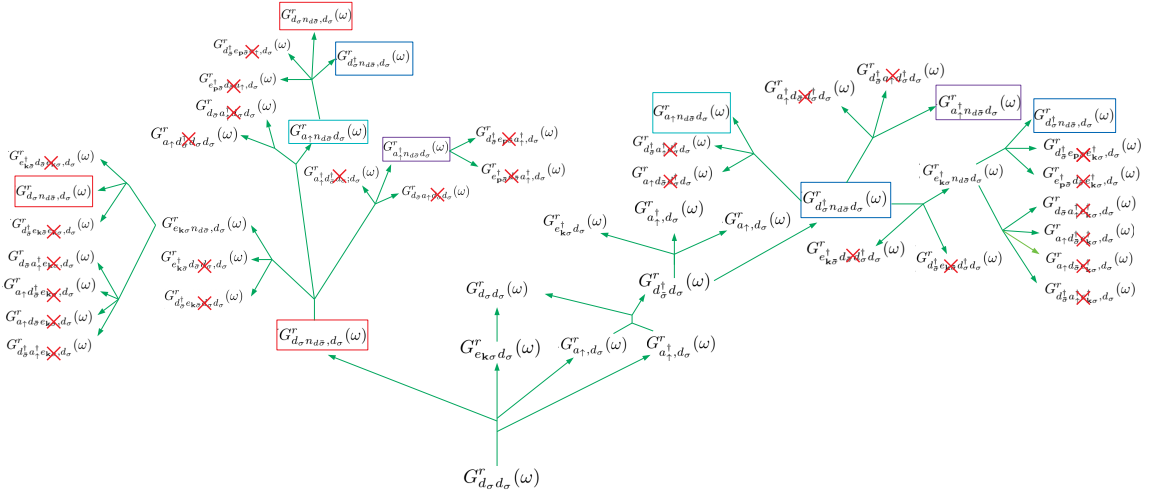


Figure 7.1: Green's functions Tree showing a bird's eye view of evolution of each Green's function under application of EOM technique. The functions with a red X were thrown away due to Hubbard-I truncation scheme.

follows

$$(\omega + \eta^+) G_{c_i c_j}^r(\omega) = \delta_{ij} + \langle\langle [c_i, \mathcal{H}]; c_j^\dagger \rangle\rangle, \quad (7.6)$$

for single-particle Green's functions, where $c_{i(j)}$ are fermionic operators belonging to Hamiltonian \mathcal{H} , which obeys the usual anticommutation relations $\{c_{i(j)}, c_{i(j)}\} = \{c_{i(j)}^\dagger, c_{i(j)}^\dagger\} = 0$ and $\{c_i, c_j^\dagger\} = \delta_{i,j}$. Thus, for the Green's function of dot:

$$(\omega + \eta^+) G_{d_\sigma d_\sigma}^r(\omega) = 1 + \langle\langle [d_\sigma, H]; d_\sigma^\dagger \rangle\rangle, \quad (7.7)$$

where H is the Hamiltonian of Eq. (7.1). after calculating $[d_\sigma, H]$, one gets:

$$\begin{aligned} (\omega - \varepsilon_{d_\sigma} + \eta^+) G_{d_\sigma d_\sigma}^r(\omega) &= 1 + U G_{d_\sigma n_{d\bar{\sigma}} d_\sigma}^r(\omega) + \sqrt{2}V \sum_{\mathbf{k}} G_{e_{\mathbf{k}\sigma} d_\sigma}^r(\omega) \\ &- t_{hp} \sum_{\bar{\sigma}} \delta_{\sigma\bar{\sigma}} G_{f_{\uparrow}, d_\sigma}^r(\omega) - \sum_{\bar{\sigma}} \delta_{\sigma\bar{\sigma}} \Delta G_{f_{\uparrow}^\dagger, d_\sigma}^r(\omega), \end{aligned} \quad (7.8)$$

wherein we can notice the presence of new Green's functions, which will be computed by applying the EOM again.

However, we draw attention for the Green's function of four operators $G_{d_\sigma n_{d\bar{\sigma}} d_\sigma}^r(\omega)$, which emerges due to many-particle correlations $n_{d,\sigma} n_{d,\bar{\sigma}}$ introduced by Coulomb charging energy in the system Hamiltonian [Eq. (7.1)], as we have discussed in chapter 3. As can be seen in Appendix B, the calculation of such a many-particle Green's function via EOM yields new ones, which, in turn generate new many-particle Green's functions. In other words, successive application of EOM in this kind of Green's functions will generate an infinite chain of others Green's functions and thus, the system can not be closed. Here, we apply the Hubbard-I truncation scheme, which allows us to describe better the Coulomb blockade regime. For suitable discussion, we kindly ask the reader to see the paper version of our paper at the end of this chapter and also go back to chapter 3.

Instead of present a step-by-step calculation of Green's functions of Eq. (7.8) with the truncation

procedure, below we present a scheme of the complete set of Green's functions to show how the system has grown by applying the EOM approach and in what point it was needed to truncate. We properly called this scheme of "*The Green's functions Tree*". Detailed calculations can be seen in Appendix B. The final Green's function of dot is shown in Eq. (17) of the paper.

7.3 Published Paper

Spin-dependent zero-bias peak in a hybrid nanowire-quantum dot system: Distinguishing isolated Majorana fermions from Andreev bound states

L. S. Ricco,^{1,*} M. de Souza,² M. S. Figueira,³ I. A. Shelykh,^{4,5} and A. C. Seridonio^{1,2,†}

¹*Departamento de Física e Química, Universidade Estadual Paulista (Unesp), Faculdade de Engenharia, 15385-000, Ilha Solteira, São Paulo, Brazil*

²*Departamento de Física, Instituto de Geociências e Ciências Exatas, Universidade Estadual Paulista (Unesp), 13506-970, Rio Claro, São Paulo, Brazil*

³*Instituto de Física, Universidade Federal Fluminense, 24210-340, Niterói, Rio de Janeiro, Brazil*

⁴*Science Institute, University of Iceland, Dunhagi-3, IS-107, Reykjavik, Iceland*

⁵*ITMO University, St. Petersburg 197101, Russia*

(Dated: May 3, 2019)

Hybrid system composed by a semiconducting nanowire with proximity-induced superconductivity and a quantum dot at the end working as spectrometer was recently used to quantify the so-called degree of Majorana nonlocality [Deng *et al.*, *Phys.Rev.B*, **98**, 085125 (2018)]. Here we demonstrate that spin-resolved density of states of the dot responsible for zero-bias conductance peak strongly depends on the separation between the Majorana bound states (MBSs) and their relative couplings with the dot and investigate how the charging energy affects the spectrum of the system in the distinct scenarios of Majorana nonlocality (topological quality). Our findings suggest that spin-resolved spectroscopy of the local density of states of the dot can be used as a powerful tool for discriminating between different scenarios of the emergence of zero-bias conductance peak.

I. INTRODUCTION

The possibility of achieving of fault-tolerant quantum computing with qubits based on Majorana bound states (MBSs)^{1,2} started a new era in the domains of mesoscopic physics and quantum information. These exotic non-Abelian excitations³ emerge as topologically protected mid-gap zero-energy modes in so-called topological superconductors^{4,5}. The topological protection stems from the separation between individual MBSs, i.e., *nonlocality*, which is also responsible for the immunity of a setup against local perturbations and consequent loss of the information due to the processes of decoherence^{3,6}. However, it should be noticed that, for practical realizations of quantum computing systems, the MBSs qubit becomes vulnerable to the decoherence process caused by local perturbations when coupled to environment^{7,8}, which can lead to unwelcome errors in the processing of quantum information.

Topological superconductivity can be realized experimentally in hybrid superconductor-semiconductor nanowires with induced proximity effect in the presence of strong spin-orbit coupling and external magnetic field, favoring the formation of superconducting (SC) triplet states^{9,10}. In these hybrid devices, manifestation of a robust zero-bias conductance peak (ZBCP) has been considered as an experimental signature of the presence of highly nonlocal MBSs emerging at the opposite ends of a nanowire^{11–15}. However, it was argued later on that other physical mechanisms such as disorder¹⁶, Kondo effect^{17,18} and formation of Andreev bound states (ABSs)^{19–28} can be responsible for the appearance of analogs of ZBCP. In particular, there is ongoing controversy²⁹ whether near zero-energy ABS, constituted by weakly overlapping MBSs, can mimic robust $2e^2/h$ ZBCP^{22,23}. Overall, there is currently consensus that observation of ZBCP

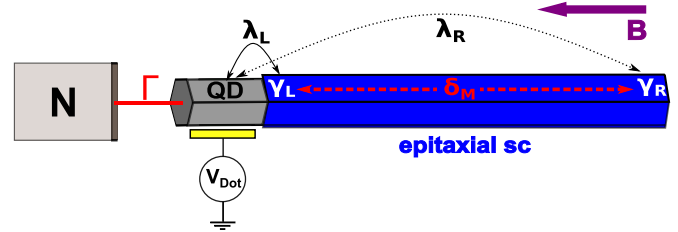


Figure 1. Sketch of the system consisting of a hybrid superconducting (SC) nanowire (blue region) coupled to a quantum dot (QD) with energy level ϵ_d , which can be tuned by application of an external gate voltage V_{Dot} . The QD is coupled to both Majorana bound states (MBSs) γ_L and γ_R at the opposite ends of SC nanowire with strengths λ_L and λ_R , respectively. The MBSs may be hybridized with each other by δ_M in the presence of an external magnetic field applied longitudinally (purple arrow) due to the finite size effects. The QD levels are broadened due to the coupling Γ with a normal metallic lead N.

only is not enough to guarantee the presence of topologically protected MBSs in the system.

A possible way to clarify the origin of ZBCP is performing tunneling spectroscopy of a quantum dot (QD)^{30,31} is assumed to be coupled to both ends of SC nanowire. In this type of experiment one can access the so-called degree of Majorana nonlocality^{14,32,33} characterizing “*how topological*” are MBSs and distinguish between the cases of well-separated MBS and near zero-energy ABSs (overlapping MBSs)^{13,21,34,35}.

Distinct from earlier works^{13,14,32,33,36}, in the present paper we analyze how charging energy of the QD single-level coupled to a normal lead affects the energy spectrum of the device sketched in the Fig. 1. To account for the correlation effects we go beyond the Hartree-Fock mean-

field approximation used by Prada *et al*³² for larger Zeeman fields, applying the method developed by Hubbard³⁷ to treat the charging energy which allows us to recover qualitatively the recent experimental profiles reported by Deng *et al*¹⁴ for a set of tunable parameters. In this sense, we demonstrate that for highly nonlocal MBSs, a plateau at zero-energy is formed in the QD density of states in the wide range of the values of the dot level and charging energies. In the case of strongly overlapping MBSs forming an ABS, the spectrum is strongly modified and this plateau disappears. Moreover, changes in MBSs degree of nonlocality strongly affect spin resolved density of states of QD, which means that spectroscopic experiment with spin-polarized local probe³⁸⁻⁴³ will allow to identify whether ZBCP is induced by topological MBSs or ABSs (overlapping Majoranas).

II. THE MODEL

The effective Hamiltonian describing the device depicted in Fig. 1 takes the following form^{32,36}

$$H = \sum_{\mathbf{k}\sigma} \varepsilon_{\mathbf{k}\sigma} e_{\mathbf{k}\sigma}^\dagger e_{\mathbf{k}\sigma} + \sum_{\sigma} \varepsilon_{d\sigma} n_{d\sigma} + U n_{d\uparrow} n_{d\downarrow} + \sqrt{2}V \sum_{\mathbf{k}\sigma} (e_{\mathbf{k}\sigma}^\dagger d_{\sigma} + d_{\sigma}^\dagger e_{\mathbf{k}\sigma}) + H_{Nw}, \quad (1)$$

where $n_{d\sigma} = d_{\sigma}^\dagger d_{\sigma}$ is the operator of the number of the electrons residing in the single-level QD, the operators $e_{\mathbf{k}\sigma}^\dagger$ ($e_{\mathbf{k}\sigma}$) correspond to the creation of the electrons (holes) in the normal (N) lead³⁶ with wave vector \mathbf{k} , spin $\sigma = \uparrow, \downarrow$ and energy $\varepsilon_{\mathbf{k}\sigma}$. The energy of an electron in the QD is spin dependent, $\varepsilon_{d\sigma} = \varepsilon_d - \sigma V_Z$, where V_Z is Zeeman energy splitting induced by an external magnetic field. U is the charging energy of the QD. The dot is coupled to the normal lead N with coupling strength $\sqrt{2}V$.

To describe the SC-nanowire hosting a pair of MBSs γ_i at the opposite ends and coupled to the QD, we use low-energy effective model developed by Prada *et. al*³², and characterized by the following Hamiltonian:

$$H_{Nw} = i\delta_M \gamma_L \gamma_R + (\lambda_L d_{\sigma} - \lambda_L^* d_{\sigma}^\dagger) \gamma_L + (\lambda_R d_{\sigma} + \lambda_R^* d_{\sigma}^\dagger) \gamma_R \quad (2)$$

where self-conjugated operators $\gamma_i = \gamma_i^\dagger$ describe localized Majorana fermions and obey the algebraic relation $\{\gamma_i, \gamma_j\} = \delta_{ij}$ ^{1,4-6}. H_{Nw} can be rewritten in the regular fermionic basis, since Majorana operators can be decomposed into pairs of normal fermionic operators, $\gamma_L = (f_{\uparrow} + f_{\uparrow}^\dagger)/\sqrt{2}$ and $\gamma_R = i(f_{\uparrow}^\dagger - f_{\uparrow})/\sqrt{2}$. The dot is coupled to the left and right MBSs, with coupling constants λ_L and λ_R , respectively. The direct hybridization δ_M between MBSs reads^{44,45}

$$\delta_M = \frac{e^{-l/2b}}{\sqrt{b}} \cos(l\sqrt{b}) E_0, \quad (3)$$

which is the function of both Zeeman energy splitting $b = V_Z/E_0$, $E_0 = (2m^* \alpha^2 \Delta_{\text{SC}}^2 / \hbar^2)^{1/3}$ and $l = L\sqrt{2m^* E_0}/\hbar$ with L being the length of the wire, m^* being electrons effective mass, α the spin-orbit coupling constant and Δ_{SC} the induced SC gap⁴⁴. The degree of MBSs nonlocality η can be defined as ratio between QD-MBSs right/left coupling strengths³²:

$$\eta^2 = \frac{|\lambda_R|}{|\lambda_L|} \quad (4)$$

This parameter can be experimentally accessed through the measurement of the conductance as a function of the gate potential changing the energy of a QD and drain-source voltage¹⁴ and estimated as the ratio between energy values in which the Majorana and QD states are on resonance (anticrossing points)³², $\eta^2 \approx \epsilon_{\text{MBS}}^\pm / \epsilon_{\text{QD}}^\pm$ [See Fig 2(d-f)].

A. Density of states calculations

Our main goal is to investigate how the spectral properties of the QD accessible in spin-resolved measurements are changing when the degree of MBSs nonlocality characterized by the parameter η ³² is modified. Hence, it is suitable to evaluate the total density of states (DOS) in the QD, which reads:

$$\text{DOS}(\omega) = \pi\Gamma \sum_{\sigma} \rho_{\sigma}(\omega), \quad (5)$$

where the constant $\Gamma = 2\pi V^2 \rho_0$ is the QD-N lead effective coupling⁴⁶, with ρ_0 being the DOS of the lead. The quantity

$$\rho_{\sigma}(\omega) = -\frac{1}{\pi} \text{Im}[G_{d,d}^{r,\sigma}(\omega)] \quad (6)$$

denotes the DOS corresponding to a given spin orientation, which is determined by the retarded Green's function of the QD $G_{d,d}^{r,\sigma}(\omega)$ in the spectral domain. The application of the equation of motion (EOM) method⁴⁷ leads to the following equation (Appendix A):

$$(\omega^+ - \varepsilon_{d\sigma} - \Sigma_{M,\sigma}^{U=0} + i\Gamma) G_{d,d}^{r,\sigma}(\omega) = 1 + U G_{d_{\sigma} n_{d\bar{\sigma}}, d_{\sigma}}^r(\omega) + U(|\lambda_L|^2 - |\lambda_R|^2) \bar{K}^{\sigma} G_{d_{\sigma} n_{d\bar{\sigma}}, d_{\sigma}}^r(\omega), \quad (7)$$

where $\omega^+ = \omega + i0^+$, $\Sigma_{M,\sigma}^{U=0} = K_1 + (|\lambda_L|^2 - |\lambda_R|^2)^2 K \bar{K}^{\sigma}$ is the self-energy³⁶ due to QD-MBSs hybridization in the absence of the charging energy, and

$$K = \frac{1}{2} \left(\frac{1}{\omega^+ + \delta_M} + \frac{1}{\omega^+ - \delta_M} \right), \quad (8)$$

$$\bar{K}^\sigma = \frac{1}{2} \left(\frac{K}{\omega^+ + \varepsilon_{d\sigma} - K_2 + i\Gamma} \right), \quad (9)$$

$$K_1 = \frac{1}{2} \cdot \left[\frac{(|\lambda_L| - |\lambda_R|)^2}{\omega^+ - \delta_M} + \frac{(|\lambda_L| + |\lambda_R|)^2}{\omega^+ + \delta_M} \right] \quad (10)$$

and

$$K_2 = \frac{1}{2} \cdot \left[\frac{(|\lambda_L| - |\lambda_R|)^2}{\omega^+ + \delta_M} + \frac{(|\lambda_L| + |\lambda_R|)^2}{\omega^+ - \delta_M} \right]. \quad (11)$$

The presence of the two-particle operator corresponding to the charging energy term in the Hamiltonian [Eq. (1)] leads to the appearance of the two particle Green's functions in the Eq. (7). The iterative application of the EOM procedure to such higher order functions will produce an infinite chain of the equations which should be truncated at some point⁴⁷. Distinct from the earlier work³² in which the charging energy of the dot was accounted for using a mean-field approximation, here we take a step further by following Hubbard-I truncation scheme³⁷. This allows us to account for the appearance of the so-called Hubbard peaks and thus describe better the physics of Coulomb blockade regime. Note, however, that in our approach Kondo-type correlations are fully neglected, and it is applicable only if $T_K/\Delta_{SC} \gtrsim 0.6$ ³² or $T \gg T_K$, wherein T_K is the Kondo temperature^{17,18}. Further details of the calculations can be found in the Appendix B.

After Hubbard-I truncation, the two-particle Green's functions take the following form:

$$G_{d_\sigma n_{d\bar{\sigma}}; d_\sigma}^r(\omega) = \frac{\langle n_{d\bar{\sigma}} \rangle}{\omega^+ - \varepsilon_{d\sigma} - U - \Sigma_{M,\sigma}^{U \neq 0} + i\Gamma}, \quad (12)$$

and

$$G_{d_\sigma^\dagger n_{d\bar{\sigma}} d_\sigma}^r(\omega) = -(|\lambda_L|^2 - |\lambda_R|^2) \bar{K}_U^\sigma G_{d_\sigma n_{d\bar{\sigma}}; d_\sigma}^r(\omega), \quad (13)$$

wherein

$$\langle n_{d\bar{\sigma}} \rangle = \int_{-\infty}^0 d\omega \rho_{\bar{\sigma}}(\omega) \quad (14)$$

gives the occupation number of the dot per spin $\bar{\sigma}$ (opposite to σ) at $T = 0$. The self-energy term provided by the presence of MBSs and charging energy U is given by

$$\Sigma_{M,\sigma}^{U \neq 0} = K_1 + (|\lambda_L|^2 - |\lambda_R|^2)^2 K \bar{K}_U^\sigma \quad (15)$$

where

$$\bar{K}_U^\sigma = \frac{1}{2} \cdot \frac{K}{\omega^+ + \varepsilon_{d\sigma} + U + K_2 + i\Gamma} \quad (16)$$

After some algebra we get from Eqs. (7), (12) and (13) the following expression for the retarded Green's function

of the dot:

$$G_{d,d}^{r,\sigma}(\omega) = \frac{\lambda(\omega, \sigma\bar{\sigma}) - U(|\lambda_L|^2 - |\lambda_R|^2)^2 \mathcal{M}(\omega, \sigma\bar{\sigma})}{\omega^+ - \varepsilon_{d\sigma} - \Sigma_{M,\sigma}^{U=0} + i\Gamma} \quad (17)$$

with

$$\lambda(\omega, \sigma\bar{\sigma}) = 1 + \frac{U \langle n_{d\bar{\sigma}} \rangle}{\omega^+ - \varepsilon_{d\sigma} - U - \Sigma_{M,\sigma}^{U \neq 0} + i\Gamma} \quad (18)$$

and

$$\mathcal{M}(\omega, \sigma\bar{\sigma}) = \frac{\langle n_{d\bar{\sigma}} \rangle \bar{K}^\sigma \bar{K}_U^\sigma}{\omega^+ - \varepsilon_{d\sigma} - U - \Sigma_{M,\sigma}^{U \neq 0} + i\Gamma}. \quad (19)$$

III. RESULTS AND DISCUSSION

We investigate the energy spectrum of the device depicted in Fig. 1 analyzing the DOS of the QD [Eq. (5)] as a function of spectral frequency ω and dot energy level ε_d for several regimes corresponding to the different ratios between the parameters of the system. The relevant parameters of our model, in units of E_0 , are the charging energy U , hybridization λ_L (λ_R) between the dot and MBS(left/right) and Zeeman energy splitting V_Z , which modulates the direct overlap δ_M between the MBSs at the opposite nanowire ends. The length of the SC was chosen as $L \approx 0.1\mu\text{m}$, in accordance with the results presented in the Ref. 44. The occupation numbers for each spin [Eq. (14)] were self-consistently computed. In all the situations, the QD-left MBS coupling strength is kept fixed ($\lambda_L = 1.0E_0$). Concerning the charging energy strength U , we follow Prada *et al.*³² effective Hamiltonian, assuming that $U > \Delta$.

Fig. 2(a) corresponds to the highest nonlocal situation ($\eta = 0$), where SC nanowire is long enough ($L \approx 2.0\mu\text{m}$) to ensure formation of isolated MBSs at the ends ($\delta_M = 0$). In this regime, the dot couples only with the left MBS ($\lambda_R = 0$). As predicted by the earlier works^{14,32,33}, the Majorana states remain unperturbed under variations of the QD energy level, since the latter can not cross the topologically protected zero-energy MBSs.

For shorter wires ($L \approx 0.4\mu\text{m}$), Fig. 2(b), DOS of the dot reveals the so-called "bowtie" profile, characteristic to the regime when the overlap between MBSs is finite and the dot is only weakly hybridized with rightmost Majorana ($\lambda_L, \delta_M \gg \lambda_R$)³². In this situation the topological protection is absent and the energies of the overlapping MBSs are strongly perturbed in the vicinity of the resonance with the QD state. The splitting of near-zero states is ruled by direct hybridization between MBSs $2\delta_M$ (See yellow bar in the panel (b)).

Fig. 2(c) demonstrates the spectra for the case of the local fermionic zero-mode ($\delta_M = 0$ and $\eta = 1$), corresponding to the highest localization of MBSs (lowest topological quality factor³³), for which any pronounced structure at $\omega = 0$ is absent.

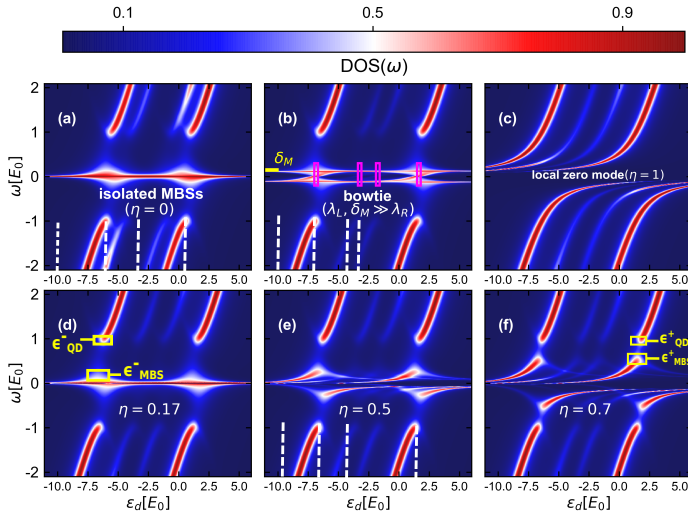


Figure 2. Color scale plots of the DOS of a QD as a function of QD energy level ε_d and spectral frequency ω for distinct regimes. In all situations we chose $U = 5E_0$ and $\lambda_L = 1.0E_0$. (a) highly nonlocal isolated MBSs ($\delta_M = \lambda_R = 0$) for $V_Z = 0.8E_0$ and $L = 2.0\mu\text{m}$; (b) bowtie profile, wherein $V_Z = 1.72E_0$, $L = 0.4\mu\text{m}$, $\delta_M = 0.12E_0$ and $\lambda_R = 0.003E_0$. (c) regular fermionic zero mode ($\lambda_L = \lambda_R = E_0$, $\delta_M = 0$), with $L = 0.4\mu\text{m}$ and $V_Z = 1.38E_0$; (d)-(f) diamond profiles ($\delta_M \ll \lambda_R, \lambda_L$), with actual nanowire length $L = 0.4\mu\text{m}$. Panel (d) exhibits the situation for $V_Z = 1.4E_0$, $\delta_M = 0.004E_0$ and $\lambda_R = 0.03E_0$. In (e) we have set $V_Z = 1.5E_0$, $\delta_M = 0.04E_0$ and $\lambda_R = 0.25E_0$, while in panel (f) $V_Z = 1.6E_0$, $\delta_M = 0.08E_0$ and $\lambda_R = 0.5E_0$.

The panels (d)-(f) of the Fig. 2 correspond to the case of the shorter SC nanowires ($L \approx 0.4\mu\text{m}$), for which $\delta_M \neq 0$ but $\delta_M \ll \lambda_R$. This regime corresponds to the situation wherein the wave function describing the right MBS moves towards the QD due to the application of the magnetic field^{15,23}. One can notice the presence of the previously reported “diamond” profiles^{14,32}. Fig. 2(d) shows the diamond lineshape for a quasi-ideal case of the isolated MBSs ($\eta = 0.17$), while panels (e) and (f) illustrate the situations where the nonlocal feature was suppressed by enhancing λ_R and, consequently η . The loss of the nonlocality ($\eta \rightarrow 1$) is related to the displacement of the right MBS (γ_R) wave function towards the left MBS, increasing the overlap between such states and enhancing the hybridization λ_R of right Majorana mode with the dot state. By comparing the Figs. 2(d)-(f), it can be noticed that ABS formation due to the strong localization of the right MBS near the QD gives rise to the disintegration of the diamond shapes. In other words, the closer $\epsilon_{\text{MBS}}^\pm$ is to ϵ_{QD}^\pm (See panels (d) and (f)), the higher is the local nature of MBSs and the lower is the topological quality of the device.

It is worth noting that the results presented in the Fig. 2 differ from analogous results of the earlier works^{14,32} due to the presence of extra crossing points appearing in the middle region of all the panels. This feature is direct outcome of the theoretical treatment af-

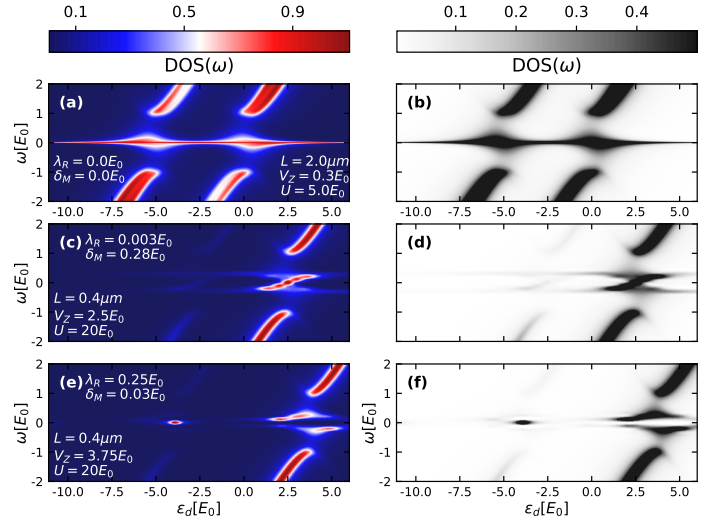


Figure 3. Color scale plots of the DOS of a QD as a function of QD energy level ε_d and spectral frequency ω for distinct regimes. In all situations we chose $\lambda_L = 1.0E_0$. Left panels show (a) isolated MBSs, (c) bowtie and (e) diamond profiles, corresponding to the cases illustrated by Fig. 2(a), (b) and (e), respectively, but for the distinct values of Zeeman splitting V_Z and charging energy U . Right panels reproduce the corresponding left ones in the reduced gray scale.

forded by Hubbard-I approximation³⁷ to charging energy term of the system Hamiltonian [Eq. (1)]. It is known that such approximation makes the condition of the transition to ferromagnetic state more restrictive compared to Hartree-Fock mean-field approximation, since it accounts for the higher order correlations thus reducing the energy of non-magnetic states with respect to ferromagnetic ones³⁷. For this reason, Hartree-Fock mean-field approximation works well for larger Zeeman fields, as previously noticed by Prada *et al*³². However, within such a mean-field approach for any value of V_Z , the information about correlated motion of electrons is only taken into account with the mean occupation⁴⁸. Hubbard-I decoupling scheme accounts for such correlated motion, which gives rise to the appearance of the so-called Hubbard peaks at $\varepsilon_{d\sigma}$ and $\varepsilon_{d\sigma} + U$, describing the regime of the Coulomb blockade. From the experimental perspective, the work of Deng *et al*¹⁴ shows the validity of the Hartree-Fock approach, since such an experiment was performed under relatively larger Zeeman fields, which are enough to resolve the QD spin-degrees of freedom. In this work, by using the Hubbard I decoupling scheme, we predict the system behavior in the scenario of weaker Zeeman splitting, which could be addressed in future experiments.

Detuning of the parameters V_Z and U from the value corresponding to the Figs. 2(a), (b) and (e) allows us to recover low-energy spectrum theoretically predicted within the Hartree-Fock mean-field approximation³², which was experimentally verified by Deng *et al*¹⁴, thus ensuring the comprehensiveness of the ap-

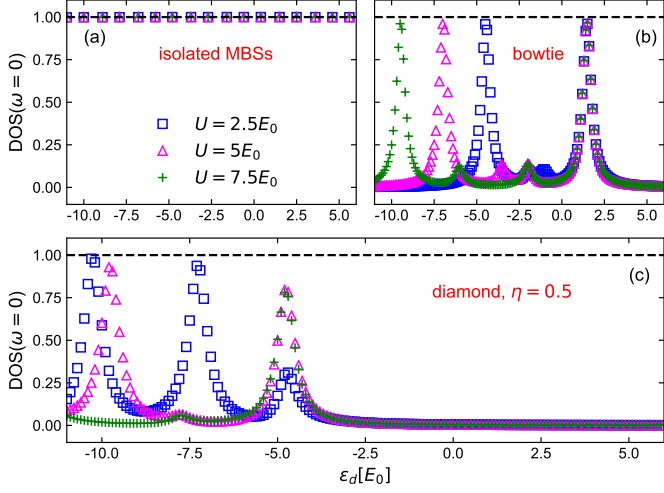


Figure 4. Density of states as a function of the QD level ε_d at $\omega = 0$ for (a) isolated MBSs, (b) bowtie and (c) diamond configurations. Plots for several values of charging energy [$U = 2.5E_0$ (blue squares), $5E_0$ (magenta triangles) and $7.5E_0$ (green crosses)] are presented.

proximation employed here. Figs. 3(a)-(b) illustrate the case of isolated MBSs, but with V_Z lower than that of Fig. 2(a). Such a Zeeman splitting is unable to resolve spin up and down states of the QD. Consequently, instead of a four-peak structure, profiles with only two peaks resembling those presented in the Fig. 4(d) of the Ref. 14 appear. Figs. 3(c)-(d) show bowtie profiles corresponding to $V_Z = 2.5E_0$ and $U = 20E_0$ and comparable to those presented in the Fig. 3(b) of Ref. 14. In the corresponding scenario only two peaks are present as well, since higher charging energy sets other peaks outside the considered range of ε_d . Increase of the value of U results in the profiles shown in the Figs. 3(e)-(f) corresponding to the diamond situation shown in the Fig. 2(e) and comparable to those presented in the Fig. 3(c) of the Ref. 14.

Fig 4 shows the DOS of the dot as a function of QD level ε_d at $\omega = 0$ for (a) isolated MBSs, (b) bowtie and (c) diamond situations, for distinct strengths of the dot charging energy [$U = 2.5E_0$ (blue squares), $5E_0$ (magenta triangles) and $7.5E_0$ (green crosses)]. In the highest nonlocal case [Fig 4(a)], the insensitivity of the zero frequency peak to the tuning of the QD level and variations of the dot charging energy is verified^{14,32,33}. There is a plateau in the total DOS characteristic to ZBCP. This scenario breaks down for the possible situation of the formation of ABS due to the overlap between MBSs [Fig 4(b-c)]. In this case the plateau in the DOS is destroyed and positions of the peaks change with variations of both position of the dot level ε_d and charging energy U . Fig 4(b) describes a linecut at $\omega = 0$ for the bowtie configuration, wherein the four resonances for $U = 5E_0$ (magenta triangles) correspond to the anticrossings between the dot level and near zero-energy states appearing in the Fig 2(b) (indicated by magenta rectangles). These

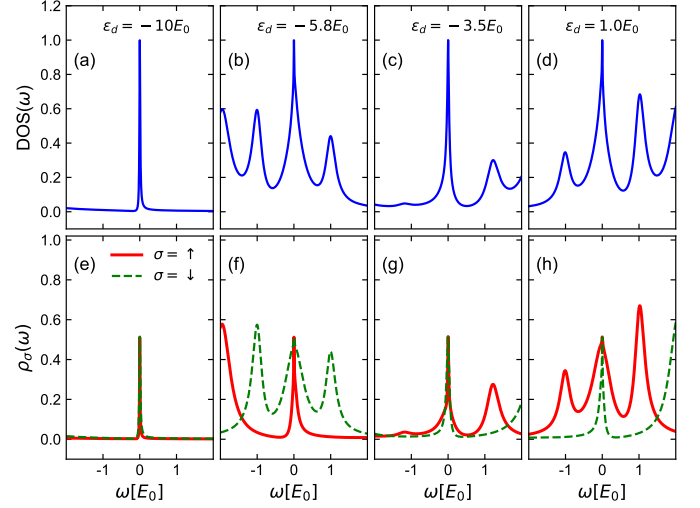


Figure 5. (a)-(d): (a)-(d): total DOS as a function of ω for MBSs (corresponding to the Fig.2(a)) for various values of ε_d corresponding to the vertical dashed white lines in Fig. 2(a). (e)-(h) spin resolved DOS $\rho_\sigma(\omega)$ for same parameters as in the panels (a)-(d)

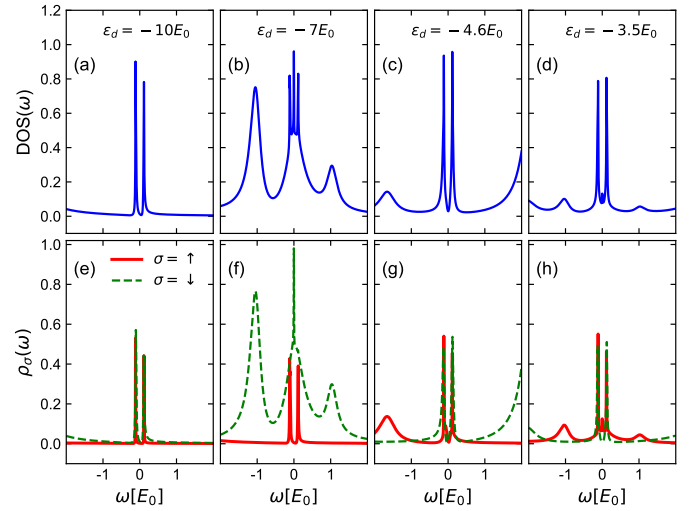


Figure 6. (a)-(d): total DOS as a function of ω for bowtie profile (corresponding to the Fig.2(b)) for various values of ε_d corresponding to the vertical dashed white lines in Fig. 2(b). (e)-(h) spin resolved DOS $\rho_\sigma(\omega)$ for same parameters as in the panels (a)-(d)

anticrossing points (resonance positions) are strongly dependent on the charging energy, since near zero-energy ABS, which can be a trivial non-protected state, is affected by the QD energy levels. Similar behavior is found for a diamond profile with degree of nonlocality $\eta = 0.5$, as it is shown in the Fig. 4(c). Moreover, the plateau depicted in the Fig. 4(a) also allows to distinguish the Majorana ZBCP from that induced by usual Kondo effect, since Kondo resonance only appears when a QD is single occupied, $\varepsilon_d < \varepsilon_F$, as verified by one of us in the

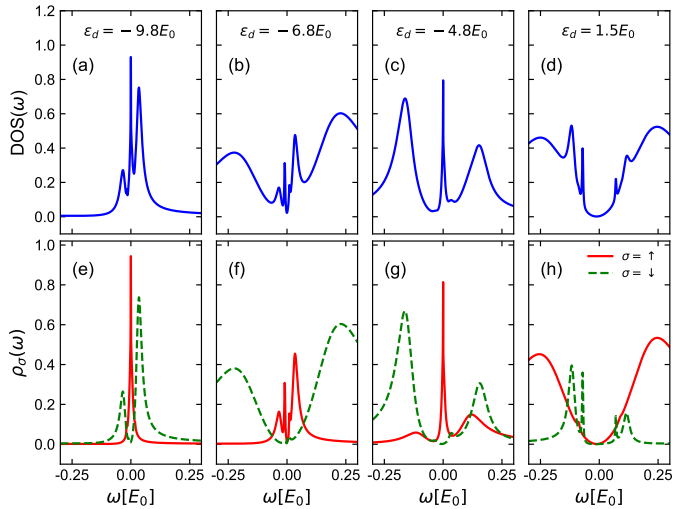


Figure 7. (a)-(d): total DOS as a function of ω for diamond profile for various values of ε_d corresponding to the vertical dashed white lines in Fig. 2(e). (e)-(h) spin resolved DOS $\rho_\sigma(\omega)$ for same parameters as in the panels (a)-(d)

Ref. 49 (see Fig. 1(g)-(i) of that paper).

The impact of each spin component to the total DOS is presented in the Figs. 5, 6 and 7 for isolated MBSs, bowtie [Fig.2(b)] and diamond [Fig.2(e)] configurations, respectively. Panels (a)-(d) of the Fig. 5 show the DOS of the dot for isolated MBSs configuration [Fig.2(a)] as a function of ω for several values of ε_d indicated by the white dashed lines in the Fig. 2(a). As can be seen, a peak at $\omega = 0$ emerges for all values of the dot energy as observed in the panels (a)-(d). Panels (e)-(h) of the same figure reveal that zero-peak structure in the total DOS is spin degenerated: at $\omega = 0$, $\rho_\uparrow = \rho_\downarrow$.

This degeneracy is broken when MBSs overlap ($\delta_M \neq 0$) and the dot hybridizes with the rightmost Majorana ($\lambda_R \neq 0$) as well, as it is demonstrated for the bowtie configuration in the Fig. 6. In this case a zero-peak structure in the total DOS emerges only when ε_d crosses zero-energy as it happens in the panel (b). In this case DOS around $\omega = 0$ becomes spin sensitive, $\rho_\uparrow \neq \rho_\downarrow$, as one can verify from the panel (f), thus suggesting the situation of the spin-dependent transport.

Diamond configuration also displays spin-dependent behavior, as it is shown in the Fig. 7. However, there is a remarkable difference from the bowtie case: the near zero-energy two-peaks having $\sigma = \uparrow$ are no longer pinned and merge with one another at $\omega = 0$ [panels (e) and (g)] for certain values of ε_d , giving rise to zero-peak structure in the DOS, as displayed in the panels (a) and (c). Such a feature is consistent with the picture of coalescing ABSs (overlapped MBSs), which can mimic the behavior MBSs under certain conditions^{21–23,34,35}. It also can be verified for the situations where the QD level does not shift the near-zero peaks describing ABSs towards $\omega = 0$ [panels(f) and (h)] and consequently there is no peak structure at zero-energy in DOS [panels (b) and

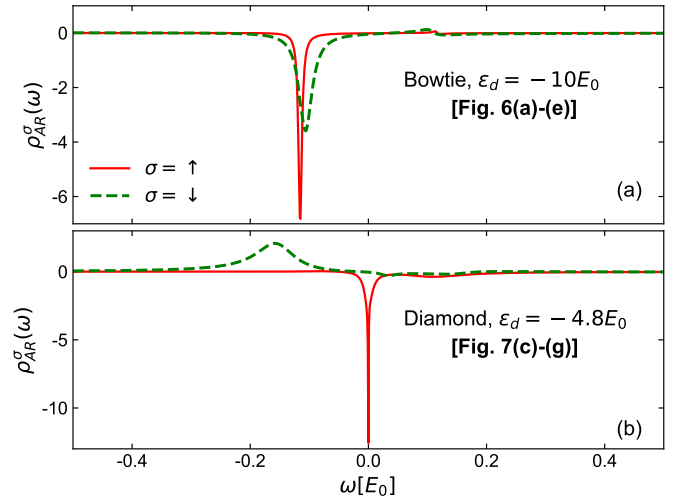


Figure 8. DOS related to AR processes for each spin component, wherein two representative situations were considered. Panel (a) depicts the same case of Figs. 6(a)-(e), while panel (b) is related to Figs. 7(c)-(g).

(d)].

It is worth noting that the presence of ABSs in the total DOS of a QD [Eq. (5)] in the results presented in the Figs. 4, 6 and 7 can be confirmed by the computation of the anomalous Green's function $G_{f_\uparrow^\dagger, d_\sigma}^r(\omega)$. The latter enters into the Green's function of the QD according to the Eq. (A4), describes the correlation between QD (d_σ^\dagger) and SC nanowire appearing due Andreev reflection (AR)^{20,50,51} and can be defined in the time domain as:⁴⁸

$$G_{f_\uparrow^\dagger, d_\sigma}^r(t-t') = -i\theta(t-t')\langle\{f_\uparrow^\dagger(t), d_\sigma^\dagger(t')\}\rangle, \quad (20)$$

wherein $\theta(t-t')$ is Heaviside function, $\{\dots, \dots\}$ denotes anticommutator and f_\uparrow^\dagger corresponds to the creation of a non-local fermion in SC nanowire, which is formed by the linear combination of the left (γ_L) and right (γ_R) MBSs, i.e., $f_\uparrow^\dagger = (\gamma_L - v\gamma_R)/\sqrt{2}$ and $f_\uparrow = (\gamma_L + v\gamma_R)/\sqrt{2}$.

AR can take place through different transport channels, once QD is coupled to the both ends of a nanowire (λ_L and $\lambda_R \neq 0$). The presence of the coupling asymmetry can give rise to the appearance of Fano antiresonances^{36,52–54} as it can be seen in the Fig. 8, where we illustrate AR process by plotting $\rho_{AR}^\sigma(\omega) = -\text{Im}\{G_{f_\uparrow^\dagger, d_\sigma}^r(\omega)\}/\pi$ for two representative “bowtie” and “diamond” configurations (see Figs. 6(a)-(e) and 7(c)-(g), respectively).

IV. CONCLUSIONS

We presented the theoretical study of MBSs nonlocality in the hybrid device sketched in the Fig. 1. It was analyzed in detail how the charging energy affects spin resolved DOS of a QD coupled with MBSs. For highly

nonlocal MBSs there is a plateau at zero-energy in the QD density of states for any values of the dot level and charging energy. For overlapping MBSs the spectrum of the dot is strongly modified. It was shown that the zero-peak structure in the DOS reveals pronounced spin dependence if MBSs become hybridized. Our findings suggest that a spin-dependent local probe may be used as a tool to resolve an outstanding problem in experimental Majorana physics: discriminating between the cases when ZBCP is due to the isolated MBSs or ABSs.

V. ACKNOWLEDGMENTS

We thank the funding Brazilian agencies CNPq (Grants No. 307573/2015-0 and No. 305668/2018-8) and São Paulo Research Foundation (FAPESP) Grant No. 2015/23539-8. IAS acknowledges support by Horizon2020 RISE project CoExAN. MdS acknowledges the Austrian Academy of Science ÖAW for the JESH fellowship and Serdar Sariciftci for the hospitality.

Appendix A: Quantum dot Green's function derivation

In this Appendix we present the main steps concerning on derivation of Eq. (7) via EOM technique. It is known that such a method can be summarized according to^{47,48}

$$(\omega + i0^+)G_{c_i c_j}^r(\omega) = \{c_i, c_j^\dagger\} + G_{[c_i, \mathcal{H}]; c_j}^r(\omega), \quad (\text{A1})$$

wherein $c_{i(j)}$ is a fermionic operator belonging to Hamiltonian \mathcal{H} . Hence, the Green's function of QD is given by:

$$(\omega + i0^+)G_{d_\sigma d_\sigma}^r(\omega) = 1 + G_{[d_\sigma, H]; d_\sigma}^r, \quad (\text{A2})$$

with

$$\begin{aligned} [d_\sigma, H] &= \varepsilon_{d_\sigma} d_\sigma + U d_\sigma n_{d\bar{\sigma}} + \sqrt{2}V \sum_{\mathbf{k}} e_{\mathbf{k}\sigma} \\ &\quad - \lambda \sum_{\bar{\sigma}} \delta_{\sigma\bar{\sigma}} f_{\uparrow} - \lambda' \sum_{\bar{\sigma}} \delta_{\sigma\bar{\sigma}} f_{\uparrow}^\dagger, \end{aligned} \quad (\text{A3})$$

where $f_{\uparrow}^\dagger(f_{\uparrow})$ stands for creation(annihilation) of a non-local fermion in the hybrid SC nanowire, since it can be rewritten as a linear combination of MBSs at opposite ends of the nanowire. Within this picture, the coupling strengths between the QD and the nonlocal fermionic site are given by $\lambda = (|\lambda_L| - |\lambda_R|)/\sqrt{2}$ and $\lambda' = (|\lambda_L| + |\lambda_R|)/\sqrt{2}$, respectively. Eq (A3) allows to

write that

$$\begin{aligned} (\omega^+ - \varepsilon_{d_\sigma})G_{d_\sigma d_\sigma}^r(\omega) &= \\ &1 + U G_{d_\sigma n_{d\bar{\sigma}}, d_\sigma}^r(\omega) + \sqrt{2}V \sum_{\mathbf{k}} G_{e_{\mathbf{k}\sigma} d_\sigma}^r(\omega) \\ &\quad - \lambda \sum_{\bar{\sigma}} \delta_{\sigma\bar{\sigma}} G_{f_{\uparrow}, d_\sigma}^r(\omega) - \lambda' \sum_{\bar{\sigma}} \delta_{\sigma\bar{\sigma}} G_{f_{\uparrow}^\dagger, d_\sigma}^r(\omega), \end{aligned} \quad (\text{A4})$$

with $\omega^+ \rightarrow \omega + i0^+$. The three last Green's functions also are obtained through straightforward application of EOM technique [Eq. (A1)], being respectively given by:

$$G_{e_{\mathbf{k}\sigma} d_\sigma}^r(\omega) = \sqrt{2}V \sum_{\mathbf{k}} \frac{1}{(\omega^+ - \varepsilon_{\mathbf{k}\sigma})} G_{d_\sigma d_\sigma}^r(\omega), \quad (\text{A5})$$

$$\begin{aligned} (\omega^+ - \delta_M)G_{f_{\uparrow} d_\sigma}^r(\omega) &= \\ &-\lambda \sum_{\bar{\sigma}} G_{d_{\bar{\sigma}} d_\sigma}^r(\omega) + \lambda' \sum_{\bar{\sigma}} G_{d_{\bar{\sigma}}^\dagger d_\sigma}^r(\omega) \end{aligned} \quad (\text{A6})$$

and

$$\begin{aligned} (\omega^+ + \delta_M)G_{f_{\uparrow}^\dagger d_\sigma}^r(\omega) &= \\ &\lambda \sum_{\bar{\sigma}} G_{d_{\bar{\sigma}}^\dagger d_\sigma}^r(\omega) - \lambda' \sum_{\bar{\sigma}} G_{d_{\bar{\sigma}} d_\sigma}^r(\omega). \end{aligned} \quad (\text{A7})$$

Substituting Eqs. (A5), (A6) and (A7) into Eq. (A4), we find

$$\begin{aligned} \left(\omega^+ - \varepsilon_{d_\sigma} + i\Gamma - \frac{\lambda^2}{\omega^+ - \delta_M} - \frac{\lambda'^2}{\omega^+ + \delta_M} \right) G_{d_\sigma d_\sigma}^r(\omega) &= \\ &1 + U G_{d_\sigma n_{d\bar{\sigma}}, d_\sigma}^r(\omega) - (2\lambda\lambda') K G_{d_\sigma^\dagger d_\sigma}^r(\omega), \end{aligned} \quad (\text{A8})$$

where K is given by Eq. (8) and Γ is the Anderson parameter⁴⁶. We now evaluate the Green's function $G_{d_\sigma^\dagger d_\sigma}^r(\omega)$, getting the following result:

$$\begin{aligned} \left(\omega^+ + \varepsilon_{d_\sigma} + i\Gamma - \frac{\lambda^2}{\omega^+ + \delta_M} - \frac{\lambda'^2}{\omega^+ - \delta_M} \right) G_{d_\sigma^\dagger d_\sigma}^r(\omega) &= \\ &-U G_{d_\sigma^\dagger n_{d\bar{\sigma}}, d_\sigma}^r(\omega) - (2\lambda\lambda') K G_{d_\sigma d_\sigma}^r(\omega). \end{aligned} \quad (\text{A9})$$

Substituting into Eq. (A8) and recognizing \bar{K}_σ [Eq. (9)], K_1 [Eq. (10)] and K_2 [Eq. (11)], is now easy to show that Eq. (A8) becomes into Eq. (7).

Appendix B: Hubbard-I Approximation

We now evaluate the two particle Green's functions of Eq. (7) according to EOM. Following Eq. (A1), we have

$$(\omega + i\eta^+)G_{d_\sigma n_{d\bar{\sigma}}, d_\sigma}^r(\omega) = \langle n_{d\bar{\sigma}} \rangle + G_{[d_\sigma n_{d\bar{\sigma}}, H]; d_\sigma}^r(\omega). \quad (\text{B1})$$

Deriving the commutator

$$\begin{aligned}
[d_{\sigma}n_{d\bar{\sigma}}, H] &= \varepsilon_{d\sigma}d_{\sigma}n_{d\bar{\sigma}} + Ud_{\sigma}n_{d\bar{\sigma}} \\
&+ \sqrt{2V} \sum_{\mathbf{k}} (-e_{\mathbf{k}\bar{\sigma}}^{\dagger}d_{\bar{\sigma}}d_{\sigma} + d_{\bar{\sigma}}^{\dagger}e_{\mathbf{k}\bar{\sigma}}d_{\sigma} + e_{\mathbf{k}\sigma}n_{d\bar{\sigma}}) \\
&+ \lambda \sum_{\bar{\sigma}} (-\delta_{\bar{\sigma}\sigma}d_{\bar{\sigma}}f_{\uparrow}^{\dagger}d_{\sigma} + \delta_{\bar{\sigma}\sigma}f_{\uparrow}d_{\bar{\sigma}}^{\dagger}d_{\sigma} - \delta_{\bar{\sigma}\sigma}f_{\uparrow}n_{d\bar{\sigma}}) \\
&+ \lambda' \sum_{\bar{\sigma}} (-\delta_{\bar{\sigma}\sigma}d_{\bar{\sigma}}f_{\uparrow}d_{\sigma} + \delta_{\bar{\sigma}\sigma}f_{\uparrow}^{\dagger}d_{\bar{\sigma}}^{\dagger}d_{\sigma} - \delta_{\bar{\sigma}\sigma}f_{\uparrow}^{\dagger}n_{d\bar{\sigma}}), \quad (\text{B2})
\end{aligned}$$

we find

$$\begin{aligned}
(\omega^+ - \varepsilon_{d\sigma} - U)G_{d_{\sigma}n_{d\bar{\sigma}}, d_{\sigma}}^r(\omega) &= \langle n_{d\bar{\sigma}} \rangle \\
&+ \sqrt{2V} \sum_{\mathbf{k}} G_{e_{\mathbf{k}\sigma}n_{d\bar{\sigma}}, d_{\sigma}}^r(\omega) + \sqrt{2V} \sum_{\mathbf{k}} G_{d_{\bar{\sigma}}^{\dagger}e_{\mathbf{k}\bar{\sigma}}d_{\sigma}d_{\sigma}}^r(\omega) \\
&- \sqrt{2V} \sum_{\mathbf{k}} G_{e_{\mathbf{k}\bar{\sigma}}^{\dagger}d_{\bar{\sigma}}d_{\sigma}, d_{\sigma}}^r(\omega) - \lambda \sum_{\bar{\sigma}} \delta_{\bar{\sigma}\sigma} G_{f_{\uparrow}n_{d\bar{\sigma}}, d_{\sigma}}^r(\omega) \\
&+ \lambda \sum_{\bar{\sigma}} \delta_{\bar{\sigma}\sigma} G_{f_{\uparrow}d_{\bar{\sigma}}^{\dagger}d_{\sigma}d_{\sigma}}^r(\omega) - \lambda \sum_{\bar{\sigma}} \delta_{\bar{\sigma}\sigma} G_{d_{\bar{\sigma}}f_{\uparrow}^{\dagger}d_{\sigma}d_{\sigma}}^r(\omega) \\
&- \lambda' \sum_{\bar{\sigma}} \delta_{\bar{\sigma}\sigma} G_{f_{\uparrow}^{\dagger}n_{d\bar{\sigma}}, d_{\sigma}}^r(\omega) + \lambda' \sum_{\bar{\sigma}} \delta_{\bar{\sigma}\sigma} G_{f_{\uparrow}^{\dagger}d_{\bar{\sigma}}^{\dagger}d_{\sigma}, d_{\sigma}}^r(\omega) \\
&- \lambda' \sum_{\bar{\sigma}} \delta_{\bar{\sigma}\sigma} G_{d_{\bar{\sigma}}f_{\uparrow}d_{\sigma}d_{\sigma}}^r(\omega). \quad (\text{B3})
\end{aligned}$$

At this point we apply the Hubbard-I decoupling scheme³⁷ by considering the following approximations:

$$G_{d_{\bar{\sigma}}^{\dagger}e_{\mathbf{k}\bar{\sigma}}d_{\sigma}d_{\sigma}}^r(\omega) \approx \langle d_{\bar{\sigma}}^{\dagger}e_{\mathbf{k}\bar{\sigma}} \rangle G_{d_{\sigma}d_{\sigma}}^r(\omega), \quad (\text{B4})$$

$$G_{e_{\mathbf{k}\bar{\sigma}}^{\dagger}d_{\bar{\sigma}}d_{\sigma}, d_{\sigma}}^r(\omega) \approx \langle e_{\mathbf{k}\bar{\sigma}}^{\dagger}d_{\bar{\sigma}} \rangle G_{d_{\sigma}d_{\sigma}}^r(\omega), \quad (\text{B5})$$

$$G_{a_{\uparrow}d_{\bar{\sigma}}^{\dagger}d_{\sigma}d_{\sigma}}^r(\omega) \approx \langle a_{\uparrow}d_{\bar{\sigma}}^{\dagger} \rangle G_{d_{\sigma}d_{\sigma}}^r(\omega), \quad (\text{B6})$$

$$G_{d_{\bar{\sigma}}a_{\uparrow}^{\dagger}d_{\sigma}d_{\sigma}}^r(\omega) \approx \langle d_{\bar{\sigma}}a_{\uparrow}^{\dagger} \rangle G_{d_{\sigma}d_{\sigma}}^r(\omega), \quad (\text{B7})$$

$$G_{a_{\uparrow}^{\dagger}d_{\bar{\sigma}}^{\dagger}d_{\sigma}, d_{\sigma}}^r(\omega) \approx \langle a_{\uparrow}^{\dagger}d_{\bar{\sigma}}^{\dagger} \rangle G_{d_{\sigma}d_{\sigma}}^r(\omega), \quad (\text{B8})$$

and

$$G_{d_{\bar{\sigma}}a_{\uparrow}d_{\sigma}d_{\sigma}}^r(\omega) \approx \langle d_{\bar{\sigma}}a_{\uparrow} \rangle G_{d_{\sigma}d_{\sigma}}^r(\omega). \quad (\text{B9})$$

Taking into account that $\langle d_{\bar{\sigma}}^{\dagger}e_{\mathbf{k}\bar{\sigma}} \rangle = \langle e_{\mathbf{k}\bar{\sigma}}^{\dagger}d_{\bar{\sigma}} \rangle$, $\langle a_{\uparrow}d_{\bar{\sigma}}^{\dagger} \rangle = \langle d_{\bar{\sigma}}a_{\uparrow}^{\dagger} \rangle$ and $\langle a_{\uparrow}^{\dagger}d_{\bar{\sigma}}^{\dagger} \rangle = \langle d_{\bar{\sigma}}a_{\uparrow} \rangle$, Eq. (B3) becomes into

$$\begin{aligned}
(\omega^+ - \varepsilon_{d\sigma} - U)G_{d_{\sigma}n_{d\bar{\sigma}}, d_{\sigma}}^r(\omega) &= \langle n_{d\bar{\sigma}} \rangle \\
&+ \sqrt{2V} \sum_{\mathbf{k}} G_{e_{\mathbf{k}\sigma}n_{d\bar{\sigma}}, d_{\sigma}}^r(\omega) - \lambda \sum_{\bar{\sigma}} \delta_{\bar{\sigma}\sigma} G_{f_{\uparrow}n_{d\bar{\sigma}}, d_{\sigma}}^r(\omega) \\
&- \lambda' \sum_{\bar{\sigma}} \delta_{\bar{\sigma}\sigma} G_{f_{\uparrow}^{\dagger}n_{d\bar{\sigma}}, d_{\sigma}}^r(\omega). \quad (\text{B10})
\end{aligned}$$

As can be seen in the procedure above, we threw away the Green's functions which describe spin-flip mechanisms between the QD level and the metallic lead, thus leading to the impossibility of catching Kondo-type correlations^{47,48}.

The other two-particle Green's functions of equation above also are found with the EOM, followed by approximations introduced by Hubbard-I procedure. Hence, we get

$$G_{e_{\mathbf{k}\sigma}n_{d\bar{\sigma}}, d_{\sigma}}^r(\omega) = \sqrt{2V} \sum_{\mathbf{k}} \frac{1}{(\omega^+ - \varepsilon_{\mathbf{k}\sigma})} G_{d_{\sigma}n_{d\bar{\sigma}}, d_{\sigma}}^r(\omega), \quad (\text{B11})$$

$$\begin{aligned}
(\omega^+ - \delta_M) \sum_{\bar{\sigma}} \delta_{\bar{\sigma}\sigma} G_{f_{\uparrow}n_{d\bar{\sigma}}, d_{\sigma}}^r(\omega) &= \\
&- \lambda G_{d_{\sigma}n_{d\bar{\sigma}}, d_{\sigma}}^r(\omega) + \lambda' G_{d_{\bar{\sigma}}^{\dagger}n_{d\bar{\sigma}}, d_{\sigma}}^r(\omega) \quad (\text{B12})
\end{aligned}$$

and

$$\begin{aligned}
(\omega^+ + \delta_M) \sum_{\bar{\sigma}} \delta_{\bar{\sigma}\sigma} G_{f_{\uparrow}^{\dagger}n_{d\bar{\sigma}}, d_{\sigma}}^r(\omega) &= \\
&\lambda G_{d_{\bar{\sigma}}^{\dagger}n_{d\bar{\sigma}}, d_{\sigma}}^r(\omega) - \lambda' G_{d_{\sigma}n_{d\bar{\sigma}}, d_{\sigma}}^r(\omega), \quad (\text{B13})
\end{aligned}$$

allowing us to find that

$$\begin{aligned}
(\omega^+ - \varepsilon_{d\sigma} - U - K1 + i\Gamma)G_{d_{\sigma}n_{d\bar{\sigma}}, d_{\sigma}}^r(\omega) &= \langle n_{d\bar{\sigma}} \rangle \\
&- (2\lambda\lambda')K G_{d_{\bar{\sigma}}^{\dagger}n_{d\bar{\sigma}}, d_{\sigma}}^r(\omega). \quad (\text{B14})
\end{aligned}$$

By adopting the same procedure described above, we evaluate $G_{d_{\bar{\sigma}}^{\dagger}n_{d\bar{\sigma}}, d_{\sigma}}^r(\omega)$, resulting in Eq. (13), which allows us to rewrite Eq. (B14) as expressed in Eq. (12). It is worth noting that turning off the QD-MBSs couplings ($\lambda = \lambda' = 0$) in Eq. (B14) and Eq. (7) allows us to recover the well-known Hubbard solution for Green's function of QD^{37,48}

$$G_{d_{\sigma}d_{\sigma}}^r(\omega) = \frac{1 - \langle n_{d\bar{\sigma}} \rangle}{\omega^+ - \varepsilon_{d\sigma} + i\Gamma} + \frac{\langle n_{d\bar{\sigma}} \rangle}{\omega^+ - \varepsilon_{d\sigma} - U + i\Gamma}. \quad (\text{B15})$$

* corresponding author: luciano.silianoricco@gmail.com

† corresponding author: acfseridonio@gmail.com

¹ R. Aguado, *Riv. Nuovo Cimento* **40**, 523 (2017).

² A. Y. Kitaev, *Physics-Uspekhi* **44**, 131 (2001).

- ³ C. Nayak, S. H. Simon, A. Stern, M. Freedman, and S. Das Sarma, *Rev. Mod. Phys.* **80**, 1083 (2008).
- ⁴ J. Alicea, *Reports on Progress in Physics* **75**, 076501 (2012).
- ⁵ S. R. Elliott and M. Franz, *Rev. Mod. Phys.* **87**, 137 (2015).
- ⁶ S. D. Sarma, M. Freedman, and C. Nayak, *Npj Quantum Information* **1**, 15001 (2015).
- ⁷ G. Goldstein and C. Chamon, *Phys. Rev. B* **84**, 205109 (2011).
- ⁸ J. C. Budich, S. Walter, and B. Trauzettel, *Phys. Rev. B* **85**, 121405 (2012).
- ⁹ R. M. Lutchyn, J. D. Sau, and S. Das Sarma, *Phys. Rev. Lett.* **105**, 077001 (2010).
- ¹⁰ Y. Oreg, G. Refael, and F. von Oppen, *Phys. Rev. Lett.* **105**, 177002 (2010).
- ¹¹ V. Mourik, K. Zuo, S. M. Frolov, S. R. Plissard, E. P. A. M. Bakkers, and L. P. Kouwenhoven, *Science* **336**, 1003 (2012).
- ¹² S. M. Albrecht, A. Higginbotham, M. Madsen, F. Kuemmeth, T. S. Jespersen, J. Nygård, P. Krogstrup, and C. Marcus, *Nature* **531**, 206 (2016).
- ¹³ M. T. Deng, S. Vaitiekėnas, E. B. Hansen, J. Danon, M. Leijnse, K. Flensberg, J. Nygård, P. Krogstrup, and C. M. Marcus, *Science* **354**, 1557 (2016).
- ¹⁴ M.-T. Deng, S. Vaitiekėnas, E. Prada, P. San-Jose, J. Nygård, P. Krogstrup, R. Aguado, and C. M. Marcus, *Phys. Rev. B* **98**, 085125 (2018).
- ¹⁵ H. Zhang, C.-X. Liu, S. Gazibegovic, D. Xu, J. A. Logan, G. Wang, N. van Loo, J. D. S. Bommer, M. W. A. de Moor, D. Car, R. L. M. Op het Veld, P. J. van Veldhoven, S. Koelling, M. A. Verheijen, M. Pendharkar, D. J. Pennachio, B. Shojaei, J. S. Lee, C. J. Palmstrøm, E. P. A. M. Bakkers, S. D. Sarma, and L. P. Kouwenhoven, *Nature* **556**, 74 (2018).
- ¹⁶ D. Bagrets and A. Altland, *Phys. Rev. Lett.* **109**, 227005 (2012).
- ¹⁷ S. M. Cronenwett, T. H. Oosterkamp, and L. P. Kouwenhoven, *Science* **281**, 540 (1998).
- ¹⁸ D. Goldhaber-Gordon, H. Shtrikman, D. Mahalu, D. Abusch-Magder, U. Meirav, and M. A. Kastner, *Nature (London)* **391**, 156 (1998).
- ¹⁹ G. Kells, D. Meidan, and P. W. Brouwer, *Phys. Rev. B* **86**, 100503 (2012).
- ²⁰ E. J. H. Lee, X. Jiang, M. Houzet, C. M. Lieber, and S. De Franceschi, *Nature Nanotechnology* **9**, 79 (2013).
- ²¹ C.-X. Liu, J. D. Sau, T. D. Stanescu, and S. Das Sarma, *Phys. Rev. B* **96**, 075161 (2017).
- ²² C. Moore, T. D. Stanescu, and S. Tewari, *Phys. Rev. B* **97**, 165302 (2018).
- ²³ C. Moore, C. Zeng, T. D. Stanescu, and S. Tewari, *ArXiv e-prints* (2018), [arXiv:1804.03164 \[cond-mat.mes-hall\]](https://arxiv.org/abs/1804.03164).
- ²⁴ J. Cayao, A. M. Black-Schaffer, E. Prada, and R. Aguado, *Beilstein Journal of Nanotechnology* **9**, 1339 (2018).
- ²⁵ P. Subhajit and B. Colin, *Scientific Reports* **8**, 11949 (2018).
- ²⁶ J. Cayao, E. Prada, P. San-Jose, and R. Aguado, *Phys. Rev. B* **91**, 024514 (2015).
- ²⁷ J. Cayao, P. San-Jose, A. M. Black-Schaffer, R. Aguado, and E. Prada, *Phys. Rev. B* **96**, 205425 (2017).
- ²⁸ P. San-Jose, J. Cayao, E. Prada, and R. Aguado, *New Journal of Physics* **15**, 075019 (2013).
- ²⁹ J. Avila, F. Peñaranda, E. Prada, P. San-Jose, and R. Aguado, *ArXiv e-prints* (2018), [arXiv:1807.04677 \[cond-mat.mes-hall\]](https://arxiv.org/abs/1807.04677).
- ³⁰ S. Hoffman, D. Chevallier, D. Loss, and J. Klinovaja, *Phys. Rev. B* **96**, 045440 (2017).
- ³¹ D. Chevallier, P. Szumniak, S. Hoffman, D. Loss, and J. Klinovaja, *Phys. Rev. B* **97**, 045404 (2018).
- ³² E. Prada, R. Aguado, and P. San-Jose, *Phys. Rev. B* **96**, 085418 (2017).
- ³³ D. J. Clarke, *Phys. Rev. B* **96**, 201109 (2017).
- ³⁴ C.-X. Liu, J. D. Sau, and S. Das Sarma, *Phys. Rev. B* **97**, 214502 (2018).
- ³⁵ M. Hell, K. Flensberg, and M. Leijnse, *Phys. Rev. B* **97**, 161401 (2018).
- ³⁶ L. S. Ricco, V. L. Campo, I. A. Shelykh, and A. C. Seridonio, *Phys. Rev. B* **98**, 075142 (2018).
- ³⁷ J. Hubbard, *Proc. R. Soc. A* **276**, 238 (1963).
- ³⁸ D. Sticlet, C. Bena, and P. Simon, *Phys. Rev. Lett.* **108**, 096802 (2012).
- ³⁹ K. Björnson, S. S. Pershoguba, A. V. Balatsky, and A. M. Black-Schaffer, *Phys. Rev. B* **92**, 214501 (2015).
- ⁴⁰ M. M. Maška and T. Domański, *Scientific Reports* **7**, 16193 (2017).
- ⁴¹ S. Jeon, Y. Xie, J. Li, Z. Wang, B. A. Bernevig, and A. Yazdani, *Science* **358**, 772 (2017).
- ⁴² J. Li, S. Jeon, Y. Xie, A. Yazdani, and B. A. Bernevig, *Phys. Rev. B* **97**, 125119 (2018).
- ⁴³ M. Serina, D. Loss, and J. Klinovaja, *Phys. Rev. B* **98**, 035419 (2018).
- ⁴⁴ J. Danon, E. B. Hansen, and K. Flensberg, *Phys. Rev. B* **96**, 125420 (2017).
- ⁴⁵ C. Fleckenstein, F. Domínguez, N. Traverso Ziani, and B. Trauzettel, *Phys. Rev. B* **97**, 155425 (2018).
- ⁴⁶ P. W. Anderson, *Phys. Rev.* **124**, 41 (1961).
- ⁴⁷ H. Haug and A. Jauho, *Quantum Kinetics in Transport and Optics of Semiconductors*, Springer Series in Solid-State Sciences (Springer Berlin Heidelberg, 2008).
- ⁴⁸ H. Bruus and K. Flensberg, *Many-Body Quantum Theory in Condensed Matter Physics: An Introduction*, Oxford Graduate Texts (Oxford University Press, 2004).
- ⁴⁹ E. Vernek, P. H. Penteado, A. C. Seridonio, and J. C. Egues, *Phys. Rev. B* **89**, 165314 (2014).
- ⁵⁰ J. Barański and T. Domański, *J. Phys.: Cond. Matter* **25**, 435305 (2013).
- ⁵¹ A. V. Balatsky, I. Vekhter, and J.-X. Zhu, *Rev. Mod. Phys.* **78**, 373 (2006).
- ⁵² A. E. Miroshnichenko, S. Flach, and Y. S. Kivshar, *Rev. Mod. Phys.* **82**, 2257 (2010).
- ⁵³ G. Fülöp, F. Domínguez, S. d'Hollosy, A. Baumgartner, P. Makk, M. H. Madsen, V. A. Guzenko, J. Nygård, C. Schönenberger, A. Levy Yeyati, and S. Csonka, *Phys. Rev. Lett.* **115**, 227003 (2015).
- ⁵⁴ A. Schuray, L. Weithofer, and P. Recher, *Phys. Rev. B* **96**, 085417 (2017).

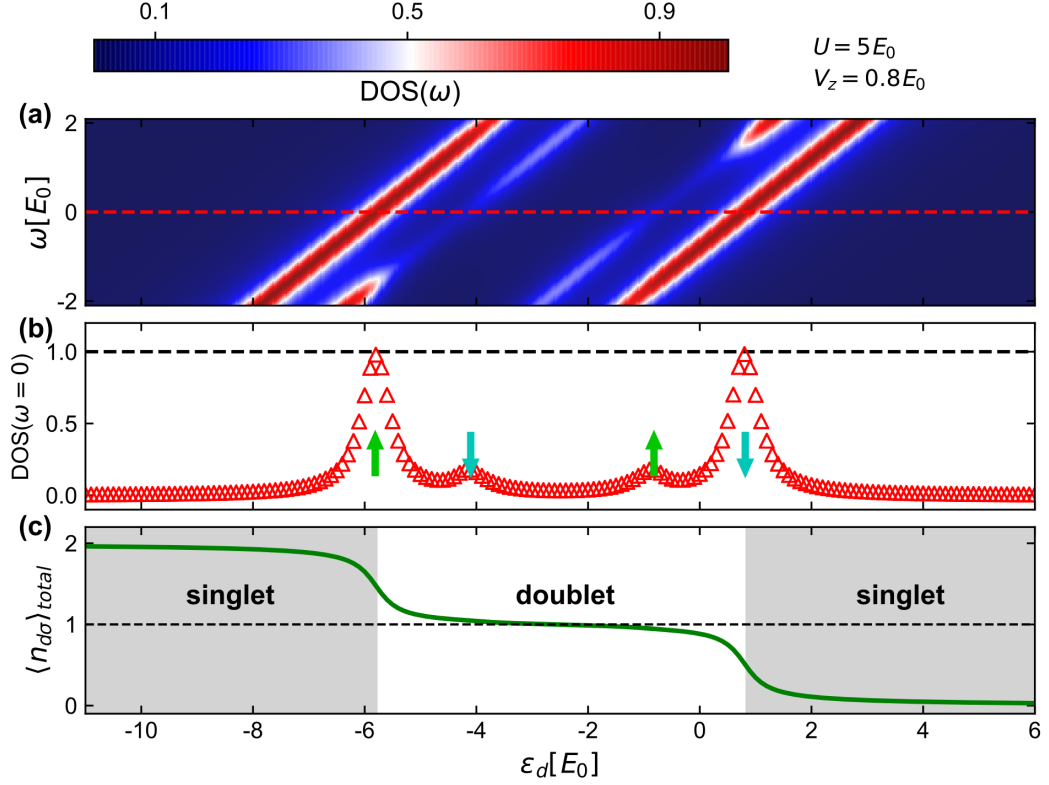


Figure 7.2: (a) Color scale plot of density of states for a QD under external magnetic field coupled to a normal lead as a function of QD energy level ϵ_d and spectral frequency ω . (b) Line cut in the above panel at $\omega = 0$ (dashed line in (a)). The arrows indicate the spin of each possible QD state. (c) Total occupation number of the QD state obtained by self-consistent numerical calculation [Eq. (14) of draft], showing a singlet-doublet-singlet transition.

7.4 Supplementary Results

To ensure the validity of our calculations, in Fig. 7.2(a) a color scale plot of DOS is shown for a QD under external magnetic field coupled to a normal lead as a function of spectral frequency ω and QD energy level ϵ_d . The two structures at negative ϵ_d correspond to the spin up and down states, respectively, since $\epsilon_{d\sigma} = \epsilon_d - \sigma V_Z$, wherein V_Z is the Zeeman energy splitting induced in the QD level due to external magnetic field. Due to the presence of charging energy U , a second possible state emerges at positive QD energies, which is also splitted up by the external field. Panel (b) of same figure exhibits a linecut in the above panel at $\omega = 0$ (dashed red line in (a)), which shows a four peak structure reflecting both the Coulomb blockade physics and Zeeman splitting processes. The arrows indicate the spin of each possible QD state. Total occupation number of the QD state obtained by self-consistent numerical calculation [Eq. (14) of draft] is depicted in Fig.7.2(c), showing a singlet-doublet-singlet transition. At first negative ϵ_d the dot presents double occupancy with opposite spins, forming a singlet state ($\langle n_{d\uparrow} \rangle = \langle n_{d\downarrow} \rangle = 1$). For intermediary values of ϵ_d (white background) the spin degeneracy is broken by the Coulomb charging energy ($\langle n_{d\uparrow} \rangle \neq \langle n_{d\downarrow} \rangle$), giving rise to a doublet state. At positive energy levels the dot is empty, ($\langle n_{d\uparrow} \rangle = \langle n_{d\downarrow} \rangle = 0$), which depicts a singlet state again.

Density of states as a function of ω keeping fixed $\epsilon_d = -2.5E_0$ in the Anderson symmetric regime ($U = 5E_0$) is displayed in Fig. 7.3, considering distinct physical situations. Inset shows DOS of each case in low-energy spectrum. The gray triangles describe the simplest situation of a QD-N lead system decoupled from the SC nanowire ($\lambda_L = \lambda_R = 0$), corresponding to the same situation explored in

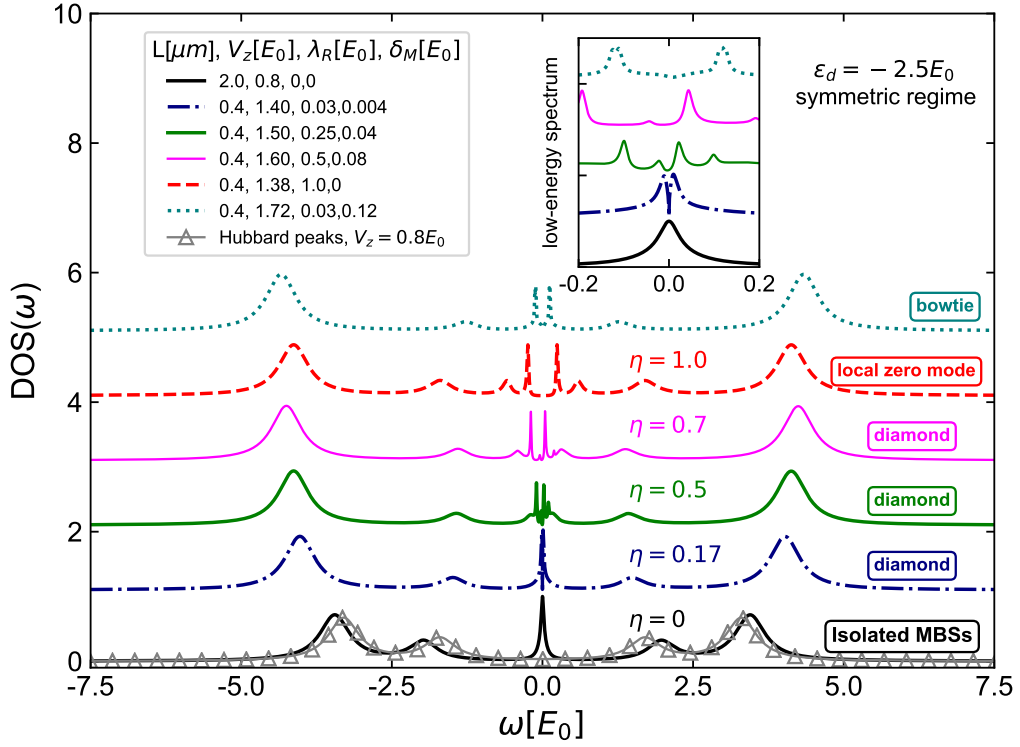


Figure 7.3: Density of states as a function of ω with $\varepsilon_d = -2.5E_0$ in the Anderson symmetric regime ($U = 5E_0$), for distinct physical situations. The curves were shifted for better visualization.

Fig. 7.2. The emergence of a four resonances characterizes the presence of both charging and Zeeman energies, being localized at $\varepsilon_{d\sigma} = \varepsilon_d - \sigma V_Z$ and $\varepsilon_{d\sigma} = \varepsilon_d + U - \sigma V_Z$. When the nanowire is long enough to ensure ideal condition of highly nonlocal MBSs (black line, $\delta_M = 0$, $\lambda_R = 0$), the emergence of a zero-bias peak is verified. However, for smaller nanowire lengths and $\lambda_R \gg \delta_M$, which is equivalent to diamond profiles of Fig. 2(d-f) of draft, a peak splitting is verified due to displacement of right MBS towards to left MBSs and finite overlap between them. These near-zero-energy resonances evidently changes with increasing η [Eq. (4) of draft] (blue dash-dotted, green and magenta lines), leading to a stronger peak splitting, which characterizes the enhancement of local nature of MBSs (formation of ABS) and therefore loss of topological protection. The extreme situation (red line) wherein $\lambda_L = \lambda_R$ and $\delta_M = 0$, describes a local fermion with zero-energy. For $\delta_M \gg \lambda_R$ (teal dotted curve), corresponding to bowtie situation of Fig. 2(c) of draft, a two-peak structure is also verified, wherein the distance between them (strength of splitting) is modulated by the direct overlap δ_M between MBSs.

Chapter 8

Conclusions

Throughout this thesis, we have studied the electronic transport features of a hybrid device composed by a quantum dot coupled to a topological superconducting nanowire hosting Majorana bound states at the ends. In a nutshell, we have shown that such a setup can be used to enlarge the discussion concerning the Majorana controversial detection, as well as having potential to be applied to the next generation of quantum devices. Related to this applications:

- In chapter 4, we have demonstrated that a setup composed by a quantum dot between two topological superconducting nanowires within the topological phase can work as a qubit storage mechanism, wherein the information is trapped by means of the so-called bound states in the continuum;
- In chapter 5, we have explored the thermoelectrical properties of a quantum dot coupled to both ends of a U-shaped Kitaev nanowire and between metallic reservoirs. Basically, we have shown that is possible to tune the heat and charge through the system by changing the coupling strengths between the nanowire and the quantum dot.

Regarding the Majorana detection:

- In chapter 6, we have studied the role of Fano interference processes in the so-called Majorana oscillations for a T-shaped hybrid setup, wherein the quantum dot hybridizes with both ends of the topological superconducting nanowire, *i.e.*, when the degree of Majorana nonlocality is taken into account. We have demonstrated that both the amplitude and shape of the Majorana oscillations depend on the bias-voltage, Fano parameter of system and the degree of Majorana nonlocality;
- In chapter 7, we have shown that the spin-resolved density of states of the quantum dot responsible for the zero-bias conductance peak strongly depends on the overlap between the MBSs at opposite ends of the topological superconducting nanowire and consequently, of the degree of Majorana nonlocality. Such a main finding suggests that spin-resolved measurements can be employed for distinguishing the trully topological Majorana bound states from the so-called Andreev bound states, for instance.

Appendix A

Obtaining the DOS of Majorana quasiparticles

In this Appendix, we provide the calculations concerning the Green's functions which describes the DOS of Majorana quasiparticles, by employing the EOM approach (Sec. 3). The results were employed to yield the findings of Sec. 4.

The DOS for Majorana operators η_1 and η_2 are given by:

$$\tilde{\rho}_{\eta_1\eta_1}(\varepsilon) = -\left(\frac{1}{\pi}\right) \text{Im} \left\{ \tilde{\mathcal{G}}_{\eta_1\eta_1}(\varepsilon) \right\} \quad (\text{A.1})$$

and

$$\tilde{\rho}_{\eta_2\eta_2}(\varepsilon) = -\left(\frac{1}{\pi}\right) \text{Im} \left\{ \tilde{\mathcal{G}}_{\eta_2\eta_2}(\varepsilon) \right\}, \quad (\text{A.2})$$

wherein the correspondent system is described by the follow Hamiltonian in the regular fermionic basis

$$\begin{aligned} \mathcal{H} = & \sum_k \varepsilon_k c_{ek}^\dagger c_{ek} + \varepsilon_1 d_1^\dagger d_1 + \sqrt{\frac{2}{\mathcal{N}}} V \sum_k (c_{ek}^\dagger d_1 + H.c.) + \frac{V_{BT}}{\mathcal{N}} \sum_{kq} c_{ek}^\dagger c_{eq} \\ & + \varepsilon_M \left(f^\dagger f - \frac{1}{2} \right) + \frac{\lambda_A}{\sqrt{2}} \left(d_1 f^\dagger + f d_1^\dagger \right) + \frac{\lambda_B}{\sqrt{2}} \left(d_1 f - d_1^\dagger f^\dagger \right), \end{aligned} \quad (\text{A.3})$$

with $\lambda_A/\sqrt{2} \equiv t$ and $\lambda_B/\sqrt{2} \equiv \Delta$ in the paper (Sec 4.2).

As can be seen in Eqs. (A.1) and (A.2) we should calculate the Green Functions for Majoranas η_1 and η_2 , given by

$$\mathcal{G}_{\eta_1\eta_1}(t) = \left(-\frac{i}{\hbar}\right) \theta(t) \mathcal{Z}^{-1} \sum_r e^{-\beta E_r} \left\langle r \left| \left[\eta_1(t), \eta_1^\dagger(0) \right]_+ \right| r \right\rangle \quad (\text{A.4})$$

and

$$\mathcal{G}_{\eta_2\eta_2}(t) = \left(-\frac{i}{\hbar}\right) \theta(t) \mathcal{Z}^{-1} \sum_r e^{-\beta E_r} \left\langle r \left| \left[\eta_2(t), \eta_2^\dagger(0) \right]_+ \right| r \right\rangle \quad (\text{A.5})$$

respectively, with the Majorana operators

$$\eta_1 = \frac{1}{\sqrt{2}}(f^\dagger + f), \quad (\text{A.6})$$

and

$$\eta_2 = i \frac{1}{\sqrt{2}} (f^\dagger - f) \quad (\text{A.7})$$

rewritten in terms of a regular fermion operator f , with $\eta_{1(2)} = \eta_{1(2)}^\dagger$.

A.1 Finding the Green's Function for the Majorana Quasiparticle η_1

$$\left[\eta_1(t), \eta_1^\dagger(0) \right]_+ = \eta_1(t)\eta_1(0) + \eta_1(0)\eta_1(t) \quad (\text{A.8})$$

$$\begin{aligned} \eta_1(t)\eta_1(0) &= \frac{1}{\sqrt{2}}(f^\dagger(t) + f(t)) \frac{1}{\sqrt{2}}(f^\dagger(0) + f(0)) \\ &= \frac{1}{2} \left(f^\dagger(t)f^\dagger(0) + f^\dagger(t)f(0) + f(t)f^\dagger(0) + f(t)f(0) \right) \end{aligned} \quad (\text{A.9})$$

$$\begin{aligned} \eta_1(0)\eta_1(t) &= \frac{1}{\sqrt{2}}(f^\dagger(0) + f(0)) \frac{1}{\sqrt{2}}(f^\dagger(t) + f(t)) \\ &= \frac{1}{2} (f^\dagger(0)f^\dagger(t) + f^\dagger(0)f(t) + f(0)f^\dagger(t) + f(0)f(t)) \end{aligned} \quad (\text{A.10})$$

$$\begin{aligned} \left[\eta_1(t), \eta_1^\dagger(0) \right]_+ &= \frac{1}{2} \left(f^\dagger(t)f^\dagger(0) + f^\dagger(t)f(0) + f(t)f^\dagger(0) + f(t)f(0) \right) \\ &+ \frac{1}{2} (f^\dagger(0)f^\dagger(t) + f^\dagger(0)f(t) + f(0)f^\dagger(t) + f(0)f(t)) \\ &= \frac{1}{2} \left(f^\dagger(t)f^\dagger(0) + f^\dagger(0)f^\dagger(t) \right) + \frac{1}{2} \left(f^\dagger(t)f(0) + f^\dagger(0)f(t) \right) \\ &+ \frac{1}{2} \left(f(t)f^\dagger(0) + f(0)f^\dagger(t) \right) + \frac{1}{2} (f(t)f(0) + f(0)f(t)) \Rightarrow \\ \left[\eta_1(t), \eta_1^\dagger(0) \right]_+ &= \frac{1}{2} \left[f^\dagger(t), f^\dagger(0) \right]_+ + \frac{1}{2} \left[f^\dagger(t), f(0) \right]_+ + \frac{1}{2} \left[f(t), f^\dagger(0) \right]_+ \\ &+ \frac{1}{2} [f(t), f(0)]_+. \end{aligned} \quad (\text{A.11})$$

By substituting Eq. (A.11) in (A.4), we obtain:

$$\begin{aligned}
 \mathcal{G}_{\eta_1\eta_1}(t) &= \frac{1}{2}\left(-\frac{i}{\hbar}\right)\theta(t)\mathcal{Z}^{-1}\sum_r e^{-\beta E_r} \left\langle r \left| [f^\dagger(t), f^\dagger(0)]_+ \right| r \right\rangle \\
 &+ \frac{1}{2}\left(-\frac{i}{\hbar}\right)\theta(t)\mathcal{Z}^{-1}\sum_r e^{-\beta E_r} \left\langle r \left| [f^\dagger(t), f(0)]_+ \right| r \right\rangle \\
 &+ \frac{1}{2}\left(-\frac{i}{\hbar}\right)\theta(t)\mathcal{Z}^{-1}\sum_r e^{-\beta E_r} \left\langle r \left| [f(t), f^\dagger(0)]_+ \right| r \right\rangle \\
 &+ \frac{1}{2}\left(-\frac{i}{\hbar}\right)\theta(t)\mathcal{Z}^{-1}\sum_r e^{-\beta E_r} \left\langle r \left| [f(t), f(0)]_+ \right| r \right\rangle, \tag{A.12}
 \end{aligned}$$

$$\mathcal{G}_{\eta_1\eta_1}(t) = \frac{1}{2}\mathcal{G}_{f^\dagger f}(t) + \frac{1}{2}\mathcal{G}_{f^\dagger f^\dagger}(t) + \frac{1}{2}\mathcal{G}_{ff}(t) + \frac{1}{2}\mathcal{G}_{ff^\dagger}(t). \tag{A.13}$$

Let us calculate the first Green function, namely $\mathcal{G}_{f^\dagger f}(t)$, defined as

$$\mathcal{G}_{f^\dagger f}(t) = \left(-\frac{i}{\hbar}\right)\theta(t)\mathcal{Z}^{-1}\sum_r e^{-\beta E_r} \left\langle r \left| [f^\dagger(t), f^\dagger(0)]_+ \right| r \right\rangle. \tag{A.14}$$

By applying the Equation of Motion (EOM) method, we obtain:

$$\begin{aligned}
 \partial_t \mathcal{G}_{f^\dagger f}(t) &= \left(-\frac{i}{\hbar}\right)\delta(t)\mathcal{Z}^{-1}\sum_r e^{-\beta E_r} \left\langle r \left| [f^\dagger(t), f^\dagger(0)]_+ \right| r \right\rangle \\
 &+ \left(-\frac{i}{\hbar}\right)\theta(t)\mathcal{Z}^{-1}\sum_r e^{-\beta E_r} \left\langle r \left| [\partial_t f^\dagger(t), f^\dagger(0)]_+ \right| r \right\rangle. \tag{A.15}
 \end{aligned}$$

We have to evolve the fermionic operator in the time, by using the Heisenberg equation:

$$\begin{aligned}
 \partial_t f^\dagger(t) &= \left(-\frac{i}{\hbar}\right) [f^\dagger, \mathcal{H}] \\
 &= \left(-\frac{i}{\hbar}\right) \left[f^\dagger, \sum_k \varepsilon_k c_{ek}^\dagger c_{ek} \right] + \left(-\frac{i}{\hbar}\right) [f^\dagger, \varepsilon_1 d_1^\dagger d_1] + \left(-\frac{i}{\hbar}\right) \left[f^\dagger, \sqrt{2}V \sum_k (c_{ek}^\dagger d_1 + H.c.) \right] \\
 &+ \left(-\frac{i}{\hbar}\right) \left[f^\dagger, V_{BT} \sum_{kq} c_{ek}^\dagger c_{eq} \right] + \left(-\frac{i}{\hbar}\right) [f^\dagger, \varepsilon_M (f^\dagger f - \frac{1}{2})] + \left(-\frac{i}{\hbar}\right) \left[f^\dagger, \frac{\lambda_A}{\sqrt{2}} (d_1 f^\dagger + f d_1^\dagger) \right] \\
 &+ \left(-\frac{i}{\hbar}\right) \left[f^\dagger, \frac{\lambda_B}{\sqrt{2}} (d_1 f - d_1^\dagger f^\dagger) \right], \tag{A.16}
 \end{aligned}$$

Due to the commutation relation with fermionic operators which belong to distinct Hilbert spaces, the equation above becomes:

$$\begin{aligned}
 \partial_t f^\dagger(t) &= \left(-\frac{i}{\hbar}\right) [f^\dagger, \mathcal{H}] \\
 &= \left(-\frac{i}{\hbar}\right) \left[f^\dagger, \varepsilon_M \left(f^\dagger f - \frac{1}{2} \right) \right] + \left(-\frac{i}{\hbar}\right) \left[f^\dagger, \frac{\lambda_A}{\sqrt{2}} (d_1 f^\dagger + f d_1^\dagger) \right] \\
 &\quad + \left(-\frac{i}{\hbar}\right) \left[f^\dagger, \frac{\lambda_B}{\sqrt{2}} (d_1 f - d_1^\dagger f^\dagger) \right], \tag{A.17}
 \end{aligned}$$

Now we calculate the commutators:

$$\begin{aligned}
 \left[f^\dagger, \varepsilon_M \left(f^\dagger f - \frac{1}{2} \right) \right] &= f^\dagger \varepsilon_M \left(f^\dagger f - \frac{1}{2} \right) - \varepsilon_M \left(f^\dagger f - \frac{1}{2} \right) f^\dagger \\
 &= \varepsilon_M f^\dagger f^\dagger f - \varepsilon_M f^\dagger f f^\dagger = \varepsilon_M f^\dagger f^\dagger f - \varepsilon_M f^\dagger (1 - f^\dagger f) \\
 &= \varepsilon_M f^\dagger f^\dagger f - \varepsilon_M f^\dagger + \varepsilon_M f^\dagger f^\dagger f \\
 &= \varepsilon_M f^\dagger f^\dagger f - \varepsilon_M f^\dagger - \varepsilon_M f^\dagger f^\dagger f = -\varepsilon_M f^\dagger. \tag{A.18}
 \end{aligned}$$

$$\begin{aligned}
 \frac{\lambda_A}{\sqrt{2}} \left[f^\dagger, (d_1 f^\dagger + f d_1^\dagger) \right] &= \frac{\lambda_A}{\sqrt{2}} (f^\dagger (d_1 f^\dagger + f d_1^\dagger) - (d_1 f^\dagger + f d_1^\dagger) f^\dagger) \\
 &= \frac{\lambda_A}{\sqrt{2}} (f^\dagger d_1 f^\dagger + f^\dagger f d_1^\dagger - d_1 f^\dagger f^\dagger - f d_1^\dagger f^\dagger) \\
 &= \frac{\lambda_A}{\sqrt{2}} (-d_1 f^\dagger f^\dagger + f^\dagger f d_1^\dagger + d_1 f^\dagger f^\dagger + f f^\dagger d_1^\dagger) \\
 &= \frac{\lambda_A}{\sqrt{2}} (f^\dagger f d_1^\dagger + f f^\dagger d_1^\dagger) = \frac{\lambda_A}{\sqrt{2}} (f^\dagger f + f f^\dagger) d_1^\dagger \\
 &= \frac{\lambda_A}{\sqrt{2}} d_1^\dagger. \tag{A.19}
 \end{aligned}$$

$$\begin{aligned}
 \frac{\lambda_B}{\sqrt{2}} \left[f^\dagger, (d_1 f - d_1^\dagger f^\dagger) \right] &= \frac{\lambda_B}{\sqrt{2}} (f^\dagger (d_1 f - d_1^\dagger f^\dagger) - (d_1 f - d_1^\dagger f^\dagger) f^\dagger) \\
 &= \frac{\lambda_B}{\sqrt{2}} (f^\dagger d_1 f - f^\dagger d_1^\dagger f^\dagger - d_1 f f^\dagger + d_1^\dagger f^\dagger f^\dagger) \\
 &= \frac{\lambda_B}{\sqrt{2}} (-d_1 f^\dagger f + d_1^\dagger f^\dagger f^\dagger - d_1 f f^\dagger - d_1^\dagger f^\dagger f^\dagger) \\
 &= \frac{\lambda_B}{\sqrt{2}} (-d_1 f^\dagger f - d_1 f f^\dagger) = -\frac{\lambda_B}{\sqrt{2}} d_1 (f^\dagger f + f f^\dagger) \\
 &= -\frac{\lambda_B}{\sqrt{2}} d_1. \tag{A.20}
 \end{aligned}$$

Thus,

$$\begin{aligned}
 \partial_t f^\dagger(t) &= \left(-\frac{i}{\hbar}\right) [f^\dagger, \mathcal{H}] \\
 &= +\left(-\frac{i}{\hbar}\right)(-\varepsilon_M) f^\dagger + \left(-\frac{i}{\hbar}\right) \frac{\lambda_A}{\sqrt{2}} d_1^\dagger + \left(-\frac{i}{\hbar}\right) \left(-\frac{\lambda_B}{\sqrt{2}}\right) d_1
 \end{aligned} \tag{A.21}$$

$$\begin{aligned}
 \partial_t \mathcal{G}_{f^\dagger f}(t) &= \left(-\frac{i}{\hbar}\right) \delta(t) \mathcal{Z}^{-1} \sum_r e^{-\beta E_r} \left\langle r \left| [f^\dagger(t), f^\dagger(0)]_+ \right| r \right\rangle \\
 &\quad - \left(-\frac{i}{\hbar}\right) \varepsilon_M \left(-\frac{i}{\hbar}\right) \theta(t) \mathcal{Z}^{-1} \sum_r e^{-\beta E_r} \left\langle r \left| [f^\dagger(t), f^\dagger(0)]_+ \right| r \right\rangle \\
 &\quad + \left(-\frac{i}{\hbar}\right) \frac{\lambda_A}{\sqrt{2}} \left(-\frac{i}{\hbar}\right) \theta(t) \mathcal{Z}^{-1} \sum_r e^{-\beta E_r} \left\langle r \left| [d_1^\dagger(t), f^\dagger(0)]_+ \right| r \right\rangle \\
 &\quad - \left(-\frac{i}{\hbar}\right) \frac{\lambda_B}{\sqrt{2}} \left(-\frac{i}{\hbar}\right) \theta(t) \mathcal{Z}^{-1} \sum_r e^{-\beta E_r} \left\langle r \left| [d_1(t), f^\dagger(0)]_+ \right| r \right\rangle \Rightarrow \\
 \partial_t \mathcal{G}_{f^\dagger f}(t) &= \left(-\frac{i}{\hbar}\right) \delta(t) \mathcal{Z}^{-1} \sum_r e^{-\beta E_r} \left\langle r \left| [f^\dagger(t), f^\dagger(0)]_+ \right| r \right\rangle \\
 &\quad - \left(-\frac{i}{\hbar}\right) \varepsilon_M \mathcal{G}_{f^\dagger f}(t) + \left(-\frac{i}{\hbar}\right) \frac{\lambda_A}{\sqrt{2}} \mathcal{G}_{d_1^\dagger f}(t) - \left(-\frac{i}{\hbar}\right) \frac{\lambda_B}{\sqrt{2}} \mathcal{G}_{d_1 f}(t).
 \end{aligned} \tag{A.22}$$

By performing the Fourier transform $\left(-\frac{i}{\hbar}\right)(\varepsilon + i\delta) \tilde{\mathcal{G}}_{AB}(\varepsilon) = \int dt \partial_t \mathcal{G}_{AB}(t) e^{-\frac{i}{\hbar}(\varepsilon + i\delta)t}$, we obtain:

$$(\varepsilon + \varepsilon_M + i\delta) \tilde{\mathcal{G}}_{f^\dagger f}(\varepsilon) = \frac{\lambda_A}{\sqrt{2}} \tilde{\mathcal{G}}_{d_1^\dagger f}(\varepsilon) - \frac{\lambda_B}{\sqrt{2}} \mathcal{G}_{d_1 f}(\varepsilon). \tag{A.23}$$

Now, let us calculate $\mathcal{G}_{f^\dagger f^\dagger}(t)$ by the same EOM approach:

$$\mathcal{G}_{f^\dagger f^\dagger}(t) = \left(-\frac{i}{\hbar}\right) \theta(t) \mathcal{Z}^{-1} \sum_r e^{-\beta E_r} \left\langle r \left| [f^\dagger(t), f(0)]_+ \right| r \right\rangle \tag{A.24}$$

$$\begin{aligned}
 \partial_t \mathcal{G}_{f^\dagger f^\dagger}(t) &= \left(-\frac{i}{\hbar}\right) \delta(t) \mathcal{Z}^{-1} \sum_r e^{-\beta E_r} \left\langle r \left| [f^\dagger(t), f(0)]_+ \right| r \right\rangle \\
 &\quad + \left(-\frac{i}{\hbar}\right) \theta(t) \mathcal{Z}^{-1} \sum_r e^{-\beta E_r} \left\langle r \left| [\partial_t f^\dagger(t), f(0)]_+ \right| r \right\rangle.
 \end{aligned} \tag{A.25}$$

But we already have found $\partial_t f^\dagger(t)$ according to the Heisenberg equation, as one can see in Eq. (A.21):

$$\begin{aligned}
 \partial_t f^\dagger(t) &= \left(-\frac{i}{\hbar}\right) [f^\dagger, \mathcal{H}] \\
 &= +\left(-\frac{i}{\hbar}\right)(-\varepsilon_M) f^\dagger + \left(-\frac{i}{\hbar}\right) \frac{\lambda_A}{\sqrt{2}} d_1^\dagger + \left(-\frac{i}{\hbar}\right) \left(-\frac{\lambda_B}{\sqrt{2}}\right) d_1.
 \end{aligned} \tag{A.26}$$

Therefore,

$$\begin{aligned}
 \partial_t \mathcal{G}_{f^\dagger f^\dagger}(t) &= \left(-\frac{i}{\hbar}\right) \delta(t) \mathcal{Z}^{-1} \sum_r e^{-\beta E_r} \left\langle r \left| \left[f^\dagger(t), f(0) \right]_+ \right| r \right\rangle \\
 &\quad - \left(-\frac{i}{\hbar}\right) \varepsilon_M \left(-\frac{i}{\hbar}\right) \theta(t) \mathcal{Z}^{-1} \sum_r e^{-\beta E_r} \left\langle r \left| \left[f^\dagger(t), f(0) \right]_+ \right| r \right\rangle \\
 &\quad + \left(-\frac{i}{\hbar}\right) \frac{\lambda_A}{\sqrt{2}} \left(-\frac{i}{\hbar}\right) \theta(t) \mathcal{Z}^{-1} \sum_r e^{-\beta E_r} \left\langle r \left| \left[d_1^\dagger(t), f(0) \right]_+ \right| r \right\rangle \\
 &\quad - \left(-\frac{i}{\hbar}\right) \frac{\lambda_B}{\sqrt{2}} \left(-\frac{i}{\hbar}\right) \theta(t) \mathcal{Z}^{-1} \sum_r e^{-\beta E_r} \left\langle r \left| \left[d_1(t), f(0) \right]_+ \right| r \right\rangle \Rightarrow \\
 \partial_t \mathcal{G}_{f^\dagger f^\dagger}(t) &= \left(-\frac{i}{\hbar}\right) \delta(t) \mathcal{Z}^{-1} \sum_r e^{-\beta E_r} \left\langle r \left| \left[f^\dagger(t), f(0) \right]_+ \right| r \right\rangle \\
 &\quad - \left(-\frac{i}{\hbar}\right) \varepsilon_M \mathcal{G}_{f^\dagger f^\dagger}(t) + \left(-\frac{i}{\hbar}\right) \frac{\lambda_A}{\sqrt{2}} \mathcal{G}_{d_1^\dagger f^\dagger}(t) - \left(-\frac{i}{\hbar}\right) \frac{\lambda_B}{\sqrt{2}} \mathcal{G}_{d_1 f^\dagger}(t).
 \end{aligned} \tag{A.27}$$

After of apply the Fourier transform in Eq. (A.27), we find

$$(\varepsilon + \varepsilon_M + i\delta) \tilde{\mathcal{G}}_{f^\dagger f^\dagger}(\varepsilon) = 1 + \frac{\lambda_A}{\sqrt{2}} \tilde{\mathcal{G}}_{d_1^\dagger f^\dagger}(\varepsilon) - \frac{\lambda_B}{\sqrt{2}} \mathcal{G}_{d_1 f^\dagger}(\varepsilon). \tag{A.28}$$

We also should calculate $\mathcal{G}_{ff}(t)$, definite as

$$\mathcal{G}_{ff}(t) = \left(-\frac{i}{\hbar}\right) \theta(t) \mathcal{Z}^{-1} \sum_r e^{-\beta E_r} \left\langle r \left| \left[f(t), f^\dagger(0) \right]_+ \right| r \right\rangle. \tag{A.29}$$

$$\begin{aligned}
 \partial_t \mathcal{G}_{ff}(t) &= \left(-\frac{i}{\hbar}\right) \delta(t) \mathcal{Z}^{-1} \sum_r e^{-\beta E_r} \left\langle r \left| \left[f(t), f^\dagger(0) \right]_+ \right| r \right\rangle \\
 &\quad + \left(-\frac{i}{\hbar}\right) \theta(t) \mathcal{Z}^{-1} \sum_r e^{-\beta E_r} \left\langle r \left| \left[\partial_t f(t), f^\dagger(0) \right]_+ \right| r \right\rangle.
 \end{aligned} \tag{A.30}$$

$$\begin{aligned}
 \partial_t f(t) &= \left(-\frac{i}{\hbar}\right) [f, \mathcal{H}] \\
 &= \left(-\frac{i}{\hbar}\right) \left[f, \sum_k \varepsilon_k c_{ek}^\dagger c_{ek} \right] + \left(-\frac{i}{\hbar}\right) [f, \varepsilon_1 d_1^\dagger d_1] + \left(-\frac{i}{\hbar}\right) \left[f, \sqrt{2}V \sum_k (c_{ek}^\dagger d_1 + H.c.) \right] \\
 &\quad + \left(-\frac{i}{\hbar}\right) \left[f, V_{BT} \sum_{kq} c_{ek}^\dagger c_{eq} \right] + \left(-\frac{i}{\hbar}\right) \left[f, \varepsilon_M \left(f^\dagger f - \frac{1}{2} \right) \right] + \left(-\frac{i}{\hbar}\right) \left[f, \frac{\lambda_A}{\sqrt{2}} (d_1 f^\dagger + f d_1^\dagger) \right] \\
 &\quad + \left(-\frac{i}{\hbar}\right) \left[f, \frac{\lambda_B}{\sqrt{2}} (d_1 f - d_1^\dagger f^\dagger) \right],
 \end{aligned} \tag{A.31}$$

$$\begin{aligned}
 \partial_t f(t) &= \left(-\frac{i}{\hbar}\right)[f, \mathcal{H}] \\
 &= \left(-\frac{i}{\hbar}\right)\left[f, \varepsilon_M \left(f^\dagger f - \frac{1}{2}\right)\right] + \left(-\frac{i}{\hbar}\right)\left[f, \frac{\lambda_A}{\sqrt{2}} \left(d_1 f^\dagger + f d_1^\dagger\right)\right] \\
 &+ \left(-\frac{i}{\hbar}\right)\left[f, \frac{\lambda_B}{\sqrt{2}} \left(d_1 f - d_1^\dagger f^\dagger\right)\right], \tag{A.32}
 \end{aligned}$$

$$\begin{aligned}
 \varepsilon_M \left[f, \left(f^\dagger f - \frac{1}{2}\right)\right] &= \varepsilon_M \left(f \left(f^\dagger f - \frac{1}{2}\right) - \left(f^\dagger f - \frac{1}{2}\right) f\right) = \varepsilon_M \left(f f^\dagger f - f^\dagger f f\right) \\
 &= \varepsilon_M \left(\left(1 - f^\dagger f\right) f - f^\dagger f f\right) = \varepsilon_M \left(\left(1 - f^\dagger f\right) f - f^\dagger f f\right) \\
 &= \varepsilon_M \left(f - f^\dagger f f + f^\dagger f f\right) = \varepsilon_M f. \tag{A.33}
 \end{aligned}$$

$$\begin{aligned}
 \frac{\lambda_A}{\sqrt{2}} \left[f, \left(d_1 f^\dagger + f d_1^\dagger\right)\right] &= \frac{\lambda_A}{\sqrt{2}} \left(f \left(d_1 f^\dagger + f d_1^\dagger\right) - \left(d_1 f^\dagger + f d_1^\dagger\right) f\right) = \frac{\lambda_A}{\sqrt{2}} \left(f d_1 f^\dagger + f f d_1^\dagger - d_1 f^\dagger f - f d_1^\dagger f\right) \\
 &= \frac{\lambda_A}{\sqrt{2}} \left(-d_1 f f^\dagger - f f d_1^\dagger - d_1 f^\dagger f + f f d_1^\dagger\right) = -\frac{\lambda_A}{\sqrt{2}} d_1 \left(f f^\dagger + f^\dagger f\right) = -\frac{\lambda_A}{\sqrt{2}} d_1. \tag{A.34}
 \end{aligned}$$

$$\begin{aligned}
 \frac{\lambda_B}{\sqrt{2}} \left[f, \left(d_1 f - d_1^\dagger f^\dagger\right)\right] &= \frac{\lambda_B}{\sqrt{2}} \left(f \left(d_1 f - d_1^\dagger f^\dagger\right) - \left(d_1 f - d_1^\dagger f^\dagger\right) f\right) = \frac{\lambda_B}{\sqrt{2}} \left(f d_1 f - f d_1^\dagger f^\dagger - d_1 f f + d_1^\dagger f^\dagger f\right) \\
 &= \frac{\lambda_B}{\sqrt{2}} \left(-d_1 f f + d_1^\dagger f f^\dagger + d_1 f f + d_1^\dagger f^\dagger f\right) = \frac{\lambda_B}{\sqrt{2}} d_1^\dagger \left(f f^\dagger + f^\dagger f\right) = \frac{\lambda_B}{\sqrt{2}} d_1^\dagger. \tag{A.35}
 \end{aligned}$$

$$\begin{aligned}
 \partial_t f(t) &= \left(-\frac{i}{\hbar}\right)[f, \mathcal{H}] \\
 &= \left(-\frac{i}{\hbar}\right)\varepsilon_M f + \left(-\frac{i}{\hbar}\right)\left(-\frac{\lambda_A}{\sqrt{2}}\right) d_1 + \left(-\frac{i}{\hbar}\right)\frac{\lambda_B}{\sqrt{2}} d_1^\dagger, \tag{A.36}
 \end{aligned}$$

$$\begin{aligned}
 \partial_t \mathcal{G}_{ff}(t) &= \left(-\frac{i}{\hbar}\right)\delta(t)\mathcal{Z}^{-1}\sum_r e^{-\beta E_r} \left\langle r \left| \left[f(t), f^\dagger(0) \right]_+ \right| r \right\rangle \\
 &+ \left(-\frac{i}{\hbar}\right)\varepsilon_M \left(-\frac{i}{\hbar}\right)\theta(t)\mathcal{Z}^{-1}\sum_r e^{-\beta E_r} \left\langle r \left| \left[f(t), f^\dagger(0) \right]_+ \right| r \right\rangle \\
 &- \left(-\frac{i}{\hbar}\right)\frac{\lambda_A}{\sqrt{2}} \left(-\frac{i}{\hbar}\right)\theta(t)\mathcal{Z}^{-1}\sum_r e^{-\beta E_r} \left\langle r \left| \left[d_1(t), f^\dagger(0) \right]_+ \right| r \right\rangle \\
 &+ \left(-\frac{i}{\hbar}\right)\frac{\lambda_B}{\sqrt{2}} \left(-\frac{i}{\hbar}\right)\theta(t)\mathcal{Z}^{-1}\sum_r e^{-\beta E_r} \left\langle r \left| \left[d_1^\dagger(t), f^\dagger(0) \right]_+ \right| r \right\rangle \tag{A.37}
 \end{aligned}$$

$$\begin{aligned}
 \partial_t \mathcal{G}_{ff}(t) &= \left(-\frac{i}{\hbar}\right) \delta(t) \mathcal{Z}^{-1} \sum_r e^{-\beta E_r} \left\langle r \left| \left[f(t), f^\dagger(0) \right]_+ \right| r \right\rangle \\
 &+ \left(-\frac{i}{\hbar}\right) \varepsilon_M \mathcal{G}_{ff}(t) - \left(-\frac{i}{\hbar}\right) \frac{\lambda_A}{\sqrt{2}} \mathcal{G}_{d_1 f}(t) + \left(-\frac{i}{\hbar}\right) \frac{\lambda_B}{\sqrt{2}} \mathcal{G}_{d_1^\dagger f}(t)
 \end{aligned} \tag{A.38}$$

According to the Fourier transform, we have

$$(\varepsilon - \varepsilon_M + i\delta) \tilde{\mathcal{G}}_{ff}(\varepsilon) = 1 - \frac{\lambda_A}{\sqrt{2}} \tilde{\mathcal{G}}_{d_1 f}(\varepsilon) + \frac{\lambda_B}{\sqrt{2}} \tilde{\mathcal{G}}_{d_1^\dagger f}(\varepsilon) \tag{A.39}$$

Similarly, we obtain $\tilde{\mathcal{G}}_{f^\dagger f}(\varepsilon)$:

$$(\varepsilon - \varepsilon_M + i\delta) \tilde{\mathcal{G}}_{f^\dagger f}(\varepsilon) = -\frac{\lambda_A}{\sqrt{2}} \tilde{\mathcal{G}}_{d_1 f^\dagger}(\varepsilon) + \frac{\lambda_B}{\sqrt{2}} \tilde{\mathcal{G}}_{d_1^\dagger f^\dagger}(\varepsilon) \tag{A.40}$$

We can regroup the mean equations up to now:

$$\tilde{\mathcal{G}}_{f^\dagger f}(\varepsilon) = \frac{\lambda_A}{\sqrt{2}} \frac{\tilde{\mathcal{G}}_{d_1^\dagger f}(\varepsilon)}{(\varepsilon + \varepsilon_M + i\delta)} - \frac{\lambda_B}{\sqrt{2}} \frac{\mathcal{G}_{d_1 f}(\varepsilon)}{(\varepsilon + \varepsilon_M + i\delta)}, \tag{A.41}$$

$$\tilde{\mathcal{G}}_{f^\dagger f^\dagger}(\varepsilon) = \frac{1}{(\varepsilon + \varepsilon_M + i\delta)} + \frac{\lambda_A}{\sqrt{2}} \frac{\tilde{\mathcal{G}}_{d_1^\dagger f^\dagger}(\varepsilon)}{(\varepsilon + \varepsilon_M + i\delta)} - \frac{\lambda_B}{\sqrt{2}} \frac{\mathcal{G}_{d_1 f^\dagger}(\varepsilon)}{(\varepsilon + \varepsilon_M + i\delta)}, \tag{A.42}$$

$$\tilde{\mathcal{G}}_{ff}(\varepsilon) = \frac{1}{(\varepsilon - \varepsilon_M + i\delta)} - \frac{\lambda_A}{\sqrt{2}} \frac{\tilde{\mathcal{G}}_{d_1 f}(\varepsilon)}{(\varepsilon - \varepsilon_M + i\delta)} + \frac{\lambda_B}{\sqrt{2}} \frac{\tilde{\mathcal{G}}_{d_1^\dagger f}(\varepsilon)}{(\varepsilon - \varepsilon_M + i\delta)}, \tag{A.43}$$

$$\tilde{\mathcal{G}}_{ff^\dagger}(\varepsilon) = -\frac{\lambda_A}{\sqrt{2}} \frac{\tilde{\mathcal{G}}_{d_1 f^\dagger}(\varepsilon)}{(\varepsilon - \varepsilon_M + i\delta)} + \frac{\lambda_B}{\sqrt{2}} \frac{\tilde{\mathcal{G}}_{d_1^\dagger f^\dagger}(\varepsilon)}{(\varepsilon - \varepsilon_M + i\delta)} \tag{A.44}$$

and

$$\mathcal{G}_{\eta_1 \eta_1}(t) = \frac{1}{2} \mathcal{G}_{f^\dagger f}(t) + \frac{1}{2} \mathcal{G}_{f^\dagger f^\dagger}(t) + \frac{1}{2} \mathcal{G}_{ff}(t) + \frac{1}{2} \mathcal{G}_{ff^\dagger}(t). \tag{A.45}$$

On the time domain:

$$\tilde{\mathcal{G}}_{\eta_1\eta_1}(\varepsilon) = \frac{1}{2}\tilde{\mathcal{G}}_{f^\dagger f}(\varepsilon) + \frac{1}{2}\tilde{\mathcal{G}}_{f^\dagger f^\dagger}(\varepsilon) + \frac{1}{2}\tilde{\mathcal{G}}_{ff}(\varepsilon) + \frac{1}{2}\tilde{\mathcal{G}}_{ff^\dagger}(\varepsilon). \quad (\text{A.46})$$

By substituting Eqs. (B.31), (A.42), (A.43) and (A.44) in Eq. (A.46), we obtain:

$$\begin{aligned} \tilde{\mathcal{G}}_{\eta_1\eta_1}(\varepsilon) &= \frac{1}{2} \left[\frac{\lambda_A}{\sqrt{2}} \frac{\tilde{\mathcal{G}}_{d_1^\dagger f}(\varepsilon)}{(\varepsilon + \varepsilon_M + i\delta)} - \frac{\lambda_B}{\sqrt{2}} \frac{\mathcal{G}_{d_1 f}(\varepsilon)}{(\varepsilon + \varepsilon_M + i\delta)} \right] \\ &+ \frac{1}{2} \left[\frac{1}{(\varepsilon + \varepsilon_M + i\delta)} + \frac{\lambda_A}{\sqrt{2}} \frac{\tilde{\mathcal{G}}_{d_1^\dagger f^\dagger}(\varepsilon)}{(\varepsilon + \varepsilon_M + i\delta)} - \frac{\lambda_B}{\sqrt{2}} \frac{\mathcal{G}_{d_1 f^\dagger}(\varepsilon)}{(\varepsilon + \varepsilon_M + i\delta)} \right] \\ &+ \frac{1}{2} \left[\frac{1}{(\varepsilon - \varepsilon_M + i\delta)} - \frac{\lambda_A}{\sqrt{2}} \frac{\tilde{\mathcal{G}}_{d_1 f}(\varepsilon)}{(\varepsilon - \varepsilon_M + i\delta)} + \frac{\lambda_B}{\sqrt{2}} \frac{\tilde{\mathcal{G}}_{d_1^\dagger f}(\varepsilon)}{(\varepsilon - \varepsilon_M + i\delta)} \right] \\ &+ \frac{1}{2} \left[-\frac{\lambda_A}{\sqrt{2}} \frac{\tilde{\mathcal{G}}_{d_1 f^\dagger}(\varepsilon)}{(\varepsilon - \varepsilon_M + i\delta)} + \frac{\lambda_B}{\sqrt{2}} \frac{\tilde{\mathcal{G}}_{d_1^\dagger f^\dagger}(\varepsilon)}{(\varepsilon - \varepsilon_M + i\delta)} \right] \\ &= \frac{1}{2} \left(\frac{1}{\varepsilon + \varepsilon_M + i\delta} + \frac{1}{\varepsilon - \varepsilon_M + i\delta} \right) \\ &+ \frac{1}{2\sqrt{2}} \left(\frac{\lambda_A}{\varepsilon + \varepsilon_M + i\delta} + \frac{\lambda_B}{\varepsilon - \varepsilon_M + i\delta} \right) \tilde{\mathcal{G}}_{d_1^\dagger f}(\varepsilon) \\ &+ \frac{1}{2\sqrt{2}} \left(\frac{\lambda_A}{\varepsilon + \varepsilon_M + i\delta} + \frac{\lambda_B}{\varepsilon - \varepsilon_M + i\delta} \right) \tilde{\mathcal{G}}_{d_1^\dagger f^\dagger}(\varepsilon) \\ &- \frac{1}{2\sqrt{2}} \left(\frac{\lambda_A}{\varepsilon - \varepsilon_M + i\delta} + \frac{\lambda_B}{\varepsilon + \varepsilon_M + i\delta} \right) \tilde{\mathcal{G}}_{d_1 f}(\varepsilon) \\ &- \frac{1}{2\sqrt{2}} \left(\frac{\lambda_A}{\varepsilon - \varepsilon_M + i\delta} + \frac{\lambda_B}{\varepsilon + \varepsilon_M + i\delta} \right) \tilde{\mathcal{G}}_{d_1 f^\dagger}(\varepsilon) \end{aligned} \quad (\text{A.47})$$

$$\begin{aligned} \tilde{\mathcal{G}}_{\eta_1\eta_1} &= K + \frac{1}{2\sqrt{2}} \left(\frac{\lambda_A}{\varepsilon + \varepsilon_M + i\delta} + \frac{\lambda_B}{\varepsilon - \varepsilon_M + i\delta} \right) (\tilde{\mathcal{G}}_{d_1^\dagger f} + \tilde{\mathcal{G}}_{d_1^\dagger f^\dagger}) \\ &- \frac{1}{2\sqrt{2}} \left(\frac{\lambda_A}{\varepsilon - \varepsilon_M + i\delta} + \frac{\lambda_B}{\varepsilon + \varepsilon_M + i\delta} \right) (\tilde{\mathcal{G}}_{d_1 f} + \tilde{\mathcal{G}}_{d_1 f^\dagger}) \end{aligned} \quad (\text{A.48})$$

Notice that we have to find four new Green functions. We start with $\tilde{\mathcal{G}}_{d_1^\dagger f}$:

$$\mathcal{G}_{d_1^\dagger f}(t) = \left(-\frac{i}{\hbar}\right)\theta(t)\mathcal{Z}^{-1}\sum_r e^{-\beta E_r} \left\langle r \left| \left[d_1^\dagger(t), f^\dagger(0) \right]_+ \right| r \right\rangle. \quad (\text{A.49})$$

$$\begin{aligned} \partial_t \mathcal{G}_{d_1^\dagger f}(t) &= \left(-\frac{i}{\hbar}\right)\delta(t)\mathcal{Z}^{-1}\sum_r e^{-\beta E_r} \left\langle r \left| \left[d_1^\dagger(t), f^\dagger(0) \right]_+ \right| r \right\rangle \\ &+ \left(-\frac{i}{\hbar}\right)\theta(t)\mathcal{Z}^{-1}\sum_r e^{-\beta E_r} \left\langle r \left| \left[\partial_t d_1^\dagger(t), f^\dagger(0) \right]_+ \right| r \right\rangle \end{aligned} \quad (\text{A.50})$$

$$\begin{aligned}
 \partial_t d_1^\dagger(t) &= \left(-\frac{i}{\hbar}\right) \left[d_1^\dagger, \mathcal{H} \right] \\
 &= \left(-\frac{i}{\hbar}\right) \left[d_1^\dagger, \sum_k \varepsilon_k c_{ek}^\dagger c_{ek} \right] + \left(-\frac{i}{\hbar}\right) \left[d_1^\dagger, \varepsilon_1 d_1^\dagger d_1 \right] + \left(-\frac{i}{\hbar}\right) \left[d_1^\dagger, \sqrt{2}V \sum_k (c_{ek}^\dagger d_1 + H.c.) \right] \\
 &+ \left(-\frac{i}{\hbar}\right) \left[d_1^\dagger, V_{BT} \sum_{kq} c_{ek}^\dagger c_{eq} \right] + \left(-\frac{i}{\hbar}\right) \left[d_1^\dagger, \varepsilon_M \left(f^\dagger f - \frac{1}{2} \right) \right] + \left(-\frac{i}{\hbar}\right) \left[d_1^\dagger, \frac{\lambda_A}{\sqrt{2}} \left(d_1 f^\dagger + f d_1^\dagger \right) \right] \\
 &+ \left(-\frac{i}{\hbar}\right) \left[d_1^\dagger, \frac{\lambda_B}{\sqrt{2}} \left(d_1 f - d_1^\dagger f^\dagger \right) \right], \tag{A.51}
 \end{aligned}$$

$$\begin{aligned}
 \partial_t d_1^\dagger(t) &= \left(-\frac{i}{\hbar}\right) \left[d_1^\dagger, \mathcal{H} \right] \\
 &= \left(-\frac{i}{\hbar}\right) \left[d_1^\dagger, \varepsilon_1 d_1^\dagger d_1 \right] + \left(-\frac{i}{\hbar}\right) \left[d_1^\dagger, \sqrt{2}V \sum_k (c_{ek}^\dagger d_1 + H.c.) \right] \\
 &+ \left(-\frac{i}{\hbar}\right) \left[d_1^\dagger, \frac{\lambda_A}{\sqrt{2}} \left(d_1 f^\dagger + f d_1^\dagger \right) \right] + \left(-\frac{i}{\hbar}\right) \left[d_1^\dagger, \frac{\lambda_B}{\sqrt{2}} \left(d_1 f - d_1^\dagger f^\dagger \right) \right] \tag{A.52}
 \end{aligned}$$

$$\begin{aligned}
 \varepsilon_1 \left[d_1^\dagger, d_1^\dagger d_1 \right] &= \varepsilon_1 \left(d_1^\dagger d_1^\dagger d_1 - d_1^\dagger d_1 d_1^\dagger \right) = \varepsilon_1 \left(d_1^\dagger d_1^\dagger d_1 - d_1^\dagger \left(1 - d_1^\dagger d_1 \right) \right) \\
 &= \varepsilon_1 \left(-d_1^\dagger d_1^\dagger d_1 - d_1^\dagger + d_1^\dagger d_1^\dagger d_1 \right) = -\varepsilon_1 d_1^\dagger \tag{A.53}
 \end{aligned}$$

$$\begin{aligned}
 \sqrt{2}V \sum_k \left[d_1^\dagger, (c_{ek}^\dagger d_1 + H.c.) \right] &= \sqrt{2}V \sum_k \left(d_1^\dagger (c_{ek}^\dagger d_1 + d_1^\dagger c_{ek}) - (c_{ek}^\dagger d_1 + d_1^\dagger c_{ek}) d_1^\dagger \right) \\
 &= \sqrt{2}V \sum_k \left(d_1^\dagger c_{ek}^\dagger d_1 + d_1^\dagger d_1^\dagger c_{ek} - c_{ek}^\dagger d_1 d_1^\dagger - d_1^\dagger c_{ek} d_1^\dagger \right) \\
 &= \sqrt{2}V \sum_k \left(-c_{ek}^\dagger d_1^\dagger d_1 - d_1^\dagger d_1^\dagger c_{ek} - c_{ek}^\dagger d_1 d_1^\dagger + d_1^\dagger d_1^\dagger c_{ek} \right) \\
 &= \sqrt{2}V \sum_k \left(-c_{ek}^\dagger \right) \left(d_1^\dagger d_1 + d_1 d_1^\dagger \right) = -\sqrt{2}V \sum_k c_{ek}^\dagger \tag{A.54}
 \end{aligned}$$

$$\begin{aligned}
 \frac{\lambda_A}{\sqrt{2}} \left[d_1^\dagger, \left(d_1 f^\dagger + f d_1^\dagger \right) \right] &= \frac{\lambda_A}{\sqrt{2}} \left(d_1^\dagger \left(d_1 f^\dagger + f d_1^\dagger \right) - \left(d_1 f^\dagger + f d_1^\dagger \right) d_1^\dagger \right) \\
 &= \frac{\lambda_A}{\sqrt{2}} \left(d_1^\dagger d_1 f^\dagger - f d_1^\dagger d_1^\dagger + d_1 d_1^\dagger f^\dagger + f d_1^\dagger d_1^\dagger \right) \\
 &= \frac{\lambda_A}{\sqrt{2}} \left(d_1^\dagger d_1 + d_1 d_1^\dagger \right) f^\dagger = \frac{\lambda_A}{\sqrt{2}} f^\dagger \tag{A.55}
 \end{aligned}$$

$$\begin{aligned}
 \frac{\lambda_B}{\sqrt{2}} \left[d_1^\dagger, (d_1 f - d_1^\dagger f^\dagger) \right] &= \frac{\lambda_B}{\sqrt{2}} \left(d_1^\dagger (d_1 f - d_1^\dagger f^\dagger) - (d_1 f - d_1^\dagger f^\dagger) d_1^\dagger \right) \\
 &= \frac{\lambda_B}{\sqrt{2}} \left(d_1^\dagger d_1 f + d_1^\dagger d_1^\dagger f^\dagger + d_1 d_1^\dagger f - d_1^\dagger d_1^\dagger f^\dagger \right) \\
 &= \frac{\lambda_B}{\sqrt{2}} \left(d_1^\dagger d_1 + d_1 d_1^\dagger \right) f = \frac{\lambda_B}{\sqrt{2}} f
 \end{aligned} \tag{A.56}$$

$$\begin{aligned}
 \partial_t d_1^\dagger(t) &= \left(-\frac{i}{\hbar}\right) \left[d_1^\dagger, \mathcal{H} \right] \\
 &= -\left(-\frac{i}{\hbar}\right) \varepsilon_1 d_1^\dagger - \left(-\frac{i}{\hbar}\right) \sqrt{2} V \sum_k c_{ek}^\dagger + \left(-\frac{i}{\hbar}\right) \frac{\lambda_A}{\sqrt{2}} f^\dagger + \left(-\frac{i}{\hbar}\right) \frac{\lambda_B}{\sqrt{2}} f
 \end{aligned} \tag{A.57}$$

$$\begin{aligned}
 \partial_t \mathcal{G}_{d_1^\dagger f}(t) &= \left(-\frac{i}{\hbar}\right) \delta(t) \mathcal{Z}^{-1} \sum_r e^{-\beta E_r} \left\langle r \left| \left[d_1^\dagger(t), f^\dagger(0) \right]_+ \right| r \right\rangle \\
 &\quad - \left(-\frac{i}{\hbar}\right) \varepsilon_1 \left\{ \left(-\frac{i}{\hbar}\right) \theta(t) \mathcal{Z}^{-1} \sum_r e^{-\beta E_r} \left\langle r \left| \left[d_1^\dagger(t), f^\dagger(0) \right]_+ \right| r \right\rangle \right\} \\
 &\quad - \left(-\frac{i}{\hbar}\right) \sqrt{2} V \sum_k \left\{ \left(-\frac{i}{\hbar}\right) \theta(t) \mathcal{Z}^{-1} \sum_r e^{-\beta E_r} \left\langle r \left| \left[c_{ek}^\dagger(t), f^\dagger(0) \right]_+ \right| r \right\rangle \right\} \\
 &\quad + \left(-\frac{i}{\hbar}\right) \frac{\lambda_A}{\sqrt{2}} \left\{ \left(-\frac{i}{\hbar}\right) \theta(t) \mathcal{Z}^{-1} \sum_r e^{-\beta E_r} \left\langle r \left| \left[f^\dagger(t), f^\dagger(0) \right]_+ \right| r \right\rangle \right\} \\
 &\quad + \left(-\frac{i}{\hbar}\right) \frac{\lambda_B}{\sqrt{2}} \left\{ \left(-\frac{i}{\hbar}\right) \theta(t) \mathcal{Z}^{-1} \sum_r e^{-\beta E_r} \left\langle r \left| \left[f(t), f^\dagger(0) \right]_+ \right| r \right\rangle \right\}
 \end{aligned} \tag{A.58}$$

$$\begin{aligned}
 \partial_t \mathcal{G}_{d_1^\dagger f}(t) &= \left(-\frac{i}{\hbar}\right) \delta(t) \mathcal{Z}^{-1} \sum_r e^{-\beta E_r} \left\langle r \left| \left[d_1^\dagger(t), f^\dagger(0) \right]_+ \right| r \right\rangle \\
 &\quad - \left(-\frac{i}{\hbar}\right) \varepsilon_1 \mathcal{G}_{d_1^\dagger f}(t) - \left(-\frac{i}{\hbar}\right) \sqrt{2} V \sum_k \mathcal{G}_{c_{ek}^\dagger f}(t) + \left(-\frac{i}{\hbar}\right) \frac{\lambda_A}{\sqrt{2}} \mathcal{G}_{f^\dagger f}(t) + \left(-\frac{i}{\hbar}\right) \frac{\lambda_B}{\sqrt{2}} \mathcal{G}_{ff}(t)
 \end{aligned} \tag{A.59}$$

By performing the Fourier transform we obtain:

$$(\varepsilon + \varepsilon_1 + i\delta) \tilde{\mathcal{G}}_{d_1^\dagger f}(\varepsilon) = -\sqrt{2} V \sum_k \tilde{\mathcal{G}}_{c_{ek}^\dagger f}(\varepsilon) + \frac{\lambda_A}{\sqrt{2}} \tilde{\mathcal{G}}_{f^\dagger f}(\varepsilon) + \frac{\lambda_B}{\sqrt{2}} \mathcal{G}_{ff}(\varepsilon) \tag{A.60}$$

Therefore, we have to calculate $\tilde{\mathcal{G}}_{c_{ek}^\dagger f}(\varepsilon)$, definite in the time domain as:

$$\mathcal{G}_{c_{ek}^\dagger f}(t) = \left(-\frac{i}{\hbar}\right)\theta(t)\mathcal{Z}^{-1}\sum_r e^{-\beta E_r} \left\langle r \left| \left[c_{ek}^\dagger(t), f^\dagger(0) \right]_+ \right| r \right\rangle \quad (\text{A.61})$$

$$\begin{aligned} \partial_t \mathcal{G}_{c_{ek}^\dagger f}(t) &= \left(-\frac{i}{\hbar}\right)\delta(t)\mathcal{Z}^{-1}\sum_r e^{-\beta E_r} \left\langle r \left| \left[c_{ek}^\dagger(t), f^\dagger(0) \right]_+ \right| r \right\rangle \\ &+ \left(-\frac{i}{\hbar}\right)\theta(t)\mathcal{Z}^{-1}\sum_r e^{-\beta E_r} \left\langle r \left| \left[\partial_t c_{ek}^\dagger(t), f^\dagger(0) \right]_+ \right| r \right\rangle \end{aligned} \quad (\text{A.62})$$

$$\begin{aligned} \partial_t c_{ek}^\dagger(t) &= \left(-\frac{i}{\hbar}\right) \left[c_{ek}^\dagger, \mathcal{H} \right] \\ &= \left(-\frac{i}{\hbar}\right) \left[c_{ek}^\dagger, \sum_k \varepsilon_k c_{ek}^\dagger c_{ek} \right] + \left(-\frac{i}{\hbar}\right) \left[c_{ek}^\dagger, \varepsilon_1 d_1^\dagger d_1 \right] + \left(-\frac{i}{\hbar}\right) \left[c_{ek}^\dagger, \sqrt{2}V \sum_k (c_{ek}^\dagger d_1 + H.c.) \right] \\ &+ \left(-\frac{i}{\hbar}\right) \left[c_{ek}^\dagger, V_{BT} \sum_{kq} c_{ek}^\dagger c_{eq} \right] + \left(-\frac{i}{\hbar}\right) \left[c_{ek}^\dagger, \varepsilon_M \left(f^\dagger f - \frac{1}{2} \right) \right] + \left(-\frac{i}{\hbar}\right) \left[c_{ek}^\dagger, \frac{\lambda_A}{\sqrt{2}} \left(d_1 f^\dagger + f d_1^\dagger \right) \right] \\ &+ \left(-\frac{i}{\hbar}\right) \left[c_{ek}^\dagger, \frac{\lambda_B}{\sqrt{2}} \left(d_1 f - d_1^\dagger f^\dagger \right) \right], \end{aligned} \quad (\text{A.63})$$

$$\begin{aligned} \partial_t c_{ek}^\dagger(t) &= \left(-\frac{i}{\hbar}\right) \left[c_{ek}^\dagger, \mathcal{H} \right] \\ &= \left(-\frac{i}{\hbar}\right) \left[c_{ek}^\dagger, \sum_k \varepsilon_k c_{ek}^\dagger c_{ek} \right] + \left(-\frac{i}{\hbar}\right) \left[c_{ek}^\dagger, \sqrt{2}V \sum_k (c_{ek}^\dagger d_1 + H.c.) \right] \\ &+ \left(-\frac{i}{\hbar}\right) \left[c_{ek}^\dagger, V_{BT} \sum_{kq} c_{ek}^\dagger c_{eq} \right] \end{aligned} \quad (\text{A.64})$$

$$\begin{aligned} \left[c_{ek}^\dagger, \sum_p \varepsilon_p c_{ep}^\dagger c_{ep} \right] &= \sum_p \varepsilon_p \left(c_{ek}^\dagger c_{ep}^\dagger c_{ep} - c_{ep}^\dagger c_{ep} c_{ek}^\dagger \right) = \sum_p \varepsilon_p \left(c_{ek}^\dagger c_{ep}^\dagger c_{ep} - c_{ep}^\dagger \left(\delta_{pk} - c_{ek}^\dagger c_{ep} \right) \right) \\ &= \sum_p \varepsilon_p \left(c_{ek}^\dagger c_{ep}^\dagger c_{ep} - \delta_{pk} c_{ep}^\dagger - c_{ek}^\dagger c_{ep}^\dagger c_{ep} \right) = -\sum_k \varepsilon_k c_{ek}^\dagger. \end{aligned} \quad (\text{A.65})$$

$$\begin{aligned}
 \left[c_{ep}^\dagger, \sqrt{2}V \sum_k (c_{ek}^\dagger d_1 + H.c.) \right] &= \sqrt{2}V \sum_k \left(c_{ep}^\dagger (c_{ek}^\dagger d_1 + d_1^\dagger c_{ek}) - (c_{ek}^\dagger d_1 + d_1^\dagger c_{ek}) c_{ep}^\dagger \right) \\
 &= \sqrt{2}V \sum_k \left(c_{ep}^\dagger c_{ek}^\dagger d_1 + c_{ep}^\dagger d_1^\dagger c_{ek} - c_{ek}^\dagger d_1 c_{ep}^\dagger - d_1^\dagger c_{ek} c_{ep}^\dagger \right) \\
 &= \sqrt{2}V \sum_k \left(-c_{ep}^\dagger c_{ek}^\dagger d_1 - d_1^\dagger c_{ep}^\dagger c_{ek} + c_{ek}^\dagger c_{ep}^\dagger d_1 - d_1^\dagger c_{ek} c_{ep}^\dagger \right) \\
 &= \sqrt{2}V \sum_k d_1^\dagger \left(c_{ep}^\dagger c_{ek} + c_{ek} c_{ep}^\dagger \right) = -\sqrt{2}V \sum_k d_1^\dagger. \quad (\text{A.66})
 \end{aligned}$$

$$\begin{aligned}
 V_{BT} \left[c_{ek}^\dagger, \sum_{pq} c_{ep}^\dagger c_{eq} \right] &= V_{BT} \sum_{pq} \left(c_{ek}^\dagger c_{ep}^\dagger c_{eq} - c_{ep}^\dagger c_{eq} c_{ek}^\dagger \right) = V_{BT} \sum_{pq} \left(c_{ek}^\dagger c_{ep}^\dagger c_{eq} - \delta_{qk} c_{ep}^\dagger + c_{ep}^\dagger c_{ek}^\dagger c_{eq} \right) \\
 &= V_{BT} \sum_{pq} \left(-c_{ek}^\dagger c_{ep}^\dagger c_{eq} - \delta_{qk} c_{ep}^\dagger + c_{ep}^\dagger c_{ek}^\dagger c_{eq} \right) = -V_{BT} \sum_{kq} c_{ek}^\dagger \quad (\text{A.67})
 \end{aligned}$$

$$\begin{aligned}
 \partial_t c_{ek}^\dagger(t) &= \left(-\frac{i}{\hbar}\right) \left[c_{ek}^\dagger, \mathcal{H} \right] \\
 &= -\left(-\frac{i}{\hbar}\right) \sum_k \varepsilon_k c_{ek}^\dagger - \left(-\frac{i}{\hbar}\right) \sqrt{2}V \sum_k d_1^\dagger - \left(-\frac{i}{\hbar}\right) V_{BT} \sum_{kq} c_{ek}^\dagger \quad (\text{A.68})
 \end{aligned}$$

$$\begin{aligned}
 \partial_t \mathcal{G}_{c_{ek}^\dagger f}^\dagger(t) &= \left(-\frac{i}{\hbar}\right) \delta(t) \mathcal{Z}^{-1} \sum_r e^{-\beta E_r} \left\langle r \left| \left[c_{ek}^\dagger(t), f^\dagger(0) \right]_+ \right| r \right\rangle \\
 &\quad - \left(-\frac{i}{\hbar}\right) \sum_k \varepsilon_k \left\langle r \left| \left[c_{ek}^\dagger(t), f^\dagger(0) \right]_+ \right| r \right\rangle \\
 &\quad - \left(-\frac{i}{\hbar}\right) \sqrt{2}V \sum_k \left\langle r \left| \left[d_1^\dagger(t), f^\dagger(0) \right]_+ \right| r \right\rangle \\
 &\quad - \left(-\frac{i}{\hbar}\right) V_{BT} \sum_{kq} \left\langle r \left| \left[c_{ek}^\dagger(t), f^\dagger(0) \right]_+ \right| r \right\rangle \quad (\text{A.69})
 \end{aligned}$$

After applying the Fourier transform, we find:

$$(\varepsilon + \varepsilon_k + i\delta) \tilde{\mathcal{G}}_{c_{ek}^\dagger f}^\dagger(\varepsilon) = -\sqrt{2}V \tilde{\mathcal{G}}_{d_1^\dagger f}^\dagger(\varepsilon) - V_{BT} \sum_q \tilde{\mathcal{G}}_{c_{eq}^\dagger f}^\dagger(\varepsilon) \quad (\text{A.70})$$

But,

$$\begin{aligned}
 \sum_k \tilde{\mathcal{G}}_{c_{ek}^\dagger f}(\varepsilon) &= -\sqrt{2}V \sum_k \frac{\tilde{\mathcal{G}}_{d_1^\dagger f}(\varepsilon)}{(\varepsilon + \varepsilon_k + i\delta)} - V_{BT} \sum_k \frac{\tilde{\mathcal{G}}_{c_{eq}^\dagger f}(\varepsilon)}{(\varepsilon + \varepsilon_k + i\delta)} \Rightarrow \\
 \left[1 + V_{BT} \sum_k \frac{1}{(\varepsilon + \varepsilon_k + i\delta)} \right] \sum_k \tilde{\mathcal{G}}_{c_{ek}^\dagger f}(\varepsilon) &= -\sqrt{2}V \sum_k \frac{1}{(\varepsilon + \varepsilon_k + i\delta)} \tilde{\mathcal{G}}_{d_1^\dagger f}(\varepsilon) \Rightarrow \\
 \sum_k \tilde{\mathcal{G}}_{c_{ek}^\dagger f}(\varepsilon) &= \frac{-\sqrt{2}V \sum_k \frac{1}{(\varepsilon + \varepsilon_k + i\delta)}}{1 + V_{BT} \sum_k \frac{1}{(\varepsilon + \varepsilon_k + i\delta)}} \tilde{\mathcal{G}}_{d_1^\dagger f}(\varepsilon). \tag{A.71}
 \end{aligned}$$

By substituting Eq. (A.71) in (A.60) we find:

$$\begin{aligned}
 (\varepsilon + \varepsilon_1 + i\delta) \tilde{\mathcal{G}}_{d_1^\dagger f}(\varepsilon) &= -\sqrt{2}V \left[\frac{-\sqrt{2}V \sum_k \frac{1}{(\varepsilon + \varepsilon_k + i\delta)}}{1 + V_{BT} \sum_k \frac{1}{(\varepsilon + \varepsilon_k + i\delta)}} \tilde{\mathcal{G}}_{d_1^\dagger f}(\varepsilon) \right] + \frac{\lambda_A}{\sqrt{2}} \tilde{\mathcal{G}}_{f^\dagger f}(\varepsilon) + \frac{\lambda_B}{\sqrt{2}} \mathcal{G}_{ff}(\varepsilon) \\
 &= \left[\frac{2V^2 \sum_k \frac{1}{(\varepsilon + \varepsilon_k + i\delta)}}{1 + V_{BT} \sum_k \frac{1}{(\varepsilon + \varepsilon_k + i\delta)}} \tilde{\mathcal{G}}_{d_1^\dagger f}(\varepsilon) \right] + \frac{\lambda_A}{\sqrt{2}} \tilde{\mathcal{G}}_{f^\dagger f}(\varepsilon) + \frac{\lambda_B}{\sqrt{2}} \mathcal{G}_{ff}(\varepsilon) \tag{A.72}
 \end{aligned}$$

We know from other calculations that $\sum_k \frac{1}{(\varepsilon + \varepsilon_k + i\delta)} = \pi \rho_0 (\bar{q} - i)$, where ρ_0 is the DOS of leads and \bar{q} is the intrinsic Fano parameter. Thus, Eq. (A.72) becomes:

$$(\varepsilon + \varepsilon_1 + i\delta) \tilde{\mathcal{G}}_{d_1^\dagger f}(\varepsilon) = \left[\frac{2V^2 \pi \rho_0 (\bar{q} - i)}{1 + V_{BT} \pi \rho_0 (\bar{q} - i)} \tilde{\mathcal{G}}_{d_1^\dagger f}(\varepsilon) \right] + \frac{\lambda_A}{\sqrt{2}} \tilde{\mathcal{G}}_{f^\dagger f}(\varepsilon) + \frac{\lambda_B}{\sqrt{2}} \mathcal{G}_{ff}(\varepsilon) \tag{A.73}$$

In the wide band limit, $\bar{q} \rightarrow 0$ and therefore

$$\begin{aligned}
 (\varepsilon + \varepsilon_1 + i\delta) \tilde{\mathcal{G}}_{d_1^\dagger f}(\varepsilon) &= \left[\frac{-i2V^2 \pi \rho_0}{(1 - iV_{BT} \pi \rho_0)} \tilde{\mathcal{G}}_{d_1^\dagger f}(\varepsilon) \right] + \frac{\lambda_A}{\sqrt{2}} \tilde{\mathcal{G}}_{f^\dagger f}(\varepsilon) + \frac{\lambda_B}{\sqrt{2}} \mathcal{G}_{ff}(\varepsilon) \\
 &= \left[\frac{-i2V^2 \pi \rho_0 (1 + iV_{BT} \pi \rho_0)}{(1 - iV_{BT} \pi \rho_0)(1 + iV_{BT} \pi \rho_0)} \tilde{\mathcal{G}}_{d_1^\dagger f}(\varepsilon) \right] + \frac{\lambda_A}{\sqrt{2}} \tilde{\mathcal{G}}_{f^\dagger f}(\varepsilon) + \frac{\lambda_B}{\sqrt{2}} \mathcal{G}_{ff}(\varepsilon) \\
 &= \left[\frac{-i2V^2 \pi \rho_0 (1 + iV_{BT} \pi \rho_0)}{1 + (V_{BT} \pi \rho_0)^2} \tilde{\mathcal{G}}_{d_1^\dagger f}(\varepsilon) \right] + \frac{\lambda_A}{\sqrt{2}} \tilde{\mathcal{G}}_{f^\dagger f}(\varepsilon) + \frac{\lambda_B}{\sqrt{2}} \mathcal{G}_{ff}(\varepsilon) \\
 &= \left[\frac{(\sqrt{x} - i) \Gamma}{1 + x} \tilde{\mathcal{G}}_{d_1^\dagger f}(\varepsilon) \right] + \frac{\lambda_A}{\sqrt{2}} \tilde{\mathcal{G}}_{f^\dagger f}(\varepsilon) + \frac{\lambda_B}{\sqrt{2}} \mathcal{G}_{ff}(\varepsilon) \\
 &= \tag{A.74}
 \end{aligned}$$

where we use $x = (V_{BT} \pi \rho_0)^2$ and $\Gamma = 2V^2 \pi \rho_0$ as Anderson parameter. Furthermore,

$$\tilde{\Sigma} = -\frac{(\sqrt{x} - i) \Gamma}{1 + x} \tag{A.75}$$

and due this Eq. (A.74) becomes:

$$(\varepsilon + \varepsilon_1 + i\delta) \tilde{\mathcal{G}}_{d_1^\dagger f}(\varepsilon) = -\tilde{\Sigma} \tilde{\mathcal{G}}_{d_1^\dagger f}(\varepsilon) + \frac{\lambda_A}{\sqrt{2}} \tilde{\mathcal{G}}_{f^\dagger f}(\varepsilon) + \frac{\lambda_B}{\sqrt{2}} \mathcal{G}_{ff}(\varepsilon),$$

$$(\varepsilon + \varepsilon_1 + \tilde{\Sigma}) \tilde{\mathcal{G}}_{d_1^\dagger f}(\varepsilon) = \frac{\lambda_A}{\sqrt{2}} \tilde{\mathcal{G}}_{f^\dagger f}(\varepsilon) + \frac{\lambda_B}{\sqrt{2}} \mathcal{G}_{ff}(\varepsilon).$$

(A.76)

Now, let's calculate $\tilde{\mathcal{G}}_{d_1^\dagger f^\dagger}(\varepsilon)$:

$$\mathcal{G}_{d_1^\dagger f^\dagger}(t) = \left(-\frac{i}{\hbar}\right) \theta(t) \mathcal{Z}^{-1} \sum_r e^{-\beta E_r} \left\langle r \left| \left[d_1^\dagger(t), f(0) \right]_+ \right| r \right\rangle. \quad (\text{A.77})$$

$$\begin{aligned} \partial_t \mathcal{G}_{d_1^\dagger f^\dagger}(t) &= \left(-\frac{i}{\hbar}\right) \delta(t) \mathcal{Z}^{-1} \sum_r e^{-\beta E_r} \left\langle r \left| \left[d_1^\dagger(t), f(0) \right]_+ \right| r \right\rangle \\ &+ \left(-\frac{i}{\hbar}\right) \theta(t) \mathcal{Z}^{-1} \sum_r e^{-\beta E_r} \left\langle r \left| \left[\partial_t d_1^\dagger(t), f(0) \right]_+ \right| r \right\rangle \end{aligned} \quad (\text{A.78})$$

$$\begin{aligned} \partial_t d_1^\dagger(t) &= \left(-\frac{i}{\hbar}\right) \left[d_1^\dagger, \mathcal{H} \right] \\ &= -\left(-\frac{i}{\hbar}\right) \varepsilon_1 d_1^\dagger - \left(-\frac{i}{\hbar}\right) \sqrt{2} V \sum_k c_{ek}^\dagger + \left(-\frac{i}{\hbar}\right) \frac{\lambda_A}{\sqrt{2}} f^\dagger + \left(-\frac{i}{\hbar}\right) \frac{\lambda_B}{\sqrt{2}} f \end{aligned} \quad (\text{A.79})$$

$$\begin{aligned} \partial_t \mathcal{G}_{d_1^\dagger f^\dagger}(t) &= \left(-\frac{i}{\hbar}\right) \delta(t) \mathcal{Z}^{-1} \sum_r e^{-\beta E_r} \left\langle r \left| \left[d_1^\dagger(t), f(0) \right]_+ \right| r \right\rangle \\ &- \left(-\frac{i}{\hbar}\right) \varepsilon_1 \left\{ \left(-\frac{i}{\hbar}\right) \theta(t) \mathcal{Z}^{-1} \sum_r e^{-\beta E_r} \left\langle r \left| \left[d_1^\dagger(t), f(0) \right]_+ \right| r \right\rangle \right\} \\ &- \left(-\frac{i}{\hbar}\right) \sqrt{2} V \sum_k \left\{ \left(-\frac{i}{\hbar}\right) \theta(t) \mathcal{Z}^{-1} \sum_r e^{-\beta E_r} \left\langle r \left| \left[c_{ek}^\dagger(t), f(0) \right]_+ \right| r \right\rangle \right\} \\ &+ \left(-\frac{i}{\hbar}\right) \frac{\lambda_A}{\sqrt{2}} \left\{ \left(-\frac{i}{\hbar}\right) \theta(t) \mathcal{Z}^{-1} \sum_r e^{-\beta E_r} \left\langle r \left| \left[f^\dagger(t), f(0) \right]_+ \right| r \right\rangle \right\} \\ &+ \left(-\frac{i}{\hbar}\right) \frac{\lambda_B}{\sqrt{2}} \left\{ \left(-\frac{i}{\hbar}\right) \theta(t) \mathcal{Z}^{-1} \sum_r e^{-\beta E_r} \left\langle r \left| \left[f(t), f(0) \right]_+ \right| r \right\rangle \right\} \end{aligned} \quad (\text{A.80})$$

$$\begin{aligned}
 \partial_t \mathcal{G}_{d_1^\dagger f^\dagger}(t) &= \left(-\frac{i}{\hbar}\right) \delta(t) \mathcal{Z}^{-1} \sum_r e^{-\beta E_r} \left\langle r \left| \left[d_1^\dagger(t), f(0) \right]_+ \right| r \right\rangle \\
 &- \left(-\frac{i}{\hbar}\right) \varepsilon_1 \mathcal{G}_{d_1^\dagger f^\dagger}(t) - \left(-\frac{i}{\hbar}\right) \sqrt{2} V \sum_k \mathcal{G}_{c_{ek}^\dagger f^\dagger}(t) + \left(-\frac{i}{\hbar}\right) \frac{\lambda_A}{\sqrt{2}} \mathcal{G}_{f^\dagger f^\dagger}(t) + \left(-\frac{i}{\hbar}\right) \frac{\lambda_B}{\sqrt{2}} \mathcal{G}_{ff^\dagger}(t)
 \end{aligned} \tag{A.81}$$

By performing the Fourier transform we obtain:

$$(\varepsilon + \varepsilon_1 + i\delta) \tilde{\mathcal{G}}_{d_1^\dagger f^\dagger}(\varepsilon) = -\sqrt{2} V \sum_k \tilde{\mathcal{G}}_{c_{ek}^\dagger f^\dagger}(\varepsilon) + \frac{\lambda_A}{\sqrt{2}} \tilde{\mathcal{G}}_{f^\dagger f^\dagger}(\varepsilon) + \frac{\lambda_B}{\sqrt{2}} \mathcal{G}_{ff^\dagger}(\varepsilon) \tag{A.82}$$

According to Eqs. (A.74) and (A.75) we obtain:

$$(\varepsilon + \varepsilon_1 + \tilde{\Sigma}) \tilde{\mathcal{G}}_{d_1^\dagger f^\dagger}(\varepsilon) = \frac{\lambda_A}{\sqrt{2}} \tilde{\mathcal{G}}_{f^\dagger f^\dagger}(\varepsilon) + \frac{\lambda_B}{\sqrt{2}} \mathcal{G}_{ff^\dagger}(\varepsilon) \tag{A.83}$$

Now, we will calculate $\tilde{\mathcal{G}}_{d_1 f}$, definite on the time domain on:

$$\mathcal{G}_{d_1 f}(t) = \left(-\frac{i}{\hbar}\right) \theta(t) \mathcal{Z}^{-1} \sum_r e^{-\beta E_r} \left\langle r \left| \left[d_1(t), f^\dagger(0) \right]_+ \right| r \right\rangle. \tag{A.84}$$

$$\begin{aligned}
 \partial_t \mathcal{G}_{d_1 f}(t) &= \left(-\frac{i}{\hbar}\right) \delta(t) \mathcal{Z}^{-1} \sum_r e^{-\beta E_r} \left\langle r \left| \left[d_1(t), f^\dagger(0) \right]_+ \right| r \right\rangle \\
 &+ \left(-\frac{i}{\hbar}\right) \theta(t) \mathcal{Z}^{-1} \sum_r e^{-\beta E_r} \left\langle r \left| \left[\partial_t d_1(t), f^\dagger(0) \right]_+ \right| r \right\rangle.
 \end{aligned} \tag{A.85}$$

$$\begin{aligned}
 \partial_t d_1(t) &= \left(-\frac{i}{\hbar}\right) [d_1, \mathcal{H}] \\
 &= \left(-\frac{i}{\hbar}\right) \left[d_1, \sum_k \varepsilon_k c_{ek}^\dagger c_{ek} \right] + \left(-\frac{i}{\hbar}\right) [d_1, \varepsilon_1 d_1^\dagger d_1] + \left(-\frac{i}{\hbar}\right) \left[d_1, \sqrt{2} V \sum_k (c_{ek}^\dagger d_1 + H.c.) \right] \\
 &+ \left(-\frac{i}{\hbar}\right) \left[d_1, V_{BT} \sum_{kq} c_{ek}^\dagger c_{eq} \right] + \left(-\frac{i}{\hbar}\right) \left[d_1, \varepsilon_M \left(f^\dagger f - \frac{1}{2} \right) \right] + \left(-\frac{i}{\hbar}\right) \left[d_1, \frac{\lambda_A}{\sqrt{2}} (d_1 f^\dagger + f d_1^\dagger) \right] \\
 &+ \left(-\frac{i}{\hbar}\right) \left[d_1, \frac{\lambda_B}{\sqrt{2}} (d_1 f - d_1^\dagger f^\dagger) \right],
 \end{aligned} \tag{A.86}$$

$$\begin{aligned}
 \partial_t d_1(t) &= \left(-\frac{i}{\hbar}\right) [d_1, \mathcal{H}] \\
 &= \left(-\frac{i}{\hbar}\right) [d_1, \varepsilon_1 d_1^\dagger d_1] + \left(-\frac{i}{\hbar}\right) \left[d_1, \sqrt{2}V \sum_k (c_{ek}^\dagger d_1 + H.c.) \right] \\
 &\quad + \left(-\frac{i}{\hbar}\right) \left[d_1, \frac{\lambda_A}{\sqrt{2}} (d_1 f^\dagger + f d_1^\dagger) \right] + \left(-\frac{i}{\hbar}\right) \left[d_1, \frac{\lambda_B}{\sqrt{2}} (d_1 f - d_1^\dagger f^\dagger) \right]
 \end{aligned} \tag{A.87}$$

$$\begin{aligned}
 [d_1, \varepsilon_1 d_1^\dagger d_1] &= \varepsilon_1 (d_1 d_1^\dagger d_1 - d_1^\dagger d_1 d_1) = \varepsilon_1 \left((1 - d_1^\dagger d_1) d_1 - d_1^\dagger d_1 d_1 \right) \\
 &= \varepsilon_1 (d_1 - d_1^\dagger d_1 d_1 + d_1^\dagger d_1 d_1) = \varepsilon_1 d_1
 \end{aligned} \tag{A.88}$$

$$\begin{aligned}
 \left[d_1, \sqrt{2}V \sum_k (c_{ek}^\dagger d_1 + d_1^\dagger c_{ek}) \right] &= \sqrt{2}V \sum_k \left(d_1 (c_{ek}^\dagger d_1 + d_1^\dagger c_{ek}) - (c_{ek}^\dagger d_1 + d_1^\dagger c_{ek}) d_1 \right) \\
 &= \sqrt{2}V \sum_k \left(d_1 c_{ek}^\dagger d_1 + d_1 d_1^\dagger c_{ek} - c_{ek}^\dagger d_1 d_1 - d_1^\dagger c_{ek} d_1 \right) \\
 &= \sqrt{2}V \sum_k \left(c_{ek}^\dagger d_1 d_1 + d_1 d_1^\dagger c_{ek} - c_{ek}^\dagger d_1 d_1 + d_1^\dagger d_1 c_{ek} \right) \\
 &= \sqrt{2}V \sum_k \left(d_1 d_1^\dagger c_{ek} + d_1^\dagger d_1 c_{ek} \right) = \sqrt{2}V \sum_k c_{ek}
 \end{aligned} \tag{A.89}$$

$$\begin{aligned}
 \frac{\lambda_A}{\sqrt{2}} [d_1, (d_1 f^\dagger + f d_1^\dagger)] &= \frac{\lambda_A}{\sqrt{2}} \left(d_1 (d_1 f^\dagger + f d_1^\dagger) - (d_1 f^\dagger + f d_1^\dagger) d_1 \right) \\
 &= \frac{\lambda_A}{\sqrt{2}} \left(d_1 d_1 f^\dagger + d_1 f d_1^\dagger - d_1 f^\dagger d_1 - f d_1^\dagger d_1 \right) \\
 &= \frac{\lambda_A}{\sqrt{2}} \left(-d_1 d_1 f^\dagger - f d_1 d_1^\dagger + d_1 d_1 f^\dagger - f d_1^\dagger d_1 \right) \\
 &= \frac{\lambda_A}{\sqrt{2}} \left(-f d_1 d_1^\dagger - f d_1^\dagger d_1 \right) = -\frac{\lambda_A}{\sqrt{2}} f
 \end{aligned} \tag{A.90}$$

$$\begin{aligned}
 \frac{\lambda_B}{\sqrt{2}} [d_1, (d_1 f - d_1^\dagger f^\dagger)] &= \frac{\lambda_B}{\sqrt{2}} \left(d_1 (d_1 f - d_1^\dagger f^\dagger) - (d_1 f - d_1^\dagger f^\dagger) d_1 \right) \\
 &= \frac{\lambda_B}{\sqrt{2}} \left(d_1 d_1 f - d_1 d_1^\dagger f^\dagger - d_1 f d_1 + d_1^\dagger f^\dagger d_1 \right) \\
 &= \frac{\lambda_B}{\sqrt{2}} \left(-d_1 d_1 f - d_1 d_1^\dagger f^\dagger + d_1 d_1 f - d_1^\dagger d_1 f^\dagger \right) \\
 &= -\frac{\lambda_B}{\sqrt{2}} f^\dagger
 \end{aligned} \tag{A.91}$$

$$\begin{aligned}
 \partial_t d_1(t) &= \left(-\frac{i}{\hbar}\right) [d_1, \mathcal{H}] \\
 &= \left(-\frac{i}{\hbar}\right) \varepsilon_1 d_1 + \left(-\frac{i}{\hbar}\right) \sqrt{2V} \sum_k c_{ek} - \left(-\frac{i}{\hbar}\right) \frac{\lambda_A}{\sqrt{2}} f - \left(-\frac{i}{\hbar}\right) \frac{\lambda_B}{\sqrt{2}} f^\dagger
 \end{aligned} \tag{A.92}$$

$$\begin{aligned}
 \partial_t \mathcal{G}_{d_1 f}(t) &= \left(-\frac{i}{\hbar}\right) \delta(t) \mathcal{Z}^{-1} \sum_r e^{-\beta E_r} \left\langle r \left| [d_1(t), f^\dagger(0)]_+ \right| r \right\rangle \\
 &+ \left(-\frac{i}{\hbar}\right) \varepsilon_1 \left\{ \left(-\frac{i}{\hbar}\right) \theta(t) \mathcal{Z}^{-1} \sum_r e^{-\beta E_r} \left\langle r \left| [d_1(t), f^\dagger(0)]_+ \right| r \right\rangle \right\} \\
 &+ \left(-\frac{i}{\hbar}\right) \sqrt{2V} \sum_k \left\{ \left(-\frac{i}{\hbar}\right) \theta(t) \mathcal{Z}^{-1} \sum_r e^{-\beta E_r} \left\langle r \left| [c_{ek}(t), f^\dagger(0)]_+ \right| r \right\rangle \right\} \\
 &- \left(-\frac{i}{\hbar}\right) \frac{\lambda_A}{\sqrt{2}} \left\{ \left(-\frac{i}{\hbar}\right) \theta(t) \mathcal{Z}^{-1} \sum_r e^{-\beta E_r} \left\langle r \left| [f(t), f^\dagger(0)]_+ \right| r \right\rangle \right\} \\
 &- \left(-\frac{i}{\hbar}\right) \frac{\lambda_B}{\sqrt{2}} \left\{ \left(-\frac{i}{\hbar}\right) \theta(t) \mathcal{Z}^{-1} \sum_r e^{-\beta E_r} \left\langle r \left| [f^\dagger(t), f^\dagger(0)]_+ \right| r \right\rangle \right\}.
 \end{aligned} \tag{A.93}$$

$$\begin{aligned}
 \partial_t \mathcal{G}_{d_1 f}(t) &= \left(-\frac{i}{\hbar}\right) \delta(t) \mathcal{Z}^{-1} \sum_r e^{-\beta E_r} \left\langle r \left| [d_1(t), f(0)]_+ \right| r \right\rangle \\
 &+ \left(-\frac{i}{\hbar}\right) \varepsilon_1 \mathcal{G}_{d_1 f}(t) + \left(-\frac{i}{\hbar}\right) \sqrt{2V} \sum_k \mathcal{G}_{c_{ek} f}(t) - \left(-\frac{i}{\hbar}\right) \frac{\lambda_A}{\sqrt{2}} \mathcal{G}_{ff}(t) \\
 &- \left(-\frac{i}{\hbar}\right) \frac{\lambda_B}{\sqrt{2}} \mathcal{G}_{f^\dagger f}(t)
 \end{aligned} \tag{A.94}$$

By using the Fourier transform property, we obtain:

$$(\varepsilon - \varepsilon_1 + i\delta) \tilde{\mathcal{G}}_{d_1 f}(\varepsilon) = \sqrt{2V} \sum_k \tilde{\mathcal{G}}_{c_{ek} f}(\varepsilon) - \frac{\lambda_A}{\sqrt{2}} \tilde{\mathcal{G}}_{ff}(\varepsilon) - \frac{\lambda_B}{\sqrt{2}} \tilde{\mathcal{G}}_{f^\dagger f}(\varepsilon) \tag{A.95}$$

As one can see in the relation above, we should calculate $\tilde{\mathcal{G}}_{c_{ek} f}(\varepsilon)$.

$$\mathcal{G}_{c_{ek} f}(t) = \left(-\frac{i}{\hbar}\right) \theta(t) \mathcal{Z}^{-1} \sum_r e^{-\beta E_r} \left\langle r \left| [c_{ek}(t), f^\dagger(0)]_+ \right| r \right\rangle \tag{A.96}$$

$$\begin{aligned}
 \partial_t \mathcal{G}_{c_{ek}f}(t) &= \left(-\frac{i}{\hbar}\right) \delta(t) \mathcal{Z}^{-1} \sum_r e^{-\beta E_r} \left\langle r \left| \left[c_{ek}(t), f^\dagger(0) \right]_+ \right| r \right\rangle \\
 &+ \left(-\frac{i}{\hbar}\right) \theta(t) \mathcal{Z}^{-1} \sum_r e^{-\beta E_r} \left\langle r \left| \left[\partial_t c_{ek}(t), f^\dagger(0) \right]_+ \right| r \right\rangle
 \end{aligned} \tag{A.97}$$

$$\begin{aligned}
 \partial_t c_{ek}(t) &= \left(-\frac{i}{\hbar}\right) [c_{ek}, \mathcal{H}] \\
 &= \left(-\frac{i}{\hbar}\right) \left[c_{ek}, \sum_k \varepsilon_k c_{ek}^\dagger c_{ek} \right] + \left(-\frac{i}{\hbar}\right) [c_{ek}, \varepsilon_1 d_1^\dagger d_1] + \left(-\frac{i}{\hbar}\right) \left[c_{ek}, \sqrt{2}V \sum_k (c_{ek}^\dagger d_1 + H.c.) \right] \\
 &+ \left(-\frac{i}{\hbar}\right) \left[c_{ek}, V_{BT} \sum_{kq} c_{ek}^\dagger c_{eq} \right] + \left(-\frac{i}{\hbar}\right) \left[c_{ek}, \varepsilon_M \left(f^\dagger f - \frac{1}{2} \right) \right] + \left(-\frac{i}{\hbar}\right) \left[c_{ek}, \frac{\lambda_A}{\sqrt{2}} (d_1 f^\dagger + f d_1^\dagger) \right] \\
 &+ \left(-\frac{i}{\hbar}\right) \left[c_{ek}, \frac{\lambda_B}{\sqrt{2}} (d_1 f - d_1^\dagger f^\dagger) \right],
 \end{aligned} \tag{A.98}$$

$$\begin{aligned}
 \partial_t c_{ek}(t) &= \left(-\frac{i}{\hbar}\right) [c_{ek}, \mathcal{H}] \\
 &= \left(-\frac{i}{\hbar}\right) \left[c_{ek}, \sum_k \varepsilon_k c_{ek}^\dagger c_{ek} \right] + \left(-\frac{i}{\hbar}\right) \left[c_{ek}, \sqrt{2}V \sum_k (c_{ek}^\dagger d_1 + H.c.) \right] \\
 &+ \left(-\frac{i}{\hbar}\right) \left[c_{ek}, V_{BT} \sum_{kq} c_{ek}^\dagger c_{eq} \right]
 \end{aligned} \tag{A.99}$$

$$\begin{aligned}
 \left[c_{ek}, \sum_p \varepsilon_p c_{ep}^\dagger c_{ep} \right] &= \sum_p \varepsilon_p (c_{ek} c_{ep}^\dagger c_{ep} - c_{ep}^\dagger c_{ep} c_{ek}) = \sum_p \varepsilon_p \left((\delta_{kp} - c_{ep}^\dagger c_{ek}) c_{ep} - c_{ep}^\dagger c_{ep} c_{ek} \right) \\
 &= \sum_p \varepsilon_p (\delta_{kp} c_{ep} - c_{ep}^\dagger c_{ek} c_{ep} + c_{ep}^\dagger c_{ek} c_{ep}) = \sum_k \varepsilon_k c_{ek}
 \end{aligned} \tag{A.100}$$

$$\begin{aligned}
 \left[c_{ek}, \sqrt{2}V \sum_p (c_{ep}^\dagger d_1 + H.c.) \right] &= \sqrt{2}V \sum_p (c_{ek} (c_{ep}^\dagger d_1 + d_1^\dagger c_{ep}) - (c_{ep}^\dagger d_1 + d_1^\dagger c_{ep}) c_{ek}) \\
 &= \sqrt{2}V \sum_p (c_{ek} c_{ep}^\dagger d_1 + c_{ek} d_1^\dagger c_{ep} - c_{ep}^\dagger d_1 c_{ek} - d_1^\dagger c_{ep} c_{ek}) \\
 &= \sqrt{2}V \sum_p (c_{ek} c_{ep}^\dagger d_1 + d_1^\dagger c_{ep} c_{ek} + c_{ep}^\dagger c_{ek} d_1 - d_1^\dagger c_{ep} c_{ek}) \\
 &= \sqrt{2}V \sum_p (c_{ek} c_{ep}^\dagger + c_{ep}^\dagger c_{ek}) d_1 = \sqrt{2}V \sum_p d_1
 \end{aligned} \tag{A.101}$$

$$\begin{aligned}
 \left[c_{ek}, V_{BT} \sum_{pq} c_{ep}^\dagger c_{eq} \right] &= V_{BT} \sum_{kq} \left(c_{ek} c_{ep}^\dagger c_{eq} - c_{ep}^\dagger c_{eq} c_{ek} \right) \\
 &= V_{BT} \sum_{kq} \left(\left(\delta_{kp} - c_{ep}^\dagger c_{ek} \right) c_{eq} - c_{ep}^\dagger c_{eq} c_{ek} \right) \\
 &= V_{BT} \sum_{kq} \left(\delta_{kp} c_{eq} + c_{ep}^\dagger c_{eq} c_{ek} - c_{ep}^\dagger c_{eq} c_{ek} \right) \\
 &= V_{BT} \sum_q c_{eq}
 \end{aligned} \tag{A.102}$$

$$\begin{aligned}
 \partial_t c_{ek}(t) &= \left(-\frac{i}{\hbar} \right) [c_{ek}, \mathcal{H}] \\
 &= \left(-\frac{i}{\hbar} \right) \sum_k \varepsilon_k c_{ek} + \left(-\frac{i}{\hbar} \right) \sqrt{2} V \sum_p d_1 + \left(-\frac{i}{\hbar} \right) V_{BT} \sum_q c_{eq}
 \end{aligned} \tag{A.103}$$

$$\begin{aligned}
 \partial_t \mathcal{G}_{cekf}(t) &= \left(-\frac{i}{\hbar} \right) \delta(t) \mathcal{Z}^{-1} \sum_r e^{-\beta E_r} \left\langle r \left| [c_{ek}(t), f^\dagger(0)]_+ \right| r \right\rangle \\
 &+ \left(-\frac{i}{\hbar} \right) \sum_k \varepsilon_k \left\{ \left(-\frac{i}{\hbar} \right) \theta(t) \mathcal{Z}^{-1} \sum_r e^{-\beta E_r} \left\langle r \left| [c_{ek}(t), f^\dagger(0)]_+ \right| r \right\rangle \right\} \\
 &+ \left(-\frac{i}{\hbar} \right) \sqrt{2} V \sum_k \left\{ \left(-\frac{i}{\hbar} \right) \theta(t) \mathcal{Z}^{-1} \sum_r e^{-\beta E_r} \left\langle r \left| [d_1(t), f^\dagger(0)]_+ \right| r \right\rangle \right\} \\
 &+ \left(-\frac{i}{\hbar} \right) V_{BT} \sum_q \left\{ \left(-\frac{i}{\hbar} \right) \theta(t) \mathcal{Z}^{-1} \sum_r e^{-\beta E_r} \left\langle r \left| [c_{eq}(t), f^\dagger(0)]_+ \right| r \right\rangle \right\}
 \end{aligned} \tag{A.104}$$

$$\begin{aligned}
 \partial_t \mathcal{G}_{cekf}(t) &= \left(-\frac{i}{\hbar} \right) \delta(t) \mathcal{Z}^{-1} \sum_r e^{-\beta E_r} \left\langle r \left| [c_{ek}(t), f^\dagger(0)]_+ \right| r \right\rangle \\
 &+ \left(-\frac{i}{\hbar} \right) \varepsilon_k \mathcal{G}_{cekf}(t) + \left(-\frac{i}{\hbar} \right) \sqrt{2} V \sum_k \mathcal{G}_{d_1 f}(t) + \left(-\frac{i}{\hbar} \right) V_{BT} \sum_q \mathcal{G}_{ceqf}(t)
 \end{aligned} \tag{A.105}$$

By performing the Fourier transform we obtain:

$$(\varepsilon - \varepsilon_k + i\delta) \tilde{\mathcal{G}}_{cekf}(\varepsilon) = \sqrt{2} V \sum_k \tilde{\mathcal{G}}_{d_1 f}(\varepsilon) + V_{BT} \sum_q \tilde{\mathcal{G}}_{ceqf}(\varepsilon) \tag{A.106}$$

We can rewrite the expression above in a better way:

$$\begin{aligned}
 (\varepsilon - \varepsilon_k + i\delta) \sum_k \tilde{\mathcal{G}}_{cekf}(\varepsilon) &= \sqrt{2}V \sum_k \tilde{\mathcal{G}}_{d1f}(\varepsilon) + V_{BT} \sum_k \tilde{\mathcal{G}}_{ceqf}(\varepsilon) \Rightarrow \\
 \tilde{\mathcal{G}}_{cekf}(\varepsilon) &= \sqrt{2}V \sum_k \frac{\tilde{\mathcal{G}}_{d1f}(\varepsilon)}{(\varepsilon - \varepsilon_k + i\delta)} + V_{BT} \sum_q \frac{\tilde{\mathcal{G}}_{ceqf}(\varepsilon)}{(\varepsilon - \varepsilon_k + i\delta)} \Rightarrow \\
 \left[1 - V_{BT} \sum_k \frac{1}{(\varepsilon - \varepsilon_k + i\delta)} \right] \tilde{\mathcal{G}}_{cekf}(\varepsilon) &= \sqrt{2}V \sum_k \frac{1}{(\varepsilon - \varepsilon_k + i\delta)} \tilde{\mathcal{G}}_{d1f}(\varepsilon),
 \end{aligned} \tag{A.107}$$

Using the same definition that we applied in Eq. (A.73) we obtain:

$$\sum_k \tilde{\mathcal{G}}_{cekf}(\varepsilon) = \frac{\sqrt{2}V\pi\rho_0(\bar{q} - i)}{1 - V_{BT}\pi\rho_0(\bar{q} - i)} \tilde{\mathcal{G}}_{d1f}(\varepsilon). \tag{A.108}$$

By substituting Eq. (A.108) in Eq. (A.95) we find:

$$\begin{aligned}
 (\varepsilon - \varepsilon_1 + i\delta) \tilde{\mathcal{G}}_{d1f}(\varepsilon) &= \sqrt{2}V \left[\frac{\sqrt{2}V\pi\rho_0(\bar{q} - i)}{1 - V_{BT}\pi\rho_0(\bar{q} - i)} \tilde{\mathcal{G}}_{d1f}(\varepsilon) \right] - \frac{\lambda_A}{\sqrt{2}} \tilde{\mathcal{G}}_{ff}(\varepsilon) - \frac{\lambda_B}{\sqrt{2}} \tilde{\mathcal{G}}_{f^\dagger f}(\varepsilon) \\
 &= \left[\frac{2V^2\pi\rho_0(\bar{q} - i)}{1 - V_{BT}\pi\rho_0(\bar{q} - i)} \tilde{\mathcal{G}}_{d1f}(\varepsilon) \right] - \frac{\lambda_A}{\sqrt{2}} \tilde{\mathcal{G}}_{ff}(\varepsilon) - \frac{\lambda_B}{\sqrt{2}} \tilde{\mathcal{G}}_{f^\dagger f}(\varepsilon). \tag{A.109}
 \end{aligned}$$

Applying the wide band limit condition, we have

$$\begin{aligned}
 (\varepsilon - \varepsilon_1 + i\delta) \tilde{\mathcal{G}}_{d1f}(\varepsilon) &= \left[\frac{-i2V^2\pi\rho_0}{1 + iV_{BT}\pi\rho_0} \tilde{\mathcal{G}}_{d1f}(\varepsilon) \right] - \frac{\lambda_A}{\sqrt{2}} \tilde{\mathcal{G}}_{ff}(\varepsilon) - \frac{\lambda_B}{\sqrt{2}} \tilde{\mathcal{G}}_{f^\dagger f}(\varepsilon) \\
 &= \left[\frac{-i2V^2\pi\rho_0(1 - iV_{BT}\pi\rho_0)}{(1 + iV_{BT}\pi\rho_0)(1 - iV_{BT}\pi\rho_0)} \tilde{\mathcal{G}}_{d1f}(\varepsilon) \right] - \frac{\lambda_A}{\sqrt{2}} \tilde{\mathcal{G}}_{ff}(\varepsilon) - \frac{\lambda_B}{\sqrt{2}} \tilde{\mathcal{G}}_{f^\dagger f}(\varepsilon) \\
 &= \left[\frac{2V^2\pi\rho_0(-i - V_{BT}\pi\rho_0)}{1 + (V_{BT}\pi\rho_0)^2} \tilde{\mathcal{G}}_{d1f}(\varepsilon) \right] - \frac{\lambda_A}{\sqrt{2}} \tilde{\mathcal{G}}_{ff}(\varepsilon) - \frac{\lambda_B}{\sqrt{2}} \tilde{\mathcal{G}}_{f^\dagger f}(\varepsilon) \\
 &= \left[\frac{-2V^2\pi\rho_0(V_{BT}\pi\rho_0 + i)}{1 + (V_{BT}\pi\rho_0)^2} \tilde{\mathcal{G}}_{d1f}(\varepsilon) \right] - \frac{\lambda_A}{\sqrt{2}} \tilde{\mathcal{G}}_{ff}(\varepsilon) - \frac{\lambda_B}{\sqrt{2}} \tilde{\mathcal{G}}_{f^\dagger f}(\varepsilon) \\
 &= \frac{-(\sqrt{x} + i)\Gamma}{1 + x} \tilde{\mathcal{G}}_{d1f}(\varepsilon) - \frac{\lambda_A}{\sqrt{2}} \tilde{\mathcal{G}}_{ff}(\varepsilon) - \frac{\lambda_B}{\sqrt{2}} \tilde{\mathcal{G}}_{f^\dagger f}(\varepsilon), \tag{A.110}
 \end{aligned}$$

But we can define:

$$\Sigma = \frac{-(\sqrt{x} + i)\Gamma}{1 + x} \tag{A.111}$$

and therefore

$$\begin{aligned}
 (\varepsilon - \varepsilon_1 - \Sigma + i\delta) \tilde{\mathcal{G}}_{d_1 f}(\varepsilon) &= -\frac{\lambda_A}{\sqrt{2}} \tilde{\mathcal{G}}_{ff}(\varepsilon) - \frac{\lambda_B}{\sqrt{2}} \tilde{\mathcal{G}}_{f^\dagger f}(\varepsilon), \\
 &=
 \end{aligned} \tag{A.112}$$

The last step in this stage is calculate $\tilde{\mathcal{G}}_{d_1 f^\dagger}$:

$$\mathcal{G}_{d_1 f^\dagger}(t) = \left(-\frac{i}{\hbar}\right) \theta(t) \mathcal{Z}^{-1} \sum_r e^{-\beta E_r} \langle r | [d_1(t), f(0)]_+ | r \rangle. \tag{A.113}$$

$$\begin{aligned}
 \partial_t \mathcal{G}_{d_1 f^\dagger}(t) &= \left(-\frac{i}{\hbar}\right) \delta(t) \mathcal{Z}^{-1} \sum_r e^{-\beta E_r} \langle r | [d_1(t), f(0)]_+ | r \rangle \\
 &+ \left(-\frac{i}{\hbar}\right) \theta(t) \mathcal{Z}^{-1} \sum_r e^{-\beta E_r} \langle r | [\partial_t d_1(t), f(0)]_+ | r \rangle.
 \end{aligned} \tag{A.114}$$

$$\begin{aligned}
 \partial_t d_1(t) &= \left(-\frac{i}{\hbar}\right) [d_1, \mathcal{H}] \\
 &= \left(-\frac{i}{\hbar}\right) \varepsilon_1 d_1 + \left(-\frac{i}{\hbar}\right) \sqrt{2} V \sum_k c_{ek} - \left(-\frac{i}{\hbar}\right) \frac{\lambda_A}{\sqrt{2}} f - \left(-\frac{i}{\hbar}\right) \frac{\lambda_B}{\sqrt{2}} f^\dagger
 \end{aligned} \tag{A.115}$$

$$\begin{aligned}
 \partial_t \mathcal{G}_{d_1 f^\dagger}(t) &= \left(-\frac{i}{\hbar}\right) \delta(t) \mathcal{Z}^{-1} \sum_r e^{-\beta E_r} \langle r | [d_1(t), f(0)]_+ | r \rangle \\
 &+ \left(-\frac{i}{\hbar}\right) \varepsilon_1 \left\{ \left(-\frac{i}{\hbar}\right) \theta(t) \mathcal{Z}^{-1} \sum_r e^{-\beta E_r} \langle r | [d_1(t), f(0)]_+ | r \rangle \right\} \\
 &+ \left(-\frac{i}{\hbar}\right) \sqrt{2} V \sum_k \left\{ \left(-\frac{i}{\hbar}\right) \theta(t) \mathcal{Z}^{-1} \sum_r e^{-\beta E_r} \langle r | [c_{ek}(t), f(0)]_+ | r \rangle \right\} \\
 &- \left(-\frac{i}{\hbar}\right) \frac{\lambda_A}{\sqrt{2}} \left\{ \left(-\frac{i}{\hbar}\right) \theta(t) \mathcal{Z}^{-1} \sum_r e^{-\beta E_r} \langle r | [f(t), f(0)]_+ | r \rangle \right\} \\
 &- \left(-\frac{i}{\hbar}\right) \frac{\lambda_B}{\sqrt{2}} \left\{ \left(-\frac{i}{\hbar}\right) \theta(t) \mathcal{Z}^{-1} \sum_r e^{-\beta E_r} \langle r | [f^\dagger(t), f(0)]_+ | r \rangle \right\}.
 \end{aligned} \tag{A.116}$$

$$\begin{aligned}
 \partial_t \mathcal{G}_{d_1 f^\dagger}(t) &= \left(-\frac{i}{\hbar}\right) \delta(t) \mathcal{Z}^{-1} \sum_r e^{-\beta E_r} \langle r | [d_1(t), f(0)]_+ | r \rangle \\
 &+ \left(-\frac{i}{\hbar}\right) \varepsilon_1 \mathcal{G}_{d_1 f^\dagger}(t) + \left(-\frac{i}{\hbar}\right) \sqrt{2} V \sum_k \mathcal{G}_{c_{ek} f^\dagger}(t) - \left(-\frac{i}{\hbar}\right) \frac{\lambda_A}{\sqrt{2}} \mathcal{G}_{ff^\dagger}(t) \\
 &- \left(-\frac{i}{\hbar}\right) \frac{\lambda_B}{\sqrt{2}} \mathcal{G}_{f^\dagger f^\dagger}(t)
 \end{aligned} \tag{A.117}$$

By applying the Fourier transform:

$$(\varepsilon - \varepsilon_1 + i\delta) \tilde{\mathcal{G}}_{d_1 f^\dagger}(\varepsilon) = \sqrt{2}V \sum_k \tilde{\mathcal{G}}_{c_{ek} f^\dagger}(\varepsilon) - \frac{\lambda_A}{\sqrt{2}} \tilde{\mathcal{G}}_{ff^\dagger}(\varepsilon) - \frac{\lambda_B}{\sqrt{2}} \tilde{\mathcal{G}}_{f^\dagger f^\dagger}(\varepsilon) \quad (\text{A.118})$$

and using the definitions of Eq. (A.110) and (A.111) we find:

$$(\varepsilon - \varepsilon_1 - \Sigma + i\delta) \tilde{\mathcal{G}}_{d_1 f^\dagger}(\varepsilon) = -\frac{\lambda_A}{\sqrt{2}} \tilde{\mathcal{G}}_{ff^\dagger}(\varepsilon) - \frac{\lambda_B}{\sqrt{2}} \tilde{\mathcal{G}}_{f^\dagger f^\dagger}(\varepsilon). \quad (\text{A.119})$$

A.1.1 Summary of mean relations

One can write down the following main relations obtained so far:

$$\begin{aligned} \tilde{\mathcal{G}}_{\eta_1 \eta_1} &= K + \frac{1}{2\sqrt{2}} \left(\frac{\lambda_A}{\varepsilon + \varepsilon_M + i\delta} + \frac{\lambda_B}{\varepsilon - \varepsilon_M + i\delta} \right) (\tilde{\mathcal{G}}_{d_1^\dagger f} + \tilde{\mathcal{G}}_{d_1^\dagger f^\dagger}) \\ &\quad - \frac{1}{2\sqrt{2}} \left(\frac{\lambda_A}{\varepsilon - \varepsilon_M + i\delta} + \frac{\lambda_B}{\varepsilon + \varepsilon_M + i\delta} \right) (\tilde{\mathcal{G}}_{d_1 f} + \tilde{\mathcal{G}}_{d_1 f^\dagger}), \end{aligned} \quad (\text{A.120})$$

$$(\varepsilon + \varepsilon_1 + \tilde{\Sigma}) \tilde{\mathcal{G}}_{d_1^\dagger f}(\varepsilon) = \frac{\lambda_A}{\sqrt{2}} \tilde{\mathcal{G}}_{f^\dagger f}(\varepsilon) + \frac{\lambda_B}{\sqrt{2}} \mathcal{G}_{ff}(\varepsilon), \quad (\text{A.121})$$

$$(\varepsilon + \varepsilon_1 + \tilde{\Sigma}) \tilde{\mathcal{G}}_{d_1^\dagger f^\dagger}(\varepsilon) = \frac{\lambda_A}{\sqrt{2}} \tilde{\mathcal{G}}_{f^\dagger f^\dagger}(\varepsilon) + \frac{\lambda_B}{\sqrt{2}} \mathcal{G}_{f^\dagger f^\dagger}(\varepsilon), \quad (\text{A.122})$$

$$\begin{aligned} (\varepsilon - \varepsilon_1 - \Sigma + i\delta) \tilde{\mathcal{G}}_{d_1 f}(\varepsilon) &= -\frac{\lambda_A}{\sqrt{2}} \tilde{\mathcal{G}}_{ff}(\varepsilon) - \frac{\lambda_B}{\sqrt{2}} \tilde{\mathcal{G}}_{f^\dagger f}(\varepsilon), \\ &= \end{aligned} \quad (\text{A.123})$$

$$(\varepsilon - \varepsilon_1 - \Sigma + i\delta) \tilde{\mathcal{G}}_{d_1 f^\dagger}(\varepsilon) = -\frac{\lambda_A}{\sqrt{2}} \tilde{\mathcal{G}}_{ff^\dagger}(\varepsilon) - \frac{\lambda_B}{\sqrt{2}} \tilde{\mathcal{G}}_{f^\dagger f^\dagger}(\varepsilon) \quad (\text{A.124})$$

$$\tilde{\mathcal{G}}_{f^\dagger f}(\varepsilon) = \frac{\lambda_A}{\sqrt{2}} \frac{\tilde{\mathcal{G}}_{d_1^\dagger f}(\varepsilon)}{(\varepsilon + \varepsilon_M + i\delta)} - \frac{\lambda_B}{\sqrt{2}} \frac{\mathcal{G}_{d_1 f}(\varepsilon)}{(\varepsilon + \varepsilon_M + i\delta)}, \quad (\text{A.125})$$

$$\tilde{\mathcal{G}}_{f^\dagger f^\dagger}(\varepsilon) = \frac{1}{(\varepsilon + \varepsilon_M + i\delta)} + \frac{\lambda_A}{\sqrt{2}} \frac{\tilde{\mathcal{G}}_{d_1^\dagger f^\dagger}(\varepsilon)}{(\varepsilon + \varepsilon_M + i\delta)} - \frac{\lambda_B}{\sqrt{2}} \frac{\mathcal{G}_{d_1 f^\dagger}(\varepsilon)}{(\varepsilon + \varepsilon_M + i\delta)}, \quad (\text{A.126})$$

$$\tilde{\mathcal{G}}_{ff}(\varepsilon) = \frac{1}{(\varepsilon - \varepsilon_M + i\delta)} - \frac{\lambda_A}{\sqrt{2}} \frac{\tilde{\mathcal{G}}_{d_1 f}(\varepsilon)}{(\varepsilon - \varepsilon_M + i\delta)} + \frac{\lambda_B}{\sqrt{2}} \frac{\tilde{\mathcal{G}}_{d_1^\dagger f}(\varepsilon)}{(\varepsilon - \varepsilon_M + i\delta)}, \quad (\text{A.127})$$

and

$$\tilde{\mathcal{G}}_{ff^\dagger}(\varepsilon) = -\frac{\lambda_A}{\sqrt{2}} \frac{\tilde{\mathcal{G}}_{d_1 f^\dagger}(\varepsilon)}{(\varepsilon - \varepsilon_M + i\delta)} + \frac{\lambda_B}{\sqrt{2}} \frac{\tilde{\mathcal{G}}_{d_1^\dagger f^\dagger}(\varepsilon)}{(\varepsilon - \varepsilon_M + i\delta)}. \quad (\text{A.128})$$

A.1.2 Grouping terms

In order to obtain $\tilde{\mathcal{G}}_{\eta_1 \eta_1}$ [see Eq. (A.120)], we have to regroup some expressions. Let's start with $\tilde{\mathcal{G}}_{d_1^\dagger f}$, where we have to use Eqs. (A.125) and (A.127):

$$\begin{aligned} (\varepsilon + \varepsilon_1 + \tilde{\Sigma}) \tilde{\mathcal{G}}_{d_1^\dagger f}(\varepsilon) &= \frac{\lambda_A}{\sqrt{2}} \left[\frac{\lambda_A}{\sqrt{2}} \frac{\tilde{\mathcal{G}}_{d_1^\dagger f}(\varepsilon)}{(\varepsilon + \varepsilon_M + i\delta)} - \frac{\lambda_B}{\sqrt{2}} \frac{\mathcal{G}_{d_1 f}(\varepsilon)}{(\varepsilon + \varepsilon_M + i\delta)} \right] \\ &+ \frac{\lambda_B}{\sqrt{2}} \left[\frac{1}{(\varepsilon - \varepsilon_M + i\delta)} - \frac{\lambda_A}{\sqrt{2}} \frac{\tilde{\mathcal{G}}_{d_1 f}(\varepsilon)}{(\varepsilon - \varepsilon_M + i\delta)} + \frac{\lambda_B}{\sqrt{2}} \frac{\tilde{\mathcal{G}}_{d_1^\dagger f}(\varepsilon)}{(\varepsilon - \varepsilon_M + i\delta)} \right] \\ &= \frac{\lambda_B}{\sqrt{2}} \frac{1}{(\varepsilon - \varepsilon_M + i\delta)} + \frac{1}{2} \left[\lambda_A^2 \frac{\tilde{\mathcal{G}}_{d_1^\dagger f}(\varepsilon)}{(\varepsilon + \varepsilon_M + i\delta)} - \lambda_A \lambda_B \frac{\mathcal{G}_{d_1 f}(\varepsilon)}{(\varepsilon + \varepsilon_M + i\delta)} \right] \\ &+ \frac{1}{2} \left[-\lambda_A \lambda_B \frac{\tilde{\mathcal{G}}_{d_1 f}(\varepsilon)}{(\varepsilon - \varepsilon_M + i\delta)} + \lambda_B^2 \frac{\tilde{\mathcal{G}}_{d_1^\dagger f}(\varepsilon)}{(\varepsilon - \varepsilon_M + i\delta)} \right] \\ &= \frac{\lambda_B}{\sqrt{2}} \frac{1}{(\varepsilon - \varepsilon_M + i\delta)} - \lambda_A \lambda_B \left[\frac{1}{2} \left(\frac{1}{\varepsilon - \varepsilon_M + i\delta} + \frac{1}{\varepsilon + \varepsilon_M + i\delta} \right) \right] \mathcal{G}_{d_1 f}(\varepsilon) \\ &+ \frac{1}{2} \left[\lambda_A^2 \frac{1}{(\varepsilon + \varepsilon_M + i\delta)} + \lambda_B^2 \frac{1}{(\varepsilon - \varepsilon_M + i\delta)} \right] \tilde{\mathcal{G}}_{d_1^\dagger f}(\varepsilon) \end{aligned} \quad (\text{A.129})$$

$$\begin{aligned}
 (\varepsilon + \varepsilon_1 + \tilde{\Sigma}) \tilde{\mathcal{G}}_{d_1^\dagger f}(\varepsilon) &= \frac{\lambda_B}{\sqrt{2}} \frac{1}{(\varepsilon - \varepsilon_M + i\delta)} - \lambda_A \lambda_B \left[\frac{1}{2} \left(\frac{1}{\varepsilon - \varepsilon_M + i\delta} + \frac{1}{\varepsilon + \varepsilon_M + i\delta} \right) \right] \mathcal{G}_{d_1 f}(\varepsilon) \\
 &+ \frac{\lambda_A^2}{2} \left[\frac{1}{(\varepsilon + \varepsilon_M + i\delta)} + \left(\frac{\lambda_B^2}{\lambda_A^2} \right) \frac{1}{(\varepsilon - \varepsilon_M + i\delta)} \right] \tilde{\mathcal{G}}_{d_1^\dagger f}(\varepsilon) \\
 &= \frac{\lambda_B}{\sqrt{2}} \frac{1}{(\varepsilon - \varepsilon_M + i\delta)} - \lambda_A \lambda_B \left[\frac{1}{2} \left(\frac{1}{\varepsilon - \varepsilon_M + i\delta} + \frac{1}{\varepsilon + \varepsilon_M + i\delta} \right) \right] \mathcal{G}_{d_1 f}(\varepsilon) \\
 &+ \frac{\lambda_A^2}{2} \left[\frac{(\varepsilon - \varepsilon_M + i\delta) \lambda_A^2 + (\varepsilon + \varepsilon_M + i\delta) \lambda_B^2}{(\varepsilon + \varepsilon_M + i\delta) (\varepsilon - \varepsilon_M + i\delta) \lambda_A^2} \right] \tilde{\mathcal{G}}_{d_1^\dagger f}(\varepsilon) \\
 &= \frac{\lambda_B}{\sqrt{2}} \frac{1}{(\varepsilon - \varepsilon_M + i\delta)} - \lambda_A \lambda_B \left[\frac{1}{2} \left(\frac{1}{\varepsilon - \varepsilon_M + i\delta} + \frac{1}{\varepsilon + \varepsilon_M + i\delta} \right) \right] \mathcal{G}_{d_1 f}(\varepsilon) \\
 &+ \frac{1}{2} \left[\frac{(\varepsilon + i\delta) (\lambda_A^2 + \lambda_B^2) - \varepsilon_M (\lambda_A^2 - \lambda_B^2)}{\varepsilon^2 - \varepsilon_M^2 + i2\varepsilon\delta - \delta^2} \right] \tilde{\mathcal{G}}_{d_1^\dagger f}(\varepsilon). \tag{A.130}
 \end{aligned}$$

$$(\varepsilon + \varepsilon_1 + \tilde{\Sigma}) \tilde{\mathcal{G}}_{d_1^\dagger f}(\varepsilon) = \frac{\lambda_B}{\sqrt{2}} \frac{1}{(\varepsilon - \varepsilon_M + i\delta)} - \lambda_A \lambda_B K \mathcal{G}_{d_1 f}(\varepsilon) + K_- \tilde{\mathcal{G}}_{d_1^\dagger f}(\varepsilon) \tag{A.131}$$

where we used $K = \frac{1}{2} \left(\frac{1}{\varepsilon - \varepsilon_M + i\delta} + \frac{1}{\varepsilon + \varepsilon_M + i\delta} \right)$ and $K_- = \frac{1}{2} \left[\frac{(\varepsilon + i\delta) (\lambda_A^2 + \lambda_B^2) - \varepsilon_M (\lambda_A^2 - \lambda_B^2)}{\varepsilon^2 - \varepsilon_M^2 + i2\varepsilon\delta - \delta^2} \right]$. Thus,

$$(\varepsilon + \varepsilon_1 + \tilde{\Sigma} - K_-) \tilde{\mathcal{G}}_{d_1^\dagger f}(\varepsilon) = \frac{\lambda_B}{\sqrt{2}} \frac{1}{(\varepsilon - \varepsilon_M + i\delta)} - \lambda_A \lambda_B K \mathcal{G}_{d_1 f}(\varepsilon) \tag{A.132}$$

Now we will obtain $\tilde{\mathcal{G}}_{d_1^\dagger f^\dagger}$. To this end we have to employ Eqs. (A.126) and (A.128):

$$\begin{aligned}
 (\varepsilon + \varepsilon_1 + \tilde{\Sigma}) \tilde{\mathcal{G}}_{d_1^\dagger f^\dagger}(\varepsilon) &= \frac{\lambda_A}{\sqrt{2}} \left[\frac{1}{(\varepsilon + \varepsilon_M + i\delta)} + \frac{\lambda_A}{\sqrt{2}} \frac{\tilde{\mathcal{G}}_{d_1^\dagger f^\dagger}(\varepsilon)}{(\varepsilon + \varepsilon_M + i\delta)} - \frac{\lambda_B}{\sqrt{2}} \frac{\mathcal{G}_{d_1 f^\dagger}(\varepsilon)}{(\varepsilon + \varepsilon_M + i\delta)} \right] \\
 &+ \frac{\lambda_B}{\sqrt{2}} \left[-\frac{\lambda_A}{\sqrt{2}} \frac{\tilde{\mathcal{G}}_{d_1 f^\dagger}(\varepsilon)}{(\varepsilon - \varepsilon_M + i\delta)} + \frac{\lambda_B}{\sqrt{2}} \frac{\tilde{\mathcal{G}}_{d_1^\dagger f^\dagger}(\varepsilon)}{(\varepsilon - \varepsilon_M + i\delta)} \right] \\
 &= \frac{\lambda_A}{\sqrt{2}} \frac{1}{(\varepsilon + \varepsilon_M + i\delta)} + \frac{1}{2} \left[\lambda_A^2 \frac{\tilde{\mathcal{G}}_{d_1^\dagger f^\dagger}(\varepsilon)}{(\varepsilon + \varepsilon_M + i\delta)} - \lambda_A \lambda_B \frac{\mathcal{G}_{d_1 f^\dagger}(\varepsilon)}{(\varepsilon + \varepsilon_M + i\delta)} \right] \\
 &+ \frac{1}{2} \left[-\lambda_A \lambda_B \frac{\tilde{\mathcal{G}}_{d_1 f^\dagger}(\varepsilon)}{(\varepsilon - \varepsilon_M + i\delta)} + \lambda_B^2 \frac{\tilde{\mathcal{G}}_{d_1^\dagger f^\dagger}(\varepsilon)}{(\varepsilon - \varepsilon_M + i\delta)} \right] \\
 &= \frac{\lambda_A}{\sqrt{2}} \frac{1}{(\varepsilon + \varepsilon_M + i\delta)} + \frac{1}{2} \left[\lambda_A^2 \frac{1}{(\varepsilon + \varepsilon_M + i\delta)} + \lambda_B^2 \frac{1}{(\varepsilon - \varepsilon_M + i\delta)} \right] \tilde{\mathcal{G}}_{d_1^\dagger f^\dagger}(\varepsilon) \\
 &- \lambda_A \lambda_B \left[\frac{1}{2} \left(\frac{1}{\varepsilon + \varepsilon_M + i\delta} + \frac{1}{\varepsilon - \varepsilon_M + i\delta} \right) \right] \mathcal{G}_{d_1 f^\dagger}(\varepsilon) \tag{A.133}
 \end{aligned}$$

Using the definitions of K and K_- , Eq. (A.133) becomes:

$$\begin{aligned}
 (\varepsilon + \varepsilon_1 + \tilde{\Sigma}) \tilde{\mathcal{G}}_{d_1^\dagger f^\dagger}(\varepsilon) &= \frac{\lambda_A}{\sqrt{2}} \frac{1}{(\varepsilon + \varepsilon_M + i\delta)} + K_- \tilde{\mathcal{G}}_{d_1^\dagger f^\dagger}(\varepsilon) \\
 &- \lambda_A \lambda_B K \mathcal{G}_{d_1 f^\dagger}(\varepsilon) \tag{A.134}
 \end{aligned}$$

$$(\varepsilon + \varepsilon_1 + \tilde{\Sigma} - K_-) \tilde{\mathcal{G}}_{d_1 f^\dagger}(\varepsilon) = \frac{\lambda_A}{\sqrt{2}} \frac{1}{(\varepsilon + \varepsilon_M + i\delta)} - \lambda_A \lambda_B K \mathcal{G}_{d_1 f^\dagger}(\varepsilon). \quad (\text{A.135})$$

Now, we will calculate $\tilde{\mathcal{G}}_{d_1 f}$:

$$\begin{aligned} (\varepsilon - \varepsilon_1 - \Sigma + i\delta) \tilde{\mathcal{G}}_{d_1 f}(\varepsilon) &= -\frac{\lambda_A}{\sqrt{2}} \left[\frac{1}{(\varepsilon - \varepsilon_M + i\delta)} - \frac{\lambda_A}{\sqrt{2}} \frac{\tilde{\mathcal{G}}_{d_1 f}(\varepsilon)}{(\varepsilon - \varepsilon_M + i\delta)} + \frac{\lambda_B}{\sqrt{2}} \frac{\tilde{\mathcal{G}}_{d_1 f^\dagger}(\varepsilon)}{(\varepsilon - \varepsilon_M + i\delta)} \right] \\ &+ -\frac{\lambda_B}{\sqrt{2}} \left[\frac{\lambda_A}{\sqrt{2}} \frac{\tilde{\mathcal{G}}_{d_1 f^\dagger}(\varepsilon)}{(\varepsilon + \varepsilon_M + i\delta)} - \frac{\lambda_B}{\sqrt{2}} \frac{\mathcal{G}_{d_1 f}(\varepsilon)}{(\varepsilon + \varepsilon_M + i\delta)} \right], \\ &= -\frac{\lambda_A}{\sqrt{2}} \frac{1}{(\varepsilon - \varepsilon_M + i\delta)} - \lambda_A \lambda_B \left[\frac{1}{2} \left(\frac{1}{\varepsilon + \varepsilon_M + i\delta} + \frac{1}{\varepsilon - \varepsilon_M + i\delta} \right) \right] \tilde{\mathcal{G}}_{d_1 f^\dagger}(\varepsilon) \\ &+ \frac{1}{2} \left[\lambda_A^2 \frac{1}{(\varepsilon - \varepsilon_M + i\delta)} + \lambda_B^2 \frac{1}{(\varepsilon + \varepsilon_M + i\delta)} \right] \tilde{\mathcal{G}}_{d_1 f}(\varepsilon) \\ &= -\frac{\lambda_A}{\sqrt{2}} \frac{1}{(\varepsilon - \varepsilon_M + i\delta)} - \lambda_A \lambda_B K \tilde{\mathcal{G}}_{d_1 f^\dagger}(\varepsilon) \\ &+ K_+ \tilde{\mathcal{G}}_{d_1 f}(\varepsilon), \end{aligned} \quad (\text{A.136})$$

where we define $K_+ = \frac{1}{2} \left[\frac{(\varepsilon + i\delta)(\lambda_A^2 + \lambda_B^2) + \varepsilon_M(\lambda_A^2 - \lambda_B^2)}{\varepsilon^2 - \varepsilon_M^2 + i2\varepsilon\delta - \delta^2} \right]$. Furthermore,

$$\tilde{\mathcal{G}}_{d_1 f^\dagger}(\varepsilon) = \frac{\frac{\lambda_B}{\sqrt{2}} \frac{1}{(\varepsilon - \varepsilon_M + i\delta)}}{(\varepsilon + \varepsilon_1 + \tilde{\Sigma} - K_-)} - \lambda_A \lambda_B \tilde{K} \mathcal{G}_{d_1 f}(\varepsilon) \quad (\text{A.137})$$

with $\tilde{K} = \frac{K}{(\varepsilon + \varepsilon_1 + \tilde{\Sigma} - K_-)}$. Thus,

$$\begin{aligned} (\varepsilon - \varepsilon_1 - \Sigma + i\delta) \tilde{\mathcal{G}}_{d_1 f}(\varepsilon) &= -\frac{\lambda_A}{\sqrt{2}} \frac{1}{(\varepsilon - \varepsilon_M + i\delta)} - \lambda_A \lambda_B K \left[\frac{\frac{\lambda_B}{\sqrt{2}} \frac{1}{(\varepsilon - \varepsilon_M + i\delta)}}{(\varepsilon + \varepsilon_1 + \tilde{\Sigma} - K_-)} - \lambda_A \lambda_B \tilde{K} \mathcal{G}_{d_1 f}(\varepsilon) \right] \\ &+ K_+ \tilde{\mathcal{G}}_{d_1 f}(\varepsilon) \\ &= -\frac{\lambda_A}{\sqrt{2}} \frac{1}{(\varepsilon - \varepsilon_M + i\delta)} - \frac{\lambda_B}{\sqrt{2}} \frac{\lambda_A \lambda_B \tilde{K}}{(\varepsilon - \varepsilon_M + i\delta)} + (\lambda_A \lambda_B)^2 K \tilde{K} \mathcal{G}_{d_1 f}(\varepsilon) \\ &+ K_+ \tilde{\mathcal{G}}_{d_1 f}(\varepsilon) \end{aligned} \quad (\text{A.138})$$

$$(\varepsilon - \varepsilon_1 - \Sigma - \Sigma_{\text{MFs}}) \tilde{\mathcal{G}}_{d_1 f}(\varepsilon) = -\frac{\lambda_A}{\sqrt{2}} \frac{(1 + \lambda_B^2 \tilde{K})}{(\varepsilon - \varepsilon_M + i\delta)} \quad (\text{A.139})$$

where $\Sigma_{\text{MFs}} = K_+ + (\lambda_A \lambda_B)^2 K \tilde{K}$. At last, we have to obtain $\tilde{\mathcal{G}}_{d_1 f^\dagger}$:

$$\begin{aligned}
 (\varepsilon - \varepsilon_1 - \Sigma + i\delta) \tilde{\mathcal{G}}_{d_1 f^\dagger}(\varepsilon) &= -\frac{\lambda_A}{\sqrt{2}} \left[-\frac{\lambda_A}{\sqrt{2}} \frac{\tilde{\mathcal{G}}_{d_1 f^\dagger}(\varepsilon)}{(\varepsilon - \varepsilon_M + i\delta)} + \frac{\lambda_B}{\sqrt{2}} \frac{\tilde{\mathcal{G}}_{d_1^\dagger f^\dagger}(\varepsilon)}{(\varepsilon - \varepsilon_M + i\delta)} \right] \\
 &\quad - \frac{\lambda_B}{\sqrt{2}} \left[\frac{1}{(\varepsilon + \varepsilon_M + i\delta)} + \frac{\lambda_A}{\sqrt{2}} \frac{\tilde{\mathcal{G}}_{d_1^\dagger f^\dagger}(\varepsilon)}{(\varepsilon + \varepsilon_M + i\delta)} - \frac{\lambda_B}{\sqrt{2}} \frac{\mathcal{G}_{d_1 f^\dagger}(\varepsilon)}{(\varepsilon + \varepsilon_M + i\delta)} \right] \\
 &= -\frac{\lambda_B}{\sqrt{2}} \frac{1}{(\varepsilon + \varepsilon_M + i\delta)} - \lambda_A \lambda_B \left[\frac{1}{2} \left(\frac{1}{\varepsilon + \varepsilon_M + i\delta} + \frac{1}{\varepsilon - \varepsilon_M + i\delta} \right) \right] \tilde{\mathcal{G}}_{d_1^\dagger f^\dagger}(\varepsilon) \\
 &\quad + \frac{1}{2} \left[\lambda_A^2 \frac{1}{(\varepsilon - \varepsilon_M + i\delta)} + \lambda_B^2 \frac{1}{(\varepsilon + \varepsilon_M + i\delta)} \right] \tilde{\mathcal{G}}_{d_1 f^\dagger}(\varepsilon) \\
 &= -\frac{\lambda_B}{\sqrt{2}} \frac{1}{(\varepsilon + \varepsilon_M + i\delta)} - \lambda_A \lambda_B K \tilde{\mathcal{G}}_{d_1^\dagger f^\dagger}(\varepsilon) + K_+ \tilde{\mathcal{G}}_{d_1 f^\dagger}(\varepsilon)
 \end{aligned} \tag{A.140}$$

But according to Eq. (B.104):

$$\tilde{\mathcal{G}}_{d_1^\dagger f^\dagger}(\varepsilon) = \frac{\frac{\lambda_A}{\sqrt{2}} \frac{1}{(\varepsilon + \varepsilon_M + i\delta)}}{(\varepsilon + \varepsilon_1 + \tilde{\Sigma} - K_-)} - \lambda_A \lambda_B \tilde{K} \mathcal{G}_{d_1 f^\dagger}(\varepsilon). \tag{A.141}$$

By substituting Eq. (A.141) in Eq. (B.109) we find:

$$\begin{aligned}
 (\varepsilon - \varepsilon_1 - \Sigma + i\delta) \tilde{\mathcal{G}}_{d_1 f^\dagger}(\varepsilon) &= -\frac{\lambda_B}{\sqrt{2}} \frac{1}{(\varepsilon + \varepsilon_M + i\delta)} + K_+ \tilde{\mathcal{G}}_{d_1 f^\dagger}(\varepsilon) \\
 &\quad - \lambda_A \lambda_B K \left[\frac{\frac{\lambda_A}{\sqrt{2}} \frac{1}{(\varepsilon + \varepsilon_M + i\delta)}}{(\varepsilon + \varepsilon_1 + \tilde{\Sigma} - K_-)} - \lambda_A \lambda_B \tilde{K} \mathcal{G}_{d_1 f^\dagger}(\varepsilon) \right] \\
 &= -\frac{\lambda_B}{\sqrt{2}} \frac{1}{(\varepsilon + \varepsilon_M + i\delta)} - \lambda_A \lambda_B \tilde{K} \frac{\lambda_A}{\sqrt{2}} \frac{1}{(\varepsilon + \varepsilon_M + i\delta)} \\
 &\quad + (\lambda_A \lambda_B)^2 K \tilde{K} \mathcal{G}_{d_1 f^\dagger}(\varepsilon) + K_+ \tilde{\mathcal{G}}_{d_1 f^\dagger}(\varepsilon)
 \end{aligned} \tag{A.142}$$

Finally:

$$(\varepsilon - \varepsilon_1 - \Sigma - \Sigma_{\text{MFs}}) \tilde{\mathcal{G}}_{d_1 f^\dagger}(\varepsilon) = -\frac{\lambda_B}{\sqrt{2}} \frac{(1 + \lambda_A^2 \tilde{K})}{(\varepsilon + \varepsilon_M + i\delta)} \tag{A.143}$$

A.1.3 Summary of Results for $\tilde{\mathcal{G}}_{\eta_1 \eta_1}$

The Green's function for the Majorana quasiparticle η_1 is given by

$$\begin{aligned}\tilde{\mathcal{G}}_{\eta_1\eta_1} &= K + \frac{1}{2\sqrt{2}} \left(\frac{\lambda_A}{\varepsilon + \varepsilon_M + i\delta} + \frac{\lambda_B}{\varepsilon - \varepsilon_M + i\delta} \right) (\tilde{\mathcal{G}}_{d_1^\dagger f} + \tilde{\mathcal{G}}_{d_1^\dagger f^\dagger}) \\ &- \frac{1}{2\sqrt{2}} \left(\frac{\lambda_A}{\varepsilon - \varepsilon_M + i\delta} + \frac{\lambda_B}{\varepsilon + \varepsilon_M + i\delta} \right) (\tilde{\mathcal{G}}_{d_1 f} + \tilde{\mathcal{G}}_{d_1 f^\dagger}),\end{aligned}\tag{A.144}$$

wherein

$$\tilde{\mathcal{G}}_{d_1 f}(\varepsilon) = \frac{-\frac{\lambda_A}{\sqrt{2}} \frac{(1+\lambda_B^2 \tilde{K})}{(\varepsilon - \varepsilon_M + i\delta)}}{(\varepsilon - \varepsilon_1 - \Sigma - \Sigma_{\text{MFs}})},\tag{A.145}$$

$$\tilde{\mathcal{G}}_{d_1 f^\dagger}(\varepsilon) = \frac{-\frac{\lambda_B}{\sqrt{2}} \frac{(1+\lambda_A^2 \tilde{K})}{(\varepsilon + \varepsilon_M + i\delta)}}{(\varepsilon - \varepsilon_1 - \Sigma - \Sigma_{\text{MFs}})},\tag{A.146}$$

$$\tilde{\mathcal{G}}_{d_1^\dagger f}(\varepsilon) = \frac{\frac{\lambda_B}{\sqrt{2}} \frac{1}{(\varepsilon - \varepsilon_M + i\delta)}}{(\varepsilon + \varepsilon_1 + \tilde{\Sigma} - K_-)} - \lambda_A \lambda_B \tilde{K} \tilde{\mathcal{G}}_{d_1 f}(\varepsilon)\tag{A.147}$$

and

$$\tilde{\mathcal{G}}_{d_1^\dagger f^\dagger}(\varepsilon) = \frac{\frac{\lambda_A}{\sqrt{2}} \frac{1}{(\varepsilon + \varepsilon_M + i\delta)}}{(\varepsilon + \varepsilon_1 + \tilde{\Sigma} - K_-)} - \lambda_A \lambda_B \tilde{K} \tilde{\mathcal{G}}_{d_1 f^\dagger}(\varepsilon),\tag{A.148}$$

with

$$\Sigma_{\text{MFs}} = K_+ + (\lambda_A \lambda_B)^2 K \tilde{K},\tag{A.149}$$

$$\tilde{K} = \frac{K}{(\varepsilon + \varepsilon_1 + \tilde{\Sigma} - K_-)},\tag{A.150}$$

$$K_{\pm} = \frac{1}{2} \left[\frac{(\varepsilon + i\delta) (\lambda_A^2 + \lambda_B^2) \pm \varepsilon_M (\lambda_A^2 - \lambda_B^2)}{\varepsilon^2 - \varepsilon_M^2 + i2\varepsilon\delta - \delta^2} \right]\tag{A.151}$$

and

$$K = \frac{1}{2} \left(\frac{1}{\varepsilon - \varepsilon_M + i\delta} + \frac{1}{\varepsilon + \varepsilon_M + i\delta} \right).\tag{A.152}$$

A.2 Finding the Green's Function for the Majorana Quasiparticle η_2

In order to obtain $\tilde{\rho}_{\eta_2\eta_2}(\varepsilon)$, we should calculate $\tilde{\mathcal{G}}_{\eta_2\eta_2}$, given by:

$$\mathcal{G}_{\eta_2\eta_2}(t) = \left(-\frac{i}{\hbar}\right)\theta(t)\mathcal{Z}^{-1}\sum_r e^{-\beta E_r} \left\langle r \left| \left[\eta_2(t), \eta_2^\dagger(0) \right]_+ \right| r \right\rangle, \quad (\text{A.153})$$

where

$$\eta_2 = i\frac{1}{\sqrt{2}}(f^\dagger - f). \quad (\text{A.154})$$

Thus, we have to calculate $\left[\eta_2(t), \eta_2^\dagger(0) \right]_+$ as follows:

$$\left[\eta_2(t), \eta_2^\dagger(0) \right]_+ = \eta_2(t)\eta_2(0) + \eta_2(0)\eta_2(t) \quad (\text{A.155})$$

$$\begin{aligned} \eta_2(t)\eta_2(0) &= i\frac{1}{\sqrt{2}}(f^\dagger(t) - f(t))i\frac{1}{\sqrt{2}}(f^\dagger(0) - f(0)) = -\frac{1}{2}(f^\dagger(t)f^\dagger(0) - f^\dagger(t)f(0) - f(t)f^\dagger(0) + f(t)f(0)) \\ &= \frac{1}{2}(-f^\dagger(t)f^\dagger(0) + f^\dagger(t)f(0) + f(t)f^\dagger(0) - f(t)f(0)) \end{aligned} \quad (\text{A.156})$$

$$\begin{aligned} \eta_2(0)\eta_2(t) &= i\frac{1}{\sqrt{2}}(f^\dagger(0) - f(0))i\frac{1}{\sqrt{2}}(f^\dagger(t) - f(t)) = -\frac{1}{2}(f^\dagger(0)f^\dagger(t) - f^\dagger(0)f(t) - f(0)f^\dagger(t) + f(0)f(t)) \\ &= \frac{1}{2}(-f^\dagger(0)f^\dagger(t) + f^\dagger(0)f(t) + f(0)f^\dagger(t) - f(0)f(t)) \end{aligned} \quad (\text{A.157})$$

$$\begin{aligned} \left[\eta_2(t), \eta_2^\dagger(0) \right]_+ &= \frac{1}{2}(-f^\dagger(t)f^\dagger(0) + f^\dagger(t)f(0) + f(t)f^\dagger(0) - f(t)f(0)) \\ &\quad + \frac{1}{2}(-f^\dagger(0)f^\dagger(t) + f^\dagger(0)f(t) + f(0)f^\dagger(t) - f(0)f(t)) \\ &= -\frac{1}{2}(f^\dagger(t)f^\dagger(0) + f^\dagger(0)f^\dagger(t)) + \frac{1}{2}(f^\dagger(t)f(0) + f^\dagger(0)f(t)) \\ &\quad + \frac{1}{2}(f(t)f^\dagger(0) + f(0)f^\dagger(t)) - \frac{1}{2}(f(t)f(0) + f(0)f(t)) \\ &= -\frac{1}{2}[f^\dagger(t), f^\dagger(0)]_+ + \frac{1}{2}[f^\dagger(t), f(0)]_+ + \frac{1}{2}[f(t), f^\dagger(0)]_+ \\ &\quad - \frac{1}{2}[f(t), f(0)]_+ \end{aligned} \quad (\text{A.158})$$

$$\left[\eta_2(t), \eta_2^\dagger(0) \right]_+ = -\frac{1}{2}[f^\dagger(t), f^\dagger(0)]_+ + \frac{1}{2}[f^\dagger(t), f(0)]_+ + \frac{1}{2}[f(t), f^\dagger(0)]_+ - \frac{1}{2}[f(t), f(0)]_+ \quad (\text{A.159})$$

By substituting Eq.(A.159) in Eq. (A.153) we obtain:

$$\begin{aligned}
 \mathcal{G}_{\eta_2\eta_2}(t) &= -\frac{1}{2}\left(-\frac{i}{\hbar}\right)\theta(t)\mathcal{Z}^{-1}\sum_r e^{-\beta E_r} \left\langle r \left| \left[f^\dagger(t), f^\dagger(0) \right]_+ \right| r \right\rangle \\
 &+ \frac{1}{2}\left(-\frac{i}{\hbar}\right)\theta(t)\mathcal{Z}^{-1}\sum_r e^{-\beta E_r} \left\langle r \left| \left[f^\dagger(t), f(0) \right]_+ \right| r \right\rangle \\
 &+ \frac{1}{2}\left(-\frac{i}{\hbar}\right)\theta(t)\mathcal{Z}^{-1}\sum_r e^{-\beta E_r} \left\langle r \left| \left[f(t), f^\dagger(0) \right]_+ \right| r \right\rangle \\
 &- \frac{1}{2}\left(-\frac{i}{\hbar}\right)\theta(t)\mathcal{Z}^{-1}\sum_r e^{-\beta E_r} \left\langle r \left| \left[f(t), f(0) \right]_+ \right| r \right\rangle
 \end{aligned} \tag{A.160}$$

Thus,

$$\mathcal{G}_{\eta_2\eta_2}(t) = -\frac{1}{2}\mathcal{G}_{f^\dagger f}(t) + \frac{1}{2}\mathcal{G}_{f^\dagger f^\dagger}(t) + \frac{1}{2}\mathcal{G}_{ff}(t) - \frac{1}{2}\mathcal{G}_{ff^\dagger}(t) \tag{A.161}$$

$$\tilde{\mathcal{G}}_{\eta_2\eta_2}(\varepsilon) = -\frac{1}{2}\tilde{\mathcal{G}}_{f^\dagger f}(\varepsilon) + \frac{1}{2}\tilde{\mathcal{G}}_{f^\dagger f^\dagger}(\varepsilon) + \frac{1}{2}\tilde{\mathcal{G}}_{ff}(\varepsilon) - \frac{1}{2}\tilde{\mathcal{G}}_{ff^\dagger}(\varepsilon) \tag{A.162}$$

But we already have obtained the Green functions above, which are given by:

$$\tilde{\mathcal{G}}_{f^\dagger f}(\varepsilon) = \frac{\lambda_A}{\sqrt{2}} \frac{\tilde{\mathcal{G}}_{d_1^\dagger f}(\varepsilon)}{(\varepsilon + \varepsilon_M + i\delta)} - \frac{\lambda_B}{\sqrt{2}} \frac{\mathcal{G}_{d_1 f}(\varepsilon)}{(\varepsilon + \varepsilon_M + i\delta)}, \tag{A.163}$$

$$\tilde{\mathcal{G}}_{f^\dagger f^\dagger}(\varepsilon) = \frac{1}{(\varepsilon + \varepsilon_M + i\delta)} + \frac{\lambda_A}{\sqrt{2}} \frac{\tilde{\mathcal{G}}_{d_1^\dagger f^\dagger}(\varepsilon)}{(\varepsilon + \varepsilon_M + i\delta)} - \frac{\lambda_B}{\sqrt{2}} \frac{\mathcal{G}_{d_1 f^\dagger}(\varepsilon)}{(\varepsilon + \varepsilon_M + i\delta)}, \tag{A.164}$$

$$\tilde{\mathcal{G}}_{ff}(\varepsilon) = \frac{1}{(\varepsilon - \varepsilon_M + i\delta)} - \frac{\lambda_A}{\sqrt{2}} \frac{\tilde{\mathcal{G}}_{d_1 f}(\varepsilon)}{(\varepsilon - \varepsilon_M + i\delta)} + \frac{\lambda_B}{\sqrt{2}} \frac{\tilde{\mathcal{G}}_{d_1^\dagger f}(\varepsilon)}{(\varepsilon - \varepsilon_M + i\delta)}, \tag{A.165}$$

$$\tilde{\mathcal{G}}_{ff^\dagger}(\varepsilon) = -\frac{\lambda_A}{\sqrt{2}} \frac{\tilde{\mathcal{G}}_{d_1 f^\dagger}(\varepsilon)}{(\varepsilon - \varepsilon_M + i\delta)} + \frac{\lambda_B}{\sqrt{2}} \frac{\tilde{\mathcal{G}}_{d_1^\dagger f^\dagger}(\varepsilon)}{(\varepsilon - \varepsilon_M + i\delta)} \tag{A.166}$$

Therefore,

$$\begin{aligned}
 \tilde{\mathcal{G}}_{\eta_2\eta_2}(\varepsilon) &= -\frac{1}{2} \left[\frac{\lambda_A}{\sqrt{2}} \frac{\tilde{\mathcal{G}}_{d_1^\dagger f}(\varepsilon)}{(\varepsilon + \varepsilon_M + i\delta)} - \frac{\lambda_B}{\sqrt{2}} \frac{\mathcal{G}_{d_1 f}(\varepsilon)}{(\varepsilon + \varepsilon_M + i\delta)} \right] \\
 &+ \frac{1}{2} \left[\frac{1}{(\varepsilon + \varepsilon_M + i\delta)} + \frac{\lambda_A}{\sqrt{2}} \frac{\tilde{\mathcal{G}}_{d_1^\dagger f^\dagger}(\varepsilon)}{(\varepsilon + \varepsilon_M + i\delta)} - \frac{\lambda_B}{\sqrt{2}} \frac{\mathcal{G}_{d_1 f^\dagger}(\varepsilon)}{(\varepsilon + \varepsilon_M + i\delta)} \right] \\
 &+ \frac{1}{2} \left[\frac{1}{(\varepsilon - \varepsilon_M + i\delta)} - \frac{\lambda_A}{\sqrt{2}} \frac{\tilde{\mathcal{G}}_{d_1 f}(\varepsilon)}{(\varepsilon - \varepsilon_M + i\delta)} + \frac{\lambda_B}{\sqrt{2}} \frac{\tilde{\mathcal{G}}_{d_1^\dagger f}(\varepsilon)}{(\varepsilon - \varepsilon_M + i\delta)} \right] \\
 &- \frac{1}{2} \left[-\frac{\lambda_A}{\sqrt{2}} \frac{\tilde{\mathcal{G}}_{d_1 f^\dagger}(\varepsilon)}{(\varepsilon - \varepsilon_M + i\delta)} + \frac{\lambda_B}{\sqrt{2}} \frac{\tilde{\mathcal{G}}_{d_1^\dagger f^\dagger}(\varepsilon)}{(\varepsilon - \varepsilon_M + i\delta)} \right] \\
 &= \frac{1}{2} \left[\frac{1}{(\varepsilon + \varepsilon_M + i\delta)} + \frac{1}{(\varepsilon - \varepsilon_M + i\delta)} \right] \\
 &+ \frac{1}{2} \left[\frac{\lambda_B}{\sqrt{2}} \frac{1}{(\varepsilon - \varepsilon_M + i\delta)} - \frac{\lambda_A}{\sqrt{2}} \frac{1}{(\varepsilon + \varepsilon_M + i\delta)} \right] \tilde{\mathcal{G}}_{d_1^\dagger f}(\varepsilon) \\
 &+ \frac{1}{2} \left[\frac{\lambda_B}{\sqrt{2}} \frac{1}{(\varepsilon + \varepsilon_M + i\delta)} - \frac{\lambda_A}{\sqrt{2}} \frac{1}{(\varepsilon - \varepsilon_M + i\delta)} \right] \tilde{\mathcal{G}}_{d_1 f}(\varepsilon) \\
 &+ \frac{1}{2} \left[\frac{\lambda_A}{\sqrt{2}} \frac{1}{(\varepsilon + \varepsilon_M + i\delta)} - \frac{\lambda_B}{\sqrt{2}} \frac{1}{(\varepsilon - \varepsilon_M + i\delta)} \right] \tilde{\mathcal{G}}_{d_1^\dagger f^\dagger}(\varepsilon) \\
 &+ \frac{1}{2} \left[\frac{\lambda_A}{\sqrt{2}} \frac{1}{(\varepsilon - \varepsilon_M + i\delta)} - \frac{\lambda_B}{\sqrt{2}} \frac{1}{(\varepsilon + \varepsilon_M + i\delta)} \right] \mathcal{G}_{d_1 f^\dagger}(\varepsilon) \tag{A.167}
 \end{aligned}$$

$$\begin{aligned}
 \tilde{\mathcal{G}}_{\eta_2\eta_2}(\varepsilon) &= K - \frac{1}{2} \left[\frac{\lambda_A}{\sqrt{2}} \frac{1}{(\varepsilon + \varepsilon_M + i\delta)} - \frac{\lambda_B}{\sqrt{2}} \frac{1}{(\varepsilon - \varepsilon_M + i\delta)} \right] \tilde{\mathcal{G}}_{d_1^\dagger f}(\varepsilon) \\
 &+ \frac{1}{2} \left[\frac{\lambda_A}{\sqrt{2}} \frac{1}{(\varepsilon + \varepsilon_M + i\delta)} - \frac{\lambda_B}{\sqrt{2}} \frac{1}{(\varepsilon - \varepsilon_M + i\delta)} \right] \tilde{\mathcal{G}}_{d_1^\dagger f^\dagger}(\varepsilon) \\
 &- \frac{1}{2} \left[\frac{\lambda_A}{\sqrt{2}} \frac{1}{(\varepsilon - \varepsilon_M + i\delta)} - \frac{\lambda_B}{\sqrt{2}} \frac{1}{(\varepsilon + \varepsilon_M + i\delta)} \right] \tilde{\mathcal{G}}_{d_1 f}(\varepsilon) \\
 &+ \frac{1}{2} \left[\frac{\lambda_A}{\sqrt{2}} \frac{1}{(\varepsilon - \varepsilon_M + i\delta)} - \frac{\lambda_B}{\sqrt{2}} \frac{1}{(\varepsilon + \varepsilon_M + i\delta)} \right] \mathcal{G}_{d_1 f^\dagger}(\varepsilon) \tag{A.168}
 \end{aligned}$$

$$\begin{aligned}
 \tilde{\mathcal{G}}_{\eta_2\eta_2}(\varepsilon) &= K + \frac{1}{2} \left[\frac{\lambda_A}{\sqrt{2}} \frac{1}{(\varepsilon + \varepsilon_M + i\delta)} - \frac{\lambda_B}{\sqrt{2}} \frac{1}{(\varepsilon - \varepsilon_M + i\delta)} \right] (\tilde{\mathcal{G}}_{d_1^\dagger f^\dagger} - \tilde{\mathcal{G}}_{d_1^\dagger f}) \\
 &+ \frac{1}{2} \left[\frac{\lambda_A}{\sqrt{2}} \frac{1}{(\varepsilon - \varepsilon_M + i\delta)} - \frac{\lambda_B}{\sqrt{2}} \frac{1}{(\varepsilon + \varepsilon_M + i\delta)} \right] (\mathcal{G}_{d_1 f^\dagger} - \tilde{\mathcal{G}}_{d_1 f}) \tag{A.169}
 \end{aligned}$$

wherein $\tilde{\mathcal{G}}_{d_1^\dagger f}$, $\tilde{\mathcal{G}}_{d_1 f}$, $\tilde{\mathcal{G}}_{d_1^\dagger f^\dagger}$ and $\mathcal{G}_{d_1 f^\dagger}$ are given by the same expressions previously calculated, as can be seen in Sec.A.1.3.

Appendix B

DOS of the Quantum Dot for the Interacting Spinfull Model within Hubbard-I Approximation

B.1 Single particle Green's functions (two operators)

Let us apply the EOM approach to obtain an expression for the Green's function of quantum dot:

$$(\omega + i\eta^+)G_{d_\sigma d_\sigma}^r(\omega) = 1 + \langle\langle [d_\sigma, \mathcal{H}_e]; d_\sigma^\dagger \rangle\rangle \quad (\text{B.1})$$

$$\begin{aligned} (\omega + i\eta^+)G_{d_\sigma d_\sigma}^r(\omega) &= 1 + \langle\langle [d_\sigma, \mathcal{H}_{\text{lead}}]; d_\sigma^\dagger \rangle\rangle + \langle\langle [d_\sigma, \mathcal{H}_{\text{dot}}]; d_\sigma^\dagger \rangle\rangle + \langle\langle [d_\sigma, \mathcal{H}_{\text{dot-lead}}]; d_\sigma^\dagger \rangle\rangle \\ &+ \langle\langle [d_\sigma, \mathcal{H}_M]; d_\sigma^\dagger \rangle\rangle \end{aligned} \quad (\text{B.2})$$

$$\begin{aligned} (\omega + i\eta^+)G_{d_\sigma d_\sigma}^r(\omega) &= 1 + \langle\langle [d_\sigma, \mathcal{H}_{\text{dot}}]; d_\sigma^\dagger \rangle\rangle + \langle\langle [d_\sigma, \mathcal{H}_{\text{dot-lead}}]; d_\sigma^\dagger \rangle\rangle \\ &+ \langle\langle [d_\sigma, \mathcal{H}_M]; d_\sigma^\dagger \rangle\rangle \end{aligned} \quad (\text{B.3})$$

$$[d_\sigma, \mathcal{H}_{\text{dot}}] = \sum_{\bar{\sigma}} \varepsilon_{d\bar{\sigma}} [d_\sigma, d_{\bar{\sigma}}^\dagger d_{\bar{\sigma}}] + U[d_\sigma, n_{d\uparrow} n_{d\downarrow}] \quad (\text{B.4})$$

$$\begin{aligned}
\sum_{\bar{\sigma}} \varepsilon_{d\bar{\sigma}} [d_{\sigma}, d_{\bar{\sigma}}^{\dagger} d_{\bar{\sigma}}] &= \sum_{\bar{\sigma}} \varepsilon_{d\bar{\sigma}} \left(d_{\sigma} d_{\bar{\sigma}}^{\dagger} d_{\bar{\sigma}} - d_{\bar{\sigma}}^{\dagger} d_{\bar{\sigma}} d_{\sigma} \right) \\
&= \sum_{\bar{\sigma}} \varepsilon_{d\bar{\sigma}} \left(\left(\delta_{\sigma\bar{\sigma}} - d_{\bar{\sigma}}^{\dagger} d_{\sigma} \right) d_{\bar{\sigma}} - d_{\bar{\sigma}}^{\dagger} d_{\bar{\sigma}} d_{\sigma} \right) \\
&= \sum_{\bar{\sigma}} \varepsilon_{d\bar{\sigma}} \left(\delta_{\sigma\bar{\sigma}} d_{\bar{\sigma}} - d_{\bar{\sigma}}^{\dagger} d_{\sigma} d_{\bar{\sigma}} - d_{\bar{\sigma}}^{\dagger} d_{\bar{\sigma}} d_{\sigma} \right) \\
&= \sum_{\bar{\sigma}} \varepsilon_{d\bar{\sigma}} \left(\delta_{\sigma\bar{\sigma}} d_{\bar{\sigma}} + d_{\bar{\sigma}}^{\dagger} d_{\bar{\sigma}} d_{\sigma} - d_{\bar{\sigma}}^{\dagger} d_{\bar{\sigma}} d_{\sigma} \right) \\
&= \varepsilon_{d\sigma} d_{\sigma}.
\end{aligned} \tag{B.5}$$

$$\begin{aligned}
U[d_{\sigma}, n_{d\uparrow} n_{d\downarrow}] &= U(d_{\sigma} n_{d\uparrow} n_{d\downarrow} - n_{d\uparrow} n_{d\downarrow} d_{\sigma}) \\
&= U(d_{\sigma} d_{\uparrow}^{\dagger} d_{\uparrow} d_{\downarrow}^{\dagger} d_{\downarrow} - d_{\uparrow}^{\dagger} d_{\uparrow} d_{\downarrow}^{\dagger} d_{\downarrow} d_{\sigma}) \\
&= U\left(\left(\delta_{\sigma\uparrow} - d_{\uparrow}^{\dagger} d_{\sigma}\right) d_{\uparrow} d_{\downarrow}^{\dagger} d_{\downarrow} - d_{\uparrow}^{\dagger} d_{\uparrow} d_{\downarrow}^{\dagger} d_{\downarrow} d_{\sigma}\right) \\
&= U\left(\delta_{\sigma\uparrow} d_{\uparrow} d_{\downarrow}^{\dagger} d_{\downarrow} - d_{\uparrow}^{\dagger} d_{\sigma} d_{\uparrow} d_{\downarrow}^{\dagger} d_{\downarrow} - d_{\uparrow}^{\dagger} d_{\uparrow} d_{\downarrow}^{\dagger} d_{\downarrow} d_{\sigma}\right) \\
&= U\left(\delta_{\sigma\uparrow} d_{\uparrow} d_{\downarrow}^{\dagger} d_{\downarrow} + d_{\uparrow}^{\dagger} d_{\uparrow} d_{\sigma} d_{\downarrow}^{\dagger} d_{\downarrow} - d_{\uparrow}^{\dagger} d_{\uparrow} d_{\downarrow}^{\dagger} d_{\downarrow} d_{\sigma}\right) \\
&= U\left(\delta_{\sigma\uparrow} d_{\uparrow} d_{\downarrow}^{\dagger} d_{\downarrow} + d_{\uparrow}^{\dagger} d_{\uparrow} \left(\delta_{\sigma\downarrow} - d_{\downarrow}^{\dagger} d_{\sigma}\right) d_{\downarrow} - d_{\uparrow}^{\dagger} d_{\uparrow} d_{\downarrow}^{\dagger} d_{\downarrow} d_{\sigma}\right) \\
&= U\left(\delta_{\sigma\uparrow} d_{\uparrow} d_{\downarrow}^{\dagger} d_{\downarrow} + \delta_{\sigma\downarrow} d_{\uparrow}^{\dagger} d_{\uparrow} d_{\downarrow} - d_{\uparrow}^{\dagger} d_{\uparrow} d_{\downarrow}^{\dagger} d_{\sigma} d_{\downarrow} - d_{\uparrow}^{\dagger} d_{\uparrow} d_{\downarrow}^{\dagger} d_{\downarrow} d_{\sigma}\right) \\
&= U\left(\delta_{\sigma\uparrow} d_{\uparrow} d_{\downarrow}^{\dagger} d_{\downarrow} + \delta_{\sigma\downarrow} d_{\uparrow}^{\dagger} d_{\uparrow} d_{\downarrow} + d_{\uparrow}^{\dagger} d_{\uparrow} d_{\downarrow}^{\dagger} d_{\downarrow} d_{\sigma} - d_{\uparrow}^{\dagger} d_{\uparrow} d_{\downarrow}^{\dagger} d_{\downarrow} d_{\sigma}\right) \\
&= U\left(\delta_{\sigma\uparrow} d_{\uparrow} d_{\downarrow}^{\dagger} d_{\downarrow} + \delta_{\sigma\downarrow} d_{\uparrow}^{\dagger} d_{\uparrow} d_{\downarrow}\right) \\
&= U\left(\delta_{\sigma\uparrow} d_{\uparrow} d_{\downarrow}^{\dagger} d_{\downarrow} + \delta_{\sigma\downarrow} d_{\downarrow} d_{\uparrow}^{\dagger} d_{\uparrow}\right) \\
&= U d_{\sigma} d_{\bar{\sigma}}^{\dagger} d_{\bar{\sigma}} = U d_{\sigma} n_{d\bar{\sigma}}.
\end{aligned} \tag{B.6}$$

where $\bar{\sigma}$ is opposite of σ , e.g, $\sigma = \uparrow$ (\downarrow), $\bar{\sigma} = \downarrow$ (\uparrow).

$$\begin{aligned}
 [d_\sigma, \mathcal{H}_{\text{dot-lead}}] &= [d_\sigma, \sqrt{2V} \sum_{\mathbf{k}\bar{\sigma}} (e_{\mathbf{k}\bar{\sigma}}^\dagger d_{\bar{\sigma}} + d_{\bar{\sigma}}^\dagger e_{\mathbf{k}\bar{\sigma}})] \\
 &= [d_\sigma, \sqrt{2V} \sum_{\mathbf{k}\bar{\sigma}} e_{\mathbf{k}\bar{\sigma}}^\dagger d_{\bar{\sigma}}] + [d_\sigma, \sqrt{2V} \sum_{\mathbf{k}\bar{\sigma}} d_{\bar{\sigma}}^\dagger e_{\mathbf{k}\bar{\sigma}}] \\
 &= \sqrt{2V} \sum_{\mathbf{k}\bar{\sigma}} (d_\sigma e_{\mathbf{k}\bar{\sigma}}^\dagger d_{\bar{\sigma}} - e_{\mathbf{k}\bar{\sigma}}^\dagger d_{\bar{\sigma}} d_\sigma) \\
 &\quad + \sqrt{2V} \sum_{\mathbf{k}\bar{\sigma}} (d_\sigma d_{\bar{\sigma}}^\dagger e_{\mathbf{k}\bar{\sigma}} - d_{\bar{\sigma}}^\dagger e_{\mathbf{k}\bar{\sigma}} d_\sigma) \\
 &= \sqrt{2V} \sum_{\mathbf{k}\bar{\sigma}} (e_{\mathbf{k}\bar{\sigma}}^\dagger d_{\bar{\sigma}} d_\sigma - e_{\mathbf{k}\bar{\sigma}}^\dagger d_{\bar{\sigma}} d_\sigma) \\
 &\quad + \sqrt{2V} \sum_{\mathbf{k}\bar{\sigma}} (e_{\mathbf{k}\bar{\sigma}} d_\sigma d_{\bar{\sigma}}^\dagger + e_{\mathbf{k}\bar{\sigma}} d_{\bar{\sigma}}^\dagger d_\sigma) \\
 &= \sqrt{2V} \sum_{\mathbf{k}\bar{\sigma}} e_{\mathbf{k}\bar{\sigma}} (d_\sigma d_{\bar{\sigma}}^\dagger + d_{\bar{\sigma}}^\dagger d_\sigma) \\
 &= \sqrt{2V} \sum_{\mathbf{k}\bar{\sigma}} e_{\mathbf{k}\bar{\sigma}} \delta_{\sigma\bar{\sigma}} = \sqrt{2V} \sum_{\mathbf{k}\bar{\sigma}} \delta_{\sigma\bar{\sigma}} e_{\mathbf{k}\bar{\sigma}} \\
 &= \sqrt{2V} \sum_{\mathbf{k}} e_{\mathbf{k}\sigma}. \tag{B.7}
 \end{aligned}$$

$$\begin{aligned}
 (\omega + \eta^+) G_{d_\sigma d_\sigma}^r(\omega) &= 1 + \varepsilon_{d_\sigma} \langle\langle d_\sigma; d_\sigma^\dagger \rangle\rangle + U \langle\langle d_\sigma n_{d\bar{\sigma}}; d_\sigma^\dagger \rangle\rangle + \sqrt{2V} \sum_{\mathbf{k}} \langle\langle e_{\mathbf{k}\sigma}; d_\sigma^\dagger \rangle\rangle \\
 &\quad + \langle\langle [d_\sigma, \mathcal{H}_M]; d_\sigma^\dagger \rangle\rangle \tag{B.8}
 \end{aligned}$$

In the equation above, we have the well-known result for a QD between metallic leads without a Kitaev wire. The novelty is due to the following commutation relations:

$$\begin{aligned}
 [d_\sigma, \mathcal{H}_M] &= \left[d_\sigma, \delta_M \left(a_\uparrow^\dagger a_\uparrow - \frac{1}{2} \right) \right] + \left[d_\sigma, t_{hp} \sum_{\bar{\sigma}} (d_{\bar{\sigma}} a_\uparrow^\dagger + a_\uparrow d_{\bar{\sigma}}^\dagger) \right] \\
 &\quad + \left[d_\sigma, \Delta \sum_{\bar{\sigma}} (d_{\bar{\sigma}} a_\uparrow + a_\uparrow^\dagger d_{\bar{\sigma}}^\dagger) \right] \tag{B.9}
 \end{aligned}$$

$$[d_\sigma, \mathcal{H}_M] = \left[d_\sigma, t_{hp} \sum_{\bar{\sigma}} (d_{\bar{\sigma}} a_\uparrow^\dagger + a_\uparrow d_{\bar{\sigma}}^\dagger) \right] + \left[d_\sigma, \Delta \sum_{\bar{\sigma}} (d_{\bar{\sigma}} a_\uparrow + a_\uparrow^\dagger d_{\bar{\sigma}}^\dagger) \right] \tag{B.10}$$

$$\begin{aligned}
[d_\sigma, t_{hp}(d_{\bar{\sigma}}a_\uparrow^\dagger + a_\uparrow d_{\bar{\sigma}}^\dagger)] &= t_{hp} \sum_{\bar{\sigma}} [d_\sigma, d_{\bar{\sigma}}a_\uparrow^\dagger] + t_{hp} \sum_{\bar{\sigma}} [d_\sigma, a_\uparrow d_{\bar{\sigma}}^\dagger] \\
&= t_{hp} \sum_{\bar{\sigma}} (d_\sigma d_{\bar{\sigma}}a_\uparrow^\dagger - d_{\bar{\sigma}}a_\uparrow^\dagger d_\sigma) \\
&+ t_{hp} \sum_{\bar{\sigma}} (d_\sigma a_\uparrow d_{\bar{\sigma}}^\dagger - a_\uparrow d_{\bar{\sigma}}^\dagger d_\sigma) \\
&= t_{hp} \sum_{\bar{\sigma}} (d_\sigma d_{\bar{\sigma}}a_\uparrow^\dagger - d_\sigma d_{\bar{\sigma}}a_\uparrow^\dagger) \\
&+ t_{hp} \sum_{\bar{\sigma}} (-d_\sigma d_{\bar{\sigma}}^\dagger a_\uparrow - d_{\bar{\sigma}}^\dagger d_\sigma a_\uparrow) \\
&= -t_{hp} \sum_{\bar{\sigma}} (d_\sigma d_{\bar{\sigma}}^\dagger + d_{\bar{\sigma}}^\dagger d_\sigma) a_\uparrow = -t_{hp} \sum_{\bar{\sigma}} \{d_\sigma, d_{\bar{\sigma}}^\dagger\} a_\uparrow \\
&= -t_{hp} \sum_{\bar{\sigma}} \delta_{\sigma\bar{\sigma}} a_\uparrow
\end{aligned} \tag{B.11}$$

$$\begin{aligned}
\left[d_\sigma, \Delta \sum_{\bar{\sigma}} (d_{\bar{\sigma}}a_\uparrow + a_\uparrow d_{\bar{\sigma}}^\dagger) \right] &= \Delta \sum_{\bar{\sigma}} [d_\sigma, d_{\bar{\sigma}}a_\uparrow] + \Delta \sum_{\bar{\sigma}} [d_\sigma, a_\uparrow d_{\bar{\sigma}}^\dagger] \\
&= \Delta \sum_{\bar{\sigma}} (d_\sigma d_{\bar{\sigma}}a_\uparrow - d_{\bar{\sigma}}a_\uparrow d_\sigma) \\
&+ \Delta \sum_{\bar{\sigma}} (d_\sigma a_\uparrow d_{\bar{\sigma}}^\dagger - a_\uparrow d_{\bar{\sigma}}^\dagger d_\sigma) \\
&= \Delta \sum_{\bar{\sigma}} (d_\sigma d_{\bar{\sigma}}a_\uparrow - d_\sigma d_{\bar{\sigma}}a_\uparrow) \\
&+ \Delta \sum_{\bar{\sigma}} (-a_\uparrow d_\sigma d_{\bar{\sigma}}^\dagger - a_\uparrow d_{\bar{\sigma}}^\dagger d_\sigma) \\
&= -\Delta \sum_{\bar{\sigma}} a_\uparrow (d_\sigma d_{\bar{\sigma}}^\dagger + d_{\bar{\sigma}}^\dagger d_\sigma) \\
&= -\Delta \sum_{\bar{\sigma}} \delta_{\sigma\bar{\sigma}} a_\uparrow^\dagger
\end{aligned} \tag{B.12}$$

$$\begin{aligned}
(\omega + \eta\eta^+)G_{d_\sigma d_\sigma}^r(\omega) &= 1 + \varepsilon_{d\sigma} \langle\langle d_\sigma; d_\sigma^\dagger \rangle\rangle + U \langle\langle d_\sigma n_{d\bar{\sigma}}; d_\sigma^\dagger \rangle\rangle + \sqrt{2}V \sum_{\mathbf{k}} \langle\langle e_{\mathbf{k}\sigma}; d_\sigma^\dagger \rangle\rangle \\
&+ -t_{hp} \sum_{\bar{\sigma}} \delta_{\sigma\bar{\sigma}} \langle\langle a_\uparrow; d_\sigma^\dagger \rangle\rangle - \Delta \sum_{\bar{\sigma}} \delta_{\sigma\bar{\sigma}} \langle\langle a_\uparrow^\dagger; d_\sigma^\dagger \rangle\rangle
\end{aligned} \tag{B.13}$$

$$\begin{aligned}
(\omega - \varepsilon_{d\sigma} + \eta\eta^+)G_{d_\sigma d_\sigma}^r(\omega) &= 1 + U G_{d_\sigma n_{d\bar{\sigma}}, d_\sigma}^r(\omega) + \sqrt{2}V \sum_{\mathbf{k}} G_{e_{\mathbf{k}\sigma} d_\sigma}^r(\omega) \\
&- t_{hp} \sum_{\bar{\sigma}} \delta_{\sigma\bar{\sigma}} G_{a_\uparrow, d_\sigma}^r(\omega) - \sum_{\bar{\sigma}} \delta_{\sigma\bar{\sigma}} \Delta G_{a_\uparrow^\dagger, d_\sigma}^r(\omega)
\end{aligned} \tag{B.14}$$

Now, let us apply the EOM to find $G_{e_{\mathbf{k}\sigma} d_\sigma}^r(\omega)$:

$$(\omega + \eta^+) G_{e_{\mathbf{k}\sigma} d_\sigma}^r(\omega) = \delta_{e_{\mathbf{k}\sigma} d_\sigma} + \langle\langle [e_{\mathbf{k}\sigma}, \mathcal{H}_e]; d_\sigma^\dagger \rangle\rangle \quad (\text{B.15})$$

$$\begin{aligned} [e_{\mathbf{k}\sigma}, \mathcal{H}_e] &= [e_{\mathbf{k}\sigma}, \mathcal{H}_{\text{lead}}] + [e_{\mathbf{k}\sigma}, \mathcal{H}_{\text{dot}}] + [e_{\mathbf{k}\sigma}, \mathcal{H}_{\text{dot-lead}}] + [e_{\mathbf{k}\sigma}, \mathcal{H}_M] \\ &= [e_{\mathbf{k}\sigma}, \mathcal{H}_{\text{lead}}] + [e_{\mathbf{k}\sigma}, \mathcal{H}_{\text{dot-lead}}] \end{aligned} \quad (\text{B.16})$$

$$\begin{aligned} [e_{\mathbf{k}\sigma}, \mathcal{H}_{\text{lead}}] &= [e_{\mathbf{k}\sigma}, \sum_{\mathbf{p}\tilde{\sigma}} \varepsilon_{\mathbf{p}\tilde{\sigma}} e_{\mathbf{p}\tilde{\sigma}}^\dagger e_{\mathbf{p}\tilde{\sigma}} + V_{SD} \sum_{\mathbf{p}, \mathbf{q}\tilde{\sigma}} e_{\mathbf{p}\tilde{\sigma}}^\dagger e_{\mathbf{q}\tilde{\sigma}}] \\ &= [e_{\mathbf{k}\sigma}, \sum_{\mathbf{p}\tilde{\sigma}} \varepsilon_{\mathbf{p}\tilde{\sigma}} e_{\mathbf{p}\tilde{\sigma}}^\dagger e_{\mathbf{p}\tilde{\sigma}}] + [e_{\mathbf{k}\sigma}, V_{SD} \sum_{\mathbf{p}, \mathbf{q}\tilde{\sigma}} e_{\mathbf{p}\tilde{\sigma}}^\dagger e_{\mathbf{q}\tilde{\sigma}}] \end{aligned} \quad (\text{B.17})$$

$$\begin{aligned} [e_{\mathbf{k}\sigma}, \sum_{\mathbf{p}\tilde{\sigma}} \varepsilon_{\mathbf{p}\tilde{\sigma}} e_{\mathbf{p}\tilde{\sigma}}^\dagger e_{\mathbf{p}\tilde{\sigma}}] &= \sum_{\mathbf{p}\tilde{\sigma}} \varepsilon_{\mathbf{p}\tilde{\sigma}} \left(e_{\mathbf{k}\sigma} e_{\mathbf{p}\tilde{\sigma}}^\dagger e_{\mathbf{p}\tilde{\sigma}} - e_{\mathbf{p}\tilde{\sigma}}^\dagger e_{\mathbf{p}\tilde{\sigma}} e_{\mathbf{k}\sigma} \right) \\ &= \sum_{\mathbf{p}\tilde{\sigma}} \varepsilon_{\mathbf{p}\tilde{\sigma}} \left(\left(\delta_{\mathbf{k}\mathbf{p}} \delta_{\sigma\tilde{\sigma}} - e_{\mathbf{p}\tilde{\sigma}}^\dagger e_{\mathbf{k}\sigma} \right) e_{\mathbf{p}\tilde{\sigma}} - e_{\mathbf{p}\tilde{\sigma}}^\dagger e_{\mathbf{p}\tilde{\sigma}} e_{\mathbf{k}\sigma} \right) \\ &= \sum_{\mathbf{p}\tilde{\sigma}} \varepsilon_{\mathbf{p}\tilde{\sigma}} \left(\delta_{\mathbf{k}\mathbf{p}} \delta_{\sigma\tilde{\sigma}} e_{\mathbf{p}\tilde{\sigma}} - e_{\mathbf{p}\tilde{\sigma}}^\dagger e_{\mathbf{k}\sigma} e_{\mathbf{p}\tilde{\sigma}} - e_{\mathbf{p}\tilde{\sigma}}^\dagger e_{\mathbf{p}\tilde{\sigma}} e_{\mathbf{k}\sigma} \right) \\ &= \sum_{\mathbf{p}\tilde{\sigma}} \varepsilon_{\mathbf{p}\tilde{\sigma}} \left(\delta_{\mathbf{k}\mathbf{p}} \delta_{\sigma\tilde{\sigma}} e_{\mathbf{p}\tilde{\sigma}} - e_{\mathbf{p}\tilde{\sigma}}^\dagger e_{\mathbf{p}\tilde{\sigma}} e_{\mathbf{k}\sigma} - e_{\mathbf{p}\tilde{\sigma}}^\dagger e_{\mathbf{p}\tilde{\sigma}} e_{\mathbf{k}\sigma} \right) \\ &= \varepsilon_{\mathbf{k}\sigma} e_{\mathbf{k}\sigma}. \end{aligned} \quad (\text{B.18})$$

$$\begin{aligned} [e_{\mathbf{k}\sigma}, V_{SD} \sum_{\mathbf{p}, \mathbf{q}\tilde{\sigma}} e_{\mathbf{p}\tilde{\sigma}}^\dagger e_{\mathbf{q}\tilde{\sigma}}] &= V_{SD} \sum_{\mathbf{p}, \mathbf{q}\tilde{\sigma}} \left(e_{\mathbf{k}\sigma} e_{\mathbf{p}\tilde{\sigma}}^\dagger e_{\mathbf{q}\tilde{\sigma}} - e_{\mathbf{p}\tilde{\sigma}}^\dagger e_{\mathbf{q}\tilde{\sigma}} e_{\mathbf{k}\sigma} \right) \\ &= V_{SD} \sum_{\mathbf{p}, \mathbf{q}\tilde{\sigma}} \left(\left(\delta_{\mathbf{k}\mathbf{p}} \delta_{\sigma\tilde{\sigma}} - e_{\mathbf{p}\tilde{\sigma}}^\dagger e_{\mathbf{k}\sigma} \right) e_{\mathbf{q}\tilde{\sigma}} - e_{\mathbf{p}\tilde{\sigma}}^\dagger e_{\mathbf{q}\tilde{\sigma}} e_{\mathbf{k}\sigma} \right) \\ &= V_{SD} \sum_{\mathbf{p}, \mathbf{q}\tilde{\sigma}} \left(\delta_{\mathbf{k}\mathbf{p}} \delta_{\sigma\tilde{\sigma}} e_{\mathbf{q}\tilde{\sigma}} + e_{\mathbf{p}\tilde{\sigma}}^\dagger e_{\mathbf{q}\tilde{\sigma}} e_{\mathbf{k}\sigma} - e_{\mathbf{p}\tilde{\sigma}}^\dagger e_{\mathbf{q}\tilde{\sigma}} e_{\mathbf{k}\sigma} \right) \\ &= V_{SD} \sum_{\mathbf{q}} e_{\mathbf{q}\sigma}. \end{aligned} \quad (\text{B.19})$$

$$\begin{aligned}
 [e_{\mathbf{k}\sigma}, \mathcal{H}_{\text{dot-lead}}] &= [e_{\mathbf{k}\sigma}, \sqrt{2}V \sum_{\mathbf{p}\bar{\sigma}} (e_{\mathbf{p}\bar{\sigma}}^\dagger d_{\bar{\sigma}} + d_{\bar{\sigma}}^\dagger e_{\mathbf{p}\bar{\sigma}})] \\
 &= [e_{\mathbf{k}\sigma}, \sqrt{2}V \sum_{\mathbf{p}\bar{\sigma}} e_{\mathbf{p}\bar{\sigma}}^\dagger d_{\bar{\sigma}}] + [e_{\mathbf{k}\sigma}, \sqrt{2}V \sum_{\mathbf{p}\bar{\sigma}} d_{\bar{\sigma}}^\dagger e_{\mathbf{p}\bar{\sigma}}] \\
 &= \sqrt{2}V \sum_{\mathbf{p}\bar{\sigma}} (e_{\mathbf{k}\sigma} e_{\mathbf{p}\bar{\sigma}}^\dagger d_{\bar{\sigma}} - e_{\mathbf{p}\bar{\sigma}}^\dagger d_{\bar{\sigma}} e_{\mathbf{k}\sigma}) \\
 &+ \sqrt{2}V \sum_{\mathbf{p}\bar{\sigma}} (e_{\mathbf{k}\sigma} d_{\bar{\sigma}}^\dagger e_{\mathbf{p}\bar{\sigma}} - d_{\bar{\sigma}}^\dagger e_{\mathbf{p}\bar{\sigma}} e_{\mathbf{k}\sigma}) \\
 &= \sqrt{2}V \sum_{\mathbf{p}\bar{\sigma}} \left((\delta_{\mathbf{p},\mathbf{k}} \delta_{\sigma\bar{\sigma}} - e_{\mathbf{p}\bar{\sigma}}^\dagger e_{\mathbf{k}\sigma}) d_{\bar{\sigma}} + e_{\mathbf{p}\bar{\sigma}}^\dagger e_{\mathbf{k}\sigma} d_{\bar{\sigma}} \right) \\
 &+ \sqrt{2}V \sum_{\mathbf{p}\bar{\sigma}} (d_{\bar{\sigma}}^\dagger e_{\mathbf{p}\bar{\sigma}} e_{\mathbf{k}\sigma} - d_{\bar{\sigma}}^\dagger e_{\mathbf{p}\bar{\sigma}} e_{\mathbf{k}\sigma}) \\
 &= \sqrt{2}V \sum_{\mathbf{p}\bar{\sigma}} (\delta_{\mathbf{p},\mathbf{k}} \delta_{\sigma\bar{\sigma}} d_{\bar{\sigma}} - \delta_{\mathbf{p},\mathbf{k}} \delta_{\sigma\bar{\sigma}} e_{\mathbf{p}\bar{\sigma}}^\dagger e_{\mathbf{k}\sigma} d_{\bar{\sigma}} + e_{\mathbf{p}\bar{\sigma}}^\dagger e_{\mathbf{k}\sigma} d_{\bar{\sigma}}) \\
 &= \sqrt{2}V (d_{\sigma} - e_{\mathbf{k}\sigma}^\dagger e_{\mathbf{k}\sigma} d_{\sigma} + e_{\mathbf{k}\sigma}^\dagger e_{\mathbf{k}\sigma} d_{\sigma}) \\
 &= \sqrt{2}V d_{\sigma}.
 \end{aligned} \tag{B.20}$$

$$(\omega + \eta^+) G_{e_{\mathbf{k}\sigma} d_{\sigma}}^r(\omega) = \varepsilon_{\mathbf{k}\sigma} \langle \langle e_{\mathbf{k}\sigma}; d_{\sigma}^\dagger \rangle \rangle + V_{SD} \sum_{\mathbf{q}} \langle \langle e_{\mathbf{q}\sigma}; d_{\sigma}^\dagger \rangle \rangle + \sqrt{2}V \langle \langle d_{\sigma}; d_{\sigma}^\dagger \rangle \rangle \tag{B.21}$$

$$(\omega - \varepsilon_{\mathbf{k}\sigma} + \eta^+) G_{e_{\mathbf{k}\sigma} d_{\sigma}}^r(\omega) = V_{SD} \sum_{\mathbf{q}} \langle \langle e_{\mathbf{q}\sigma}; d_{\sigma}^\dagger \rangle \rangle + \sqrt{2}V \langle \langle d_{\sigma}; d_{\sigma}^\dagger \rangle \rangle \tag{B.22}$$

$$(\omega - \varepsilon_{\mathbf{k}\sigma} + \eta^+) G_{e_{\mathbf{k}\sigma} d_{\sigma}}^r(\omega) - V_{SD} \sum_{\mathbf{k}} G_{e_{\mathbf{k}\sigma} d_{\sigma}}^r(\omega) = \sqrt{2}V G_{d_{\sigma} d_{\sigma}}^r(\omega) \tag{B.23}$$

Let us divide the expression above by $(\omega - \varepsilon_{\mathbf{k}\sigma} + \eta^+)$:

$$G_{e_{\mathbf{k}\sigma} d_{\sigma}}^r(\omega) - V_{SD} \sum_{\mathbf{k}} \frac{G_{e_{\mathbf{k}\sigma} d_{\sigma}}^r(\omega)}{(\omega - \varepsilon_{\mathbf{k}\sigma} + \eta^+)} = \frac{\sqrt{2}V G_{d_{\sigma} d_{\sigma}}^r(\omega)}{(\omega - \varepsilon_{\mathbf{k}\sigma} + \eta^+)} \tag{B.24}$$

$$\left[1 - \sum_{\mathbf{k}} \frac{V_{SD}}{(\omega - \varepsilon_{\mathbf{k}\sigma} + \eta^+)} \right] G_{e_{\mathbf{k}\sigma} d_{\sigma}}^r(\omega) = \frac{\sqrt{2}V G_{d_{\sigma} d_{\sigma}}^r(\omega)}{(\omega - \varepsilon_{\mathbf{k}\sigma} + \eta^+)} \tag{B.25}$$

$$G_{e_{\mathbf{k}\sigma} d_{\sigma}}^r(\omega) = \frac{\sqrt{2}V (\omega - \varepsilon_{\mathbf{k}\sigma} + \eta^+)^{-1}}{\left[1 - \sum_{\mathbf{k}} \frac{V_{SD}}{(\omega - \varepsilon_{\mathbf{k}\sigma} + \eta^+)} \right]} G_{d_{\sigma} d_{\sigma}}^r(\omega) \tag{B.26}$$

Substituting the expression above into Eq.(B.14):

$$\begin{aligned}
 (\omega - \varepsilon_{d\sigma} + \eta^+) G_{d_\sigma d_\sigma}^r(\omega) &= 1 + U G_{d_\sigma n_{d\bar{\sigma}}, d_\sigma}^r(\omega) + \sum_{\mathbf{k}} \frac{2V^2(\omega - \varepsilon_{\mathbf{k}\sigma} + \eta^+)^{-1}}{\left[1 - \sum_{\mathbf{k}} \frac{V_{SD}}{(\omega - \varepsilon_{\mathbf{k}\sigma} + \eta^+)}\right]} G_{d_\sigma d_\sigma}^r(\omega) \\
 &- t_{hp} \sum_{\bar{\sigma}} \delta_{\sigma\bar{\sigma}} G_{a_\uparrow, d_\sigma}^r(\omega) - \Delta \sum_{\bar{\sigma}} \delta_{\sigma\bar{\sigma}} G_{a_\uparrow, d_\sigma}^r(\omega)
 \end{aligned} \tag{B.27}$$

As we have shown in previous works:

$$\sum_{\mathbf{k}} \left(\frac{1}{\omega - \varepsilon_{\mathbf{k}\sigma} + \eta^+} \right) = -i\pi \rho_{\mathbf{k}\sigma}(\omega) \tag{B.28}$$

in the wide-band limit, where $\rho_{\mathbf{k}\sigma}(\omega) = \left(\frac{1}{\pi}\right) \sum_{\mathbf{k}} \delta(\omega - \varepsilon_{\mathbf{k}\sigma})$ is the DOS of metallic leads. Thus,

$$\begin{aligned}
 (\omega - \varepsilon_{d\sigma} + \eta^+) G_{d_\sigma d_\sigma}^r(\omega) &= 1 + U G_{d_\sigma n_{d\bar{\sigma}}, d_\sigma}^r(\omega) + \frac{2V^2(-i\pi \rho_{\mathbf{k}\sigma}(\omega))}{[1 - V_{SD}(-i\pi \rho_{\mathbf{k}\sigma}(\omega))]} G_{d_\sigma d_\sigma}^r(\omega) \\
 &- \sum_{\bar{\sigma}} \delta_{\sigma\bar{\sigma}} t_{hp} G_{a_\uparrow, d_\sigma}^r(\omega) - \sum_{\bar{\sigma}} \delta_{\sigma\bar{\sigma}} \Delta G_{a_\uparrow, d_\sigma}^r(\omega)
 \end{aligned} \tag{B.29}$$

$$\begin{aligned}
 (\omega - \varepsilon_{d\sigma} + \eta^+) G_{d_\sigma d_\sigma}^r(\omega) &= 1 + U G_{d_\sigma n_{d\bar{\sigma}}, d_\sigma}^r(\omega) - \frac{i2V^2\pi \rho_{\mathbf{k}\sigma}(\omega)}{[1 + i(V_{SD}\pi \rho_{\mathbf{k}\sigma}(\omega))]} G_{d_\sigma d_\sigma}^r(\omega) \\
 &- t_{hp} \sum_{\bar{\sigma}} \delta_{\sigma\bar{\sigma}} G_{a_\uparrow, d_\sigma}^r(\omega) - \sum_{\bar{\sigma}} \delta_{\sigma\bar{\sigma}} \Delta G_{a_\uparrow, d_\sigma}^r(\omega)
 \end{aligned} \tag{B.30}$$

However, the Anderson parameter $\Gamma_\sigma = 2V^2\pi \rho_{\mathbf{k}\sigma}(\omega)$.

$$\begin{aligned}
 (\omega - \varepsilon_{d\sigma} + \eta^+) G_{d_\sigma d_\sigma}^r(\omega) &= 1 + U G_{d_\sigma n_{d\bar{\sigma}}, d_\sigma}^r(\omega) - \frac{i\Gamma_\sigma}{[1 + i(V_{SD}\pi \rho_{\mathbf{k}\sigma}(\omega))]} G_{d_\sigma d_\sigma}^r(\omega) \\
 &- t_{hp} \sum_{\bar{\sigma}} \delta_{\sigma\bar{\sigma}} G_{a_\uparrow, d_\sigma}^r(\omega) - \Delta \sum_{\bar{\sigma}} \delta_{\sigma\bar{\sigma}} G_{a_\uparrow, d_\sigma}^r(\omega)
 \end{aligned} \tag{B.31}$$

Let us label $\sqrt{x} = V_{SD}\pi \rho_{\mathbf{k}\sigma}(\omega)$:

$$\begin{aligned}
 \frac{-i\Gamma_\sigma [1 - i\sqrt{x}]}{[1 + i\sqrt{x}][1 - i\sqrt{x}]} &= \frac{-i\Gamma_\sigma - \sqrt{x}\Gamma_\sigma}{1 + x} \\
 &= \frac{-(i + \sqrt{x})\Gamma_\sigma}{1 + x} \\
 &= -\frac{\sqrt{x}\Gamma_\sigma}{1 + x} - i\frac{\Gamma_\sigma}{1 + x}
 \end{aligned} \tag{B.32}$$

$$\Sigma_\sigma = -\frac{\sqrt{x}\Gamma_\sigma}{1 + x} - i\frac{\Gamma_\sigma}{1 + x} = \text{Re}(\Sigma_\sigma) + \text{Im}(\Sigma_\sigma) \tag{B.33}$$

$$\begin{aligned}
 (\omega - \varepsilon_{d\sigma} + \eta\eta^+)G_{d\sigma d\sigma}^r(\omega) &= 1 + UG_{d\sigma n_{d\bar{\sigma}}, d\sigma}^r(\omega) + \Sigma_{\sigma}G_{d\sigma d\sigma}^r(\omega) \\
 &- t_{hp} \sum_{\bar{\sigma}} \delta_{\sigma\bar{\sigma}} G_{a_{\uparrow}d\sigma}^r(\omega) - \Delta \sum_{\bar{\sigma}} \delta_{\sigma\bar{\sigma}} G_{a_{\uparrow}^{\dagger}d\sigma}^r(\omega)
 \end{aligned} \tag{B.34}$$

$$(\omega - \varepsilon_{d\sigma} - \Sigma_{\sigma} + \eta\eta^+)G_{d\sigma d\sigma}^r(\omega) = 1 + UG_{d\sigma n_{d\bar{\sigma}}, d\sigma}^r(\omega) - t_{hp} \sum_{\bar{\sigma}} \delta_{\sigma\bar{\sigma}} G_{a_{\uparrow}d\sigma}^r(\omega) - \Delta \sum_{\bar{\sigma}} \delta_{\sigma\bar{\sigma}} G_{a_{\uparrow}^{\dagger}d\sigma}^r(\omega) \tag{B.35}$$

Below, we present the calculations for the Green's functions related to the *Kitaev wire*:

$$(\omega + \eta\eta^+)G_{a_{\uparrow}d\sigma}^r(\omega) = \langle\langle [a_{\uparrow}, \mathcal{H}_e]; d_{\sigma}^{\dagger} \rangle\rangle \tag{B.36}$$

$$\begin{aligned}
 [a_{\uparrow}, \mathcal{H}_e] &= [a_{\uparrow}, \mathcal{H}_{\text{lead}}] + [a_{\uparrow}, \mathcal{H}_{\text{dot}}] + [a_{\uparrow}, \mathcal{H}_{\text{dot-lead}}] + [a_{\uparrow}, \mathcal{H}_M] \\
 &= [a_{\uparrow}, \mathcal{H}_M]
 \end{aligned} \tag{B.37}$$

$$\begin{aligned}
 [a_{\uparrow}, \mathcal{H}_M] &= \left[a_{\uparrow}, \delta_M \left(a_{\uparrow}^{\dagger} a_{\uparrow} - \frac{1}{2} \right) \right] + \left[a_{\uparrow}, t_{hp} \sum_{\bar{\sigma}} (d_{\bar{\sigma}} a_{\uparrow}^{\dagger} + a_{\uparrow} d_{\bar{\sigma}}^{\dagger}) \right] \\
 &+ \left[a_{\uparrow}, \Delta \sum_{\bar{\sigma}} (d_{\bar{\sigma}} a_{\uparrow} + a_{\uparrow}^{\dagger} d_{\bar{\sigma}}^{\dagger}) \right]
 \end{aligned} \tag{B.38}$$

$$\begin{aligned}
 \left[a_{\uparrow}, \delta_M \left(a_{\uparrow}^{\dagger} a_{\uparrow} - \frac{1}{2} \right) \right] &= \delta_M (a_{\uparrow} a_{\uparrow}^{\dagger} a_{\uparrow} - a_{\uparrow}^{\dagger} a_{\uparrow} a_{\uparrow}) \\
 &= \delta_M \left((1 - a_{\uparrow}^{\dagger} a_{\uparrow}) a_{\uparrow} - a_{\uparrow}^{\dagger} a_{\uparrow} a_{\uparrow} \right) \\
 &= \delta_M (a_{\uparrow} - a_{\uparrow}^{\dagger} a_{\uparrow} a_{\uparrow} + a_{\uparrow}^{\dagger} a_{\uparrow} a_{\uparrow}) \\
 &= \delta_M a_{\uparrow}
 \end{aligned} \tag{B.39}$$

$$\begin{aligned}
\sum_{\bar{\sigma}} [a_{\uparrow}, t_{hp}(d_{\bar{\sigma}}a_{\uparrow}^{\dagger} + a_{\uparrow}d_{\bar{\sigma}}^{\dagger})] &= t_{hp} \sum_{\bar{\sigma}} [a_{\uparrow}, d_{\bar{\sigma}}a_{\uparrow}^{\dagger}] + t_{hp} \sum_{\bar{\sigma}} [a_{\uparrow}, a_{\uparrow}d_{\bar{\sigma}}^{\dagger}] \\
&= t_{hp} \sum_{\bar{\sigma}} (a_{\uparrow}d_{\bar{\sigma}}a_{\uparrow}^{\dagger} - d_{\bar{\sigma}}a_{\uparrow}^{\dagger}a_{\uparrow}) \\
&\quad + t_{hp} \sum_{\bar{\sigma}} (a_{\uparrow}a_{\uparrow}d_{\bar{\sigma}}^{\dagger} - a_{\uparrow}d_{\bar{\sigma}}^{\dagger}a_{\uparrow}) \\
&= t_{hp} \sum_{\bar{\sigma}} (-d_{\bar{\sigma}}a_{\uparrow}a_{\uparrow}^{\dagger} - d_{\bar{\sigma}}a_{\uparrow}^{\dagger}a_{\uparrow}) \\
&\quad + t_{hp} \sum_{\bar{\sigma}} (-a_{\uparrow}a_{\uparrow}d_{\bar{\sigma}}^{\dagger} + a_{\uparrow}a_{\uparrow}d_{\bar{\sigma}}^{\dagger}) \\
&= t_{hp} \sum_{\bar{\sigma}} (-d_{\bar{\sigma}}) (a_{\uparrow}a_{\uparrow}^{\dagger} + a_{\uparrow}^{\dagger}a_{\uparrow}) \\
&= t_{hp} \sum_{\bar{\sigma}} (-d_{\bar{\sigma}}). \tag{B.40}
\end{aligned}$$

$$\begin{aligned}
\sum_{\bar{\sigma}} [a_{\uparrow}, \Delta(d_{\bar{\sigma}}a_{\uparrow} + a_{\uparrow}^{\dagger}d_{\bar{\sigma}}^{\dagger})] &= \Delta \sum_{\bar{\sigma}} [a_{\uparrow}, d_{\bar{\sigma}}a_{\uparrow}] + \Delta \sum_{\bar{\sigma}} [a_{\uparrow}, a_{\uparrow}^{\dagger}d_{\bar{\sigma}}^{\dagger}] \\
&= \Delta \sum_{\bar{\sigma}} (a_{\uparrow}d_{\bar{\sigma}}a_{\uparrow} - d_{\bar{\sigma}}a_{\uparrow}a_{\uparrow}) \\
&\quad + \Delta \sum_{\bar{\sigma}} (a_{\uparrow}a_{\uparrow}^{\dagger}d_{\bar{\sigma}}^{\dagger} - a_{\uparrow}^{\dagger}d_{\bar{\sigma}}^{\dagger}a_{\uparrow}) \\
&= \Delta \sum_{\bar{\sigma}} (d_{\bar{\sigma}}a_{\uparrow}a_{\uparrow} - d_{\bar{\sigma}}a_{\uparrow}a_{\uparrow}) \\
&\quad + \Delta \sum_{\bar{\sigma}} (a_{\uparrow}a_{\uparrow}^{\dagger}d_{\bar{\sigma}}^{\dagger} - a_{\uparrow}^{\dagger}d_{\bar{\sigma}}^{\dagger}a_{\uparrow}) \\
&= \Delta \sum_{\bar{\sigma}} (a_{\uparrow}a_{\uparrow}^{\dagger}d_{\bar{\sigma}}^{\dagger} + a_{\uparrow}^{\dagger}a_{\uparrow}d_{\bar{\sigma}}^{\dagger}) \\
&= \Delta \sum_{\bar{\sigma}} (a_{\uparrow}a_{\uparrow}^{\dagger} + a_{\uparrow}^{\dagger}a_{\uparrow}) d_{\bar{\sigma}}^{\dagger} \\
&= \Delta \sum_{\bar{\sigma}} d_{\bar{\sigma}}^{\dagger}. \tag{B.41}
\end{aligned}$$

$$(\omega + i\eta^+) G_{a_{\uparrow}d_{\sigma}}^r(\omega) = \langle\langle \delta_{\mathbf{M}} a_{\uparrow}; d_{\sigma}^{\dagger} \rangle\rangle + \sum_{\bar{\sigma}} \langle\langle t_{hp}(-d_{\bar{\sigma}}); d_{\sigma}^{\dagger} \rangle\rangle + \sum_{\sigma} \langle\langle \Delta d_{\bar{\sigma}}^{\dagger}; d_{\sigma}^{\dagger} \rangle\rangle \tag{B.42}$$

$$(\omega - \delta_{\mathbf{M}} + i\eta^+) G_{a_{\uparrow}d_{\sigma}}^r(\omega) = -t_{hp} \sum_{\bar{\sigma}} G_{d_{\bar{\sigma}}d_{\sigma}}^r(\omega) + \Delta \sum_{\bar{\sigma}} G_{d_{\bar{\sigma}}^{\dagger}d_{\sigma}}^r(\omega) \tag{B.43}$$

$$(\omega + i\eta^+) G_{a_{\uparrow}^{\dagger}d_{\sigma}}^r(\omega) = \langle\langle [a_{\uparrow}^{\dagger}, \mathcal{H}_e]; d_{\sigma}^{\dagger} \rangle\rangle \tag{B.44}$$

$$\begin{aligned}
 [a_{\uparrow}^{\dagger}, \mathcal{H}_e] &= [a_{\uparrow}^{\dagger}, \mathcal{H}_{\text{lead}}] + [a_{\uparrow}^{\dagger}, \mathcal{H}_{\text{dot}}] + [a_{\uparrow}^{\dagger}, \mathcal{H}_{\text{dot-lead}}] + [a_{\uparrow}^{\dagger}, \mathcal{H}_M] \\
 &= [a_{\uparrow}^{\dagger}, \mathcal{H}_M]
 \end{aligned} \tag{B.45}$$

$$\begin{aligned}
 [a_{\uparrow}^{\dagger}, \mathcal{H}_M] &= \left[a_{\uparrow}^{\dagger}, \delta_M \left(a_{\uparrow}^{\dagger} a_{\uparrow} - \frac{1}{2} \right) \right] + \left[a_{\uparrow}^{\dagger}, t_{hp} \sum_{\sigma} (d_{\sigma} a_{\uparrow}^{\dagger} + a_{\uparrow}^{\dagger} d_{\sigma}^{\dagger}) \right] \\
 &+ \left[a_{\uparrow}^{\dagger}, \Delta \sum_{\sigma} (d_{\sigma} a_{\uparrow} + a_{\uparrow}^{\dagger} d_{\sigma}^{\dagger}) \right]
 \end{aligned} \tag{B.46}$$

$$\begin{aligned}
 \left[a_{\uparrow}^{\dagger}, \delta_M \left(a_{\uparrow}^{\dagger} a_{\uparrow} - \frac{1}{2} \right) \right] &= \delta_M (a_{\uparrow}^{\dagger} a_{\uparrow}^{\dagger} a_{\uparrow} - a_{\uparrow}^{\dagger} a_{\uparrow} a_{\uparrow}^{\dagger}) \\
 &= \delta_M (a_{\uparrow}^{\dagger} a_{\uparrow}^{\dagger} a_{\uparrow} - a_{\uparrow}^{\dagger} (1 - a_{\uparrow}^{\dagger} a_{\uparrow})) \\
 &= \delta_M (a_{\uparrow}^{\dagger} a_{\uparrow}^{\dagger} a_{\uparrow} - a_{\uparrow}^{\dagger} + a_{\uparrow}^{\dagger} a_{\uparrow}^{\dagger} a_{\uparrow}) \\
 &= -\delta_M a_{\uparrow}^{\dagger}.
 \end{aligned} \tag{B.47}$$

$$\begin{aligned}
 [a_{\uparrow}^{\dagger}, t_{hp} (d_{\bar{\sigma}} a_{\uparrow}^{\dagger} + a_{\uparrow}^{\dagger} d_{\bar{\sigma}}^{\dagger})] &= t_{hp} [a_{\uparrow}^{\dagger}, d_{\bar{\sigma}} a_{\uparrow}^{\dagger}] + t_{hp} [a_{\uparrow}^{\dagger}, a_{\uparrow}^{\dagger} d_{\bar{\sigma}}^{\dagger}] \\
 &= t_{hp} (a_{\uparrow}^{\dagger} d_{\bar{\sigma}} a_{\uparrow}^{\dagger} - d_{\bar{\sigma}} a_{\uparrow}^{\dagger} a_{\uparrow}^{\dagger}) \\
 &+ t_{hp} (a_{\uparrow}^{\dagger} a_{\uparrow}^{\dagger} d_{\bar{\sigma}}^{\dagger} - a_{\uparrow}^{\dagger} d_{\bar{\sigma}}^{\dagger} a_{\uparrow}^{\dagger}) \\
 &= t_{hp} (d_{\bar{\sigma}} a_{\uparrow}^{\dagger} a_{\uparrow}^{\dagger} - d_{\bar{\sigma}} a_{\uparrow}^{\dagger} a_{\uparrow}^{\dagger}) \\
 &+ t_{hp} (a_{\uparrow}^{\dagger} a_{\uparrow}^{\dagger} d_{\bar{\sigma}}^{\dagger} + a_{\uparrow}^{\dagger} a_{\uparrow}^{\dagger} d_{\bar{\sigma}}^{\dagger}) \\
 &= t_{hp} (a_{\uparrow}^{\dagger} a_{\uparrow} + a_{\uparrow} a_{\uparrow}^{\dagger}) d_{\bar{\sigma}}^{\dagger} \\
 &= t_{hp} d_{\bar{\sigma}}^{\dagger}.
 \end{aligned} \tag{B.48}$$

$$\begin{aligned}
 [a_{\uparrow}^{\dagger}, \Delta (d_{\bar{\sigma}} a_{\uparrow} + a_{\uparrow}^{\dagger} d_{\bar{\sigma}}^{\dagger})] &= \Delta [a_{\uparrow}^{\dagger}, d_{\bar{\sigma}} a_{\uparrow}] + \Delta [a_{\uparrow}^{\dagger}, a_{\uparrow}^{\dagger} d_{\bar{\sigma}}^{\dagger}] \\
 &= \Delta (a_{\uparrow}^{\dagger} d_{\bar{\sigma}} a_{\uparrow} - d_{\bar{\sigma}} a_{\uparrow} a_{\uparrow}^{\dagger}) \\
 &+ \Delta (a_{\uparrow}^{\dagger} a_{\uparrow}^{\dagger} d_{\bar{\sigma}}^{\dagger} - a_{\uparrow}^{\dagger} d_{\bar{\sigma}}^{\dagger} a_{\uparrow}^{\dagger}) \\
 &= \Delta (-d_{\bar{\sigma}} a_{\uparrow}^{\dagger} a_{\uparrow} - d_{\bar{\sigma}} a_{\uparrow} a_{\uparrow}^{\dagger}) \\
 &+ \Delta (a_{\uparrow}^{\dagger} a_{\uparrow}^{\dagger} d_{\bar{\sigma}}^{\dagger} - a_{\uparrow}^{\dagger} a_{\uparrow}^{\dagger} d_{\bar{\sigma}}^{\dagger}) \\
 &= \Delta (-d_{\bar{\sigma}}) (a_{\uparrow}^{\dagger} a_{\uparrow} + a_{\uparrow} a_{\uparrow}^{\dagger}) \\
 &= -\Delta d_{\bar{\sigma}}.
 \end{aligned} \tag{B.49}$$

$$(\omega + \eta\eta^+)G_{a_{\uparrow}^{\dagger}d_{\sigma}}^r(\omega) = -\delta_M \langle \langle a_{\uparrow}^{\dagger}; d_{\sigma}^{\dagger} \rangle \rangle + t_{hp} \sum_{\bar{\sigma}} \langle \langle d_{\bar{\sigma}}^{\dagger}; d_{\sigma}^{\dagger} \rangle \rangle - \Delta \sum_{\bar{\sigma}} \langle \langle d_{\bar{\sigma}}; d_{\sigma}^{\dagger} \rangle \rangle \quad (\text{B.50})$$

$$(\omega + \delta_M + \eta\eta^+)G_{a_{\uparrow}^{\dagger}d_{\sigma}}^r(\omega) = t_{hp} \sum_{\bar{\sigma}} \langle \langle d_{\bar{\sigma}}^{\dagger}; d_{\sigma}^{\dagger} \rangle \rangle - \Delta \sum_{\bar{\sigma}} \langle \langle d_{\bar{\sigma}}; d_{\sigma}^{\dagger} \rangle \rangle \quad (\text{B.51})$$

$$(\omega + \delta_M + \eta\eta^+)G_{a_{\uparrow}^{\dagger}d_{\sigma}}^r(\omega) = \sum_{\bar{\sigma}} t_{hp} G_{d_{\bar{\sigma}}^{\dagger}d_{\sigma}}^r(\omega) - \sum_{\bar{\sigma}} \Delta G_{d_{\bar{\sigma}}d_{\sigma}}^r(\omega) \quad (\text{B.52})$$

From Eqs.(B.43) and (B.52):

$$G_{a_{\uparrow}d_{\sigma}}^r(\omega) = -\frac{t_{hp} \sum_{\bar{\sigma}} G_{d_{\bar{\sigma}}d_{\sigma}}^r(\omega)}{(\omega - \delta_M + \eta\eta^+)} + \frac{\Delta \sum_{\bar{\sigma}} G_{d_{\bar{\sigma}}^{\dagger}d_{\sigma}}^r(\omega)}{(\omega - \delta_M + \eta\eta^+)} \quad (\text{B.53})$$

$$G_{a_{\uparrow}^{\dagger}d_{\sigma}}^r(\omega) = \frac{t_{hp} \sum_{\bar{\sigma}} G_{d_{\bar{\sigma}}^{\dagger}d_{\sigma}}^r(\omega)}{(\omega + \delta_M + \eta\eta^+)} - \frac{\Delta \sum_{\bar{\sigma}} G_{d_{\bar{\sigma}}d_{\sigma}}^r(\omega)}{(\omega + \delta_M + \eta\eta^+)} \quad (\text{B.54})$$

Let us substitute them in Eq.(B.35):

$$\begin{aligned} (\omega - \varepsilon_{d\sigma} - \Sigma_{\sigma} + \eta\eta^+)G_{d_{\sigma}d_{\sigma}}^r(\omega) &= 1 + UG_{d_{\sigma}n_{d\bar{\sigma}},d_{\sigma}}^r(\omega) \\ &- \sum_{\bar{\sigma}} \delta_{\sigma\bar{\sigma}} t_{hp} \left[-\frac{t_{hp} \sum_{\bar{\sigma}} G_{d_{\bar{\sigma}}d_{\sigma}}^r(\omega)}{(\omega - \delta_M + \eta\eta^+)} + \frac{\Delta \sum_{\bar{\sigma}} G_{d_{\bar{\sigma}}^{\dagger}d_{\sigma}}^r(\omega)}{(\omega - \delta_M + \eta\eta^+)} \right] \\ &- \sum_{\bar{\sigma}} \delta_{\sigma\bar{\sigma}} \Delta \left[\frac{t_{hp} \sum_{\bar{\sigma}} G_{d_{\bar{\sigma}}^{\dagger}d_{\sigma}}^r(\omega)}{(\omega + \delta_M + \eta\eta^+)} - \frac{\Delta \sum_{\bar{\sigma}} G_{d_{\bar{\sigma}}d_{\sigma}}^r(\omega)}{(\omega + \delta_M + \eta\eta^+)} \right] \end{aligned} \quad (\text{B.55})$$

$$\begin{aligned} (\omega - \varepsilon_{d\sigma} - \Sigma_{\sigma} + \eta\eta^+)G_{d_{\sigma}d_{\sigma}}^r(\omega) &= 1 + UG_{d_{\sigma}n_{d\bar{\sigma}},d_{\sigma}}^r(\omega) \\ &+ \sum_{\bar{\sigma}\bar{\sigma}} \delta_{\sigma\bar{\sigma}} \frac{(t_{hp})^2 G_{d_{\bar{\sigma}}d_{\sigma}}^r(\omega)}{(\omega - \delta_M + \eta\eta^+)} - \sum_{\bar{\sigma}\bar{\sigma}} \delta_{\sigma\bar{\sigma}} \frac{t_{hp} \Delta G_{d_{\bar{\sigma}}^{\dagger}d_{\sigma}}^r(\omega)}{(\omega - \delta_M + \eta\eta^+)} \\ &- \sum_{\bar{\sigma}\bar{\sigma}} \delta_{\sigma\bar{\sigma}} \frac{t_{hp} \Delta G_{d_{\bar{\sigma}}^{\dagger}d_{\sigma}}^r(\omega)}{(\omega + \delta_M + \eta\eta^+)} + \sum_{\bar{\sigma}\bar{\sigma}} \delta_{\sigma\bar{\sigma}} \frac{(\Delta)^2 G_{d_{\bar{\sigma}}d_{\sigma}}^r(\omega)}{(\omega + \delta_M + \eta\eta^+)} \end{aligned} \quad (\text{B.56})$$

$$\begin{aligned} (\omega - \varepsilon_{d\sigma} - \Sigma_{\sigma} + \eta\eta^+)G_{d_{\sigma}d_{\sigma}}^r(\omega) &= 1 + UG_{d_{\sigma}n_{d\bar{\sigma}},d_{\sigma}}^r(\omega) \\ &- t_{hp} \Delta \left[\frac{1}{(\omega + \delta_M + \eta\eta^+)} + \frac{1}{(\omega - \delta_M + \eta\eta^+)} \right] G_{d_{\bar{\sigma}}^{\dagger}d_{\sigma}}^r(\omega) \\ &+ \left[\frac{(t_{hp})^2}{(\omega - \delta_M + \eta\eta^+)} + \frac{(\Delta)^2}{(\omega + \delta_M + \eta\eta^+)} \right] G_{d_{\sigma}d_{\sigma}}^r(\omega) \end{aligned} \quad (\text{B.57})$$

$$K = \left[\frac{1}{(\omega + \delta_M + \eta\eta^+)} + \frac{1}{(\omega - \delta_M + \eta\eta^+)} \right] \quad (\text{B.58})$$

$$\begin{aligned}
 (\omega - \varepsilon_{d\sigma} - \Sigma_\sigma + i\eta^+)G_{d_\sigma d_\sigma}^r(\omega) &= 1 + UG_{d_\sigma n_{d\bar{\sigma}}, d_\sigma}^r(\omega) - t_{hp}\Delta KG_{d_\sigma^\dagger d_\sigma}^r(\omega) \\
 &+ \left[\frac{(t_{hp})^2}{(\omega - \delta_M + i\eta^+)} + \frac{(\Delta)^2}{(\omega + \delta_M + i\eta^+)} \right] G_{d_\sigma d_\sigma}^r(\omega).
 \end{aligned} \tag{B.59}$$

According to the equation above, both spins couple with the Kitaev wire. To find $G_{d_\sigma d_\sigma}^r(\omega)$, we also must obtain $G_{d_\sigma^\dagger d_\sigma}^r(\omega)$, which is performed below. According to Eq.(??):

$$(\omega + i\eta^+)G_{d_\sigma^\dagger d_\sigma}^r(\omega) = \{d_\sigma^\dagger, d_\sigma^\dagger\} + \langle\langle [d_\sigma^\dagger, \mathcal{H}_e]; d_\sigma^\dagger \rangle\rangle \tag{B.60}$$

$$(\omega + i\eta^+)G_{d_\sigma^\dagger d_\sigma}^r(\omega) = \langle\langle [d_\sigma^\dagger, \mathcal{H}_e]; d_\sigma^\dagger \rangle\rangle \tag{B.61}$$

$$\begin{aligned}
 [d_\sigma^\dagger, \mathcal{H}_e] &= [d_\sigma^\dagger, \mathcal{H}_{\text{lead}}] + [d_\sigma^\dagger, \mathcal{H}_{\text{dot}}] + [d_\sigma^\dagger, \mathcal{H}_{\text{dot-lead}}] + [d_\sigma^\dagger, \mathcal{H}_M] \\
 &= [d_\sigma^\dagger, \mathcal{H}_{\text{dot}}] + [d_\sigma^\dagger, \mathcal{H}_{\text{dot-lead}}] + [d_\sigma^\dagger, \mathcal{H}_M]
 \end{aligned} \tag{B.62}$$

$$[d_\sigma^\dagger, \mathcal{H}_{\text{dot}}] = [d_\sigma^\dagger, \sum_\sigma \varepsilon_{d\sigma} d_\sigma^\dagger d_\sigma] + [d_\sigma^\dagger, U n_{d\uparrow} n_{d\downarrow}] \tag{B.63}$$

$$\begin{aligned}
 [d_\sigma^\dagger, \sum_{\bar{\sigma}} \varepsilon_{d\bar{\sigma}} d_{\bar{\sigma}}^\dagger d_{\bar{\sigma}}] &= \sum_{\bar{\sigma}} \varepsilon_{d\bar{\sigma}} (d_\sigma^\dagger d_{\bar{\sigma}}^\dagger d_{\bar{\sigma}} - d_{\bar{\sigma}}^\dagger d_{\bar{\sigma}} d_\sigma^\dagger) \\
 &= \sum_{\bar{\sigma}} \varepsilon_{d\bar{\sigma}} (d_\sigma^\dagger d_{\bar{\sigma}}^\dagger d_{\bar{\sigma}} - d_{\bar{\sigma}}^\dagger (\delta_{\bar{\sigma}\sigma} - d_\sigma^\dagger d_{\bar{\sigma}})) \\
 &= \sum_{\bar{\sigma}} \varepsilon_{d\bar{\sigma}} (d_\sigma^\dagger d_{\bar{\sigma}}^\dagger d_{\bar{\sigma}} - \delta_{\bar{\sigma}\sigma} d_{\bar{\sigma}}^\dagger + d_{\bar{\sigma}}^\dagger d_\sigma^\dagger d_{\bar{\sigma}}) \\
 &= \sum_{\bar{\sigma}} \varepsilon_{d\bar{\sigma}} (d_\sigma^\dagger d_{\bar{\sigma}}^\dagger d_{\bar{\sigma}} - \delta_{\bar{\sigma}\sigma} d_{\bar{\sigma}}^\dagger - d_\sigma^\dagger d_{\bar{\sigma}}^\dagger d_{\bar{\sigma}}) \\
 &= \sum_{\bar{\sigma}} \varepsilon_{d\bar{\sigma}} (-\delta_{\bar{\sigma}\sigma} d_{\bar{\sigma}}^\dagger) \\
 &= -\varepsilon_{d\sigma} d_\sigma^\dagger.
 \end{aligned} \tag{B.64}$$

$$\begin{aligned}
[d_\sigma^\dagger, U n_{d\uparrow} n_{d\downarrow}] &= U \left(d_\uparrow^\dagger n_{d\uparrow} n_{d\downarrow} - n_{d\uparrow} n_{d\downarrow} d_\uparrow^\dagger \right) \\
&= U \left(d_\sigma^\dagger d_\uparrow^\dagger d_\uparrow d_\downarrow^\dagger d_\downarrow - d_\uparrow^\dagger d_\uparrow d_\downarrow^\dagger d_\downarrow d_\sigma^\dagger \right) \\
&= U \left(d_\sigma^\dagger d_\uparrow^\dagger d_\uparrow d_\downarrow^\dagger d_\downarrow - d_\uparrow^\dagger d_\uparrow d_\downarrow^\dagger \left(\delta_{\sigma\downarrow} - d_\sigma^\dagger d_\downarrow \right) \right) \\
&= U \left(d_\sigma^\dagger d_\uparrow^\dagger d_\uparrow d_\downarrow^\dagger d_\downarrow - \delta_{\sigma\downarrow} d_\uparrow^\dagger d_\uparrow d_\downarrow^\dagger + d_\uparrow^\dagger d_\uparrow d_\downarrow^\dagger d_\sigma^\dagger d_\downarrow \right) \\
&= U \left(d_\sigma^\dagger d_\uparrow^\dagger d_\uparrow d_\downarrow^\dagger d_\downarrow - \delta_{\sigma\downarrow} d_\downarrow^\dagger d_\uparrow^\dagger d_\uparrow - d_\uparrow^\dagger d_\uparrow d_\sigma^\dagger d_\downarrow^\dagger d_\downarrow \right) \\
&= U \left(d_\sigma^\dagger d_\uparrow^\dagger d_\uparrow d_\downarrow^\dagger d_\downarrow - \delta_{\sigma\downarrow} d_\downarrow^\dagger d_\uparrow^\dagger d_\uparrow - d_\uparrow^\dagger \left(\delta_{\sigma\uparrow} - d_\sigma^\dagger d_\uparrow \right) d_\downarrow^\dagger d_\downarrow \right) \\
&= U \left(d_\sigma^\dagger d_\uparrow^\dagger d_\uparrow d_\downarrow^\dagger d_\downarrow - \delta_{\sigma\downarrow} d_\downarrow^\dagger d_\uparrow^\dagger d_\uparrow - \delta_{\sigma\uparrow} d_\uparrow^\dagger d_\downarrow^\dagger d_\downarrow - d_\sigma^\dagger d_\uparrow^\dagger d_\uparrow d_\downarrow^\dagger d_\downarrow \right) \\
&= U \left(-\delta_{\sigma\downarrow} d_\downarrow^\dagger d_\uparrow^\dagger d_\uparrow - \delta_{\sigma\uparrow} d_\uparrow^\dagger d_\downarrow^\dagger d_\downarrow \right) \\
&= -U d_\sigma^\dagger n_{d\bar{\sigma}}.
\end{aligned} \tag{B.65}$$

$$\begin{aligned}
[d_\uparrow^\dagger, \mathcal{H}_{\text{dot-lead}}] &= [d_{\bar{\sigma}}^\dagger, \sqrt{2V} \sum_{\mathbf{k}\sigma} (e_{\mathbf{k}\sigma}^\dagger d_\sigma + d_\sigma^\dagger e_{\mathbf{k}\sigma})] \\
&= \sqrt{2V} \sum_{\mathbf{k}\sigma} [d_{\bar{\sigma}}^\dagger, e_{\mathbf{k}\sigma}^\dagger d_\sigma] + \sqrt{2V} \sum_{\mathbf{k}\sigma} [d_{\bar{\sigma}}^\dagger, d_\sigma^\dagger e_{\mathbf{k}\sigma}] \\
&= \sqrt{2V} \sum_{\mathbf{k}\sigma} \left(d_{\bar{\sigma}}^\dagger e_{\mathbf{k}\sigma}^\dagger d_\sigma - e_{\mathbf{k}\sigma}^\dagger d_\sigma d_{\bar{\sigma}}^\dagger \right) \\
&+ \sqrt{2V} \sum_{\mathbf{k}\sigma} \left(d_{\bar{\sigma}}^\dagger d_\sigma^\dagger e_{\mathbf{k}\sigma} - d_\sigma^\dagger e_{\mathbf{k}\sigma} d_{\bar{\sigma}}^\dagger \right) \\
&= \sqrt{2V} \sum_{\mathbf{k}\sigma} \left(-e_{\mathbf{k}\sigma}^\dagger d_{\bar{\sigma}}^\dagger d_\sigma - e_{\mathbf{k}\sigma}^\dagger d_\sigma d_{\bar{\sigma}}^\dagger \right) \\
&+ \sqrt{2V} \sum_{\mathbf{k}\sigma} \left(d_{\bar{\sigma}}^\dagger d_\sigma^\dagger e_{\mathbf{k}\sigma} - d_{\bar{\sigma}}^\dagger d_\sigma^\dagger e_{\mathbf{k}\sigma} \right) \\
&= \sqrt{2V} \sum_{\mathbf{k}\sigma} \left(-e_{\mathbf{k}\sigma}^\dagger \right) \left(d_{\bar{\sigma}}^\dagger d_\sigma + d_\sigma d_{\bar{\sigma}}^\dagger \right) \\
&= \sqrt{2V} \sum_{\mathbf{k}\bar{\sigma}} \delta_{\sigma\bar{\sigma}} \left(-e_{\mathbf{k}\bar{\sigma}}^\dagger \right) \\
&= \sqrt{2V} \sum_{\mathbf{k}} \left(-e_{\mathbf{k}\sigma}^\dagger \right).
\end{aligned} \tag{B.66}$$

$$\begin{aligned}
(\omega + \eta^+) G_{d_\sigma^\dagger d_\sigma}^r(\omega) &= \langle\langle -\varepsilon_{d\sigma} d_\sigma^\dagger; d_\sigma^\dagger \rangle\rangle + \langle\langle \sqrt{2V} \sum_{\mathbf{k}} (-e_{\mathbf{k}\sigma}^\dagger); d_\sigma^\dagger \rangle\rangle + \langle\langle -U d_\sigma^\dagger n_{d\bar{\sigma}}; d_\sigma^\dagger \rangle\rangle \\
&+ \langle\langle [d_\sigma^\dagger, \mathcal{H}_M]; d_\sigma^\dagger \rangle\rangle
\end{aligned} \tag{B.67}$$

$$\begin{aligned}
 (\omega + \varepsilon_{d\sigma} + i\eta^+) G_{d\sigma^\dagger d\sigma}^r(\omega) &= -\sqrt{2}V \sum_{\mathbf{k}} G_{e_{\mathbf{k}\sigma}^\dagger d\sigma}^r(\omega) - U G_{d\sigma^\dagger n_{d\bar{\sigma}} d\sigma}^r(\omega) \\
 &+ \langle\langle [d_{\sigma}^\dagger, \mathcal{H}_M]; d_{\sigma}^\dagger \rangle\rangle.
 \end{aligned} \tag{B.68}$$

$$\begin{aligned}
 [d_{\sigma}^\dagger, \mathcal{H}_M] &= \left[d_{\sigma}^\dagger, \delta_M \left(a_{\uparrow}^\dagger a_{\uparrow} - \frac{1}{2} \right) \right] + \left[d_{\sigma}^\dagger, t_{hp} \sum_{\bar{\sigma}} (d_{\bar{\sigma}} a_{\uparrow}^\dagger + a_{\uparrow} d_{\bar{\sigma}}^\dagger) \right] \\
 &+ \left[d_{\sigma}^\dagger, \Delta \sum_{\bar{\sigma}} (d_{\bar{\sigma}} a_{\uparrow} + a_{\uparrow}^\dagger d_{\bar{\sigma}}^\dagger) \right]
 \end{aligned} \tag{B.69}$$

$$[d_{\sigma}^\dagger, \mathcal{H}_M] = \left[d_{\sigma}^\dagger, t_{hp} \sum_{\bar{\sigma}} (d_{\bar{\sigma}} a_{\uparrow}^\dagger + a_{\uparrow} d_{\bar{\sigma}}^\dagger) \right] + \left[d_{\sigma}^\dagger, \Delta \sum_{\bar{\sigma}} (d_{\bar{\sigma}} a_{\uparrow} + a_{\uparrow}^\dagger d_{\bar{\sigma}}^\dagger) \right] \tag{B.70}$$

$$\begin{aligned}
 \left[d_{\sigma}^\dagger, t_{hp} \sum_{\bar{\sigma}} (d_{\bar{\sigma}} a_{\uparrow}^\dagger + a_{\uparrow} d_{\bar{\sigma}}^\dagger) \right] &= t_{hp} \sum_{\bar{\sigma}} [d_{\sigma}^\dagger, d_{\bar{\sigma}} a_{\uparrow}^\dagger] + t_{hp} \sum_{\bar{\sigma}} [d_{\sigma}^\dagger, a_{\uparrow} d_{\bar{\sigma}}^\dagger] \\
 &= t_{hp} \sum_{\bar{\sigma}} (d_{\sigma}^\dagger d_{\bar{\sigma}} a_{\uparrow}^\dagger - d_{\bar{\sigma}} a_{\uparrow}^\dagger d_{\sigma}^\dagger) \\
 &+ t_{hp} \sum_{\bar{\sigma}} (d_{\sigma}^\dagger a_{\uparrow} d_{\bar{\sigma}}^\dagger - a_{\uparrow} d_{\bar{\sigma}}^\dagger d_{\sigma}^\dagger) \\
 &= t_{hp} \sum_{\bar{\sigma}} (d_{\sigma}^\dagger d_{\bar{\sigma}} + d_{\bar{\sigma}} d_{\sigma}^\dagger) a_{\uparrow}^\dagger \\
 &+ t_{hp} \sum_{\bar{\sigma}} (a_{\uparrow} d_{\bar{\sigma}}^\dagger d_{\sigma}^\dagger - a_{\uparrow} d_{\bar{\sigma}}^\dagger d_{\sigma}^\dagger) \\
 &= t_{hp} \sum_{\bar{\sigma}} \delta_{\sigma\bar{\sigma}} a_{\uparrow}^\dagger
 \end{aligned} \tag{B.71}$$

$$\begin{aligned}
 \left[d_{\sigma}^\dagger, \Delta \sum_{\bar{\sigma}} (d_{\bar{\sigma}} a_{\uparrow} + a_{\uparrow}^\dagger d_{\bar{\sigma}}^\dagger) \right] &= \Delta \sum_{\bar{\sigma}} [d_{\sigma}^\dagger, d_{\bar{\sigma}} a_{\uparrow}] + \Delta \sum_{\bar{\sigma}} [d_{\sigma}^\dagger, a_{\uparrow}^\dagger d_{\bar{\sigma}}^\dagger] \\
 &= \Delta \sum_{\bar{\sigma}} (d_{\sigma}^\dagger d_{\bar{\sigma}} a_{\uparrow} - d_{\bar{\sigma}} a_{\uparrow} d_{\sigma}^\dagger) \\
 &+ \Delta \sum_{\bar{\sigma}} (d_{\sigma}^\dagger a_{\uparrow}^\dagger d_{\bar{\sigma}}^\dagger - a_{\uparrow}^\dagger d_{\bar{\sigma}}^\dagger d_{\sigma}^\dagger) \\
 &= \Delta \sum_{\bar{\sigma}} (d_{\sigma}^\dagger d_{\bar{\sigma}} + d_{\bar{\sigma}} d_{\sigma}^\dagger) a_{\uparrow} \\
 &+ \Delta \sum_{\bar{\sigma}} (a_{\uparrow}^\dagger d_{\bar{\sigma}}^\dagger d_{\sigma}^\dagger - a_{\uparrow}^\dagger d_{\bar{\sigma}}^\dagger d_{\sigma}^\dagger) \\
 &= \Delta \sum_{\bar{\sigma}} \delta_{\sigma\bar{\sigma}} a_{\uparrow}
 \end{aligned} \tag{B.72}$$

$$\begin{aligned}
 (\omega + \varepsilon_{d\sigma} + \eta^+) G_{d_{\bar{\sigma}}^{\dagger} d_{\sigma}}^r(\omega) &= -\sqrt{2}V \sum_{\mathbf{k}} G_{e_{\mathbf{k}\sigma}^{\dagger} d_{\sigma}}^r(\omega) - U G_{d_{\bar{\sigma}}^{\dagger} n_{d\bar{\sigma}} d_{\sigma}}^r(\omega) \\
 &+ \langle\langle t_{hp} a_{\sigma}^{\dagger}; d_{\sigma}^{\dagger} \rangle\rangle + \langle\langle \Delta a_{\sigma}; d_{\sigma}^{\dagger} \rangle\rangle
 \end{aligned} \tag{B.73}$$

$$\begin{aligned}
 (\omega + \varepsilon_{d\sigma} + \eta^+) G_{d_{\bar{\sigma}}^{\dagger} d_{\sigma}}^r(\omega) &= -\sqrt{2}V \sum_{\mathbf{k}} G_{e_{\mathbf{k}\sigma}^{\dagger} d_{\sigma}}^r(\omega) - U G_{d_{\bar{\sigma}}^{\dagger} n_{d\bar{\sigma}} d_{\sigma}}^r(\omega) \\
 &+ t_{hp} \sum_{\bar{\sigma}} \delta_{\bar{\sigma}\bar{\sigma}} G_{a_{\sigma}^{\dagger} d_{\sigma}}^r(\omega) + \Delta \sum_{\bar{\sigma}} \delta_{\bar{\sigma}\bar{\sigma}} G_{a_{\sigma} d_{\sigma}}^r(\omega)
 \end{aligned} \tag{B.74}$$

$$(\omega + \eta^+) G_{e_{\mathbf{k}\sigma}^{\dagger} d_{\sigma}}^r(\omega) = \{e_{\mathbf{k}\sigma}^{\dagger}, d_{\sigma}^{\dagger}\} + \langle\langle [e_{\mathbf{k}\sigma}^{\dagger}, \mathcal{H}_e]; d_{\sigma}^{\dagger} \rangle\rangle = \langle\langle [e_{\mathbf{k}\sigma}^{\dagger}, \mathcal{H}_e]; d_{\sigma}^{\dagger} \rangle\rangle \tag{B.75}$$

$$\begin{aligned}
 [e_{\mathbf{k}\sigma}^{\dagger}, \mathcal{H}_e] &= [e_{\mathbf{k}\sigma}^{\dagger}, \mathcal{H}_{\text{lead}}] + [e_{\mathbf{k}\sigma}^{\dagger}, \mathcal{H}_{\text{dot}}] + [e_{\mathbf{k}\sigma}^{\dagger}, \mathcal{H}_{\text{dot-lead}}] + [e_{\mathbf{k}\sigma}^{\dagger}, \mathcal{H}_M] \\
 &= [e_{\mathbf{k}\sigma}^{\dagger}, \mathcal{H}_{\text{lead}}] + [e_{\mathbf{k}\sigma}^{\dagger}, \mathcal{H}_{\text{dot-lead}}]
 \end{aligned} \tag{B.76}$$

$$\begin{aligned}
 [e_{\mathbf{k}\sigma}^{\dagger}, \mathcal{H}_{\text{lead}}] &= [e_{\mathbf{k}\sigma}^{\dagger}, \sum_{\mathbf{p}\bar{\sigma}} \varepsilon_{\mathbf{p}\bar{\sigma}} e_{\mathbf{p}\bar{\sigma}}^{\dagger} e_{\mathbf{p}\bar{\sigma}} + V_{SD} \sum_{\mathbf{p}, \mathbf{q}\bar{\sigma}} e_{\mathbf{p}\bar{\sigma}}^{\dagger} e_{\mathbf{q}\bar{\sigma}}] \\
 &= [e_{\mathbf{k}\sigma}^{\dagger}, \sum_{\mathbf{p}\bar{\sigma}} \varepsilon_{\mathbf{p}\bar{\sigma}} e_{\mathbf{p}\bar{\sigma}}^{\dagger} e_{\mathbf{p}\bar{\sigma}}] + [e_{\mathbf{k}\sigma}^{\dagger}, V_{SD} \sum_{\mathbf{p}, \mathbf{q}\bar{\sigma}} e_{\mathbf{p}\bar{\sigma}}^{\dagger} e_{\mathbf{q}\bar{\sigma}}]
 \end{aligned} \tag{B.77}$$

$$\begin{aligned}
 [e_{\mathbf{k}\sigma}^{\dagger}, \sum_{\mathbf{p}\bar{\sigma}} \varepsilon_{\mathbf{p}\bar{\sigma}} e_{\mathbf{p}\bar{\sigma}}^{\dagger} e_{\mathbf{p}\bar{\sigma}}] &= \sum_{\mathbf{p}\bar{\sigma}} \varepsilon_{\mathbf{p}\bar{\sigma}} \left(e_{\mathbf{k}\sigma}^{\dagger} e_{\mathbf{p}\bar{\sigma}}^{\dagger} e_{\mathbf{p}\bar{\sigma}} - e_{\mathbf{p}\bar{\sigma}}^{\dagger} e_{\mathbf{p}\bar{\sigma}} e_{\mathbf{k}\sigma}^{\dagger} \right) \\
 &= \sum_{\mathbf{p}\bar{\sigma}} \varepsilon_{\mathbf{p}\bar{\sigma}} \left(-e_{\mathbf{p}\bar{\sigma}}^{\dagger} e_{\mathbf{k}\sigma}^{\dagger} e_{\mathbf{p}\bar{\sigma}} - e_{\mathbf{p}\bar{\sigma}}^{\dagger} e_{\mathbf{p}\bar{\sigma}} e_{\mathbf{k}\sigma}^{\dagger} \right) \\
 &= \sum_{\mathbf{p}\bar{\sigma}} \varepsilon_{\mathbf{p}\bar{\sigma}} \left(-e_{\mathbf{p}\bar{\sigma}}^{\dagger} \left(\delta_{\mathbf{k}\mathbf{p}} \delta_{\sigma\bar{\sigma}} - e_{\mathbf{p}\bar{\sigma}} e_{\mathbf{k}\sigma}^{\dagger} \right) - e_{\mathbf{p}\bar{\sigma}}^{\dagger} e_{\mathbf{p}\bar{\sigma}} e_{\mathbf{k}\sigma}^{\dagger} \right) \\
 &= \sum_{\mathbf{p}\bar{\sigma}} \varepsilon_{\mathbf{p}\bar{\sigma}} \left(-\delta_{\mathbf{k}\mathbf{p}} \delta_{\sigma\bar{\sigma}} e_{\mathbf{p}\bar{\sigma}}^{\dagger} + e_{\mathbf{p}\bar{\sigma}}^{\dagger} e_{\mathbf{p}\bar{\sigma}} e_{\mathbf{k}\sigma}^{\dagger} - e_{\mathbf{p}\bar{\sigma}}^{\dagger} e_{\mathbf{p}\bar{\sigma}} e_{\mathbf{k}\sigma}^{\dagger} \right) \\
 &= \sum_{\mathbf{p}\bar{\sigma}} \varepsilon_{\mathbf{p}\bar{\sigma}} \left(-\delta_{\mathbf{k}\mathbf{p}} \delta_{\sigma\bar{\sigma}} e_{\mathbf{p}\bar{\sigma}}^{\dagger} \right) \\
 &= \varepsilon_{\mathbf{k}\sigma} \left(-e_{\mathbf{k}\sigma}^{\dagger} \right).
 \end{aligned} \tag{B.78}$$

$$\begin{aligned}
[e_{\mathbf{k}\sigma}^\dagger, V_{SD} \sum_{\mathbf{p}, \mathbf{q}\bar{\sigma}} e_{\mathbf{p}\bar{\sigma}}^\dagger e_{\mathbf{q}\bar{\sigma}}] &= V_{SD} \sum_{\mathbf{p}, \mathbf{q}\bar{\sigma}} \left(e_{\mathbf{k}\sigma}^\dagger e_{\mathbf{p}\bar{\sigma}}^\dagger e_{\mathbf{q}\bar{\sigma}} - e_{\mathbf{p}\bar{\sigma}}^\dagger e_{\mathbf{q}\bar{\sigma}} e_{\mathbf{k}\sigma}^\dagger \right) \\
&= V_{SD} \sum_{\mathbf{p}, \mathbf{q}\bar{\sigma}} \left(-e_{\mathbf{p}\bar{\sigma}}^\dagger e_{\mathbf{k}\sigma}^\dagger e_{\mathbf{q}\bar{\sigma}} - e_{\mathbf{p}\bar{\sigma}}^\dagger e_{\mathbf{q}\bar{\sigma}} e_{\mathbf{k}\sigma}^\dagger \right) \\
&= V_{SD} \sum_{\mathbf{p}, \mathbf{q}\bar{\sigma}} \left(-e_{\mathbf{p}\bar{\sigma}}^\dagger \left(\delta_{\mathbf{k}\mathbf{q}} \delta_{\sigma\bar{\sigma}} - e_{\mathbf{q}\bar{\sigma}} e_{\mathbf{k}\sigma}^\dagger \right) - e_{\mathbf{p}\bar{\sigma}}^\dagger e_{\mathbf{q}\bar{\sigma}} e_{\mathbf{k}\sigma}^\dagger \right) \\
&= V_{SD} \sum_{\mathbf{p}, \mathbf{q}\bar{\sigma}} \left(-\delta_{\mathbf{k}\mathbf{q}} \delta_{\sigma\bar{\sigma}} e_{\mathbf{p}\bar{\sigma}}^\dagger + e_{\mathbf{p}\bar{\sigma}}^\dagger e_{\mathbf{q}\bar{\sigma}} e_{\mathbf{k}\sigma}^\dagger - e_{\mathbf{p}\bar{\sigma}}^\dagger e_{\mathbf{q}\bar{\sigma}} e_{\mathbf{k}\sigma}^\dagger \right) \\
&= V_{SD} \sum_{\mathbf{p}} \left(-e_{\mathbf{p}\sigma}^\dagger \right).
\end{aligned}$$

$$\begin{aligned}
[e_{\mathbf{k}\sigma}^\dagger, \mathcal{H}_{\text{dot-lead}}] &= [e_{\mathbf{k}\sigma}^\dagger, \sqrt{2}V \sum_{\mathbf{p}\bar{\sigma}} (e_{\mathbf{p}\bar{\sigma}}^\dagger d_{\bar{\sigma}} + d_{\bar{\sigma}}^\dagger e_{\mathbf{p}\bar{\sigma}})] \\
&= [e_{\mathbf{k}\sigma}^\dagger, \sqrt{2}V \sum_{\mathbf{p}\bar{\sigma}} e_{\mathbf{p}\bar{\sigma}}^\dagger d_{\bar{\sigma}}] + [e_{\mathbf{k}\sigma}^\dagger, \sqrt{2}V \sum_{\mathbf{p}\bar{\sigma}} d_{\bar{\sigma}}^\dagger e_{\mathbf{p}\bar{\sigma}}] \\
&= \sqrt{2}V \sum_{\mathbf{p}\bar{\sigma}} \left(e_{\mathbf{k}\sigma}^\dagger e_{\mathbf{p}\bar{\sigma}}^\dagger d_{\bar{\sigma}} - e_{\mathbf{p}\bar{\sigma}}^\dagger d_{\bar{\sigma}} e_{\mathbf{k}\sigma}^\dagger \right) \\
&+ \sqrt{2}V \sum_{\mathbf{p}\bar{\sigma}} \left(e_{\mathbf{k}\sigma}^\dagger d_{\bar{\sigma}}^\dagger e_{\mathbf{p}\bar{\sigma}} - d_{\bar{\sigma}}^\dagger e_{\mathbf{p}\bar{\sigma}} e_{\mathbf{k}\sigma}^\dagger \right) \\
&= \sqrt{2}V \sum_{\mathbf{p}\bar{\sigma}} \left(e_{\mathbf{k}\sigma}^\dagger e_{\mathbf{p}\bar{\sigma}}^\dagger d_{\bar{\sigma}} - e_{\mathbf{k}\sigma}^\dagger e_{\mathbf{p}\bar{\sigma}}^\dagger d_{\bar{\sigma}} \right) \\
&+ \sqrt{2}V \sum_{\mathbf{p}\bar{\sigma}} \left(-d_{\bar{\sigma}}^\dagger e_{\mathbf{k}\sigma}^\dagger e_{\mathbf{p}\bar{\sigma}} - d_{\bar{\sigma}}^\dagger e_{\mathbf{p}\bar{\sigma}} e_{\mathbf{k}\sigma}^\dagger \right) \\
&= \sqrt{2}V \sum_{\mathbf{p}\bar{\sigma}} \left(-d_{\bar{\sigma}}^\dagger \right) \left(e_{\mathbf{k}\sigma}^\dagger e_{\mathbf{p}\bar{\sigma}} + e_{\mathbf{p}\bar{\sigma}} e_{\mathbf{k}\sigma}^\dagger \right) \\
&= \sqrt{2}V \sum_{\mathbf{p}\bar{\sigma}} \left(-d_{\bar{\sigma}}^\dagger \right) \delta_{\mathbf{k}\mathbf{p}} \delta_{\bar{\sigma}\sigma} \\
&= \sqrt{2}V \left(-d_{\bar{\sigma}}^\dagger \right). \tag{B.79}
\end{aligned}$$

$$\begin{aligned}
(\omega + \eta^+) G_{e_{\mathbf{k}\sigma}^\dagger d_\sigma}^r(\omega) &= \langle\langle \varepsilon_{\mathbf{k}\sigma} (-e_{\mathbf{k}\sigma}^\dagger); d_\sigma^\dagger \rangle\rangle + \langle\langle V_{SD} \sum_{\mathbf{p}} (-e_{\mathbf{p}\sigma}^\dagger); d_\sigma^\dagger \rangle\rangle + \langle\langle \sqrt{2}V - d_\sigma^\dagger; d_\sigma^\dagger \rangle\rangle \\
&= -\varepsilon_{\mathbf{k}\sigma} \langle\langle e_{\mathbf{k}\sigma}^\dagger; d_\sigma^\dagger \rangle\rangle - V_{SD} \sum_{\mathbf{k}} \langle\langle e_{\mathbf{k}\sigma}^\dagger; d_\sigma^\dagger \rangle\rangle - \sqrt{2}V \langle\langle d_\sigma^\dagger; d_\sigma^\dagger \rangle\rangle \tag{B.80}
\end{aligned}$$

$$(\omega + \varepsilon_{\mathbf{k}\sigma} + \eta^+) G_{e_{\mathbf{k}\sigma}^\dagger d_\sigma}^r(\omega) = -V_{SD} \sum_{\mathbf{k}} G_{e_{\mathbf{k}\sigma}^\dagger d_\sigma}^r(\omega) - \sqrt{2}V G_{d_\sigma^\dagger d_\sigma}^r(\omega) \tag{B.81}$$

Let us divide the expression above by $(\omega + \varepsilon_{\mathbf{k}\sigma} + \eta^+)$:

$$\begin{aligned}
 G_{e_{\mathbf{k}\sigma}^\dagger d_\sigma}^r(\omega) &= -\frac{V_{SD} \sum_{\mathbf{k}} G_{e_{\mathbf{k}\sigma}^\dagger d_\sigma}^r(\omega)}{(\omega + \varepsilon_{\mathbf{k}\sigma} + i\eta^+)} - \frac{\sqrt{2}V G_{d_\sigma^\dagger d_\sigma}^r(\omega)}{(\omega + \varepsilon_{\mathbf{k}\sigma} + i\eta^+)} \\
 \left[1 + (V_{SD}) \sum_{\mathbf{k}} \frac{1}{(\omega + \varepsilon_{\mathbf{k}\sigma} + i\eta^+)} \right] G_{e_{\mathbf{k}\sigma}^\dagger d_\sigma}^r(\omega) &= -\frac{\sqrt{2}V G_{d_\sigma^\dagger d_\sigma}^r(\omega)}{(\omega + \varepsilon_{\mathbf{k}\sigma} + i\eta^+)} \\
 G_{e_{\mathbf{k}\sigma}^\dagger d_\sigma}^r(\omega) &= -\frac{\sqrt{2}V G_{d_\sigma^\dagger d_\sigma}^r(\omega)(\omega + \varepsilon_{\mathbf{k}\sigma} + i\eta^+)^{-1}}{\left[1 + (V_{SD}) \sum_{\mathbf{k}} \frac{1}{(\omega + \varepsilon_{\mathbf{k}\sigma} + i\eta^+)} \right]} \tag{B.82}
 \end{aligned}$$

Substituting such a relation into Eq.(B.74), we get

$$\begin{aligned}
 (\omega + \varepsilon_{d\sigma} + i\eta^+) G_{d_\sigma^\dagger d_\sigma}^r(\omega) &= \sum_{\mathbf{k}} \frac{2V^2(\omega + \varepsilon_{\mathbf{k}\sigma} + i\eta^+)^{-1} G_{d_\sigma^\dagger d_\sigma}^r(\omega)}{\left[1 + (V_{SD}) \sum_{\mathbf{k}} \frac{1}{(\omega + \varepsilon_{\mathbf{k}\sigma} + i\eta^+)} \right]} - U G_{d_\sigma^\dagger n_{d\bar{\sigma}} d_\sigma}^r(\omega) \\
 &+ t_{hp} \sum_{\bar{\sigma}} \delta_{\sigma\bar{\sigma}} G_{a_\dagger d_\sigma}^r(\omega) + \Delta \sum_{\bar{\sigma}} \delta_{\sigma\bar{\sigma}} G_{a_\uparrow d_\sigma}^r(\omega) \tag{B.83}
 \end{aligned}$$

As we have done previously,

$$\sum_{\mathbf{k}} \left(\frac{1}{\omega + \varepsilon_{\mathbf{k}\sigma} + i\eta^+} \right) = -i\pi \rho_{\mathbf{k}\sigma}(\omega) \tag{B.84}$$

$$\begin{aligned}
 (\omega + \varepsilon_{d\sigma} + i\eta^+) G_{d_\sigma^\dagger d_\sigma}^r(\omega) &= \frac{2V^2 (-i\pi \rho_{\mathbf{k}\sigma}(\omega)) G_{d_\sigma^\dagger d_\sigma}^r(\omega)}{\left[1 + (V_{SD}) (-i\pi \rho_{\mathbf{k}\sigma}(\omega)) \right]} - U G_{d_\sigma^\dagger n_{d\bar{\sigma}} d_\sigma}^r(\omega) \\
 &+ t_{hp} \sum_{\bar{\sigma}} \delta_{\sigma\bar{\sigma}} G_{a_\dagger d_\sigma}^r(\omega) + \Delta \sum_{\bar{\sigma}} \delta_{\sigma\bar{\sigma}} G_{a_\uparrow d_\sigma}^r(\omega) \tag{B.85}
 \end{aligned}$$

$$\begin{aligned}
 (\omega + \varepsilon_{d\sigma} + i\eta^+) G_{d_\sigma^\dagger d_\sigma}^r(\omega) &= \frac{(-i2V^2 \pi \rho_{\mathbf{k}\sigma}(\omega)) G_{d_\sigma^\dagger d_\sigma}^r(\omega)}{\left[1 + (V_{SD}) (-i\pi \rho_{\mathbf{k}\sigma}(\omega)) \right]} - U G_{d_\sigma^\dagger n_{d\bar{\sigma}} d_\sigma}^r(\omega) \\
 &+ t_{hp} \sum_{\bar{\sigma}} \delta_{\sigma\bar{\sigma}} G_{a_\dagger d_\sigma}^r(\omega) + \Delta \sum_{\bar{\sigma}} \delta_{\sigma\bar{\sigma}} G_{a_\uparrow d_\sigma}^r(\omega) \tag{B.86}
 \end{aligned}$$

$$\begin{aligned}
 (\omega + \varepsilon_{d\sigma} + i\eta^+) G_{d_\sigma^\dagger d_\sigma}^r(\omega) &= \frac{(-i2V^2 \pi \rho_{\mathbf{k}\sigma}(\omega)) G_{d_\sigma^\dagger d_\sigma}^r(\omega)}{\left[1 + (V_{SD}) (-i\pi \rho_{\mathbf{k}\sigma}(\omega)) \right]} - U G_{d_\sigma^\dagger n_{d\bar{\sigma}} d_\sigma}^r(\omega) \\
 &+ t_{hp} \sum_{\bar{\sigma}} \delta_{\sigma\bar{\sigma}} G_{a_\dagger d_\sigma}^r(\omega) + \Delta \sum_{\bar{\sigma}} \delta_{\sigma\bar{\sigma}} G_{a_\uparrow d_\sigma}^r(\omega) \tag{B.87}
 \end{aligned}$$

Following previous definitions, $\Gamma_\sigma = 2V^2 \pi \rho_{\mathbf{k}\sigma}(\omega)$.

$$\begin{aligned}
 (\omega + \varepsilon_{d\sigma} + \eta^+) G_{d_\sigma^\dagger d_\sigma}^r(\omega) &= \frac{-i\Gamma_\sigma G_{d_\sigma^\dagger d_\sigma}^r(\omega)}{(1 - iV_{SD}\pi\rho_{\mathbf{k}\sigma}(\omega))} - U G_{d_\sigma^\dagger n_{d\bar{\sigma}} d_\sigma}^r(\omega) \\
 &+ t_{hp} \sum_{\tilde{\sigma}} \delta_{\sigma\tilde{\sigma}} G_{a_\uparrow^\dagger d_\sigma}^r(\omega) + \Delta \sum_{\tilde{\sigma}} \delta_{\sigma\tilde{\sigma}} G_{a_\uparrow d_\sigma}^r(\omega)
 \end{aligned} \quad (\text{B.88})$$

As we have stated, $V_{SD}\pi\rho_{\mathbf{k}\sigma}(\omega) = \sqrt{x}$. Thus,

$$\begin{aligned}
 (\omega + \varepsilon_{d\sigma} + \eta^+) G_{d_\sigma^\dagger d_\sigma}^r(\omega) &= \frac{-i\Gamma_\uparrow G_{d_\sigma^\dagger d_\sigma}^r(\omega)}{(1 - i\sqrt{x})} - U G_{d_\sigma^\dagger n_{d\bar{\sigma}} d_\sigma}^r(\omega) \\
 &+ t_{hp} \sum_{\tilde{\sigma}} \delta_{\sigma\tilde{\sigma}} G_{a_\uparrow^\dagger d_\sigma}^r(\omega) + \Delta \sum_{\tilde{\sigma}} \delta_{\sigma\tilde{\sigma}} G_{a_\uparrow d_\sigma}^r(\omega)
 \end{aligned} \quad (\text{B.89})$$

$$\frac{-i\Gamma_\sigma}{(1 - i\sqrt{x})} \frac{(1 + i\sqrt{x})}{(1 + i\sqrt{x})} = \frac{-i\Gamma_\sigma (1 + i\sqrt{x})}{(1 + x)} = \frac{\sqrt{x}\Gamma_\sigma}{(1 + x)} - \frac{i\Gamma_\sigma}{(1 + x)} \quad (\text{B.90})$$

Comparing with Eq.(B.32):

$$-\left(\frac{\sqrt{x}\Gamma_\sigma}{(1 + x)} - \frac{i\Gamma_\sigma}{(1 + x)} \right) = -\frac{\sqrt{x}\Gamma_\sigma}{(1 + x)} + \frac{i\Gamma_\sigma}{(1 + x)} = \bar{\Sigma}_\uparrow \quad (\text{B.91})$$

$$\boxed{\bar{\Sigma}_\sigma = \text{Re}(\Sigma_\sigma) - \text{Im}(\Sigma_\sigma)} \quad (\text{B.92})$$

with

$$\text{Re}(\Sigma_\sigma) = -\frac{\sqrt{x}\Gamma_\sigma}{1 + x} \quad (\text{B.93})$$

$$\text{Im}(\Sigma_\sigma) = -\frac{i\Gamma_\sigma}{1 + x} \quad (\text{B.94})$$

Thus,

$$\begin{aligned}
 (\omega + \varepsilon_{d\sigma} + \eta^+) G_{d_\sigma^\dagger d_\sigma}^r(\omega) &= -\bar{\Sigma}_\sigma G_{d_\sigma^\dagger d_\sigma}^r(\omega) - U G_{d_\sigma^\dagger n_{d\bar{\sigma}} d_\sigma}^r(\omega) \\
 &+ t_{hp} \sum_{\tilde{\sigma}} \delta_{\sigma\tilde{\sigma}} G_{a_\uparrow^\dagger d_\sigma}^r(\omega) + \Delta \sum_{\tilde{\sigma}} \delta_{\sigma\tilde{\sigma}} G_{a_\uparrow d_\sigma}^r(\omega),
 \end{aligned} \quad (\text{B.95})$$

$$\boxed{(\omega + \varepsilon_{d\sigma} + \bar{\Sigma}_\uparrow + \eta^+) G_{d_\sigma^\dagger d_\sigma}^r(\omega) = -U G_{d_\sigma^\dagger n_{d\bar{\sigma}} d_\sigma}^r(\omega) + t_{hp} \sum_{\tilde{\sigma}} \delta_{\sigma\tilde{\sigma}} G_{a_\uparrow^\dagger d_\sigma}^r(\omega) + \Delta \sum_{\tilde{\sigma}} \delta_{\sigma\tilde{\sigma}} G_{a_\uparrow d_\sigma}^r(\omega).} \quad (\text{B.96})$$

From Eqs.(B.43) and (B.52):

$$G_{a_{\uparrow}d_{\sigma}}^r(\omega) = -\frac{t_{hp} \sum_{\bar{\sigma}} G_{d_{\bar{\sigma}}d_{\sigma}}^r(\omega)}{(\omega - \delta_M + i\eta^+)} + \frac{\Delta \sum_{\bar{\sigma}} G_{d_{\bar{\sigma}}^{\dagger}d_{\sigma}}^r(\omega)}{(\omega - \delta_M + i\eta^+)} \quad (\text{B.97})$$

$$G_{a_{\uparrow}^{\dagger}d_{\sigma}}^r(\omega) = \frac{t_{hp} \sum_{\bar{\sigma}} G_{d_{\bar{\sigma}}^{\dagger}d_{\sigma}}^r(\omega)}{(\omega + \delta_M + i\eta^+)} - \frac{\Delta \sum_{\bar{\sigma}} G_{d_{\bar{\sigma}}d_{\sigma}}^r(\omega)}{(\omega + \delta_M + i\eta^+)} \quad (\text{B.98})$$

$$\begin{aligned} (\omega + \varepsilon_{d\sigma} + \bar{\Sigma}_{\uparrow} + i\eta^+)G_{d_{\sigma}^{\dagger}d_{\sigma}}^r(\omega) &= -UG_{d_{\sigma}^{\dagger}n_{d\bar{\sigma}}d_{\sigma}}^r(\omega) \\ &+ t_{hp} \sum_{\bar{\sigma}} \delta_{\sigma\bar{\sigma}} \left[\frac{t_{hp} \sum_{\bar{\sigma}} G_{d_{\bar{\sigma}}^{\dagger}d_{\sigma}}^r(\omega)}{(\omega + \delta_M + i\eta^+)} - \frac{\Delta \sum_{\bar{\sigma}} G_{d_{\bar{\sigma}}d_{\sigma}}^r(\omega)}{(\omega + \delta_M + i\eta^+)} \right] \\ &+ \Delta \sum_{\bar{\sigma}} \delta_{\sigma\bar{\sigma}} \left[-\frac{t_{hp} \sum_{\bar{\sigma}} G_{d_{\bar{\sigma}}d_{\sigma}}^r(\omega)}{(\omega - \delta_M + i\eta^+)} + \frac{\Delta \sum_{\bar{\sigma}} G_{d_{\bar{\sigma}}^{\dagger}d_{\sigma}}^r(\omega)}{(\omega - \delta_M + i\eta^+)} \right] \end{aligned} \quad (\text{B.99})$$

$$\begin{aligned} (\omega + \varepsilon_{d\sigma} + \bar{\Sigma}_{\uparrow} + i\eta^+)G_{d_{\sigma}^{\dagger}d_{\sigma}}^r(\omega) &= -UG_{d_{\sigma}^{\dagger}n_{d\bar{\sigma}}d_{\sigma}}^r(\omega) \\ &+ \sum_{\bar{\sigma}} \delta_{\sigma\bar{\sigma}} \left[\frac{(t_{hp})^2}{(\omega + \delta_M + i\eta^+)} + \frac{(\Delta)^2}{(\omega - \delta_M + i\eta^+)} \right] G_{d_{\bar{\sigma}}^{\dagger}d_{\sigma}}^r(\omega) \\ &- t_{hp}\Delta \sum_{\bar{\sigma}} \delta_{\sigma\bar{\sigma}} \left[\frac{1}{(\omega - \delta_M + i\eta^+)} + \frac{1}{(\omega + \delta_M + i\eta^+)} \right] G_{d_{\bar{\sigma}}d_{\sigma}}^r(\omega) \end{aligned} \quad (\text{B.100})$$

$$\begin{aligned} (\omega + \varepsilon_{d\sigma} + \bar{\Sigma}_{\uparrow} + i\eta^+)G_{d_{\sigma}^{\dagger}d_{\sigma}}^r(\omega) &= -UG_{d_{\sigma}^{\dagger}n_{d\bar{\sigma}}d_{\sigma}}^r(\omega) - t_{hp}\Delta KG_{d_{\sigma}d_{\sigma}}^r(\omega) \\ &+ \left[\frac{(t_{hp})^2}{(\omega + \delta_M + i\eta^+)} + \frac{(\Delta)^2}{(\omega - \delta_M + i\eta^+)} \right] G_{d_{\sigma}^{\dagger}d_{\sigma}}^r(\omega) \end{aligned} \quad (\text{B.101})$$

Now, we have the following relations between Green's functions:

$$\begin{aligned} (\omega - \varepsilon_{d\sigma} - \Sigma_{\sigma} + i\eta^+)G_{d_{\sigma}d_{\sigma}}^r(\omega) &= 1 + UG_{d_{\sigma}n_{d\bar{\sigma}}d_{\sigma}}^r(\omega) - t_{hp}\Delta KG_{d_{\sigma}^{\dagger}d_{\sigma}}^r(\omega) \\ &+ \left[\frac{(t_{hp})^2}{(\omega - \delta_M + i\eta^+)} + \frac{(\Delta)^2}{(\omega + \delta_M + i\eta^+)} \right] G_{d_{\sigma}d_{\sigma}}^r(\omega). \end{aligned} \quad (\text{B.102})$$

$$\begin{aligned} (\omega + \varepsilon_{d\sigma} + \bar{\Sigma}_{\uparrow} + i\eta^+)G_{d_{\sigma}^{\dagger}d_{\sigma}}^r(\omega) &= -UG_{d_{\sigma}^{\dagger}n_{d\bar{\sigma}}d_{\sigma}}^r(\omega) - t_{hp}\Delta KG_{d_{\sigma}d_{\sigma}}^r(\omega) \\ &+ \left[\frac{(t_{hp})^2}{(\omega + \delta_M + i\eta^+)} + \frac{(\Delta)^2}{(\omega - \delta_M + i\eta^+)} \right] G_{d_{\sigma}^{\dagger}d_{\sigma}}^r(\omega) \end{aligned} \quad (\text{B.103})$$

B.2 Hubbard-I approximation (1st order)

It is known that a mean field approximation is valid in the regime where $\Gamma \gg U$. Otherwise, a better approximation is required to catch the effects introduced by the electronic correlation. In this section we derive the so-called Hubbard-I approximation, which is valid when the temperature of the system is bigger than the characteristic Kondo temperature ($T \gg T_K$). Such approximation allows to verify the Hubbard peaks arising due to Coulomb interaction.

Let us start from Eqs.(B.102) and (B.103):

$$(\omega^+ - \varepsilon_{d\sigma} - \Sigma_\sigma)G_{d_\sigma d_\sigma}^r(\omega) = 1 + UG_{d_\sigma n_{d\bar{\sigma}}, d_\sigma}^r(\omega) - t_{hp}\Delta K G_{d_\sigma d_\sigma}^r(\omega) + K_1 G_{d_\sigma d_\sigma}^r(\omega), \quad (\text{B.104})$$

$$(\omega^+ + \varepsilon_{d\sigma} + \bar{\Sigma}_\sigma - K_2)G_{d_\sigma d_\sigma}^r(\omega) = -UG_{d_\sigma n_{d\bar{\sigma}}, d_\sigma}^r(\omega) - t_{hp}\Delta K G_{d_\sigma d_\sigma}^r(\omega) \quad (\text{B.105})$$

From Eq.(B.105):

$$G_{d_\sigma d_\sigma}^r(\omega) = -\frac{UG_{d_\sigma n_{d\bar{\sigma}}, d_\sigma}^r(\omega)}{(\omega^+ + \varepsilon_{d\sigma} + \bar{\Sigma}_\sigma - K_2)} - \frac{t_{hp}\Delta K G_{d_\sigma d_\sigma}^r(\omega)}{(\omega^+ + \varepsilon_{d\sigma} + \bar{\Sigma}_\sigma - K_2)} \Rightarrow$$

$$G_{d_\sigma d_\sigma}^r(\omega) = -\frac{UG_{d_\sigma n_{d\bar{\sigma}}, d_\sigma}^r(\omega)}{(\omega^+ + \varepsilon_{d\sigma} + \bar{\Sigma}_\sigma - K_2)} - t_{hp}\Delta \bar{K}^\sigma G_{d_\sigma d_\sigma}^r(\omega) \quad (\text{B.106})$$

Let us substitute Eq.(B.106) into Eq.(B.104):

$$(\omega^+ - \varepsilon_{d\sigma} - \Sigma_\sigma)G_{d_\sigma d_\sigma}^r(\omega) = 1 + UG_{d_\sigma n_{d\bar{\sigma}}, d_\sigma}^r(\omega) + K_1 G_{d_\sigma d_\sigma}^r(\omega) - t_{hp}\Delta K \left[-\frac{UG_{d_\sigma n_{d\bar{\sigma}}, d_\sigma}^r(\omega)}{(\omega^+ + \varepsilon_{d\sigma} + \bar{\Sigma}_\sigma - K_2)} - t_{hp}\Delta \bar{K}^\sigma G_{d_\sigma d_\sigma}^r(\omega) \right] \Rightarrow$$

$$(\omega^+ - \varepsilon_{d\sigma} - \Sigma_\sigma)G_{d_\sigma d_\sigma}^r(\omega) = 1 + UG_{d_\sigma n_{d\bar{\sigma}}, d_\sigma}^r(\omega) + K_1 G_{d_\sigma d_\sigma}^r(\omega) + Ut_{hp}\Delta \bar{K} G_{d_\sigma n_{d\bar{\sigma}}, d_\sigma}^r(\omega) + (t_{hp}\Delta)^2 K \bar{K}^\sigma G_{d_\sigma d_\sigma}^r(\omega) \Rightarrow (\text{B.107})$$

$$(\omega^+ - \varepsilon_{d\sigma} - \Sigma_\sigma)G_{d_\sigma d_\sigma}^r(\omega) = 1 + UG_{d_\sigma n_{d\bar{\sigma}}, d_\sigma}^r(\omega) + \underbrace{[K_1 + (t_{hp}\Delta)^2 K \bar{K}^\sigma]}_{\Sigma_{M,\sigma}^{U=0}} G_{d_\sigma d_\sigma}^r(\omega) + Ut_{hp}\Delta \bar{K} G_{d_\sigma n_{d\bar{\sigma}}, d_\sigma}^r(\omega) \Rightarrow \quad (\text{B.108})$$

$$(\omega^+ - \varepsilon_{d\sigma} - \Sigma_\sigma - \Sigma_{M,\sigma}^{U=0})G_{d_\sigma d_\sigma}^r(\omega) = 1 + UG_{d_\sigma n_{d\bar{\sigma}}, d_\sigma}^r(\omega) + Ut_{hp}\Delta\bar{K}G_{d_\sigma^\dagger n_{d\bar{\sigma}} d_\sigma}^r(\omega) \quad (\text{B.109})$$

The equation above has two many-particle Green's functions (four operators): $G_{d_\sigma n_{d\bar{\sigma}}, d_\sigma}^r(\omega)$ and $G_{d_\sigma^\dagger n_{d\bar{\sigma}} d_\sigma}^r(\omega)$. Below we present the procedure to apply the Hubbard-I decoupling in both of them.

B.2.1 EOM and decoupling scheme in $G_{d_\sigma n_{d\bar{\sigma}}, d_\sigma}^r(\omega)$

The many-particle retarded Green's function is defined as:

$$G_{c_i n_{c_k} c_j}^r(t, t') = -i\theta(t - t') \left\langle \left\{ c_i(t) c_k^\dagger(t) c_k(t), c_j^\dagger(t') \right\} \right\rangle, \quad t > t' \quad (\text{B.110})$$

where $n_{c_k} = c_k^\dagger c_k$ is the number operator. Using the Zubarev notation:

$$G_{c_i n_{c_k} c_j}^r(\omega) = \langle \langle c_i c_k^\dagger c_k; c_j^\dagger \rangle \rangle \quad (\text{B.111})$$

Thus, the EOM technique can be summarized as:

$$(\omega + i\eta^+)G_{c_i n_{c_k} c_j}^r(\omega) = \langle \{c_i n_{c_k}, c_j^\dagger\} \rangle + \langle \langle [c_i n_{c_k}, \mathcal{H}]; c_j^\dagger \rangle \rangle \quad (\text{B.112})$$

Let us apply the EOM procedure in order to obtain $G_{d_\sigma n_{d\bar{\sigma}}, d_\sigma}^r(\omega)$:

$$(\omega + i\eta^+)G_{d_\sigma n_{d\bar{\sigma}}, d_\sigma}^r(\omega) = \langle \{d_\sigma n_{d\bar{\sigma}}, d_\sigma^\dagger\} \rangle + \langle \langle [d_\sigma n_{d\bar{\sigma}}, \mathcal{H}_e]; d_\sigma^\dagger \rangle \rangle \quad (\text{B.113})$$

$$\begin{aligned} \langle \{d_\sigma n_{d\bar{\sigma}}, d_\sigma^\dagger\} \rangle &= \left\langle \left(d_\sigma n_{d\bar{\sigma}} d_\sigma^\dagger + d_\sigma^\dagger d_\sigma n_{d\bar{\sigma}} \right) \right\rangle \\ &= \left\langle \left(d_\sigma d_\sigma^\dagger d_\sigma n_{d\bar{\sigma}} + d_\sigma^\dagger d_\sigma n_{d\bar{\sigma}} \right) \right\rangle \\ &= \left\langle \left(d_\sigma d_\sigma^\dagger d_\sigma^\dagger d_\sigma + d_\sigma^\dagger d_\sigma n_{d\bar{\sigma}} \right) \right\rangle \\ &= \left\langle \left(d_\sigma d_\sigma^\dagger + d_\sigma^\dagger d_\sigma \right) n_{d\bar{\sigma}} \right\rangle \\ &= \langle n_{d\bar{\sigma}} \rangle \end{aligned} \quad (\text{B.114})$$

$$(\omega + i\eta^+)G_{d_\sigma n_{d\bar{\sigma}}, d_\sigma}^r(\omega) = \langle n_{d\bar{\sigma}} \rangle + \langle \langle [d_\sigma n_{d\bar{\sigma}}, \mathcal{H}_e]; d_\sigma^\dagger \rangle \rangle \quad (\text{B.115})$$

$$\begin{aligned} [d_\sigma n_{d\bar{\sigma}}, \mathcal{H}_e] &= [d_\sigma n_{d\bar{\sigma}}, \mathcal{H}_{\text{lead}}] + [d_\sigma n_{d\bar{\sigma}}, \mathcal{H}_{\text{dot}}] + [d_\sigma n_{d\bar{\sigma}}, \mathcal{H}_{\text{dot-lead}}] + [d_\sigma n_{d\bar{\sigma}}, \mathcal{H}_M] \\ &= [d_\sigma n_{d\bar{\sigma}}, \mathcal{H}_{\text{dot}}] + [d_\sigma n_{d\bar{\sigma}}, \mathcal{H}_{\text{dot-lead}}] + [d_\sigma n_{d\bar{\sigma}}, \mathcal{H}_M]. \end{aligned} \quad (\text{B.116})$$

$$[d_\sigma n_{d\bar{\sigma}}, \mathcal{H}_{\text{dot}}] = [d_\sigma n_{d\bar{\sigma}}, \sum_{\bar{\sigma}} \varepsilon_{d\bar{\sigma}} d_\sigma^\dagger d_{\bar{\sigma}}] + [d_\sigma n_{d\bar{\sigma}}, U n_{d\uparrow} n_{d\downarrow}] \quad (\text{B.117})$$

$$\begin{aligned}
(III) & : U \left(d_{\uparrow}^{\dagger} d_{\uparrow} d_{\sigma} d_{\downarrow}^{\dagger} d_{\downarrow} d_{\bar{\sigma}}^{\dagger} d_{\bar{\sigma}} - d_{\uparrow}^{\dagger} d_{\uparrow} d_{\downarrow}^{\dagger} d_{\downarrow} d_{\sigma} d_{\bar{\sigma}}^{\dagger} d_{\bar{\sigma}} \right) \\
& = U \left(d_{\uparrow}^{\dagger} d_{\uparrow} \left(\delta_{\sigma\downarrow} - d_{\downarrow}^{\dagger} d_{\sigma} \right) d_{\downarrow} d_{\bar{\sigma}}^{\dagger} d_{\bar{\sigma}} - d_{\uparrow}^{\dagger} d_{\uparrow} d_{\downarrow}^{\dagger} d_{\downarrow} d_{\sigma} d_{\bar{\sigma}}^{\dagger} d_{\bar{\sigma}} \right) \\
& = U \left(\delta_{\sigma\downarrow} d_{\uparrow}^{\dagger} d_{\uparrow} d_{\downarrow} d_{\bar{\sigma}}^{\dagger} d_{\bar{\sigma}} + d_{\uparrow}^{\dagger} d_{\uparrow} d_{\downarrow}^{\dagger} d_{\downarrow} d_{\sigma} d_{\bar{\sigma}}^{\dagger} d_{\bar{\sigma}} - d_{\uparrow}^{\dagger} d_{\uparrow} d_{\downarrow}^{\dagger} d_{\downarrow} d_{\sigma} d_{\bar{\sigma}}^{\dagger} d_{\bar{\sigma}} \right) \\
& = U \delta_{\sigma\downarrow} d_{\uparrow}^{\dagger} d_{\uparrow} d_{\downarrow} d_{\bar{\sigma}}^{\dagger} d_{\bar{\sigma}}
\end{aligned} \tag{B.120}$$

Let us consider $\sigma = \uparrow$:

$$(I) : \delta_{\downarrow\uparrow} d_{\uparrow} d_{\downarrow}^{\dagger} d_{\uparrow} d_{\downarrow}^{\dagger} d_{\downarrow} - \delta_{\downarrow\uparrow} d_{\uparrow} d_{\downarrow}^{\dagger} d_{\downarrow} d_{\uparrow}^{\dagger} d_{\downarrow} + \delta_{\downarrow\downarrow} d_{\uparrow} d_{\downarrow}^{\dagger} d_{\uparrow} d_{\downarrow}^{\dagger} d_{\downarrow} = d_{\uparrow} d_{\downarrow}^{\dagger} d_{\uparrow} d_{\downarrow}^{\dagger} d_{\downarrow} \tag{B.121}$$

$$(II) : U \left(-\delta_{\downarrow\downarrow} d_{\uparrow} d_{\downarrow}^{\dagger} d_{\uparrow} d_{\downarrow}^{\dagger} d_{\downarrow} + \delta_{\uparrow\uparrow} d_{\uparrow} d_{\downarrow}^{\dagger} d_{\downarrow} d_{\uparrow}^{\dagger} d_{\downarrow} \right) = -d_{\uparrow} d_{\downarrow}^{\dagger} d_{\uparrow} d_{\downarrow}^{\dagger} d_{\downarrow} + d_{\uparrow} d_{\downarrow}^{\dagger} d_{\downarrow} d_{\uparrow}^{\dagger} d_{\downarrow} \tag{B.122}$$

$$(III) : U \delta_{\sigma\downarrow} d_{\uparrow}^{\dagger} d_{\uparrow} d_{\downarrow} d_{\bar{\sigma}}^{\dagger} d_{\bar{\sigma}} = 0$$

Thus,

$$\begin{aligned}
[d_{\sigma} n_{d\bar{\sigma}}, U n_{d\uparrow} n_{d\downarrow}] & = U \left(d_{\uparrow} d_{\downarrow}^{\dagger} d_{\uparrow} d_{\downarrow}^{\dagger} d_{\downarrow} - d_{\uparrow} d_{\downarrow}^{\dagger} d_{\uparrow} d_{\downarrow}^{\dagger} d_{\downarrow} + d_{\uparrow} d_{\downarrow}^{\dagger} d_{\downarrow} d_{\uparrow}^{\dagger} d_{\downarrow} \right) \\
& = U d_{\uparrow} d_{\downarrow}^{\dagger} d_{\downarrow} d_{\uparrow}^{\dagger} d_{\downarrow} \\
& = U d_{\sigma} n_{d\bar{\sigma}}.
\end{aligned} \tag{B.123}$$

wherein we have used $n_{d\bar{\sigma}} n_{d\bar{\sigma}} = n_{d\bar{\sigma}}$.

$$\begin{aligned}
[d_{\sigma} n_{d\bar{\sigma}}, \mathcal{H}_{\text{dot-lead}}] & = [d_{\sigma} n_{d\bar{\sigma}}, \sqrt{2}V \sum_{\mathbf{k}\bar{\sigma}} (e_{\mathbf{k}\bar{\sigma}}^{\dagger} d_{\bar{\sigma}} + d_{\bar{\sigma}}^{\dagger} e_{\mathbf{k}\bar{\sigma}})] \\
& = \underbrace{\sqrt{2}V \sum_{\mathbf{k}\bar{\sigma}} [d_{\sigma} n_{d\bar{\sigma}}, e_{\mathbf{k}\bar{\sigma}}^{\dagger} d_{\bar{\sigma}}]}_I + \underbrace{\sqrt{2}V \sum_{\mathbf{k}\bar{\sigma}} [d_{\sigma} n_{d\bar{\sigma}}, d_{\bar{\sigma}}^{\dagger} e_{\mathbf{k}\bar{\sigma}}]}_{II}
\end{aligned} \tag{B.124}$$

$$\begin{aligned}
(\omega + \eta^+) G_{d_\sigma n_{d\bar{\sigma}}, d_\sigma}^r(\omega) &= \langle n_{d\bar{\sigma}} \rangle + \langle \langle \varepsilon_{d\sigma} d_\sigma n_{d\bar{\sigma}}; d_\sigma^\dagger \rangle \rangle + \langle \langle U d_\sigma n_{d\bar{\sigma}}; d_\sigma^\dagger \rangle \rangle + \langle \langle -\sqrt{2}V \sum_{\mathbf{k}} e_{\mathbf{k}\bar{\sigma}}^\dagger d_{\bar{\sigma}} d_\sigma; d_\sigma^\dagger \rangle \rangle \\
&+ \sqrt{2}V \sum_{\mathbf{k}} \langle \langle d_{\bar{\sigma}}^\dagger e_{\mathbf{k}\bar{\sigma}} d_\sigma; d_\sigma^\dagger \rangle \rangle + \sqrt{2}V \sum_{\mathbf{k}} \langle \langle e_{\mathbf{k}\sigma} n_{d\bar{\sigma}}; d_\sigma^\dagger \rangle \rangle + \langle \langle [d_\sigma n_{d\bar{\sigma}}, \mathcal{H}_M]; d_\sigma^\dagger \rangle \rangle \\
(\omega + \eta^+) G_{d_\sigma n_{d\bar{\sigma}}, d_\sigma}^r(\omega) &= \langle n_{d\bar{\sigma}} \rangle + \varepsilon_{d\sigma} \langle \langle d_\sigma n_{d\bar{\sigma}}; d_\sigma^\dagger \rangle \rangle + U \langle \langle d_\sigma n_{d\bar{\sigma}}; d_\sigma^\dagger \rangle \rangle - \sqrt{2}V \sum_{\mathbf{k}} \langle \langle e_{\mathbf{k}\bar{\sigma}}^\dagger d_{\bar{\sigma}} d_\sigma; d_\sigma^\dagger \rangle \rangle \\
&+ \sqrt{2}V \sum_{\mathbf{k}} \langle \langle d_{\bar{\sigma}}^\dagger e_{\mathbf{k}\bar{\sigma}} d_\sigma; d_\sigma^\dagger \rangle \rangle + \sqrt{2}V \sum_{\mathbf{k}} \langle \langle e_{\mathbf{k}\sigma} n_{d\bar{\sigma}}; d_\sigma^\dagger \rangle \rangle + \langle \langle [d_\sigma n_{d\bar{\sigma}}, \mathcal{H}_M]; d_\sigma^\dagger \rangle \rangle
\end{aligned} \tag{B.128}$$

$$\begin{aligned}
(\omega - \varepsilon_{d\sigma} - U + \eta^+) G_{d_\sigma n_{d\bar{\sigma}}, d_\sigma}^r(\omega) &= \langle n_{d\bar{\sigma}} \rangle + \sqrt{2}V \sum_{\mathbf{k}} \left[G_{d_{\bar{\sigma}}^\dagger e_{\mathbf{k}\bar{\sigma}} d_\sigma d_\sigma}^r(\omega) - G_{e_{\mathbf{k}\bar{\sigma}}^\dagger d_{\bar{\sigma}} d_\sigma, d_\sigma}^r(\omega) + G_{e_{\mathbf{k}\sigma} n_{d\bar{\sigma}}, d_\sigma}^r(\omega) \right] \\
&+ \langle \langle [d_\sigma n_{d\bar{\sigma}}, \mathcal{H}_M]; d_\sigma^\dagger \rangle \rangle
\end{aligned} \tag{B.129}$$

The first line of equation above is the well-known set of equations for an interacting dot between metallic leads. The novelty is introduced by the term in second line, related to the presence of Kitaev wire.

$$\begin{aligned}
[d_\sigma n_{d\bar{\sigma}}, \mathcal{H}_M] &= \left[d_\sigma n_{d\bar{\sigma}}, \delta_M \left(a_\uparrow^\dagger a_\uparrow - \frac{1}{2} \right) \right] + \left[d_\sigma n_{d\bar{\sigma}}, t_{hp} \sum_{\bar{\sigma}} (d_{\bar{\sigma}} a_\uparrow^\dagger + a_\uparrow d_{\bar{\sigma}}^\dagger) \right] \\
&+ \left[d_\sigma n_{d\bar{\sigma}}, \Delta \sum_{\bar{\sigma}} (d_{\bar{\sigma}} a_\uparrow + a_\uparrow^\dagger d_{\bar{\sigma}}^\dagger) \right] \\
&= \left[d_\sigma n_{d\bar{\sigma}}, t_{hp} \sum_{\bar{\sigma}} (d_{\bar{\sigma}} a_\uparrow^\dagger + a_\uparrow d_{\bar{\sigma}}^\dagger) \right] + \left[d_\sigma n_{d\bar{\sigma}}, \Delta \sum_{\bar{\sigma}} (d_{\bar{\sigma}} a_\uparrow + a_\uparrow^\dagger d_{\bar{\sigma}}^\dagger) \right]
\end{aligned} \tag{B.130}$$

$$\left[d_\sigma n_{d\bar{\sigma}}, t_{hp} \sum_{\bar{\sigma}} (d_{\bar{\sigma}} a_\uparrow^\dagger + a_\uparrow d_{\bar{\sigma}}^\dagger) \right] = t_{hp} \sum_{\bar{\sigma}} \left[d_\sigma n_{d\bar{\sigma}}, d_{\bar{\sigma}} a_\uparrow^\dagger \right] + t_{hp} \sum_{\bar{\sigma}} \left[d_\sigma n_{d\bar{\sigma}}, a_\uparrow d_{\bar{\sigma}}^\dagger \right], \tag{B.131}$$

$$\begin{aligned}
t_{hp} \sum_{\bar{\sigma}} \left[d_{\sigma} n_{d\bar{\sigma}}, d_{\bar{\sigma}} a_{\uparrow}^{\dagger} \right] &= t_{hp} \sum_{\bar{\sigma}} \left(d_{\sigma} n_{d\bar{\sigma}} d_{\bar{\sigma}} a_{\uparrow}^{\dagger} - d_{\bar{\sigma}} a_{\uparrow}^{\dagger} d_{\sigma} n_{d\bar{\sigma}} \right) \\
&= t_{hp} \sum_{\bar{\sigma}} \left(d_{\sigma} d_{\bar{\sigma}}^{\dagger} d_{\bar{\sigma}} d_{\bar{\sigma}} a_{\uparrow}^{\dagger} + d_{\bar{\sigma}} d_{\sigma} d_{\bar{\sigma}}^{\dagger} d_{\bar{\sigma}} a_{\uparrow}^{\dagger} \right) \\
&= t_{hp} \sum_{\bar{\sigma}} \left(-d_{\sigma} \left(\delta_{\bar{\sigma}\bar{\sigma}} - d_{\bar{\sigma}} d_{\bar{\sigma}}^{\dagger} \right) d_{\bar{\sigma}} a_{\uparrow}^{\dagger} + d_{\bar{\sigma}} d_{\sigma} d_{\bar{\sigma}}^{\dagger} d_{\bar{\sigma}} a_{\uparrow}^{\dagger} \right) \\
&= t_{hp} \sum_{\bar{\sigma}} \left(-\delta_{\bar{\sigma}\bar{\sigma}} d_{\sigma} d_{\bar{\sigma}} a_{\uparrow}^{\dagger} - d_{\bar{\sigma}} d_{\sigma} d_{\bar{\sigma}}^{\dagger} d_{\bar{\sigma}} a_{\uparrow}^{\dagger} + d_{\bar{\sigma}} d_{\sigma} d_{\bar{\sigma}}^{\dagger} d_{\bar{\sigma}} a_{\uparrow}^{\dagger} \right) \\
&= t_{hp} \sum_{\bar{\sigma}} \left(-\delta_{\bar{\sigma}\bar{\sigma}} d_{\bar{\sigma}} a_{\uparrow}^{\dagger} d_{\sigma} \right), \tag{B.132}
\end{aligned}$$

$$\begin{aligned}
t_{hp} \sum_{\bar{\sigma}} \left[d_{\sigma} n_{d\bar{\sigma}}, a_{\uparrow} d_{\bar{\sigma}}^{\dagger} \right] &= t_{hp} \sum_{\bar{\sigma}} \left(d_{\sigma} n_{d\bar{\sigma}} a_{\uparrow} d_{\bar{\sigma}}^{\dagger} - a_{\uparrow} d_{\bar{\sigma}}^{\dagger} d_{\sigma} n_{d\bar{\sigma}} \right) \\
&= t_{hp} \sum_{\bar{\sigma}} \left(d_{\sigma} d_{\bar{\sigma}}^{\dagger} d_{\bar{\sigma}} a_{\uparrow} d_{\bar{\sigma}}^{\dagger} - a_{\uparrow} d_{\bar{\sigma}}^{\dagger} d_{\sigma} d_{\bar{\sigma}}^{\dagger} d_{\bar{\sigma}} \right) \\
&= t_{hp} \sum_{\bar{\sigma}} \left(-a_{\uparrow} d_{\sigma} d_{\bar{\sigma}}^{\dagger} d_{\bar{\sigma}} d_{\bar{\sigma}}^{\dagger} - a_{\uparrow} d_{\bar{\sigma}}^{\dagger} d_{\sigma} d_{\bar{\sigma}}^{\dagger} d_{\bar{\sigma}} \right) \\
&= t_{hp} \sum_{\bar{\sigma}} \left(-a_{\uparrow} d_{\sigma} d_{\bar{\sigma}}^{\dagger} \left(\delta_{\bar{\sigma}\bar{\sigma}} - d_{\bar{\sigma}}^{\dagger} d_{\bar{\sigma}} \right) - a_{\uparrow} d_{\bar{\sigma}}^{\dagger} d_{\sigma} d_{\bar{\sigma}}^{\dagger} d_{\bar{\sigma}} \right) \\
&= t_{hp} \sum_{\bar{\sigma}} \left(-\delta_{\bar{\sigma}\bar{\sigma}} a_{\uparrow} d_{\sigma} d_{\bar{\sigma}}^{\dagger} - a_{\uparrow} d_{\sigma} d_{\bar{\sigma}}^{\dagger} d_{\bar{\sigma}}^{\dagger} d_{\bar{\sigma}} - a_{\uparrow} d_{\bar{\sigma}}^{\dagger} d_{\sigma} d_{\bar{\sigma}}^{\dagger} d_{\bar{\sigma}} \right) \\
&= t_{hp} \sum_{\bar{\sigma}} \left(-\delta_{\bar{\sigma}\bar{\sigma}} a_{\uparrow} d_{\sigma} d_{\bar{\sigma}}^{\dagger} - a_{\uparrow} \left(\delta_{\bar{\sigma}\bar{\sigma}} - d_{\bar{\sigma}}^{\dagger} d_{\bar{\sigma}} \right) d_{\bar{\sigma}}^{\dagger} d_{\bar{\sigma}} - a_{\uparrow} d_{\bar{\sigma}}^{\dagger} d_{\sigma} d_{\bar{\sigma}}^{\dagger} d_{\bar{\sigma}} \right) \\
&= t_{hp} \sum_{\bar{\sigma}} \left(\delta_{\bar{\sigma}\bar{\sigma}} a_{\uparrow} d_{\bar{\sigma}}^{\dagger} d_{\sigma} - \delta_{\bar{\sigma}\bar{\sigma}} d_{\bar{\sigma}}^{\dagger} d_{\bar{\sigma}} a_{\uparrow} + a_{\uparrow} d_{\bar{\sigma}}^{\dagger} d_{\sigma} d_{\bar{\sigma}}^{\dagger} d_{\bar{\sigma}} - a_{\uparrow} d_{\bar{\sigma}}^{\dagger} d_{\sigma} d_{\bar{\sigma}}^{\dagger} d_{\bar{\sigma}} \right) \\
&= t_{hp} \sum_{\bar{\sigma}} \left(\delta_{\bar{\sigma}\bar{\sigma}} a_{\uparrow} d_{\bar{\sigma}}^{\dagger} d_{\sigma} - \delta_{\bar{\sigma}\bar{\sigma}} d_{\bar{\sigma}}^{\dagger} d_{\bar{\sigma}} a_{\uparrow} \right), \tag{B.133}
\end{aligned}$$

$$\left[d_{\sigma} n_{d\bar{\sigma}}, t_{hp} \sum_{\bar{\sigma}} (d_{\bar{\sigma}} a_{\uparrow}^{\dagger} + a_{\uparrow} d_{\bar{\sigma}}^{\dagger}) \right] = t_{hp} \sum_{\bar{\sigma}} \left(-\delta_{\bar{\sigma}\bar{\sigma}} d_{\bar{\sigma}} a_{\uparrow}^{\dagger} d_{\sigma} + \delta_{\bar{\sigma}\bar{\sigma}} a_{\uparrow} d_{\bar{\sigma}}^{\dagger} d_{\sigma} - \delta_{\bar{\sigma}\bar{\sigma}} a_{\uparrow} n_{d\bar{\sigma}} \right) \tag{B.134}$$

$$\left[d_{\sigma} n_{d\bar{\sigma}}, \Delta \sum_{\bar{\sigma}} (d_{\bar{\sigma}} a_{\uparrow} + a_{\uparrow} d_{\bar{\sigma}}^{\dagger}) \right] = \Delta \sum_{\bar{\sigma}} [d_{\sigma} n_{d\bar{\sigma}}, d_{\bar{\sigma}} a_{\uparrow}] + \Delta \sum_{\bar{\sigma}} [d_{\sigma} n_{d\bar{\sigma}}, a_{\uparrow} d_{\bar{\sigma}}^{\dagger}], \tag{B.135}$$

$$\begin{aligned}
 \Delta \sum_{\bar{\sigma}} [d_{\sigma} n_{d\bar{\sigma}}, d_{\bar{\sigma}} a_{\uparrow}] &= \Delta \sum_{\bar{\sigma}} \left(d_{\sigma} d_{\bar{\sigma}}^{\dagger} d_{\bar{\sigma}} d_{\bar{\sigma}} a_{\uparrow} - d_{\bar{\sigma}} a_{\uparrow} d_{\sigma} d_{\bar{\sigma}}^{\dagger} d_{\bar{\sigma}} \right) \\
 &= \Delta \sum_{\bar{\sigma}} \left(-d_{\sigma} d_{\bar{\sigma}}^{\dagger} d_{\bar{\sigma}} d_{\bar{\sigma}} a_{\uparrow} + d_{\bar{\sigma}} d_{\sigma} d_{\bar{\sigma}}^{\dagger} d_{\bar{\sigma}} a_{\uparrow} \right) \\
 &= \Delta \sum_{\bar{\sigma}} \left(-d_{\sigma} \left(\delta_{\bar{\sigma}\bar{\sigma}} - d_{\bar{\sigma}} d_{\bar{\sigma}}^{\dagger} \right) d_{\bar{\sigma}} a_{\uparrow} + d_{\bar{\sigma}} d_{\sigma} d_{\bar{\sigma}}^{\dagger} d_{\bar{\sigma}} a_{\uparrow} \right) \\
 &= \Delta \sum_{\bar{\sigma}} \left(-\delta_{\bar{\sigma}\bar{\sigma}} d_{\sigma} d_{\bar{\sigma}} a_{\uparrow} - d_{\bar{\sigma}} d_{\sigma} d_{\bar{\sigma}}^{\dagger} d_{\bar{\sigma}} a_{\uparrow} + d_{\bar{\sigma}} d_{\sigma} d_{\bar{\sigma}}^{\dagger} d_{\bar{\sigma}} a_{\uparrow} \right) \\
 &= \Delta \sum_{\bar{\sigma}} \left(-\delta_{\bar{\sigma}\bar{\sigma}} d_{\bar{\sigma}} a_{\uparrow} d_{\sigma} \right), \tag{B.136}
 \end{aligned}$$

$$\begin{aligned}
 \Delta \sum_{\bar{\sigma}} [d_{\sigma} n_{d\bar{\sigma}}, a_{\uparrow}^{\dagger} d_{\bar{\sigma}}^{\dagger}] &= \Delta \sum_{\bar{\sigma}} \left(d_{\sigma} d_{\bar{\sigma}}^{\dagger} d_{\bar{\sigma}} a_{\uparrow}^{\dagger} d_{\bar{\sigma}}^{\dagger} - a_{\uparrow}^{\dagger} d_{\bar{\sigma}}^{\dagger} d_{\sigma} d_{\bar{\sigma}}^{\dagger} d_{\bar{\sigma}} \right) \\
 &= \Delta \sum_{\bar{\sigma}} \left(-a_{\uparrow}^{\dagger} d_{\sigma} d_{\bar{\sigma}}^{\dagger} \left(\delta_{\bar{\sigma}\bar{\sigma}} - d_{\bar{\sigma}}^{\dagger} d_{\bar{\sigma}} \right) - a_{\uparrow}^{\dagger} d_{\bar{\sigma}}^{\dagger} d_{\sigma} d_{\bar{\sigma}}^{\dagger} d_{\bar{\sigma}} \right) \\
 &= \Delta \sum_{\bar{\sigma}} \left(-\delta_{\bar{\sigma}\bar{\sigma}} a_{\uparrow}^{\dagger} d_{\sigma} d_{\bar{\sigma}}^{\dagger} - a_{\uparrow}^{\dagger} \left(\delta_{\bar{\sigma}\sigma} - d_{\bar{\sigma}}^{\dagger} d_{\sigma} \right) d_{\bar{\sigma}}^{\dagger} d_{\bar{\sigma}} - a_{\uparrow}^{\dagger} d_{\bar{\sigma}}^{\dagger} d_{\sigma} d_{\bar{\sigma}}^{\dagger} d_{\bar{\sigma}} \right) \\
 &= \Delta \sum_{\bar{\sigma}} \left(-\delta_{\bar{\sigma}\bar{\sigma}} a_{\uparrow}^{\dagger} d_{\sigma} d_{\bar{\sigma}}^{\dagger} - \delta_{\bar{\sigma}\sigma} d_{\bar{\sigma}}^{\dagger} d_{\bar{\sigma}} a_{\uparrow}^{\dagger} + a_{\uparrow}^{\dagger} d_{\bar{\sigma}}^{\dagger} d_{\sigma} d_{\bar{\sigma}}^{\dagger} d_{\bar{\sigma}} - a_{\uparrow}^{\dagger} d_{\bar{\sigma}}^{\dagger} d_{\sigma} d_{\bar{\sigma}}^{\dagger} d_{\bar{\sigma}} \right) \\
 &= \Delta \sum_{\bar{\sigma}} \left(\delta_{\bar{\sigma}\bar{\sigma}} a_{\uparrow}^{\dagger} d_{\bar{\sigma}}^{\dagger} d_{\sigma} - \delta_{\bar{\sigma}\sigma} d_{\bar{\sigma}}^{\dagger} d_{\bar{\sigma}} a_{\uparrow}^{\dagger} \right), \tag{B.137}
 \end{aligned}$$

$$\left[d_{\sigma} n_{d\bar{\sigma}}, \Delta \sum_{\bar{\sigma}} (d_{\bar{\sigma}} a_{\uparrow} + a_{\uparrow}^{\dagger} d_{\bar{\sigma}}^{\dagger}) \right] = \Delta \sum_{\bar{\sigma}} \left(-\delta_{\bar{\sigma}\bar{\sigma}} d_{\bar{\sigma}} a_{\uparrow} d_{\sigma} + \delta_{\bar{\sigma}\bar{\sigma}} a_{\uparrow}^{\dagger} d_{\bar{\sigma}}^{\dagger} d_{\sigma} - \delta_{\bar{\sigma}\sigma} a_{\uparrow}^{\dagger} n_{d\bar{\sigma}} \right). \tag{B.138}$$

Thus,

$$\begin{aligned}
 (\omega^{+} - \varepsilon_{d\sigma} - U) G_{d_{\sigma} n_{d\bar{\sigma}}, d_{\sigma}}^r(\omega) &= \langle n_{d\bar{\sigma}} \rangle \\
 &+ \sqrt{2V} \sum_{\mathbf{k}} \left[G_{d_{\bar{\sigma}}^{\dagger} e_{\mathbf{k}\bar{\sigma}} d_{\sigma} d_{\sigma}}^r(\omega) - G_{e_{\mathbf{k}\bar{\sigma}}^{\dagger} d_{\bar{\sigma}} d_{\sigma}, d_{\sigma}}^r(\omega) + G_{e_{\mathbf{k}\sigma}^{\dagger} n_{d\bar{\sigma}}, d_{\sigma}}^r(\omega) \right] \\
 &+ t_{hp} \sum_{\bar{\sigma}} \delta_{\bar{\sigma}\bar{\sigma}} \langle \langle a_{\uparrow} d_{\bar{\sigma}}^{\dagger} d_{\sigma}; d_{\bar{\sigma}}^{\dagger} \rangle \rangle - t_{hp} \sum_{\bar{\sigma}} \delta_{\bar{\sigma}\bar{\sigma}} \langle \langle d_{\bar{\sigma}} a_{\uparrow}^{\dagger} d_{\sigma}; d_{\bar{\sigma}}^{\dagger} \rangle \rangle \\
 &- t_{hp} \sum_{\bar{\sigma}} \delta_{\bar{\sigma}\sigma} \langle \langle a_{\uparrow} n_{d\bar{\sigma}}; d_{\bar{\sigma}}^{\dagger} \rangle \rangle \\
 &+ \Delta \sum_{\bar{\sigma}} \delta_{\bar{\sigma}\bar{\sigma}} \langle \langle a_{\uparrow}^{\dagger} d_{\bar{\sigma}}^{\dagger} d_{\sigma}; d_{\bar{\sigma}}^{\dagger} \rangle \rangle - \Delta \sum_{\bar{\sigma}} \delta_{\bar{\sigma}\bar{\sigma}} \langle \langle d_{\bar{\sigma}} a_{\uparrow}^{\dagger} d_{\sigma}; d_{\bar{\sigma}}^{\dagger} \rangle \rangle \\
 &- \Delta \sum_{\bar{\sigma}} \delta_{\bar{\sigma}\sigma} \langle \langle a_{\uparrow}^{\dagger} d_{\bar{\sigma}}^{\dagger} d_{\bar{\sigma}}; d_{\bar{\sigma}}^{\dagger} \rangle \rangle \tag{B.139}
 \end{aligned}$$

$$\begin{aligned}
(\omega^+ - \varepsilon_{d\sigma} - U)G_{d_\sigma n_{d\bar{\sigma}}, d_\sigma}^r(\omega) &= \langle n_{d\bar{\sigma}} \rangle \\
&+ \sqrt{2V} \sum_{\mathbf{k}} \left[G_{d_\sigma^\dagger e_{\mathbf{k}\bar{\sigma}} d_\sigma d_\sigma}^r(\omega) - G_{e_{\mathbf{k}\bar{\sigma}}^\dagger d_\sigma d_\sigma, d_\sigma}^r(\omega) + G_{e_{\mathbf{k}\bar{\sigma}} n_{d\bar{\sigma}}, d_\sigma}^r(\omega) \right] \\
&+ t_{hp} \sum_{\bar{\sigma}} \delta_{\bar{\sigma}\bar{\sigma}} G_{a_\uparrow d_\sigma^\dagger d_\sigma d_\sigma}^r(\omega) - t_{hp} \sum_{\bar{\sigma}} \delta_{\bar{\sigma}\bar{\sigma}} G_{d_\sigma a_\uparrow^\dagger d_\sigma d_\sigma}^r(\omega) \\
&- t_{hp} \sum_{\bar{\sigma}} \delta_{\bar{\sigma}\bar{\sigma}} G_{a_\uparrow n_{d\bar{\sigma}} d_\sigma}^r(\omega) \\
&+ \Delta \sum_{\bar{\sigma}} \delta_{\bar{\sigma}\bar{\sigma}} G_{a_\uparrow^\dagger d_\sigma^\dagger d_\sigma; d_\sigma}^r(\omega) - \Delta \sum_{\bar{\sigma}} \delta_{\bar{\sigma}\bar{\sigma}} G_{d_\sigma a_\uparrow d_\sigma}^r(\omega) \\
&- \Delta \sum_{\bar{\sigma}} \delta_{\bar{\sigma}\bar{\sigma}} G_{a_\uparrow^\dagger n_{d\bar{\sigma}} d_\sigma}^r(\omega) \tag{B.140}
\end{aligned}$$

$$\begin{aligned}
(\omega^+ - \varepsilon_{d\sigma} - U)G_{d_\sigma n_{d\bar{\sigma}}, d_\sigma}^r(\omega) &= \langle n_{d\bar{\sigma}} \rangle \\
&+ \sqrt{2V} \sum_{\mathbf{k}} \left[G_{d_\sigma^\dagger e_{\mathbf{k}\bar{\sigma}} d_\sigma d_\sigma}^r(\omega) - G_{e_{\mathbf{k}\bar{\sigma}}^\dagger d_\sigma d_\sigma, d_\sigma}^r(\omega) + G_{e_{\mathbf{k}\bar{\sigma}} n_{d\bar{\sigma}}, d_\sigma}^r(\omega) \right] \\
&+ t_{hp} \sum_{\bar{\sigma}} \left[\delta_{\bar{\sigma}\bar{\sigma}} G_{a_\uparrow d_\sigma^\dagger d_\sigma d_\sigma}^r(\omega) - \delta_{\bar{\sigma}\bar{\sigma}} G_{d_\sigma a_\uparrow^\dagger d_\sigma d_\sigma}^r(\omega) - \delta_{\bar{\sigma}\bar{\sigma}} G_{a_\uparrow n_{d\bar{\sigma}} d_\sigma}^r(\omega) \right] \\
&+ \Delta \sum_{\bar{\sigma}} \left[\delta_{\bar{\sigma}\bar{\sigma}} G_{a_\uparrow^\dagger d_\sigma^\dagger d_\sigma; d_\sigma}^r(\omega) - \delta_{\bar{\sigma}\bar{\sigma}} G_{d_\sigma a_\uparrow d_\sigma}^r(\omega) - \delta_{\bar{\sigma}\bar{\sigma}} G_{a_\uparrow^\dagger n_{d\bar{\sigma}} d_\sigma}^r(\omega) \right] \tag{B.141}
\end{aligned}$$

We draw attention for this point of the calculus, wherein we will apply the first step of Hubbard-I approximation, consisting of truncate the following many-particle Green's functions:

$$G_{d_\sigma^\dagger e_{\mathbf{k}\bar{\sigma}} d_\sigma d_\sigma}^r(\omega) = \langle d_\sigma^\dagger e_{\mathbf{k}\bar{\sigma}} \rangle G_{d_\sigma d_\sigma}^r(\omega), \tag{B.142}$$

$$G_{e_{\mathbf{k}\bar{\sigma}}^\dagger d_\sigma d_\sigma, d_\sigma}^r(\omega) = \langle e_{\mathbf{k}\bar{\sigma}}^\dagger d_\sigma \rangle G_{d_\sigma d_\sigma}^r(\omega), \tag{B.143}$$

$$G_{a_\uparrow d_\sigma^\dagger d_\sigma d_\sigma}^r(\omega) = \langle a_\uparrow d_\sigma^\dagger \rangle G_{d_\sigma d_\sigma}^r(\omega), \tag{B.144}$$

$$G_{d_\sigma a_\uparrow^\dagger d_\sigma d_\sigma}^r(\omega) = \langle d_\sigma a_\uparrow^\dagger \rangle G_{d_\sigma d_\sigma}^r(\omega), \tag{B.145}$$

$$G_{a_\uparrow^\dagger d_\sigma^\dagger d_\sigma; d_\sigma}^r(\omega) = \langle a_\uparrow^\dagger d_\sigma^\dagger \rangle G_{d_\sigma d_\sigma}^r(\omega), \tag{B.146}$$

$$G_{d_\sigma a_\uparrow d_\sigma d_\sigma}^r(\omega) = \langle d_\sigma a_\uparrow \rangle G_{d_\sigma d_\sigma}^r(\omega). \tag{B.147}$$

Then,

$$\begin{aligned}
(\omega^+ - \varepsilon_{d\sigma} - U)G_{d_\sigma n_{d\bar{\sigma}}, d_\sigma}^r(\omega) &= \langle n_{d\bar{\sigma}} \rangle \\
&+ \sqrt{2V} \sum_{\mathbf{k}} \left[\langle d_{\bar{\sigma}}^\dagger e_{\mathbf{k}\bar{\sigma}} \rangle G_{d_\sigma d_\sigma}^r(\omega) - \langle e_{\mathbf{k}\bar{\sigma}}^\dagger d_{\bar{\sigma}} \rangle G_{d_\sigma d_\sigma}^r(\omega) + G_{e_{\mathbf{k}\sigma} n_{d\bar{\sigma}}, d_\sigma}^r(\omega) \right] \\
&+ t_{hp} \sum_{\bar{\sigma}} \left[\delta_{\bar{\sigma}\bar{\sigma}} \langle a_\uparrow d_{\bar{\sigma}}^\dagger \rangle G_{d_\sigma d_\sigma}^r(\omega) - \delta_{\bar{\sigma}\bar{\sigma}} \langle d_{\bar{\sigma}} a_\uparrow^\dagger \rangle G_{d_\sigma d_\sigma}^r(\omega) - \delta_{\bar{\sigma}\sigma} G_{a_\uparrow n_{d\bar{\sigma}}, d_\sigma}^r(\omega) \right] \\
&+ \Delta \sum_{\bar{\sigma}} \left[\delta_{\bar{\sigma}\bar{\sigma}} \langle a_\uparrow^\dagger d_{\bar{\sigma}}^\dagger \rangle G_{d_\sigma d_\sigma}^r(\omega) - \delta_{\bar{\sigma}\bar{\sigma}} \langle d_{\bar{\sigma}} a_\uparrow \rangle G_{d_\sigma d_\sigma}^r(\omega) - \delta_{\bar{\sigma}\sigma} G_{a_\uparrow^\dagger n_{d\bar{\sigma}}, d_\sigma}^r(\omega) \right]
\end{aligned} \tag{B.148}$$

However,

$$\langle d_{\bar{\sigma}}^\dagger e_{\mathbf{k}\bar{\sigma}} \rangle G_{d_\sigma d_\sigma}^r(\omega) = \langle e_{\mathbf{k}\bar{\sigma}}^\dagger d_{\bar{\sigma}} \rangle G_{d_\sigma d_\sigma}^r(\omega) \tag{B.149}$$

$$\delta_{\bar{\sigma}\bar{\sigma}} \langle a_\uparrow d_{\bar{\sigma}}^\dagger \rangle G_{d_\sigma d_\sigma}^r(\omega) = \delta_{\bar{\sigma}\bar{\sigma}} \langle d_{\bar{\sigma}} a_\uparrow^\dagger \rangle G_{d_\sigma d_\sigma}^r(\omega) \tag{B.150}$$

$$\delta_{\bar{\sigma}\bar{\sigma}} \langle a_\uparrow^\dagger d_{\bar{\sigma}}^\dagger \rangle G_{d_\sigma d_\sigma}^r(\omega) = \delta_{\bar{\sigma}\bar{\sigma}} \langle d_{\bar{\sigma}} a_\uparrow \rangle G_{d_\sigma d_\sigma}^r(\omega) \tag{B.151}$$

Thus,

$$\begin{aligned}
(\omega^+ - \varepsilon_{d\sigma} - U)G_{d_\sigma n_{d\bar{\sigma}}, d_\sigma}^r(\omega) &= \langle n_{d\bar{\sigma}} \rangle + \sqrt{2V} \sum_{\mathbf{k}} G_{e_{\mathbf{k}\sigma} n_{d\bar{\sigma}}, d_\sigma}^r(\omega) - t_{hp} \sum_{\bar{\sigma}} \delta_{\bar{\sigma}\sigma} G_{a_\uparrow n_{d\bar{\sigma}}, d_\sigma}^r(\omega) \\
&- \Delta \sum_{\bar{\sigma}} \delta_{\bar{\sigma}\sigma} G_{a_\uparrow^\dagger n_{d\bar{\sigma}}, d_\sigma}^r(\omega)
\end{aligned} \tag{B.152}$$

Following the Hubbard-I proposal, let us apply the EOM to obtain $G_{e_{\mathbf{k}\sigma} n_{d\bar{\sigma}}, d_\sigma}^r(\omega)$:

$$(\omega + \eta^+)G_{e_{\mathbf{k}\sigma} n_{d\bar{\sigma}}, d_\sigma}^r(\omega) = \langle \{e_{\mathbf{k}\sigma} n_{d\bar{\sigma}}, d_\sigma^\dagger\} \rangle + \langle \langle [e_{\mathbf{k}\sigma} n_{d\bar{\sigma}}, \mathcal{H}_e]; d_\sigma^\dagger \rangle \rangle \tag{B.153}$$

$$\begin{aligned}
\langle \{e_{\mathbf{k}\sigma} n_{d\bar{\sigma}}, d_\sigma^\dagger\} \rangle &= \langle e_{\mathbf{k}\sigma} n_{d\bar{\sigma}} d_\sigma^\dagger + d_\sigma^\dagger e_{\mathbf{k}\sigma} n_{d\bar{\sigma}} \rangle \\
&= \langle e_{\mathbf{k}\sigma} d_\sigma^\dagger d_{\bar{\sigma}} d_\sigma^\dagger + d_\sigma^\dagger e_{\mathbf{k}\sigma} n_{d\bar{\sigma}} \rangle \\
&= \langle -d_\sigma^\dagger e_{\mathbf{k}\sigma} d_{\bar{\sigma}}^\dagger d_{\bar{\sigma}} + d_\sigma^\dagger e_{\mathbf{k}\sigma} n_{d\bar{\sigma}} \rangle \\
&= 0.
\end{aligned} \tag{B.154}$$

$$(\omega + \eta^+)G_{e_{\mathbf{k}\sigma} n_{d\bar{\sigma}}, d_\sigma}^r(\omega) = \langle \langle [e_{\mathbf{k}\sigma} n_{d\bar{\sigma}}, \mathcal{H}_e]; d_\sigma^\dagger \rangle \rangle \tag{B.155}$$

$$[e_{\mathbf{k}\sigma} n_{d\bar{\sigma}}, \mathcal{H}_e] = [e_{\mathbf{k}\sigma} n_{d\bar{\sigma}}, \mathcal{H}_{\text{lead}}] + [e_{\mathbf{k}\sigma} n_{d\bar{\sigma}}, \mathcal{H}_{\text{dot}}] + [e_{\mathbf{k}\sigma} n_{d\bar{\sigma}}, \mathcal{H}_{\text{dot-lead}}] + [e_{\mathbf{k}\sigma} n_{d\bar{\sigma}}, \mathcal{H}_M] \tag{B.156}$$

$$[e_{\mathbf{k}\sigma}n_{d\bar{\sigma}}, \mathcal{H}_{\text{lead}}] = [e_{\mathbf{k}\sigma}n_{d\bar{\sigma}}, \sum_{\mathbf{p}\bar{\sigma}} \varepsilon_{\mathbf{p}\bar{\sigma}} e_{\mathbf{p}\bar{\sigma}}^\dagger e_{\mathbf{p}\bar{\sigma}}] + [e_{\mathbf{k}\sigma}n_{d\bar{\sigma}}, V_{SD} \sum_{\mathbf{p}, \mathbf{q}\bar{\sigma}} e_{\mathbf{p}\bar{\sigma}}^\dagger e_{\mathbf{q}\bar{\sigma}}] \quad (\text{B.157})$$

$$\begin{aligned} [e_{\mathbf{k}\sigma}n_{d\bar{\sigma}}, \sum_{\mathbf{p}\bar{\sigma}} \varepsilon_{\mathbf{p}\bar{\sigma}} e_{\mathbf{p}\bar{\sigma}}^\dagger e_{\mathbf{p}\bar{\sigma}}] &= \sum_{\mathbf{p}\bar{\sigma}} \varepsilon_{\mathbf{p}\bar{\sigma}} \left(e_{\mathbf{k}\sigma}n_{d\bar{\sigma}} e_{\mathbf{p}\bar{\sigma}}^\dagger e_{\mathbf{p}\bar{\sigma}} - e_{\mathbf{p}\bar{\sigma}}^\dagger e_{\mathbf{p}\bar{\sigma}} e_{\mathbf{k}\sigma}n_{d\bar{\sigma}} \right) \\ &= \sum_{\mathbf{p}\bar{\sigma}} \varepsilon_{\mathbf{p}\bar{\sigma}} \left(e_{\mathbf{k}\sigma} e_{\mathbf{p}\bar{\sigma}}^\dagger e_{\mathbf{p}\bar{\sigma}} n_{d\bar{\sigma}} - e_{\mathbf{p}\bar{\sigma}}^\dagger e_{\mathbf{p}\bar{\sigma}} e_{\mathbf{k}\sigma} n_{d\bar{\sigma}} \right) \\ &= \sum_{\mathbf{p}\bar{\sigma}} \varepsilon_{\mathbf{p}\bar{\sigma}} \left(e_{\mathbf{k}\sigma} e_{\mathbf{p}\bar{\sigma}}^\dagger e_{\mathbf{p}\bar{\sigma}} n_{d\bar{\sigma}} + e_{\mathbf{p}\bar{\sigma}}^\dagger e_{\mathbf{k}\sigma} e_{\mathbf{p}\bar{\sigma}} n_{d\bar{\sigma}} \right) \\ &= \sum_{\mathbf{p}\bar{\sigma}} \varepsilon_{\mathbf{p}\bar{\sigma}} \left(e_{\mathbf{k}\sigma} e_{\mathbf{p}\bar{\sigma}}^\dagger e_{\mathbf{p}\bar{\sigma}} n_{d\bar{\sigma}} + \left(\delta_{\mathbf{p}\mathbf{k}} \delta_{\bar{\sigma}\sigma} - e_{\mathbf{k}\sigma} e_{\mathbf{p}\bar{\sigma}}^\dagger \right) e_{\mathbf{p}\bar{\sigma}} n_{d\bar{\sigma}} \right) \\ &= \sum_{\mathbf{p}\bar{\sigma}} \varepsilon_{\mathbf{p}\bar{\sigma}} \left(e_{\mathbf{k}\sigma} e_{\mathbf{p}\bar{\sigma}}^\dagger e_{\mathbf{p}\bar{\sigma}} n_{d\bar{\sigma}} + \delta_{\mathbf{p}\mathbf{k}} \delta_{\bar{\sigma}\sigma} e_{\mathbf{p}\bar{\sigma}} n_{d\bar{\sigma}} - e_{\mathbf{k}\sigma} e_{\mathbf{p}\bar{\sigma}}^\dagger e_{\mathbf{p}\bar{\sigma}} n_{d\bar{\sigma}} \right) \\ &= \varepsilon_{\mathbf{k}\sigma} (e_{\mathbf{k}\sigma} n_{d\bar{\sigma}}) \end{aligned} \quad (\text{B.158})$$

$$\begin{aligned} [e_{\mathbf{k}\sigma}n_{d\bar{\sigma}}, V_{SD} \sum_{\mathbf{p}, \mathbf{q}\bar{\sigma}} e_{\mathbf{p}\bar{\sigma}}^\dagger e_{\mathbf{q}\bar{\sigma}}] &= V_{SD} \sum_{\mathbf{p}, \mathbf{q}\bar{\sigma}} \left(e_{\mathbf{k}\sigma}n_{d\bar{\sigma}} e_{\mathbf{p}\bar{\sigma}}^\dagger e_{\mathbf{q}\bar{\sigma}} - e_{\mathbf{p}\bar{\sigma}}^\dagger e_{\mathbf{q}\bar{\sigma}} e_{\mathbf{k}\sigma}n_{d\bar{\sigma}} \right) \\ &= V_{SD} \sum_{\mathbf{p}, \mathbf{q}\bar{\sigma}} \left(e_{\mathbf{k}\sigma} e_{\mathbf{p}\bar{\sigma}}^\dagger e_{\mathbf{q}\bar{\sigma}} n_{d\bar{\sigma}} - e_{\mathbf{p}\bar{\sigma}}^\dagger e_{\mathbf{q}\bar{\sigma}} e_{\mathbf{k}\sigma} n_{d\bar{\sigma}} \right) \\ &= V_{SD} \sum_{\mathbf{p}, \mathbf{q}\bar{\sigma}} \left(e_{\mathbf{k}\sigma} e_{\mathbf{p}\bar{\sigma}}^\dagger e_{\mathbf{q}\bar{\sigma}} n_{d\bar{\sigma}} + e_{\mathbf{p}\bar{\sigma}}^\dagger e_{\mathbf{k}\sigma} e_{\mathbf{q}\bar{\sigma}} n_{d\bar{\sigma}} \right) \\ &= V_{SD} \sum_{\mathbf{p}, \mathbf{q}\bar{\sigma}} \left(e_{\mathbf{k}\sigma} e_{\mathbf{p}\bar{\sigma}}^\dagger e_{\mathbf{q}\bar{\sigma}} n_{d\bar{\sigma}} + \left(\delta_{\mathbf{p}\mathbf{k}} \delta_{\bar{\sigma}\sigma} - e_{\mathbf{k}\sigma} e_{\mathbf{p}\bar{\sigma}}^\dagger \right) e_{\mathbf{q}\bar{\sigma}} n_{d\bar{\sigma}} \right) \\ &= V_{SD} \sum_{\mathbf{p}, \mathbf{q}\bar{\sigma}} \left(e_{\mathbf{k}\sigma} e_{\mathbf{p}\bar{\sigma}}^\dagger e_{\mathbf{q}\bar{\sigma}} n_{d\bar{\sigma}} + \delta_{\mathbf{p}\mathbf{k}} \delta_{\bar{\sigma}\sigma} e_{\mathbf{q}\bar{\sigma}} n_{d\bar{\sigma}} - e_{\mathbf{k}\sigma} e_{\mathbf{p}\bar{\sigma}}^\dagger e_{\mathbf{q}\bar{\sigma}} n_{d\bar{\sigma}} \right) \\ &= V_{SD} \sum_{\mathbf{q}} (e_{\mathbf{q}\bar{\sigma}} n_{d\bar{\sigma}}). \end{aligned} \quad (\text{B.159})$$

$$[e_{\mathbf{k}\sigma}n_{d\bar{\sigma}}, \mathcal{H}_{\text{dot}}] = [e_{\mathbf{k}\sigma}n_{d\bar{\sigma}}, \sum_{\bar{\sigma}} \varepsilon_{d\bar{\sigma}} d_{\bar{\sigma}}^\dagger d_{\bar{\sigma}}] + [e_{\mathbf{k}\sigma}n_{d\bar{\sigma}}, U n_{d\uparrow} n_{d\downarrow}] \quad (\text{B.160})$$

$$\begin{aligned}
[e_{\mathbf{k}\sigma} n_{d\bar{\sigma}}, \sum_{\bar{\sigma}} \varepsilon_{d\bar{\sigma}} d_{\bar{\sigma}}^{\dagger} d_{\bar{\sigma}}] &= \sum_{\bar{\sigma}} \varepsilon_{d\bar{\sigma}} \left(e_{\mathbf{k}\sigma} n_{d\bar{\sigma}} d_{\bar{\sigma}}^{\dagger} d_{\bar{\sigma}} - d_{\bar{\sigma}}^{\dagger} d_{\bar{\sigma}} e_{\mathbf{k}\sigma} n_{d\bar{\sigma}} \right) \\
&= \sum_{\bar{\sigma}} \varepsilon_{d\bar{\sigma}} \left(e_{\mathbf{k}\sigma} d_{\bar{\sigma}}^{\dagger} d_{\bar{\sigma}} d_{\bar{\sigma}}^{\dagger} d_{\bar{\sigma}} - e_{\mathbf{k}\sigma} d_{\bar{\sigma}}^{\dagger} d_{\bar{\sigma}} n_{d\bar{\sigma}} \right) \\
&= \sum_{\bar{\sigma}} \varepsilon_{d\bar{\sigma}} \left(e_{\mathbf{k}\sigma} d_{\bar{\sigma}}^{\dagger} \left(\delta_{\bar{\sigma}\bar{\sigma}} - d_{\bar{\sigma}}^{\dagger} d_{\bar{\sigma}} \right) d_{\bar{\sigma}} - e_{\mathbf{k}\sigma} d_{\bar{\sigma}}^{\dagger} d_{\bar{\sigma}} n_{d\bar{\sigma}} \right) \\
&= \sum_{\bar{\sigma}} \varepsilon_{d\bar{\sigma}} \left(\delta_{\bar{\sigma}\bar{\sigma}} e_{\mathbf{k}\sigma} d_{\bar{\sigma}}^{\dagger} d_{\bar{\sigma}} - e_{\mathbf{k}\sigma} d_{\bar{\sigma}}^{\dagger} d_{\bar{\sigma}}^{\dagger} d_{\bar{\sigma}} d_{\bar{\sigma}} - e_{\mathbf{k}\sigma} d_{\bar{\sigma}}^{\dagger} d_{\bar{\sigma}} n_{d\bar{\sigma}} \right) \\
&= \sum_{\bar{\sigma}} \varepsilon_{d\bar{\sigma}} \left(\delta_{\bar{\sigma}\bar{\sigma}} e_{\mathbf{k}\sigma} d_{\bar{\sigma}}^{\dagger} d_{\bar{\sigma}} - e_{\mathbf{k}\sigma} d_{\bar{\sigma}}^{\dagger} d_{\bar{\sigma}}^{\dagger} d_{\bar{\sigma}} d_{\bar{\sigma}} - e_{\mathbf{k}\sigma} d_{\bar{\sigma}}^{\dagger} d_{\bar{\sigma}} n_{d\bar{\sigma}} \right) \\
&= \sum_{\bar{\sigma}} \varepsilon_{d\bar{\sigma}} \left(\delta_{\bar{\sigma}\bar{\sigma}} e_{\mathbf{k}\sigma} d_{\bar{\sigma}}^{\dagger} d_{\bar{\sigma}} - e_{\mathbf{k}\sigma} d_{\bar{\sigma}}^{\dagger} \left(\delta_{\bar{\sigma}\bar{\sigma}} - d_{\bar{\sigma}}^{\dagger} d_{\bar{\sigma}} \right) d_{\bar{\sigma}} - e_{\mathbf{k}\sigma} d_{\bar{\sigma}}^{\dagger} d_{\bar{\sigma}} n_{d\bar{\sigma}} \right) \\
&= \sum_{\bar{\sigma}} \varepsilon_{d\bar{\sigma}} \left(\delta_{\bar{\sigma}\bar{\sigma}} e_{\mathbf{k}\sigma} d_{\bar{\sigma}}^{\dagger} d_{\bar{\sigma}} - \delta_{\bar{\sigma}\bar{\sigma}} e_{\mathbf{k}\sigma} d_{\bar{\sigma}}^{\dagger} d_{\bar{\sigma}} + e_{\mathbf{k}\sigma} d_{\bar{\sigma}}^{\dagger} d_{\bar{\sigma}} d_{\bar{\sigma}}^{\dagger} d_{\bar{\sigma}} - e_{\mathbf{k}\sigma} d_{\bar{\sigma}}^{\dagger} d_{\bar{\sigma}} n_{d\bar{\sigma}} \right) \\
&= \sum_{\bar{\sigma}} \varepsilon_{d\bar{\sigma}} \left(\delta_{\bar{\sigma}\bar{\sigma}} e_{\mathbf{k}\sigma} d_{\bar{\sigma}}^{\dagger} d_{\bar{\sigma}} - \delta_{\bar{\sigma}\bar{\sigma}} e_{\mathbf{k}\sigma} d_{\bar{\sigma}}^{\dagger} d_{\bar{\sigma}} \right) \\
&= \varepsilon_{d\bar{\sigma}} \left(e_{\mathbf{k}\bar{\sigma}} d_{\bar{\sigma}}^{\dagger} d_{\bar{\sigma}} - e_{\mathbf{k}\bar{\sigma}} d_{\bar{\sigma}}^{\dagger} d_{\bar{\sigma}} \right) = 0. \tag{B.161}
\end{aligned}$$

$$\begin{aligned}
 I : \sqrt{2}V \sum_{\mathbf{k}\bar{\sigma}} [e_{\mathbf{k}\sigma} n_{d\bar{\sigma}}, e_{\mathbf{k}\bar{\sigma}}^\dagger d_{\bar{\sigma}}] &= \sqrt{2}V \sum_{\mathbf{p}\bar{\sigma}} \left(e_{\mathbf{k}\sigma} n_{d\bar{\sigma}} e_{\mathbf{p}\bar{\sigma}}^\dagger d_{\bar{\sigma}} - e_{\mathbf{p}\bar{\sigma}}^\dagger d_{\bar{\sigma}} e_{\mathbf{k}\sigma} n_{d\bar{\sigma}} \right) \\
 &= \sqrt{2}V \sum_{\mathbf{p}\bar{\sigma}} \left(e_{\mathbf{k}\sigma} d_{\bar{\sigma}}^\dagger d_{\bar{\sigma}} e_{\mathbf{p}\bar{\sigma}}^\dagger d_{\bar{\sigma}} + e_{\mathbf{p}\bar{\sigma}}^\dagger e_{\mathbf{k}\sigma} d_{\bar{\sigma}} n_{d\bar{\sigma}} \right) \\
 &= \sqrt{2}V \sum_{\mathbf{p}\bar{\sigma}} \left(e_{\mathbf{k}\sigma} e_{\mathbf{p}\bar{\sigma}}^\dagger d_{\bar{\sigma}}^\dagger d_{\bar{\sigma}} d_{\bar{\sigma}} + e_{\mathbf{p}\bar{\sigma}}^\dagger e_{\mathbf{k}\sigma} d_{\bar{\sigma}} n_{d\bar{\sigma}} \right) \\
 &= \sqrt{2}V \sum_{\mathbf{p}\bar{\sigma}} \left(-e_{\mathbf{k}\sigma} e_{\mathbf{p}\bar{\sigma}}^\dagger \left(\delta_{\bar{\sigma}\bar{\sigma}} - d_{\bar{\sigma}} d_{\bar{\sigma}}^\dagger \right) d_{\bar{\sigma}} + e_{\mathbf{p}\bar{\sigma}}^\dagger e_{\mathbf{k}\sigma} d_{\bar{\sigma}} n_{d\bar{\sigma}} \right) \\
 &= \sqrt{2}V \sum_{\mathbf{p}\bar{\sigma}} \left(-\delta_{\bar{\sigma}\bar{\sigma}} e_{\mathbf{k}\sigma} e_{\mathbf{p}\bar{\sigma}}^\dagger d_{\bar{\sigma}} + e_{\mathbf{k}\sigma} e_{\mathbf{p}\bar{\sigma}}^\dagger d_{\bar{\sigma}} d_{\bar{\sigma}}^\dagger d_{\bar{\sigma}} + e_{\mathbf{p}\bar{\sigma}}^\dagger e_{\mathbf{k}\sigma} d_{\bar{\sigma}} n_{d\bar{\sigma}} \right) \\
 &= \sqrt{2}V \sum_{\mathbf{p}\bar{\sigma}} \left(-\delta_{\bar{\sigma}\bar{\sigma}} e_{\mathbf{k}\sigma} e_{\mathbf{p}\bar{\sigma}}^\dagger d_{\bar{\sigma}} + \left(e_{\mathbf{k}\sigma} e_{\mathbf{p}\bar{\sigma}}^\dagger + e_{\mathbf{p}\bar{\sigma}}^\dagger e_{\mathbf{k}\sigma} \right) d_{\bar{\sigma}} d_{\bar{\sigma}}^\dagger d_{\bar{\sigma}} \right) \\
 &= \sqrt{2}V \sum_{\mathbf{p}\bar{\sigma}} \left(-\delta_{\bar{\sigma}\bar{\sigma}} e_{\mathbf{k}\sigma} e_{\mathbf{p}\bar{\sigma}}^\dagger d_{\bar{\sigma}} + \delta_{\mathbf{k}\mathbf{p}} \delta_{\bar{\sigma}\bar{\sigma}} d_{\bar{\sigma}} d_{\bar{\sigma}}^\dagger d_{\bar{\sigma}} \right) \\
 &= \sqrt{2}V \left(-e_{\mathbf{k}\bar{\sigma}}^\dagger d_{\bar{\sigma}} e_{\mathbf{k}\sigma} + d_{\sigma} d_{\bar{\sigma}}^\dagger d_{\bar{\sigma}} \right). \tag{B.164}
 \end{aligned}$$

$$\begin{aligned}
 II : \sqrt{2}V \sum_{\mathbf{p}\bar{\sigma}} [e_{\mathbf{k}\sigma} n_{d\bar{\sigma}}, d_{\bar{\sigma}}^\dagger e_{\mathbf{p}\bar{\sigma}}] &= \sqrt{2}V \sum_{\mathbf{p}\bar{\sigma}} \left(e_{\mathbf{k}\sigma} n_{d\bar{\sigma}} d_{\bar{\sigma}}^\dagger e_{\mathbf{p}\bar{\sigma}} - d_{\bar{\sigma}}^\dagger e_{\mathbf{p}\bar{\sigma}} e_{\mathbf{k}\sigma} n_{d\bar{\sigma}} \right) \\
 &= \sqrt{2}V \sum_{\mathbf{p}\bar{\sigma}} \left(e_{\mathbf{p}\bar{\sigma}} e_{\mathbf{k}\sigma} d_{\bar{\sigma}}^\dagger d_{\bar{\sigma}} d_{\bar{\sigma}}^\dagger - e_{\mathbf{p}\bar{\sigma}} e_{\mathbf{k}\sigma} d_{\bar{\sigma}}^\dagger n_{d\bar{\sigma}} \right) \\
 &= \sqrt{2}V \sum_{\mathbf{p}\bar{\sigma}} \left(e_{\mathbf{p}\bar{\sigma}} e_{\mathbf{k}\sigma} d_{\bar{\sigma}}^\dagger \left(\delta_{\bar{\sigma}\bar{\sigma}} - d_{\bar{\sigma}}^\dagger d_{\bar{\sigma}} \right) - e_{\mathbf{p}\bar{\sigma}} e_{\mathbf{k}\sigma} d_{\bar{\sigma}}^\dagger n_{d\bar{\sigma}} \right) \\
 &= \sqrt{2}V \sum_{\mathbf{p}\bar{\sigma}} \left(\delta_{\bar{\sigma}\bar{\sigma}} e_{\mathbf{p}\bar{\sigma}} e_{\mathbf{k}\sigma} d_{\bar{\sigma}}^\dagger - e_{\mathbf{p}\bar{\sigma}} e_{\mathbf{k}\sigma} d_{\bar{\sigma}}^\dagger d_{\bar{\sigma}}^\dagger d_{\bar{\sigma}} - e_{\mathbf{p}\bar{\sigma}} e_{\mathbf{k}\sigma} d_{\bar{\sigma}}^\dagger n_{d\bar{\sigma}} \right) \\
 &= \sqrt{2}V \sum_{\mathbf{p}\bar{\sigma}} \left(\delta_{\bar{\sigma}\bar{\sigma}} e_{\mathbf{p}\bar{\sigma}} e_{\mathbf{k}\sigma} d_{\bar{\sigma}}^\dagger + e_{\mathbf{p}\bar{\sigma}} e_{\mathbf{k}\sigma} d_{\bar{\sigma}}^\dagger n_{d\bar{\sigma}} - e_{\mathbf{p}\bar{\sigma}} e_{\mathbf{k}\sigma} d_{\bar{\sigma}}^\dagger n_{d\bar{\sigma}} \right) \\
 &= \sqrt{2}V \sum_{\mathbf{p}\bar{\sigma}} \left(\delta_{\bar{\sigma}\bar{\sigma}} e_{\mathbf{p}\bar{\sigma}} e_{\mathbf{k}\sigma} d_{\bar{\sigma}}^\dagger + e_{\mathbf{p}\bar{\sigma}} e_{\mathbf{k}\sigma} d_{\bar{\sigma}}^\dagger n_{d\bar{\sigma}} - e_{\mathbf{p}\bar{\sigma}} e_{\mathbf{k}\sigma} d_{\bar{\sigma}}^\dagger n_{d\bar{\sigma}} \right) \\
 &= \sqrt{2}V \left(d_{\bar{\sigma}}^\dagger e_{\mathbf{k}\bar{\sigma}} e_{\mathbf{k}\sigma} \right). \tag{B.165}
 \end{aligned}$$

$$[e_{\mathbf{k}\sigma} n_{d\bar{\sigma}}, \mathcal{H}_{\text{dot-lead}}] = \sqrt{2}V \left(-e_{\mathbf{k}\bar{\sigma}}^\dagger d_{\bar{\sigma}} e_{\mathbf{k}\sigma} + d_{\sigma} d_{\bar{\sigma}}^\dagger d_{\bar{\sigma}} + d_{\bar{\sigma}}^\dagger e_{\mathbf{k}\bar{\sigma}} e_{\mathbf{k}\sigma} \right) \tag{B.166}$$

$$\begin{aligned}
 (\omega + \eta^+) G_{e_{\mathbf{k}\sigma} n_{d\bar{\sigma}}, d_{\sigma}}^r(\omega) &= \langle\langle \varepsilon_{\mathbf{k}\sigma} (e_{\mathbf{k}\sigma} n_{d\bar{\sigma}}); d_{\sigma}^\dagger \rangle\rangle + \langle\langle V_{SD} \sum_{\mathbf{q}} (e_{\mathbf{q}\sigma} n_{d\bar{\sigma}}); d_{\sigma}^\dagger \rangle\rangle + \langle\langle \sqrt{2}V \left(-e_{\mathbf{k}\bar{\sigma}}^\dagger d_{\bar{\sigma}} e_{\mathbf{k}\sigma} \right); d_{\sigma}^\dagger \rangle\rangle \\
 &+ \langle\langle \sqrt{2}V \left(d_{\sigma} d_{\bar{\sigma}}^\dagger d_{\bar{\sigma}} \right); d_{\sigma}^\dagger \rangle\rangle + \langle\langle \sqrt{2}V \left(d_{\bar{\sigma}}^\dagger e_{\mathbf{k}\bar{\sigma}} e_{\mathbf{k}\sigma} \right); d_{\sigma}^\dagger \rangle\rangle \\
 &+ \langle\langle [e_{\mathbf{k}\sigma} n_{d\bar{\sigma}}, \mathcal{H}_M]; d_{\sigma}^\dagger \rangle\rangle \tag{B.167}
 \end{aligned}$$

$$\begin{aligned}
(\omega - \varepsilon_{\mathbf{k}\sigma} + \eta^+) G_{e_{\mathbf{k}\sigma} n_{d\bar{\sigma}}, d_\sigma}^r(\omega) &= V_{SD} \sum_{\mathbf{k}} G_{e_{\mathbf{k}\sigma} n_{d\bar{\sigma}}, d_\sigma}^r(\omega) - \sqrt{2} V G_{e_{\mathbf{k}\bar{\sigma}}^\dagger d_{\bar{\sigma}} e_{\mathbf{k}\sigma}, d_\sigma}^r(\omega) \\
&+ \sqrt{2} V G_{d_\sigma n_{d\bar{\sigma}}, d_\sigma}^r(\omega) + \sqrt{2} V G_{d_{\bar{\sigma}}^\dagger e_{\mathbf{k}\bar{\sigma}} e_{\mathbf{k}\sigma}, d_\sigma}^r(\omega) \\
&+ \langle\langle [e_{\mathbf{k}\sigma} n_{d\bar{\sigma}}, \mathcal{H}_M]; d_\sigma^\dagger \rangle\rangle
\end{aligned} \tag{B.168}$$

Before calculating the commutation relation of last line of equation above, let us apply the Hubbard-I decoupling as follows:

$$\begin{aligned}
(\omega - \varepsilon_{\mathbf{k}\sigma} + \eta^+) G_{e_{\mathbf{k}\sigma} n_{d\bar{\sigma}}, d_\sigma}^r(\omega) &= V_{SD} \sum_{\mathbf{k}} G_{e_{\mathbf{k}\sigma} n_{d\bar{\sigma}}, d_\sigma}^r(\omega) - \sqrt{2} V \langle e_{\mathbf{k}\bar{\sigma}}^\dagger d_{\bar{\sigma}} \rangle G_{e_{\mathbf{k}\sigma}, d_\sigma}^r(\omega) \\
&+ \sqrt{2} V G_{d_\sigma n_{d\bar{\sigma}}, d_\sigma}^r(\omega) + \sqrt{2} V \langle d_{\bar{\sigma}}^\dagger e_{\mathbf{k}\bar{\sigma}} \rangle G_{e_{\mathbf{k}\sigma}, d_\sigma}^r(\omega) \\
&+ \langle\langle [e_{\mathbf{k}\sigma} n_{d\bar{\sigma}}, \mathcal{H}_M]; d_\sigma^\dagger \rangle\rangle
\end{aligned} \tag{B.169}$$

since $\langle e_{\mathbf{k}\bar{\sigma}}^\dagger d_{\bar{\sigma}} \rangle G_{e_{\mathbf{k}\sigma}, d_\sigma}^r(\omega) = \langle d_{\bar{\sigma}}^\dagger e_{\mathbf{k}\bar{\sigma}} \rangle G_{e_{\mathbf{k}\sigma}, d_\sigma}^r(\omega)$.

$$\begin{aligned}
(\omega - \varepsilon_{\mathbf{k}\sigma} + \eta^+) G_{e_{\mathbf{k}\sigma} n_{d\bar{\sigma}}, d_\sigma}^r(\omega) &= V_{SD} \sum_{\mathbf{k}} G_{e_{\mathbf{k}\sigma} n_{d\bar{\sigma}}, d_\sigma}^r(\omega) + \sqrt{2} V G_{d_\sigma n_{d\bar{\sigma}}, d_\sigma}^r(\omega) \\
&+ \langle\langle [e_{\mathbf{k}\sigma} n_{d\bar{\sigma}}, \mathcal{H}_M]; d_\sigma^\dagger \rangle\rangle
\end{aligned} \tag{B.170}$$

Now, let us calculate $\langle\langle [e_{\mathbf{k}\sigma} n_{d\bar{\sigma}}, \mathcal{H}_M]; d_\sigma^\dagger \rangle\rangle$:

$$\begin{aligned}
[e_{\mathbf{k}\sigma} n_{d\bar{\sigma}}, \mathcal{H}_M] &= \left[e_{\mathbf{k}\sigma} n_{d\bar{\sigma}}, \delta_M \left(a_\uparrow^\dagger a_\uparrow - \frac{1}{2} \right) \right] + \left[e_{\mathbf{k}\sigma} n_{d\bar{\sigma}}, t_{hp} \sum_{\bar{\sigma}} (d_{\bar{\sigma}} a_\uparrow^\dagger + a_\uparrow d_{\bar{\sigma}}^\dagger) \right] \\
&+ \left[e_{\mathbf{k}\sigma} n_{d\bar{\sigma}}, \Delta \sum_{\bar{\sigma}} (d_{\bar{\sigma}} a_\uparrow + a_\uparrow^\dagger d_{\bar{\sigma}}^\dagger) \right]
\end{aligned} \tag{B.171}$$

$$\begin{aligned}
\left[e_{\mathbf{k}\sigma} n_{d\bar{\sigma}}, \delta_M \left(a_\uparrow^\dagger a_\uparrow - \frac{1}{2} \right) \right] &= \delta_M \left(e_{\mathbf{k}\sigma} n_{d\bar{\sigma}} a_\uparrow^\dagger a_\uparrow - a_\uparrow^\dagger a_\uparrow e_{\mathbf{k}\sigma} n_{d\bar{\sigma}} \right) \\
&= \delta_M \left(a_\uparrow^\dagger a_\uparrow e_{\mathbf{k}\sigma} n_{d\bar{\sigma}} - a_\uparrow^\dagger a_\uparrow e_{\mathbf{k}\sigma} n_{d\bar{\sigma}} \right) \\
&= 0.
\end{aligned} \tag{B.172}$$

$$\left[e_{\mathbf{k}\sigma} n_{d\bar{\sigma}}, t_{hp} \sum_{\bar{\sigma}} (d_{\bar{\sigma}} a_\uparrow^\dagger + a_\uparrow d_{\bar{\sigma}}^\dagger) \right] = \underbrace{t_{hp} \sum_{\bar{\sigma}} \left[e_{\mathbf{k}\sigma} n_{d\bar{\sigma}}, d_{\bar{\sigma}} a_\uparrow^\dagger \right]}_I + \underbrace{t_{hp} \sum_{\bar{\sigma}} \left[e_{\mathbf{k}\sigma} n_{d\bar{\sigma}}, a_\uparrow d_{\bar{\sigma}}^\dagger \right]}_{II} \tag{B.173}$$

$$\begin{aligned}
I : t_{hp} \sum_{\bar{\sigma}} \left[e_{\mathbf{k}\sigma} n_{d\bar{\sigma}}, d_{\bar{\sigma}} a_{\uparrow}^{\dagger} \right] &= t_{hp} \sum_{\bar{\sigma}} \left(e_{\mathbf{k}\sigma} n_{d\bar{\sigma}} d_{\bar{\sigma}} a_{\uparrow}^{\dagger} - d_{\bar{\sigma}} a_{\uparrow}^{\dagger} e_{\mathbf{k}\sigma} n_{d\bar{\sigma}} \right) \\
&= t_{hp} \sum_{\bar{\sigma}} \left(e_{\mathbf{k}\sigma} d_{\bar{\sigma}}^{\dagger} d_{\bar{\sigma}} d_{\bar{\sigma}} a_{\uparrow}^{\dagger} - e_{\mathbf{k}\sigma} d_{\bar{\sigma}} a_{\uparrow}^{\dagger} n_{d\bar{\sigma}} \right) \\
&= t_{hp} \sum_{\bar{\sigma}} \left(-e_{\mathbf{k}\sigma} d_{\bar{\sigma}}^{\dagger} d_{\bar{\sigma}} d_{\bar{\sigma}} a_{\uparrow}^{\dagger} - e_{\mathbf{k}\sigma} d_{\bar{\sigma}} a_{\uparrow}^{\dagger} n_{d\bar{\sigma}} \right) \\
&= t_{hp} \sum_{\bar{\sigma}} \left(-e_{\mathbf{k}\sigma} \left(\delta_{\bar{\sigma}\bar{\sigma}} - d_{\bar{\sigma}} d_{\bar{\sigma}}^{\dagger} \right) d_{\bar{\sigma}} a_{\uparrow}^{\dagger} - e_{\mathbf{k}\sigma} d_{\bar{\sigma}} a_{\uparrow}^{\dagger} n_{d\bar{\sigma}} \right) \\
&= t_{hp} \sum_{\bar{\sigma}} \left(-\delta_{\bar{\sigma}\bar{\sigma}} e_{\mathbf{k}\sigma} d_{\bar{\sigma}} a_{\uparrow}^{\dagger} + e_{\mathbf{k}\sigma} d_{\bar{\sigma}} a_{\uparrow}^{\dagger} n_{d\bar{\sigma}} - e_{\mathbf{k}\sigma} d_{\bar{\sigma}} a_{\uparrow}^{\dagger} n_{d\bar{\sigma}} \right) \\
&= t_{hp} \sum_{\bar{\sigma}} \left(-\delta_{\bar{\sigma}\bar{\sigma}} d_{\bar{\sigma}} a_{\uparrow}^{\dagger} e_{\mathbf{k}\sigma} \right). \tag{B.174}
\end{aligned}$$

$$\begin{aligned}
II : t_{hp} \sum_{\bar{\sigma}} \left[e_{\mathbf{k}\sigma} n_{d\bar{\sigma}}, a_{\uparrow} d_{\bar{\sigma}}^{\dagger} \right] &= t_{hp} \sum_{\bar{\sigma}} \left(e_{\mathbf{k}\sigma} n_{d\bar{\sigma}} a_{\uparrow} d_{\bar{\sigma}}^{\dagger} - a_{\uparrow} d_{\bar{\sigma}}^{\dagger} e_{\mathbf{k}\sigma} n_{d\bar{\sigma}} \right) \\
&= t_{hp} \sum_{\bar{\sigma}} \left(-a_{\uparrow} e_{\mathbf{k}\sigma} d_{\bar{\sigma}}^{\dagger} \left(\delta_{\bar{\sigma}\bar{\sigma}} - d_{\bar{\sigma}}^{\dagger} d_{\bar{\sigma}} \right) - a_{\uparrow} d_{\bar{\sigma}}^{\dagger} e_{\mathbf{k}\sigma} n_{d\bar{\sigma}} \right) \\
&= t_{hp} \sum_{\bar{\sigma}} \left(-\delta_{\bar{\sigma}\bar{\sigma}} a_{\uparrow} e_{\mathbf{k}\sigma} d_{\bar{\sigma}}^{\dagger} + a_{\uparrow} d_{\bar{\sigma}}^{\dagger} e_{\mathbf{k}\sigma} d_{\bar{\sigma}}^{\dagger} d_{\bar{\sigma}} - a_{\uparrow} d_{\bar{\sigma}}^{\dagger} e_{\mathbf{k}\sigma} n_{d\bar{\sigma}} \right) \\
&= t_{hp} \sum_{\bar{\sigma}} \left(\delta_{\bar{\sigma}\bar{\sigma}} a_{\uparrow} d_{\bar{\sigma}}^{\dagger} e_{\mathbf{k}\sigma} \right). \tag{B.175}
\end{aligned}$$

$$\left[e_{\mathbf{k}\sigma} n_{d\bar{\sigma}}, t_{hp} \sum_{\bar{\sigma}} (d_{\bar{\sigma}} a_{\uparrow}^{\dagger} + a_{\uparrow} d_{\bar{\sigma}}^{\dagger}) \right] = t_{hp} \sum_{\bar{\sigma}} \delta_{\bar{\sigma}\bar{\sigma}} \left(-d_{\bar{\sigma}} a_{\uparrow}^{\dagger} e_{\mathbf{k}\sigma} + a_{\uparrow} d_{\bar{\sigma}}^{\dagger} e_{\mathbf{k}\sigma} \right). \tag{B.176}$$

$$\left[e_{\mathbf{k}\sigma} n_{d\bar{\sigma}}, \Delta \sum_{\bar{\sigma}} (d_{\bar{\sigma}} a_{\uparrow} + a_{\uparrow} d_{\bar{\sigma}}^{\dagger}) \right] = \underbrace{\Delta \sum_{\bar{\sigma}} [e_{\mathbf{k}\sigma} n_{d\bar{\sigma}}, d_{\bar{\sigma}} a_{\uparrow}]}_I + \underbrace{\Delta \sum_{\bar{\sigma}} [e_{\mathbf{k}\sigma} n_{d\bar{\sigma}}, a_{\uparrow} d_{\bar{\sigma}}^{\dagger}]}_{II} \tag{B.177}$$

$$\begin{aligned}
I : \Delta \sum_{\bar{\sigma}} [e_{\mathbf{k}\sigma} n_{d\bar{\sigma}}, d_{\bar{\sigma}} a_{\uparrow}] &= \Delta \sum_{\bar{\sigma}} \left(e_{\mathbf{k}\sigma} n_{d\bar{\sigma}} d_{\bar{\sigma}} a_{\uparrow} - d_{\bar{\sigma}} a_{\uparrow} e_{\mathbf{k}\sigma} n_{d\bar{\sigma}} \right) \\
&= \Delta \sum_{\bar{\sigma}} \left(-a_{\uparrow} e_{\mathbf{k}\sigma} d_{\bar{\sigma}}^{\dagger} d_{\bar{\sigma}} d_{\bar{\sigma}} - d_{\bar{\sigma}} a_{\uparrow} e_{\mathbf{k}\sigma} n_{d\bar{\sigma}} \right) \\
&= \Delta \sum_{\bar{\sigma}} \left(-a_{\uparrow} e_{\mathbf{k}\sigma} \left(\delta_{\bar{\sigma}\bar{\sigma}} - d_{\bar{\sigma}} d_{\bar{\sigma}}^{\dagger} \right) d_{\bar{\sigma}} - d_{\bar{\sigma}} a_{\uparrow} e_{\mathbf{k}\sigma} n_{d\bar{\sigma}} \right) \\
&= \Delta \sum_{\bar{\sigma}} \left(-\delta_{\bar{\sigma}\bar{\sigma}} a_{\uparrow} e_{\mathbf{k}\sigma} d_{\bar{\sigma}} + d_{\bar{\sigma}} a_{\uparrow} e_{\mathbf{k}\sigma} n_{d\bar{\sigma}} - d_{\bar{\sigma}} a_{\uparrow} e_{\mathbf{k}\sigma} n_{d\bar{\sigma}} \right) \\
&= \Delta \sum_{\bar{\sigma}} \left(\delta_{\bar{\sigma}\bar{\sigma}} a_{\uparrow} d_{\bar{\sigma}} e_{\mathbf{k}\sigma} \right). \tag{B.178}
\end{aligned}$$

$$\begin{aligned}
 II : \Delta \sum_{\tilde{\sigma}} \left[e_{\mathbf{k}\sigma} n_{d\tilde{\sigma}}, a_{\uparrow}^{\dagger} d_{\sigma}^{\dagger} \right] &= \Delta \sum_{\tilde{\sigma}} \left(e_{\mathbf{k}\sigma} n_{d\tilde{\sigma}} a_{\uparrow}^{\dagger} d_{\sigma}^{\dagger} - a_{\uparrow}^{\dagger} d_{\sigma}^{\dagger} e_{\mathbf{k}\sigma} n_{d\tilde{\sigma}} \right) \\
 &= \Delta \sum_{\tilde{\sigma}} \left(-a_{\uparrow}^{\dagger} e_{\mathbf{k}\sigma} d_{\tilde{\sigma}}^{\dagger} d_{\tilde{\sigma}} d_{\sigma}^{\dagger} - a_{\uparrow}^{\dagger} d_{\sigma}^{\dagger} e_{\mathbf{k}\sigma} n_{d\tilde{\sigma}} \right) \\
 &= \Delta \sum_{\tilde{\sigma}} \left(-a_{\uparrow}^{\dagger} e_{\mathbf{k}\sigma} d_{\tilde{\sigma}}^{\dagger} \left(\delta_{\tilde{\sigma}\tilde{\sigma}} - d_{\sigma}^{\dagger} d_{\tilde{\sigma}} \right) - a_{\uparrow}^{\dagger} d_{\sigma}^{\dagger} e_{\mathbf{k}\sigma} n_{d\tilde{\sigma}} \right) \\
 &= \Delta \sum_{\tilde{\sigma}} \left(-\delta_{\tilde{\sigma}\tilde{\sigma}} a_{\uparrow}^{\dagger} e_{\mathbf{k}\sigma} d_{\tilde{\sigma}}^{\dagger} + a_{\uparrow}^{\dagger} e_{\mathbf{k}\sigma} d_{\tilde{\sigma}}^{\dagger} d_{\sigma}^{\dagger} d_{\tilde{\sigma}} - a_{\uparrow}^{\dagger} d_{\sigma}^{\dagger} e_{\mathbf{k}\sigma} n_{d\tilde{\sigma}} \right) \\
 &= \Delta \sum_{\tilde{\sigma}} \left(-\delta_{\tilde{\sigma}\tilde{\sigma}} d_{\tilde{\sigma}}^{\dagger} a_{\uparrow}^{\dagger} e_{\mathbf{k}\sigma} + a_{\uparrow}^{\dagger} d_{\sigma}^{\dagger} e_{\mathbf{k}\sigma} n_{d\tilde{\sigma}} - a_{\uparrow}^{\dagger} d_{\sigma}^{\dagger} e_{\mathbf{k}\sigma} n_{d\tilde{\sigma}} \right) \\
 &= \Delta \sum_{\tilde{\sigma}} \left(-\delta_{\tilde{\sigma}\tilde{\sigma}} d_{\tilde{\sigma}}^{\dagger} a_{\uparrow}^{\dagger} e_{\mathbf{k}\sigma} \right). \tag{B.179}
 \end{aligned}$$

$$\left[e_{\mathbf{k}\sigma} n_{d\tilde{\sigma}}, \Delta \sum_{\tilde{\sigma}} (d_{\tilde{\sigma}} a_{\uparrow} + a_{\uparrow}^{\dagger} d_{\tilde{\sigma}}^{\dagger}) \right] = \Delta \sum_{\tilde{\sigma}} \delta_{\tilde{\sigma}\tilde{\sigma}} \left(a_{\uparrow} d_{\tilde{\sigma}} e_{\mathbf{k}\sigma} - d_{\tilde{\sigma}}^{\dagger} a_{\uparrow}^{\dagger} e_{\mathbf{k}\sigma} \right). \tag{B.180}$$

$$\begin{aligned}
 (\omega - \varepsilon_{\mathbf{k}\sigma} + \eta^+) G_{e_{\mathbf{k}\sigma} n_{d\tilde{\sigma}}, d_{\sigma}}^r(\omega) &= V_{SD} \sum_{\mathbf{k}} G_{e_{\mathbf{k}\sigma} n_{d\tilde{\sigma}}, d_{\sigma}}^r(\omega) + \sqrt{2}V G_{d_{\sigma} n_{d\tilde{\sigma}}, d_{\sigma}}^r(\omega) \\
 &+ t_{hp} \left(-\sum_{\tilde{\sigma}} \delta_{\tilde{\sigma}\tilde{\sigma}} \right) \langle \langle d_{\tilde{\sigma}} a_{\uparrow}^{\dagger} e_{\mathbf{k}\sigma}; d_{\sigma}^{\dagger} \rangle \rangle + t_{hp} \sum_{\tilde{\sigma}} \delta_{\tilde{\sigma}\tilde{\sigma}} \langle \langle a_{\uparrow} d_{\tilde{\sigma}}^{\dagger} e_{\mathbf{k}\sigma}; d_{\sigma}^{\dagger} \rangle \rangle \\
 &+ \Delta \sum_{\tilde{\sigma}} \delta_{\tilde{\sigma}\tilde{\sigma}} \langle \langle a_{\uparrow} d_{\tilde{\sigma}} e_{\mathbf{k}\sigma}; d_{\sigma}^{\dagger} \rangle \rangle + \Delta \left(-\sum_{\tilde{\sigma}} \delta_{\tilde{\sigma}\tilde{\sigma}} \right) \langle \langle d_{\tilde{\sigma}}^{\dagger} a_{\uparrow}^{\dagger} e_{\mathbf{k}\sigma}; d_{\sigma}^{\dagger} \rangle \rangle \tag{B.181}
 \end{aligned}$$

$$\begin{aligned}
 (\omega - \varepsilon_{\mathbf{k}\sigma} + \eta^+) G_{e_{\mathbf{k}\sigma} n_{d\tilde{\sigma}}, d_{\sigma}}^r(\omega) &= V_{SD} \sum_{\mathbf{k}} G_{e_{\mathbf{k}\sigma} n_{d\tilde{\sigma}}, d_{\sigma}}^r(\omega) + \sqrt{2}V G_{d_{\sigma} n_{d\tilde{\sigma}}, d_{\sigma}}^r(\omega) \\
 &+ t_{hp} \left(-\sum_{\tilde{\sigma}} \delta_{\tilde{\sigma}\tilde{\sigma}} \right) G_{d_{\tilde{\sigma}} a_{\uparrow}^{\dagger} e_{\mathbf{k}\sigma}, d_{\sigma}}^r(\omega) + t_{hp} \sum_{\tilde{\sigma}} \delta_{\tilde{\sigma}\tilde{\sigma}} G_{a_{\uparrow} d_{\tilde{\sigma}}^{\dagger} e_{\mathbf{k}\sigma}, d_{\sigma}}^r(\omega) \\
 &+ \Delta \sum_{\tilde{\sigma}} \delta_{\tilde{\sigma}\tilde{\sigma}} G_{a_{\uparrow} d_{\tilde{\sigma}} e_{\mathbf{k}\sigma}, d_{\sigma}}^r(\omega) + \Delta \left(-\sum_{\tilde{\sigma}} \delta_{\tilde{\sigma}\tilde{\sigma}} \right) G_{d_{\tilde{\sigma}}^{\dagger} a_{\uparrow}^{\dagger} e_{\mathbf{k}\sigma}, d_{\sigma}}^r(\omega) \tag{B.182}
 \end{aligned}$$

$$\begin{aligned}
 (\omega - \varepsilon_{\mathbf{k}\sigma} + \eta^+) G_{e_{\mathbf{k}\sigma} n_{d\tilde{\sigma}}, d_{\sigma}}^r(\omega) &= V_{SD} \sum_{\mathbf{k}} G_{e_{\mathbf{k}\sigma} n_{d\tilde{\sigma}}, d_{\sigma}}^r(\omega) + \sqrt{2}V G_{d_{\sigma} n_{d\tilde{\sigma}}, d_{\sigma}}^r(\omega) \\
 &+ (-1) t_{hp} \sum_{\tilde{\sigma}} \delta_{\tilde{\sigma}\tilde{\sigma}} \langle \langle d_{\tilde{\sigma}} a_{\uparrow}^{\dagger} \rangle \rangle G_{e_{\mathbf{k}\sigma}, d_{\sigma}}^r(\omega) + t_{hp} \sum_{\tilde{\sigma}} \delta_{\tilde{\sigma}\tilde{\sigma}} \langle \langle a_{\uparrow} d_{\tilde{\sigma}}^{\dagger} \rangle \rangle G_{e_{\mathbf{k}\sigma}, d_{\sigma}}^r(\omega) \\
 &+ \Delta \sum_{\tilde{\sigma}} \delta_{\tilde{\sigma}\tilde{\sigma}} \langle \langle a_{\uparrow} d_{\tilde{\sigma}} \rangle \rangle G_{e_{\mathbf{k}\sigma}, d_{\sigma}}^r(\omega) - \Delta \sum_{\tilde{\sigma}} \delta_{\tilde{\sigma}\tilde{\sigma}} \langle \langle d_{\tilde{\sigma}}^{\dagger} a_{\uparrow}^{\dagger} \rangle \rangle G_{e_{\mathbf{k}\sigma}, d_{\sigma}}^r(\omega) \tag{B.183}
 \end{aligned}$$

Thus,

$$(\omega - \varepsilon_{\mathbf{k}\sigma} + \eta^+) G_{e_{\mathbf{k}\sigma} n_{d\bar{\sigma}}, d_\sigma}^r(\omega) = V_{SD} \sum_{\mathbf{k}} G_{e_{\mathbf{k}\sigma} n_{d\bar{\sigma}}, d_\sigma}^r(\omega) + \sqrt{2}V G_{d_\sigma n_{d\bar{\sigma}}, d_\sigma}^r(\omega) \quad (\text{B.184})$$

Let us divide the equation above by $(\omega - \varepsilon_{\mathbf{k}\sigma} + \eta^+)$:

$$G_{e_{\mathbf{k}\sigma} n_{d\bar{\sigma}}, d_\sigma}^r(\omega) = V_{SD} \sum_{\mathbf{k}} \frac{G_{e_{\mathbf{k}\sigma} n_{d\bar{\sigma}}, d_\sigma}^r(\omega)}{(\omega - \varepsilon_{\mathbf{k}\sigma} + \eta^+)} + \sqrt{2}V \frac{G_{d_\sigma n_{d\bar{\sigma}}, d_\sigma}^r(\omega)}{(\omega - \varepsilon_{\mathbf{k}\sigma} + \eta^+)} \quad (\text{B.185})$$

$$G_{e_{\mathbf{k}\sigma} n_{d\bar{\sigma}}, d_\sigma}^r(\omega) = \sqrt{2}V \frac{(\omega - \varepsilon_{\mathbf{k}\sigma} + \eta^+)^{-1}}{\left[1 - V_{SD} \sum_{\mathbf{k}} \left(\frac{1}{\omega - \varepsilon_{\mathbf{k}\sigma} + \eta^+}\right)\right]} G_{d_\sigma n_{d\bar{\sigma}}, d_\sigma}^r(\omega) \quad (\text{B.186})$$

Substituting such a result in Eq.(B.152):

$$\begin{aligned} (\omega - \varepsilon_{d\sigma} - U + \eta^+) G_{d_\sigma n_{d\bar{\sigma}}, d_\sigma}^r(\omega) &= \langle n_{d\bar{\sigma}} \rangle + 2V^2 \sum_{\mathbf{k}} \frac{(\omega - \varepsilon_{\mathbf{k}\sigma} + \eta^+)^{-1}}{\left[1 - V_{SD} \sum_{\mathbf{k}} \left(\frac{1}{\omega - \varepsilon_{\mathbf{k}\sigma} + \eta^+}\right)\right]} G_{d_\sigma n_{d\bar{\sigma}}, d_\sigma}^r(\omega) \\ &\quad - \sum_{\bar{\sigma}} \delta_{\bar{\sigma}\sigma} t_{hp} G_{a_\uparrow n_{d\bar{\sigma}}, d_\sigma}^r(\omega) - \sum_{\bar{\sigma}} \delta_{\bar{\sigma}\sigma} \Delta G_{a_\uparrow^\dagger n_{d\bar{\sigma}}, d_\sigma}^r(\omega) \end{aligned} \quad (\text{B.187})$$

As we have performed previously $\sum_{\mathbf{k}} \left(\frac{1}{\omega - \varepsilon_{\mathbf{k}\sigma} + \eta^+}\right) = -i\pi\rho_{\mathbf{k}\sigma}(\omega)$.

$$\begin{aligned} (\omega - \varepsilon_{d\sigma} - U + \eta^+) G_{d_\sigma n_{d\bar{\sigma}}, d_\sigma}^r(\omega) &= \langle n_{d\bar{\sigma}} \rangle + \frac{(-i2V^2\pi\rho_{\mathbf{k}\sigma}(\omega))}{[1 + i(V_{SD}\pi\rho_{\mathbf{k}\sigma}(\omega))]} G_{d_\sigma n_{d\bar{\sigma}}, d_\sigma}^r(\omega) \\ &\quad - \sum_{\bar{\sigma}} \delta_{\bar{\sigma}\sigma} t_{hp} G_{a_\uparrow n_{d\bar{\sigma}}, d_\sigma}^r(\omega) - \sum_{\bar{\sigma}} \delta_{\bar{\sigma}\sigma} \Delta G_{a_\uparrow^\dagger n_{d\bar{\sigma}}, d_\sigma}^r(\omega) \\ &= \langle n_{d\bar{\sigma}} \rangle + \frac{(-i\Gamma_\sigma)}{[1 + i\sqrt{x}]} G_{d_\sigma n_{d\bar{\sigma}}, d_\sigma}^r(\omega) \\ &\quad - \sum_{\bar{\sigma}} \delta_{\bar{\sigma}\sigma} t_{hp} G_{a_\uparrow n_{d\bar{\sigma}}, d_\sigma}^r(\omega) - \sum_{\bar{\sigma}} \delta_{\bar{\sigma}\sigma} \Delta G_{a_\uparrow^\dagger n_{d\bar{\sigma}}, d_\sigma}^r(\omega) \\ &= \langle n_{d\bar{\sigma}} \rangle + \Sigma_\sigma G_{d_\sigma n_{d\bar{\sigma}}, d_\sigma}^r(\omega) \\ &\quad - \sum_{\bar{\sigma}} \delta_{\bar{\sigma}\sigma} t_{hp} G_{a_\uparrow n_{d\bar{\sigma}}, d_\sigma}^r(\omega) - \sum_{\bar{\sigma}} \delta_{\bar{\sigma}\sigma} \Delta G_{a_\uparrow^\dagger n_{d\bar{\sigma}}, d_\sigma}^r(\omega) \end{aligned} \quad (\text{B.188})$$

in which we have used the definition of Eq.(B.32). Thus,

$$\boxed{(\omega^+ - \varepsilon_{d\sigma} - U - \Sigma_\sigma) G_{d_\sigma n_{d\bar{\sigma}}, d_\sigma}^r(\omega) = \langle n_{d\bar{\sigma}} \rangle - t_{hp} \sum_{\bar{\sigma}} \delta_{\bar{\sigma}\sigma} G_{a_\uparrow n_{d\bar{\sigma}}, d_\sigma}^r(\omega) - \Delta \sum_{\bar{\sigma}} \delta_{\bar{\sigma}\sigma} G_{a_\uparrow^\dagger n_{d\bar{\sigma}}, d_\sigma}^r(\omega)} \quad (\text{B.189})$$

Now, we will obtain $G_{a_\uparrow n_{d\bar{\sigma}}, d_\sigma}^r(\omega)$:

$$(\omega + \eta^+) G_{a_\uparrow n_{d\bar{\sigma}}, d_\sigma}^r(\omega) = \langle \{a_\uparrow n_{d\bar{\sigma}}, d_\sigma^\dagger\} \rangle + \langle \langle [a_\uparrow n_{d\bar{\sigma}}, \mathcal{H}_e]; d_\sigma^\dagger \rangle \rangle \quad (\text{B.190})$$

$$\begin{aligned}
\langle \{a_{\uparrow} n_{d\bar{\sigma}}, d_{\sigma}^{\dagger}\} \rangle &= \langle a_{\uparrow} n_{d\bar{\sigma}} d_{\sigma}^{\dagger} + d_{\sigma}^{\dagger} a_{\uparrow} n_{d\bar{\sigma}} \rangle \\
&= \langle a_{\uparrow} d_{\bar{\sigma}}^{\dagger} d_{\bar{\sigma}} d_{\sigma}^{\dagger} - a_{\uparrow} d_{\sigma}^{\dagger} n_{d\bar{\sigma}} \rangle \\
&= \langle a_{\uparrow} d_{\sigma}^{\dagger} d_{\bar{\sigma}}^{\dagger} d_{\bar{\sigma}} - a_{\uparrow} d_{\sigma}^{\dagger} n_{d\bar{\sigma}} \rangle \\
&= \langle a_{\uparrow} d_{\sigma}^{\dagger} n_{d\bar{\sigma}} - a_{\uparrow} d_{\sigma}^{\dagger} n_{d\bar{\sigma}} \rangle \\
&= 0.
\end{aligned} \tag{B.191}$$

$$(\omega + i\eta^+) G_{a_{\uparrow} n_{d\bar{\sigma}}, d_{\sigma}}^r(\omega) = \langle \langle [a_{\uparrow} n_{d\bar{\sigma}}, \mathcal{H}_e]; d_{\sigma}^{\dagger} \rangle \rangle \tag{B.192}$$

$$\begin{aligned}
[a_{\uparrow} n_{d\bar{\sigma}}, \mathcal{H}_e] &= [a_{\uparrow} n_{d\bar{\sigma}}, \mathcal{H}_{\text{lead}}] + [a_{\uparrow} n_{d\bar{\sigma}}, \mathcal{H}_{\text{dot}}] + [a_{\uparrow} n_{d\bar{\sigma}}, \mathcal{H}_{\text{dot-lead}}] + [a_{\uparrow} n_{d\bar{\sigma}}, \mathcal{H}_M] \\
&= [a_{\uparrow} n_{d\bar{\sigma}}, \mathcal{H}_{\text{dot}}] + [a_{\uparrow} n_{d\bar{\sigma}}, \mathcal{H}_{\text{dot-lead}}] + [a_{\uparrow} n_{d\bar{\sigma}}, \mathcal{H}_M]
\end{aligned} \tag{B.193}$$

$$[a_{\uparrow} n_{d\bar{\sigma}}, \mathcal{H}_{\text{dot}}] = [a_{\uparrow} n_{d\bar{\sigma}}, \sum_{\sigma} \varepsilon_{d\sigma} d_{\sigma}^{\dagger} d_{\sigma}] + [a_{\uparrow} n_{d\bar{\sigma}}, U n_{d\uparrow} n_{d\downarrow}] \tag{B.194}$$

$$\begin{aligned}
[a_{\uparrow} n_{d\bar{\sigma}}, \sum_{\sigma} \varepsilon_{d\sigma} d_{\sigma}^{\dagger} d_{\sigma}] &= \sum_{\sigma} \varepsilon_{d\sigma} (a_{\uparrow} n_{d\bar{\sigma}} d_{\sigma}^{\dagger} d_{\sigma} - d_{\sigma}^{\dagger} d_{\sigma} a_{\uparrow} n_{d\bar{\sigma}}) \\
&= \sum_{\sigma} \varepsilon_{d\sigma} (a_{\uparrow} d_{\bar{\sigma}}^{\dagger} d_{\bar{\sigma}} d_{\sigma}^{\dagger} d_{\sigma} - a_{\uparrow} d_{\sigma}^{\dagger} d_{\sigma} n_{d\bar{\sigma}}) \\
&= \sum_{\sigma} \varepsilon_{d\sigma} (a_{\uparrow} d_{\bar{\sigma}}^{\dagger} (\delta_{\sigma\bar{\sigma}} - d_{\sigma}^{\dagger} d_{\bar{\sigma}}) d_{\sigma} - a_{\uparrow} d_{\sigma}^{\dagger} d_{\sigma} n_{d\bar{\sigma}}) \\
&= \sum_{\sigma} \varepsilon_{d\sigma} (\delta_{\sigma\bar{\sigma}} a_{\uparrow} d_{\bar{\sigma}}^{\dagger} d_{\sigma} - a_{\uparrow} d_{\bar{\sigma}}^{\dagger} d_{\sigma}^{\dagger} d_{\bar{\sigma}} d_{\sigma} - a_{\uparrow} d_{\sigma}^{\dagger} d_{\sigma} n_{d\bar{\sigma}}) \\
&= \sum_{\sigma} \varepsilon_{d\sigma} (\delta_{\sigma\bar{\sigma}} a_{\uparrow} d_{\bar{\sigma}}^{\dagger} d_{\sigma} - a_{\uparrow} d_{\sigma}^{\dagger} d_{\bar{\sigma}}^{\dagger} d_{\sigma} d_{\bar{\sigma}} - a_{\uparrow} d_{\sigma}^{\dagger} d_{\sigma} n_{d\bar{\sigma}}) \\
&= \sum_{\sigma} \varepsilon_{d\sigma} (\delta_{\sigma\bar{\sigma}} a_{\uparrow} d_{\bar{\sigma}}^{\dagger} d_{\sigma} - a_{\uparrow} d_{\sigma}^{\dagger} (\delta_{\sigma\bar{\sigma}} - d_{\sigma} d_{\bar{\sigma}}^{\dagger}) d_{\bar{\sigma}} - a_{\uparrow} d_{\sigma}^{\dagger} d_{\sigma} n_{d\bar{\sigma}}) \\
&= \sum_{\sigma} \varepsilon_{d\sigma} (\delta_{\sigma\bar{\sigma}} a_{\uparrow} d_{\bar{\sigma}}^{\dagger} d_{\sigma} - \delta_{\sigma\bar{\sigma}} a_{\uparrow} d_{\sigma}^{\dagger} d_{\bar{\sigma}} + a_{\uparrow} d_{\sigma}^{\dagger} d_{\sigma} n_{d\bar{\sigma}} - a_{\uparrow} d_{\sigma}^{\dagger} d_{\sigma} n_{d\bar{\sigma}}) \\
&= \varepsilon_{d\bar{\sigma}} (a_{\uparrow} d_{\bar{\sigma}}^{\dagger} d_{\bar{\sigma}} - a_{\uparrow} d_{\bar{\sigma}}^{\dagger} d_{\bar{\sigma}}) = 0.
\end{aligned} \tag{B.195}$$

$$\begin{aligned}
[a_{\uparrow}n_{d\bar{\sigma}}, \mathcal{H}_{\text{dot-lead}}] &= [a_{\uparrow}n_{d\bar{\sigma}}, \sqrt{2V} \sum_{\mathbf{p}\bar{\sigma}} (e_{\mathbf{p}\bar{\sigma}}^{\dagger}d_{\bar{\sigma}} + d_{\bar{\sigma}}^{\dagger}e_{\mathbf{p}\bar{\sigma}})] \\
&= \underbrace{\sqrt{2V} \sum_{\mathbf{p}\bar{\sigma}} [a_{\uparrow}n_{d\bar{\sigma}}, e_{\mathbf{p}\bar{\sigma}}^{\dagger}d_{\bar{\sigma}}]}_I + \underbrace{\sqrt{2V} \sum_{\mathbf{p}\bar{\sigma}} [a_{\uparrow}n_{d\bar{\sigma}}, d_{\bar{\sigma}}^{\dagger}e_{\mathbf{p}\bar{\sigma}}]}_{II} \quad (\text{B.198})
\end{aligned}$$

$$\begin{aligned}
I : \sqrt{2V} \sum_{\mathbf{p}\bar{\sigma}} [a_{\uparrow}n_{d\bar{\sigma}}, e_{\mathbf{p}\bar{\sigma}}^{\dagger}d_{\bar{\sigma}}] &= \sqrt{2V} \sum_{\mathbf{p}\bar{\sigma}} (a_{\uparrow}n_{d\bar{\sigma}}e_{\mathbf{p}\bar{\sigma}}^{\dagger}d_{\bar{\sigma}} - e_{\mathbf{p}\bar{\sigma}}^{\dagger}d_{\bar{\sigma}}a_{\uparrow}n_{d\bar{\sigma}}) \\
&= \sqrt{2V} \sum_{\mathbf{p}\bar{\sigma}} (a_{\uparrow}e_{\mathbf{p}\bar{\sigma}}^{\dagger}d_{\bar{\sigma}}^{\dagger}d_{\bar{\sigma}}d_{\bar{\sigma}} - a_{\uparrow}e_{\mathbf{p}\bar{\sigma}}^{\dagger}d_{\bar{\sigma}}n_{d\bar{\sigma}}) \\
&= \sqrt{2V} \sum_{\mathbf{p}\bar{\sigma}} (-a_{\uparrow}e_{\mathbf{p}\bar{\sigma}}^{\dagger}(\delta_{\bar{\sigma}\bar{\sigma}} - d_{\bar{\sigma}}d_{\bar{\sigma}}^{\dagger})d_{\bar{\sigma}} - a_{\uparrow}e_{\mathbf{p}\bar{\sigma}}^{\dagger}d_{\bar{\sigma}}n_{d\bar{\sigma}}) \\
&= \sqrt{2V} \sum_{\mathbf{p}\bar{\sigma}} (-\delta_{\bar{\sigma}\bar{\sigma}}a_{\uparrow}e_{\mathbf{p}\bar{\sigma}}^{\dagger}d_{\bar{\sigma}} + a_{\uparrow}e_{\mathbf{p}\bar{\sigma}}^{\dagger}d_{\bar{\sigma}}n_{d\bar{\sigma}} - a_{\uparrow}e_{\mathbf{p}\bar{\sigma}}^{\dagger}d_{\bar{\sigma}}n_{d\bar{\sigma}}) \\
&= \sqrt{2V} \sum_{\mathbf{p}} (-a_{\uparrow}e_{\mathbf{p}\bar{\sigma}}^{\dagger}d_{\bar{\sigma}}). \quad (\text{B.199})
\end{aligned}$$

$$\begin{aligned}
II \sqrt{2V} \sum_{\mathbf{p}\bar{\sigma}} [a_{\uparrow}n_{d\bar{\sigma}}, d_{\bar{\sigma}}^{\dagger}e_{\mathbf{p}\bar{\sigma}}] &= \sqrt{2V} \sum_{\mathbf{p}\bar{\sigma}} (a_{\uparrow}n_{d\bar{\sigma}}d_{\bar{\sigma}}^{\dagger}e_{\mathbf{p}\bar{\sigma}} - d_{\bar{\sigma}}^{\dagger}e_{\mathbf{p}\bar{\sigma}}a_{\uparrow}n_{d\bar{\sigma}}) \\
&= \sqrt{2V} \sum_{\mathbf{p}\bar{\sigma}} (e_{\mathbf{p}\bar{\sigma}}a_{\uparrow}d_{\bar{\sigma}}^{\dagger}d_{\bar{\sigma}}d_{\bar{\sigma}}^{\dagger} - e_{\mathbf{p}\bar{\sigma}}a_{\uparrow}d_{\bar{\sigma}}^{\dagger}n_{d\bar{\sigma}}) \\
&= \sqrt{2V} \sum_{\mathbf{p}\bar{\sigma}} (e_{\mathbf{p}\bar{\sigma}}a_{\uparrow}d_{\bar{\sigma}}^{\dagger}(\delta_{\bar{\sigma}\bar{\sigma}} - d_{\bar{\sigma}}^{\dagger}d_{\bar{\sigma}}) - e_{\mathbf{p}\bar{\sigma}}a_{\uparrow}d_{\bar{\sigma}}^{\dagger}n_{d\bar{\sigma}}) \\
&= \sqrt{2V} \sum_{\mathbf{p}\bar{\sigma}} (\delta_{\bar{\sigma}\bar{\sigma}}e_{\mathbf{p}\bar{\sigma}}a_{\uparrow}d_{\bar{\sigma}}^{\dagger} + e_{\mathbf{p}\bar{\sigma}}a_{\uparrow}d_{\bar{\sigma}}^{\dagger}n_{d\bar{\sigma}} - e_{\mathbf{p}\bar{\sigma}}a_{\uparrow}d_{\bar{\sigma}}^{\dagger}n_{d\bar{\sigma}}) \\
&= \sqrt{2V} \sum_{\mathbf{p}} (e_{\mathbf{p}\bar{\sigma}}a_{\uparrow}d_{\bar{\sigma}}^{\dagger}). \quad (\text{B.200})
\end{aligned}$$

$$[a_{\uparrow}n_{d\bar{\sigma}}, \mathcal{H}_{\text{dot-lead}}] = \sqrt{2V} \sum_{\mathbf{p}} (-e_{\mathbf{p}\bar{\sigma}}^{\dagger}d_{\bar{\sigma}}a_{\uparrow} + d_{\bar{\sigma}}^{\dagger}e_{\mathbf{p}\bar{\sigma}}a_{\uparrow}). \quad (\text{B.201})$$

$$\begin{aligned}
[a_{\uparrow}n_{d\bar{\sigma}}, \mathcal{H}_{\text{M}}] &= \left[a_{\uparrow}n_{d\bar{\sigma}}, \delta_{\text{M}} \left(a_{\uparrow}^{\dagger}a_{\uparrow} - \frac{1}{2} \right) \right] + \left[a_{\uparrow}n_{d\bar{\sigma}}, t_{hp} \sum_{\bar{\sigma}} (d_{\bar{\sigma}}a_{\uparrow}^{\dagger} + a_{\uparrow}d_{\bar{\sigma}}^{\dagger}) \right] \\
&+ \left[a_{\uparrow}n_{d\bar{\sigma}}, \Delta \sum_{\bar{\sigma}} (d_{\bar{\sigma}}a_{\uparrow} + a_{\uparrow}d_{\bar{\sigma}}^{\dagger}) \right], \quad (\text{B.202})
\end{aligned}$$

$$\begin{aligned}
\left[a_{\uparrow} n_{d\bar{\sigma}}, \delta_{\mathbf{M}} \left(a_{\uparrow}^{\dagger} a_{\uparrow} - \frac{1}{2} \right) \right] &= \delta_{\mathbf{M}} \left(a_{\uparrow} n_{d\bar{\sigma}} a_{\uparrow}^{\dagger} a_{\uparrow} - a_{\uparrow}^{\dagger} a_{\uparrow} a_{\uparrow} n_{d\bar{\sigma}} \right) \\
&= \delta_{\mathbf{M}} \left(a_{\uparrow} a_{\uparrow}^{\dagger} a_{\uparrow} n_{d\bar{\sigma}} + a_{\uparrow}^{\dagger} a_{\uparrow} a_{\uparrow} n_{d\bar{\sigma}} \right) \\
&= \delta_{\mathbf{M}} \left(\left(a_{\uparrow} a_{\uparrow}^{\dagger} + a_{\uparrow}^{\dagger} a_{\uparrow} \right) a_{\uparrow} n_{d\bar{\sigma}} \right) \\
&= \delta_{\mathbf{M}} \left(a_{\uparrow} n_{d\bar{\sigma}} \right). \tag{B.203}
\end{aligned}$$

$$\left[a_{\uparrow} n_{d\bar{\sigma}}, t_{hp} \sum_{\bar{\sigma}} (d_{\bar{\sigma}} a_{\uparrow}^{\dagger} + a_{\uparrow} d_{\bar{\sigma}}^{\dagger}) \right] = \underbrace{t_{hp} \sum_{\bar{\sigma}} \left[a_{\uparrow} n_{d\bar{\sigma}}, d_{\bar{\sigma}} a_{\uparrow}^{\dagger} \right]}_I + \underbrace{t_{hp} \sum_{\bar{\sigma}} \left[a_{\uparrow} n_{d\bar{\sigma}}, a_{\uparrow} d_{\bar{\sigma}}^{\dagger} \right]}_{II} \tag{B.204}$$

$$\begin{aligned}
I : t_{hp} \sum_{\bar{\sigma}} \left[a_{\uparrow} n_{d\bar{\sigma}}, d_{\bar{\sigma}} a_{\uparrow}^{\dagger} \right] &= t_{hp} \sum_{\bar{\sigma}} \left(a_{\uparrow} n_{d\bar{\sigma}} d_{\bar{\sigma}} a_{\uparrow}^{\dagger} - d_{\bar{\sigma}} a_{\uparrow}^{\dagger} a_{\uparrow} n_{d\bar{\sigma}} \right) \\
&= t_{hp} \sum_{\bar{\sigma}} \left(a_{\uparrow} a_{\uparrow}^{\dagger} d_{\bar{\sigma}}^{\dagger} d_{\bar{\sigma}} d_{\bar{\sigma}} - a_{\uparrow}^{\dagger} a_{\uparrow} d_{\bar{\sigma}} n_{d\bar{\sigma}} \right) \\
&= t_{hp} \sum_{\bar{\sigma}} \left(a_{\uparrow} a_{\uparrow}^{\dagger} \left(\delta_{\bar{\sigma}\bar{\sigma}} - d_{\bar{\sigma}} d_{\bar{\sigma}}^{\dagger} \right) d_{\bar{\sigma}} - a_{\uparrow}^{\dagger} a_{\uparrow} d_{\bar{\sigma}} n_{d\bar{\sigma}} \right) \\
&= t_{hp} \sum_{\bar{\sigma}} \left(\delta_{\bar{\sigma}\bar{\sigma}} a_{\uparrow} a_{\uparrow}^{\dagger} d_{\bar{\sigma}} - a_{\uparrow} a_{\uparrow}^{\dagger} d_{\bar{\sigma}} n_{d\bar{\sigma}} - a_{\uparrow}^{\dagger} a_{\uparrow} d_{\bar{\sigma}} n_{d\bar{\sigma}} \right) \\
&= t_{hp} \sum_{\bar{\sigma}} \left(\delta_{\bar{\sigma}\bar{\sigma}} a_{\uparrow} a_{\uparrow}^{\dagger} d_{\bar{\sigma}} - \left(1 - a_{\uparrow}^{\dagger} a_{\uparrow} \right) d_{\bar{\sigma}} n_{d\bar{\sigma}} - a_{\uparrow}^{\dagger} a_{\uparrow} d_{\bar{\sigma}} n_{d\bar{\sigma}} \right) \\
&= t_{hp} \sum_{\bar{\sigma}} \left(\delta_{\bar{\sigma}\bar{\sigma}} a_{\uparrow} a_{\uparrow}^{\dagger} d_{\bar{\sigma}} - d_{\uparrow} n_{d\bar{\sigma}} + a_{\uparrow}^{\dagger} a_{\uparrow} d_{\bar{\sigma}} n_{d\bar{\sigma}} - a_{\uparrow}^{\dagger} a_{\uparrow} d_{\bar{\sigma}} n_{d\bar{\sigma}} \right) \\
&= t_{hp} \sum_{\bar{\sigma}} \left(\delta_{\bar{\sigma}\bar{\sigma}} d_{\bar{\sigma}} a_{\uparrow} a_{\uparrow}^{\dagger} - d_{\bar{\sigma}} n_{d\bar{\sigma}} \right) \tag{B.205}
\end{aligned}$$

$$\begin{aligned}
II : t_{hp} \sum_{\bar{\sigma}} \left[a_{\uparrow} n_{d\bar{\sigma}}, a_{\uparrow} d_{\bar{\sigma}}^{\dagger} \right] &= t_{hp} \sum_{\bar{\sigma}} \left(a_{\uparrow} n_{d\bar{\sigma}} a_{\uparrow} d_{\bar{\sigma}}^{\dagger} - a_{\uparrow} d_{\bar{\sigma}}^{\dagger} a_{\uparrow} n_{d\bar{\sigma}} \right) \\
&= t_{hp} \sum_{\bar{\sigma}} \left(a_{\uparrow} a_{\uparrow} d_{\bar{\sigma}}^{\dagger} d_{\bar{\sigma}} d_{\bar{\sigma}}^{\dagger} - a_{\uparrow} a_{\uparrow} d_{\bar{\sigma}}^{\dagger} n_{d\bar{\sigma}} \right) \\
&= t_{hp} \sum_{\bar{\sigma}} \left(a_{\uparrow} a_{\uparrow} d_{\bar{\sigma}}^{\dagger} \left(\delta_{\bar{\sigma}\bar{\sigma}} - d_{\bar{\sigma}}^{\dagger} d_{\bar{\sigma}} \right) - a_{\uparrow} a_{\uparrow} d_{\bar{\sigma}}^{\dagger} n_{d\bar{\sigma}} \right) \\
&= t_{hp} \sum_{\bar{\sigma}} \left(\delta_{\bar{\sigma}\bar{\sigma}} a_{\uparrow} a_{\uparrow} d_{\bar{\sigma}}^{\dagger} + a_{\uparrow} a_{\uparrow} d_{\bar{\sigma}}^{\dagger} d_{\bar{\sigma}} d_{\bar{\sigma}}^{\dagger} - a_{\uparrow} a_{\uparrow} d_{\bar{\sigma}}^{\dagger} n_{d\bar{\sigma}} \right) \\
&= t_{hp} \sum_{\bar{\sigma}} \left(\delta_{\bar{\sigma}\bar{\sigma}} a_{\uparrow} a_{\uparrow} d_{\bar{\sigma}}^{\dagger} + a_{\uparrow} a_{\uparrow} d_{\bar{\sigma}}^{\dagger} d_{\bar{\sigma}} d_{\bar{\sigma}}^{\dagger} - a_{\uparrow} a_{\uparrow} d_{\bar{\sigma}}^{\dagger} n_{d\bar{\sigma}} \right) \\
&= t_{hp} \sum_{\bar{\sigma}} \left(-\delta_{\bar{\sigma}\bar{\sigma}} a_{\uparrow} d_{\bar{\sigma}}^{\dagger} a_{\uparrow} \right). \tag{B.206}
\end{aligned}$$

$$\left[a_{\uparrow} n_{d\bar{\sigma}}, t_{hp} \sum_{\bar{\sigma}} (d_{\bar{\sigma}} a_{\uparrow}^{\dagger} + a_{\uparrow} d_{\bar{\sigma}}^{\dagger}) \right] = t_{hp} \sum_{\bar{\sigma}} \left(\delta_{\bar{\sigma}\bar{\sigma}} d_{\bar{\sigma}} a_{\uparrow} a_{\uparrow}^{\dagger} - d_{\bar{\sigma}} n_{d\bar{\sigma}} - \delta_{\bar{\sigma}\bar{\sigma}} a_{\uparrow} d_{\bar{\sigma}}^{\dagger} a_{\uparrow} \right) \quad (\text{B.207})$$

$$\left[a_{\uparrow} n_{d\bar{\sigma}}, \Delta \sum_{\bar{\sigma}} (d_{\bar{\sigma}} a_{\uparrow} + a_{\uparrow}^{\dagger} d_{\bar{\sigma}}^{\dagger}) \right] = \underbrace{\Delta \sum_{\bar{\sigma}} [a_{\uparrow} n_{d\bar{\sigma}}, d_{\bar{\sigma}} a_{\uparrow}]}_I + \underbrace{\Delta \sum_{\bar{\sigma}} [a_{\uparrow} n_{d\bar{\sigma}}, a_{\uparrow}^{\dagger} d_{\bar{\sigma}}^{\dagger}]}_{II} \quad (\text{B.208})$$

$$\begin{aligned} I : \Delta \sum_{\bar{\sigma}} [a_{\uparrow} n_{d\bar{\sigma}}, d_{\bar{\sigma}} a_{\uparrow}] &= \Delta \sum_{\bar{\sigma}} (a_{\uparrow} n_{d\bar{\sigma}} d_{\bar{\sigma}} a_{\uparrow} - d_{\bar{\sigma}} a_{\uparrow} a_{\uparrow} n_{d\bar{\sigma}}) \\ &= \Delta \sum_{\bar{\sigma}} (a_{\uparrow} a_{\uparrow}^{\dagger} d_{\bar{\sigma}}^{\dagger} d_{\bar{\sigma}} d_{\bar{\sigma}} - a_{\uparrow} a_{\uparrow} d_{\bar{\sigma}} n_{d\bar{\sigma}}) \\ &= \Delta \sum_{\bar{\sigma}} (a_{\uparrow} a_{\uparrow} (\delta_{\bar{\sigma}\bar{\sigma}} - d_{\bar{\sigma}} d_{\bar{\sigma}}^{\dagger}) d_{\bar{\sigma}} - a_{\uparrow} a_{\uparrow} d_{\bar{\sigma}} n_{d\bar{\sigma}}) \\ &= \Delta \sum_{\bar{\sigma}} (\delta_{\bar{\sigma}\bar{\sigma}} a_{\uparrow} a_{\uparrow} d_{\bar{\sigma}} - a_{\uparrow} a_{\uparrow} d_{\bar{\sigma}} d_{\bar{\sigma}}^{\dagger} d_{\bar{\sigma}} - a_{\uparrow} a_{\uparrow} d_{\bar{\sigma}} n_{d\bar{\sigma}}) \\ &= \Delta \sum_{\bar{\sigma}} (\delta_{\bar{\sigma}\bar{\sigma}} a_{\uparrow} a_{\uparrow} d_{\bar{\sigma}} + a_{\uparrow} a_{\uparrow} d_{\bar{\sigma}} n_{d\bar{\sigma}} - a_{\uparrow} a_{\uparrow} d_{\bar{\sigma}} n_{d\bar{\sigma}}) \\ &= \Delta \sum_{\bar{\sigma}} (\delta_{\bar{\sigma}\bar{\sigma}} a_{\uparrow} a_{\uparrow} d_{\bar{\sigma}}). \end{aligned} \quad (\text{B.209})$$

$$\begin{aligned} II : \Delta \sum_{\bar{\sigma}} [a_{\uparrow} n_{d\bar{\sigma}}, a_{\uparrow}^{\dagger} d_{\bar{\sigma}}^{\dagger}] &= \Delta \sum_{\bar{\sigma}} (a_{\uparrow} n_{d\bar{\sigma}} a_{\uparrow}^{\dagger} d_{\bar{\sigma}}^{\dagger} - a_{\uparrow}^{\dagger} d_{\bar{\sigma}}^{\dagger} a_{\uparrow} n_{d\bar{\sigma}}) \\ &= \Delta \sum_{\bar{\sigma}} (a_{\uparrow} a_{\uparrow}^{\dagger} d_{\bar{\sigma}}^{\dagger} d_{\bar{\sigma}} d_{\bar{\sigma}}^{\dagger} + a_{\uparrow}^{\dagger} a_{\uparrow} d_{\bar{\sigma}}^{\dagger} n_{d\bar{\sigma}}) \\ &= \Delta \sum_{\bar{\sigma}} (a_{\uparrow} a_{\uparrow}^{\dagger} d_{\bar{\sigma}}^{\dagger} (\delta_{\bar{\sigma}\bar{\sigma}} - d_{\bar{\sigma}}^{\dagger} d_{\bar{\sigma}}) + a_{\uparrow}^{\dagger} a_{\uparrow} d_{\bar{\sigma}}^{\dagger} n_{d\bar{\sigma}}) \\ &= \Delta \sum_{\bar{\sigma}} (\delta_{\bar{\sigma}\bar{\sigma}} a_{\uparrow} a_{\uparrow}^{\dagger} d_{\bar{\sigma}}^{\dagger} + a_{\uparrow} a_{\uparrow}^{\dagger} d_{\bar{\sigma}}^{\dagger} d_{\bar{\sigma}} d_{\bar{\sigma}}^{\dagger} + a_{\uparrow}^{\dagger} a_{\uparrow} d_{\bar{\sigma}}^{\dagger} n_{d\bar{\sigma}}) \\ &= \Delta \sum_{\bar{\sigma}} (\delta_{\bar{\sigma}\bar{\sigma}} a_{\uparrow} a_{\uparrow}^{\dagger} d_{\bar{\sigma}}^{\dagger} + (1 - a_{\uparrow}^{\dagger} a_{\uparrow}) d_{\bar{\sigma}}^{\dagger} n_{d\bar{\sigma}} + a_{\uparrow}^{\dagger} a_{\uparrow} d_{\bar{\sigma}}^{\dagger} n_{d\bar{\sigma}}) \\ &= \Delta \sum_{\bar{\sigma}} (\delta_{\bar{\sigma}\bar{\sigma}} a_{\uparrow} a_{\uparrow}^{\dagger} d_{\bar{\sigma}}^{\dagger} + d_{\bar{\sigma}}^{\dagger} n_{d\bar{\sigma}} - a_{\uparrow}^{\dagger} a_{\uparrow} d_{\bar{\sigma}}^{\dagger} n_{d\bar{\sigma}} + a_{\uparrow}^{\dagger} a_{\uparrow} d_{\bar{\sigma}}^{\dagger} n_{d\bar{\sigma}}) \\ &= \Delta \sum_{\bar{\sigma}} (\delta_{\bar{\sigma}\bar{\sigma}} a_{\uparrow} a_{\uparrow}^{\dagger} d_{\bar{\sigma}}^{\dagger} + d_{\bar{\sigma}}^{\dagger} n_{d\bar{\sigma}}). \end{aligned} \quad (\text{B.210})$$

$$\begin{aligned}
 (\omega + \eta\eta^+)G_{a_\uparrow n_{d\bar{\sigma}}, d_\sigma}^r(\omega) &= \sqrt{2}V \sum_{\mathbf{p}} \left(-\langle\langle e_{\mathbf{p}\bar{\sigma}}^\dagger d_{\bar{\sigma}} a_\uparrow; d_\sigma^\dagger \rangle\rangle + \langle\langle d_{\bar{\sigma}}^\dagger e_{\mathbf{p}\bar{\sigma}} a_\uparrow; d_\sigma^\dagger \rangle\rangle \right) \\
 &+ \delta_M \langle\langle a_\uparrow n_{d\bar{\sigma}}; d_\sigma^\dagger \rangle\rangle - t_{hp} \sum_{\bar{\sigma}} \langle\langle d_\sigma n_{d\bar{\sigma}}; d_\sigma^\dagger \rangle\rangle \\
 &+ t_{hp} \sum_{\bar{\sigma}} \delta_{\bar{\sigma}\bar{\sigma}} \left(\langle\langle d_{\bar{\sigma}} a_\uparrow a_\uparrow^\dagger; d_\sigma^\dagger \rangle\rangle - \langle\langle a_\uparrow d_{\bar{\sigma}}^\dagger a_\uparrow; d_\sigma^\dagger \rangle\rangle \right) \\
 &+ \Delta \sum_{\bar{\sigma}} \langle\langle d_{\bar{\sigma}}^\dagger n_{d\bar{\sigma}}; d_\sigma^\dagger \rangle\rangle - \Delta \sum_{\bar{\sigma}} \delta_{\bar{\sigma}\bar{\sigma}} \langle\langle a_\uparrow a_\uparrow d_{\bar{\sigma}}; d_\sigma^\dagger \rangle\rangle \\
 &+ \Delta \sum_{\bar{\sigma}} \delta_{\bar{\sigma}\bar{\sigma}} \langle\langle a_\uparrow a_\uparrow^\dagger d_{\bar{\sigma}}^\dagger; d_\sigma^\dagger \rangle\rangle \tag{B.211}
 \end{aligned}$$

$$\begin{aligned}
 (\omega - \delta_M + \eta\eta^+)G_{a_\uparrow n_{d\bar{\sigma}}, d_\sigma}^r(\omega) &= \sqrt{2}V \sum_{\mathbf{p}} \left(-G_{e_{\mathbf{p}\bar{\sigma}}^\dagger d_{\bar{\sigma}} a_\uparrow, d_\sigma}^r(\omega) + G_{d_{\bar{\sigma}}^\dagger e_{\mathbf{p}\bar{\sigma}} a_\uparrow, d_\sigma}^r(\omega) \right) \\
 &+ t_{hp} \sum_{\bar{\sigma}} \left(-G_{d_{\bar{\sigma}} n_{d\bar{\sigma}}, d_\sigma}^r(\omega) + \delta_{\bar{\sigma}\bar{\sigma}} G_{d_{\bar{\sigma}} a_\uparrow a_\uparrow^\dagger, d_\sigma}^r(\omega) - \delta_{\bar{\sigma}\bar{\sigma}} G_{a_\uparrow d_{\bar{\sigma}}^\dagger a_\uparrow, d_\sigma}^r(\omega) \right) \\
 &+ \Delta \sum_{\bar{\sigma}} \left(G_{d_{\bar{\sigma}}^\dagger n_{d\bar{\sigma}}, d_\sigma}^r(\omega) + \delta_{\bar{\sigma}\bar{\sigma}} G_{d_{\bar{\sigma}} a_\uparrow a_\uparrow, d_\sigma}^r(\omega) - \delta_{\bar{\sigma}\bar{\sigma}} G_{a_\uparrow d_{\bar{\sigma}}^\dagger a_\uparrow, d_\sigma}^r(\omega) \right) \tag{B.212}
 \end{aligned}$$

As can be shown in Eq.(B.189), the Green's function above is multiplied by $\sum_{\bar{\sigma}} \delta_{\bar{\sigma}\sigma}$ and therefore is nonzero just for $\bar{\sigma} = \sigma$. Hence,

$$\begin{aligned}
 (\omega - \delta_M + \eta\eta^+) \sum_{\bar{\sigma}} \delta_{\bar{\sigma}\sigma} G_{a_\uparrow n_{d\bar{\sigma}}, d_\sigma}^r(\omega) &= \sqrt{2}V \sum_{\mathbf{p}} \sum_{\bar{\sigma}} \delta_{\bar{\sigma}\sigma} \left(-G_{e_{\mathbf{p}\bar{\sigma}}^\dagger d_{\bar{\sigma}} a_\uparrow, d_\sigma}^r(\omega) + G_{d_{\bar{\sigma}}^\dagger e_{\mathbf{p}\bar{\sigma}} a_\uparrow, d_\sigma}^r(\omega) \right) \\
 &+ t_{hp} \sum_{\bar{\sigma}} \delta_{\bar{\sigma}\sigma} \left(-G_{d_{\bar{\sigma}} n_{d\bar{\sigma}}, d_\sigma}^r(\omega) + \delta_{\bar{\sigma}\bar{\sigma}} G_{d_{\bar{\sigma}} a_\uparrow a_\uparrow^\dagger, d_\sigma}^r(\omega) - \delta_{\bar{\sigma}\bar{\sigma}} G_{a_\uparrow d_{\bar{\sigma}}^\dagger a_\uparrow, d_\sigma}^r(\omega) \right) \\
 &+ \Delta \sum_{\bar{\sigma}} \delta_{\bar{\sigma}\sigma} \left(G_{d_{\bar{\sigma}}^\dagger n_{d\bar{\sigma}}, d_\sigma}^r(\omega) + \delta_{\bar{\sigma}\bar{\sigma}} G_{d_{\bar{\sigma}} a_\uparrow a_\uparrow, d_\sigma}^r(\omega) - \delta_{\bar{\sigma}\bar{\sigma}} G_{a_\uparrow d_{\bar{\sigma}}^\dagger a_\uparrow, d_\sigma}^r(\omega) \right) \tag{B.213}
 \end{aligned}$$

$$\begin{aligned}
 (\omega - \delta_M + \eta\eta^+) \sum_{\bar{\sigma}} \delta_{\bar{\sigma}\sigma} G_{a_\uparrow n_{d\bar{\sigma}}, d_\sigma}^r(\omega) &= \sqrt{2}V \sum_{\mathbf{p}} \left(-G_{e_{\mathbf{p}\bar{\sigma}}^\dagger d_{\bar{\sigma}} a_\uparrow, d_\sigma}^r(\omega) + G_{d_{\bar{\sigma}}^\dagger e_{\mathbf{p}\bar{\sigma}} a_\uparrow, d_\sigma}^r(\omega) \right) \\
 &- t_{hp} G_{d_\sigma n_{d\bar{\sigma}}, d_\sigma}^r(\omega) + \Delta G_{d_\sigma^\dagger n_{d\bar{\sigma}}, d_\sigma}^r(\omega) \tag{B.214}
 \end{aligned}$$

At this point, we apply the decoupling scheme as follows:

$$\begin{aligned}
 (\omega - \delta_M + \eta\eta^+) \sum_{\bar{\sigma}} \delta_{\bar{\sigma}\sigma} G_{a_\uparrow n_{d\bar{\sigma}}, d_\sigma}^r(\omega) &= \sqrt{2}V \sum_{\mathbf{p}} \left(-\langle e_{\mathbf{p}\bar{\sigma}}^\dagger d_{\bar{\sigma}} \rangle G_{a_\uparrow, d_\sigma}^r(\omega) + \langle d_{\bar{\sigma}}^\dagger e_{\mathbf{p}\bar{\sigma}} \rangle G_{a_\uparrow, d_\sigma}^r(\omega) \right) \\
 &- t_{hp} G_{d_\sigma n_{d\bar{\sigma}}, d_\sigma}^r(\omega) + \Delta G_{d_\sigma^\dagger n_{d\bar{\sigma}}, d_\sigma}^r(\omega) \tag{B.215}
 \end{aligned}$$

$$\begin{aligned}
 (\omega - \delta_M + \eta^+) \sum_{\bar{\sigma}} \delta_{\bar{\sigma}\sigma} G_{a_{\uparrow} n_{d\bar{\sigma}}, d_{\sigma}}^r(\omega) &= \sqrt{2}V \sum_{\mathbf{p}} \left(-\langle e_{\mathbf{p}\bar{\sigma}}^{\dagger} d_{\bar{\sigma}} \rangle G_{a_{\uparrow}, d_{\sigma}}^r(\omega) + \langle d_{\bar{\sigma}}^{\dagger} e_{\mathbf{p}\bar{\sigma}} \rangle G_{a_{\uparrow}, d_{\sigma}}^r(\omega) \right) \\
 &\quad - t_{hp} G_{d_{\sigma} n_{d\bar{\sigma}}, d_{\sigma}}^r(\omega) + \Delta G_{d_{\sigma}^{\dagger} n_{d\bar{\sigma}}, d_{\sigma}}^r(\omega)
 \end{aligned} \tag{B.216}$$

$$\boxed{\sum_{\bar{\sigma}} \delta_{\bar{\sigma}\sigma} G_{a_{\uparrow} n_{d\bar{\sigma}}, d_{\sigma}}^r(\omega) = -\frac{t_{hp} G_{d_{\sigma} n_{d\bar{\sigma}}, d_{\sigma}}^r(\omega)}{(\omega^+ - \delta_M)} + \frac{\Delta G_{d_{\sigma}^{\dagger} n_{d\bar{\sigma}}, d_{\sigma}}^r(\omega)}{(\omega^+ - \delta_M)}} \tag{B.217}$$

Now, we calculate $G_{a_{\uparrow} n_{d\bar{\sigma}}, d_{\sigma}}^r(\omega)$:

$$(\omega + \eta^+) G_{a_{\uparrow} n_{d\bar{\sigma}}, d_{\sigma}}^r(\omega) = \langle \{a_{\uparrow}^{\dagger} n_{d\bar{\sigma}}, d_{\sigma}^{\dagger}\} \rangle + \langle \langle [a_{\uparrow}^{\dagger} n_{d\bar{\sigma}}, \mathcal{H}_e]; d_{\sigma}^{\dagger} \rangle \rangle \tag{B.218}$$

$$\begin{aligned}
 \langle \{a_{\uparrow}^{\dagger} n_{d\bar{\sigma}}, d_{\sigma}^{\dagger}\} \rangle &= \langle a_{\uparrow}^{\dagger} n_{d\bar{\sigma}} d_{\sigma}^{\dagger} + d_{\sigma}^{\dagger} a_{\uparrow}^{\dagger} n_{d\bar{\sigma}} \rangle \\
 &= \langle a_{\uparrow}^{\dagger} d_{\bar{\sigma}}^{\dagger} d_{\bar{\sigma}} d_{\sigma}^{\dagger} - a_{\uparrow}^{\dagger} d_{\sigma}^{\dagger} n_{d\bar{\sigma}} \rangle \\
 &= \langle a_{\uparrow}^{\dagger} d_{\sigma}^{\dagger} d_{\bar{\sigma}}^{\dagger} d_{\bar{\sigma}} - a_{\uparrow}^{\dagger} d_{\sigma}^{\dagger} n_{d\bar{\sigma}} \rangle \\
 &= \langle a_{\uparrow}^{\dagger} d_{\sigma}^{\dagger} n_{d\bar{\sigma}} - a_{\uparrow}^{\dagger} d_{\sigma}^{\dagger} n_{d\bar{\sigma}} \rangle \\
 &= 0.
 \end{aligned} \tag{B.219}$$

$$(\omega + \eta^+) G_{a_{\uparrow} n_{d\bar{\sigma}}, d_{\sigma}}^r(\omega) = \langle \langle [a_{\uparrow}^{\dagger} n_{d\bar{\sigma}}, \mathcal{H}_e]; d_{\sigma}^{\dagger} \rangle \rangle \tag{B.220}$$

$$\begin{aligned}
 [a_{\uparrow}^{\dagger} n_{d\bar{\sigma}}, \mathcal{H}_e] &= [a_{\uparrow}^{\dagger} n_{d\bar{\sigma}}, \mathcal{H}_{\text{lead}}] + [a_{\uparrow}^{\dagger} n_{d\bar{\sigma}}, \mathcal{H}_{\text{dot}}] + [a_{\uparrow}^{\dagger} n_{d\bar{\sigma}}, \mathcal{H}_{\text{dot-lead}}] + [a_{\uparrow}^{\dagger} n_{d\bar{\sigma}}, \mathcal{H}_M] \\
 &= [a_{\uparrow}^{\dagger} n_{d\bar{\sigma}}, \mathcal{H}_{\text{dot}}] + [a_{\uparrow}^{\dagger} n_{d\bar{\sigma}}, \mathcal{H}_{\text{dot-lead}}] + [a_{\uparrow}^{\dagger} n_{d\bar{\sigma}}, \mathcal{H}_M]
 \end{aligned} \tag{B.221}$$

$$[a_{\uparrow}^{\dagger} n_{d\bar{\sigma}}, \mathcal{H}_{\text{dot}}] = [a_{\uparrow}^{\dagger} n_{d\bar{\sigma}}, \sum_{\sigma} \varepsilon_{d\sigma} d_{\sigma}^{\dagger} d_{\sigma}] + [a_{\uparrow}^{\dagger} n_{d\bar{\sigma}}, U n_{d\uparrow} n_{d\downarrow}] = 0, \tag{B.222}$$

since $[a_{\uparrow} n_{d\bar{\sigma}}, \mathcal{H}_{\text{dot}}] = 0$.

$$\begin{aligned}
 [a_{\uparrow}^{\dagger} n_{d\bar{\sigma}}, \mathcal{H}_{\text{dot-lead}}] &= [a_{\uparrow}^{\dagger} n_{d\bar{\sigma}}, \sqrt{2}V \sum_{\mathbf{p}\bar{\sigma}} (e_{\mathbf{p}\bar{\sigma}}^{\dagger} d_{\bar{\sigma}} + d_{\bar{\sigma}}^{\dagger} e_{\mathbf{p}\bar{\sigma}})] \\
 &= \underbrace{\sqrt{2}V \sum_{\mathbf{p}\bar{\sigma}} [a_{\uparrow}^{\dagger} n_{d\bar{\sigma}}, e_{\mathbf{p}\bar{\sigma}}^{\dagger} d_{\bar{\sigma}}]}_I + \underbrace{\sqrt{2}V \sum_{\mathbf{p}\bar{\sigma}} [a_{\uparrow}^{\dagger} n_{d\bar{\sigma}}, d_{\bar{\sigma}}^{\dagger} e_{\mathbf{p}\bar{\sigma}}]}_{II}
 \end{aligned} \tag{B.223}$$

Based on the result of Eq.(B.201):

$$[a_{\uparrow}^{\dagger} n_{d\bar{\sigma}}, \mathcal{H}_{\text{dot-lead}}] = \sqrt{2}V \sum_{\mathbf{p}} \left(-e_{\mathbf{p}\bar{\sigma}}^{\dagger} d_{\bar{\sigma}} a_{\uparrow}^{\dagger} + d_{\bar{\sigma}}^{\dagger} e_{\mathbf{p}\bar{\sigma}} a_{\uparrow}^{\dagger} \right). \quad (\text{B.224})$$

Further,

$$\begin{aligned} [a_{\uparrow}^{\dagger} n_{d\bar{\sigma}}, \mathcal{H}_{\text{M}}] &= \left[a_{\uparrow}^{\dagger} n_{d\bar{\sigma}}, \delta_{\text{M}} \left(a_{\uparrow}^{\dagger} a_{\uparrow} - \frac{1}{2} \right) \right] + \left[a_{\uparrow}^{\dagger} n_{d\bar{\sigma}}, t_{hp} \sum_{\bar{\sigma}} (d_{\bar{\sigma}} a_{\uparrow}^{\dagger} + a_{\uparrow} d_{\bar{\sigma}}^{\dagger}) \right] \\ &+ \left[a_{\uparrow}^{\dagger} n_{d\bar{\sigma}}, \Delta \sum_{\bar{\sigma}} (d_{\bar{\sigma}} a_{\uparrow} + a_{\uparrow}^{\dagger} d_{\bar{\sigma}}^{\dagger}) \right], \end{aligned} \quad (\text{B.225})$$

$$\begin{aligned} \left[a_{\uparrow}^{\dagger} n_{d\bar{\sigma}}, \delta_{\text{M}} \left(a_{\uparrow}^{\dagger} a_{\uparrow} - \frac{1}{2} \right) \right] &= \delta_{\text{M}} \left(a_{\uparrow}^{\dagger} n_{d\bar{\sigma}} a_{\uparrow}^{\dagger} a_{\uparrow} - a_{\uparrow}^{\dagger} a_{\uparrow} a_{\uparrow}^{\dagger} n_{d\bar{\sigma}} \right) \\ &= \delta_{\text{M}} \left(-a_{\uparrow}^{\dagger} a_{\uparrow}^{\dagger} a_{\uparrow} n_{d\bar{\sigma}} - a_{\uparrow}^{\dagger} a_{\uparrow} a_{\uparrow}^{\dagger} n_{d\bar{\sigma}} \right) \\ &= \delta_{\text{M}} \left(-a_{\uparrow}^{\dagger} \left(a_{\uparrow}^{\dagger} a_{\uparrow} + a_{\uparrow} a_{\uparrow}^{\dagger} \right) n_{d\bar{\sigma}} \right) \\ &= \delta_{\text{M}} \left(-a_{\uparrow}^{\dagger} n_{d\bar{\sigma}} \right). \end{aligned} \quad (\text{B.226})$$

$$\left[a_{\uparrow}^{\dagger} n_{d\bar{\sigma}}, \sum_{\bar{\sigma}} (d_{\bar{\sigma}} a_{\uparrow}^{\dagger} + a_{\uparrow} d_{\bar{\sigma}}^{\dagger}) \right] = \underbrace{t_{hp} \sum_{\bar{\sigma}} \left[a_{\uparrow}^{\dagger} n_{d\bar{\sigma}}, d_{\bar{\sigma}} a_{\uparrow}^{\dagger} \right]}_I + \underbrace{t_{hp} \sum_{\bar{\sigma}} \left[a_{\uparrow}^{\dagger} n_{d\bar{\sigma}}, a_{\uparrow} d_{\bar{\sigma}}^{\dagger} \right]}_{II} \quad (\text{B.227})$$

$$\begin{aligned} I : t_{hp} \sum_{\bar{\sigma}} \left[a_{\uparrow}^{\dagger} n_{d\bar{\sigma}}, d_{\bar{\sigma}} a_{\uparrow}^{\dagger} \right] &= t_{hp} \sum_{\bar{\sigma}} \left(a_{\uparrow}^{\dagger} n_{d\bar{\sigma}} d_{\bar{\sigma}} a_{\uparrow}^{\dagger} - d_{\bar{\sigma}} a_{\uparrow}^{\dagger} a_{\uparrow}^{\dagger} n_{d\bar{\sigma}} \right) \\ &= t_{hp} \sum_{\bar{\sigma}} \left(a_{\uparrow}^{\dagger} d_{\bar{\sigma}}^{\dagger} d_{\bar{\sigma}} d_{\bar{\sigma}} a_{\uparrow}^{\dagger} - d_{\bar{\sigma}} a_{\uparrow}^{\dagger} a_{\uparrow}^{\dagger} n_{d\bar{\sigma}} \right) \\ &= t_{hp} \sum_{\bar{\sigma}} \left(a_{\uparrow}^{\dagger} a_{\uparrow}^{\dagger} \left(\delta_{\bar{\sigma}\bar{\sigma}} - d_{\bar{\sigma}} d_{\bar{\sigma}}^{\dagger} \right) d_{\bar{\sigma}} - a_{\uparrow}^{\dagger} a_{\uparrow}^{\dagger} d_{\bar{\sigma}} n_{d\bar{\sigma}} \right) \\ &= t_{hp} \sum_{\bar{\sigma}} \left(\delta_{\bar{\sigma}\bar{\sigma}} a_{\uparrow}^{\dagger} a_{\uparrow}^{\dagger} d_{\bar{\sigma}} - a_{\uparrow}^{\dagger} a_{\uparrow}^{\dagger} d_{\bar{\sigma}} d_{\bar{\sigma}}^{\dagger} d_{\bar{\sigma}} + a_{\uparrow}^{\dagger} a_{\uparrow}^{\dagger} d_{\bar{\sigma}} n_{d\bar{\sigma}} \right) \\ &= t_{hp} \sum_{\bar{\sigma}} \left(\delta_{\bar{\sigma}\bar{\sigma}} a_{\uparrow}^{\dagger} a_{\uparrow}^{\dagger} d_{\bar{\sigma}} \right) \end{aligned} \quad (\text{B.228})$$

$$\begin{aligned}
II : t_{hp} \sum_{\bar{\sigma}} \left[a_{\uparrow}^{\dagger} n_{d\bar{\sigma}}, a_{\uparrow} d_{\bar{\sigma}}^{\dagger} \right] &= t_{hp} \sum_{\bar{\sigma}} \left(a_{\uparrow}^{\dagger} n_{d\bar{\sigma}} a_{\uparrow} d_{\bar{\sigma}}^{\dagger} - a_{\uparrow} d_{\bar{\sigma}}^{\dagger} a_{\uparrow}^{\dagger} n_{d\bar{\sigma}} \right) \\
&= t_{hp} \sum_{\bar{\sigma}} \left(a_{\uparrow}^{\dagger} a_{\uparrow} d_{\bar{\sigma}}^{\dagger} d_{\bar{\sigma}} d_{\bar{\sigma}}^{\dagger} + a_{\uparrow} a_{\uparrow}^{\dagger} d_{\bar{\sigma}}^{\dagger} n_{d\bar{\sigma}} \right) \\
&= t_{hp} \sum_{\bar{\sigma}} \left(a_{\uparrow}^{\dagger} a_{\uparrow} d_{\bar{\sigma}}^{\dagger} \left(\delta_{\bar{\sigma}\bar{\sigma}} - d_{\bar{\sigma}}^{\dagger} d_{\bar{\sigma}} \right) + a_{\uparrow} a_{\uparrow}^{\dagger} d_{\bar{\sigma}}^{\dagger} n_{d\bar{\sigma}} \right) \\
&= t_{hp} \sum_{\bar{\sigma}} \left(-\delta_{\bar{\sigma}\bar{\sigma}} a_{\uparrow}^{\dagger} d_{\bar{\sigma}}^{\dagger} a_{\uparrow} - a_{\uparrow}^{\dagger} a_{\uparrow} d_{\bar{\sigma}}^{\dagger} d_{\bar{\sigma}}^{\dagger} d_{\bar{\sigma}} + a_{\uparrow} a_{\uparrow}^{\dagger} d_{\bar{\sigma}}^{\dagger} n_{d\bar{\sigma}} \right) \\
&= t_{hp} \sum_{\bar{\sigma}} \left(-\delta_{\bar{\sigma}\bar{\sigma}} a_{\uparrow}^{\dagger} d_{\bar{\sigma}}^{\dagger} a_{\uparrow} + a_{\uparrow}^{\dagger} a_{\uparrow} d_{\bar{\sigma}}^{\dagger} d_{\bar{\sigma}}^{\dagger} d_{\bar{\sigma}} + a_{\uparrow} a_{\uparrow}^{\dagger} d_{\bar{\sigma}}^{\dagger} n_{d\bar{\sigma}} \right) \\
&= t_{hp} \sum_{\bar{\sigma}} \left(-\delta_{\bar{\sigma}\bar{\sigma}} a_{\uparrow}^{\dagger} d_{\bar{\sigma}}^{\dagger} a_{\uparrow} + \left(a_{\uparrow}^{\dagger} a_{\uparrow} + a_{\uparrow} a_{\uparrow}^{\dagger} \right) d_{\bar{\sigma}}^{\dagger} n_{d\bar{\sigma}} \right) \\
&= t_{hp} \sum_{\bar{\sigma}} \left(d_{\bar{\sigma}}^{\dagger} n_{d\bar{\sigma}} - \delta_{\bar{\sigma}\bar{\sigma}} a_{\uparrow}^{\dagger} d_{\bar{\sigma}}^{\dagger} a_{\uparrow} \right) \tag{B.229}
\end{aligned}$$

$$\left[a_{\uparrow}^{\dagger} n_{d\bar{\sigma}}, \sum_{\bar{\sigma}} (d_{\bar{\sigma}} a_{\uparrow}^{\dagger} + a_{\uparrow} d_{\bar{\sigma}}^{\dagger}) \right] = t_{hp} \sum_{\bar{\sigma}} \left(\delta_{\bar{\sigma}\bar{\sigma}} a_{\uparrow}^{\dagger} a_{\uparrow}^{\dagger} d_{\bar{\sigma}} - \delta_{\bar{\sigma}\bar{\sigma}} a_{\uparrow}^{\dagger} d_{\bar{\sigma}}^{\dagger} a_{\uparrow} + d_{\bar{\sigma}}^{\dagger} n_{d\bar{\sigma}} \right). \tag{B.230}$$

$$\left[a_{\uparrow}^{\dagger} n_{d\bar{\sigma}}, \Delta \sum_{\bar{\sigma}} (d_{\bar{\sigma}} a_{\uparrow} + a_{\uparrow}^{\dagger} d_{\bar{\sigma}}^{\dagger}) \right] = \underbrace{\Delta \sum_{\bar{\sigma}} \left[a_{\uparrow}^{\dagger} n_{d\bar{\sigma}}, d_{\bar{\sigma}} a_{\uparrow} \right]}_I + \underbrace{\Delta \sum_{\bar{\sigma}} \left[a_{\uparrow}^{\dagger} n_{d\bar{\sigma}}, a_{\uparrow}^{\dagger} d_{\bar{\sigma}}^{\dagger} \right]}_{II} \tag{B.231}$$

$$\begin{aligned}
I : \Delta \sum_{\bar{\sigma}} \left[a_{\uparrow}^{\dagger} n_{d\bar{\sigma}}, d_{\bar{\sigma}} a_{\uparrow} \right] &= \Delta \sum_{\bar{\sigma}} \left(a_{\uparrow}^{\dagger} n_{d\bar{\sigma}} d_{\bar{\sigma}} a_{\uparrow} - d_{\bar{\sigma}} a_{\uparrow} a_{\uparrow}^{\dagger} n_{d\bar{\sigma}} \right) \\
&= \Delta \sum_{\bar{\sigma}} \left(a_{\uparrow}^{\dagger} d_{\bar{\sigma}}^{\dagger} d_{\bar{\sigma}} d_{\bar{\sigma}} a_{\uparrow} - d_{\bar{\sigma}} a_{\uparrow} a_{\uparrow}^{\dagger} n_{d\bar{\sigma}} \right) \\
&= \Delta \sum_{\bar{\sigma}} \left(a_{\uparrow}^{\dagger} a_{\uparrow} d_{\bar{\sigma}}^{\dagger} d_{\bar{\sigma}} d_{\bar{\sigma}} - a_{\uparrow} a_{\uparrow}^{\dagger} d_{\bar{\sigma}} n_{d\bar{\sigma}} \right) \\
&= \Delta \sum_{\bar{\sigma}} \left(a_{\uparrow}^{\dagger} a_{\uparrow} \left(\delta_{\bar{\sigma}\bar{\sigma}} - d_{\bar{\sigma}}^{\dagger} d_{\bar{\sigma}} \right) d_{\bar{\sigma}} - a_{\uparrow} a_{\uparrow}^{\dagger} d_{\bar{\sigma}} n_{d\bar{\sigma}} \right) \\
&= \Delta \sum_{\bar{\sigma}} \left(\delta_{\bar{\sigma}\bar{\sigma}} a_{\uparrow}^{\dagger} a_{\uparrow} d_{\bar{\sigma}} - a_{\uparrow}^{\dagger} a_{\uparrow} d_{\bar{\sigma}} d_{\bar{\sigma}}^{\dagger} d_{\bar{\sigma}} - a_{\uparrow} a_{\uparrow}^{\dagger} d_{\bar{\sigma}} n_{d\bar{\sigma}} \right) \\
&= \Delta \sum_{\bar{\sigma}} \left(\delta_{\bar{\sigma}\bar{\sigma}} a_{\uparrow}^{\dagger} a_{\uparrow} d_{\bar{\sigma}} - \left(a_{\uparrow}^{\dagger} a_{\uparrow} + a_{\uparrow} a_{\uparrow}^{\dagger} \right) d_{\bar{\sigma}} n_{d\bar{\sigma}} \right) \\
&= \Delta \sum_{\bar{\sigma}} \left(\delta_{\bar{\sigma}\bar{\sigma}} a_{\uparrow}^{\dagger} a_{\uparrow} d_{\bar{\sigma}} - d_{\bar{\sigma}} n_{d\bar{\sigma}} \right). \tag{B.232}
\end{aligned}$$

$$\begin{aligned}
 II : \Delta \sum_{\bar{\sigma}} \left[a_{\uparrow}^{\dagger} n_{d\bar{\sigma}}, a_{\uparrow}^{\dagger} d_{\bar{\sigma}}^{\dagger} \right] &= \Delta \left(a_{\uparrow}^{\dagger} n_{d\bar{\sigma}} a_{\uparrow}^{\dagger} d_{\bar{\sigma}}^{\dagger} - a_{\uparrow}^{\dagger} d_{\bar{\sigma}}^{\dagger} a_{\uparrow}^{\dagger} n_{d\bar{\sigma}} \right) \\
 &= \Delta \left(a_{\uparrow}^{\dagger} d_{\bar{\sigma}}^{\dagger} d_{\bar{\sigma}} a_{\uparrow}^{\dagger} d_{\bar{\sigma}}^{\dagger} - a_{\uparrow}^{\dagger} a_{\uparrow}^{\dagger} d_{\bar{\sigma}}^{\dagger} n_{d\bar{\sigma}} \right) \\
 &= \Delta \left(a_{\uparrow}^{\dagger} a_{\uparrow}^{\dagger} d_{\bar{\sigma}}^{\dagger} \left(\delta_{\bar{\sigma}\bar{\sigma}} - d_{\uparrow}^{\dagger} d_{\bar{\sigma}} \right) - a_{\uparrow}^{\dagger} a_{\uparrow}^{\dagger} d_{\bar{\sigma}}^{\dagger} n_{d\bar{\sigma}} \right) \\
 &= \Delta \left(\delta_{\bar{\sigma}\bar{\sigma}} a_{\uparrow}^{\dagger} a_{\uparrow}^{\dagger} d_{\bar{\sigma}}^{\dagger} - a_{\uparrow}^{\dagger} a_{\uparrow}^{\dagger} d_{\bar{\sigma}}^{\dagger} d_{\bar{\sigma}}^{\dagger} d_{\bar{\sigma}} - a_{\uparrow}^{\dagger} a_{\uparrow}^{\dagger} d_{\bar{\sigma}}^{\dagger} n_{d\bar{\sigma}} \right) \\
 &= \Delta \left(\delta_{\bar{\sigma}\bar{\sigma}} a_{\uparrow}^{\dagger} a_{\uparrow}^{\dagger} d_{\bar{\sigma}}^{\dagger} + a_{\uparrow}^{\dagger} a_{\uparrow}^{\dagger} d_{\bar{\sigma}}^{\dagger} d_{\bar{\sigma}}^{\dagger} d_{\bar{\sigma}} - a_{\uparrow}^{\dagger} a_{\uparrow}^{\dagger} d_{\bar{\sigma}}^{\dagger} n_{d\bar{\sigma}} \right) \\
 &= \Delta \left(\delta_{\bar{\sigma}\bar{\sigma}} a_{\uparrow}^{\dagger} a_{\uparrow}^{\dagger} d_{\bar{\sigma}}^{\dagger} \right). \tag{B.233}
 \end{aligned}$$

$$\left[a_{\uparrow}^{\dagger} n_{d\bar{\sigma}}, \Delta \sum_{\bar{\sigma}} (d_{\bar{\sigma}} a_{\uparrow} + a_{\uparrow}^{\dagger} d_{\bar{\sigma}}^{\dagger}) \right] = \Delta \left(\delta_{\bar{\sigma}\bar{\sigma}} a_{\uparrow}^{\dagger} a_{\uparrow}^{\dagger} d_{\bar{\sigma}} - d_{\bar{\sigma}} n_{d\bar{\sigma}} + \delta_{\bar{\sigma}\bar{\sigma}} a_{\uparrow}^{\dagger} a_{\uparrow}^{\dagger} d_{\bar{\sigma}}^{\dagger} \right). \tag{B.234}$$

$$\begin{aligned}
 (\omega + i\eta^+) G_{a_{\uparrow}^{\dagger} n_{d\bar{\sigma}}, d_{\sigma}}^r(\omega) &= \sqrt{2}V \sum_{\mathbf{p}} \left(-\langle\langle e_{\mathbf{p}\bar{\sigma}}^{\dagger} d_{\bar{\sigma}} a_{\uparrow}^{\dagger}; d_{\sigma}^{\dagger} \rangle\rangle + \langle\langle d_{\bar{\sigma}}^{\dagger} e_{\mathbf{p}\bar{\sigma}} a_{\uparrow}^{\dagger}; d_{\sigma}^{\dagger} \rangle\rangle \right) \\
 &+ (-\delta_{\mathbf{M}}) \langle\langle a_{\uparrow}^{\dagger} n_{d\bar{\sigma}}; d_{\sigma}^{\dagger} \rangle\rangle + t_{hp} \sum_{\bar{\sigma}} \langle\langle d_{\bar{\sigma}}^{\dagger} n_{d\bar{\sigma}}; d_{\sigma}^{\dagger} \rangle\rangle \\
 &+ t_{hp} \sum_{\bar{\sigma}} \delta_{\bar{\sigma}\bar{\sigma}} \left(\langle\langle a_{\uparrow}^{\dagger} a_{\uparrow}^{\dagger} d_{\bar{\sigma}}; d_{\sigma}^{\dagger} \rangle\rangle - \langle\langle a_{\uparrow}^{\dagger} d_{\bar{\sigma}}^{\dagger} a_{\uparrow}; d_{\sigma}^{\dagger} \rangle\rangle \right) \\
 &- \Delta \sum_{\bar{\sigma}} \langle\langle d_{\bar{\sigma}} n_{d\bar{\sigma}}; d_{\sigma}^{\dagger} \rangle\rangle - \Delta \sum_{\bar{\sigma}} \delta_{\bar{\sigma}\bar{\sigma}} \langle\langle a_{\uparrow}^{\dagger} a_{\uparrow}^{\dagger} d_{\bar{\sigma}}^{\dagger}; d_{\sigma}^{\dagger} \rangle\rangle \\
 &+ \Delta \sum_{\bar{\sigma}} \delta_{\bar{\sigma}\bar{\sigma}} \langle\langle a_{\uparrow}^{\dagger} a_{\uparrow} d_{\bar{\sigma}}; d_{\sigma}^{\dagger} \rangle\rangle \tag{B.235}
 \end{aligned}$$

As can be noticed Eq.(B.189), $G_{a_{\uparrow}^{\dagger} n_{d\bar{\sigma}}, d_{\sigma}}^r(\omega)$ also is multiplied by $\sum_{\bar{\sigma}} \delta_{\bar{\sigma}\bar{\sigma}}$. Hence, the same cancellation process of Eq.(B.213) occurs in Eq.(B.235), yielding

$$\begin{aligned}
 (\omega + \delta_{\mathbf{M}} + i\eta^+) \sum_{\bar{\sigma}} \delta_{\bar{\sigma}\bar{\sigma}} G_{a_{\uparrow}^{\dagger} n_{d\bar{\sigma}}, d_{\sigma}}^r(\omega) &= \sqrt{2}V \sum_{\mathbf{p}} \left(-G_{e_{\mathbf{p}\bar{\sigma}}^{\dagger} d_{\bar{\sigma}} a_{\uparrow}^{\dagger}, d_{\sigma}}^r(\omega) + G_{d_{\bar{\sigma}}^{\dagger} e_{\mathbf{p}\bar{\sigma}} a_{\uparrow}^{\dagger}, d_{\sigma}}^r(\omega) \right) \\
 &+ t_{hp} G_{d_{\bar{\sigma}}^{\dagger} n_{d\bar{\sigma}}, d_{\sigma}}^r(\omega) - \Delta G_{d_{\sigma} n_{d\bar{\sigma}}, d_{\sigma}}^r(\omega) \tag{B.236}
 \end{aligned}$$

Applying the decoupling scheme:

$$\begin{aligned}
 (\omega^+ + \delta_{\mathbf{M}}) \sum_{\bar{\sigma}} \delta_{\bar{\sigma}\bar{\sigma}} G_{a_{\uparrow}^{\dagger} n_{d\bar{\sigma}}, d_{\sigma}}^r(\omega) &= \sqrt{2}V \sum_{\mathbf{p}} \left(-\langle e_{\mathbf{p}\bar{\sigma}}^{\dagger} d_{\bar{\sigma}} \rangle G_{a_{\uparrow}^{\dagger}, d_{\sigma}}^r(\omega) + \langle d_{\bar{\sigma}}^{\dagger} e_{\mathbf{p}\bar{\sigma}} \rangle G_{a_{\uparrow}^{\dagger}, d_{\sigma}}^r(\omega) \right) \\
 &+ t_{hp} G_{d_{\bar{\sigma}}^{\dagger} n_{d\bar{\sigma}}, d_{\sigma}}^r(\omega) - \Delta G_{d_{\sigma} n_{d\bar{\sigma}}, d_{\sigma}}^r(\omega) \Rightarrow \tag{B.237}
 \end{aligned}$$

$$\boxed{\sum_{\bar{\sigma}} \delta_{\bar{\sigma}\sigma} G_{a_{\uparrow}^{\dagger} n_{d\bar{\sigma}}, d_{\sigma}}^r(\omega) = \frac{t_{hp} G_{d_{\sigma}^{\dagger} n_{d\bar{\sigma}}, d_{\sigma}}^r(\omega)}{(\omega^{+} + \delta_M)} - \frac{\Delta G_{d_{\sigma} n_{d\bar{\sigma}}, d_{\sigma}}^r(\omega)}{(\omega^{+} + \delta_M)}} \quad (\text{B.238})$$

Below, we list the main results obtained so far, which come from Eqs.(B.189), (B.217) and (B.238):

$$(\omega^{+} - \varepsilon_{d\sigma} - U - \Sigma_{\sigma}) G_{d_{\sigma} n_{d\bar{\sigma}}, d_{\sigma}}^r(\omega) + t_{hp} \sum_{\bar{\sigma}} \delta_{\bar{\sigma}\sigma} G_{a_{\uparrow}^{\dagger} n_{d\bar{\sigma}}, d_{\sigma}}^r(\omega) + \Delta \sum_{\bar{\sigma}} \delta_{\bar{\sigma}\sigma} G_{d_{\sigma}^{\dagger} n_{d\bar{\sigma}}, d_{\sigma}}^r(\omega) = \langle n_{d\bar{\sigma}} \rangle, \quad (\text{B.239})$$

$$\sum_{\bar{\sigma}} \delta_{\bar{\sigma}\sigma} G_{a_{\uparrow}^{\dagger} n_{d\bar{\sigma}}, d_{\sigma}}^r(\omega) = -\frac{t_{hp} G_{d_{\sigma} n_{d\bar{\sigma}}, d_{\sigma}}^r(\omega)}{(\omega^{+} - \delta_M)} + \frac{\Delta G_{d_{\sigma}^{\dagger} n_{d\bar{\sigma}}, d_{\sigma}}^r(\omega)}{(\omega^{+} - \delta_M)}, \quad (\text{B.240})$$

$$\sum_{\bar{\sigma}} \delta_{\bar{\sigma}\sigma} G_{d_{\sigma}^{\dagger} n_{d\bar{\sigma}}, d_{\sigma}}^r(\omega) = \frac{t_{hp} G_{d_{\sigma}^{\dagger} n_{d\bar{\sigma}}, d_{\sigma}}^r(\omega)}{(\omega^{+} + \delta_M)} - \frac{\Delta G_{d_{\sigma} n_{d\bar{\sigma}}, d_{\sigma}}^r(\omega)}{(\omega^{+} + \delta_M)}. \quad (\text{B.241})$$

The Eqs. (B.240) and (B.241) can be substituted in Eq.(B.239):

$$\begin{aligned} (\omega^{+} - \varepsilon_{d\sigma} - U - \Sigma_{\sigma}) G_{d_{\sigma} n_{d\bar{\sigma}}, d_{\sigma}}^r(\omega) + t_{hp} \left[-\frac{t_{hp} G_{d_{\sigma} n_{d\bar{\sigma}}, d_{\sigma}}^r(\omega)}{(\omega^{+} - \delta_M)} + \frac{\Delta G_{d_{\sigma}^{\dagger} n_{d\bar{\sigma}}, d_{\sigma}}^r(\omega)}{(\omega^{+} - \delta_M)} \right] \\ + \Delta \left[\frac{t_{hp} G_{d_{\sigma}^{\dagger} n_{d\bar{\sigma}}, d_{\sigma}}^r(\omega)}{(\omega^{+} + \delta_M)} - \frac{\Delta G_{d_{\sigma} n_{d\bar{\sigma}}, d_{\sigma}}^r(\omega)}{(\omega^{+} + \delta_M)} \right] = \langle n_{d\bar{\sigma}} \rangle \Rightarrow \end{aligned}$$

$$\begin{aligned} (\omega^{+} - \varepsilon_{d\sigma} - U - \Sigma_{\sigma}) G_{d_{\sigma} n_{d\bar{\sigma}}, d_{\sigma}}^r(\omega) - \left[\frac{t_{hp}^2}{(\omega^{+} - \delta_M)} + \frac{\Delta^2}{(\omega^{+} + \delta_M)} \right] G_{d_{\sigma} n_{d\bar{\sigma}}, d_{\sigma}}^r(\omega) \\ + t_{hp} \Delta \left[\frac{1}{(\omega^{+} - \delta_M)} + \frac{1}{(\omega^{+} + \delta_M)} \right] G_{d_{\sigma}^{\dagger} n_{d\bar{\sigma}}, d_{\sigma}}^r(\omega) = \langle n_{d\bar{\sigma}} \rangle \end{aligned} \quad (\text{B.242})$$

Using the same definitions of Eqs.(B.189), (B.217) and (B.238) into the equation above, we find:

$$\boxed{(\omega^{+} - \varepsilon_{d\sigma} - U - \Sigma_{\sigma}) G_{d_{\sigma} n_{d\bar{\sigma}}, d_{\sigma}}^r(\omega) - K_1 G_{d_{\sigma} n_{d\bar{\sigma}}, d_{\sigma}}^r(\omega) + t_{hp} \Delta K G_{d_{\sigma}^{\dagger} n_{d\bar{\sigma}}, d_{\sigma}}^r(\omega) = \langle n_{d\bar{\sigma}} \rangle} \quad (\text{B.243})$$

B.2.2 EOM and decoupling scheme in $G_{d_{\sigma}^{\dagger} n_{d\bar{\sigma}}, d_{\sigma}}^r(\omega)$

Continuing our endeavor to find the Green's function $G_{dd}^{\sigma}(\omega)$, we now proceed to find $G_{d_{\sigma}^{\dagger} n_{d\bar{\sigma}}, d_{\sigma}}^r(\omega)$, following the same steps of previous section. Let us start with:

$$(\omega + v\eta^{+}) G_{d_{\sigma}^{\dagger} n_{d\bar{\sigma}}, d_{\sigma}}^r(\omega) = \langle \{d_{\sigma}^{\dagger} n_{d\bar{\sigma}}, d_{\sigma}^{\dagger}\} \rangle + \langle \langle [d_{\sigma}^{\dagger} n_{d\bar{\sigma}}, \mathcal{H}_e]; d_{\sigma}^{\dagger} \rangle \rangle \quad (\text{B.244})$$

$$\begin{aligned}
\langle \{d_{\sigma}^{\dagger} n_{d\bar{\sigma}}, d_{\sigma}^{\dagger}\} \rangle &= \langle d_{\sigma}^{\dagger} n_{d\bar{\sigma}} d_{\sigma}^{\dagger} + d_{\sigma}^{\dagger} d_{\sigma}^{\dagger} n_{d\bar{\sigma}} \rangle \\
&= \langle d_{\sigma}^{\dagger} d_{\bar{\sigma}}^{\dagger} d_{\bar{\sigma}} d_{\sigma}^{\dagger} + d_{\sigma}^{\dagger} d_{\sigma}^{\dagger} n_{d\bar{\sigma}} \rangle \\
&= \langle d_{\sigma}^{\dagger} d_{\bar{\sigma}}^{\dagger} (\delta_{\sigma\bar{\sigma}} - d_{\sigma}^{\dagger} d_{\bar{\sigma}}) + d_{\sigma}^{\dagger} d_{\sigma}^{\dagger} n_{d\bar{\sigma}} \rangle \\
&= \langle \delta_{\sigma\bar{\sigma}} d_{\sigma}^{\dagger} d_{\bar{\sigma}}^{\dagger} - d_{\sigma}^{\dagger} d_{\bar{\sigma}}^{\dagger} d_{\sigma}^{\dagger} d_{\bar{\sigma}} + d_{\sigma}^{\dagger} d_{\sigma}^{\dagger} n_{d\bar{\sigma}} \rangle \\
&= \langle \delta_{\sigma\bar{\sigma}} d_{\sigma}^{\dagger} d_{\bar{\sigma}}^{\dagger} - d_{\sigma}^{\dagger} d_{\sigma}^{\dagger} d_{\bar{\sigma}}^{\dagger} d_{\bar{\sigma}} + d_{\sigma}^{\dagger} d_{\sigma}^{\dagger} n_{d\bar{\sigma}} \rangle \\
&= \delta_{\sigma\bar{\sigma}} \langle d_{\sigma}^{\dagger} d_{\bar{\sigma}}^{\dagger} \rangle = 0, \quad \text{since } \delta_{\sigma\bar{\sigma}} = 0
\end{aligned} \tag{B.245}$$

$$(\omega + \eta\eta^+) G_{d_{\sigma}^{\dagger} n_{d\bar{\sigma}} d_{\sigma}}^r(\omega) = \langle \langle [d_{\sigma}^{\dagger} n_{d\bar{\sigma}}, \mathcal{H}_e]; d_{\sigma}^{\dagger} \rangle \rangle \tag{B.246}$$

$$\begin{aligned}
[d_{\sigma}^{\dagger} n_{d\bar{\sigma}}, \mathcal{H}_e] &= [d_{\sigma}^{\dagger} n_{d\bar{\sigma}}, \mathcal{H}_{\text{lead}}] + [d_{\sigma}^{\dagger} n_{d\bar{\sigma}}, \mathcal{H}_{\text{dot}}] + [d_{\sigma}^{\dagger} n_{d\bar{\sigma}}, \mathcal{H}_{\text{dot-lead}}] + [d_{\sigma}^{\dagger} n_{d\bar{\sigma}}, \mathcal{H}_{\text{M}}] \\
&= [d_{\sigma}^{\dagger} n_{d\bar{\sigma}}, \mathcal{H}_{\text{dot}}] + [d_{\sigma}^{\dagger} n_{d\bar{\sigma}}, \mathcal{H}_{\text{dot-lead}}] + [d_{\sigma}^{\dagger} n_{d\bar{\sigma}}, \mathcal{H}_{\text{M}}].
\end{aligned} \tag{B.247}$$

$$[d_{\sigma}^{\dagger} n_{d\bar{\sigma}}, \mathcal{H}_{\text{dot}}] = [d_{\sigma}^{\dagger} n_{d\bar{\sigma}}, \sum_{\bar{\sigma}} \varepsilon_{d\bar{\sigma}} d_{\bar{\sigma}}^{\dagger} d_{\bar{\sigma}}] + [d_{\sigma}^{\dagger} n_{d\bar{\sigma}}, U n_{d\uparrow} n_{d\downarrow}] \tag{B.248}$$

$$\begin{aligned}
II & : U \left(-\delta_{\downarrow\bar{\sigma}} d_{\sigma}^{\dagger} d_{\uparrow}^{\dagger} d_{\downarrow}^{\dagger} d_{\bar{\sigma}} - d_{\uparrow}^{\dagger} d_{\sigma}^{\dagger} d_{\uparrow}^{\dagger} d_{\downarrow}^{\dagger} d_{\bar{\sigma}}^{\dagger} d_{\bar{\sigma}} - d_{\uparrow}^{\dagger} d_{\uparrow}^{\dagger} d_{\downarrow}^{\dagger} d_{\sigma}^{\dagger} d_{\bar{\sigma}}^{\dagger} d_{\bar{\sigma}} \right) \\
& = U \left(-\delta_{\downarrow\bar{\sigma}} d_{\sigma}^{\dagger} d_{\uparrow}^{\dagger} d_{\downarrow}^{\dagger} d_{\bar{\sigma}} - d_{\uparrow}^{\dagger} \left(\delta_{\sigma\uparrow} - d_{\uparrow} d_{\sigma}^{\dagger} \right) d_{\downarrow}^{\dagger} d_{\downarrow}^{\dagger} d_{\bar{\sigma}}^{\dagger} d_{\bar{\sigma}} \right) \\
& + U \left(-d_{\uparrow}^{\dagger} d_{\uparrow}^{\dagger} d_{\downarrow}^{\dagger} d_{\sigma}^{\dagger} d_{\bar{\sigma}}^{\dagger} d_{\bar{\sigma}} \right) \\
& = U \left(-\delta_{\downarrow\bar{\sigma}} d_{\sigma}^{\dagger} d_{\uparrow}^{\dagger} d_{\downarrow}^{\dagger} d_{\bar{\sigma}} - \delta_{\sigma\uparrow} d_{\uparrow}^{\dagger} d_{\downarrow}^{\dagger} d_{\downarrow}^{\dagger} d_{\bar{\sigma}}^{\dagger} d_{\bar{\sigma}} - d_{\uparrow}^{\dagger} d_{\uparrow}^{\dagger} d_{\downarrow}^{\dagger} d_{\sigma}^{\dagger} d_{\bar{\sigma}}^{\dagger} d_{\bar{\sigma}} \right) \\
& + U \left(-d_{\uparrow}^{\dagger} d_{\uparrow}^{\dagger} d_{\downarrow}^{\dagger} d_{\sigma}^{\dagger} d_{\bar{\sigma}}^{\dagger} d_{\bar{\sigma}} \right) \\
& = U \left(-\delta_{\downarrow\bar{\sigma}} d_{\sigma}^{\dagger} d_{\uparrow}^{\dagger} d_{\downarrow}^{\dagger} d_{\bar{\sigma}} - \delta_{\sigma\uparrow} d_{\uparrow}^{\dagger} d_{\downarrow}^{\dagger} d_{\downarrow}^{\dagger} d_{\bar{\sigma}}^{\dagger} d_{\bar{\sigma}} \right) \\
& + U \left(-d_{\uparrow}^{\dagger} d_{\uparrow}^{\dagger} d_{\downarrow}^{\dagger} \left(\delta_{\sigma\downarrow} - d_{\downarrow} d_{\sigma}^{\dagger} \right) d_{\bar{\sigma}}^{\dagger} d_{\bar{\sigma}} - d_{\uparrow}^{\dagger} d_{\uparrow}^{\dagger} d_{\downarrow}^{\dagger} d_{\sigma}^{\dagger} d_{\bar{\sigma}}^{\dagger} d_{\bar{\sigma}} \right) \\
& = U \left(-\delta_{\downarrow\bar{\sigma}} d_{\sigma}^{\dagger} d_{\uparrow}^{\dagger} d_{\downarrow}^{\dagger} d_{\bar{\sigma}} - \delta_{\sigma\uparrow} d_{\uparrow}^{\dagger} d_{\downarrow}^{\dagger} d_{\downarrow}^{\dagger} d_{\bar{\sigma}}^{\dagger} d_{\bar{\sigma}} \right) \\
& + U \left(-\delta_{\sigma\downarrow} d_{\uparrow}^{\dagger} d_{\uparrow}^{\dagger} d_{\downarrow}^{\dagger} d_{\bar{\sigma}}^{\dagger} d_{\bar{\sigma}} + d_{\uparrow}^{\dagger} d_{\uparrow}^{\dagger} d_{\downarrow}^{\dagger} d_{\sigma}^{\dagger} d_{\bar{\sigma}}^{\dagger} d_{\bar{\sigma}} - d_{\uparrow}^{\dagger} d_{\uparrow}^{\dagger} d_{\downarrow}^{\dagger} d_{\sigma}^{\dagger} d_{\bar{\sigma}}^{\dagger} d_{\bar{\sigma}} \right) \\
& = U \left(-\delta_{\downarrow\bar{\sigma}} d_{\sigma}^{\dagger} d_{\uparrow}^{\dagger} d_{\downarrow}^{\dagger} d_{\bar{\sigma}} - \delta_{\sigma\uparrow} d_{\uparrow}^{\dagger} d_{\downarrow}^{\dagger} d_{\downarrow}^{\dagger} d_{\bar{\sigma}}^{\dagger} d_{\bar{\sigma}} - \delta_{\sigma\downarrow} d_{\uparrow}^{\dagger} d_{\uparrow}^{\dagger} d_{\downarrow}^{\dagger} d_{\bar{\sigma}}^{\dagger} d_{\bar{\sigma}} \right), \tag{B.251}
\end{aligned}$$

$$\begin{aligned}
[d_{\sigma}^{\dagger} n_{d\bar{\sigma}}, U n_{d\uparrow} n_{d\downarrow}] & = U \left(\delta_{\uparrow\bar{\sigma}} d_{\sigma}^{\dagger} d_{\bar{\sigma}}^{\dagger} d_{\uparrow}^{\dagger} d_{\downarrow}^{\dagger} d_{\downarrow} - \delta_{\uparrow\bar{\sigma}} d_{\sigma}^{\dagger} d_{\uparrow}^{\dagger} d_{\bar{\sigma}}^{\dagger} d_{\downarrow}^{\dagger} d_{\downarrow} + \delta_{\downarrow\bar{\sigma}} d_{\sigma}^{\dagger} d_{\uparrow}^{\dagger} d_{\uparrow}^{\dagger} d_{\bar{\sigma}}^{\dagger} d_{\downarrow} \right) \\
& + U \left(-\delta_{\downarrow\bar{\sigma}} d_{\sigma}^{\dagger} d_{\uparrow}^{\dagger} d_{\downarrow}^{\dagger} d_{\bar{\sigma}} - \delta_{\sigma\uparrow} d_{\uparrow}^{\dagger} d_{\downarrow}^{\dagger} d_{\downarrow}^{\dagger} d_{\bar{\sigma}}^{\dagger} d_{\bar{\sigma}} - \delta_{\sigma\downarrow} d_{\uparrow}^{\dagger} d_{\uparrow}^{\dagger} d_{\downarrow}^{\dagger} d_{\bar{\sigma}}^{\dagger} d_{\bar{\sigma}} \right) \tag{B.252}
\end{aligned}$$

For $\sigma = \uparrow$:

$$\begin{aligned}
[d_{\sigma}^{\dagger} n_{d\bar{\sigma}}, U n_{d\uparrow} n_{d\downarrow}] & = U \left(d_{\uparrow}^{\dagger} d_{\uparrow}^{\dagger} d_{\uparrow}^{\dagger} d_{\downarrow}^{\dagger} d_{\downarrow} - d_{\uparrow}^{\dagger} d_{\uparrow}^{\dagger} d_{\uparrow}^{\dagger} d_{\downarrow}^{\dagger} d_{\downarrow} - d_{\uparrow}^{\dagger} d_{\downarrow}^{\dagger} d_{\downarrow}^{\dagger} d_{\downarrow} \right) \\
& = U \left(-d_{\uparrow}^{\dagger} d_{\downarrow}^{\dagger} d_{\downarrow}^{\dagger} d_{\downarrow} \right) \\
& = U \left(-d_{\sigma}^{\dagger} n_{d\bar{\sigma}} \right), \text{ where we have used } n_{d\bar{\sigma}} n_{d\bar{\sigma}} = n_{d\bar{\sigma}}. \tag{B.253}
\end{aligned}$$

$$\begin{aligned}
[d_{\sigma}^{\dagger} n_{d\bar{\sigma}}, \mathcal{H}_{\text{dot-lead}}] & = [d_{\sigma}^{\dagger} n_{d\bar{\sigma}}, \sqrt{2V} \sum_{\mathbf{k}\bar{\sigma}} (e_{\mathbf{k}\bar{\sigma}}^{\dagger} d_{\bar{\sigma}} + d_{\bar{\sigma}}^{\dagger} e_{\mathbf{k}\bar{\sigma}})] \\
& = \underbrace{\sqrt{2V} \sum_{\mathbf{k}\bar{\sigma}} [d_{\sigma}^{\dagger} n_{d\bar{\sigma}}, e_{\mathbf{k}\bar{\sigma}}^{\dagger} d_{\bar{\sigma}}]}_I + \underbrace{\sqrt{2V} \sum_{\mathbf{k}\bar{\sigma}} [d_{\sigma}^{\dagger} n_{d\bar{\sigma}}, d_{\bar{\sigma}}^{\dagger} e_{\mathbf{k}\bar{\sigma}}]}_{II} \tag{B.254}
\end{aligned}$$

$$\begin{aligned}
(\omega + \eta^+) G_{d_\sigma^\dagger n_{d\bar{\sigma}} d_\sigma}^r(\omega) &= -\varepsilon_{d\sigma} \langle \langle d_\sigma^\dagger n_{d\bar{\sigma}}; d_\sigma^\dagger \rangle \rangle - U \langle \langle d_\sigma^\dagger n_{d\bar{\sigma}}; d_\sigma^\dagger \rangle \rangle - \sqrt{2}V \sum_{\mathbf{k}} \langle \langle e_{\mathbf{k}\bar{\sigma}}^\dagger n_{d\bar{\sigma}}; d_\sigma^\dagger \rangle \rangle \\
&+ \sqrt{2}V \sum_{\mathbf{k}} \left(\langle \langle d_\sigma^\dagger e_{\mathbf{k}\bar{\sigma}} d_\sigma^\dagger; d_\sigma^\dagger \rangle \rangle - \langle \langle e_{\mathbf{k}\bar{\sigma}}^\dagger d_\sigma d_\sigma^\dagger; d_\sigma^\dagger \rangle \rangle \right) \\
&+ \langle \langle [d_\sigma^\dagger n_{d\bar{\sigma}}, \mathcal{H}_M]; d_\sigma^\dagger \rangle \rangle
\end{aligned} \tag{B.258}$$

$$\begin{aligned}
(\omega^+ + \varepsilon_{d\sigma} + U) G_{d_\sigma^\dagger n_{d\bar{\sigma}} d_\sigma}^r(\omega) &= -\sqrt{2}V \sum_{\mathbf{k}} G_{e_{\mathbf{k}\bar{\sigma}}^\dagger n_{d\bar{\sigma}} d_\sigma}^r(\omega) \\
&+ \sqrt{2}V \sum_{\mathbf{k}} \left(G_{d_\sigma^\dagger e_{\mathbf{k}\bar{\sigma}} d_\sigma^\dagger d_\sigma}^r(\omega) - G_{e_{\mathbf{k}\bar{\sigma}}^\dagger d_\sigma d_\sigma^\dagger d_\sigma}^r(\omega) \right) \\
&+ \langle \langle [d_\sigma^\dagger n_{d\bar{\sigma}}, \mathcal{H}_M]; d_\sigma^\dagger \rangle \rangle
\end{aligned} \tag{B.259}$$

$$\begin{aligned}
[d_\sigma^\dagger n_{d\bar{\sigma}}, \mathcal{H}_M] &= \left[d_\sigma^\dagger n_{d\bar{\sigma}}, \delta_M \left(a_\uparrow^\dagger a_\uparrow - \frac{1}{2} \right) \right] + \left[d_\sigma^\dagger n_{d\bar{\sigma}}, t_{hp} \sum_{\bar{\sigma}} (d_{\bar{\sigma}} a_\uparrow^\dagger + a_\uparrow d_{\bar{\sigma}}^\dagger) \right] \\
&+ \left[d_\sigma^\dagger n_{d\bar{\sigma}}, \Delta \sum_{\bar{\sigma}} (d_{\bar{\sigma}} a_\uparrow + a_\uparrow^\dagger d_{\bar{\sigma}}^\dagger) \right] \\
&= \left[d_\sigma^\dagger n_{d\bar{\sigma}}, t_{hp} \sum_{\bar{\sigma}} (d_{\bar{\sigma}} a_\uparrow^\dagger + a_\uparrow d_{\bar{\sigma}}^\dagger) \right] + \left[d_\sigma^\dagger n_{d\bar{\sigma}}, \Delta \sum_{\bar{\sigma}} (d_{\bar{\sigma}} a_\uparrow + a_\uparrow^\dagger d_{\bar{\sigma}}^\dagger) \right]
\end{aligned} \tag{B.260}$$

$$\left[d_\sigma^\dagger n_{d\bar{\sigma}}, t_{hp} \sum_{\bar{\sigma}} (d_{\bar{\sigma}} a_\uparrow^\dagger + a_\uparrow d_{\bar{\sigma}}^\dagger) \right] = \underbrace{t_{hp} \sum_{\bar{\sigma}} [d_\sigma^\dagger n_{d\bar{\sigma}}, d_{\bar{\sigma}} a_\uparrow^\dagger]}_I + \underbrace{t_{hp} \sum_{\bar{\sigma}} [d_\sigma^\dagger n_{d\bar{\sigma}}, a_\uparrow d_{\bar{\sigma}}^\dagger]}_{II} \tag{B.261}$$

$$\begin{aligned}
I : t_{hp} \sum_{\bar{\sigma}} \left[d_{\sigma}^{\dagger} n_{d\bar{\sigma}}, d_{\bar{\sigma}} a_{\uparrow}^{\dagger} \right] &= t_{hp} \sum_{\bar{\sigma}} \left(d_{\sigma}^{\dagger} n_{d\bar{\sigma}} d_{\bar{\sigma}} a_{\uparrow}^{\dagger} - d_{\bar{\sigma}} a_{\uparrow}^{\dagger} d_{\sigma}^{\dagger} n_{d\bar{\sigma}} \right) \\
&= t_{hp} \sum_{\bar{\sigma}} \left(d_{\sigma}^{\dagger} d_{\bar{\sigma}}^{\dagger} d_{\bar{\sigma}} d_{\bar{\sigma}} a_{\uparrow}^{\dagger} - d_{\bar{\sigma}} a_{\uparrow}^{\dagger} d_{\sigma}^{\dagger} n_{d\bar{\sigma}} \right) \\
&= t_{hp} \sum_{\bar{\sigma}} \left(-a_{\uparrow}^{\dagger} d_{\sigma}^{\dagger} d_{\bar{\sigma}}^{\dagger} d_{\bar{\sigma}} d_{\bar{\sigma}} - d_{\bar{\sigma}} a_{\uparrow}^{\dagger} d_{\sigma}^{\dagger} n_{d\bar{\sigma}} \right) \\
&= t_{hp} \sum_{\bar{\sigma}} \left(-a_{\uparrow}^{\dagger} d_{\sigma}^{\dagger} \left(\delta_{\bar{\sigma}\bar{\sigma}} - d_{\bar{\sigma}} d_{\bar{\sigma}}^{\dagger} \right) d_{\bar{\sigma}} - d_{\bar{\sigma}} a_{\uparrow}^{\dagger} d_{\sigma}^{\dagger} n_{d\bar{\sigma}} \right) \\
&= t_{hp} \sum_{\bar{\sigma}} \left(-\delta_{\bar{\sigma}\bar{\sigma}} a_{\uparrow}^{\dagger} d_{\sigma}^{\dagger} d_{\bar{\sigma}} + a_{\uparrow}^{\dagger} d_{\sigma}^{\dagger} d_{\bar{\sigma}} d_{\bar{\sigma}}^{\dagger} d_{\bar{\sigma}} - d_{\bar{\sigma}} a_{\uparrow}^{\dagger} d_{\sigma}^{\dagger} n_{d\bar{\sigma}} \right) \\
&= t_{hp} \sum_{\bar{\sigma}} \left(-\delta_{\bar{\sigma}\bar{\sigma}} a_{\uparrow}^{\dagger} d_{\sigma}^{\dagger} d_{\bar{\sigma}} + a_{\uparrow}^{\dagger} \left(\delta_{\bar{\sigma}\sigma} - d_{\bar{\sigma}} d_{\sigma}^{\dagger} \right) d_{\bar{\sigma}}^{\dagger} d_{\bar{\sigma}} - d_{\bar{\sigma}} a_{\uparrow}^{\dagger} d_{\sigma}^{\dagger} n_{d\bar{\sigma}} \right) \\
&= t_{hp} \sum_{\bar{\sigma}} \left(-\delta_{\bar{\sigma}\bar{\sigma}} a_{\uparrow}^{\dagger} d_{\sigma}^{\dagger} d_{\bar{\sigma}} + \delta_{\bar{\sigma}\sigma} a_{\uparrow}^{\dagger} d_{\bar{\sigma}}^{\dagger} d_{\bar{\sigma}} + d_{\bar{\sigma}} a_{\uparrow}^{\dagger} d_{\sigma}^{\dagger} n_{d\bar{\sigma}} - d_{\bar{\sigma}} a_{\uparrow}^{\dagger} d_{\sigma}^{\dagger} n_{d\bar{\sigma}} \right) \\
&= t_{hp} \sum_{\bar{\sigma}} \left(-\delta_{\bar{\sigma}\bar{\sigma}} d_{\bar{\sigma}} a_{\uparrow}^{\dagger} d_{\sigma}^{\dagger} + \delta_{\bar{\sigma}\sigma} a_{\uparrow}^{\dagger} d_{\bar{\sigma}}^{\dagger} d_{\bar{\sigma}} \right). \tag{B.262}
\end{aligned}$$

$$\begin{aligned}
II : t_{hp} \sum_{\bar{\sigma}} \left[d_{\sigma}^{\dagger} n_{d\bar{\sigma}}, a_{\uparrow} d_{\bar{\sigma}}^{\dagger} \right] &= t_{hp} \sum_{\bar{\sigma}} \left(d_{\sigma}^{\dagger} n_{d\bar{\sigma}} a_{\uparrow} d_{\bar{\sigma}}^{\dagger} - a_{\uparrow} d_{\bar{\sigma}}^{\dagger} d_{\sigma}^{\dagger} n_{d\bar{\sigma}} \right) \\
&= t_{hp} \sum_{\bar{\sigma}} \left(d_{\sigma}^{\dagger} d_{\bar{\sigma}}^{\dagger} d_{\bar{\sigma}} a_{\uparrow} d_{\bar{\sigma}}^{\dagger} - a_{\uparrow} d_{\bar{\sigma}}^{\dagger} d_{\sigma}^{\dagger} n_{d\bar{\sigma}} \right) \\
&= t_{hp} \sum_{\bar{\sigma}} \left(-a_{\uparrow} d_{\sigma}^{\dagger} d_{\bar{\sigma}}^{\dagger} d_{\bar{\sigma}} d_{\bar{\sigma}}^{\dagger} - a_{\uparrow} d_{\bar{\sigma}}^{\dagger} d_{\sigma}^{\dagger} n_{d\bar{\sigma}} \right) \\
&= t_{hp} \sum_{\bar{\sigma}} \left(-a_{\uparrow} d_{\sigma}^{\dagger} d_{\bar{\sigma}}^{\dagger} \left(\delta_{\bar{\sigma}\bar{\sigma}} - d_{\bar{\sigma}}^{\dagger} d_{\bar{\sigma}} \right) - a_{\uparrow} d_{\bar{\sigma}}^{\dagger} d_{\sigma}^{\dagger} n_{d\bar{\sigma}} \right) \\
&= t_{hp} \sum_{\bar{\sigma}} \left(-\delta_{\bar{\sigma}\bar{\sigma}} a_{\uparrow} d_{\sigma}^{\dagger} d_{\bar{\sigma}}^{\dagger} + a_{\uparrow} d_{\bar{\sigma}}^{\dagger} d_{\sigma}^{\dagger} n_{d\bar{\sigma}} - a_{\uparrow} d_{\bar{\sigma}}^{\dagger} d_{\sigma}^{\dagger} n_{d\bar{\sigma}} \right) \\
&= t_{hp} \sum_{\bar{\sigma}} \delta_{\bar{\sigma}\bar{\sigma}} a_{\uparrow} d_{\bar{\sigma}}^{\dagger} d_{\sigma}^{\dagger}. \tag{B.263}
\end{aligned}$$

$$\left[d_{\sigma}^{\dagger} n_{d\bar{\sigma}}, t_{hp} \sum_{\bar{\sigma}} (d_{\bar{\sigma}} a_{\uparrow}^{\dagger} + a_{\uparrow} d_{\bar{\sigma}}^{\dagger}) \right] = t_{hp} \sum_{\bar{\sigma}} \left(-\delta_{\bar{\sigma}\bar{\sigma}} d_{\bar{\sigma}} a_{\uparrow}^{\dagger} d_{\sigma}^{\dagger} + \delta_{\bar{\sigma}\bar{\sigma}} a_{\uparrow} d_{\bar{\sigma}}^{\dagger} d_{\sigma}^{\dagger} + \delta_{\bar{\sigma}\sigma} a_{\uparrow}^{\dagger} d_{\bar{\sigma}}^{\dagger} d_{\bar{\sigma}} \right) \tag{B.264}$$

$$\left[d_{\sigma}^{\dagger} n_{d\bar{\sigma}}, \Delta \sum_{\bar{\sigma}} (d_{\bar{\sigma}} a_{\uparrow} + a_{\uparrow}^{\dagger} d_{\bar{\sigma}}^{\dagger}) \right] = \underbrace{\Delta \sum_{\bar{\sigma}} \left[d_{\sigma}^{\dagger} n_{d\bar{\sigma}}, d_{\bar{\sigma}} a_{\uparrow} \right]}_I + \underbrace{\Delta \sum_{\bar{\sigma}} \left[d_{\sigma}^{\dagger} n_{d\bar{\sigma}}, a_{\uparrow}^{\dagger} d_{\bar{\sigma}}^{\dagger} \right]}_{II} \tag{B.265}$$

$$\begin{aligned}
 I : \Delta \sum_{\bar{\sigma}} \left[d_{\sigma}^{\dagger} n_{d\bar{\sigma}}, d_{\bar{\sigma}} a_{\uparrow} \right] &= \Delta \sum_{\bar{\sigma}} \left(d_{\sigma}^{\dagger} d_{\bar{\sigma}}^{\dagger} d_{\bar{\sigma}} d_{\bar{\sigma}} a_{\uparrow} - d_{\bar{\sigma}} a_{\uparrow} d_{\sigma}^{\dagger} n_{d\bar{\sigma}} \right) \\
 &= \Delta \sum_{\bar{\sigma}} \left(-a_{\uparrow} d_{\sigma}^{\dagger} d_{\bar{\sigma}}^{\dagger} d_{\bar{\sigma}} d_{\bar{\sigma}} - d_{\bar{\sigma}} a_{\uparrow} d_{\sigma}^{\dagger} n_{d\bar{\sigma}} \right) \\
 &= \Delta \sum_{\bar{\sigma}} \left(-\delta_{\bar{\sigma}\bar{\sigma}} a_{\uparrow} d_{\sigma}^{\dagger} d_{\bar{\sigma}} + a_{\uparrow} \left(\delta_{\bar{\sigma}\sigma} - d_{\bar{\sigma}} d_{\sigma}^{\dagger} \right) d_{\bar{\sigma}}^{\dagger} d_{\bar{\sigma}} - d_{\bar{\sigma}} a_{\uparrow} d_{\sigma}^{\dagger} n_{d\bar{\sigma}} \right) \\
 &= \Delta \sum_{\bar{\sigma}} \left(-\delta_{\bar{\sigma}\bar{\sigma}} a_{\uparrow} d_{\sigma}^{\dagger} d_{\bar{\sigma}} + \delta_{\bar{\sigma}\sigma} a_{\uparrow} d_{\bar{\sigma}}^{\dagger} d_{\bar{\sigma}} - a_{\uparrow} d_{\bar{\sigma}} d_{\sigma}^{\dagger} d_{\bar{\sigma}} - d_{\bar{\sigma}} a_{\uparrow} d_{\sigma}^{\dagger} n_{d\bar{\sigma}} \right) \\
 &= \Delta \sum_{\bar{\sigma}} \left(\delta_{\bar{\sigma}\bar{\sigma}} a_{\uparrow} d_{\bar{\sigma}} d_{\sigma}^{\dagger} + \delta_{\bar{\sigma}\sigma} a_{\uparrow} d_{\bar{\sigma}}^{\dagger} d_{\bar{\sigma}} \right). \tag{B.266}
 \end{aligned}$$

$$\begin{aligned}
 II : \Delta \sum_{\bar{\sigma}} \left[d_{\sigma}^{\dagger} n_{d\bar{\sigma}}, a_{\uparrow}^{\dagger} d_{\bar{\sigma}}^{\dagger} \right] &= \Delta \sum_{\bar{\sigma}} \left(d_{\sigma}^{\dagger} d_{\bar{\sigma}}^{\dagger} d_{\bar{\sigma}} a_{\uparrow}^{\dagger} d_{\bar{\sigma}}^{\dagger} - a_{\uparrow}^{\dagger} d_{\bar{\sigma}}^{\dagger} d_{\sigma}^{\dagger} n_{d\bar{\sigma}} \right) \\
 &= \Delta \sum_{\bar{\sigma}} \left(-a_{\uparrow}^{\dagger} d_{\sigma}^{\dagger} d_{\bar{\sigma}}^{\dagger} d_{\bar{\sigma}} d_{\bar{\sigma}}^{\dagger} - a_{\uparrow}^{\dagger} d_{\bar{\sigma}}^{\dagger} d_{\sigma}^{\dagger} n_{d\bar{\sigma}} \right) \\
 &= \Delta \sum_{\bar{\sigma}} \left(-a_{\uparrow}^{\dagger} d_{\sigma}^{\dagger} d_{\bar{\sigma}}^{\dagger} \left(\delta_{\bar{\sigma}\bar{\sigma}} - d_{\bar{\sigma}}^{\dagger} d_{\bar{\sigma}} \right) - a_{\uparrow}^{\dagger} d_{\bar{\sigma}}^{\dagger} d_{\sigma}^{\dagger} n_{d\bar{\sigma}} \right) \\
 &= \Delta \sum_{\bar{\sigma}} \left(-\delta_{\bar{\sigma}\bar{\sigma}} a_{\uparrow}^{\dagger} d_{\sigma}^{\dagger} d_{\bar{\sigma}}^{\dagger} + a_{\uparrow}^{\dagger} d_{\bar{\sigma}}^{\dagger} d_{\sigma}^{\dagger} d_{\bar{\sigma}}^{\dagger} d_{\bar{\sigma}} - a_{\uparrow}^{\dagger} d_{\bar{\sigma}}^{\dagger} d_{\sigma}^{\dagger} n_{d\bar{\sigma}} \right) \\
 &= \Delta \sum_{\bar{\sigma}} \left(-\delta_{\bar{\sigma}\bar{\sigma}} d_{\bar{\sigma}}^{\dagger} a_{\uparrow}^{\dagger} d_{\sigma}^{\dagger} \right). \tag{B.267}
 \end{aligned}$$

$$\left[d_{\sigma}^{\dagger} n_{d\bar{\sigma}}, \Delta \sum_{\bar{\sigma}} (d_{\bar{\sigma}} a_{\uparrow} + a_{\uparrow}^{\dagger} d_{\bar{\sigma}}^{\dagger}) \right] = \Delta \sum_{\bar{\sigma}} \left(\delta_{\bar{\sigma}\bar{\sigma}} a_{\uparrow} d_{\bar{\sigma}} d_{\sigma}^{\dagger} - \delta_{\bar{\sigma}\bar{\sigma}} d_{\bar{\sigma}}^{\dagger} a_{\uparrow}^{\dagger} d_{\sigma}^{\dagger} + \delta_{\bar{\sigma}\sigma} a_{\uparrow} d_{\bar{\sigma}}^{\dagger} d_{\sigma} \right) \tag{B.268}$$

$$\begin{aligned}
 (\omega + \varepsilon_{d\sigma} + U + \eta^{\dagger}) G_{d_{\sigma}^{\dagger} n_{d\bar{\sigma}} d_{\sigma}}^r(\omega) &= -\sqrt{2}V \sum_{\mathbf{k}} G_{e_{\mathbf{k}\bar{\sigma}}^{\dagger} n_{d\bar{\sigma}} d_{\sigma}}^r(\omega) + \sqrt{2}V \sum_{\mathbf{k}} \left(G_{d_{\bar{\sigma}}^{\dagger} e_{\mathbf{k}\bar{\sigma}} d_{\sigma}^{\dagger} d_{\sigma}}^r(\omega) - G_{e_{\mathbf{k}\bar{\sigma}}^{\dagger} d_{\bar{\sigma}} d_{\sigma}^{\dagger} d_{\sigma}}^r(\omega) \right) \\
 &+ t_{hp} \sum_{\bar{\sigma}} \left(\delta_{\bar{\sigma}\bar{\sigma}} G_{a_{\uparrow}^{\dagger} d_{\bar{\sigma}} d_{\sigma}^{\dagger} d_{\sigma}}^r(\omega) - \delta_{\bar{\sigma}\bar{\sigma}} G_{d_{\bar{\sigma}}^{\dagger} a_{\uparrow} d_{\sigma}^{\dagger} d_{\sigma}}^r(\omega) + \delta_{\bar{\sigma}\sigma} G_{a_{\uparrow}^{\dagger} n_{d\bar{\sigma}} d_{\sigma}}^r(\omega) \right) \\
 &+ \Delta \sum_{\bar{\sigma}} \left(\delta_{\bar{\sigma}\bar{\sigma}} G_{a_{\uparrow} d_{\bar{\sigma}} d_{\sigma}^{\dagger} d_{\sigma}}^r(\omega) - \delta_{\bar{\sigma}\bar{\sigma}} G_{d_{\bar{\sigma}}^{\dagger} a_{\uparrow} d_{\sigma}^{\dagger} d_{\sigma}}^r(\omega) + \delta_{\bar{\sigma}\sigma} G_{a_{\uparrow} n_{d\bar{\sigma}} d_{\sigma}}^r(\omega) \right) \tag{B.269}
 \end{aligned}$$

At this point, we truncate some Green's function in same way that we have done in Eq.(B.141):

$$G_{d_{\bar{\sigma}}^{\dagger} e_{\mathbf{k}\bar{\sigma}} d_{\sigma}^{\dagger} d_{\sigma}}^r(\omega) = \langle d_{\bar{\sigma}}^{\dagger} e_{\mathbf{k}\bar{\sigma}} \rangle G_{d_{\bar{\sigma}}^{\dagger} d_{\sigma}}^r(\omega), \tag{B.270}$$

$$G_{e_{\mathbf{k}\bar{\sigma}}^{\dagger} d_{\bar{\sigma}} d_{\sigma}^{\dagger} d_{\sigma}}^r(\omega) = \langle e_{\mathbf{k}\bar{\sigma}} d_{\bar{\sigma}} \rangle G_{d_{\bar{\sigma}}^{\dagger} d_{\sigma}}^r(\omega), \tag{B.271}$$

$$G_{a_{\uparrow}^{\dagger}d_{\bar{\sigma}}d_{\sigma}^{\dagger}}^r(\omega) = \langle a_{\uparrow}^{\dagger}d_{\bar{\sigma}} \rangle G_{d_{\bar{\sigma}}^{\dagger}d_{\sigma}}^r(\omega), \quad (\text{B.272})$$

$$G_{d_{\bar{\sigma}}^{\dagger}a_{\uparrow}d_{\sigma}^{\dagger}}^r(\omega) = \langle d_{\bar{\sigma}}^{\dagger}a_{\uparrow} \rangle G_{d_{\bar{\sigma}}^{\dagger}d_{\sigma}}^r(\omega), \quad (\text{B.273})$$

$$G_{a_{\uparrow}d_{\bar{\sigma}}d_{\sigma}^{\dagger}}^r(\omega) = \langle a_{\uparrow}d_{\bar{\sigma}} \rangle G_{d_{\bar{\sigma}}^{\dagger}d_{\sigma}}^r(\omega), \quad (\text{B.274})$$

$$G_{d_{\bar{\sigma}}^{\dagger}a_{\uparrow}^{\dagger}d_{\sigma}^{\dagger}}^r(\omega) = \langle d_{\bar{\sigma}}^{\dagger}a_{\uparrow}^{\dagger} \rangle G_{d_{\bar{\sigma}}^{\dagger}d_{\sigma}}^r(\omega). \quad (\text{B.275})$$

But,

$$\langle d_{\bar{\sigma}}^{\dagger}e_{\mathbf{k}\bar{\sigma}} \rangle G_{d_{\bar{\sigma}}^{\dagger}d_{\sigma}}^r(\omega) = \langle e_{\mathbf{k}\bar{\sigma}}^{\dagger}d_{\bar{\sigma}} \rangle G_{d_{\bar{\sigma}}^{\dagger}d_{\sigma}}^r(\omega) \quad (\text{B.276})$$

$$\langle a_{\uparrow}^{\dagger}d_{\bar{\sigma}} \rangle G_{d_{\bar{\sigma}}^{\dagger}d_{\sigma}}^r(\omega) = \langle d_{\bar{\sigma}}^{\dagger}a_{\uparrow} \rangle G_{d_{\bar{\sigma}}^{\dagger}d_{\sigma}}^r(\omega) \quad (\text{B.277})$$

$$\langle a_{\uparrow}d_{\bar{\sigma}} \rangle G_{d_{\bar{\sigma}}^{\dagger}d_{\sigma}}^r(\omega) = \langle d_{\bar{\sigma}}^{\dagger}a_{\uparrow}^{\dagger} \rangle G_{d_{\bar{\sigma}}^{\dagger}d_{\sigma}}^r(\omega) \quad (\text{B.278})$$

Thus,

$$(\omega^+ + \varepsilon_{d\sigma} + U)G_{d_{\bar{\sigma}}^{\dagger}n_{d\bar{\sigma}}d_{\sigma}}^r(\omega) = \left(-\sqrt{2}V\right) \sum_{\mathbf{k}} G_{e_{\mathbf{k}\bar{\sigma}}^{\dagger}n_{d\bar{\sigma}}d_{\sigma}}^r(\omega) + t_{hp} \sum_{\bar{\sigma}} \delta_{\bar{\sigma}\sigma} G_{a_{\uparrow}^{\dagger}n_{d\bar{\sigma}}d_{\sigma}}^r(\omega) + \Delta \sum_{\bar{\sigma}} \delta_{\bar{\sigma}\sigma} G_{a_{\uparrow}n_{d\bar{\sigma}}d_{\sigma}}^r(\omega) \quad (\text{B.279})$$

We already have obtained $\sum_{\bar{\sigma}} \delta_{\bar{\sigma}\sigma} G_{a_{\uparrow}^{\dagger}n_{d\bar{\sigma}}d_{\sigma}}^r(\omega)$ [Eq.(B.241)] and $\sum_{\bar{\sigma}} \delta_{\bar{\sigma}\sigma} G_{a_{\uparrow}n_{d\bar{\sigma}}d_{\sigma}}^r(\omega)$ [Eq.(B.240)]:

$$\sum_{\bar{\sigma}} \delta_{\bar{\sigma}\sigma} G_{a_{\uparrow}n_{d\bar{\sigma}}d_{\sigma}}^r(\omega) = -\frac{t_{hp}G_{d_{\sigma}n_{d\bar{\sigma}}d_{\sigma}}^r(\omega)}{(\omega^+ - \delta_{\mathbf{M}})} + \frac{\Delta G_{d_{\bar{\sigma}}^{\dagger}n_{d\bar{\sigma}}d_{\sigma}}^r(\omega)}{(\omega^+ - \delta_{\mathbf{M}})}, \quad (\text{B.280})$$

$$\sum_{\bar{\sigma}} \delta_{\bar{\sigma}\sigma} G_{a_{\uparrow}^{\dagger}n_{d\bar{\sigma}}d_{\sigma}}^r(\omega) = \frac{t_{hp}G_{d_{\bar{\sigma}}^{\dagger}n_{d\bar{\sigma}}d_{\sigma}}^r(\omega)}{(\omega^+ + \delta_{\mathbf{M}})} - \frac{\Delta G_{d_{\sigma}n_{d\bar{\sigma}}d_{\sigma}}^r(\omega)}{(\omega^+ + \delta_{\mathbf{M}})}. \quad (\text{B.281})$$

Let us substitute them into Eq.(B.279):

$$\begin{aligned} (\omega^+ + \varepsilon_{d\sigma} + U)G_{d_{\bar{\sigma}}^{\dagger}n_{d\bar{\sigma}}d_{\sigma}}^r(\omega) - t_{hp} \left[\frac{t_{hp}G_{d_{\bar{\sigma}}^{\dagger}n_{d\bar{\sigma}}d_{\sigma}}^r(\omega)}{(\omega^+ + \delta_{\mathbf{M}})} - \frac{\Delta G_{d_{\sigma}n_{d\bar{\sigma}}d_{\sigma}}^r(\omega)}{(\omega^+ + \delta_{\mathbf{M}})} \right] \\ - \Delta \left[-\frac{t_{hp}G_{d_{\sigma}n_{d\bar{\sigma}}d_{\sigma}}^r(\omega)}{(\omega^+ - \delta_{\mathbf{M}})} + \frac{\Delta G_{d_{\bar{\sigma}}^{\dagger}n_{d\bar{\sigma}}d_{\sigma}}^r(\omega)}{(\omega^+ - \delta_{\mathbf{M}})} \right] = \left(-\sqrt{2}V\right) \sum_{\mathbf{k}} G_{e_{\mathbf{k}\bar{\sigma}}^{\dagger}n_{d\bar{\sigma}}d_{\sigma}}^r(\omega) \Rightarrow \end{aligned}$$

$$\begin{aligned}
 (\omega^+ + \varepsilon_{d\sigma} + U)G_{d_\sigma^\dagger n_{d\bar{\sigma}} d_\sigma}^r(\omega) - \left[\frac{t_{hp}^2}{(\omega^+ + \delta_M)} + \frac{\Delta^2}{(\omega^+ - \delta_M)} \right] G_{d_\sigma^\dagger n_{d\bar{\sigma}} d_\sigma}^r(\omega) \\
 + t_{hp}\Delta \left[\frac{1}{(\omega^+ + \delta_M)} + \frac{1}{(\omega^+ - \delta_M)} \right] G_{d_\sigma n_{d\bar{\sigma}} d_\sigma}^r(\omega) = \left(-\sqrt{2}V \right) \sum_{\mathbf{k}} G_{e_{\mathbf{k}\sigma}^\dagger n_{d\bar{\sigma}} d_\sigma}^r(\omega)
 \end{aligned} \tag{B.282}$$

$$(\omega^+ + \varepsilon_{d\sigma} + U)G_{d_\sigma^\dagger n_{d\bar{\sigma}} d_\sigma}^r(\omega) - K_2 G_{d_\sigma^\dagger n_{d\bar{\sigma}} d_\sigma}^r(\omega) + t_{hp}\Delta K G_{d_\sigma n_{d\bar{\sigma}} d_\sigma}^r(\omega) = \left(-\sqrt{2}V \right) \sum_{\mathbf{k}} G_{e_{\mathbf{k}\sigma}^\dagger n_{d\bar{\sigma}} d_\sigma}^r(\omega)$$

(B.283)

where we have used the definitions of Eqs.(??) and (??). Following the Hubbard-I decoupling procedure, we should calculate $G_{e_{\mathbf{k}\sigma}^\dagger n_{d\bar{\sigma}} d_\sigma}^r(\omega)$:

$$(\omega + \eta^+) G_{e_{\mathbf{k}\sigma}^\dagger n_{d\bar{\sigma}} d_\sigma}^r(\omega) = \langle \{ e_{\mathbf{k}\sigma}^\dagger n_{d\bar{\sigma}}, d_\sigma^\dagger \} \rangle + \langle \langle [e_{\mathbf{k}\sigma}^\dagger n_{d\bar{\sigma}}, \mathcal{H}_e]; d_\sigma^\dagger \rangle \rangle \tag{B.284}$$

$$\begin{aligned}
 \langle \{ e_{\mathbf{k}\sigma}^\dagger n_{d\bar{\sigma}}, d_\sigma^\dagger \} \rangle &= \langle e_{\mathbf{k}\sigma}^\dagger n_{d\bar{\sigma}} d_\sigma^\dagger + d_\sigma^\dagger e_{\mathbf{k}\sigma}^\dagger n_{d\bar{\sigma}} \rangle \\
 &= \langle -d_\sigma^\dagger e_{\mathbf{k}\sigma}^\dagger n_{d\bar{\sigma}} + d_\sigma^\dagger e_{\mathbf{k}\sigma}^\dagger n_{d\bar{\sigma}} \rangle \\
 &= 0.
 \end{aligned} \tag{B.285}$$

$$(\omega + \eta^+) G_{e_{\mathbf{k}\sigma}^\dagger n_{d\bar{\sigma}} d_\sigma}^r(\omega) = \langle \langle [e_{\mathbf{k}\sigma}^\dagger n_{d\bar{\sigma}}, \mathcal{H}_e]; d_\sigma^\dagger \rangle \rangle \tag{B.286}$$

$$[e_{\mathbf{k}\sigma}^\dagger n_{d\bar{\sigma}}, \mathcal{H}_e] = [e_{\mathbf{k}\sigma}^\dagger n_{d\bar{\sigma}}, \mathcal{H}_{\text{lead}}] + [e_{\mathbf{k}\sigma}^\dagger n_{d\bar{\sigma}}, \mathcal{H}_{\text{dot}}] + [e_{\mathbf{k}\sigma}^\dagger n_{d\bar{\sigma}}, \mathcal{H}_{\text{dot-lead}}] + [e_{\mathbf{k}\sigma}^\dagger n_{d\bar{\sigma}}, \mathcal{H}_M] \tag{B.287}$$

$$[e_{\mathbf{k}\sigma}^\dagger n_{d\bar{\sigma}}, \mathcal{H}_{\text{lead}}] = [e_{\mathbf{k}\sigma}^\dagger n_{d\bar{\sigma}}, \sum_{\mathbf{p}\bar{\sigma}} \varepsilon_{\mathbf{p}\bar{\sigma}} e_{\mathbf{p}\bar{\sigma}}^\dagger e_{\mathbf{p}\bar{\sigma}}] + [e_{\mathbf{k}\sigma}^\dagger n_{d\bar{\sigma}}, V_{SD} \sum_{\mathbf{p}, \mathbf{q}\bar{\sigma}} e_{\mathbf{p}\bar{\sigma}}^\dagger e_{\mathbf{q}\bar{\sigma}}] \tag{B.288}$$

$$\begin{aligned}
 [e_{\mathbf{k}\sigma}^\dagger n_{d\bar{\sigma}}, \sum_{\mathbf{p}\bar{\sigma}} \varepsilon_{\mathbf{p}\bar{\sigma}} e_{\mathbf{p}\bar{\sigma}}^\dagger e_{\mathbf{p}\bar{\sigma}}] &= \sum_{\mathbf{p}\bar{\sigma}} \varepsilon_{\mathbf{p}\bar{\sigma}} \left(e_{\mathbf{k}\sigma}^\dagger n_{d\bar{\sigma}} e_{\mathbf{p}\bar{\sigma}}^\dagger e_{\mathbf{p}\bar{\sigma}} - e_{\mathbf{p}\bar{\sigma}}^\dagger e_{\mathbf{p}\bar{\sigma}} e_{\mathbf{k}\sigma}^\dagger n_{d\bar{\sigma}} \right) \\
 &= \sum_{\mathbf{p}\bar{\sigma}} \varepsilon_{\mathbf{p}\bar{\sigma}} \left(e_{\mathbf{k}\sigma}^\dagger e_{\mathbf{p}\bar{\sigma}}^\dagger e_{\mathbf{p}\bar{\sigma}} n_{d\bar{\sigma}} - e_{\mathbf{p}\bar{\sigma}}^\dagger e_{\mathbf{p}\bar{\sigma}} e_{\mathbf{k}\sigma}^\dagger n_{d\bar{\sigma}} \right) \\
 &= \sum_{\mathbf{p}\bar{\sigma}} \varepsilon_{\mathbf{p}\bar{\sigma}} \left(e_{\mathbf{k}\sigma}^\dagger e_{\mathbf{p}\bar{\sigma}}^\dagger e_{\mathbf{p}\bar{\sigma}} n_{d\bar{\sigma}} - e_{\mathbf{p}\bar{\sigma}}^\dagger \left(\delta_{\mathbf{k}\mathbf{p}} \delta_{\sigma\bar{\sigma}} - e_{\mathbf{k}\sigma}^\dagger e_{\mathbf{p}\bar{\sigma}} \right) n_{d\bar{\sigma}} \right) \\
 &= \sum_{\mathbf{p}\bar{\sigma}} \varepsilon_{\mathbf{p}\bar{\sigma}} \left(e_{\mathbf{k}\sigma}^\dagger e_{\mathbf{p}\bar{\sigma}}^\dagger e_{\mathbf{p}\bar{\sigma}} n_{d\bar{\sigma}} - \delta_{\mathbf{k}\mathbf{p}} \delta_{\sigma\bar{\sigma}} e_{\mathbf{p}\bar{\sigma}}^\dagger n_{d\bar{\sigma}} + e_{\mathbf{p}\bar{\sigma}}^\dagger e_{\mathbf{k}\sigma}^\dagger e_{\mathbf{p}\bar{\sigma}} n_{d\bar{\sigma}} \right) \\
 &= \sum_{\mathbf{p}\bar{\sigma}} \varepsilon_{\mathbf{p}\bar{\sigma}} \left(e_{\mathbf{k}\sigma}^\dagger e_{\mathbf{p}\bar{\sigma}}^\dagger e_{\mathbf{p}\bar{\sigma}} n_{d\bar{\sigma}} - \delta_{\mathbf{k}\mathbf{p}} \delta_{\sigma\bar{\sigma}} e_{\mathbf{p}\bar{\sigma}}^\dagger n_{d\bar{\sigma}} - e_{\mathbf{k}\sigma}^\dagger e_{\mathbf{p}\bar{\sigma}}^\dagger e_{\mathbf{p}\bar{\sigma}} n_{d\bar{\sigma}} \right) \\
 &= \varepsilon_{\mathbf{k}\sigma} \left(-e_{\mathbf{k}\sigma}^\dagger n_{d\bar{\sigma}} \right). \tag{B.289}
 \end{aligned}$$

$$\begin{aligned}
 [e_{\mathbf{k}\sigma}^\dagger n_{d\bar{\sigma}}, V_{SD} \sum_{\mathbf{p}, \mathbf{q}\bar{\sigma}} e_{\mathbf{p}\bar{\sigma}}^\dagger e_{\mathbf{q}\bar{\sigma}}] &= V_{SD} \sum_{\mathbf{p}, \mathbf{q}\bar{\sigma}} \left(e_{\mathbf{k}\sigma}^\dagger n_{d\bar{\sigma}} e_{\mathbf{p}\bar{\sigma}}^\dagger e_{\mathbf{q}\bar{\sigma}} - e_{\mathbf{p}\bar{\sigma}}^\dagger e_{\mathbf{q}\bar{\sigma}} e_{\mathbf{k}\sigma}^\dagger n_{d\bar{\sigma}} \right) \\
 &= V_{SD} \sum_{\mathbf{p}, \mathbf{q}\bar{\sigma}} \left(e_{\mathbf{k}\sigma}^\dagger e_{\mathbf{p}\bar{\sigma}}^\dagger e_{\mathbf{q}\bar{\sigma}} n_{d\bar{\sigma}} - e_{\mathbf{p}\bar{\sigma}}^\dagger e_{\mathbf{q}\bar{\sigma}} e_{\mathbf{k}\sigma}^\dagger n_{d\bar{\sigma}} \right) \\
 &= V_{SD} \sum_{\mathbf{p}, \mathbf{q}\bar{\sigma}} \left(e_{\mathbf{k}\sigma}^\dagger e_{\mathbf{p}\bar{\sigma}}^\dagger e_{\mathbf{q}\bar{\sigma}} n_{d\bar{\sigma}} - e_{\mathbf{p}\bar{\sigma}}^\dagger \left(\delta_{\mathbf{k}\mathbf{q}} \delta_{\sigma\bar{\sigma}} - e_{\mathbf{k}\sigma}^\dagger e_{\mathbf{q}\bar{\sigma}} \right) n_{d\bar{\sigma}} \right) \\
 &= V_{SD} \sum_{\mathbf{p}, \mathbf{q}\bar{\sigma}} \left(e_{\mathbf{k}\sigma}^\dagger e_{\mathbf{p}\bar{\sigma}}^\dagger e_{\mathbf{q}\bar{\sigma}} n_{d\bar{\sigma}} - \delta_{\mathbf{k}\mathbf{q}} \delta_{\sigma\bar{\sigma}} e_{\mathbf{p}\bar{\sigma}}^\dagger n_{d\bar{\sigma}} + e_{\mathbf{p}\bar{\sigma}}^\dagger e_{\mathbf{k}\sigma}^\dagger e_{\mathbf{q}\bar{\sigma}} n_{d\bar{\sigma}} \right) \\
 &= V_{SD} \sum_{\mathbf{p}, \mathbf{q}\bar{\sigma}} \left(e_{\mathbf{k}\sigma}^\dagger e_{\mathbf{p}\bar{\sigma}}^\dagger e_{\mathbf{q}\bar{\sigma}} n_{d\bar{\sigma}} - \delta_{\mathbf{k}\mathbf{q}} \delta_{\sigma\bar{\sigma}} e_{\mathbf{p}\bar{\sigma}}^\dagger n_{d\bar{\sigma}} - e_{\mathbf{k}\sigma}^\dagger e_{\mathbf{p}\bar{\sigma}}^\dagger e_{\mathbf{q}\bar{\sigma}} n_{d\bar{\sigma}} \right) \\
 &= V_{SD} \sum_{\mathbf{q}} \left(-e_{\mathbf{p}\bar{\sigma}}^\dagger n_{d\bar{\sigma}} \right). \tag{B.290}
 \end{aligned}$$

$$[e_{\mathbf{k}\sigma}^\dagger n_{d\bar{\sigma}}, \mathcal{H}_{\text{lead}}] = \varepsilon_{\mathbf{k}\sigma} \left(-e_{\mathbf{k}\sigma}^\dagger n_{d\bar{\sigma}} \right) + V_{SD} \sum_{\mathbf{q}} \left(-e_{\mathbf{p}\bar{\sigma}}^\dagger n_{d\bar{\sigma}} \right). \tag{B.291}$$

$$[e_{\mathbf{k}\sigma}^\dagger n_{d\bar{\sigma}}, \mathcal{H}_{\text{dot}}] = [e_{\mathbf{k}\sigma}^\dagger n_{d\bar{\sigma}}, \sum_{\bar{\sigma}} \varepsilon_{d\bar{\sigma}} d_{\bar{\sigma}}^\dagger d_{\bar{\sigma}}] + [e_{\mathbf{k}\sigma}^\dagger n_{d\bar{\sigma}}, U n_{d\uparrow} n_{d\downarrow}] = 0. \tag{B.292}$$

since $[e_{\mathbf{k}\sigma}^\dagger n_{d\bar{\sigma}}, \mathcal{H}_{\text{dot}}] = 0$.

$$\begin{aligned}
 [e_{\mathbf{k}\sigma}^\dagger n_{d\bar{\sigma}}, \mathcal{H}_{\text{dot-lead}}] &= [e_{\mathbf{k}\sigma}^\dagger n_{d\bar{\sigma}}, \sqrt{2}V \sum_{\mathbf{p}\bar{\sigma}} (e_{\mathbf{p}\bar{\sigma}}^\dagger d_{\bar{\sigma}} + d_{\bar{\sigma}}^\dagger e_{\mathbf{p}\bar{\sigma}})] \\
 &= \underbrace{\sqrt{2}V \sum_{\mathbf{p}\bar{\sigma}} [e_{\mathbf{k}\sigma}^\dagger n_{d\bar{\sigma}}, e_{\mathbf{p}\bar{\sigma}}^\dagger d_{\bar{\sigma}}]}_I + \underbrace{\sqrt{2}V \sum_{\mathbf{p}\bar{\sigma}} [e_{\mathbf{k}\sigma}^\dagger n_{d\bar{\sigma}}, d_{\bar{\sigma}}^\dagger e_{\mathbf{p}\bar{\sigma}}]}_{II} \tag{B.293}
 \end{aligned}$$

$$\begin{aligned}
 I : \sqrt{2}V \sum_{\mathbf{p}\bar{\sigma}} [e_{\mathbf{k}\sigma}^\dagger n_{d\bar{\sigma}}, e_{\mathbf{p}\bar{\sigma}}^\dagger d_{\bar{\sigma}}] &= \sqrt{2}V \sum_{\mathbf{p}\bar{\sigma}} \left(e_{\mathbf{k}\sigma}^\dagger n_{d\bar{\sigma}} e_{\mathbf{p}\bar{\sigma}}^\dagger d_{\bar{\sigma}} - e_{\mathbf{p}\bar{\sigma}}^\dagger d_{\bar{\sigma}} e_{\mathbf{k}\sigma}^\dagger n_{d\bar{\sigma}} \right) \\
 &= \sqrt{2}V \sum_{\mathbf{p}\bar{\sigma}} \left(-e_{\mathbf{p}\bar{\sigma}}^\dagger e_{\mathbf{k}\sigma}^\dagger d_{\bar{\sigma}}^\dagger d_{\bar{\sigma}} d_{\bar{\sigma}} + e_{\mathbf{p}\bar{\sigma}}^\dagger e_{\mathbf{k}\sigma}^\dagger d_{\bar{\sigma}} n_{d\bar{\sigma}} \right) \\
 &= \sqrt{2}V \sum_{\mathbf{p}\bar{\sigma}} \left(e_{\mathbf{p}\bar{\sigma}}^\dagger e_{\mathbf{k}\sigma}^\dagger \left(\delta_{\bar{\sigma}\bar{\sigma}} - d_{\bar{\sigma}}^\dagger d_{\bar{\sigma}} \right) d_{\bar{\sigma}} + e_{\mathbf{p}\bar{\sigma}}^\dagger e_{\mathbf{k}\sigma}^\dagger d_{\bar{\sigma}} n_{d\bar{\sigma}} \right) \\
 &= \sqrt{2}V \sum_{\mathbf{p}\bar{\sigma}} \left(\delta_{\bar{\sigma}\bar{\sigma}} e_{\mathbf{p}\bar{\sigma}}^\dagger e_{\mathbf{k}\sigma}^\dagger d_{\bar{\sigma}} - e_{\mathbf{p}\bar{\sigma}}^\dagger e_{\mathbf{k}\sigma}^\dagger d_{\bar{\sigma}} n_{d\bar{\sigma}} + e_{\mathbf{p}\bar{\sigma}}^\dagger e_{\mathbf{k}\sigma}^\dagger d_{\bar{\sigma}} n_{d\bar{\sigma}} \right) \\
 &= \sqrt{2}V \sum_{\mathbf{p}} \left(-e_{\mathbf{p}\bar{\sigma}}^\dagger d_{\bar{\sigma}} e_{\mathbf{k}\sigma}^\dagger \right). \tag{B.294}
 \end{aligned}$$

$$\begin{aligned}
 II : \sqrt{2}V \sum_{\mathbf{p}\bar{\sigma}} [e_{\mathbf{k}\sigma}^\dagger n_{d\bar{\sigma}}, d_{\bar{\sigma}}^\dagger e_{\mathbf{p}\bar{\sigma}}] &= \sqrt{2}V \sum_{\mathbf{p}\bar{\sigma}} \left(e_{\mathbf{k}\sigma}^\dagger n_{d\bar{\sigma}} d_{\bar{\sigma}}^\dagger e_{\mathbf{p}\bar{\sigma}} - d_{\bar{\sigma}}^\dagger e_{\mathbf{p}\bar{\sigma}} e_{\mathbf{k}\sigma}^\dagger n_{d\bar{\sigma}} \right) \\
 &= \sqrt{2}V \sum_{\mathbf{p}\bar{\sigma}} \left(-e_{\mathbf{k}\sigma}^\dagger e_{\mathbf{p}\bar{\sigma}} d_{\bar{\sigma}}^\dagger d_{\bar{\sigma}} d_{\bar{\sigma}}^\dagger - e_{\mathbf{p}\bar{\sigma}} e_{\mathbf{k}\sigma}^\dagger d_{\bar{\sigma}}^\dagger n_{d\bar{\sigma}} \right) \\
 &= \sqrt{2}V \sum_{\mathbf{p}\bar{\sigma}} \left(-e_{\mathbf{k}\sigma}^\dagger e_{\mathbf{p}\bar{\sigma}} d_{\bar{\sigma}}^\dagger d_{\bar{\sigma}} d_{\bar{\sigma}}^\dagger - e_{\mathbf{p}\bar{\sigma}} e_{\mathbf{k}\sigma}^\dagger d_{\bar{\sigma}}^\dagger n_{d\bar{\sigma}} \right) \\
 &= \sqrt{2}V \sum_{\mathbf{p}\bar{\sigma}} \left(-\left(\delta_{\bar{\sigma}\bar{\sigma}} e_{\mathbf{k}\sigma}^\dagger e_{\mathbf{p}\bar{\sigma}} d_{\bar{\sigma}}^\dagger - e_{\mathbf{k}\sigma}^\dagger e_{\mathbf{p}\bar{\sigma}} d_{\bar{\sigma}}^\dagger d_{\bar{\sigma}}^\dagger d_{\bar{\sigma}} \right) - e_{\mathbf{p}\bar{\sigma}} e_{\mathbf{k}\sigma}^\dagger d_{\bar{\sigma}}^\dagger n_{d\bar{\sigma}} \right) \\
 &= \sqrt{2}V \sum_{\mathbf{p}\bar{\sigma}} \left(-\delta_{\bar{\sigma}\bar{\sigma}} e_{\mathbf{k}\sigma}^\dagger e_{\mathbf{p}\bar{\sigma}} d_{\bar{\sigma}}^\dagger + e_{\mathbf{k}\sigma}^\dagger e_{\mathbf{p}\bar{\sigma}} d_{\bar{\sigma}}^\dagger d_{\bar{\sigma}}^\dagger d_{\bar{\sigma}} - e_{\mathbf{p}\bar{\sigma}} e_{\mathbf{k}\sigma}^\dagger d_{\bar{\sigma}}^\dagger n_{d\bar{\sigma}} \right) \\
 &= \sqrt{2}V \sum_{\mathbf{p}\bar{\sigma}} \left(-\delta_{\bar{\sigma}\bar{\sigma}} e_{\mathbf{k}\sigma}^\dagger e_{\mathbf{p}\bar{\sigma}} d_{\bar{\sigma}}^\dagger - \left(e_{\mathbf{k}\sigma}^\dagger e_{\mathbf{p}\bar{\sigma}} + e_{\mathbf{p}\bar{\sigma}} e_{\mathbf{k}\sigma}^\dagger \right) d_{\bar{\sigma}}^\dagger d_{\bar{\sigma}}^\dagger d_{\bar{\sigma}} \right) \\
 &= \sqrt{2}V \sum_{\mathbf{p}\bar{\sigma}} \left(\delta_{\bar{\sigma}\bar{\sigma}} d_{\bar{\sigma}}^\dagger e_{\mathbf{p}\bar{\sigma}} e_{\mathbf{k}\sigma}^\dagger - \delta_{\mathbf{k}\mathbf{p}} \delta_{\bar{\sigma}\bar{\sigma}} d_{\bar{\sigma}}^\dagger d_{\bar{\sigma}}^\dagger d_{\bar{\sigma}} \right) \\
 &= \sqrt{2}V \left(\sum_{\mathbf{p}\bar{\sigma}} \delta_{\bar{\sigma}\bar{\sigma}} d_{\bar{\sigma}}^\dagger e_{\mathbf{p}\bar{\sigma}} e_{\mathbf{k}\sigma}^\dagger - \sum_{\mathbf{p}\bar{\sigma}} \delta_{\mathbf{k}\mathbf{p}} \delta_{\bar{\sigma}\bar{\sigma}} d_{\bar{\sigma}}^\dagger d_{\bar{\sigma}}^\dagger d_{\bar{\sigma}} \right) \\
 &= \sqrt{2}V \left(\sum_{\mathbf{p}} d_{\bar{\sigma}}^\dagger e_{\mathbf{p}\bar{\sigma}} e_{\mathbf{k}\sigma}^\dagger - d_{\bar{\sigma}}^\dagger d_{\bar{\sigma}}^\dagger d_{\bar{\sigma}} \right) \\
 &= \sqrt{2}V \left(\sum_{\mathbf{p}} d_{\bar{\sigma}}^\dagger e_{\mathbf{p}\bar{\sigma}} e_{\mathbf{k}\sigma}^\dagger - d_{\bar{\sigma}}^\dagger n_{d\bar{\sigma}} \right). \tag{B.295}
 \end{aligned}$$

$$[e_{\mathbf{k}\sigma}^\dagger n_{d\bar{\sigma}}, \mathcal{H}_{\text{dot-lead}}] = \sqrt{2}V \sum_{\mathbf{p}} \left(-e_{\mathbf{p}\bar{\sigma}}^\dagger d_{\bar{\sigma}} e_{\mathbf{k}\sigma}^\dagger + d_{\bar{\sigma}}^\dagger e_{\mathbf{p}\bar{\sigma}} e_{\mathbf{k}\sigma}^\dagger \right) - \sqrt{2}V d_{\bar{\sigma}}^\dagger n_{d\bar{\sigma}}. \tag{B.296}$$

$$\begin{aligned}
(\omega + \eta^+) G_{e_{\mathbf{k}\sigma}^\dagger n_{d\bar{\sigma}}, d_\sigma}^r(\omega) &= (-\varepsilon_{\mathbf{k}\sigma}) \langle \langle e_{\mathbf{k}\sigma}^\dagger n_{d\bar{\sigma}}; d_\sigma^\dagger \rangle \rangle + \left(-V_{SD} \sum_{\mathbf{q}} \right) \langle \langle e_{\mathbf{p}\sigma}^\dagger n_{d\bar{\sigma}}; d_\sigma^\dagger \rangle \rangle - \sqrt{2}V \langle \langle d_\sigma^\dagger n_{d\bar{\sigma}}; d_\sigma^\dagger \rangle \rangle \\
&+ \sqrt{2}V \sum_{\mathbf{p}} \langle \langle d_\sigma^\dagger e_{\mathbf{p}\bar{\sigma}} e_{\mathbf{k}\sigma}^\dagger; d_\sigma^\dagger \rangle \rangle + \left(-\sqrt{2}V \sum_{\mathbf{p}} \right) \langle \langle e_{\mathbf{p}\bar{\sigma}}^\dagger d_\sigma e_{\mathbf{k}\sigma}^\dagger; d_\sigma^\dagger \rangle \rangle \\
&+ \langle \langle [e_{\mathbf{k}\sigma}^\dagger n_{d\bar{\sigma}}, \mathcal{H}_M]; d_\sigma^\dagger \rangle \rangle
\end{aligned} \tag{B.297}$$

$$\begin{aligned}
(\omega + \varepsilon_{\mathbf{k}\sigma} + \eta^+) G_{e_{\mathbf{k}\sigma}^\dagger n_{d\bar{\sigma}}, d_\sigma}^r(\omega) &= \left(-V_{SD} \sum_{\mathbf{k}} \right) G_{e_{\mathbf{k}\sigma}^\dagger n_{d\bar{\sigma}}, d_\sigma}^r(\omega) - \sqrt{2}V G_{d_\sigma^\dagger n_{d\bar{\sigma}}, d_\sigma}^r(\omega) \\
&+ \sqrt{2}V \sum_{\mathbf{p}} G_{d_\sigma^\dagger e_{\mathbf{p}\bar{\sigma}} e_{\mathbf{k}\sigma}^\dagger, d_\sigma}^r(\omega) + \left(-\sqrt{2}V \sum_{\mathbf{p}} \right) G_{e_{\mathbf{p}\bar{\sigma}}^\dagger d_\sigma e_{\mathbf{k}\sigma}^\dagger, d_\sigma}^r(\omega) \\
&+ \langle \langle [e_{\mathbf{k}\sigma}^\dagger n_{d\bar{\sigma}}, \mathcal{H}_M]; d_\sigma^\dagger \rangle \rangle
\end{aligned} \tag{B.298}$$

Before calculating the commutation relation of last line of equation above, let us apply the Hubbard-I decoupling as follows:

$$\begin{aligned}
(\omega + \varepsilon_{\mathbf{k}\sigma} + \eta^+) G_{e_{\mathbf{k}\sigma}^\dagger n_{d\bar{\sigma}}, d_\sigma}^r(\omega) &= -V_{SD} \sum_{\mathbf{k}} G_{e_{\mathbf{k}\sigma}^\dagger n_{d\bar{\sigma}}, d_\sigma}^r(\omega) - \sqrt{2}V G_{d_\sigma^\dagger n_{d\bar{\sigma}}, d_\sigma}^r(\omega) \\
&+ \sqrt{2}V \sum_{\mathbf{p}} \langle d_\sigma^\dagger e_{\mathbf{p}\bar{\sigma}} \rangle G_{e_{\mathbf{k}\sigma}^\dagger, d_\sigma}^r(\omega) - \sqrt{2}V \sum_{\mathbf{p}} \langle e_{\mathbf{p}\bar{\sigma}}^\dagger d_\sigma \rangle G_{e_{\mathbf{k}\sigma}^\dagger, d_\sigma}^r(\omega) \\
&+ \langle \langle [e_{\mathbf{k}\sigma}^\dagger n_{d\bar{\sigma}}, \mathcal{H}_M]; d_\sigma^\dagger \rangle \rangle
\end{aligned} \tag{B.299}$$

$$\begin{aligned}
(\omega + \varepsilon_{\mathbf{k}\sigma} + \eta^+) G_{e_{\mathbf{k}\sigma}^\dagger n_{d\bar{\sigma}}, d_\sigma}^r(\omega) &= -V_{SD} \sum_{\mathbf{k}} G_{e_{\mathbf{k}\sigma}^\dagger n_{d\bar{\sigma}}, d_\sigma}^r(\omega) - \sqrt{2}V G_{d_\sigma^\dagger n_{d\bar{\sigma}}, d_\sigma}^r(\omega) \\
&+ \sqrt{2}V \sum_{\mathbf{p}} \langle d_\sigma^\dagger e_{\mathbf{p}\bar{\sigma}} \rangle G_{e_{\mathbf{k}\sigma}^\dagger, d_\sigma}^r(\omega) - \sqrt{2}V \sum_{\mathbf{p}} \langle e_{\mathbf{p}\bar{\sigma}}^\dagger d_\sigma \rangle G_{e_{\mathbf{k}\sigma}^\dagger, d_\sigma}^r(\omega) \\
&+ \langle \langle [e_{\mathbf{k}\sigma}^\dagger n_{d\bar{\sigma}}, \mathcal{H}_M]; d_\sigma^\dagger \rangle \rangle
\end{aligned} \tag{B.300}$$

$$\begin{aligned}
(\omega + \varepsilon_{\mathbf{k}\sigma} + \eta^+) G_{e_{\mathbf{k}\sigma}^\dagger n_{d\bar{\sigma}}, d_\sigma}^r(\omega) &= -V_{SD} \sum_{\mathbf{k}} G_{e_{\mathbf{k}\sigma}^\dagger n_{d\bar{\sigma}}, d_\sigma}^r(\omega) - \sqrt{2}V G_{d_\sigma^\dagger n_{d\bar{\sigma}}, d_\sigma}^r(\omega) \\
&+ \langle \langle [e_{\mathbf{k}\sigma}^\dagger n_{d\bar{\sigma}}, \mathcal{H}_M]; d_\sigma^\dagger \rangle \rangle
\end{aligned} \tag{B.301}$$

Now, let us calculate $\langle \langle [e_{\mathbf{k}\sigma}^\dagger n_{d\bar{\sigma}}, \mathcal{H}_M]; d_\sigma^\dagger \rangle \rangle$:

$$\begin{aligned}
 [e_{\mathbf{k}\sigma}^\dagger n_{d\bar{\sigma}}, \mathcal{H}_M] &= \left[e_{\mathbf{k}\sigma}^\dagger n_{d\bar{\sigma}}, \delta_M \left(a_\uparrow^\dagger a_\uparrow - \frac{1}{2} \right) \right] + \left[e_{\mathbf{k}\sigma}^\dagger n_{d\bar{\sigma}}, t_{hp} \sum_{\bar{\sigma}} (d_{\bar{\sigma}} a_\uparrow^\dagger + a_\uparrow d_{\bar{\sigma}}^\dagger) \right] \\
 &+ \left[e_{\mathbf{k}\sigma}^\dagger n_{d\bar{\sigma}}, \Delta \sum_{\bar{\sigma}} (d_{\bar{\sigma}} a_\uparrow + a_\uparrow^\dagger d_{\bar{\sigma}}^\dagger) \right]
 \end{aligned} \tag{B.302}$$

$$\begin{aligned}
 \left[e_{\mathbf{k}\sigma}^\dagger n_{d\bar{\sigma}}, \delta_M \left(a_\uparrow^\dagger a_\uparrow - \frac{1}{2} \right) \right] &= \delta_M \left(e_{\mathbf{k}\sigma}^\dagger n_{d\bar{\sigma}} a_\uparrow^\dagger a_\uparrow - a_\uparrow^\dagger a_\uparrow e_{\mathbf{k}\sigma}^\dagger n_{d\bar{\sigma}} \right) \\
 &= \delta_M \left(a_\uparrow^\dagger a_\uparrow e_{\mathbf{k}\sigma}^\dagger n_{d\bar{\sigma}} - a_\uparrow^\dagger a_\uparrow e_{\mathbf{k}\sigma}^\dagger n_{d\bar{\sigma}} \right) \\
 &= 0.
 \end{aligned} \tag{B.303}$$

$$\left[e_{\mathbf{k}\sigma}^\dagger n_{d\bar{\sigma}}, t_{hp} \sum_{\bar{\sigma}} (d_{\bar{\sigma}} a_\uparrow^\dagger + a_\uparrow d_{\bar{\sigma}}^\dagger) \right] = \underbrace{t_{hp} \sum_{\bar{\sigma}} [e_{\mathbf{k}\sigma}^\dagger n_{d\bar{\sigma}}, d_{\bar{\sigma}} a_\uparrow^\dagger]}_I + \underbrace{t_{hp} \sum_{\bar{\sigma}} [e_{\mathbf{k}\sigma}^\dagger n_{d\bar{\sigma}}, a_\uparrow d_{\bar{\sigma}}^\dagger]}_{II} \tag{B.304}$$

$$\begin{aligned}
 I : t_{hp} \sum_{\bar{\sigma}} [e_{\mathbf{k}\sigma}^\dagger n_{d\bar{\sigma}}, d_{\bar{\sigma}} a_\uparrow^\dagger] &= t_{hp} \sum_{\bar{\sigma}} \left(e_{\mathbf{k}\sigma}^\dagger n_{d\bar{\sigma}} d_{\bar{\sigma}} a_\uparrow^\dagger - d_{\bar{\sigma}} a_\uparrow^\dagger e_{\mathbf{k}\sigma}^\dagger n_{d\bar{\sigma}} \right) \\
 &= t_{hp} \sum_{\bar{\sigma}} \left(e_{\mathbf{k}\sigma}^\dagger d_{\bar{\sigma}}^\dagger d_{\bar{\sigma}} d_{\bar{\sigma}} a_\uparrow^\dagger - e_{\mathbf{k}\sigma}^\dagger d_{\bar{\sigma}} a_\uparrow^\dagger n_{d\bar{\sigma}} \right) \\
 &= t_{hp} \sum_{\bar{\sigma}} \left(-e_{\mathbf{k}\sigma}^\dagger d_{\bar{\sigma}}^\dagger d_{\bar{\sigma}} d_{\bar{\sigma}} a_\uparrow^\dagger - e_{\mathbf{k}\sigma}^\dagger d_{\bar{\sigma}} a_\uparrow^\dagger n_{d\bar{\sigma}} \right) \\
 &= t_{hp} \sum_{\bar{\sigma}} \left(-e_{\mathbf{k}\sigma}^\dagger \left(\delta_{\bar{\sigma}\bar{\sigma}} - d_{\bar{\sigma}} d_{\bar{\sigma}}^\dagger \right) d_{\bar{\sigma}} a_\uparrow^\dagger - e_{\mathbf{k}\sigma}^\dagger d_{\bar{\sigma}} a_\uparrow^\dagger n_{d\bar{\sigma}} \right) \\
 &= t_{hp} \sum_{\bar{\sigma}} \left(-\delta_{\bar{\sigma}\bar{\sigma}} e_{\mathbf{k}\sigma}^\dagger d_{\bar{\sigma}} a_\uparrow^\dagger + e_{\mathbf{k}\sigma}^\dagger d_{\bar{\sigma}} a_\uparrow^\dagger n_{d\bar{\sigma}} - e_{\mathbf{k}\sigma}^\dagger d_{\bar{\sigma}} a_\uparrow^\dagger n_{d\bar{\sigma}} \right) \\
 &= t_{hp} \sum_{\bar{\sigma}} \left(-\delta_{\bar{\sigma}\bar{\sigma}} d_{\bar{\sigma}} a_\uparrow^\dagger e_{\mathbf{k}\sigma}^\dagger \right).
 \end{aligned} \tag{B.305}$$

$$\begin{aligned}
 II : t_{hp} \sum_{\bar{\sigma}} [e_{\mathbf{k}\sigma}^\dagger n_{d\bar{\sigma}}, a_\uparrow d_{\bar{\sigma}}^\dagger] &= t_{hp} \sum_{\bar{\sigma}} \left(e_{\mathbf{k}\sigma}^\dagger n_{d\bar{\sigma}} a_\uparrow d_{\bar{\sigma}}^\dagger - a_\uparrow d_{\bar{\sigma}}^\dagger e_{\mathbf{k}\sigma}^\dagger n_{d\bar{\sigma}} \right) \\
 &= t_{hp} \sum_{\bar{\sigma}} \left(-a_\uparrow e_{\mathbf{k}\sigma}^\dagger d_{\bar{\sigma}}^\dagger \left(\delta_{\bar{\sigma}\bar{\sigma}} - d_{\bar{\sigma}}^\dagger d_{\bar{\sigma}} \right) - a_\uparrow d_{\bar{\sigma}}^\dagger e_{\mathbf{k}\sigma}^\dagger n_{d\bar{\sigma}} \right) \\
 &= t_{hp} \sum_{\bar{\sigma}} \left(-\delta_{\bar{\sigma}\bar{\sigma}} a_\uparrow e_{\mathbf{k}\sigma}^\dagger d_{\bar{\sigma}}^\dagger + a_\uparrow d_{\bar{\sigma}}^\dagger e_{\mathbf{k}\sigma}^\dagger d_{\bar{\sigma}}^\dagger d_{\bar{\sigma}} - a_\uparrow d_{\bar{\sigma}}^\dagger e_{\mathbf{k}\sigma}^\dagger n_{d\bar{\sigma}} \right) \\
 &= t_{hp} \sum_{\bar{\sigma}} \delta_{\bar{\sigma}\bar{\sigma}} a_\uparrow d_{\bar{\sigma}}^\dagger e_{\mathbf{k}\sigma}^\dagger.
 \end{aligned} \tag{B.306}$$

$$\left[e_{\mathbf{k}\bar{\sigma}}^\dagger n_{d\bar{\sigma}}, t_{hp} \sum_{\bar{\sigma}} (d_{\bar{\sigma}} a_{\uparrow}^\dagger + a_{\uparrow} d_{\bar{\sigma}}^\dagger) \right] = t_{hp} \sum_{\bar{\sigma}} \left(-\delta_{\bar{\sigma}\bar{\sigma}} d_{\bar{\sigma}} a_{\uparrow}^\dagger e_{\mathbf{k}\bar{\sigma}}^\dagger + \delta_{\bar{\sigma}\bar{\sigma}} a_{\uparrow} d_{\bar{\sigma}}^\dagger e_{\mathbf{k}\bar{\sigma}}^\dagger \right). \quad (\text{B.307})$$

$$\left[e_{\mathbf{k}\bar{\sigma}}^\dagger n_{d\bar{\sigma}}, \Delta \sum_{\bar{\sigma}} (d_{\bar{\sigma}} a_{\uparrow} + a_{\uparrow} d_{\bar{\sigma}}^\dagger) \right] = \underbrace{\Delta \sum_{\bar{\sigma}} [e_{\mathbf{k}\bar{\sigma}}^\dagger n_{d\bar{\sigma}}, d_{\bar{\sigma}} a_{\uparrow}]}_I + \underbrace{\Delta \sum_{\bar{\sigma}} [e_{\mathbf{k}\bar{\sigma}}^\dagger n_{d\bar{\sigma}}, a_{\uparrow} d_{\bar{\sigma}}^\dagger]}_{II} \quad (\text{B.308})$$

$$\begin{aligned} I : \Delta \sum_{\bar{\sigma}} [e_{\mathbf{k}\bar{\sigma}}^\dagger n_{d\bar{\sigma}}, d_{\bar{\sigma}} a_{\uparrow}] &= \Delta \sum_{\bar{\sigma}} \left(e_{\mathbf{k}\bar{\sigma}}^\dagger n_{d\bar{\sigma}} d_{\bar{\sigma}} a_{\uparrow} - d_{\bar{\sigma}} a_{\uparrow} e_{\mathbf{k}\bar{\sigma}}^\dagger n_{d\bar{\sigma}} \right) \\ &= \Delta \sum_{\bar{\sigma}} \left(-a_{\uparrow} e_{\mathbf{k}\bar{\sigma}}^\dagger d_{\bar{\sigma}}^\dagger d_{\bar{\sigma}} d_{\bar{\sigma}} - d_{\bar{\sigma}} a_{\uparrow} e_{\mathbf{k}\bar{\sigma}}^\dagger n_{d\bar{\sigma}} \right) \\ &= \Delta \sum_{\bar{\sigma}} \left(-a_{\uparrow} e_{\mathbf{k}\bar{\sigma}}^\dagger \left(\delta_{\bar{\sigma}\bar{\sigma}} - d_{\bar{\sigma}} d_{\bar{\sigma}}^\dagger \right) d_{\bar{\sigma}} - d_{\bar{\sigma}} a_{\uparrow} e_{\mathbf{k}\bar{\sigma}}^\dagger n_{d\bar{\sigma}} \right) \\ &= \Delta \sum_{\bar{\sigma}} \left(-\delta_{\bar{\sigma}\bar{\sigma}} a_{\uparrow} e_{\mathbf{k}\bar{\sigma}}^\dagger d_{\bar{\sigma}} + d_{\bar{\sigma}} a_{\uparrow} e_{\mathbf{k}\bar{\sigma}}^\dagger n_{d\bar{\sigma}} - d_{\bar{\sigma}} a_{\uparrow} e_{\mathbf{k}\bar{\sigma}}^\dagger n_{d\bar{\sigma}} \right) \\ &= \Delta \sum_{\bar{\sigma}} \left(\delta_{\bar{\sigma}\bar{\sigma}} a_{\uparrow} d_{\bar{\sigma}} e_{\mathbf{k}\bar{\sigma}}^\dagger \right). \end{aligned} \quad (\text{B.309})$$

$$\begin{aligned} II : \Delta \sum_{\bar{\sigma}} [e_{\mathbf{k}\bar{\sigma}}^\dagger n_{d\bar{\sigma}}, a_{\uparrow} d_{\bar{\sigma}}^\dagger] &= \Delta \sum_{\bar{\sigma}} \left(e_{\mathbf{k}\bar{\sigma}}^\dagger n_{d\bar{\sigma}} a_{\uparrow} d_{\bar{\sigma}}^\dagger - a_{\uparrow} d_{\bar{\sigma}}^\dagger e_{\mathbf{k}\bar{\sigma}}^\dagger n_{d\bar{\sigma}} \right) \\ &= \Delta \sum_{\bar{\sigma}} \left(-a_{\uparrow} e_{\mathbf{k}\bar{\sigma}}^\dagger d_{\bar{\sigma}}^\dagger d_{\bar{\sigma}} d_{\bar{\sigma}}^\dagger - a_{\uparrow} d_{\bar{\sigma}}^\dagger e_{\mathbf{k}\bar{\sigma}}^\dagger n_{d\bar{\sigma}} \right) \\ &= \Delta \sum_{\bar{\sigma}} \left(-a_{\uparrow} e_{\mathbf{k}\bar{\sigma}}^\dagger d_{\bar{\sigma}}^\dagger \left(\delta_{\bar{\sigma}\bar{\sigma}} - d_{\bar{\sigma}}^\dagger d_{\bar{\sigma}} \right) - a_{\uparrow} d_{\bar{\sigma}}^\dagger e_{\mathbf{k}\bar{\sigma}}^\dagger n_{d\bar{\sigma}} \right) \\ &= \Delta \sum_{\bar{\sigma}} \left(-\delta_{\bar{\sigma}\bar{\sigma}} a_{\uparrow} e_{\mathbf{k}\bar{\sigma}}^\dagger d_{\bar{\sigma}}^\dagger + a_{\uparrow} e_{\mathbf{k}\bar{\sigma}}^\dagger d_{\bar{\sigma}}^\dagger d_{\bar{\sigma}}^\dagger d_{\bar{\sigma}} - a_{\uparrow} d_{\bar{\sigma}}^\dagger e_{\mathbf{k}\bar{\sigma}}^\dagger n_{d\bar{\sigma}} \right) \\ &= \Delta \sum_{\bar{\sigma}} \left(-\delta_{\bar{\sigma}\bar{\sigma}} d_{\bar{\sigma}}^\dagger a_{\uparrow} e_{\mathbf{k}\bar{\sigma}}^\dagger + a_{\uparrow} d_{\bar{\sigma}}^\dagger e_{\mathbf{k}\bar{\sigma}}^\dagger n_{d\bar{\sigma}} - a_{\uparrow} d_{\bar{\sigma}}^\dagger e_{\mathbf{k}\bar{\sigma}}^\dagger n_{d\bar{\sigma}} \right) \\ &= \Delta \sum_{\bar{\sigma}} \left(-\delta_{\bar{\sigma}\bar{\sigma}} d_{\bar{\sigma}}^\dagger a_{\uparrow} e_{\mathbf{k}\bar{\sigma}}^\dagger \right). \end{aligned} \quad (\text{B.310})$$

$$\left[e_{\mathbf{k}\bar{\sigma}}^\dagger n_{d\bar{\sigma}}, \Delta \sum_{\bar{\sigma}} (d_{\bar{\sigma}} a_{\uparrow} + a_{\uparrow} d_{\bar{\sigma}}^\dagger) \right] = \Delta \sum_{\bar{\sigma}} \left(\delta_{\bar{\sigma}\bar{\sigma}} a_{\uparrow} d_{\bar{\sigma}} e_{\mathbf{k}\bar{\sigma}}^\dagger - \delta_{\bar{\sigma}\bar{\sigma}} d_{\bar{\sigma}}^\dagger a_{\uparrow} e_{\mathbf{k}\bar{\sigma}}^\dagger \right). \quad (\text{B.311})$$

$$\begin{aligned}
(\omega + \varepsilon_{\mathbf{k}\sigma} + \eta^+) G_{e_{\mathbf{k}\sigma}^\dagger n_{d\bar{\sigma}}, d_\sigma}^r(\omega) &= -V_{SD} \sum_{\mathbf{k}} G_{e_{\mathbf{k}\sigma}^\dagger n_{d\bar{\sigma}}, d_\sigma}^r(\omega) - \sqrt{2}V G_{d_\sigma^\dagger n_{d\bar{\sigma}}, d_\sigma}^r(\omega) \\
&+ t_{hp} \sum_{\bar{\sigma}} \delta_{\bar{\sigma}\bar{\sigma}} \left(-\langle\langle d_{\bar{\sigma}} a_{\uparrow}^\dagger e_{\mathbf{k}\sigma}^\dagger; d_\sigma^\dagger \rangle\rangle + \langle\langle a_{\uparrow} d_{\bar{\sigma}}^\dagger e_{\mathbf{k}\sigma}^\dagger; d_\sigma^\dagger \rangle\rangle \right) \\
&+ \Delta \sum_{\bar{\sigma}} \delta_{\bar{\sigma}\bar{\sigma}} \left(\langle\langle a_{\uparrow} d_{\bar{\sigma}} e_{\mathbf{k}\sigma}^\dagger; d_\sigma^\dagger \rangle\rangle - \langle\langle d_{\bar{\sigma}}^\dagger a_{\uparrow}^\dagger e_{\mathbf{k}\sigma}^\dagger; d_\sigma^\dagger \rangle\rangle \right) \quad (\text{B.312})
\end{aligned}$$

$$\begin{aligned}
(\omega + \varepsilon_{\mathbf{k}\sigma} + \eta^+) G_{e_{\mathbf{k}\sigma}^\dagger n_{d\bar{\sigma}}, d_\sigma}^r(\omega) &= -V_{SD} \sum_{\mathbf{k}} G_{e_{\mathbf{k}\sigma}^\dagger n_{d\bar{\sigma}}, d_\sigma}^r(\omega) - \sqrt{2}V G_{d_\sigma^\dagger n_{d\bar{\sigma}}, d_\sigma}^r(\omega) \\
&+ t_{hp} \sum_{\bar{\sigma}} \delta_{\bar{\sigma}\bar{\sigma}} \left(-G_{d_{\bar{\sigma}} a_{\uparrow}^\dagger e_{\mathbf{k}\sigma}^\dagger, d_\sigma}^r(\omega) + G_{a_{\uparrow} d_{\bar{\sigma}}^\dagger e_{\mathbf{k}\sigma}^\dagger, d_\sigma}^r(\omega) \right) \\
&+ \Delta \sum_{\bar{\sigma}} \delta_{\bar{\sigma}\bar{\sigma}} \left(G_{a_{\uparrow} d_{\bar{\sigma}} e_{\mathbf{k}\sigma}^\dagger, d_\sigma}^r(\omega) - G_{d_{\bar{\sigma}}^\dagger a_{\uparrow}^\dagger e_{\mathbf{k}\sigma}^\dagger, d_\sigma}^r(\omega) \right) \quad (\text{B.313})
\end{aligned}$$

Let us apply the decoupling:

$$\begin{aligned}
(\omega + \varepsilon_{\mathbf{k}\sigma} + \eta^+) G_{e_{\mathbf{k}\sigma}^\dagger n_{d\bar{\sigma}}, d_\sigma}^r(\omega) &= -V_{SD} \sum_{\mathbf{k}} G_{e_{\mathbf{k}\sigma}^\dagger n_{d\bar{\sigma}}, d_\sigma}^r(\omega) - \sqrt{2}V G_{d_\sigma^\dagger n_{d\bar{\sigma}}, d_\sigma}^r(\omega) \\
&+ t_{hp} \sum_{\bar{\sigma}} \delta_{\bar{\sigma}\bar{\sigma}} \left(-\langle d_{\bar{\sigma}} a_{\uparrow}^\dagger \rangle G_{e_{\mathbf{k}\sigma}^\dagger, d_\sigma}^r(\omega) + \langle a_{\uparrow} d_{\bar{\sigma}}^\dagger \rangle G_{e_{\mathbf{k}\sigma}^\dagger, d_\sigma}^r(\omega) \right) \\
&+ \Delta \sum_{\bar{\sigma}} \delta_{\bar{\sigma}\bar{\sigma}} \left(\langle a_{\uparrow} d_{\bar{\sigma}} \rangle G_{e_{\mathbf{k}\sigma}^\dagger, d_\sigma}^r(\omega) - \langle d_{\bar{\sigma}}^\dagger a_{\uparrow}^\dagger \rangle G_{e_{\mathbf{k}\sigma}^\dagger, d_\sigma}^r(\omega) \right) \quad (\text{B.314})
\end{aligned}$$

$$\begin{aligned}
(\omega + \varepsilon_{\mathbf{k}\sigma} + \eta^+) G_{e_{\mathbf{k}\sigma}^\dagger n_{d\bar{\sigma}}, d_\sigma}^r(\omega) &= -V_{SD} \sum_{\mathbf{k}} G_{e_{\mathbf{k}\sigma}^\dagger n_{d\bar{\sigma}}, d_\sigma}^r(\omega) - \sqrt{2}V G_{d_\sigma^\dagger n_{d\bar{\sigma}}, d_\sigma}^r(\omega) \\
&+ t_{hp} \sum_{\bar{\sigma}} \delta_{\bar{\sigma}\bar{\sigma}} \left(-\langle d_{\bar{\sigma}} a_{\uparrow}^\dagger \rangle G_{e_{\mathbf{k}\sigma}^\dagger, d_\sigma}^r(\omega) + \langle a_{\uparrow} d_{\bar{\sigma}}^\dagger \rangle G_{e_{\mathbf{k}\sigma}^\dagger, d_\sigma}^r(\omega) \right) \\
&+ \Delta \sum_{\bar{\sigma}} \delta_{\bar{\sigma}\bar{\sigma}} \left(\langle a_{\uparrow} d_{\bar{\sigma}} \rangle G_{e_{\mathbf{k}\sigma}^\dagger, d_\sigma}^r(\omega) - \langle d_{\bar{\sigma}}^\dagger a_{\uparrow}^\dagger \rangle G_{e_{\mathbf{k}\sigma}^\dagger, d_\sigma}^r(\omega) \right) \quad (\text{B.315})
\end{aligned}$$

$$(\omega^+ + \varepsilon_{\mathbf{k}\sigma}) G_{e_{\mathbf{k}\sigma}^\dagger n_{d\bar{\sigma}}, d_\sigma}^r(\omega) = -V_{SD} \sum_{\mathbf{k}} G_{e_{\mathbf{k}\sigma}^\dagger n_{d\bar{\sigma}}, d_\sigma}^r(\omega) - \sqrt{2}V G_{d_\sigma^\dagger n_{d\bar{\sigma}}, d_\sigma}^r(\omega) \div (\omega^+ + \varepsilon_{\mathbf{k}\sigma})$$

$$\left[1 + V_{SD} \sum_{\mathbf{k}} \left(\frac{1}{\omega^+ + \varepsilon_{\mathbf{k}\sigma}} \right) \right] G_{e_{\mathbf{k}\sigma}^\dagger n_{d\bar{\sigma}}, d_\sigma}^r(\omega) = \frac{-\sqrt{2}V G_{d_\sigma^\dagger n_{d\bar{\sigma}}, d_\sigma}^r(\omega)}{(\omega^+ + \varepsilon_{\mathbf{k}\sigma})} \quad (\text{B.316})$$

$$\boxed{G_{e_{\mathbf{k}\sigma}^\dagger n_{d\bar{\sigma}}, d_\sigma}^r(\omega) = -\frac{\sqrt{2}V(\omega^+ + \varepsilon_{\mathbf{k}\sigma})^{-1} G_{d_\sigma^\dagger n_{d\bar{\sigma}}, d_\sigma}^r(\omega)}{\left[1 + V_{SD} \sum_{\mathbf{k}} \left(\frac{1}{\omega^+ + \varepsilon_{\mathbf{k}\sigma}} \right) \right]}} \quad (\text{B.317})$$

Now, we substitute this result into Eq.(B.283):

$$(\omega^+ + \varepsilon_{d\sigma} + U - K_2)G_{d_\sigma^\dagger n_{d\bar{\sigma}} d_\sigma}^r(\omega) + t_{hp}\Delta K G_{d_\sigma n_{d\bar{\sigma}}, d_\sigma}^r(\omega) = \frac{2V^2 \sum_{\mathbf{k}} (\omega^+ + \varepsilon_{\mathbf{k}\sigma})^{-1} G_{d_\sigma^\dagger n_{d\bar{\sigma}}, d_\sigma}^r(\omega)}{\left[1 + V_{SD} \sum_{\mathbf{k}} \left(\frac{1}{\omega^+ + \varepsilon_{\mathbf{k}\sigma}}\right)\right]} \quad (\text{B.318})$$

As previously defined, $\sum_{\mathbf{k}} \left(\frac{1}{\omega^+ + \varepsilon_{\mathbf{k}\sigma} + i\eta^+}\right) = -i\pi\rho_{\mathbf{k}\sigma}(\omega)$ and $\Gamma_\sigma = 2V^2\pi\rho_{\mathbf{k}\sigma}(\omega)$. Thus,

$$(\omega^+ + \varepsilon_{d\sigma} + U - K_2)G_{d_\sigma^\dagger n_{d\bar{\sigma}} d_\sigma}^r(\omega) + t_{hp}\Delta K G_{d_\sigma n_{d\bar{\sigma}}, d_\sigma}^r(\omega) = \frac{-\Gamma_\sigma G_{d_\sigma^\dagger n_{d\bar{\sigma}}, d_\sigma}^r(\omega)}{[1 - i(V_{SD}\pi\rho_{\mathbf{k}\sigma}(\omega))]} \Rightarrow \quad (\text{B.319})$$

$$(\omega^+ + \varepsilon_{d\sigma} + U - K_2)G_{d_\sigma^\dagger n_{d\bar{\sigma}} d_\sigma}^r(\omega) + t_{hp}\Delta K G_{d_\sigma n_{d\bar{\sigma}}, d_\sigma}^r(\omega) = \frac{-\Gamma_\sigma G_{d_\sigma^\dagger n_{d\bar{\sigma}}, d_\sigma}^r(\omega)}{[1 - i\sqrt{x}]}, \quad (\text{B.320})$$

with $x = (V_{SD}\pi\rho_{\mathbf{k}\sigma}(\omega))^2$. Further,

$$\frac{-i\Gamma_\sigma}{(1 - i\sqrt{x})} \frac{(1 + i\sqrt{x})}{(1 + i\sqrt{x})} = \frac{-i\Gamma_\sigma (1 + i\sqrt{x})}{(1 + x)} = \frac{\sqrt{x}\Gamma_\sigma}{(1 + x)} - \frac{i\Gamma_\sigma}{(1 + x)} \quad (\text{B.321})$$

Comparing with Eq.(A.43):

$$-\left(\frac{\sqrt{x}\Gamma_\sigma}{(1 + x)} - \frac{i\Gamma_\sigma}{(1 + x)}\right) = -\frac{\sqrt{x}\Gamma_\sigma}{(1 + x)} + \frac{i\Gamma_\sigma}{(1 + x)} = \bar{\Sigma}_\sigma \quad (\text{B.322})$$

$$\boxed{\bar{\Sigma}_\sigma = \text{Re}(\Sigma_\sigma) - \text{Im}(\Sigma_\sigma)} \quad (\text{B.323})$$

with

$$\text{Re}(\Sigma_\sigma) = -\frac{\sqrt{x}\Gamma_\sigma}{1 + x} \quad (\text{B.324})$$

$$\text{Im}(\Sigma_\sigma) = -\frac{i\Gamma_\sigma}{1 + x} \quad (\text{B.325})$$

Therefore,

$$(\omega^+ + \varepsilon_{d\sigma} + U - K_2)G_{d_\sigma^\dagger n_{d\bar{\sigma}} d_\sigma}^r(\omega) + t_{hp}\Delta K G_{d_\sigma n_{d\bar{\sigma}}, d_\sigma}^r(\omega) = -\bar{\Sigma}_\sigma G_{d_\sigma^\dagger n_{d\bar{\sigma}}, d_\sigma}^r(\omega) \Rightarrow$$

$$(\omega^+ + \varepsilon_{d\sigma} + U + \bar{\Sigma}_\sigma - K_2)G_{d_\sigma^\dagger n_{d\bar{\sigma}} d_\sigma}^r(\omega) + t_{hp}\Delta K G_{d_\sigma n_{d\bar{\sigma}}, d_\sigma}^r(\omega) = 0 \Rightarrow$$

$$G_{d_\sigma^\dagger n_{d\bar{\sigma}} d_\sigma}^r(\omega) + \frac{t_{hp}\Delta K}{(\omega^+ + \varepsilon_{d\sigma} + U + \bar{\Sigma}_\sigma - K_2)} G_{d_\sigma n_{d\bar{\sigma}}, d_\sigma}^r(\omega) = 0 \quad (\text{B.326})$$

$$\boxed{G_{d_\sigma^\dagger n_{d\bar{\sigma}} d_\sigma}^r(\omega) + t_{hp}\Delta \bar{K}_U^\sigma G_{d_\sigma n_{d\bar{\sigma}}, d_\sigma}^r(\omega) = 0} \quad (\text{B.327})$$

wherein we recognize

$$\bar{K}_U^\sigma = \frac{K}{(\omega^+ + \varepsilon_{d\sigma} + U + \bar{\Sigma}_\sigma - K_2)} \quad (\text{B.328})$$

B.2.3 Resulting system of Green's functions

After deriving the many-particle Green's functions with the EOM technique and Hubbard-I approximation, we get the following result:

$$(\omega^+ - \varepsilon_{d\sigma} - U - \Sigma_\sigma)G_{d_\sigma n_{d\bar{\sigma}}, d_\sigma}^r(\omega) - K_1 G_{d_\sigma n_{d\bar{\sigma}}, d_\sigma}^r(\omega) + t_{hp}\Delta K G_{d_\sigma^\dagger n_{d\bar{\sigma}}, d_\sigma}^r(\omega) = \langle n_{d\bar{\sigma}} \rangle \quad (\text{B.329})$$

$$G_{d_\sigma^\dagger n_{d\bar{\sigma}} d_\sigma}^r(\omega) + t_{hp}\Delta \bar{K}_U^\sigma G_{d_\sigma n_{d\bar{\sigma}}, d_\sigma}^r(\omega) = 0 \quad (\text{B.330})$$

Let us substitute Eq.(B.330) into Eq.(B.329):

$$(\omega^+ - \varepsilon_{d\sigma} - U - \Sigma_\sigma)G_{d_\sigma n_{d\bar{\sigma}}, d_\sigma}^r(\omega) - K_1 G_{d_\sigma n_{d\bar{\sigma}}, d_\sigma}^r(\omega) + t_{hp}\Delta K (-t_{hp}\Delta \bar{K}_U^\sigma G_{d_\sigma n_{d\bar{\sigma}}, d_\sigma}^r(\omega)) = \langle n_{d\bar{\sigma}} \rangle \Rightarrow$$

$$(\omega^+ - \varepsilon_{d\sigma} - U - \Sigma_\sigma)G_{d_\sigma n_{d\bar{\sigma}}, d_\sigma}^r(\omega) - K_1 G_{d_\sigma n_{d\bar{\sigma}}, d_\sigma}^r(\omega) - (t_{hp}\Delta)^2 K \bar{K}_U^\sigma G_{d_\sigma n_{d\bar{\sigma}}, d_\sigma}^r(\omega) = \langle n_{d\bar{\sigma}} \rangle \Rightarrow$$

$$(\omega^+ - \varepsilon_{d\sigma} - U - \Sigma_\sigma)G_{d_\sigma n_{d\bar{\sigma}}, d_\sigma}^r(\omega) - \left[K_1 + (t_{hp}\Delta)^2 K \bar{K}_U^\sigma \right] G_{d_\sigma n_{d\bar{\sigma}}, d_\sigma}^r(\omega) = \langle n_{d\bar{\sigma}} \rangle \quad (\text{B.331})$$

We recognize the Majorana self-energy modified by the presence of electronic correlation

$$\Sigma_{M,\sigma}^{U \neq 0} = K_1 + (t_{hp}\Delta)^2 K \bar{K}_U^\sigma \quad (\text{B.332})$$

Hence,

$$G_{d_\sigma n_{d\bar{\sigma}}, d_\sigma}^r(\omega) = \frac{\langle n_{d\bar{\sigma}} \rangle}{(\omega^+ - \varepsilon_{d\sigma} - U - \Sigma_{M,\sigma}^{U \neq 0} - \Sigma_\sigma)} \quad (\text{B.333})$$

B.2.4 Results for Hubbard-I approximation

Finally, we have the following relations to evolve to an expression for $G_{d_\sigma d_\sigma}^r(\omega)$:

$$(\omega^+ - \varepsilon_{d\sigma} - \Sigma_\sigma - \Sigma_{M,\sigma}^{U=0})G_{d_\sigma d_\sigma}^r(\omega) = 1 + UG_{d_\sigma n_{d\bar{\sigma}}, d_\sigma}^r(\omega) + Ut_{hp}\Delta\bar{K}G_{d_\sigma^\dagger n_{d\bar{\sigma}} d_\sigma}^r(\omega) \quad (\text{B.334})$$

$$(\omega^+ - \varepsilon_{d\sigma} - U - \Sigma_{M,\sigma}^{U\neq 0} - \Sigma_\sigma)G_{d_\sigma n_{d\bar{\sigma}}, d_\sigma}^r(\omega) = \langle n_{d\bar{\sigma}} \rangle \quad (\text{B.335})$$

$$G_{d_\sigma^\dagger n_{d\bar{\sigma}} d_\sigma}^r(\omega) + t_{hp}\Delta\bar{K}_U^\sigma G_{d_\sigma n_{d\bar{\sigma}}, d_\sigma}^r(\omega) = 0 \quad (\text{B.336})$$

From Eqs.(B.335) and (B.336):

$$\boxed{G_{d_\sigma^\dagger n_{d\bar{\sigma}} d_\sigma}^r(\omega) = \frac{-t_{hp}\Delta\bar{K}_U^\sigma \langle n_{d\bar{\sigma}} \rangle}{\omega^+ - \varepsilon_{d\sigma} - U - \Sigma_{M,\sigma}^{U\neq 0} - \Sigma_\sigma}} \quad (\text{B.337})$$

Thus,

$$\begin{aligned} (\omega^+ - \varepsilon_{d\sigma} - \Sigma_\sigma - \Sigma_{M,\sigma}^{U=0})G_{d_\sigma d_\sigma}^r(\omega) &= 1 + U \left[\frac{\langle n_{d\bar{\sigma}} \rangle}{\omega^+ - \varepsilon_{d\sigma} - U - \Sigma_{M,\sigma}^{U\neq 0} - \Sigma_\sigma} \right] \\ &+ Ut_{hp}\Delta\bar{K} \left[\frac{-t_{hp}\Delta\bar{K}_U^\sigma \langle n_{d\bar{\sigma}} \rangle}{\omega^+ - \varepsilon_{d\sigma} - U - \Sigma_{M,\sigma}^{U\neq 0} - \Sigma_\sigma} \right] \Rightarrow \\ (\omega^+ - \varepsilon_{d\sigma} - \Sigma_\sigma - \Sigma_{M,\sigma}^{U=0})G_{d_\sigma d_\sigma}^r(\omega) &= 1 + \frac{U\langle n_{d\bar{\sigma}} \rangle}{\left(\omega^+ - \varepsilon_{d\sigma} - U - \Sigma_{M,\sigma}^{U\neq 0} - \Sigma_\sigma\right)} - \frac{U(t_{hp}\Delta)^2 \langle n_{d\bar{\sigma}} \rangle \bar{K} \bar{K}_U^\sigma}{\left(\omega^+ - \varepsilon_{d\sigma} - U - \Sigma_{M,\sigma}^{U\neq 0} - \Sigma_\sigma\right)} \end{aligned} \quad (\text{B.338})$$

Let us label

$$\boxed{\lambda(\omega, \sigma\bar{\sigma}) = 1 + \frac{U\langle n_{d\bar{\sigma}} \rangle}{\left(\omega^+ - \varepsilon_{d\sigma} - U - \Sigma_{M,\sigma}^{U\neq 0} - \Sigma_\sigma\right)}} \quad (\text{B.339})$$

and

$$\boxed{\mathcal{M}(\omega, \sigma\bar{\sigma}) = \frac{\langle n_{d\bar{\sigma}} \rangle \bar{K}^\sigma \bar{K}_U^\sigma}{\left(\omega^+ - \varepsilon_{d\sigma} - U - \Sigma_{M,\sigma}^{U\neq 0} - \Sigma_\sigma\right)}} \quad (\text{B.340})$$

$$(\omega^+ - \varepsilon_{d\sigma} - \Sigma_\sigma - \Sigma_{M,\sigma}^{U=0})G_{d_\sigma d_\sigma}^r(\omega) = \lambda(\omega, \sigma\bar{\sigma}) - U(t_{hp}\Delta)^2 \mathcal{M}(\omega, \sigma\bar{\sigma}) \quad (\text{B.341})$$

Finally, the Green's function of the QD considering the Hubbard-I approximation is given by:

$$G_d(\omega, \sigma) = \frac{\lambda(\omega, \sigma \bar{\sigma}) - U(t_{hp}\Delta)^2 \mathcal{M}(\omega, \sigma \bar{\sigma})}{\omega^+ - \varepsilon_{d\sigma} - \Sigma_\sigma - \Sigma_{M,\sigma}^{U=0}} \quad (\text{B.342})$$

with

$$\begin{aligned} \Sigma_{M,\sigma}^{U=0} &= K_1 + (t_{hp}\Delta)^2 K \bar{K}^\sigma & \Sigma_{M,\sigma}^{U \neq 0} &= K_1 + (t_{hp}\Delta)^2 K \bar{K}_U^\sigma \\ \bar{K}_U^\sigma &= \frac{K}{(\omega^+ + \varepsilon_{d\sigma} + U + \bar{\Sigma}_\sigma - K_2)} & \bar{K}^\sigma &= \frac{K}{(\omega^+ + \varepsilon_{d\sigma} + \bar{\Sigma}_\sigma - K_2)} \\ K_1 &= \frac{(t_{hp})^2}{(\omega^+ - \delta_M)} + \frac{(\Delta)^2}{(\omega^+ + \delta_M)} & K_2 &= \frac{(t_{hp})^2}{(\omega^+ + \delta_M)} + \frac{(\Delta)^2}{(\omega^+ - \delta_M)} \end{aligned} \quad (\text{B.343})$$

$$K = \frac{1}{(\omega^+ - \delta_M)} + \frac{1}{(\omega^+ + \delta_M)} \quad (\text{B.344})$$

and $\Sigma_\sigma = -\frac{\sqrt{x}\Gamma_\sigma}{1+x} - i\frac{\Gamma_\sigma}{1+x}$, $\bar{\Sigma}_\sigma = -\frac{\sqrt{x}\Gamma_\sigma}{1+x} + i\frac{\Gamma_\sigma}{1+x}$, with $\Gamma_\sigma = 2V^2\pi\rho_{k\sigma}(\omega)$ as being the Anderson broadening.

Appendix C

Curriculum Vitae and List of Publications

Education

- **2016 - Present**

PhD degree in Science Materials with emphasis in Condensed Matter Physics

Institution: UNESP, School of Natural Sciences and Engineering, Ilha Solteira, Brazil.

Thesis: Majorana bound states in hybrid quantum dot-topological superconducting nanowires: detection and applications

Supervisor: Prof. Dr. Antonio Carlos Ferreira Seridonio

Grant: São Paulo Research Foundation (FAPESP), 2015/23539-8.

- **2014 - 2016**

Msc degree in Science Materials with emphasis in Condensed Matter Physics

Institution: UNESP, School of Natural Sciences and Engineering, Ilha Solteira, Brazil.

Dissertation: Fano Interference in quantum dots assisted by Majorana fermions.

Supervisor: Prof. Dr. Antonio Carlos Ferreira Seridonio

Grant: São Paulo Research Foundation (FAPESP), 2014/14143-0.

- **2009 - 2013**

B.S. degree in Physics (Exchange Program, 2010-2012)

Institution: Faculty of Sciences and Technology, University of Coimbra (FCTUC), Coimbra, Portugal.

Institution: UNESP, School of Natural Sciences and Engineering, Ilha Solteira, Brazil.

List of Publications

1. **L. S. RICCO**, M. de Souza, M. S. Figueira, I. A. Shelykh, A. C. Seridonio. Spin-dependent zero-bias peak in a hybrid nanowire-quantum dot system: Distinguishing isolated Majorana fermions from Andreev bound states. *Phys. Rev. B* 99, 155159 (2019);

2. **RICCO L. S.**, Campo, V. L., Shelykh, I. A. and Seridonio, A. C. Majorana oscillations modulated by Fano interference and degree of nonlocality in a topological superconducting-nanowire-quantum-dot system. *Phys. Rev. B*, 98, 075142 (2018);
3. **RICCO, L. S.** Dessotti, F. A., Shelykh, I. A., Figueira, M.S., and Seridonio, A. C. Tuning of heat and charge transport by Majorana fermions. *Scientific Reports*, 8, p. 1-8 (2018);
4. Campo, V. L., **RICCO, L. S.** and Seridonio, A. C. Isolating Majorana fermions with finite Kitaev nanowires and temperature: Universality of the zero-bias conductance. *Phys. Rev. B*, 96, 045135 (2017);
5. Marques, Y., Obispo, A. E., **RICCO, L. S.**, de Souza, M., Shelykh, I. A., Seridonio, A. C. Antibonding ground state of adatom molecules in bulk Dirac semimetals. *Phys. Rev. B*, 96, 041112 (2017);
6. Guessi, L. H., Dessotti, F. A., Marques, Y., **RICCO, L. S.**, Pereira, G. M., Menegasso, P., de Souza, M. and Seridonio, A. C. Encrypting Majorana fermion qubits as bound states in the continuum. *Phys. Rev. B*, 96, 041114 (2017);
7. Dessotti, F.A., **RICCO, L.S.**, Marques, Y., Machado, R.S., Guessi, L.H., Figueira, M.S., de Souza, M., Seridonio, A.C. Fano fingerprints of Majoranas in Kitaev dimers of superconducting adatoms. *Phys. E*, v. 00, p. 1-9 (2016);
8. **RICCO, L.S.**, Marques, Y., Dessotti, F. A., Machado, R. S., de Souza, M., Seridonio, A. C. Decay of bound states in the continuum of Majorana fermions induced by vacuum fluctuations: Proposal of qubit technology. *Phys. Rev. B*, 93, 165116 (2016);
9. Dessotti, F. A., **RICCO, L. S.**, Marques, Y., Guessi, L. H., Yoshida, M., Figueira M. S., de Souza, M., Sodano, P. and Seridonio, A. C. Unveiling Majorana quasiparticles by a quantum phase transition: Proposal of a current switch. *Phys. Rev. B*, 94, 125426 (2016);
10. Marques, Y., **RICCO, L. S.**, Dessotti F. A., Machado, R. S., Shelykh, I. A., de Souza, M. and Seridonio, A. C. Realization of anomalous multiferroicity in free-standing graphene with magnetic adatoms. *Phys. Rev. B*, 94, 205119 (2016);
11. Guessi, L. H., Machado, R. S., Marques, Y., **RICCO, L. S.**, Kristinsson, K., Yoshida, M., Shelykh, I. A., de Souza, M. and Seridonio, A. C. Catching the bound states in the continuum of a phantom atom in graphene. *Phys. Rev. B*, 92, 045409 (2015);
12. Guessi, L. H., Marques, Y., Machado, R. S., Kristinsson, K., **RICCO, L. S.**, Shelykh, I. A., Figueira M. S., de Souza, M. and Seridonio, A. C. Quantum phase transition triggering magnetic bound states in the continuum in graphene. *Phys. Rev. B*, 92, 245107 (2015);
13. **RICCO L. S.**, Marques, Y., Dessotti, F.A., de Souza, M., Seridonio, A.C. Effect of interdots electronic repulsion in the Majorana signature for a double dot interferometer. *Phys. E*, 78, p. 25-30 (2015);

14. Dessotti, F. A., **RICCO, L. S.**, de Souza, M., Souza, F. M. and Seridonio, A. C. Probing the antisymmetric Fano interference assisted by a Majorana fermion. *Journal of Applied Physics*, 116, 173701 (2014).